

ADVANCES IN NON-ALCOHOLIC FATTY LIVER DISEASE THERAPEUTICS: PATHOGENIC MECHANISMS AND TARGETS

EDITED BY: Ana Blas-García and Francisco Javier Cubero
PUBLISHED IN: Frontiers in Pharmacology





frontiers

Frontiers eBook Copyright Statement

The copyright in the text of individual articles in this eBook is the property of their respective authors or their respective institutions or funders. The copyright in graphics and images within each article may be subject to copyright of other parties. In both cases this is subject to a license granted to Frontiers.

The compilation of articles constituting this eBook is the property of Frontiers.

Each article within this eBook, and the eBook itself, are published under the most recent version of the Creative Commons CC-BY licence.

The version current at the date of publication of this eBook is CC-BY 4.0. If the CC-BY licence is updated, the licence granted by Frontiers is automatically updated to the new version.

When exercising any right under the CC-BY licence, Frontiers must be attributed as the original publisher of the article or eBook, as applicable.

Authors have the responsibility of ensuring that any graphics or other materials which are the property of others may be included in the CC-BY licence, but this should be checked before relying on the CC-BY licence to reproduce those materials. Any copyright notices relating to those materials must be complied with.

Copyright and source acknowledgement notices may not be removed and must be displayed in any copy, derivative work or partial copy which includes the elements in question.

All copyright, and all rights therein, are protected by national and international copyright laws. The above represents a summary only. For further information please read Frontiers' Conditions for Website Use and Copyright Statement, and the applicable CC-BY licence.

ISSN 1664-8714

ISBN 978-2-83250-858-9

DOI 10.3389/978-2-83250-858-9

About Frontiers

Frontiers is more than just an open-access publisher of scholarly articles: it is a pioneering approach to the world of academia, radically improving the way scholarly research is managed. The grand vision of Frontiers is a world where all people have an equal opportunity to seek, share and generate knowledge. Frontiers provides immediate and permanent online open access to all its publications, but this alone is not enough to realize our grand goals.

Frontiers Journal Series

The Frontiers Journal Series is a multi-tier and interdisciplinary set of open-access, online journals, promising a paradigm shift from the current review, selection and dissemination processes in academic publishing. All Frontiers journals are driven by researchers for researchers; therefore, they constitute a service to the scholarly community. At the same time, the Frontiers Journal Series operates on a revolutionary invention, the tiered publishing system, initially addressing specific communities of scholars, and gradually climbing up to broader public understanding, thus serving the interests of the lay society, too.

Dedication to Quality

Each Frontiers article is a landmark of the highest quality, thanks to genuinely collaborative interactions between authors and review editors, who include some of the world's best academicians. Research must be certified by peers before entering a stream of knowledge that may eventually reach the public - and shape society; therefore, Frontiers only applies the most rigorous and unbiased reviews. Frontiers revolutionizes research publishing by freely delivering the most outstanding research, evaluated with no bias from both the academic and social point of view. By applying the most advanced information technologies, Frontiers is catapulting scholarly publishing into a new generation.

What are Frontiers Research Topics?

Frontiers Research Topics are very popular trademarks of the Frontiers Journals Series: they are collections of at least ten articles, all centered on a particular subject. With their unique mix of varied contributions from Original Research to Review Articles, Frontiers Research Topics unify the most influential researchers, the latest key findings and historical advances in a hot research area! Find out more on how to host your own Frontiers Research Topic or contribute to one as an author by contacting the Frontiers Editorial Office: frontiersin.org/about/contact

ADVANCES IN NON-ALCOHOLIC FATTY LIVER DISEASE THERAPEUTICS: PATHOGENIC MECHANISMS AND TARGETS

Topic Editors:

Ana Blas-García, University of Valencia, Spain

Francisco Javier Cubero, Complutense University of Madrid, Spain

Citation: Blas-García, A., Cubero, F. J., eds. (2022). Advances in Non-Alcoholic Fatty Liver Disease Therapeutics: Pathogenic Mechanisms and Targets. Lausanne: Frontiers Media SA. doi: 10.3389/978-2-83250-858-9

Table of Contents

- 05 Editorial: Advances in Non-Alcoholic Fatty Liver Disease Therapeutics: Pathogenic Mechanisms and Targets**
Ana Blas-García and Francisco Javier Cubero
- 08 Transcriptomic Analysis Reveals the Protective Effects of Empagliflozin on Lipid Metabolism in Nonalcoholic Fatty Liver Disease**
Yuting Ma, Chengxia Kan, Hongyan Qiu, Yongping Liu, Ningning Hou, Fang Han, Junfeng Shi and Xiaodong Sun
- 22 Regulation of Lipid Metabolism by Lamin in Mutation-Related Diseases**
Yue Peng, Qianyu Tang, Fan Xiao and Nian Fu
- 34 Pharmacological Effects and Molecular Protective Mechanisms of Astragalus Polysaccharides on Nonalcoholic Fatty Liver Disease**
Jing Zhang and Quansheng Feng
- 45 Regression of Liver Steatosis Following Phosphatidylcholine Administration: A Review of Molecular and Metabolic Pathways Involved**
D. Osipova, K. Kokoreva, L. Lazebnik, E. Golovanova, Ch. Pavlov, A. Dukhanin, S. Orlova and K. Starostin
- 55 Elevated Serum Regulator of Calcineurin 2 is Associated With an Increased Risk of Non-Alcoholic Fatty Liver Disease**
Xia Fang, Hongya Wang, Xiaozhen Tan, Ting Ye, Yong Xu and Jiahao Fan
- 67 NUSAP1 Could be a Potential Target for Preventing NAFLD Progression to Liver Cancer**
Taofei Zeng, Guanglei Chen, Xinbo Qiao, Hui Chen, Lisha Sun, Qingtian Ma, Na Li, Junqi Wang, Chaoliu Dai and Feng Xu
- 81 Rifaximin Ameliorates Non-alcoholic Steatohepatitis in Mice Through Regulating gut Microbiome-Related Bile Acids**
Jie Jian, Mei-Tong Nie, Baoyu Xiang, Hui Qian, Chuan Yin, Xin Zhang, Menghui Zhang, Xuan Zhu and Wei-Fen Xie
- 93 Celastrol: An Update on Its Hepatoprotective Properties and the Linked Molecular Mechanisms**
Mengzhen Li, Faren Xie, Lu Wang, Guoxue Zhu, Lian-Wen Qi and Shujun Jiang
- 108 FGF9 Alleviates the Fatty Liver Phenotype by Regulating Hepatic Lipid Metabolism**
Fanrong Zhao, Lei Zhang, Menglin Zhang, Jincan Huang, Jun Zhang and Yongsheng Chang
- 120 Revealing the Mechanism of Huazhi Rougan Granule in the Treatment of Nonalcoholic Fatty Liver Through Intestinal Flora Based on 16S rRNA, Metagenomic Sequencing and Network Pharmacology**
Yingying Liu, Yingying Tan, Jiaqi Huang, Chao Wu, Xiaotian Fan, Antony Stalin, Shan Lu, Haojia Wang, Jingyuan Zhang, Fanqin Zhang, Zhishan Wu, Bing Li, Zhihong Huang, Meilin Chen, Guoliang Cheng, Yanfang Mou and Jiarui Wu

- 139** *Obeticholic Acid Induces Hepatotoxicity Via FXR in the NAFLD Mice*
Chuangzhen Lin, Bingqing Yu, Lixin Chen, Zhaohui Zhang, Weixiang Ye, Hui Zhong, Wenke Bai, Yuping Yang and Biao Nie
- 149** *Mendelian Randomization Rules Out Causation Between Inflammatory Bowel Disease and Non-Alcoholic Fatty Liver Disease*
Lanlan Chen, Zhongqi Fan, Xiaodong Sun, Wei Qiu, Yuguo Chen, Jianpeng Zhou and Guoyue Lv
- 157** *Targeting Thyroid Hormone/Thyroid Hormone Receptor Axis: An Attractive Therapy Strategy in Liver Diseases*
Qianyu Tang, Min Zeng, Linxi Chen and Nian Fu
- 173** *Multi-Omics Reveals Inhibitory Effect of Baicalein on Non-Alcoholic Fatty Liver Disease in Mice*
Ping Li, Jianran Hu, Hongmei Zhao, Jing Feng and Baofeng Chai



OPEN ACCESS

EDITED AND REVIEWED BY

Angelo A. Izzo,
University of Naples Federico II, Italy

*CORRESPONDENCE

Ana Blas-García,
ana.blas@uv.es
Francisco Javier Cubero,
fcubero@ucom.es

SPECIALTY SECTION

This article was submitted to
Gastrointestinal and Hepatic
Pharmacology,
a section of the journal
Frontiers in Pharmacology

RECEIVED 17 October 2022

ACCEPTED 31 October 2022

PUBLISHED 10 November 2022

CITATION

Blas-García A and Cubero FJ (2022),
Editorial: Advances in non-alcoholic
fatty liver disease therapeutics:
Pathogenic mechanisms and targets.
Front. Pharmacol. 13:1072353.
doi: 10.3389/fphar.2022.1072353

COPYRIGHT

© 2022 Blas-García and Cubero. This is
an open-access article distributed
under the terms of the [Creative
Commons Attribution License \(CC BY\)](#).
The use, distribution or reproduction in
other forums is permitted, provided the
original author(s) and the copyright
owner(s) are credited and that the
original publication in this journal is
cited, in accordance with accepted
academic practice. No use, distribution
or reproduction is permitted which does
not comply with these terms.

Editorial: Advances in non-alcoholic fatty liver disease therapeutics: Pathogenic mechanisms and targets

Ana Blas-García^{1,2,3*} and Francisco Javier Cubero^{3,4,5*}

¹Department of Physiology, Faculty of Medicine, University of Valencia, Valencia, Spain, ²FISABIO (Fundación para el Fomento de la Investigación Sanitaria y Biomédica de la Comunidad Valenciana), Valencia, Spain, ³Centro de Investigación Biomédica en Red de Enfermedades Hepáticas y Digestivas (CIBEREHD), Madrid, Spain, ⁴Department of Immunology, Ophthalmology and ENT, Complutense University School of Medicine, Madrid, Spain, ⁵Instituto de Investigación Sanitaria Gregorio Marañón (IIISGM), Madrid, Spain

KEYWORDS

NAFLD, liver, therapy, gut, microbiome, NASH

Editorial on the Research Topic

[Advances in non-alcoholic fatty liver disease therapeutics: Pathogenic mechanisms and targets](#)

Non-alcoholic fatty liver disease (NAFLD) is a leading cause of advanced liver diseases worldwide and an increasing clinical and economic burden. As its complex pathophysiology and heterogeneity of disease phenotypes result in a lack of therapeutic approaches for NAFLD, efforts must continue to develop effective treatments for patients with advanced non-alcoholic steatohepatitis (NASH) and prevention methods for individuals at high risk of NAFLD and progressive liver disease.

As editors of this Research Topic, it was a joy to review a wide range of interesting manuscripts in relation to the novel targets and therapies for NAFLD. In total about 100 basic scientists and clinicians from different countries contributed 14 originals or review articles about current perspectives in novel targets and approaches for NAFLD resolution and prevention. In the current editorial we summarize the main contributions and take-home messages within each of the accepted articles.

[Ma et al.](#) analyzed the impact of empagliflozin, a novel type of sodium-glucose co-transporter two inhibitor, in a murine model of NAFLD. Transcriptomic analysis revealed that empagliflozin significantly decreased lipid synthesis and improved lipid metabolism, thereby enhancing triglyceride transfer, lipolysis and microsomal mitochondrial β -oxidation. Control trials with patients are needed with this already approved drug.

[Osipova et al.](#) reviewed the literature of the use of essential phospholipids (EPLs) rich in phosphatidylcholine (PCH) as a treatment option for fatty liver disease, demonstrating a robust clinical utility. This review nicely explored the potential molecular and metabolic pathways involved in the positive effects of PCH on steatosis regression.

The regulatory mechanisms of mutations in the lamin gene in lipid alterations in human disease is reviewed by Peng et al. Nuclear lamins, known as type 5 intermediate fibers, are composed of lamin A, lamin C, lamin B1, and lamin B2, which are encoded by *LMNA* and *LMNB* genes, respectively. Importantly, mutations in nuclear lamins not only participate in lipid disorders but also in different human diseases, such as lipodystrophy, metabolic-associated fatty liver disease, and dilated cardiomyopathy. Targeting nuclear lamins may be a potent therapeutic avenue for lipid metabolic disorders and human diseases in the future.

The study by Zeng et al. identified key genes linking NAFLD fibrosis and hepatocellular carcinoma (HCC) through analysis and experimental verification using two GEO datasets. The results suggested that common differentially expressed genes (DEGs) were strongly associated with the glucocorticoid receptor pathway, regulation of transmembrane transporter activity, peroxisome, and proteoglycan biosynthetic process. Interestingly, the expression of nucleolar and spindle associated protein 1 (NUSAP1) was highly expressed in both human hepatic cell lines and NAFLD models at mRNA and protein level. These data revealed that modulation of NUSAP1 may be a therapeutic target for preventing NAFLD progression to liver cancer.

Fang et al. evaluated calcineurin 2 (RCAN2) expression in the liver of mice with hepatic steatosis and in the serum of NAFLD patients. They found that elevated serum RCAN2 levels were associated with an increased risk of NAFLD, suggesting that serum RCAN2, and especially the ratio between serum RCAN2 and liver enzymes, might be a candidate diagnostic marker for NAFLD.

Jian et al. showed that rifaximin greatly ameliorated hepatic steatosis, lobular inflammation, and fibrogenesis in mice with methionine and choline deficient diet-induced NASH via alteration of the gut microbiome. Rifaximin treatment may therefore be a promising approach for NASH therapy in humans.

Zhao et al. demonstrated that overexpression of fibroblast growth factor-9 (FGF9) in the liver of diet-induced obese mice inhibits the expression of genes involved in lipogenesis and increases the expression of genes involved in fatty acid oxidation, thereby reducing cellular lipid accumulation. Thus, targeting FGF9 might be exploited to treat NAFLD and metabolic syndrome.

The review by Zhang and Feng summarized the actual knowledge on the potential use of *Astragalus* polysaccharides (APS) for basic research, pharmacological development, and therapeutic applications in the management of NAFLD.

The pharmacological function and the underlying mechanisms of celastrol in the prevention and treatment of liver diseases including NAFLD, liver injury, and liver cancer

was comprehensively reviewed by Li et al. Both preclinical and clinical studies are required to accelerate the clinical transformation of celastrol in a feasible treatment option.

Growing evidence suggests that thyroid hormone/thyroid hormone receptor (TH/TR) axis participates in hepatic metabolism, specifically in NAFLD, liver fibrosis, and in the progression of acute liver failure and alcoholic liver disease. Therefore, Tang et al. present pros and cons for the TH/TR axis as a prospecting target to cure hepatic diseases.

Huazhi Rougan Granule (HRG) is commonly used in the clinical treatment of NAFLD because it can reduce hepatic lipid deposition and regulate intestinal flora, thus exerting a protective mechanism. In a murine model, Liu et al. showed that the mechanism of HRG in the treatment of NAFLD through intestinal flora is mainly reflected in the biological process of gene function and related to infectious diseases, immune systems, and signal transduction pathways.

Lin et al. investigated the role of farnesoid X receptor (FXR) in the high-dose obeticholic acid (OCA)-induced hepatotoxicity in a NAFLD mouse model. In their study, the authors showed that high-dose OCA induces cholesterol accumulation in livers via the upregulation of genes involved in cholesterol acquisition and the downregulation of genes regulating cholesterol degradation in liver, leading to the production of IL-1 β and an FXR-mediated inflammatory response.

Chen et al. explored the causal relationship between NAFLD and inflammatory bowel disease (IBD) using a multivariable Mendelian randomization analysis. This study ruled out the causal relationship between these two pathologies, suggesting therapeutics targeting NAFLD might not work for IBD and *vice versa*.

Finally, the study by Li et al. analyzed the protective effect of oral administration of baicalein, a natural flavonoid with multiple biological activities, on NAFLD in high-fat diet murine models. Multi-omics analysis revealed that baicalein might affect lipid metabolism in liver via regulating the ecological structure of gut microbiota in NAFLD mice.

Altogether, this Research Topic deepens in novel mechanisms, drugs and targets for the treatment of NAFLD/NASH.

Author contributions

All authors listed have made a substantial, direct, and intellectual contribution to the work and approved it for publication.

Funding

This work was supported by the MICINN Retos PID 2020-117941RB-I00, co-funded with FEDER funds, COST Action

CA17112, Instituto de Salud Carlos III (CIBER CB06/04/0071 and CB06/04/0082), Generalitat Valenciana (AICO 2021/017 and CIPROM/2021/044) and FISABIO (UGP-21-236). The research group belongs to the validated Research Groups Ref. 970935 Liver Pathophysiology, 920631 Lymphocyte Immunobiology and IBL-6 (imas12-associated).

Acknowledgments

The authors thank all researchers that have contributed to this Research Topic, the expert referees who reviewed submissions in a constructive manner and the Editorial office team of Frontiers for its kind support and assistance.

Conflict of interest

The authors declare that the research was conducted in the absence of any commercial or financial relationships that could be construed as a potential conflict of interest.

Publisher's note

All claims expressed in this article are solely those of the authors and do not necessarily represent those of their affiliated organizations, or those of the publisher, the editors and the reviewers. Any product that may be evaluated in this article, or claim that may be made by its manufacturer, is not guaranteed or endorsed by the publisher.



Transcriptomic Analysis Reveals the Protective Effects of Empagliflozin on Lipid Metabolism in Nonalcoholic Fatty Liver Disease

Yuting Ma^{1,2,3†}, Chengxia Kan^{1,2,3†}, Hongyan Qiu^{1,2,3†}, Yongping Liu^{1,2,3}, Ningning Hou^{1,2}, Fang Han⁴, Junfeng Shi^{1,2,3*} and Xiaodong Sun^{1,2,3*}

¹Department of Endocrinology and Metabolism, Affiliated Hospital of Weifang Medical University, Weifang, China, ²Branch of Shandong Provincial Clinical Research Center for Diabetes and Metabolic Diseases, Weifang, China, ³Clinical Research Center, Affiliated Hospital of Weifang Medical University, Weifang, China, ⁴Department of Pathology, Affiliated Hospital of Weifang Medical University, Weifang, China

OPEN ACCESS

Edited by:

Francisco Javier Cubero,
Complutense University of Madrid,
Spain

Reviewed by:

Stefania Di Mauro,
University of Catania, Italy
Carlos Sanz Garcia,
Complutense University of Madrid,
Spain

*Correspondence:

Junfeng Shi
jfsi@wfmuc.edu.cn
Xiaodong Sun
xiaodong.sun@wfmuc.edu.cn

[†]These authors have contributed
equally to this work and share first
authorship

Specialty section:

This article was submitted to
Gastrointestinal and Hepatic
Pharmacology,
a section of the journal
Frontiers in Pharmacology

Received: 12 October 2021

Accepted: 06 December 2021

Published: 21 December 2021

Citation:

Ma Y, Kan C, Qiu H, Liu Y, Hou N,
Han F, Shi J and Sun X (2021)
Transcriptomic Analysis Reveals the
Protective Effects of Empagliflozin on
Lipid Metabolism in Nonalcoholic Fatty
Liver Disease.
Front. Pharmacol. 12:793586.
doi: 10.3389/fphar.2021.793586

Empagliflozin is a novel type of sodium-glucose cotransporter two inhibitor with diverse beneficial effects in the treatment of nonalcoholic fatty liver disease (NAFLD). Although empagliflozin impacts NAFLD by regulating lipid metabolism, the underlying mechanism has not been fully elucidated. In this study, we investigated transcriptional regulation pathways affected by empagliflozin in a mouse model of NAFLD. In this study, NAFLD was established in male C57BL/6J mice by administration of a high-fat diet; it was then treated with empagliflozin and whole transcriptome analysis was conducted. Gene expression levels detected by transcriptome analysis were then verified by quantitative real-time polymerase chain reaction, protein levels detected by Western Blot. Differential expression genes screened from RNA-Seq data were enriched in lipid metabolism and synthesis. The Gene Set Enrichment Analysis (GSEA) results showed decreased lipid synthesis and improved lipid metabolism. Empagliflozin improved NAFLD through enhanced triglyceride transfer, triglyceride lipolysis and microsomal mitochondrial β -oxidation. This study provides new insights concerning the mechanisms by which sodium-glucose cotransporter two inhibitors impact NAFLD, particularly in terms of liver lipid metabolism. The lipid metabolism-related genes identified in this experiment provide robust evidence for further analyses of the mechanism by which empagliflozin impacts NAFLD.

Keywords: empagliflozin, NAFLD, obesity, lipid, transcriptome

INTRODUCTION

Nonalcoholic fatty liver disease (NAFLD) is a common chronic liver disease, characterized by a broad spectrum of clinical manifestations (e.g., hepatic steatosis, fibrosis, cirrhosis, and hepatocellular carcinoma) (Rinella, 2015; Manne et al., 2018). Importantly, NAFLD affects one-quarter of adults worldwide (Zhou et al., 2019). Metabolic diseases (e.g., obesity and type 2 diabetes) have been associated with greater NAFLD risk in previous studies (Perumpail et al., 2017). Considering the increasing morbidity of obesity and diabetes, the prevalences of NAFLD and advanced liver disease are expected to increase (Cotter and Rinella, 2020). Lipid metabolism disorders have essential roles in NAFLD occurrence and progression (Mato et al., 2019; Di et al., 2021). For example, hepatic steatosis (a typical symptom of NAFLD) results from lipid

acquisition that exceeds lipid disposal (Ipsen et al., 2018). Considering that the liver has a central role in lipid synthesis and metabolism, it is important to study drug prevention and treatment of NAFLD from the perspective of liver lipid metabolism. Recently, SGLT2i has become a focus because of beneficial effect on reduced serum transaminase activities (Seko et al., 2018). Furthermore, several pilot studies showed SGLT2i had a significant reduction in liver transaminases, body weight, and the fatty liver index in NAFLD patients (Komiya et al., 2016; Seko et al., 2017). Therefore, the efficacy of SGLT2 inhibitor on NASH/NAFLD can be expected.

Sodium-glucose cotransporter 2 (SGLT2) inhibitors are effective hypoglycemic drugs that function by inhibiting glucose reabsorption in proximal renal tubules. SGLT2 inhibitors improve glycemic status in patients with type 2 diabetes; they also contribute to weight loss and body fat reduction (Szekeres et al., 2021). Multiple studies have reported that SGLT2 inhibitor treatments reduce serum cholesterol and triglyceride (TG) levels (Hayashi et al., 2017; Calapkulu et al., 2019); they also increase lipolysis, liver fatty acid oxidation, and ketogenesis (Osataphan et al., 2019). Empagliflozin (EMP), a novel anti-hyperglycemic agent (**Supplementary Figure S1**), is a type of SGLT2 inhibitor (Frampton, 2018). Although EMP was designed as a hypoglycemic drug, it also has an important effect on lipid metabolism and has been shown to reduce liver fat in NAFLD (Kuchay et al., 2018). Studies by Xu et al. revealed that EMP contributes to weight loss through increased fat utilization and browning. Furthermore, reductions of obesity-related inflammation by EMP have been associated with M2 macrophage polarization (Xu et al., 2017; Xu et al., 2019). Additionally, recent studies indicated SGLT2i decreased body weight and lipid profiles, including total cholesterol (TC) and TG (Al-Sharea et al., 2018; Matsubayashi et al., 2020; Liu et al., 2021). However, there is a few researches illustrating how EMP regulated the progress of TG accumulation and associated triglyceride molecules.

Triglyceride molecule is the main form of storage and transport of fatty acids in cells and plasma. Fatty acid activation is catalyzed by long-chain acyl-CoA synthetase (ACSL) family of enzymes and microsomal G3P acyltransferase (GPAT) enzymes catalyzed G3P pathway, which is the main way to synthesize TG (Cohen and Fisher, 2013). The triglyceride transfer protein (MTP) combined with TG to form VLDL particles (Cohen and Fisher, 2013). Furthermore, adipose triglyceride lipase (ATGL, also known as PNPLA2), a rate-limiting step of TG lipolysis in adipocytes was activated by the comparative gene identification-58 (CGI-58) (Lass et al., 2006). Liver specific resection of CGI-58 can lead to NAFLD phenotype in mice, including hepatic steatosis and hepatic fibrosis (Guo et al., 2013). The patatin-like phospholipase domain-containing 3 (PNPLA3) has a genetic association with NAFLD, and mice showed accumulation of inactive PNPLA3 in lipid droplets and increased steatosis in high-fat diet feeding (Smagris et al., 2015). Hepatic TG can be oxidized by multiple pathways. Mitochondrial β -oxidation is the main route in hepatocytes (Musso et al., 2009). The expression of genes including mitochondrial β -oxidation is regulated largely by PPAR α

activity. PGC1 α and BAF60a form a complex to regulate activity of PPAR α transcriptional in the liver (Li et al., 2008).

Moreover, with the rapid development of RNAseq technology, transcriptome analysis of NAFLD is increasing. Previous investigations suggested lipid metabolism plays a major role in NAFLD (Xu et al., 2021). However, the molecular mechanisms underlying EMP-mediated NAFLD protection of hepatic lipid metabolism have not been fully elucidated. Here, we investigated signaling pathways impacted by EMP in a mouse model of NAFLD and explored the mechanisms and triglyceride molecules underlying the effects of EMP on liver lipid metabolism and synthesis.

MATERIALS AND METHODS

Animal Model and Drug Administration

All animal experiments in this study were approved by the Animal Ethics Committee of Weifang Medical University and adhered to national guidelines for experiments involving laboratory animals. Six-week-old male C57BL/6J mice (weight, 21 ± 0.8 g) were purchased from Pengyue Co., Ltd. (Jinan, China). All mice were housed under a 12-h day/night cycle at constant temperature (approximately 22°C) and suitable humidity (45–70%). As previous study (Han et al., 2020), the CT group ($n = 8$) was fed a regular diet (320 kcal per 100 g) (Pengyue Co., Ltd. Jinan, China), and the HFD ($n = 8$) and EMP groups ($n = 8$) were fed a high-fat diet (54.05% fat, 15.10% protein, and 30.85% carbohydrate; 529.8 kcal per 100 g) (Fanbo Biotechnology Co., Ltd., Shanghai, China) for 20 weeks. After the 12 weeks of feeding, the EMP group underwent further intragastric administration of EMP (10 mg/kg/day) for 8 weeks, whereas CT and HFD groups received same volume of saline for 8 weeks. After successive drug administration for 8 weeks, the mice were given 2% barbiturate sodium (40 mg/kg, ip) after 12 h of fasting. Body composition of the mice were measured by Body Composition Analysis (Bruker Minispec LF50, German). Blood samples were collected. Livers were also rapidly isolated and cut into several small pieces; two pieces of liver were fixed with formalin, then subjected to hematoxylin-eosin (HE) staining and Oil Red O staining. Plasma triglycerides and liver triglycerides were measured using triglyceride assay kit from Jiancheng (Nanjing, China). The remaining liver tissues were stored at -80°C for RNA extraction.

Total RNA Extraction, cDNA Library Construction, and RNA Sequencing

Total RNA was extracted and purified from liver tissue using TRIzol, in accordance with the manufacturer's instructions (Invitrogen, United States). Bioanalyzer 2,100 (Agilent, United States) and NanoDrop ND-1000 (NanoDrop, United States) equipment were used to assess total RNA quantity and quality. Poly (A) RNA was purified twice using Dynabeads Oligo (dT) (Thermo Fisher, United States). The resulting RNA was fragmented using a Magnesium RNA Fragmentation Module (NEB, United States) at 94°C for 5–7 min. RNA was used as a template for cDNA synthesis by

TABLE 1 | The sequence of the primers for qRT-PCR.

| Gene | Forward primer (5'-3') | Reverse primer (5'-3') |
|----------------|-------------------------|-------------------------|
| ACSL3 | AACCAAGTATCTTCAACACCATC | AGTCCGGTTTGGAAGTACAG |
| ACSL5 | TCCTGACGTTTGGAACGGC | CTCCCTCAATCCCCACAGAC |
| CGI-58 | TGGGGTTTTCTGAGCGAC | GGTTAAAGGGAGTCAATGCTGC |
| Cyp2g1 | GCACCTTTGTTTGTCTTGCCTG | TCCAAAAACGGTATTGGTGTG |
| Fam131c | CCTCTCTGGATGACGAAGAACT | TGTCCTGAAGGTAGATGCTCTC |
| Fdps | GGAGGTCTAGAGTACAATGCC | AAGCCTGGAGCAGTTCTACAC |
| GPAT1 | ACAGTTGGCACAATAGACGTTT | CCTTCCATTTCAGTGTTCGAGA |
| Hmgcs1 | AACTGGTGCAGAAATCTCTAGC | GGTTGAATAGCTCAGAACTAGCC |
| Hr | CCCCTGTGAACGGCATTGT | CCCCTCCAAAAGGGAGCAG |
| HSL | CCAGCCTGAGGGCTTACTG | CTCCATTGACTGTGACATCTCG |
| MTP | CTCTTGGCAGTGCTTTTCTCT | GAGCTTGTATAGCCGCTCATT |
| PGC-1 α | TATGGAGTGACATAGAGTGTCT | CCACTTCAATCCACCCAGAAAG |
| PNPLA3 | TCACCTTCGTGTGCACTCTC | CCTGGAGCCCGTCTCTGAT |
| PPAR α | AGAGCCCATCTGTCTCTCTC | ACTGGTAGTCTGCAAAACCAA |
| Rdh1 | GTCATGGGCCGAATGTCTTTC | GCCTGTCACTACTTGTACACAA |
| Smpd3 | TTTGCTTTTCTCGGGTTCATC | TTGTCTTCTAGCCGGGAGTAG |
| Sox9 | GAGCCGGATCTGAAGAGGGA | GCTTGACGTGTGGCTTGTTC |
| Sqle | ATAAGAAATGCGGGGATGTCAC | ATATCCGAGAAGGCAGCGAAC |
| β -actin | GGCTGTATCCCCTCCATCG | CCAGTTGGTAACAATGCCATGT |

SuperScript™ II Reverse transcriptase (Invitrogen). Single- or dual-index adapters were ligated to the fragments; AMPureXP beads were used for size selection. The mean insert size in the final cDNA library was 300 ± 50 bp. RNA-Seq was performed by Illumina NovaSeq™ 6,000 (LC Bio Technology Co., Ltd. China); 150-bp paired-end sequences were generated.

Quantification of RNA and Analysis of Differential Expression

FastQC was used to assess sequence quality. After removal of low-quality reads, the remaining 150-bp paired-end sequences were reassembled and mapped to the *Mus musculus* genome by HISAT2 (Kim et al., 2015). The transcripts were merged from sequences by StringTie (Pertea et al., 2015). To assure quality of RNA, we finally chosen five samples per group for further study. Genes with low expression levels were discarded when their minimum expression thresholds were below one count per million (CPM) in all 15 samples. The expression data were normalized by trimmed mean of M-values (TMM) using the edgeR package in Bioconductor (Robinson et al., 2010); counts of sequences were transformed to \log_2 (CPM) values for subsequent estimation of gene expression levels. Differentially expressed genes (DEGs) were identified using the limma package in R (Ritchie et al., 2015) with the following settings: fold change >2 or < -2 , and $p < 0.01$.

Analysis of Enrichment, PPI and GSEA

Gene Ontology (GO) (Young et al., 2010) and Kyoto Encyclopedia of Genes and Genomes (KEGG) (Kanehisa et al., 2008) analyses of DEGs were conducted using the clusterProfiler package in R (Yu et al., 2012). DEGs were integrated with mouse protein-protein interaction (PPI) networks using STRING. PPI networks were analyzed by Cytoscape 3.8.0 (Shannon et al., 2003). Gene Set Enrichment Analysis (GSEA) was used for additional pathway analyses; forward regression was then performed (Subramanian et al., 2005).

Real-Time Quantitative PCR

DEGs related to lipid metabolism and synthesis were subjected to validation by qPCR. Total RNA was extracted as described above for RNA-Seq analysis. cDNA was obtained using the PrimerScript™ RT reagent Kit with gDNA Eraser (TaKaRa, Japan). qPCR was performed using TB Green™ Premix Ex Taq™ (TaKaRa). Primers of target genes were synthesized by Sangon Biotech (China); Table 1 shows the sequences of primers used in this study. All relative expression levels of RNA were calculated based on Ct values, then normalized to the levels of β -actin (Liu et al., 2011) as follows: $2^{-[\Delta Ct = Ct(\text{target genes}) - Ct(\beta\text{-actin})]}$.

Western Blot

Total protein from liver tissues were lysed in ice-cold Lysis buffer (Whole Cell Lysis Assay, KeyGEN, China), and the total protein concentration was quantified by a BCA Protein Assay Kit (Solarbio, China). Equal amounts of protein were electrophoresed on 10% SDS-PAGE gels and transferred to PVDF membranes. After blocking with 5% BSA, the membranes were incubated with primary antibodies (FDPS, HMGCS1 1:1,000, Proteintech) overnight at 4°C. After washing, membranes were soaked in the secondary antibodies (Anti-rabbit IgG HRP-linked, 1:5,000, Anti-mouse IgG HRP-linked, 1:5,000) for 1 h β -actin was used as an internal control. Immunoblots were then visualized by enhanced chemiluminescence (ECL) using ImageQuant LAS 5000 (GE Healthcare) and analyzed using ImageJ.

Oil Red O Staining and H&E Staining

Mice were anesthetized by intraperitoneal injection of 2% sodium pentobarbital and 4% buffered neutral formalin solution was used to fix their liver tissues for 24 h. Tissue sections were subjected to H&E staining and Oil Red O staining, in accordance with standard protocols. The images were obtained using a microscope (CKX53, Olympus).

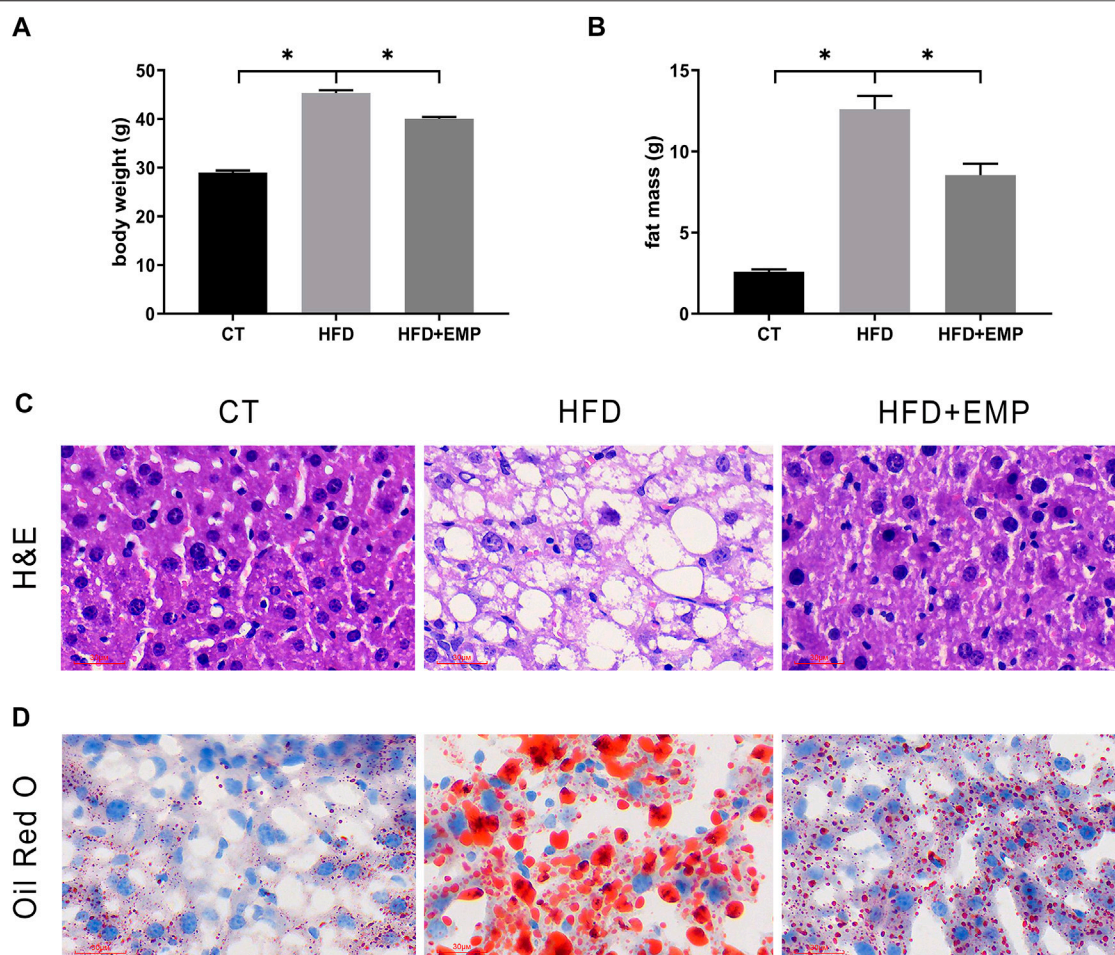


FIGURE 1 | Effect of EMP on mice. The impact of EMP on body weight **(A)** and fat mass **(B)**. Liver histological examination with H&E (200 \times) **(C)** and Oil Red O staining **(D)**. Data are presented as means \pm SEM, * $p < 0.05$, Scale bar: 30 μ m.

Statistics

Statistical analysis of this study was conducted by GraphPad Prism 7.0. Normality test was performed by Shapiro-Wilk normality test. Normally distributed data were presented as the means \pm SEM. One-way ANOVA followed by Dunnett's *post-hoc* test was performed when data involved in all three groups. Abnormally distributed data are displayed as the median and interquartile intervals, and the distributions between groups were compared with the non-parametric Kruskal-Wallis test. p values < 0.05 were considered significant.

RESULTS

Effects of EMP on Mouse Body Weight and Liver Pathology

All mice were acclimated for 1 week, then randomly separated into CT, HFD, and EMP groups. However, the CT + EMP group is not included in our study. Because our previous study had reported EMP does not have an effect on body weight, fat mass, plasma lipids (Sun et al., 2020). Also, a previous study consistent with our study indicated EMP does

TABLE 2 | Biometric and blood parameters of rats in the studied groups.

| Group | CT | HFD | EMP |
|-------------------------|------------------|--------------------------------|-------------------------------|
| Initial body weight (g) | 22.17 \pm 0.23 | 22.03 \pm 0.19 | 21.73 \pm 0.30 |
| Final body weight (g) | 28.97 \pm 0.45 | 45.37 \pm 0.58 ^a | 40.00 \pm 0.42 ^b |
| Initial fat mass (g) | 1.28 \pm 0.03 | 1.29 \pm 0.01 | 1.26 \pm 0.03 |
| Final fat mass (g) | 2.59 \pm 0.15 | 12.59 \pm 0.84 ^a | 8.55 \pm 0.69 ^b |
| FBG (mmol/L) | 5.23 \pm 0.93 | 7.21 \pm 1.39 | 6.85 \pm 0.63 |
| triglycerides (mg/dl) | 34.25 \pm 6.23 | 52.40 \pm 4.78 ^a | 50.06 \pm 6.06 |
| ALT (U/L) | 40.10 \pm 1.97 | 159.7 \pm 18.86 ^a | 45.3 \pm 3.52 ^b |
| AST (U/L) | 45.23 \pm 6.41 | 78.06 \pm 9.33 ^a | 31.2 \pm 3.79 ^b |

Data are shown as mean \pm SEM.

^a $p < 0.05$ vs CT.

^b $p < 0.05$ vs HFD.

not alter liver metabolism and biochemical parameters (Petito-da-Silva et al., 2019). Therefore, we did not establish the CT + EMP group. After 20 weeks of high-fat diet treatment, the weight and fat mass were significantly higher in the HFD and EMP groups than in the CT group. After 8 weeks of intragastric administration of EMP, the weight and fat

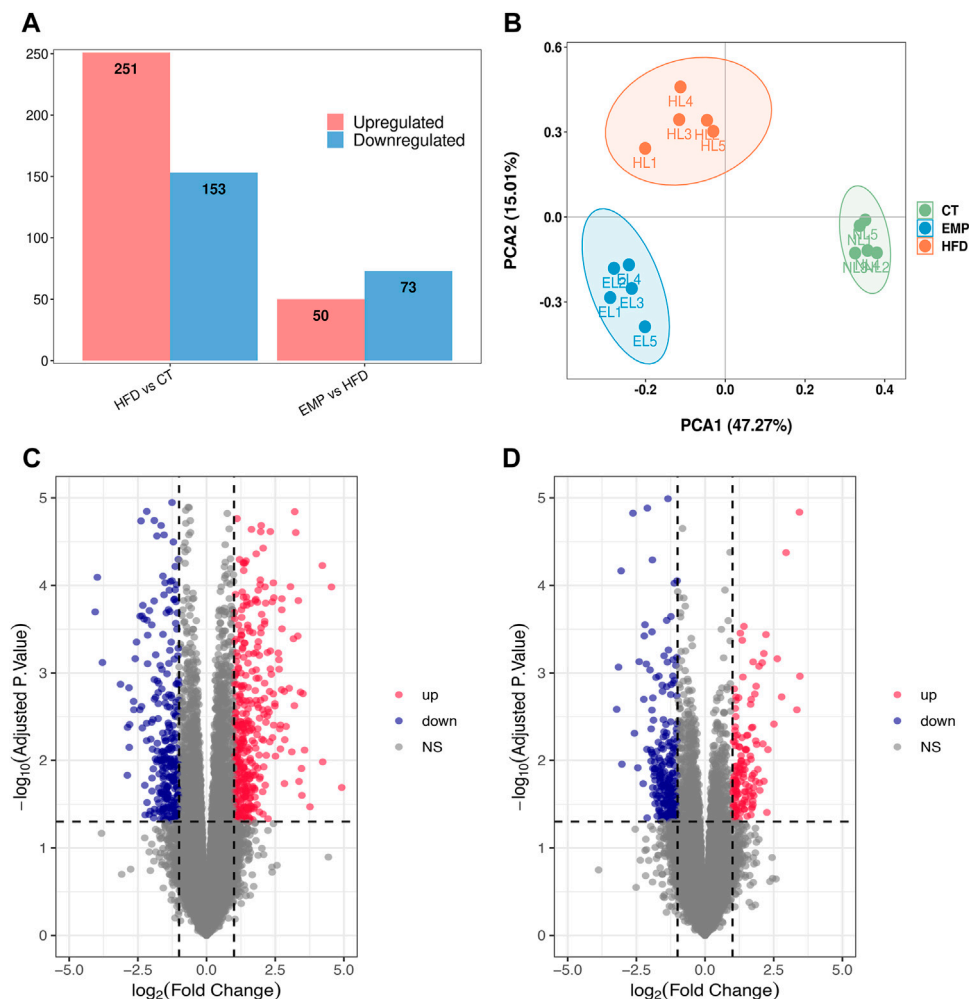


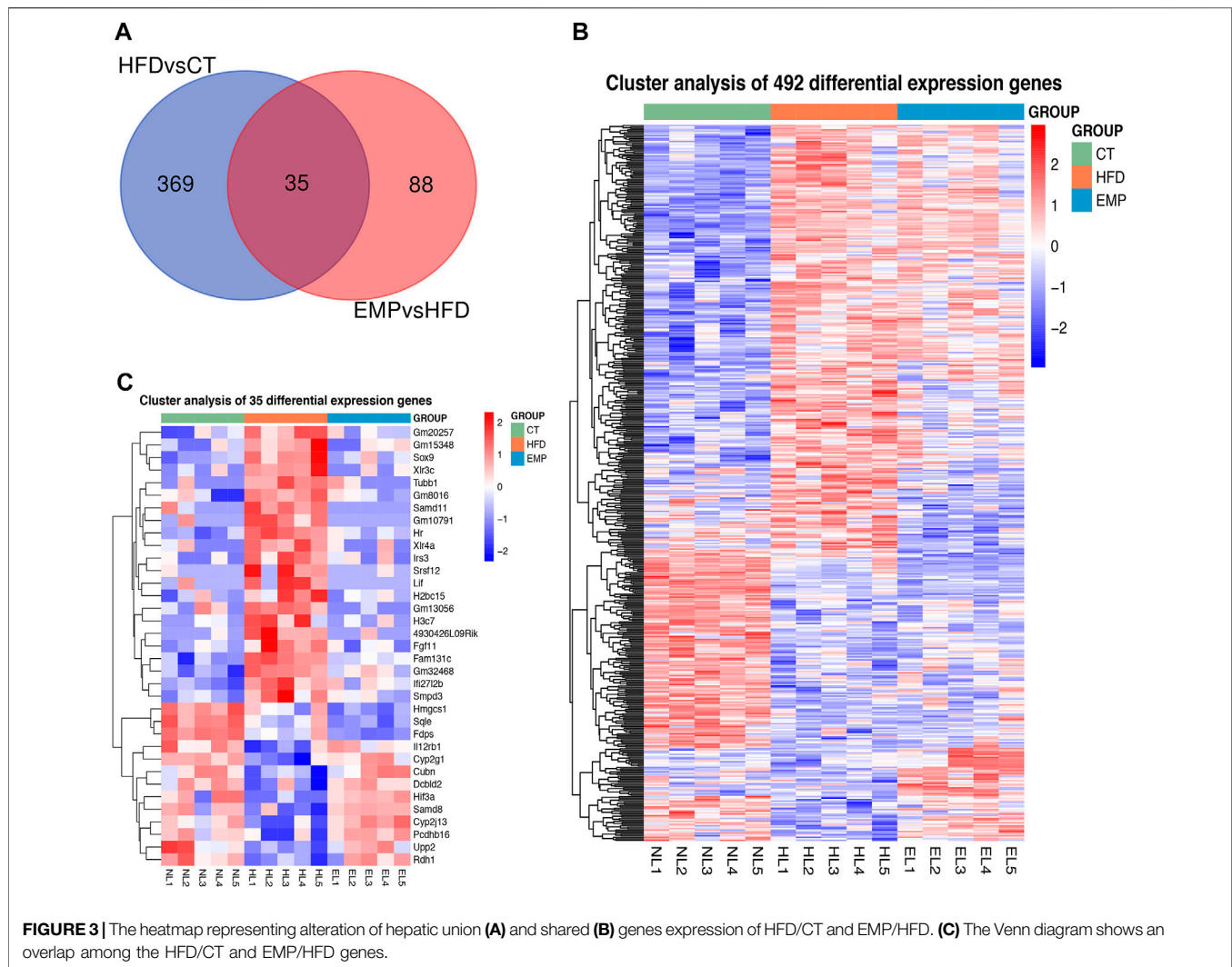
FIGURE 2 | Comparison of transcriptome profiling. **(A)** The gene number of up-regulation and down-regulation in HFD/CT and EMP/HFD. **(B)** PCA analysis of three groups. **(C)** The volcano plots for the distribution of differently expressed genes between HFD and CT group. Blue represents a down-regulation in expression, red represents upregulation and gray represents no significance when compared with control. **(D)** The volcano plots for the distribution of differently expressed genes between EMP and HFD group.

mass were decreased in the EMP group, compared with the HFD group (**Figure 1A, B, Table 2**). To access the liver metabolism caused by HFD, we measured alanine aminotransferase (ALT), aspartate aminotransferase (AST) and plasma TG levels. The results showed EMP alleviated increased liver injury with reducing AST, ALT and plasma TG levels (**Table 2**). Liver changes were observed by H&E and Oil Red O staining (**Figures 1C,D**). Liver tissue structure was normal in the CT group, with distinguishable edges and clear outlines. HFD mice showed prominent diffuse hepatic steatosis with nuclear condensation, cytoplasmic looseness, and increased lipid contents; all of these abnormalities were ameliorated by EMP treatment (**Figure 1**).

Identification of Differentially Expressed Genes Across Disease and Drug

Here, we performed RNA-Seq using liver tissue from NAFLD model mice that had received EMP to explore the mechanisms

underlying the effects of EMP on lipid metabolism and synthesis. We first investigated the liver tissue transcriptome profile in mice with regular and high-fat diets to determine gene expression changes during NAFLD. In total, 404 DEGs were observed in the HFD group, compared with the CT group; these consisted of 251 upregulated genes and 153 downregulated genes (**Figures 2A,C**). To understand how EMP treatment affects NAFLD, we compared transcriptome profiles between the HFD and EMP groups. Compared with the HFD group, 123 DEGs were observed in the EMP group; these consisted of 50 upregulated genes and 73 downregulated genes (**Figures 2A,D**). We investigated repeatability among samples using principal components analysis (PCA). The PCA results were displayed in a two-dimensional image format (**Figure 2B**), showing the degrees of separation among samples and groups. Notably, spatial separation trends were observed between HFD and CT groups, as well as between EMP and HFD groups. The findings indicated



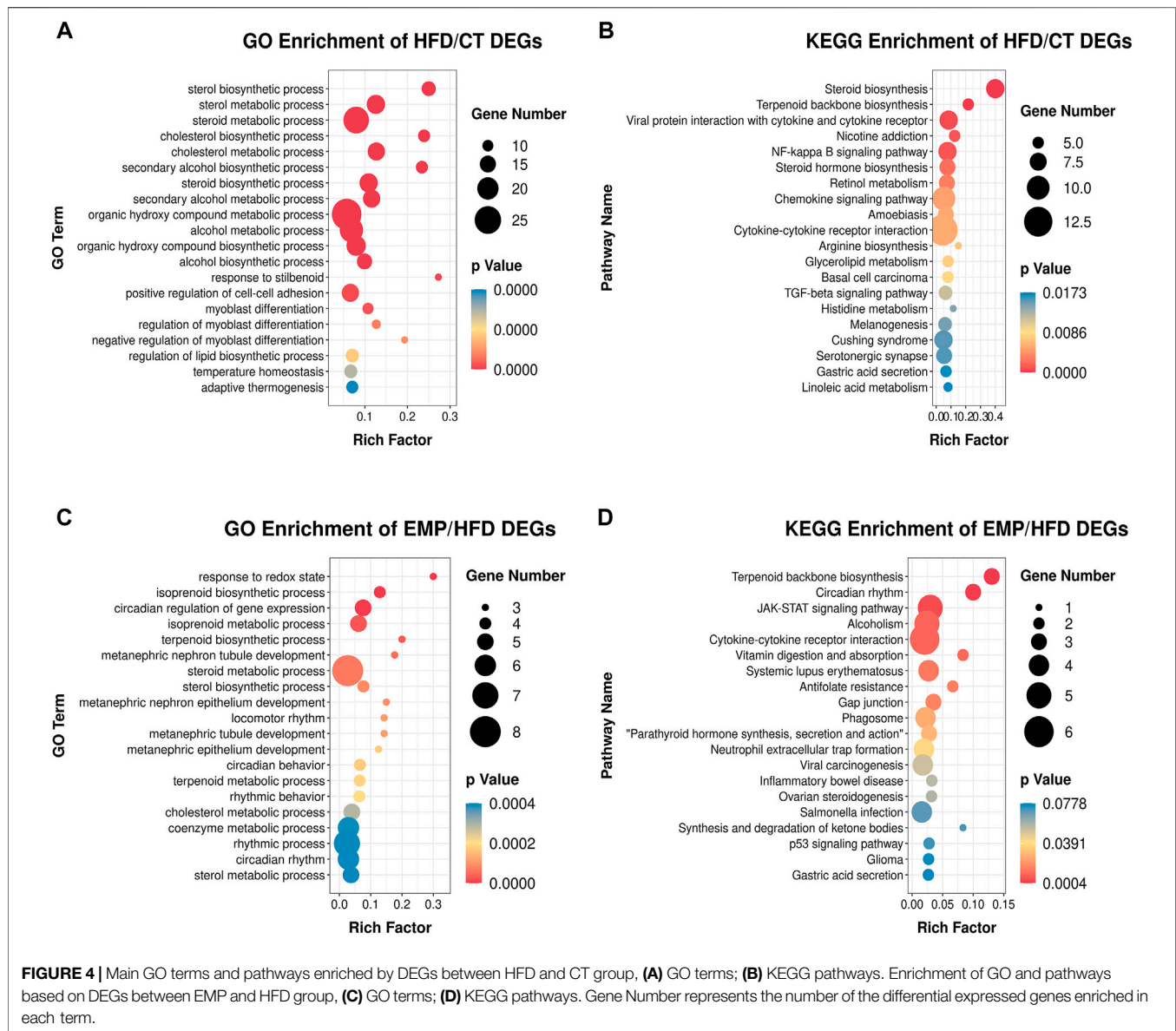
significant differences in gene expression patterns among the three groups; sample correlation was high within each group. The union and shared DEGs (492 and 35 genes) were displayed in the Venn diagram (Figure 3A). The gene expression profiles of union and shared DEGs exhibited apparent gene expression variations among the CT, HFD, and EMP groups (Figures 3B,C).

GO and KEGG Pathway Analysis

The expression levels of 404 genes were significantly changed in the HFD group compared with the CT group. GO enrichment analysis showed that the DEGs affected by HFD were mainly involved in the “sterol biosynthetic process,” “sterol metabolic process,” “steroid metabolic process,” “cholesterol biosynthetic process,” “cholesterol metabolic process,” “secondary alcohol biosynthetic process,” and “steroid biosynthetic process” categories (Figure 4A). Moreover, KEGG pathway analysis showed that these DEGs were mainly enriched in “steroid biosynthesis” and “terpenoid backbone biosynthesis” pathways (Figure 4B). These results suggested that the HFD treatment primarily affected lipid

synthesis and metabolism. Our results are consistent with previous studies which also revealed lipid biosynthetic and lipid metabolic process were enriched in the biological process (Chen et al., 2021; Xu et al., 2021). These results indicate a large proportion of dysregulated protein-coding genes in the transcriptome of a NAFLD liver, associated with glycolipid metabolism. However, there is no study exploring the effect of EMP on HFD-induced NAFLD.

Thus, we established HFD-EMP group to further analysis the potential biological processes. We identified 123 DEGs that were significantly changed in the EMP group, compared with the HFD group. GO enrichment analysis showed that the DEGs were mainly involved in “response to redox state,” “isoprenoid biosynthetic process,” “isoprenoid metabolic process,” “terpenoid biosynthetic process,” “steroid metabolic process,” and “sterol biosynthetic process” categories (Figure 4C). The KEGG pathway analysis indicated that these DEGs were mainly enriched in “terpenoid backbone biosynthesis” and “JAK-STAT signaling” pathways (Figure 4D). These results indicated that EMP mainly affects lipid oxidation and metabolism.



PPI Network and GSEA Analysis

Gene expression data and PPI networks were used in combination to identify the regulated parts of the network in the drug treatment. This process created a PPI network involving DEGs of the EMP and HFD groups, such that the edges connecting co-expressed genes were preserved. To identify the “communities” and “hubs” of the subnetworks, we analyzed the differentially expressed parts of the transcriptome. This analysis revealed multiple communities that contained either up- or downregulated genes associated with EMP treatment (Figure 5).

Next, we used GSEA to identify the differentially expressed pathways associated with EMP treatment. Although PPI network analysis identified co-regulated gene communities, GSEA showed additional pathways that were differentially associated with histological severity. In total, 12 pathways were affected by EMP treatment (FDR <0.05, Figure 6A). The full set of

pathways identified in this experiment is provided in Table 3. Four pathways were associated with lipid metabolism and synthesis: “ovarian steroidogenesis” (upregulated), “arachidonic acid metabolism” (upregulated), “terpenoid backbone biosynthesis” (downregulated), and “linoleic acid metabolism” (upregulated) (Figures 6B–E).

EMP Reduced Lipid Metabolism Through Increasing TG Lipolysis and Mitochondrial β -oxidation

Consistent with previous studies, HFD mice showed significantly high TG content both in serum and liver (Figure 7A/B, Table 2), however, there was a decrease trend between HFD mice and EMP mice but no significant difference ($p > 0.05$). To further explore the underlying triglyceride molecules among groups, we detect

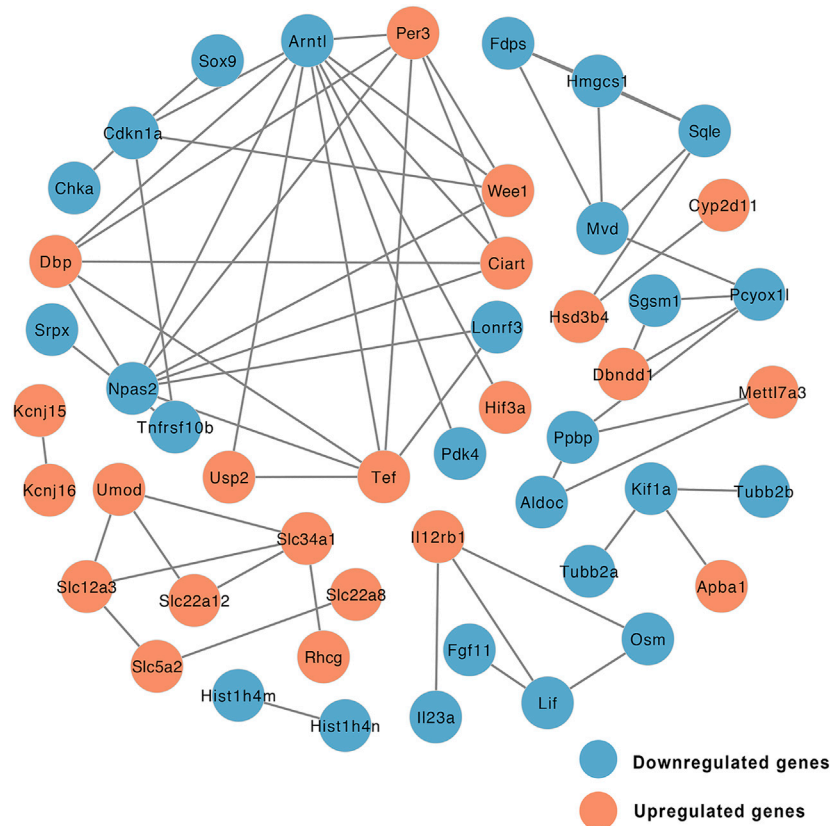


FIGURE 5 | Network of protein-protein interaction (PPI) of DEGs between EMP and HFD group (orange node: upregulated genes, blue node: downregulated genes).

the genes expressions of triglyceride metabolism and transport. As showed in **Figure Figure7C**, EMP had no effect on these genes (ACSL3, ACSL5, GPAT1) involved in the synthesis of TG. Compared with control group, HFD mice had lower expression of MTP, CGI-58, HSL, PNPLA3, meaning decreased triglyceride transfer and TG lipolysis (**Figures 7D,E**). However, these effects were reversed by EMP treatment. Moreover, EMP also enhanced these decreased-mitochondrial β -oxidation factors (including PPAR α , PGC1 α), which were overtly suppressed by HFD (**Figure7F**). To further explore whether RNA-seq data was consistent with protein level, we choose the most relevant genes in lipid metabolism to detect protein level through Western Blot analysis. As expected, the protein level of FDPS and HMGCS1 was downregulated in mice after treatment of EMP (**Figures 7G,H**).

qPCR Assessment of DEGs

To confirm the gene expression levels observed in RNA-Seq analysis, we chose nine genes that were mainly associated with lipid metabolism and synthesis (*Smpd3*, *Fdps*, *Hmgcs1*, *Rdh1*, *Sox9*, *HR*, *Sqle*, *Fam131c*, *Cyp2g1*). qPCR results were generally consistent with the RNA-Seq findings (**Figure 8A**). As showed in **Figure 8B**, the mRNA expression of *Fam131c*, *Sox9*, *Smpd3* was upregulated in HFD groups compared with control group, these

effects were reversed after treatment of EMP. Moreover, we found the expression of *Fdps*, *Hmgcs1*, *HR*, *Sqle* were downregulated in HFD-induced mice, however, these results were not reversed in EMP group.

DISCUSSION

This study investigated the effects of EMP on NAFLD. We found that EMP attenuated liver fat content and improved lipid metabolism by regulating genes related to lipid generation, transfer, lipolysis and oxidation. Our results provide a snapshot of the transcriptionally regulated pathways affected by EMP treatment for NAFLD; they may be important candidate pathways for alleviating disease. Additionally, the results provide insights concerning how these pathways interact to inhibit disease.

EMP is a novel type of antihyperglycemic drug that inhibits glucose reabsorption in proximal renal tubules. In addition to its effects on glycemic status in patients with type 2 diabetes, it contributes to weight loss and body fat reduction (Sun et al., 2020; Szekeres et al., 2021). Recently, clinical trials have reported SGLT-2i had beneficial effects on NAFLD, as evidenced by the remarkably reduced ALT, AST, triglycerides, hepatic insulin

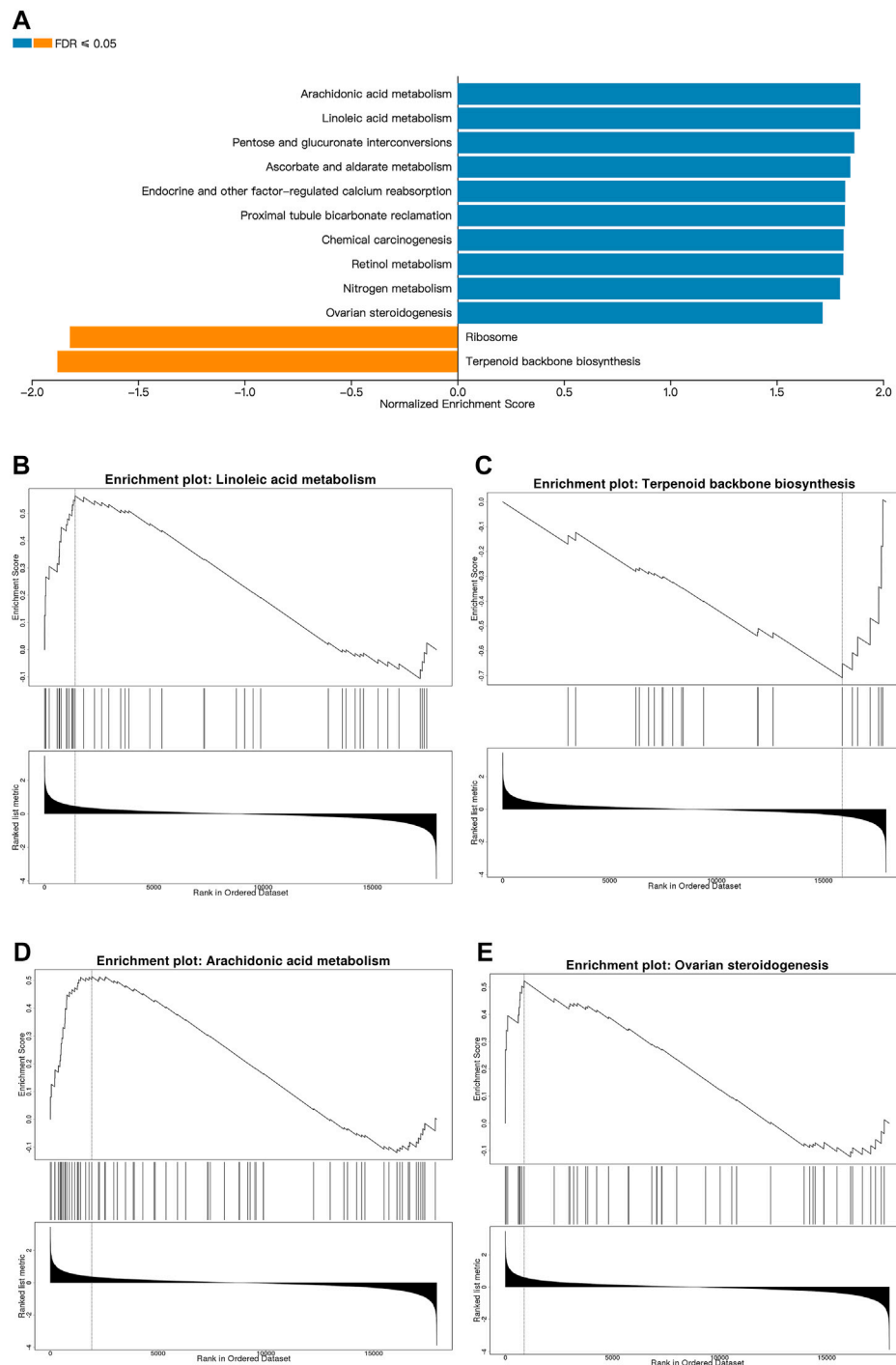


FIGURE 6 | Metabolic pathways affected by EMP. **(A)** The top Reactome gene sets that are up- and down-regulated with respect to EMP treatment based on normalized enrichment scores (NES) for EMP/HFD genes. **(B–E)** Pathways related to lipid metabolism and synthesis which are selected from **(A)**. (orange: upregulated pathways, blue: downregulated pathways, FDR ≤ 0.01).

sensitivity indices (Ranjbar et al., 2019; Kahl et al., 2020). Of note, in EMPA-REG OUTCOME trial and E-LIFT trial also showed that treatment with empagliflozin significantly reduced liver enzymes and liver fat (Sattar et al., 2018; Kim and Lee, 2020). It also increases energy consumption, thermogenesis, and

expression of uncoupling protein one in brown fat (Xu et al., 2017). Importantly, EMP attenuates NAFLD by activating autophagy and reducing ER stress and apoptosis (Nasiri-Ansari et al., 2021). Thus, these effects have emerged as important underlying mechanisms in NAFLD development

TABLE 3 | The full set of pathways identified.

| Gene set | Description | ES | NES | p value | FDR |
|----------|---|-------|-------|---------|------|
| mmu04913 | Ovarian steroidogenesis | 0.52 | 1.72 | 0.00 | 0.04 |
| mmu00590 | Arachidonic acid metabolism | 0.51 | 1.89 | 0.00 | 0.04 |
| mmu03010 | Ribosome | -0.49 | -1.82 | 0.00 | 0.03 |
| mmu00900 | Terpenoid backbone biosynthesis | -0.71 | -1.88 | 0.00 | 0.03 |
| mmu04961 | Endocrine and other factor-regulated calcium reabsorption | 0.57 | 1.82 | 0.00 | 0.03 |
| mmu00591 | Linoleic acid metabolism | 0.56 | 1.89 | 0.00 | 0.02 |
| mmu00053 | Ascorbate and aldarate metabolism | 0.63 | 1.85 | 0.00 | 0.02 |
| mmu04964 | Proximal tubule bicarbonate reclamation | 0.67 | 1.82 | 0.00 | 0.02 |
| mmu00040 | Pentose and glucuronate interconversions | 0.62 | 1.87 | 0.00 | 0.02 |
| mmu00910 | Nitrogen metabolism | 0.70 | 1.80 | 0.00 | 0.02 |
| mmu05204 | Chemical carcinogenesis | 0.48 | 1.81 | 0.00 | 0.02 |
| mmu00830 | Retinol metabolism | 0.48 | 1.81 | 0.00 | 0.02 |

and progression. In the present study, we found that 8-weeks treatment with EMP reduced body weight and fat mass, while alleviating HFD-induced liver injury. These results confirm the protective effects of EMP in a model of NAFLD.

The liver is essential for lipid synthesis and regulation of lipid metabolism. Healthy liver function involves balanced adjustment of lipid metabolism through multiple biological processes. In NAFLD, the compensatory enhancement of fatty acid oxidation is insufficient to normalize the lipid level; it may promote cell and tissue damage, as well as disease progression, by enhancing oxidative stress (Ipsen et al., 2018). In our study, we found that EMP reduced triglyceride level both in serum and liver through enhanced triglyceride transfer, TG lipolysis and microsomal mitochondrial β -oxidation. Previous studies identified DEGs that were associated with NAFLD onset and progression. Moreover, some studies examined gene expression using transcriptome data from liver biopsies of affected patients (Wruck et al., 2015). The findings revealed that many functional pathways and genes exhibited significant associations with NAFLD; many of these pathways and genes were related to lipid metabolism. Here, we used RNA-Seq to investigate the major pathways and genes involved in the effects of EMP on lipid synthesis and metabolism. Subsequent bioinformatics assays identified 123 DEGs with significant changes in expression levels after EMP treatment.

A previous study confirmed that overexpression of sex-determining region Y-box 9 (SOX9) enhanced lipogenesis and expression of PPAR γ in sebocytes (Shi et al., 2017). In addition, HR lysine demethylase and nuclear receptor corepressor (HR) may be a adipogenic transcription factor by regulating the expression of PPAR γ to generate white adipogenesis (Kumpf et al., 2012). PPAR γ is the primary inducer of adipogenesis (Li et al., 2018) and regulates adipocyte differentiation. In our study, SOX9 mRNA levels were significantly reduced in the EMP group. We speculate EMP treatment inhibited SOX9 expression, which led to reduced lipogenesis in the liver. These changes reduced PPAR γ expression, thereby inhibiting adipocyte differentiation. Sphingomyelins (SMs) have been reported as potential biomarkers for diagnosis of hepatic steatosis (Li et al., 2014). Additionally, a transcriptome analysis involved in mouse models of NAFLD and liver tissues from patients had reported the expression of SOX9 and SMPD3 (Teufel et al., 2016). In this study, sphingomyelin phosphodiesterase 3 (SMPD3) was inhibited in the EMP group, which may have led to increased

SM expression. This finding conflicts with the results of a previous study (Zhang et al., 2019), in which SMPD3 had a lower expression level in tyloxapol-treated mice, then increased after treatment. This inconsistency is presumably because the animal models were established using different methods. The final biosynthetic product of the 3-hydroxy-3-methylglutaryl-CoA synthase 1 (HMGCS1) pathway is cholesterol. HMGCS1 is upregulated by galectin-7 (Gal-7); subsequent HMGCS1 activity increases the accumulation of cellular cholesterol (Fujimoto et al., 2021). Squalene monooxygenase (SQLE) is a critical regulatory point in the cholesterol synthesis pathway (Howe et al., 2017). Farnesyl diphosphate synthase (FDPS) and cytochrome P450 family 2g1 (CYP2G1) are both associated with lipid and cholesterol biosynthesis (Wang et al., 2017). In the present study, the expression levels of HMGCS1, SQLE, and FDPS were highest in the CT group and lowest in the EMP group. These gene expression differences provide important insights into the mechanisms by which EMP affects the liver. Family with sequence similarity 131c (FAM131C) is a group of human N-myristoylated proteins; protein N-myristoylation is required for proper targeting of SAMM50 to mitochondria (Takamitsu et al., 2015). Some studies have shown that overexpression of SAMM50 enhances fatty acid oxidation and reduces intracellular lipid accumulation (Li et al., 2021). In contrast, we found that the *Fam131c* expression level increased in the HFD group but decreased in the EMP group. Retinol dehydrogenase 1 (RDH1) is one of several enzymes that catalyze the conversion of retinol into all-trans-retinoic acid (atRA). RDH1 can suppress adiposity by promoting brown adipose generation (Krois et al., 2019). In this study, RDH1 expression levels differed between RNA-Seq and qPCR, presumably because of differences in the technical protocols.

Overall, we found that EMP treatment could reverse the activities of NAFLD-associated pathways. These transformations mainly involved reduction of lipid metabolism and synthesis pathways in the liver. Our results indicate that EMP treatment alleviates fat accumulation and slightly affects inflammation in NAFLD. GO and KEGG enrichment were performed to analyze these DEGs, with the aim of clarifying the mechanism by which EMP affects lipid synthesis and metabolism in the liver. Our findings showed that EMP mainly affects the response to redox state,

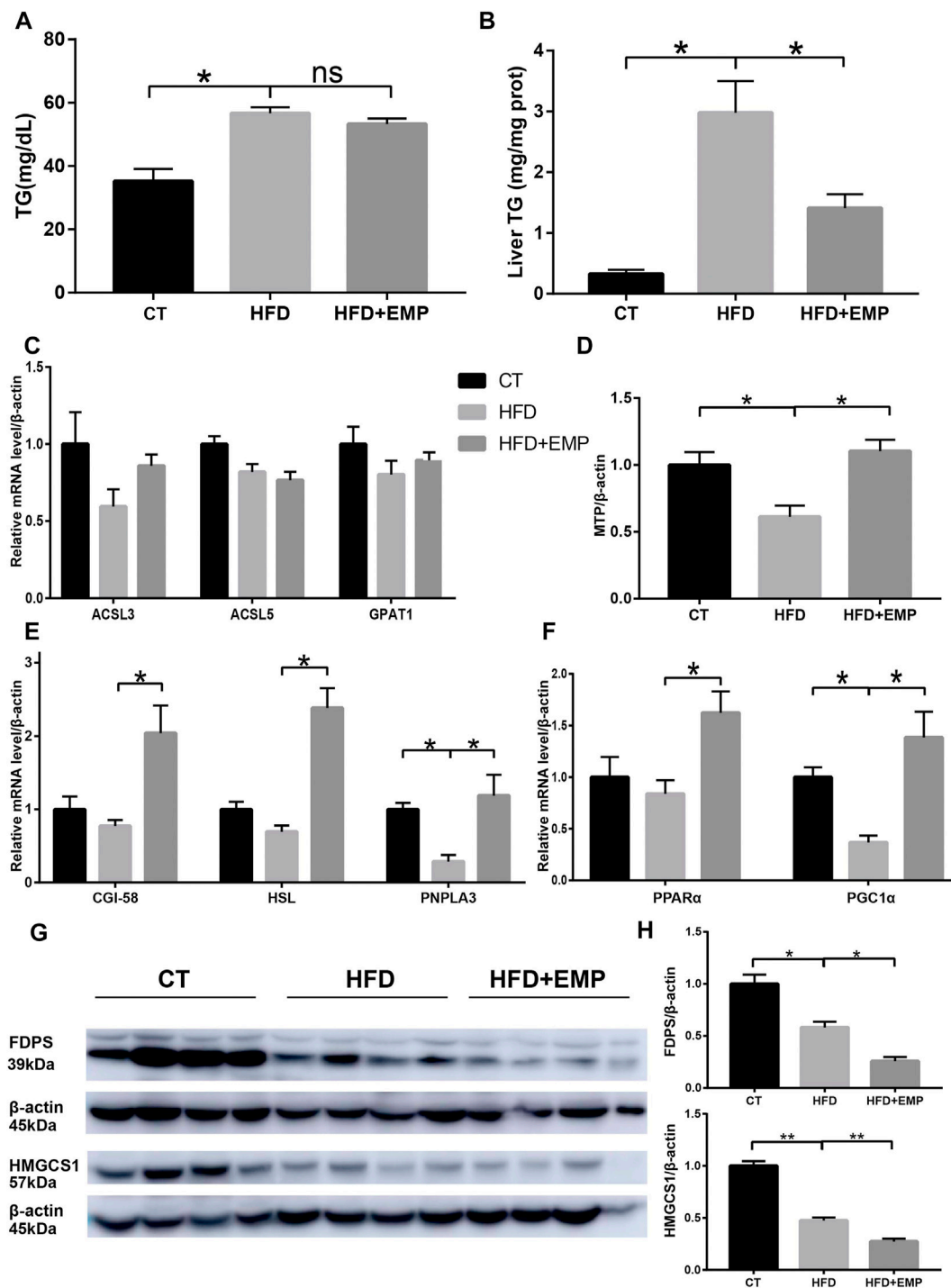


FIGURE 7 | Empagliflozin reduced triglyceride level both in serum (A) and liver (B) through enhanced triglyceride transfer (D), lipolysis (E) and microsomal mitochondrial β -oxidation (F). Empagliflozin had no effect on the synthesis genes of triglyceride (C). Western-blot analysis showed the protein levels of FDPS and HMGCS1 (G and H), which were the most relevant genes in lipid metabolism. Equal loading of protein was verified by probing β -actin. Data represent means \pm SEM. * $p < 0.05$, ** $p < 0.01$, $n = (4-6)$.

triglyceride transfer, TG lipolysis and microsomal mitochondrial β -oxidation, and JAK-STAT signaling pathways. Importantly, EMP reduced lipid accumulation and alleviated pathological changes involved in NAFLD.

These changes may be related to the regulation of lipid oxidation-associated gene expression by EMP. However, we only established the relation between mechanisms of EMP and NAFLD, but which cell type (hepatocytes, macrophages or

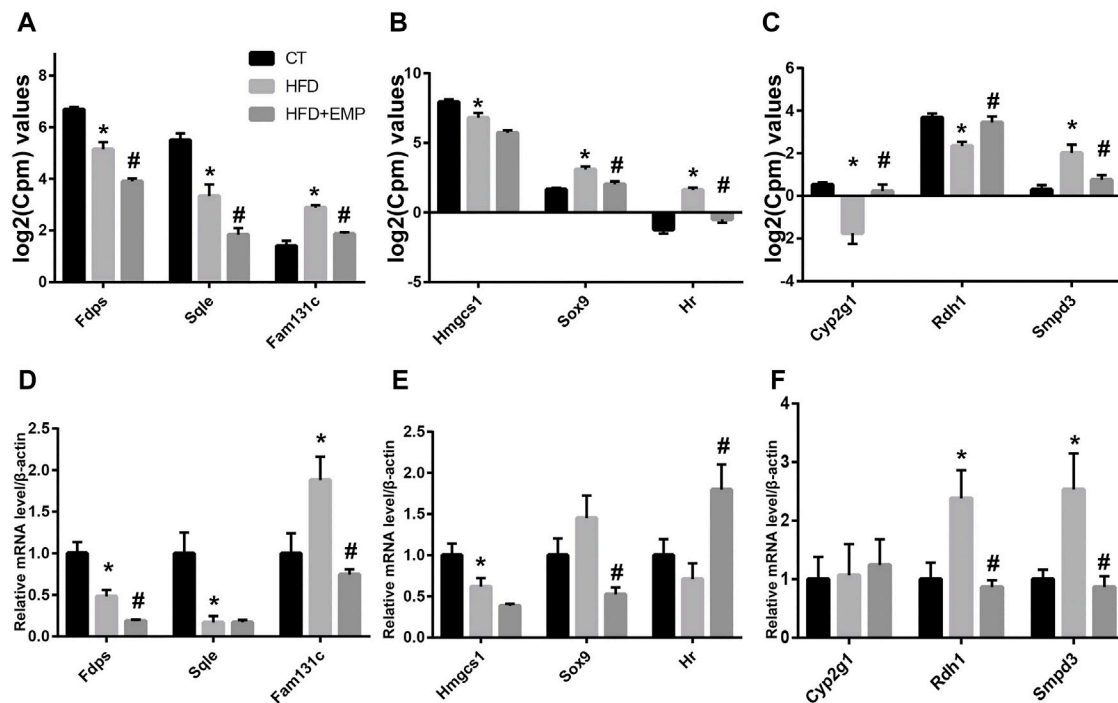


FIGURE 8 | Quantitative real-time PCR validation of RNA-seq analysis of DEGs. Graphs represent $\log_2(\text{CPM})$ values of gene expression levels (A–C) in RNA-seq data and mRNA levels normalized to β -actin, * $p < 0.05$ vs. CT, # $p < 0.05$ vs. HFD, $n = 5$, (D–F) from quantitative real-time PCR data. Data are presented as means \pm SEM, * $p < 0.05$ vs. CT, # $p < 0.05$ vs. HFD, $n = (4–6)$.

hepatic stellate cells) in liver for lipid metabolism and synthesis is not determined in this work. Therefore, we will focus this limitation in the next research.

In summary, our results provide snapshot of the transcriptionally regulated pathways affected by EMP treatment for NAFLD; these may be important candidate pathways for treatment to slow the progression of NAFLD. Additionally, our findings provide insights concerning how these pathways interact to inhibit disease. Our research provides new insights concerning the mechanisms by which SGLT inhibitors impact NAFLD, particularly in terms of liver metabolism. The genes identified in this experiment provide robust evidence for further analyses of the mechanism by which EMP impacts NAFLD.

DATA AVAILABILITY STATEMENT

The datasets presented in this study can be found in online repositories. The names of the repository/repositories and accession number(s) can be found below: <https://www.ncbi.nlm.nih.gov/>, PRJNA770493.

ETHICS STATEMENT

The animal study was reviewed and approved by Animal Ethics Committee of Weifang Medical University.

AUTHOR CONTRIBUTIONS

YM, CK and HQ collected the data, conducted the analysis, and drafted the manuscript. XBC designed the study and conducted the analysis. YL, FH and NH directed the study's analytic strategy and reviewed the manuscript. XS and JS designed the entire study and revised the manuscript. All authors read and approved the final manuscript.

FUNDING

This work was supported by the National Natural Science Foundation of China (81870593), Natural Science Foundation of Shandong Province of China (ZR2020MH106, ZR202102240146), Shandong Province Higher Educational Science and Technology Program for Youth Innovation (2020KJL004) and Quality Improvement of Postgraduate Education in Shandong Province (SDYAL19156).

SUPPLEMENTARY MATERIAL

The Supplementary Material for this article can be found online at: <https://www.frontiersin.org/articles/10.3389/fphar.2021.793586/full#supplementary-material>

REFERENCES

- Al-Sharea, A., Murphy, A. J., Huggins, L. A., Hu, Y., Goldberg, I. J., and Nagareddy, P. R. (2018). SGLT2 Inhibition Reduces Atherosclerosis by Enhancing Lipoprotein Clearance in Ldlr^{-/-} Type 1 Diabetic Mice. *Atherosclerosis* 271, 166–176. doi:10.1016/j.atherosclerosis.2018.02.028
- Calapkulu, M., Cander, S., Gul, O. O., and Ersoy, C. (2019). Lipid Profile in Type 2 Diabetic Patients with New Dapagliflozin Treatment; Actual Clinical Experience Data of Six Months Retrospective Lipid Profile from Single center. *Diabetes Metab. Syndr.* 13, 1031–1034. doi:10.1016/j.dsx.2019.01.016
- Chen, X., Tang, Y., Chen, S., Ling, W., and Wang, Q. (2021). IGFBP-2 as a Biomarker in NAFLD Improves Hepatic Steatosis: an Integrated Bioinformatics and Experimental Study. *Endocr. Connect.* 10, 1315–1325. doi:10.1530/EC-21-0353
- Cohen, D. E., and Fisher, E. A. (2013). Lipoprotein Metabolism, Dyslipidemia, and Nonalcoholic Fatty Liver Disease. *Semin. Liver Dis.* 33, 380–388. doi:10.1055/s-0033-1358519
- Cotter, T. G., and Rinella, M. (2020). Nonalcoholic Fatty Liver Disease 2020: The State of the Disease. *Gastroenterology* 158, 1851–1864. doi:10.1053/j.gastro.2020.01.052
- Di Mauro, S., Salomone, F., Scamporrino, A., Filippello, A., Morisco, F., Guido, M., et al. (2021). Coffee Restores Expression of lncRNAs Involved in Steatosis and Fibrosis in a Mouse Model of NAFLD. *Nutrients* 13, 2952. doi:10.3390/nu13092952
- Frampton, J. E. (2018). Empagliflozin: A Review in Type 2 Diabetes. *Drugs* 78, 1037–1048. doi:10.1007/s40265-018-0937-z
- Fujimoto, N., Akiyama, M., Satoh, Y., and Tajima, S. (2021). Interaction of Galectin-7 with HMGC1 *In Vitro* May Facilitate Cholesterol Deposition in Cultured Keratinocytes. *J. Invest. Dermatol.* S0022-202X, 02085–02086. doi:10.1016/j.jid.2021.04.038
- Guo, F., Ma, Y., Kadegowda, A. K., Betters, J. L., Xie, P., Liu, G., et al. (2013). Deficiency of Liver Comparative Gene Identification-58 Causes Steatohepatitis and Fibrosis in Mice. *J. Lipid Res.* 54, 2109–2120. doi:10.1194/jlr.M035519
- Han, X., Ding, C., Zhang, G., Pan, R., Liu, Y., Huang, N., et al. (2020). Liraglutide Ameliorates Obesity-Related Nonalcoholic Fatty Liver Disease by Regulating Sestrin2-Mediated Nrf2/HO-1 Pathway. *Biochem. Biophys. Res. Commun.* 525, 895–901. doi:10.1016/j.bbrc.2020.03.032
- Hayashi, T., Fukui, T., Nakanishi, N., Yamamoto, S., Tomoyasu, M., Osamura, A., et al. (2017). Dapagliflozin Decreases Small Dense Low-Density Lipoprotein-Cholesterol and Increases High-Density Lipoprotein 2-cholesterol in Patients with Type 2 Diabetes: Comparison with Sitagliptin. *Cardiovasc. Diabetol.* 16, 8. doi:10.1186/s12933-016-0491-5
- Howe, V., Sharpe, L. J., Prabhu, A. V., and Brown, A. J. (2017). New Insights into Cellular Cholesterol Acquisition: Promoter Analysis of Human HMGR and SQLE, Two Key Control Enzymes in Cholesterol Synthesis. *Biochim. Biophys. Acta Mol. Cel Biol Lipids* 1862, 647–657. doi:10.1016/j.bbalip.2017.03.009
- Ipsen, D. H., Lykkesfeldt, J., and Tveden-Nyborg, P. (2018). Molecular Mechanisms of Hepatic Lipid Accumulation in Non-alcoholic Fatty Liver Disease. *Cell. Mol. Life Sci.* 75, 3313–3327. doi:10.1007/s00018-018-2860-6
- Kahl, S., Gancheva, S., Straßburger, K., Herder, C., Machann, J., Katsuyama, H., et al. (2020). Empagliflozin Effectively Lowers Liver Fat Content in Well-Controlled Type 2 Diabetes: A Randomized, Double-Blind, Phase 4, Placebo-Controlled Trial. *Diabetes Care* 43, 298–305. doi:10.2337/dc19-0641
- Kanehisa, M., Araki, M., Goto, S., Hattori, M., Hirakawa, M., Itoh, M., et al. (2008). KEGG for Linking Genomes to Life and the Environment. *Nucleic Acids Res.* 36, D480–D484. doi:10.1093/nar/gkm882
- Kim, D., Langmead, B., and Salzberg, S. L. (2015). HISAT: a Fast Spliced Aligner with Low Memory Requirements. *Nat. Methods* 12, 357–360. doi:10.1038/nmeth.3317
- Kim, K. S., and Lee, B. W. (2020). Beneficial Effect of Anti-diabetic Drugs for Nonalcoholic Fatty Liver Disease. *Clin. Mol. Hepatol.* 26, 430–443. doi:10.3350/cmh.2020.0137
- Komiya, C., Tsuchiya, K., Shiba, K., Miyachi, Y., Furuke, S., Shimazu, N., et al. (2016). Ipragliflozin Improves Hepatic Steatosis in Obese Mice and Liver Dysfunction in Type 2 Diabetic Patients Irrespective of Body Weight Reduction. *PLoS ONE* 11, e0151511. doi:10.1371/journal.pone.0151511
- Krois, C. R., Vuckovic, M. G., Huang, P., Zaversnik, C., Liu, C. S., Gibson, C. E., et al. (2019). RDH1 Suppresses Adiposity by Promoting Brown Adipose Adaptation to Fasting and Re-feeding. *Cel. Mol. Life Sci.* 76, 2425–2447. doi:10.1007/s00018-019-03046-z
- Kuchay, M. S., Krishan, S., Mishra, S. K., Farooqui, K. J., Singh, M. K., Wasir, J. S., et al. (2018). Effect of Empagliflozin on Liver Fat in Patients with Type 2 Diabetes and Nonalcoholic Fatty Liver Disease: A Randomized Controlled Trial (E-LIFT Trial). *Diabetes Care* 41, 1801–1808. doi:10.2337/dc18-0165
- Kumpf, S., Mihlan, M., Goginashvili, A., Grandl, G., Gehart, H., Godel, A., et al. (2012). Hairless Promotes PPAR γ Expression and Is Required for white Adipogenesis. *EMBO Rep.* 13, 1012–1020. doi:10.1038/embor.2012.133
- Lass, A., Zimmermann, R., Haemmerle, G., Riederer, M., Schoiswohl, G., Schweiger, M., et al. (2006). Adipose Triglyceride Lipase-Mediated Lipolysis of Cellular Fat Stores Is Activated by CGI-58 and Defective in Charnin-Dorfman Syndrome. *Cell Metab* 3, 309–319. doi:10.1016/j.cmet.2006.03.005
- Li, J. F., Qu, F., Zheng, S. J., Wu, H. L., Liu, M., Liu, S., et al. (2014). Elevated Plasma Sphingomyelin (D18:1/22:0) Is Closely Related to Hepatic Steatosis in Patients with Chronic Hepatitis C Virus Infection. *Eur. J. Clin. Microbiol. Infect. Dis.* 33, 1725–1732. doi:10.1007/s10096-014-2123-x
- Li, S., Liu, C., Li, N., Hao, T., Han, T., Hill, D. E., et al. (2008). Genome-wide Coactivation Analysis of PGC-1 α Identifies BAF60a as a Regulator of Hepatic Lipid Metabolism. *Cel Metab* 8, 105–117. doi:10.1016/j.cmet.2008.06.013
- Li, Y., Jin, D., Xie, W., Wen, L., Chen, W., Xu, J., et al. (2018). PPAR- γ and Wnt Regulate the Differentiation of MSCs into Adipocytes and Osteoblasts Respectively. *Curr. Stem Cel Res Ther* 13, 185–192. doi:10.2174/1574888X12666171012141908
- Li, Z., Shen, W., Wu, G., Qin, C., Zhang, Y., Wang, Y., et al. (2021). The Role of SAMM50 in Non-alcoholic Fatty Liver Disease: from Genetics to Mechanisms. *FEBS Open Bio* 11, 1893–1906. doi:10.1002/2211-5463.13146
- Liu, W., Xu, G., Ma, J., Jia, W., Li, J., Chen, K., et al. (2011). Osteopontin as a Key Mediator for Vascogenic Mimicry in Hepatocellular Carcinoma. *Tohoku J. Exp. Med.* 224, 29–39. doi:10.1620/tjem.224.29
- Liu, Y., Xu, J., Wu, M., Xu, B., and Kang, L. (2021). Empagliflozin Protects against Atherosclerosis Progression by Modulating Lipid Profiles and Sympathetic Activity. *Lipids Health Dis.* 20, 5. doi:10.1186/s12944-021-01430-y
- Manne, V., Handa, P., and Kowdley, K. V. (2018). Pathophysiology of Nonalcoholic Fatty Liver Disease/Nonalcoholic Steatohepatitis. *Clin. Liver Dis.* 22, 23–37. doi:10.1016/j.cld.2017.08.007
- Mato, J. M., Alonso, C., Noureddin, M., and Lu, S. C. (2019). Biomarkers and Subtypes of Deranged Lipid Metabolism in Non-alcoholic Fatty Liver Disease. *World J. Gastroenterol.* 25, 3009–3020. doi:10.3748/wjg.v25.i24.3009
- Matsubayashi, Y., Yoshida, A., Suganami, H., Osawa, T., Furukawa, K., Suzuki, H., et al. (2020). Association of Increased Hepatic Insulin Clearance and Change in Serum Triglycerides or β -hydroxybutyrate Concentration via the Sodium/glucose-Cotransporter 2 Inhibitor Tofogliflozin. *Diabetes Obes. Metab.* 22, 947–956. doi:10.1111/dom.13980
- Musso, G., Gambino, R., and Cassader, M. (2009). Recent Insights into Hepatic Lipid Metabolism in Non-alcoholic Fatty Liver Disease (NAFLD). *Prog. Lipid Res.* 48, 1–26. doi:10.1016/j.plipres.2008.08.001
- Nasiri-Ansari, N., Nikolopoulou, C., Papoutsis, K., Kyrrou, I., Mantzoros, C. S., Kyriakopoulos, G., et al. (2021). Empagliflozin Attenuates Non-alcoholic Fatty Liver Disease (NAFLD) in High Fat Diet Fed ApoE(-/-) Mice by Activating Autophagy and Reducing ER Stress and Apoptosis. *Int. J. Mol. Sci.* 22, 818. doi:10.3390/ijms22020818
- Osataphan, S., Macchi, C., Singhal, G., Chimene-Weiss, J., Sales, V., Kozuka, C., et al. (2019). SGLT2 Inhibition Reprograms Systemic Metabolism via FGF21-dependent and -independent Mechanisms. *JCI Insight* 4, e123130. doi:10.1172/jci.insight.123130
- Pertea, M., Pertea, G. M., Antonescu, C. M., Chang, T. C., Mendell, J. T., and Salzberg, S. L. (2015). StringTie Enables Improved Reconstruction of a Transcriptome from RNA-Seq Reads. *Nat. Biotechnol.* 33, 290–295. doi:10.1038/nbt.3122
- Perumpail, B. J., Khan, M. A., Yoo, E. R., Cholaneril, G., Kim, D., and Ahmed, A. (2017). Clinical Epidemiology and Disease burden of Nonalcoholic Fatty Liver Disease. *World J. Gastroenterol.* 23, 8263–8276. doi:10.3748/wjg.v23.i47.8263
- Petito-da-Silva, T. I., Souza-Mello, V., and Barbosa-da-Silva, S. (2019). Empagliflozin Mitigates NAFLD in High-Fat-Fed Mice by Alleviating Insulin

- Resistance, Lipogenesis and ER Stress. *Mol. Cel. Endocrinol.* 498, 110539. doi:10.1016/j.mce.2019.110539
- Ranjbar, G., Mikhailidis, D. P., and Sahebkar, A. (2019). Effects of Newer Antidiabetic Drugs on Nonalcoholic Fatty Liver and Steatohepatitis: Think Out of the Box!. *Metabolism* 101, 154001. doi:10.1016/j.metabol.2019.154001
- Rinella, M. E. (2015). Nonalcoholic Fatty Liver Disease: a Systematic Review. *JAMA* 313, 2263–2273. doi:10.1001/jama.2015.5370
- Ritchie, M. E., Phipson, B., Wu, D., Hu, Y., Law, C. W., Shi, W., et al. (2015). Limma powers Differential Expression Analyses for RNA-Sequencing and Microarray Studies. *Nucleic Acids Res.* 43, e47. doi:10.1093/nar/gkv007
- Robinson, M. D., McCarthy, D. J., and Smyth, G. K. (2010). edgeR: a Bioconductor Package for Differential Expression Analysis of Digital Gene Expression Data. *Bioinformatics* 26, 139–140. doi:10.1093/bioinformatics/btp616
- Sattar, N., Fitchett, D., Hantel, S., George, J. T., and Zinman, B. (2018). Empagliflozin Is Associated with Improvements in Liver Enzymes Potentially Consistent with Reductions in Liver Fat: Results from Randomised Trials Including the EMPA-REG OUTCOME® Trial. *Diabetologia* 61, 2155–2163. doi:10.1007/s00125-018-4702-3
- Seko, Y., Sumida, Y., Sasaki, K., Itoh, Y., Iijima, H., Hashimoto, T., et al. (2018). Effects of Canagliflozin, an SGLT2 Inhibitor, on Hepatic Function in Japanese Patients with Type 2 Diabetes Mellitus: Pooled and Subgroup Analyses of Clinical Trials. *J. Gastroenterol.* 53, 140–151. doi:10.1007/s00535-017-1364-8
- Seko, Y., Sumida, Y., Tanaka, S., Mori, K., Taketani, H., Ishiba, H., et al. (2017). Effect of Sodium Glucose Cotransporter 2 Inhibitor on Liver Function Tests in Japanese Patients with Non-alcoholic Fatty Liver Disease and Type 2 Diabetes Mellitus. *Hepatol. Res.* 47, 1072–1078. doi:10.1111/hepr.12834
- Shannon, P., Markiel, A., Ozier, O., Baliga, N. S., Wang, J. T., Ramage, D., et al. (2003). Cytoscape: a Software Environment for Integrated Models of Biomolecular Interaction Networks. *Genome Res.* 13, 2498–2504. doi:10.1101/gr.1239303
- Shi, G., Wang, T. T., Quan, J. H., Li, S. J., Zhang, M. F., Liao, P. Y., et al. (2017). Sox9 Facilitates Proliferation, Differentiation and Lipogenesis in Primary Cultured Human Sebocytes. *J. Dermatol. Sci.* 85, 44–50. doi:10.1016/j.jdermsci.2016.10.005
- Smagris, E., BasuRay, S., Li, J., Huang, Y., Lai, K. M., Gromada, J., et al. (2015). Pnpla3^{1148M} Knockin Mice Accumulate PNPLA3 on Lipid Droplets and Develop Hepatic Steatosis. *Hepatology* 61, 108–118. doi:10.1002/hep.27242
- Subramanian, A., Tamayo, P., Mootha, V. K., Mukherjee, S., Ebert, B. L., Gillette, M. A., et al. (2005). Gene Set Enrichment Analysis: a Knowledge-Based Approach for Interpreting Genome-wide Expression Profiles. *Proc. Natl. Acad. Sci. U S A* 102, 15545–15550. doi:10.1073/pnas.0506580102
- Sun, X., Han, F., Lu, Q., Li, X., Ren, D., Zhang, J., et al. (2020). Empagliflozin Ameliorates Obesity-Related Cardiac Dysfunction by Regulating Sestrin2-Mediated AMPK-mTOR Signaling and Redox Homeostasis in High-Fat Diet-Induced Obese Mice. *Diabetes* 69, 1292–1305. doi:10.2337/db19-0991
- Szekeres, Z., Toth, K., and Szabados, E. (2021). The Effects of SGLT2 Inhibitors on Lipid Metabolism. *Metabolites* 11, 87. doi:10.3390/metabo11020087
- Takamitsu, E., Otsuka, M., Haebara, T., Yano, M., Matsuzaki, K., Kobuchi, H., et al. (2015). Identification of Human N-Myristoylated Proteins from Human Complementary DNA Resources by Cell-free and Cellular Metabolic Labeling Analyses. *PLoS ONE* 10, e0136360. doi:10.1371/journal.pone.0136360
- Teufel, A., Itzel, T., Erhart, W., Brosch, M., Wang, X. Y., Kim, Y. O., et al. (2016). Comparison of Gene Expression Patterns between Mouse Models of Nonalcoholic Fatty Liver Disease and Liver Tissues from Patients. *Gastroenterology* 151, 513–e0. doi:10.1053/j.gastro.2016.05.051
- Wang, C. C., Yen, J. H., Cheng, Y. C., Lin, C. Y., Hsieh, C. T., Gau, R. J., et al. (2017). Polygala Tenuifolia Extract Inhibits Lipid Accumulation in 3T3-L1 Adipocytes and High-Fat Diet-Induced Obese Mouse Model and Affects Hepatic Transcriptome and Gut Microbiota Profiles. *Food Nutr. Res.* 61, 1379861. doi:10.1080/16546628.2017.1379861
- Wruck, W., Kashofer, K., Rehman, S., Daskalaki, A., Berg, D., Gralka, E., et al. (2015). Multi-omic Profiles of Human Non-alcoholic Fatty Liver Disease Tissue Highlight Heterogenic Phenotypes. *Sci. Data* 2, 150068. doi:10.1038/sdata.2015.68
- Xu, L., Nagata, N., Chen, G., Nagashimada, M., Zhuge, F., Ni, Y., et al. (2019). Empagliflozin Reverses Obesity and Insulin Resistance through Fat Browning and Alternative Macrophage Activation in Mice Fed a High-Fat Diet. *BMJ Open Diabetes Res. Care* 7, e000783. doi:10.1136/bmjdr-2019-000783
- Xu, L., Nagata, N., Nagashimada, M., Zhuge, F., Ni, Y., Chen, G., et al. (2017). SGLT2 Inhibition by Empagliflozin Promotes Fat Utilization and Browning and Attenuates Inflammation and Insulin Resistance by Polarizing M2 Macrophages in Diet-Induced Obese Mice. *EBioMedicine* 20, 137–149. doi:10.1016/j.ebiom.2017.05.028
- Xu, L., Yin, L., Qi, Y., Tan, X., Gao, M., and Peng, J. (2021). 3D Disorganization and Rearrangement of Genome Provide Insights into Pathogenesis of NAFLD by Integrated Hi-C, Nanopore, and RNA Sequencing. *Acta Pharm. Sin B* 11, 3150–3164. doi:10.1016/j.apsb.2021.03.022
- Young, M. D., Wakefield, M. J., Smyth, G. K., and Oshlack, A. (2010). Gene Ontology Analysis for RNA-Seq: Accounting for Selection Bias. *Genome Biol.* 11, R14. doi:10.1186/gb-2010-11-2-r14
- Yu, G., Wang, L. G., Han, Y., and He, Q. Y. (2012). clusterProfiler: an R Package for Comparing Biological Themes Among Gene Clusters. *OMICS* 16, 284–287. doi:10.1089/omi.2011.0118
- Zhang, T., Zhao, Q., Xiao, X., Yang, R., Hu, D., Zhu, X., et al. (2019). Modulation of Lipid Metabolism by Celastrol. *J. Proteome Res.* 18, 1133–1144. doi:10.1021/acs.jproteome.8b00797
- Zhou, J. H., Cai, J. J., She, Z. G., and Li, H. L. (2019). Noninvasive Evaluation of Nonalcoholic Fatty Liver Disease: Current Evidence and Practice. *World J. Gastroenterol.* 25, 1307–1326. doi:10.3748/wjg.v25.i11.1307

Conflict of Interest: The authors declare that the research was conducted in the absence of any commercial or financial relationships that could be construed as a potential conflict of interest.

Publisher's Note: All claims expressed in this article are solely those of the authors and do not necessarily represent those of their affiliated organizations, or those of the publisher, the editors and the reviewers. Any product that may be evaluated in this article, or claim that may be made by its manufacturer, is not guaranteed or endorsed by the publisher.

Copyright © 2021 Ma, Kan, Qiu, Liu, Hou, Han, Shi and Sun. This is an open-access article distributed under the terms of the Creative Commons Attribution License (CC BY). The use, distribution or reproduction in other forums is permitted, provided the original author(s) and the copyright owner(s) are credited and that the original publication in this journal is cited, in accordance with accepted academic practice. No use, distribution or reproduction is permitted which does not comply with these terms.



Regulation of Lipid Metabolism by Lamin in Mutation-Related Diseases

Yue Peng^{1†}, Qianyu Tang^{1†}, Fan Xiao^{2*} and Nian Fu^{1,2*}

¹The Affiliated Nanhua Hospital, Department of Gastroenterology, Hunan Provincial Clinical Research Center of Metabolic Associated Fatty Liver Disease, Hengyang, China, ²The Affiliated Nanhua Hospital, Clinical Research Institute, Hengyang Medical School, University of South China, Hengyang, China

OPEN ACCESS

Edited by:

Ana Blas-García,
University of Valencia, Spain

Reviewed by:

Giuseppe Novelli,
University of Rome Tor Vergata, Italy
Joshi Stephen,
Baylor College of Medicine,
United States

*Correspondence:

Nian Fu
2002funian@163.com
Fan Xiao
xiaof-usc@foxmail.com

[†]These authors have contributed
equally to this work

Specialty section:

This article was submitted to
Gastrointestinal and Hepatic
Pharmacology,
a section of the journal
Frontiers in Pharmacology

Received: 23 November 2021

Accepted: 24 January 2022

Published: 25 February 2022

Citation:

Peng Y, Tang Q, Xiao F and Fu N
(2022) Regulation of Lipid Metabolism
by Lamin in Mutation-
Related Diseases.
Front. Pharmacol. 13:820857.
doi: 10.3389/fphar.2022.820857

Nuclear lamins, known as type 5 intermediate fibers, are composed of lamin A, lamin C, lamin B1, and lamin B2, which are encoded by *LMNA* and *LMNB* genes, respectively. Importantly, mutations in nuclear lamins not only participate in lipid disorders but also in the human diseases, such as lipodystrophy, metabolic-associated fatty liver disease, and dilated cardiomyopathy. Among those diseases, the mechanism of lamin has been widely discussed. Thereby, this review mainly focuses on the regulatory mechanism of the mutations in the lamin gene in lipid alterations and the human diseases. Considering the protean actions, targeting nuclear lamins may be a potent therapeutic avenue for lipid metabolic disorders and human diseases in the future.

Keywords: nuclear lamins, lipid metabolism, human diseases, mutation of lamin, lipodystrophy

INTRODUCTION

The nuclear lamina (NL) is fibrin network structure located in the lower layer of nuclear membrane, which is primarily composed of lamin A, C, B1, and B2 in mammalian cells. Lamins A and C are classified as type A encoded by *LMNA* while B1 and B2 as type B encoded by *LMNB1* and *LMNB2*, separately (Figure 1). As a major component of the nuclear lamina, lamin is responsible for maintaining the nuclear shape, transducing signals, organizing chromatin, repairing DNA, and pyroptosis (de Leeuw et al., 2018; Stiekema et al., 2020). In structure, lamin, which serves as a V-type intermediate filaggrin (IFS), forms the main cytoskeleton of the nucleus. Like all IFS, a V-type IFS has three components, mainly including an amino acid domain at the head, a helix domain at the center, and a carboxy-terminal domain at the tail. Additionally, the unique characteristics of these subcomponents mainly include a nuclear localization signal (NLS), IG folding domain, and CaaX motif (C = cysteine, A = aliphatic residue, X = any residue) (Gruenbaum and Medalia, 2015; Dittmer and Misteli, 2011) (Figure 2). Surprisingly, the CaaX motif is a vital post-translational modification site for lipid metabolism (Kuchay et al., 2019). Therefore, considering the above structure of lamin, lamin may be an indispensable part in maintaining lipid homeostasis.

Indeed, the structure of lamin is of great importance to lipid metabolism. The dysfunction of lamin leads to numerous pathologies, mainly affecting the structure of the nuclear membrane, lipid synthesis genes, transcription factors, degenerative pathology, fat distribution, malnutrition, and aging (Östlund et al., 2020; Kim et al., 2018; Afonso et al., 2016; Ruiz de Eguino et al., 2012; Padiath and Fu, 2010). So, the abnormality of lamin elicits a series of metabolic disorders, the most common of which is lipodystrophy (Maraldi et al., 2011). The correlation between lamin and lipid metabolism has been well elucidated. For instance, the overexpression (OE) of lamin B1 downregulates the expression of lipid synthesis genes and the content of myelin-enriched lipids, ultimately increasing the risk of autosomal dominant leukodystrophy (ADLD) (Östlund et al., 2020). Also, NF-κB is activated by lamin A/C, subsequently boosting proinflammatory genes, such as Il6, Tnf, Ccl2, and

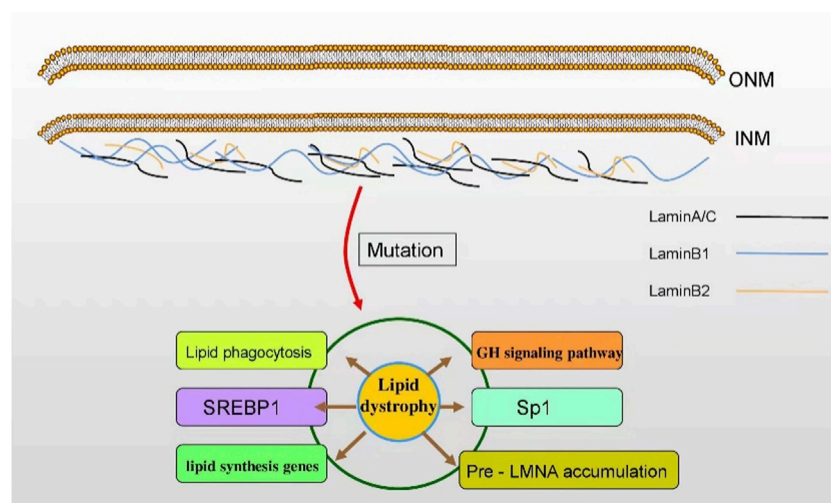


FIGURE 1 | The subtypes and roles of lamin. Lamin A/C, lamin B1, and lamin B2 are the fibrin network structures located at the lower layer of the inner nuclear membrane. Lamin is responsible for maintaining the nuclear shape, participating in signal transduction, organizing chromatin, repairing DNA, and inducing apoptosis. The mutation of LMN genes affect lipid dystrophy in various human diseases. INM: inner nuclear membrane; ONM: outer nuclear membrane.

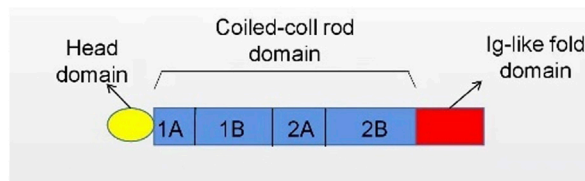


FIGURE 2 | The structure of lamin. Nuclear lamins contain three domains: a head domain, a coiled-coil rod domain, and an Ig-like fold domain.

Nos2, and finally promoting the development of obesity-induced insulin resistance in adipose tissue macrophages (ATMs) (Kim et al., 2018). As lamin always interferes with lipid metabolism, it is plausible that lamin-mediated lipid disorders may be intimately correlated with human diseases. Indeed, accumulating evidence has demonstrated that the mutations in the lamin gene play an important role on human diseases. Lamin genes are susceptible to

mutate, hundreds of which are correlated to the human diseases. Furthermore, it is noteworthy that 17% of those diseases are lipodystrophy. Lipodystrophy syndrome is a rare heterogeneous disease characterized by systemic or partial fat atrophy with metabolic complications, which include insulin resistance, diabetes mellitus (DM), female hyperandrogenia, fatty liver, and dyslipidemia. Then, numerous studies have shown that lamin mutations are of great importance in human lipodystrophy syndrome (Table 1). More specifically speaking, lamin A/C mutation, prelamin A maturation, and lamin B mutation or deregulation have been proven to be the reasons or significant related factors of human lipodystrophy syndrome (Guénantin et al., 2014; Laver et al., 2018). Since lamin is associated with various lipid-related physiological alterations, more emphasis should be placed on the mechanism of the nuclear lamins in human diseases. Herein, this review summarizes the molecular mechanisms of lamin mutation-associated diseases concerning lipid metabolism.

TABLE 1 | Nuclear lamina-related diseases about genetic lipodystrophy syndromes.

| Lipodystrophy type | Genetic mutation | Clinical phenotype |
|--|----------------------|---|
| Familial partial lipodystrophy type 2 (FPLD2) | LMNA (151660 AD) | Gradual loss of fat from the limbs and trunk, “cushingoid” appearance due to neck and face sparing, muscular dystrophy, dilated cardiomyopathy |
| Hutchinson–Gilford progeria syndrome (HGPS) | LMNA (176670 AD) | Generalized loss of subcutaneous fat, progeroid features |
| Mandibuloacral dysplasia with lipodystrophy (MAD type A) | LMNA (248370 AR) | Mandibular and clavicular hypoplasia, acro-osteolysis. Distal and truncal lipoatrophy, progeroid features |
| Mandibuloacral dysplasia with lipodystrophy (MAD type B) | ZMPSTE24 (608612 AR) | Mandibular and clavicular hypoplasia, acro-osteolysis. More generalized loss of fat, premature renal failure, progeroid features |
| Atypical Werner syndrome (AWS) | LMNA (150330 AR) | Partial or generalized loss of subcutaneous fat, progeroid features |
| Adult-onset demyelinating leukodystrophy (ADLD) | LMNB1 (169500 AD) | Downregulates the expression of genes associated with lipid synthesis, which in turn leads to a decrease in myelin-rich lipids |
| Acquired partial lipodystrophy (APL) | LMNB2 (608709 AD) | Gradual symmetrical subcutaneous fat loss, starting in the face and progressing down the upper part of the body. Subcutaneous fat in the lower abdomen and legs is significantly reduced, while fat storage in the gluteal area and lower limbs tends to be retained or increased |

THE REGULATORY MECHANISMS IN HUMAN DISEASES BY MUTATION OF LAMIN GENES

In the human disease spectrum, hundreds of mutations in the *LMNA* gene have been identified and are associated with more than a dozen human diseases, especially including lipodystrophy (Gonzalo et al., 2017). Lipodystrophy is a series of heterogeneous diseases characterized by the loss of selective adipose tissue or loss of functional adipose cells, thus leading to dyslipidemia and heterotopic steatosis (Hafidi et al., 2019). Specifically speaking, autosomal dominant mutations in *LMNA* genes are strongly correlated with familial partial lipodystrophy type 2 (FPLD type 2) (Hegele et al., 2000; Jéru et al., 2017). Additionally, the autosomal recessive mutation of *LMNA* gene is related to mandibuloacral dysplasia (MAD), which causes changes in lipid metabolism (Bagias et al., 2020). Besides, the mutation of *LMN* gene also elicits a dozen of diseases, including FPLD, Hutchinson–Gilford progeria syndrome (HGPS), metabolic associated fatty liver disease (MAFLD), MAD, dilated cardiomyopathy (DCM), autosomal dominant leukodystrophy (ADLD), acquired partial lipodystrophy (APL), Barraquer–Simons (BSS) syndrome, atypical Werner syndrome (WS), limb girdle muscular dystrophy type 1b (LGMD1B), and the autosomal dominant form of Emery–Dreifuss muscular dystrophy (AD-EDMD). In recent years, the regulatory mechanism of lamin mutation has been gradually elucidated. However, the understanding of the regulatory mechanism of mutated lamin in human diseases is not entirely clear, which is still being explored. The study on the regulatory mechanism of lamin mutation is helpful to reveal the importance of lamin in human diseases.

LAMINA/C MUTATION-RELATED DISEASES

The Mutation of *LMNA* Increases Prelamin A Accumulation

FPLD2, a large genetic and phenotypic variation first reported in the 1970s, is characterized by the progressive loss of subcutaneous adipose tissue in the limbs and trunk, accumulation of fat in the face and neck, and severe metabolic disorders, including insulin resistance, glucose intolerance, diabetes, dyslipidemia, and steatohepatitis (Dunnigan et al., 1974; Köbberling et al., 1975; Krawiec et al., 2016). Interestingly, *LMNA* R482W and R482Q are common pathogenic variants in FPLD type 2 (Özen et al., 2020). FPLD and HGPS both belong to premature aging diseases and exhibit a significant loss of subcutaneous adipose tissue. More intriguingly, the pathogenesis of HGPS is caused by the *LMNA* mutation, preventing the conversion of prelamins A to mature lamin A, thereby leading to the accumulation of prelamins A. Later, a large number of studies reported the pathogenesis of lipodystrophy in FPLD roots in the accumulation of prelamins A by mutated *LMNA*, which is similar to the pathogenesis of HGPS (Capanni et al., 2005; Bidault et al., 2013; Afonso et al., 2016).

Conversely, Tu et al. (2016) doubted that most of the mutated sites of *LMNA* mutation in FPLD are not located in the key sequence for lamin A processing. In addition to this, some of these commercial antibodies bind nonspecifically to other proteins. To reconfirm the mechanisms involved, the monoclonal antibodies against prelamins A made by Tu were used for four subjects with *LMNA* mutations in lipodystrophy. Surprisingly, no evidence of prelamins A accumulation was found. As a result, Tu et al. suggested that the missense mutations of *LMNA* in FPLD cannot lead to an accumulation of prelamins A.

Meanwhile, a growing number of studies have shown that the function of lamin is not only at the cellular level but also in disease states is controlled by the PTMs of proteins, including phosphorylation (Machowska et al., 2015), SUMOylation (Moriuchi et al., 2016), glycosylation (Snider and Omary, 2014), farnesylation (Farnsworth et al., 1989), methylation (Rao et al., 2019), o-glucNAcylation (Alfaro et al., 2012; Wang et al., 2012; Simon et al., 2018), succinylation (Weinert et al., 2013), and ubiquitination (Wagner et al., 2011; Povlsen et al., 2012). Farnesylation is special among many PTMs in the regulation of prelamins A. Specifically speaking, pre-*LMNA* (the precursor of mature *LMNA*) and B-type *LMN* are a farnylation on the cysteine residues of carboxy-terminal-Caax motifs (Weber et al., 1989). Moreover, the three terminal amino acids on type A and type B *LMN* were subjected to zinc metalloproteinases (ZMPSTE24; prelamins A) or RAS-converting enzyme 1 (Rce1; *LMNB1* and B2) and cleaved by methylated α -carboxyl groups (Winter-Vann and Casey, 2005). Interestingly, *LMNC* is not able to be farnylated due to lack of the -Caax motif (Goldberg et al., 2008; Adam et al., 2013; Jung et al., 2013). Therefore, ZMPSTE24 is essential for prelamins A to become a mature lamin A. Afonso et al. (2016) discovered that the expression of ZMPSTE24 decreases in FPLD cells, but it is not clear why *LMNA/C* missense mutation affected the expression of ZMPSTE24. Therefore, for lipid dystrophy caused by *LMNA* mutation in FPLD, does *LMNA* mutation cause prelamins A accumulation? If there is an accumulation of prelamins A, is it caused by *LMNA* mutation that reduces the expression of ZMPSTE24?

In short, there is much evidence that the accumulation of prelamins A by mutated *LMNA* causes FPLD and HGPS. Since prelamins A has a paradoxical role in the occurrence and development of FPLD and HGPS, the relevant regulatory mechanism of *LMNA* mutation remains to be further explored.

The Mutated Lamin Elicits Dynamic Recombination of Nuclear Layer Networks

The rupture of lamina is an early event and a prerequisite of lipogenesis and lipocyte differentiation. To understand the underlying regulatory networks, Verstraeten et al. (2011) have found broken lamina, the loss of lamin, and emerin proteins at the 10th day of fat cell differentiation. Eight days after that, the proportion of cells expressing lamins increase while lamin A/C protein levels remain low in the whole. Thus, the re-expression of lamin subtypes increases the plasticity of nuclear membrane to indentations under lipid stress, ultimately causing a reorganization

of the cellular infrastructure. Moreover, progerin, a farnylated protein resulting from *LMNA* mutation, can harden the nucleus and reduce the reorganization, finally wiping the differentiation of lipocytes. Lipid accumulation happens, while low progerin expresses (Najdi et al., 2021). In short, targeting progerin may be an effective method to improve lipid disorders.

The Mutation of *LMNA* Enhances Lipophagy

Lipophagy is mainly manifested as the interaction of the autophagosome membrane with LC3. Then, the lipid droplets (LDs) are selectively delivered to the lysis chamber for degradation by the autophagic protein (Singh and Cuervo, 2012; Wang, 2016; Kloska et al., 2020; Shin, 2020). In a recent study, Chad A. Cowan et al. (Friesen and Cowan, 2018) discovered that in lipolysis, the proportion of LC3-II and LC3-I, the level of ATG7 protein significantly stimulates *LMNA* R482W mutant cells, thereby indicating that autophagosome formation increases in FPLD2 adipocytes. As described above, reduced fat production, increased lipolysis, and increased autophagy may be intimately related to the lipid abnormalities of FPLD2. As a result, *LMNA* mutation promotes lipophagy, while the deeper connection between the lamin gene and lipophagy needs more exploration.

The Lamin A/C Activates Liver Growth Hormone Receptor Signals

MAFLD, a clinicopathological syndrome, is characterized by an excessive deposition of fat in liver cells caused by non-alcohol and other clear liver damage factors and is closely related to metabolic stress liver injury (Mantovani and Dalbeni, 2020). Recently, Vargas et al. (Mahdi et al., 2020) indicated that a case of MAFLD patient was derived from the D300N *LMNA* mutation of FPLD, which surprisingly suggested that the mutation of the lamin gene may progress to steatosis, therefore eliciting MAFLD. Accordingly, the subsequent genetic testing and the risk of MAFLD should be taken seriously in FPLD-diagnosed patients. Beyond that, the change of lamin protein may also contribute to the occurrence and development of MAFLD. Recent research reported that the specific lamin A/C deficiency of hepatocellular in mice induces spontaneous liver injury and increases the susceptibility to steatohepatitis fed with high-fat diets in mice (Kwan et al., 2017). Considering the fact mentioned above, it is plausible that lamin protein is intimately correlated with MAFLD.

Indeed, the regulatory mechanism of lamin in MAFLD has been gradually elucidated. Nevertheless, the understanding of the regulatory mechanism remains unclear. It has been found that the deficiency of lamin A/C upregulates stat1 mRNA and protein levels and blocks the phosphorylation of Janus kinase 2 (JAK2), transcription activator (Stat 5) and extracellular regulated protein kinases (ERKs) mediated by the liver growth hormone (GH) receptor signal, thus downregulating the expression of stat5-dependent male-specific genes, ultimately promoting excessive fatty acids, inflammation, and fibrosis in hepatocytes and exacerbating the progression of MAFLD (Kwan et al., 2017) (Figure 3).

In general, the mutation of the *LMNA* gene induces MAFLD. Similarly, the GH signal pathway and stat1 mediated by lamin A/C play protective roles in delaying MAFLD progression. Nevertheless, the regulatory mechanism of lamin in MAFLD remains to be further studied.

Prelamin A Segregates SREBP1 at Nuclear Margin

MAD, an extremely rare autosomal recessive disorder, is mainly manifested as bone abnormalities, premature aging, and lipodystrophy (Bagias et al., 2020). Growing evidence suggests that the lamin mutation may be a vital part in the lipid changes of MAD. Firstly, a study hinted that a single amino acid substitution in laminin A/C causes MAD (Novelli et al., 2002). In addition, the two defects in MAD are the mutation of *LMNA* or *ZMPSTE24* genes and are named as type A or B MAD, respectively. Intriguingly, it has been found that the different types of MAD also cause various fat changes. Specifically speaking, type A MAD (MADA) loses fat in the extremities, while fat deposits in the neck and trunk are normal or excessive; type B MAD (MADB) forms subcutaneous fat loss that resulted from a typical mutation in the *ZMPSTE24* gene (Cenni et al., 2018). The above evidence shows that the mutated lamin is intimately correlated with lipid disorders in MAD. Moreover, some studies have demonstrated that the regulatory mechanism of prelamin A plays an important role in MAD.

Indeed, some studies have demonstrated that prelamin A plays an important role in regulating lipid homeostasis. Lattanzi et al. (Capanni et al., 2005) reported that prelamin A accumulated in Dunnigan familial partial lipodystrophy, mandibuloacral dysplasia, and atypical Werner syndrome, which are three laminopathies characterized by lipodystrophic phenotypes. Furthermore, prelamin A precursors specifically accumulate in dystrophic cells and lipodystrophic cells and colocalize with cholesterol regulatory element binding protein 1 (SREBP1) (SREBP1: The key regulators of lipid metabolism, involved in adipocyte differentiation, are expressed at high levels in adipose tissue, and stimulates the expression of a variety of adipogenic genes, including FAS, acetyl-CoA carboxylase, stearoyl-coenzyme A desaturase1, and lipoprotein lipase (Li et al., 2016). Lattanzi et al. also suggested that not mature lamin A/C but rather prelamin A interacts with SREBP1. The mechanism is that prelamin A isolates SREBP1 at the nuclear border, thereby declining the activation of peroxisome proliferator activated receptor gamma (PPAR gamma) via inhibiting active SREBP1, thus impairing pre-adipocyte differentiation (Capanni et al., 2005).

In conclusion, the lamin mutation leads to lipid changes in MAD. Also, prelamin A interacts with SREBP1, thus affecting the actions of pre-adipocytes. However, the understanding of the lipid-regulated mechanism of lamin is not entirely clear, which is still being explored.

Prelamin A and Sp1 Effects on Adipogenesis

To investigate the effect of lamin on transcriptional factors, research shows that lipodystrophy can not only result from

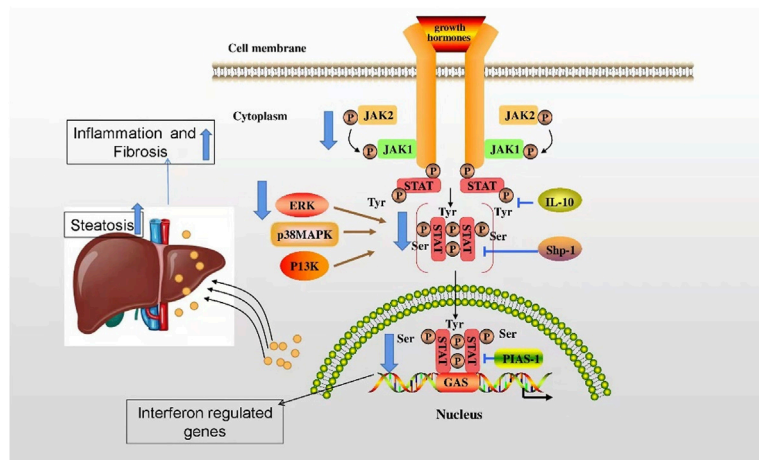


FIGURE 3 | The regulatory mechanism of lamin in alleviation of MAFLD. The deficiency of lamin A/C upregulates stat1 mRNA and protein levels and blocks JAK2, Stat 5, and ERK mediated by the liver GH receptor signal, thus downregulating the expression of stat5-dependent male-specific genes, ultimately promoting excessive fatty acids, inflammation, and fibrosis in hepatocytes and exacerbating the progression of MAFLD.

lamin mutation but also from the use of human immunodeficiency virus protease inhibitors (PIs). Under PI treatment in human mesenchymal stem cells (hMSC), impaired adipogenesis is due to an interaction between accumulated prelamin A and Sp1 transcription factors, finally altering extracellular matrix gene expression (Ruiz de Eguino et al., 2012). In general, the interaction between prelamin A and Sp1 exacerbates *LMNA*-linked lipostrophy. Nevertheless, the regulatory mechanism between lamin and transcriptional factors in human diseases remains to be further studied.

The Activation of Tumor Protein 53

DCM is characterized by a progressive conduction system disease, arrhythmia, and systolic impairment (Captur et al., 2018). It has been studied that cyclin-dependent kinase inhibitor 2A (CDKN2A), a downstream target of the E2F pathway, is responsible for activation. *LMNA* D300N, associated with DCM, results from E2F/DNA damage/TP53 activation. This axis can be a potential intervention target for DCM in laminopathies (Augusto et al., 2020). Furthermore, the impaired crosstalk between endothelial cells (ECs) and cardiomyocytes (CMs) can contribute to the pathogenesis of *LMNA*-related DCM (Sayed et al., 2020). The other sites of cardiac involvement in DCM contain missense lamin A/C mutation (Arg60Gly) (Porcu et al., 2021).

LMINB1 MUTATION-RELATED DISEASES

Lamin B1 Downregulates Lipid Synthesis Genes

ADLD is a slow-progressing but fatal neurological disorder in 40–50-year-old adults, usually accompanied by symptoms of autonomic nervous dysfunction, followed by ataxia and cognitive impairment and even the loss of myelin sheath in the central nervous system (CNS) (Chrast et al., 2011; Giorgio

et al., 2015). Interestingly, ADLD is the only disease associated with the lamin B1 gene (Padiath, 2019). Otherwise, the pathogenesis of ADLD is overexpressed lamin B1 protein levels due to *LMNB1* gene replication or upstream deletion (Takamori et al., 2018). In addition, lamin B1 OE targets oligodendrocytes, thus decreasing the production of myelin sheaths in the CNS. Furthermore, Rolyan et al. also discovered that lamin B1 OE mice exhibit severe demyelination, axon damage, and neuron loss due to the decreased gene expression of lipid synthesis pathways that play an important role in myelin regulation, ultimately depleting myelin-rich lipids (Rolyan et al., 2015). Indeed, the myelin genes required for oligodendrocyte maturation are sensitively influenced by the nuclear membrane (Lin et al., 2011). However, another study indicated that increased lamin B1 alters the chromatin associated with the region of the nuclear layer, therefore affecting the structure of the nuclear membrane and myelin-related genes (Padiath and Fu, 2010).

In conclusion, the expression of lamin B1 exacerbates ADLD. Despite considerable studies that are accessible, more experiments are necessitated about the lipid-related effects of lamin.

LMINB2 MUTATION-RELATED DISEASES

Overactivation of the Complement System

Mutations in the *LMNB2* have been associated with APL, also known as BSS syndrome, which usually begins in childhood or adolescence. Fat loss in BSS is typically characterized by gradual symmetrical subcutaneous fat loss, starting in the face and progressing down the upper part of the body. The subcutaneous fat in the lower abdomen and legs is significantly reduced, while fat storage in the gluteal area and lower limbs tends to be retained or increased (Hegele et al., 2006; Oliveira et al., 2016). CORVILLO et al. analyzed clinical, immunological, and histological events in an 11-year-old girl

with BSS during a 5-year follow-up, and their results suggest that the overactivation of the complement system in adipose tissue may be responsible for fat loss in BSS patients (Corvillo et al., 2020).

THE REGULATORY MECHANISMS ARE STILL UNCLEAR

WS or atypical WS is a rare autosomal recessive disorder caused by inherited mutations in the *WRN* gene and *LMNA* gene, respectively (Rossi et al., 2010; Wang et al., 2018). In atypical WS associated with the R133L mutation of the *LMNA* gene, the severity of metabolic complications is positively related to the degree of lipodystrophy (Doh et al., 2009). In addition, Garg et al. investigated the body fat distribution pattern and metabolic abnormalities in two patients with atypical WS carrying R133L heterozygous *LMNA* mutations. Both patients with *LMNA* mutations had a unique distribution of body fat, with patient 1 having a fat loss limited to the distal portion of the limbs and an increase in fat deposition in the trunk region, whereas patient 2 had a significant decrease in body fat. In summary, patients with atypical Werner syndrome caused by R133L heterozygous *LMNA* mutations may present with different types of lipodystrophies, which may present with partial or total body fat loss. Partial lipodystrophy can be further divided into two distinct patterns: one involves the entire limb, mainly including familial partial lipodystrophy, the Dunnigan type, and mandibular dysplasia, while the other happens to involve only the distal limb region (Muchir et al., 2000). However, the regulatory mechanism needs to be further discovered.

Emery–Dreifuss muscular dystrophy (EDMD) is a severe muscular disorder characterized by the early contracture of the elbows, slowly progressive muscle weakness, and cardiomyopathy with conduction block (Onishi et al., 2002). Lamin A/C defects occur both in X-EDMD and AD-EDMD (Niebroj-Dobosz et al., 2003). Lamin A is not only required for lamin B receptor (LBR) retention but also for the localization of transcriptional RNA pol II in muscle cells (Reichart et al., 2004).

Limb girdle muscular dystrophy (LGMD), a type of muscular dystrophy (MD), is manifested as the progressive weakness of muscles (Rajoria et al., 2021). Though the regulatory mechanism is still unclear, a survey has reported that the lipid changes of LGMD are similar to FPLD in skeletal muscle metabolism, mainly exhibiting incomplete fatty acid oxidation and upregulated ketogenesis, which may result from a common underlying cause of muscular metabolic disorders (Boschmann et al., 2010). Actually, LGMD1B is same as FPLD and EDMD (Morris, 2001). Besides, LGMD1B and AD-EDMD are allelic disorders (Muchir et al., 2000).

CONCLUSION

As a component of nucleus, lamin plays an important role in maintaining nuclear shape, mechanical signaling, stabilizing chromatin, regulating gene expression, and promoting cell

cycle progression. Here, we amply review the possible mechanisms of innate or acquired lipid abnormalities caused by lamin in the human diseases, mainly including increased prelamin A accumulation, a dynamic recombination of nuclear layer networks, enhanced lipophagy, activated liver growth hormone receptor signals, segregated SREBP1 at the nuclear margin, adipogenesis, lipid synthesis genes, overactivated complement system, and activated TP53. Those are the targets for lipid defects caused by lamin alterations. Nevertheless, the regulatory mechanism of lamin in lipid metabolism and human diseases remains to be further studied. As a result, targeting lamin should be considered for treating human diseases, which may be a promising disease-reversing strategy for patients.

PROSPECTION

Lipolysis and autophagy are two central catabolic pathways of lipid decomposition (Zechner et al., 2017). Lipolysis depends on the direct activation of lipase related to LDs, such as adipose triglyceride lipase (ATGL), hormone-sensitive lipase (HSL), and monoglycerol lipase (MGL). In addition, LDs interact with ATGL activators and inhibitors and then provide energy and basic materials for the synthesis of cell membranes and hormones in the body (Onal et al., 2017). Another lysosomal autophagy pathway that plays an important role in lipid degradation is called lipid autophagy, or lipophagy for short. Lipophagy requires cargo identification accomplished by the interaction between the autophagosome membrane with LC3. Subsequently, LDs are selectively delivered to the lysis chamber for degradation by the autophagic protein (Singh and Cuervo, 2012; Wang, 2016; Kloska et al., 2020; Shin, 2020). Thus, the dysregulation of lipophagy can lead to an abnormal deposition of lipids, therefore seriously affecting cell function and dynamic balance, ultimately resulting in cell death and a variety of diseases, including non-alcoholic fatty liver disease, coronary heart disease, and even cancer (Johnson and Stolzing, 2019).

Nuclear autophagy, a new type of selective autophagy, is responsible for selectively removing damaged or unnecessary nuclear substances in cells (Fu et al., 2018). Nuclear autophagy happens in a variety of conditions, including starvation, rapamycin-induced TORC1 inactivation, nuclear vacuolar junction (NVJ) expansion, and nuclear fibrillary lamina defects (Bo Otto and Thumm, 2020). In 2009, it was first reported that *LMNA/C* is involved in the development of mammalian nuclear autophagy. Additionally, some nuclear components exist in perinuclear autophagosomes and lysosomes (Park et al., 2009). Dou et al. also found a large amount of endogenous LC3 and a small amount of lipidated LC3-II in the nucleus. Lamin B1 interacts with LC3 to induce nuclear autophagy, which may be enhanced by lipidated LC3 (Dou et al., 2015) (Figure 4). Additionally, the NEM1-spo7/Pah1 axis is very important in the lipid synthesis axis. Meanwhile, this axis is also an important factor to induce nuclear autophagy and correct the localization of micronucleus autophagy factor NVJ1 and nuclear autophagy receptor Atg39 (Rahman et al., 2018; Mirheydari et al., 2020).

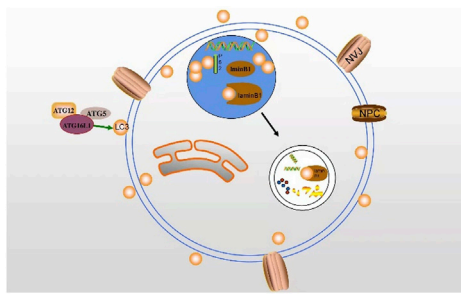


FIGURE 4 | The interaction between LC3 and lamin B1 may induce nuclear autophagy. LC3 transports autophagy membrane and substrate via binding to lamin B1 in the nucleus.

Combined with the above literature, it is not difficult to find that nuclear autophagy is significantly correlated with lipid metabolism. For instance, lamin participates in the occurrence and development of nuclear autophagy by interacting with LC3, and the latter one is an essential factor in the process of lipophagy. As a result, the nuclear autophagy and lipophagy involved in lamin may be not independent of each other, although the specific correlation mechanism and the relationship between lamin-dependent nuclear autophagy and lipid metabolism deserve to be further studied.

Apart from autophagy, apoptosis is another form of cell death. Apoptosis is characterized by caspase activation, DNA cleavage, and membrane surface modifications that enable apoptotic and phagocytic cells to be recognized, as well as morphological changes such as chromatin concentration and nuclear fragmentation (Jung et al., 2020a). Importantly, lamin also seems to act in the relationship between apoptosis and lipid metabolism. In nonadipose tissues such as liver, heart, kidney, muscle, and islet, the harmful effects caused by excessive accumulation of fat on these organs or systems are called lipotoxicity, which can induce programmed cell death, and lipid apoptosis is the main cellular consequence of lipotoxicity (Schaffer, 2016; Zhang et al., 2019). In all, the involvement of lamins in nuclear autophagy and apoptosis is also a promising point for lipodystrophy and deserves to be further explored in the future.

Chromatin concentration is a nuclear modification characteristic of the active apoptotic phase that follows DNA cleavage and the hydrolysis of certain nuclear proteins by proteases in the caspase family. The cysteine aspartate protease family (caspase) is the main factor affecting protein hydrolysis in the process of apoptosis. The apoptotic caspase can be divided into two types: the initiation of caspase, including caspase-8, -9, and -10, and the execution of caspase, including caspase-3, -6, and -7. Caspase-3 and caspase-6 are responsible for the cleavage of nuclear proteins PARP and lamin, respectively. Among many apoptosis-related proteins, the hydrolysis of PARP by caspase-3 is considered as an early indicator of apoptosis. The early cleavage and rapid processing of lamin B by caspase-6 are regarded as a marker of apoptosis (Villa et al., 1997; Buendia et al., 1999; Eron et al., 2017; Jung et al., 2020b). Meanwhile, lamin A can also be

cleaved as a substrate of caspase-6. Studies have shown that caspase-3 cleaves caspase-6 first in normal cell apoptosis, and caspase-6 cleaves lamin A/C before apoptosis (Capo-Chichi et al., 2018). Only when lamin A/C is cleaved by caspase-6 can chromosomal DNA fully coagulate during apoptosis (Yan et al., 2021) (Figure 5). Lamin plays a key role in apoptosis, while the specific mechanism of the involvement of lamin in lipid apoptosis remains to be further studied. For instance, if adipocytes show apoptosis in lipodystrophy, then silencing caspase may prevent its interference with lamin expression, subsequently ameliorating lipid defects.

In MAD, we review the interaction between prelamin A and SREBP1, suggesting that prelamin A sequesters SREBP1 at the nuclear border and restricts the translocation of some transcription factors into the nucleus, thereby reducing the pool of normally activated active SREBP1 and leading to the dysdifferentiation of adipocytes (Capanni et al., 2005). Meanwhile, it has been reported that SREBP1c (one of the subtypes of SREBP1) modified by SUMO1 (small ubiquitin-like modifier, also named SUMOylation, is a crucial post-translational modification that exhibits a strong effect on DNA repair, transcriptional regulation, protein stability, and cell cycle progression) can repress the transcriptional activity of SREBP1c and inhibits lipid production (Pichler et al., 2017; Zeng et al., 2020). Similarly, several lamin A domains can also be modified by SUMOylation. Two typical mutations cause lipid dystrophy (LMNA P.g465d and P.K486N), while only the atypical FPLD2-related p. r482W mutation shows a decrease in lamin A sumoylation. This may provide an alternative mechanism for these atypical lipodystrophies (Simon et al., 2013).

The distribution of adipose tissue is not entirely alike in various types of lipodystrophy. Moreover, the special distribution is an ongoing research. Additionally, the major

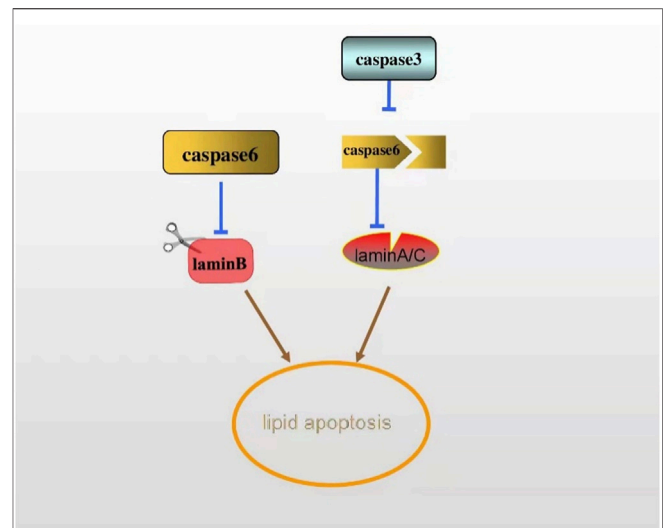


FIGURE 5 | The early cleavage of lamin B by caspase-6 is regarded as a marker of apoptosis. Lamin A can also be a substrate of caspase-6. In apoptosis, caspase-6 is cleaved by caspase-3, thus cleaving lamin A/C, ultimately activating the apoptosis.

foregone mutated genes in lipid disorders encode proteins forming lipid droplets (Meehan et al., 2016). However, not only the connections between genetic mutation and fat loss but also the cure strategies still need to be discovered. Metreleptin, a recombinant analog of human leptin, is the only drug approved for the treatment of metabolic complications associated with lipodystrophy. This compound is used for the replacement of lipodystrophy accompanied by leptin deficiency without HIV infection (Chevalier et al., 2021). Nonetheless, except for Japan, no country authorizes metreleptin as a drug for lipid issues. Worse, it is not entirely clear whether metreleptin is a benefit or not to lipodystrophy syndrome with normal leptin levels (Oral et al., 2019). Worse still, various complications in the treatment of lipodystrophy have shown to us all. Notably, the most common of which includes weight loss, abdominal pain, hypoglycemia, fatigue, headache, a loss of appetite, injection site reactions (bruising and hives), anti-leptin antibodies, T-cell lymphoma, and infection (Tchang et al., 2015). Even so, metreleptin treatment powerfully alleviates metabolic abnormalities such as hyperglycemia, hypertriglyceridemia, increased hepatic fat content, and elevated liver enzymes alanine transaminase and aspartate transaminase and corrects the hyperphagia of leptin deficiency in patients with generalized lipodystrophy (Akinci and Akinci, 2015).

REFERENCES

- Adam, S. A., Butin-Israeli, V., Cleland, M. M., Shimi, T., and Goldman, R. D. (2013). Disruption of Lamin B1 and Lamin B2 Processing and Localization by Farnesyltransferase Inhibitors. *Nucleus* 4 (2), 142–150. doi:10.4161/nucl.24089
- Afonso, P., Auclair, M., Boccara, F., Vantyghem, M. C., Katlama, C., Capeau, J., et al. (2016). LMNA Mutations Resulting in Lipodystrophy and HIV Protease Inhibitors Trigger Vascular Smooth Muscle Cell Senescence and Calcification: Role of ZMPSTE24 Downregulation. *Atherosclerosis* 245, 200–211. doi:10.1016/j.atherosclerosis.2015.12.012
- Akinci, G., and Akinci, B. (2015). Metreleptin Treatment in Patients with Non-HIV Associated Lipodystrophy. *Recent Pat Endocr. Metab. Immune Drug Discov.* 9 (2), 74–78. doi:10.2174/157489281166615111142554
- Alfaro, J. F., Gong, C. X., Monroe, M. E., Aldrich, J. T., Clauss, T. R., Purvine, S. O., et al. (2012). Tandem Mass Spectrometry Identifies many Mouse Brain O-GlcNAcylated Proteins Including EGF Domain-specific O-GlcNAc Transferase Targets. *Proc. Natl. Acad. Sci. U S A.* 109 (19), 7280–7285. doi:10.1073/pnas.1200425109
- Augusto, J. B., Eiros, R., Nakou, E., Moura-Ferreira, S., Treibel, T. A., Captur, G., et al. (2020). Dilated Cardiomyopathy and Arrhythmogenic Left Ventricular Cardiomyopathy: a Comprehensive Genotype-Imaging Phenotype Study. *Eur. Heart J. Cardiovasc. Imaging* 21 (3), 326–336. doi:10.1093/ehjci/jez188
- Bagias, C., Xiarchou, A., Bargiota, A., and Tigas, S. (2020). Familial Partial Lipodystrophy (FPLD): Recent Insights. *Diabetes Metab. Syndr. Obes.* 13, 1531–1544. doi:10.2147/DMSO.S206053
- Bidault, G., Garcia, M., Vantyghem, M. C., Ducluzeau, P. H., Morichon, R., Thiagarajah, K., et al. (2013). Lipodystrophy-linked LMNA p.R482W Mutation Induces Clinical Early Atherosclerosis and *In Vitro* Endothelial Dysfunction. *Arterioscler Thromb. Vasc. Biol.* 33 (9), 2162–2171. doi:10.1161/ATVBAHA.113.301933
- Bo Otto, F., and Thumm, M. (2020). Nucleophagy-Implications for Microautophagy and Health. *Int. J. Mol. Sci.* 21 (12). doi:10.3390/ijms21124506
- Boschmann, M., Engeli, S., Moro, C., Luedtke, A., Adams, F., Gorgelniak, K., et al. (2010). LMNA Mutations, Skeletal Muscle Lipid Metabolism, and Insulin Resistance. *J. Clin. Endocrinol. Metab.* 95 (4), 1634–1643. doi:10.1210/jc.2009-1293
- Buendia, B., Santa-Maria, A., and Courvalin, J. C. (1999). Caspase-dependent Proteolysis of Integral and Peripheral Proteins of Nuclear Membranes and Nuclear Pore Complex Proteins during Apoptosis. *J. Cell Sci.* 112 (Pt 11), 1743–1753. doi:10.1242/jcs.112.11.1743
- Capanni, C., Mattioli, E., Columbaro, M., Lucarelli, E., Parnaik, V. K., Novelli, G., et al. (2005). Altered Pre-lamin A Processing Is a Common Mechanism Leading to Lipodystrophy. *Hum. Mol. Genet.* 14 (11), 1489–1502. doi:10.1093/hmg/ddi158
- Capo-Chichi, C. D., Cai, K. Q., and Xu, X. X. (2018). Overexpression and Cytoplasmic Localization of Caspase-6 Is Associated with Lamin A Degradation in Set of Ovarian Cancers. *Biomark Res.* 6, 30. doi:10.1186/s40364-018-0144-9
- Captur, G., Arbustini, E., Bonne, G., Syrris, P., Mills, K., Wahbi, K., et al. (2018). Lamin and the Heart. *Heart* 104 (6), 468–479. doi:10.1136/heartjnl-2017-312338
- Cenni, V., D'Apice, M. R., Garagnani, P., Columbaro, M., Novelli, G., Franceschi, C., et al. (2018). Mandibuloacral Dysplasia: A Premature Ageing Disease with Aspects of Physiological Ageing. *Ageing Res. Rev.* 42, 1–13. doi:10.1016/j.arr.2017.12.001
- Chevalier, B., Lemaître, M., Leguier, L., Mapihan, K. L., Douillard, C., Jannin, A., et al. (2021). Metreleptin Treatment of Non-HIV Lipodystrophy Syndromes. *Presse Med.* 50 (3), 104070. doi:10.1016/j.lpm.2021.104070
- Chrast, R., Saher, G., Nave, K. A., and Verheijen, M. H. (2011). Lipid Metabolism in Myelinating Glial Cells: Lessons from Human Inherited Disorders and Mouse Models. *J. Lipid Res.* 52 (3), 419–434. doi:10.1194/jlr.R009761
- Corvillo, F., Nozal, P., López-Lera, A., De Miguel, M. P., Piñero-Fernández, J. A., De Lucas, R., et al. (2020). Evidence of Ongoing Complement Activation on Adipose Tissue from an 11-Year-Old Girl with Barraquer-Simons Syndrome. *J. Dermatol.* 47 (12), 1439–1444. doi:10.1111/1346-8138.15570
- de Leeuw, R., Gruenbaum, Y., and Medalia, O. (2018). Nuclear Lamins: Thin Filaments with Major Functions. *Trends Cell Biol.* 28 (1), 34–45. doi:10.1016/j.tcb.2017.08.004
- Dittmer, T. A., and Misteli, T. (2011). The Lamin Protein Family. *Genome Biol.* 12 (5), 222. doi:10.1186/gb-2011-12-5-222

AUTHOR CONTRIBUTIONS

YP wrote the manuscript and QT searched for references. FX and NF was responsible for revising the manuscript.

FUNDING

This work was jointly supported by the Natural Science Foundation of Hunan Province (2021JJ30628), Clinical medical technology innovation guidance project of Hunan Province (2020SK51904), Natural Science Foundation of Hunan Province (grant number 2019JJ50556), Postgraduate Scientific Research Innovation Project of Hunan Province (CX20210979), Scientific research project of University of South China (Documents of the university of south China (2019)02), the Innovative Province Construction Special Project of Hunan Province (2021SK4031).

- Doh, Y. J., Kim, H. K., Jung, E. D., Choi, S. H., Kim, J. G., Kim, B. W., et al. (2009). Novel LMNA Gene Mutation in a Patient with Atypical Werner's Syndrome. *Korean J. Intern. Med.* 24 (1), 68–72. doi:10.3904/kjim.2009.24.1.68
- Dou, Z., Xu, C., Donahue, G., Shimi, T., Pan, J. A., Zhu, J., et al. (2015). Autophagy Mediates Degradation of Nuclear Lamina. *Nature* 527 (7576), 105–109. doi:10.1038/nature15548
- Dunnigan, M. G., Cochrane, M. A., Kelly, A., and Scott, J. W. (1974). Familial Lipotrophic Diabetes with Dominant Transmission. A New Syndrome. *Q. J. Med.* 43 (169), 33–48.
- Eron, S. J., Raghupathi, K., and Hardy, J. A. (2017). Dual Site Phosphorylation of Caspase-7 by PAK2 Blocks Apoptotic Activity by Two Distinct Mechanisms. *Structure* 25 (1), 27–39. doi:10.1016/j.str.2016.11.001
- Farnsworth, C. C., Wolda, S. L., Gelb, M. H., and Glomset, J. A. (1989). Human Lamin B Contains a Farnesylated Cysteine Residue. *J. Biol. Chem.* 264 (34), 20422–20429. doi:10.1016/s0021-9258(19)47079-8
- Friesen, M., and Cowan, C. A. (2018). FPLD2 LMNA Mutation R482W Dysregulates iPSC-Derived Adipocyte Function and Lipid Metabolism. *Biochem. Biophys. Res. Commun.* 495 (1), 254–260. doi:10.1016/j.bbrc.2017.11.008
- Fu, N., Yang, X., and Chen, L. (2018). Nucleophagy Plays a Major Role in Human Diseases. *Curr. Drug Targets* 19 (15), 1767–1773. doi:10.2174/1389450119666180518112350
- Giorgio, E., Robyr, D., Spielmann, M., Ferrero, E., Di Gregorio, E., Imperiale, D., et al. (2015). A Large Genomic Deletion Leads to Enhancer Adoption by the Lamin B1 Gene: a Second Path to Autosomal Dominant Adult-Onset Demyelinating Leukodystrophy (ADLD). *Hum. Mol. Genet.* 24 (11), 3143–3154. doi:10.1093/hmg/ddv065
- Goldberg, M. W., Huttenlauch, I., Hutchison, C. J., and Stick, R. (2008). Filaments Made from A- and B-type Lamins Differ in Structure and Organization. *J. Cell Sci* 121 (Pt 2), 215–225. doi:10.1242/jcs.022020
- Gonzalo, S., Kreienkamp, R., and Askjaer, P. (2017). Hutchinson-Gilford Progeria Syndrome: A Premature Aging Disease Caused by LMNA Gene Mutations. *Ageing Res. Rev.* 33, 18–29. doi:10.1016/j.arr.2016.06.007
- Gruenbaum, Y., and Medalia, O. (2015). Lamins: the Structure and Protein Complexes. *Curr. Opin. Cell Biol* 32, 7–12. doi:10.1016/j.ccb.2014.09.009
- Guénant, A. C., Briand, N., Bidault, G., Afonso, P., Béréziat, V., Vatié, C., et al. (2014). Nuclear Envelope-Related Lipodystrophies. *Semin. Cell Dev Biol* 29, 148–157. doi:10.1016/j.semdb.2013.12.015
- Hafidi, M. E., Buelna-Chontal, M., Sánchez-Muñoz, F., and Carbó, R. (2019). Adipogenesis: A Necessary but Harmful Strategy. *Int. J. Mol. Sci.* 20 (15). doi:10.3390/ijms20153657
- Hegele, R. A., Cao, H., Huff, M. W., and Anderson, C. M. (2000). LMNA R482Q Mutation in Partial Lipodystrophy Associated with Reduced Plasma Leptin Concentration. *J. Clin. Endocrinol. Metab.* 85 (9), 3089–3093. doi:10.1210/jcem.85.9.6768
- Hegele, R. A., Cao, H., Liu, D. M., Costain, G. A., Charlton-Menys, V., Rodger, N. W., et al. (2006). Sequencing of the Reannotated LMNB2 Gene Reveals Novel Mutations in Patients with Acquired Partial Lipodystrophy. *Am. J. Hum. Genet.* 79 (2), 383–389. doi:10.1086/505885
- Jéru, I., Vatié, C., Araujo-Vilar, D., Vigouroux, C., and Lasclos, O. (2017). Clinical Utility Gene Card for: Familial Partial Lipodystrophy. *Eur. J. Hum. Genet.* 25 (2). doi:10.1038/ejhg.2016.102
- Johnson, A. A., and Stolz, A. (2019). The Role of Lipid Metabolism in Aging, Lifespan Regulation, and Age-Related Disease. *Ageing Cell* 18 (6), e13048. doi:10.1111/ace.13048
- Jung, H. J., Nobumori, C., Goulbourne, C. N., Tu, Y., Lee, J. M., Tatar, A., et al. (2013). Farnesylation of Lamin B1 Is Important for Retention of Nuclear Chromatin during Neuronal Migration. *Proc. Natl. Acad. Sci. U S A* 110 (21), E1923–E1932. doi:10.1073/pnas.1303916110
- Jung, J. H., Lee, H. J., Kim, J. H., Sim, D. Y., Im, E., Kim, S., et al. (2020). Colocalization of MID1IP1 and C-Myc Is Critically Involved in Liver Cancer Growth via Regulation of Ribosomal Protein L5 and L11 and CNOT2. *Cells* 9 (4), 985. doi:10.3390/cells9040985
- Jung, S., Jeong, H., and Yu, S. W. (2020). Autophagy as a Decisive Process for Cell Death. *Exp. Mol. Med.* 52 (6), 921–930. doi:10.1038/s12276-020-0455-4
- Kim, Y., Bayona, P. W., Kim, M., Chang, J., Hong, S., Park, Y., et al. (2018). Macrophage Lamin A/C Regulates Inflammation and the Development of Obesity-Induced Insulin Resistance. *Front. Immunol.* 9, 696. doi:10.3389/fimmu.2018.00696
- Kloska, A., Węsierska, M., Malinowska, M., Gabig-Cimińska, M., and Jakóbkiewicz-Banecka, J. (2020). Lipophagy and Lipolysis Status in Lipid Storage and Lipid Metabolism Diseases. *Int. J. Mol. Sci.* 21 (17), 6113. doi:10.3390/ijms21176113
- Köbberling, J., Willms, B., Kattermann, R., and Creutzfeldt, W. (1975). Lipodystrophy of the Extremities. A Dominantly Inherited Syndrome Associated with Lipatrophic Diabetes. *Humangenetik* 29 (2), 111–120. doi:10.1007/BF00430347
- Krawiec, P., Melges, B., Pac-Kożuchowska, E., Mroczkowska-Juchkiewicz, A., and Czerska, K. (2016). Fitting the Pieces of the Puzzle Together: a Case Report of the Dunnigan-type of Familial Partial Lipodystrophy in the Adolescent Girl. *BMC Pediatr.* 16, 38. doi:10.1186/s12887-016-0581-2
- Kuchay, S., Wang, H., Marzio, A., Jain, K., Homer, H., Fehrenbacher, N., et al. (2019). GGTase3 Is a Newly Identified Geranylgeranyltransferase Targeting a Ubiquitin Ligase. *Nat. Struct. Mol. Biol.* 26 (7), 628–636. doi:10.1038/s41594-019-0249-3
- Kwan, R., Brady, G. F., Brzozowski, M., Weerasinghe, S. V., Martin, H., Park, M. J., et al. (2017). Hepatocyte-Specific Deletion of Mouse Lamin A/C Leads to Male-Selective Steatohepatitis. *Cell Mol Gastroenterol Hepatol* 4 (3), 365–383. doi:10.1016/j.jcmgh.2017.06.005
- Laver, T. W., Patel, K. A., Colclough, K., Curran, J., Dale, J., Davis, N., et al. (2018). PLIN1 Haploinsufficiency Is Not Associated with Lipodystrophy. *J. Clin. Endocrinol. Metab.* 103 (9), 3225–3230. doi:10.1210/je.2017-02662
- Li, X., Yang, M., Li, Z., Xue, M., Shanguan, Z., Ou, Z., et al. (2016). Fructus Xanthii Improves Lipid Homeostasis in the Epididymal Adipose Tissue of Rats Fed a High-Fat Diet. *Mol. Med. Rep.* 13 (1), 787–795. doi:10.3892/mmr.2015.4628
- Lin, S. T., Ptáček, L. J., and Fu, Y. H. (2011). Adult-onset Autosomal Dominant Leukodystrophy: Linking Nuclear Envelope to Myelin. *J. Neurosci.* 31 (4), 1163–1166. doi:10.1523/JNEUROSCI.5994-10.2011
- Machowska, M., Piekarczyk, K., and Rzepecki, R. (2015). Regulation of Lamin Properties and Functions: Does Phosphorylation Do it All?. *Open Biol.* 5 (11). doi:10.1098/rsob.150094
- Mahdi, L., Kahn, A., Dhamija, R., and Vargas, H. E. (2020). Hepatic Steatosis Resulting from LMNA-Associated Familial Lipodystrophy. *ACG Case Rep. J.* 7 (4), e00375. doi:10.14309/crj.0000000000000375
- Mantovani, A., and Dalbeni, A. (2020). NAFLD, MAFLD and DAFLD. *Dig. Liver Dis.* 52 (12), 1519–1520. doi:10.1016/j.dld.2020.09.013
- Maraldi, N. M., Capanni, C., Cenni, V., Fini, M., and Lattanzi, G. (2011). Laminopathies and Lamin-Associated Signaling Pathways. *J. Cell Biochem* 112 (4), 979–992. doi:10.1002/jcb.22992
- Meehan, C. A., Cochran, E., Kassai, A., Brown, R. J., and Gorden, P. (2016). Metreleptin for Injection to Treat the Complications of Leptin Deficiency in Patients with Congenital or Acquired Generalized Lipodystrophy. *Expert Rev. Clin. Pharmacol.* 9 (1), 59–68. doi:10.1586/17512433.2016.1096772
- Mirheydari, M., Dey, P., Stuke, G. J., Park, Y., Han, G. S., and Carman, G. M. (2020). The Spo7 Sequence LLI Is Required for Nem1-Spo7/Pah1 Phosphatase cascade Function in Yeast Lipid Metabolism. *J. Biol. Chem.* 295 (33), 11473–11485. doi:10.1074/jbc.RA120.014129
- Moriuchi, T., Kuroda, M., Kusumoto, F., Osumi, T., and Hirose, F. (2016). Lamin A Reassembly at the End of Mitosis Is Regulated by its SUMO-Interacting Motif. *Exp. Cell Res* 342 (1), 83–94. doi:10.1016/j.yexcr.2016.02.016
- Morris, G. E. (2001). The Role of the Nuclear Envelope in Emery-Dreifuss Muscular Dystrophy. *Trends Mol. Med.* 7 (12), 572–577. doi:10.1016/s1471-4914(01)02128-1
- Muchir, A., Bonne, G., van der Kooi, A. J., van Meegen, M., Baas, F., Bolhuis, P. A., et al. (2000). Identification of Mutations in the Gene Encoding Lamins A/C in Autosomal Dominant Limb Girdle Muscular Dystrophy with Atrioventricular Conduction Disturbances (LGMD1B). *Hum. Mol. Genet.* 9 (9), 1453–1459. doi:10.1093/hmg/9.9.1453
- Najdi, F., Krüger, P., and Djabali, K. (2021). Impact of Progerin Expression on Adipogenesis in Hutchinson-Gilford Progeria Skin-Derived Precursor Cells. *Cells* 10 (7). doi:10.3390/cells10071598
- Niebroj-Dobosz, I., Fidzińska, A., and Hausmanowa-Petrusewicz, I. (2003). Expression of Emerin and Lamins in Muscle of Patients with Different Forms of Emery-Dreifuss Muscular Dystrophy. *Acta Myol* 22 (2), 52–57.
- Novelli, G., Muchir, A., Sangiulio, F., Helbling-Leclerc, A., D'Apice, M. R., Massart, C., et al. (2002). Mandibuloacral Dysplasia Is Caused by a

- Mutation in LMNA-Encoding Lamin A/C. *Am. J. Hum. Genet.* 71 (2), 426–431. doi:10.1086/341908
- Oliveira, J., Freitas, P., Lau, E., and Carvalho, D. (2016). Barraquer-Simons Syndrome: a Rare Form of Acquired Lipodystrophy. *BMC Res. Notes* 9, 175. doi:10.1186/s13104-016-1975-9
- Onal, G., Kutlu, O., Gozuacik, D., and Dokmeci Emre, S. (2017). Lipid Droplets in Health and Disease. *Lipids Health Dis.* 16 (1), 128. doi:10.1186/s12944-017-0521-7
- Onishi, Y., Higuchi, J., Ogawa, T., Namekawa, A., Hayashi, H., Odakura, H., et al. (2002). The First Japanese Case of Autosomal Dominant Emery-Dreifuss Muscular Dystrophy with a Novel Mutation in the Lamin A/C Gene. *Rinsho Shinkeigaku* 42 (2), 140–144.
- Oral, E. A., Gorden, P., Cochran, E., Araújo-Vilar, D., Savage, D. B., Long, A., et al. (2019). Long-term Effectiveness and Safety of Metreleptin in the Treatment of Patients with Partial Lipodystrophy. *Endocrine* 64 (3), 500–511. doi:10.1007/s12020-019-01862-8
- Östlund, C., Hernandez-Ono, A., and Shin, J. Y. (2020). The Nuclear Envelope in Lipid Metabolism and Pathogenesis of NAFLD. *Biology (Basel)* 9 (10), 338. doi:10.3390/biology9100338
- Özen, S., Akıncı, B., and Oral, E. A. (2020). Current Diagnosis, Treatment and Clinical Challenges in the Management of Lipodystrophy Syndromes in Children and Young People. *J. Clin. Res. Pediatr. Endocrinol.* 12 (1), 17–28. doi:10.4274/jcrpe.galenos.2019.2019.0124
- Padiath, Q. S. (2019). Autosomal Dominant Leukodystrophy: A Disease of the Nuclear Lamina. *Front. Cel. Dev. Biol.* 7, 41. doi:10.3389/fcell.2019.00041
- Padiath, Q. S., and Fu, Y. H. (2010). Autosomal Dominant Leukodystrophy Caused by Lamin B1 Duplications a Clinical and Molecular Case Study of Altered Nuclear Function and Disease. *Methods Cel Biol* 98, 337–357. doi:10.1016/S0091-679X(10)98014-X
- Park, Y. E., Hayashi, Y. K., Bonne, G., Arimura, T., Noguchi, S., Nonaka, I., et al. (2009). Autophagic Degradation of Nuclear Components in Mammalian Cells. *Autophagy* 5 (6), 795–804. doi:10.4161/auto.8901
- Pichler, A., Fatouros, C., Lee, H., and Eisenhardt, N. (2017). SUMO Conjugation - a Mechanistic View. *Biomol. Concepts* 8 (1), 13–36. doi:10.1515/bmc-2016-0030
- Porcu, M., Corda, M., Pasqualucci, D., Binaghi, G., Sanna, N., Matta, G., et al. (2021). A Very Long-Term Observation of a Family with Dilated Cardiomyopathy and Overlapping Phenotype from Lamin A/C Mutation. *J. Cardiovasc. Med. (Hagerstown)* 22 (1), 53–58. doi:10.2459/JCM.0000000000001060
- Povlsen, L. K., Beli, P., Wagner, S. A., Poulsen, S. L., Sylvestersen, K. B., Poulsen, J. W., et al. (2012). Systems-wide Analysis of Ubiquitylation Dynamics Reveals a Key Role for PAF15 Ubiquitylation in DNA-Damage Bypass. *Nat. Cel Biol* 14 (10), 1089–1098. doi:10.1038/ncb2579
- Rahman, M. A., Mostofa, M. G., and Ushimaru, T. (2018). The Nem1/Spo7-Pah1/lipin axis Is Required for Autophagy Induction after TORC1 Inactivation. *FEBS J.* 285 (10), 1840–1860. doi:10.1111/febs.14448
- Rajoria, K., Singh, S. K., and Dadhich, S. (2021). Ayurvedic Management in Limb Girdle Muscular Dystrophy - A Case Report. *J. Ayurveda Integr. Med.* 13, 100486. doi:10.1016/j.jaim.2021.07.002
- Rao, R. A., Ketkar, A. A., Kedia, N., Krishnamoorthy, V. K., Lakshmanan, V., Kumar, P., et al. (2019). KMT1 Family Methyltransferases Regulate Heterochromatin-Nuclear Periphery Tethering via Histone and Non-histone Protein Methylation. *EMBO Rep.* 20 (5), e43260. doi:10.15252/embr.201643260
- Reichart, B., Klafke, R., Dreger, C., Krüger, E., Motsch, I., Ewald, A., et al. (2004). Expression and Localization of Nuclear Proteins in Autosomal-Dominant Emery-Dreifuss Muscular Dystrophy with LMNA R377H Mutation. *BMC Cel Biol* 5, 12. doi:10.1186/1471-2121-5-12
- Rolyan, H., Tyurina, Y. Y., Hernandez, M., Amoscatto, A. A., Sparvero, L. J., Nmezi, B. C., et al. (2015). Defects of Lipid Synthesis Are Linked to the Age-dependent Demyelination Caused by Lamin B1 Overexpression. *J. Neurosci.* 35 (34), 12002–12017. doi:10.1523/JNEUROSCI.1668-15.2015
- Rossi, M. L., Ghosh, A. K., and Bohr, V. A. (2010). Roles of Werner Syndrome Protein in protection of Genome Integrity. *DNA Repair (Amst)* 9 (3), 331–344. doi:10.1016/j.dnarep.2009.12.011
- Ruiz de Eguino, G., Infante, A., Schlangen, K., Aransay, A. M., Fullaondo, A., Soriano, M., et al. (2012). Sp1 Transcription Factor Interaction with Accumulated Prelamin a Impairs Adipose Lineage Differentiation in Human Mesenchymal Stem Cells: Essential Role of Sp1 in the Integrity of Lipid Vesicles. *Stem Cell Transl Med* 1 (4), 309–321. doi:10.5966/sctm.2011-0010
- Sayed, N., Liu, C., Ameen, M., Himmati, F., Zhang, J. Z., Khanamiri, S., et al. (2020). Clinical Trial in a Dish Using iPSCs Shows Lovastatin Improves Endothelial Dysfunction and Cellular Cross-Talk in LMNA Cardiomyopathy. *Sci. Transl Med.* 12 (554), eaax9276. doi:10.1126/scitranslmed.aax9276
- Schaffer, J. E. (2016). Lipotoxicity: Many Roads to Cell Dysfunction and Cell Death: Introduction to a Thematic Review Series. *J. Lipid Res.* 57 (8), 1327–1328. doi:10.1194/jlr.E069880
- Shin, D. W. (2020). Lipophagy: Molecular Mechanisms and Implications in Metabolic Disorders. *Mol. Cell* 43 (8), 686–693. doi:10.14348/molcells.2020.0046
- Simon, D. N., Domaradzki, T., Hofmann, W. A., and Wilson, K. L. (2013). Lamin A Tail Modification by SUMO1 Is Disrupted by Familial Partial Lipodystrophy-Causing Mutations. *Mol. Biol. Cel* 24 (3), 342–350. doi:10.1091/mbc.E12-07-0527
- Simon, D. N., Wriston, A., Fan, Q., Shabanowitz, J., Florwick, A., Dharmaraj, T., et al. (2018). OGT (O-GlcNAc Transferase) Selectively Modifies Multiple Residues Unique to Lamin A. *Cells* 7 (5). doi:10.3390/cells7050044
- Singh, R., and Cuervo, A. M. (2012). Lipophagy: Connecting Autophagy and Lipid Metabolism. *Int. J. Cel Biol* 2012, 282041. doi:10.1155/2012/282041
- Snider, N. T., and Omary, M. B. (2014). Post-translational Modifications of Intermediate Filament Proteins: Mechanisms and Functions. *Nat. Rev. Mol. Cel Biol* 15 (3), 163–177. doi:10.1038/nrm3753
- Stiekema, M., van Zandvoort, M. A. M. J., Ramaekers, F. C. S., and Broers, J. L. V. (2020). Structural and Mechanical Aberrations of the Nuclear Lamina in Disease. *Cells* 9 (8). doi:10.3390/cells9081884
- Takamori, Y., Hirahara, Y., Wakabayashi, T., Mori, T., Koike, T., Kataoka, Y., et al. (2018). Differential Expression of Nuclear Lamin Subtypes in the Neural Cells of the Adult Rat Cerebral Cortex. *IBRO Rep.* 5, 99–109. doi:10.1016/j.ibror.2018.11.001
- Tchang, B. G., Shukla, A. P., and Aronne, L. J. (2015). Metreleptin and Generalized Lipodystrophy and Evolving Therapeutic Perspectives. *Expert Opin. Biol. Ther.* 15 (7), 1061–1075. doi:10.1517/14712598.2015.1052789
- Tu, Y., Sánchez-Iglesias, S., Araújo-Vilar, D., Fong, L. G., and Young, S. G. (2016). LMNA Missense Mutations Causing Familial Partial Lipodystrophy Do Not lead to an Accumulation of Prelamin A. *Nucleus* 7 (5), 512–521. doi:10.1080/19491034.2016.1242542
- Verstraeten, V. L., Renes, J., Ramaekers, F. C., Kamps, M., Kuijpers, H. J., Verheyen, F., et al. (2011). Reorganization of the Nuclear Lamina and Cytoskeleton in Adipogenesis. *Histochem. Cel Biol* 135 (3), 251–261. doi:10.1007/s00418-011-0792-4
- Villa, P., Kaufmann, S. H., and Earnshaw, W. C. (1997). Caspases and Caspase Inhibitors. *Trends Biochem. Sci.* 22 (10), 388–393. doi:10.1016/s0968-0004(97)01107-9
- Wagner, S. A., Beli, P., Weinert, B. T., Nielsen, M. L., Cox, J., Mann, M., et al. (2011). A Proteome-wide, Quantitative Survey of *In Vivo* Ubiquitylation Sites Reveals Widespread Regulatory Roles. *Mol. Cel Proteomics* 10 (10), M111–M013284. doi:10.1074/mcp.M111.013284
- Wang, C. W. (2016). Lipid Droplets, Lipophagy, and beyond. *Biochim. Biophys. Acta* 1861 (8 Pt B), 793–805. doi:10.1016/j.bbalip.2015.12.010
- Wang, L. R., Radonjic, A., Dillio, A. A., McIntyre, A. D., and Hegele, R. A. (2018). A De Novo POLD1 Mutation Associated with Mandibular Hypoplasia, Deafness, Progeroid Features, and Lipodystrophy Syndrome in a Family with Werner Syndrome. *J. Investig. Med. High Impact Case Rep.* 6, 2324709618786770. doi:10.1177/2324709618786770
- Wang, S., Huang, X., Sun, D., Xin, X., Pan, Q., Peng, S., et al. (2012). Extensive Crosstalk between O-GlcNAcylation and Phosphorylation Regulates Akt Signaling. *PLoS One* 7 (5), e37427. doi:10.1371/journal.pone.0037427
- Weber, K., Plessmann, U., and Traub, P. (1989). Maturation of Nuclear Lamin A Involves a Specific Carboxy-Terminal Trimming, Which Removes the Polyisoprenylation Site from the Precursor; Implications for the Structure of the Nuclear Lamina. *FEBS Lett.* 257 (2), 411–414. doi:10.1016/0014-5793(89)81584-4
- Weinert, B. T., Schölz, C., Wagner, S. A., Iesmantavicius, V., Su, D., Daniel, J. A., et al. (2013). Lysine Succinylation Is a Frequently Occurring Modification in

- Prokaryotes and Eukaryotes and Extensively Overlaps with Acetylation. *Cell Rep* 4 (4), 842–851. doi:10.1016/j.celrep.2013.07.024
- Winter-Vann, A. M., and Casey, P. J. (2005). Post-prenylation-processing Enzymes as New Targets in Oncogenesis. *Nat. Rev. Cancer* 5 (5), 405–412. doi:10.1038/nrc1612
- Yan, J., Xie, Y., Si, J., Gan, L., Li, H., Sun, C., et al. (2021). Crosstalk of the Caspase Family and Mammalian Target of Rapamycin Signaling. *Ijms* 22 (2), 817. doi:10.3390/ijms22020817
- Zechner, R., Madeo, F., and Kratky, D. (2017). Cytosolic Lipolysis and Lipophagy: Two Sides of the Same coin. *Nat. Rev. Mol. Cel Biol* 18 (11), 671–684. doi:10.1038/nrm.2017.76
- Zeng, M., Liu, W., Hu, Y., and Fu, N. (2020). Sumoylation in Liver Disease. *Clin. Chim. Acta* 510, 347–353. doi:10.1016/j.cca.2020.07.044
- Zhang, E., Lu, X., Yin, S., Yan, M., Lu, S., Fan, L., et al. (2019). The Functional Role of Bax/Bak in Palmitate-Induced Lipoapoptosis. *Food Chem. Toxicol.* 123, 268–274. doi:10.1016/j.fct.2018.11.011

Conflict of Interest: The authors declare that the research was conducted in the absence of any commercial or financial relationships that could be construed as a potential conflict of interest.

Publisher's Note: All claims expressed in this article are solely those of the authors and do not necessarily represent those of their affiliated organizations, or those of the publisher, the editors and the reviewers. Any product that may be evaluated in this article, or claim that may be made by its manufacturer, is not guaranteed or endorsed by the publisher.

Copyright © 2022 Peng, Tang, Xiao and Fu. This is an open-access article distributed under the terms of the Creative Commons Attribution License (CC BY). The use, distribution or reproduction in other forums is permitted, provided the original author(s) and the copyright owner(s) are credited and that the original publication in this journal is cited, in accordance with accepted academic practice. No use, distribution or reproduction is permitted which does not comply with these terms.

GLOSSARY

ADLD autosomal dominant leukodystrophy

AD-EDMD autosomal dominant form of Emery–Dreifuss muscular dystrophy

APL acquired partial lipodystrophy

ATGL adipose triglyceride lipase

BSS Barraquer–Simons syndrome

CDKN2A cyclin-dependent kinase inhibitor 2A

CNS central nervous system

CMs cardiomyocytes

DM diabetes mellitus

DCM dilated cardiomyopathy

ECs endothelial cells

EDMD Emery–Dreifuss muscular dystrophy

ERK extracellular regulated protein kinase

GH growth hormone

HSL hormone-sensitive lipase

hMSC human mesenchymal stem cell

HGPS Hutchinson–Gilford progeria syndrome

IFS intermediate filaggrin

INM inner nuclear membrane

JAK2 Janus kinase 2

LGMD limb girdle muscular dystrophy

LGMD1B limb girdle muscular dystrophy type 1b

LD lipid droplet

LBR lamin B receptor

MADA type A mandibuloacral dysplasia

MADB type B mandibuloacral dysplasia

MAD mandibular sacral dysplasia

MAFLD metabolic associated fatty liver disease

MD muscular dystrophy

MGL monoglycerol lipase

NLS nuclear localization signal

NVJ nuclear vacuolar junction

ONM outer nuclear membrane

OE overexpression

PPAR gamma peroxisome proliferator activated receptor gamma

PI protease inhibitor

PTMs post-translational modification

SUMOylation small ubiquitin-like modifier

Stat5 transcription activator

SREBP1 cholesterol regulatory element binding protein 1

WS Werner syndrome

ZMPSTE24 zinc metalloproteinase



Pharmacological Effects and Molecular Protective Mechanisms of Astragalus Polysaccharides on Nonalcoholic Fatty Liver Disease

Jing Zhang and Quansheng Feng*

College of Basic Medicine, Chengdu University of Traditional Chinese Medicine, Chengdu, China

OPEN ACCESS

Edited by:

Francisco Javier Cubero,
Complutense University of Madrid,
Spain

Reviewed by:

Hyeon-Geug Kim,
Indiana University, United States
Xiu Zhou,
Wuyi University, China

*Correspondence:

Quansheng Feng
fengqs118@163.com

Specialty section:

This article was submitted to
Gastrointestinal and Hepatic
Pharmacology,
a section of the journal
Frontiers in Pharmacology

Received: 14 January 2022

Accepted: 07 February 2022

Published: 03 March 2022

Citation:

Zhang J and Feng Q (2022)
Pharmacological Effects and Molecular
Protective Mechanisms of Astragalus
Polysaccharides on Nonalcoholic Fatty
Liver Disease.
Front. Pharmacol. 13:854674.
doi: 10.3389/fphar.2022.854674

Nonalcoholic fatty liver disease (NAFLD) has been renamed metabolic dysfunction-associated fatty liver disease (MAFLD), a condition for which there is now no authorized treatment. The search for new medications to treat MAFLD made from natural substances is gaining traction. The function of anti-oxidant, anti-inflammation, hypoglycaemic, antiviral, hypolipidemic, and immunomodulatory actions of Astragalus polysaccharides (APS), a chemical molecule isolated from Astragalus membranaceus, has become the focus of therapeutic attention. We have a large number of papers on the pharmacological effects of APS on NAFLD that have never been systematically reviewed before. According to our findings, APS may help to slow the progression of non-alcoholic fatty liver disease (NAFL) to non-alcoholic steatohepatitis (NASH). Lipid metabolism, insulin resistance (IR), oxidative stress (OS), endoplasmic reticulum stress (ERS), inflammation, fibrosis, autophagy, and apoptosis are some of the pathogenic pathways involved. SIRT1/PPAR α /FGF21, PI3K/AKT/IRS-1, AMPK/ACC, mTOR/4EBP-1/S6K1, GRP78/IRE-1/JNK, AMPK/PGC-1/NRF1, TLR4/MyD88/NF- κ B, and TGF- β /Smad pathways were the most common molecular protective mechanisms. All of the information presented in this review suggests that APS is a natural medication with a lot of promise for NAFLD, but more study, bioavailability studies, medicine type and dosage, and clinical proof are needed. This review could be useful for basic research, pharmacological development, and therapeutic applications of APS in the management of MAFLD.

Keywords: astragalus polysaccharides, metabolic dysfunction-associated fatty liver disease, nonalcoholic fatty liver disease, lipid metabolism, insulin resistance, inflammation, oxidative stress, endoplasmic reticulum stress

1 INTRODUCTION

In addition to being caused by alcohol and other definitive factors, metabolic dysfunction-associated fatty liver disease, formerly known as nonalcoholic fatty liver disease (NAFLD) (Eslam et al., 2020a; Eslam et al., 2020b), is a clinical-pathological syndrome characterized by steatosis of hepatic parenchymal cells and inflammation in the liver lobes linked to insulin resistance and hereditary predisposition. It is further divided into non-alcoholic fatty liver disease (NAFL) and non-alcoholic steatohepatitis (NASH) based on liver histological changes (Ratzliff et al., 2010; Younossi et al., 2018; Eslam et al., 2020b). The related pathogenic process is complex and cascaded-connected, as the “two-hit” theory suggests (Friedman et al., 2018). Fat buildup in the liver is the first essential step in the development of NAFLD. The second hit from NAFL to NASH is triggered by inflammatory

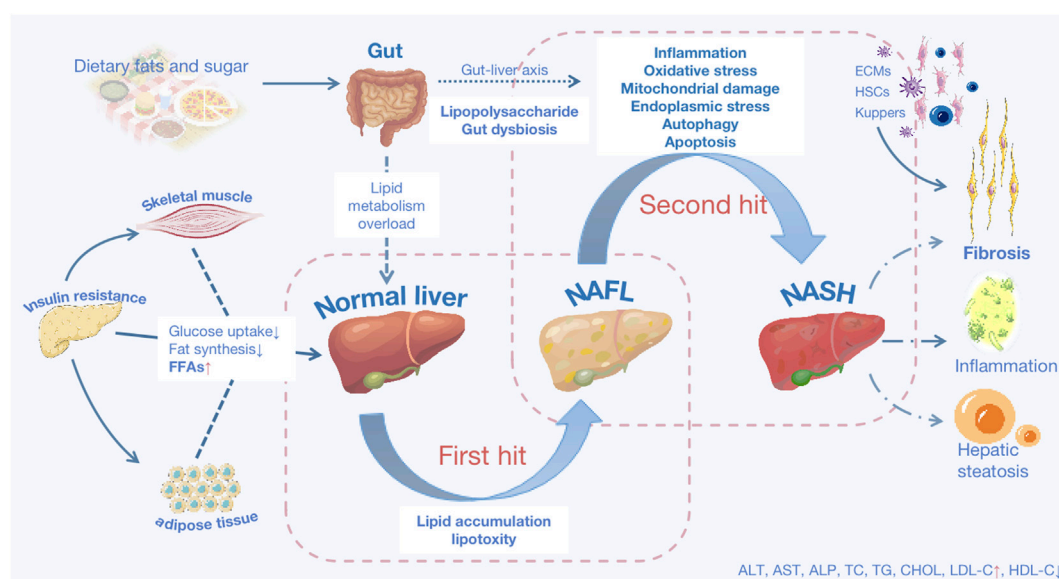


FIGURE 1 | The basic pathological mechanisms of NAFLD. NAFLD is characterized as either non-alcoholic fatty liver disease (NAFL) or non-alcoholic steatohepatitis (NASH) predicated on histological characteristics. Lipid accumulation (LA) is the first hit, and with that lipotoxicity triggered, mainly results from three sources: increased visceral adipose tissue lipolysis, hepatic *de novo* lipid (DNL) production activation, and excessive fat and calorie intake from diets. Insulin resistance, visceral adiposity, and atherogenic are all linked to aberrant LA. Deficient insulin sensitivity in adipose tissue and skeletal muscle, resulting in decreased fat synthesis and glucose uptake, an increase in the quantity of free fatty acids (FFAs) in the blood. FFAs enter the liver as a result of metabolic overload, which is the primary site of fat production. Oxidative stress, endoplasmic reticulum stress, mitochondrial damage, inflammatory reactions, fibrosis, and other factors all contribute to the second hit. Excessive deposition of extracellular matrix (ECM), activation of hepatic stellate cells (HSCs) and kupffer cells contribute to fibrosis in long-term chronic inflammatory reactions. Steatosis causes autophagy and apoptosis in hepatocytes. AST: aspartate transaminase; ALT: alanine aminotransferase; ALP: alkaline phosphatase; TC: total cholesterol; TG: triacylglycerol; CHOL: cholesterol; LDL-C: low-density lipoprotein cholesterol; HDL-C: high-density lipoprotein cholesterol.

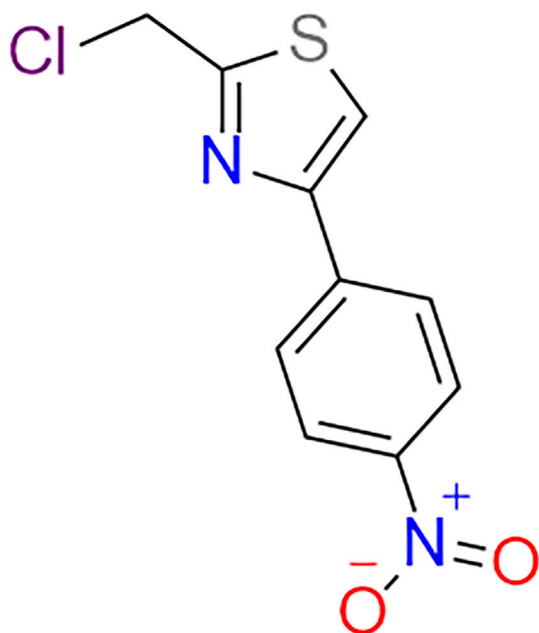


FIGURE 2 | The chemical construction of APS.

reactions, oxidative stress (OS), endoplasmic reticulum (ER) stress, mitochondrial damage, fibrogenesis, and disturbance of the gut flora, among other factors (Pierantonelli and Svegliati-

Baroni, 2019) (As shown in **Figure 1**). NAFLD is the most common chronic liver disease, threatening nearly a quarter of the world's population (Lonardo et al., 2016), and it will progress to cirrhosis and liver cancer in advanced stages, yet there is still no approved medication to treat it. Therefore, research is urgent and high-profile.

Chinese herbal medicine, which is a tremendous treasure trove of human medical development, has indeed demonstrated tangible advantages in the treatment of liver illness. Using contemporary technologies to excavate this treasure trove of potent medicinal components, more and more small-molecule compounds have been discovered from Chinese herbs, such as Flos inulae (Yang et al., 2021), Forsythiaside A (Gong et al., 2021), and Baicalin (Hu et al., 2021). Astragalus membranaceus (AM), also known in China as *Huangqi*, has been used to replenish qi and blood for over two millennia and is suitable for deficiency disorders (Auyeung et al., 2016). Astragalus polysaccharides (2-(Chloromethyl)-4-(4-Nitrophenyl)-1,3-Thiazole, APS) (As shown in **Figure 2**), a key active ingredient isolated from AM that contains over 200 constituents (Guo et al., 2019), has received a lot of attention over the past 2 decades. A slew of recent pharmacology studies has shown its benefits on blood lipids and glucose management, and it has anti-inflammation, anti-oxidative stress, anti-fibrosis, liver protection, anti-tumor, and immunoregulatory capabilities (Qi et al., 2017; Chen et al., 2020), all of which are linked to the pathogenic

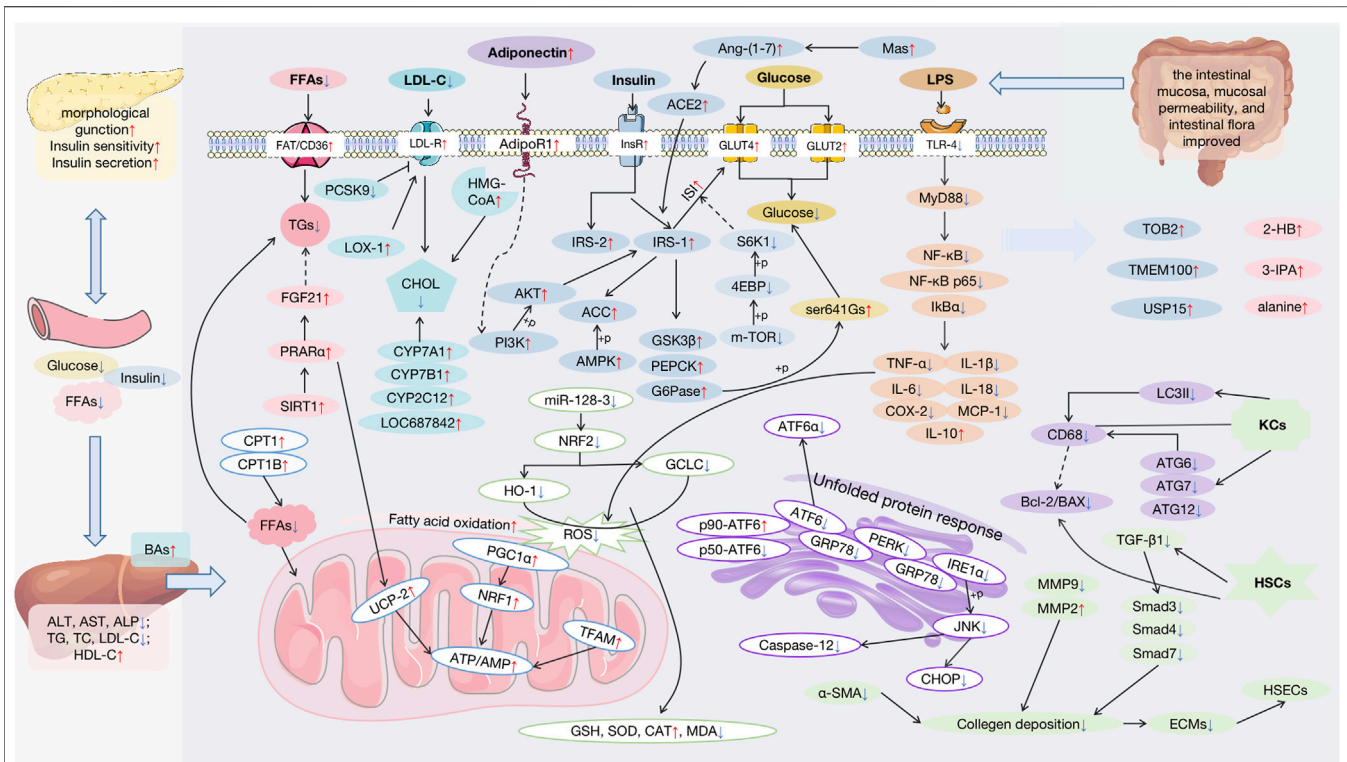


FIGURE 3 | Pharmacological effects and molecular mechanisms of APS against NAFLD. FFAs: free fatty acids; AST: aspartate transaminase; ALT: alanine aminotransferase; ALP: alkaline phosphatase; TG: triglyceride; TC: total cholesterol; LDL-C: low-density lipoprotein cholesterol; HDL-C: high-density lipoprotein cholesterol; BAs: bile acids; FGF21: fibroblast growth factor 21; PPARα: peroxisome proliferator-activated receptor alpha; SIRT1: stimulating the sirtuin 1; CPT1: carnitine palmitoyltransferase 1; LDL-R: low-density lipoprotein receptor; PCSK9: proprotein convertase subtilisin/kexin type; LOX-1: oxidized-LDL receptor-1; CHOL: cholesterol; CYP: cholesterol hydroxylase; HMG-CoA: 3-hydroxy-3-methyl glutaryl coenzyme A reductase; InsR: insulin receptor; Ang-(1-7): angiotensin-(1-7); ACE2: angiotensin-converting enzyme 2; IRS: insulin receptor substrates; ACC: acetyl-CoA carboxylase; AMPK: AMP-activated protein kinase; AKT: protein kinase B; PI3K: the phosphatidylinositol-3 kinase; GSK3β: the glycogen synthase kinase 3beta; PEPCK: the phosphoenolpyruvate carboxyl kinase; G6Pase: the gluconeogenic enzymes glucose 6-phosphatase; S6K1: S6 kinase 1; 4EBP: 4E-binding protein; GRP78: glucose-regulated protein 78; ATF6: transcription factor 6; PERK: protein kinase-like endoplasmic reticulum kinase; IRE1α: inositol-requiring enzyme 1; JNK: the c-Jun N-terminal kinase; CHOP: C/EBP-homologous protein; NRF1: the nuclear factor erythroid 2-like 1; HO-1: heme Oxygenase-1; GCLC: glutamate-cysteine ligase; ROS: reactive oxygen species; PGC1α: the peroxisome proliferator-activated receptor γ coactivator 1; NRF2: nuclear erythroid-derived 2-related factor 2; UCP-2: uncoupling protein 2; TFAM: the mitochondrial transcription factor A; GSH: glutathione; SOD: superoxide dismutase; CAT: peroxidase catalase; MDA: malondialdehyde; LPS: lipopolysaccharide; TLR4: toll-like receptor 4; MyD88: the adaptor protein myeloid differentiation primary response 88; NF-κB: the nuclear factor-kappa B; IκBα: inhibitory kappa B alpha; TNF-α: tumor necrosis factor-alpha; IL-1β: interleukin-1β; IL-6: interleukin-6; IL-18: interleukin-18; COX-2: cyclooxygenase-2; MCP-1: monocyte chemoattractant protein-1; IL-10: interleukin-10; LC3II: protein II light chain 3; ATG: recombinant autophagy-related protein; KCs: hepatic stellate cells; HSCs: hepatic sinusoidal endothelial cells; TGF-β1: transforming growth factor-β1; ECM: extracellular matrix; TOB2: transducer of ErbB2.2; USP15: the ubiquitin-specific proteases 15; 2-HB: 2-hemoglobin; 3-IPA: 3-indolepropionic acid.

mechanism of NAFLD. These NAFLD pathogenic processes are interconnected, promote each other, and share underlying mediators and pathways.

Multi-components, multi-targets, and multi-pathways all seem to be advantages for Chinese medicine. Obtained from experimental evidence on APS and the complex pathophysiology of NAFLD, we assume the potential efficacy of APS for NAFLD. A complete assessment of pharmacological data, particularly on molecular protective mechanisms, is required to stimulate further study and to understand the potential of this medicine; consequently, we wrote this work to encourage further exploration and understanding of its potential.

In this work we intend to provide a complete review of APS's pharmacological effects and advancements in molecular mechanism works of literature in NAFLD. The flaws in

existing development research are also explored, as well as prospective study directions.

2 PHARMACOLOGICAL EFFECTS AND MOLECULAR MECHANISMS OF ASTRAGALUS POLYSACCHARIDES AGAINST NONALCOHOLIC FATTY LIVER DISEASE

A plethora of research indicates that APS appear to be effective on NAFLD. (As shown in **Supplementary Table S1**). Serum aspartate transaminase, alanine aminotransferase, and alkaline phosphatase, which indicate liver injury, were all reversed in the

study (Hamid et al., 2017a; Hamid et al., 2017b; Sun et al., 2019). Through various mechanisms, APS may exert liver-protecting functions, including improving insulin resistance (IR) and lipid metabolism; inhibiting OS, ER, and mitochondrial injury; providing anti-inflammatory and anti-fibrosis functions; and regulating autophagy and apoptosis, and the main targets modulated by APS are shown in **Figure 3**.

2.1 Lipid Metabolism

The first crucial step in the development of NAFLD is lipids-aberrant accumulation in the liver. Triglycerides (TGs), phospholipids, glycolipids, cholesterol (CHOL), and cholesterol ester are lipids that are part of the cell structure and play a role in cellular homeostasis, cell-cell interaction, and inflammation and immune modulation (Marra and Svegliati-Baroni, 2018). Fatty liver accumulation is caused by a lipid deposition and removal imbalance to toxic lipids species including TGs, free fatty acids (FFAs), lysophosphatidylcholine, ceramides, and free cholesterol (Fch), which results in lipotoxicity and glucotoxicity (Marchesini et al., 2016; Marra and Svegliati-Baroni, 2018; Régnier et al., 2019).

APS could inhibit the synthesis and accumulation of TGs by regulating the transport and breakdown of FFAs (Mao and Ouyang, 2007; Song et al., 2014). FFAs determine the synthesis of TGs, and APS could increase the FA translocator/receptor FAT/CD36 to promote this synthesis (Song et al., 2014). Meanwhile, carnitine palmitoyltransferase 1 (CPT1) and fatty acid oxidation rate-limiting enzyme gene CPT1B increased (Cui et al., 2015b), which helped increase FFA decomposition as a rate-limiting enzyme of long-chain FFAs entering the human mitochondrial inner membrane to speed up the fatty acid oxidation process.

APS may also play a role in the synthesis, catalysis, and metabolism of CHOL. Total cholesterol, Fch, and low-density lipoprotein (LDL) cholesterol levels fell after APS intervention (Cui et al., 2015a; Yan Y. et al., 2020; Wang and Sun, 2021), while high-density lipoprotein (HDL) cholesterol levels increased to move CHOL out (Chen et al., 2018; Cai et al., 2020). The LDL receptor pathway is responsible for the breakdown of LDL, which is a cholesterol-rich lipoprotein. APS could reduce proprotein convertase subtilisin/kexin type 9 (PCSK9) levels via the PPAR- β/γ pathway to increase the expression of low-density lipoprotein receptors (LDL-R) to reduce lipid deposition (Zou, 2016; Sabatine, 2019), and oxidized-LDL receptor-1 (LOX-1) increased to improve lipid disorder (Cui et al., 2015b). It is reported PCSK9 also has a mutually beneficial interaction with LOX-1 and induces the secretion of pro-inflammation cytokines by regulating toll-like receptor 4 (TLR4) expression and NF- κ B activation (Ding et al., 2020). It is thought that viscous polysaccharides can lower cholesterol and bile acids (BAs) absorption, which is restricted by APS (Cheng et al., 2011; Cui et al., 2015b; Sun et al., 2019). By inhibiting 3-hydroxy-3-methyl glutaryl-coenzyme A reductase, a rate-limiting enzyme in hepatocyte cholesterol synthesis catalyzing the creation of mevalonic acid, APS may lower CHOL synthesis (Cheng, 2010). To enhance BAs secretion, APS could stimulate the expression of cytochrome P450 (CYP) enzymes such as

cholesterol 7-hydroxylase (CYP7A1), cholesterol 7-hydroxylase (CYP7B1), CYP2C12, and LOC687842 (Cheng, 2010; Cheng et al., 2011; Cui et al., 2015b). The alternate pathway to BAs begins with the 27-hydroxylation of cholesterol as the initial step in the liver or extrahepatic tissues, followed by CYP7B1-dependent oxidation in the 7-position (Leoni and Caccia, 2011; Kakiyama et al., 2020). CYP7A1 could transfer cholesterol to HDL particles, which are then returned to the liver for conversion into BAs. CYP2C12 and LOC687842 belong to the family of cytochrome P450 as short hairpin RNA, which participate in the metabolism of the linoleic acid pathway (Elfaki et al., 2018).

By stimulating the sirtuin 1 (SIRT1)/peroxisome proliferator-activated receptor alpha (PPAR α)/Fibroblast growth factor 21 (FGF21) pathway, APS could alleviate lipid metabolism disorder, notably, by increasing hepatic glycolipid metabolism, reducing inflammation, and lipid droplet deposition (Gu et al., 2015). PPAR α is mainly involved in the catabolism of hepatic lipids and bile acids metabolism, fatty acid uptake, and activation, which affects intracellular fatty acid-binding and mitochondrial fatty acid oxidation (Burri et al., 2010). FGF21 and SIRT1 interact with PPAR α to regulate hepatic glycolipid metabolism, OS, and inflammation and may serve as a biological target in NAFLD to improve IR (Ding et al., 2017).

Furthermore, Li et al. discovered the three following distinct metabolites in the APS treatment group and high-fat diet model mice: 3-indole propionic acid, 2-hemoglobin, and alanine, which may ameliorate lipid droplets, but there is no further evidence to support its exact mechanism (Li et al., 2019).

2.2 Insulin Resistance

Insulin sensitivity in muscle and adipose tissue declines in the IR state, glucose delivery to these tissues decreases, and FFAs are liberated into the systemic circulation. To compensate for high blood glucose (BG) levels, pancreatic beta cells release more insulin, resulting in hyperinsulinemia. Despite being primarily insulin-sensitive and being exposed to high concentrations of BG, TGs, FFAs, and insulin, the liver enters a hyper-anabolic state when it continues to generate and store lipids, all of which is improved by APS (Gu et al., 2015; He et al., 2016). APS may help injured islets regain their morphological function and maintain a balance of normal insulin output and compensatory insulin secretion (Gu et al., 2015; Hong et al., 2020; Liu et al., 2020).

APS may increase ISI by stimulating the phosphorylation of insulin receptor substrates (IRS) and aiding the transit of glucose transporters (GLUTs) from the nucleus to the cell membrane, promoting glucose transfer and boosting insulin utilization (Zou et al., 2009; Sun, 2012; Ye et al., 2014; Sun et al., 2019). Insulin insufficiency is characterized by a lack of receptors and a reduction in GLUTs. APS may phosphorylate IRS-1 by the phosphatidylinositol-3 kinase (PI3K)/protein kinase B (PKB, also known as Akt) signal pathway to promote the activation of the AMPK/acetyl-CoA carboxylase (ACC) pathway and its downstream targets, glycogen synthase kinase 3 β (GSK3 β), phosphoenolpyruvate carboxyl kinase (PEPCK), and gluconeogenic enzymes glucose 6-phosphatase (G6Pase) phosphorylation, to improve glucose metabolism (Sun et al.,

2019). The metabolic function of insulin is mainly achieved through the PI3K signal pathway, which binds to the insulin receptor to phosphorylate IRS, leading to Akt phosphorylation; it exerts the biological effects of insulin to promote glucose uptake and glucose homeostasis in the liver. PEPCK and G6Pase regulate gluconeogenesis (Liu Q. et al., 2017), GSK3 β could inhibit glycogen synthesis, and the synthesis also reduced results from ser641GS phosphorylation activated by APS (Zou et al., 2007). AMPK is the main energy sensor that regulates the dynamic balance of ATP/AMP levels up-regulated and phosphorylated by APS (Zou et al., 2009; Zou, 2010; Sun et al., 2019). Lipoglycometabolism, insulin sensitivity, and plasma glucose regulation are all dependent on it (Smith et al., 2016). APS might boost IRS-1 and Akt phosphorylation, triggering the PI3k signal transduction pathway to improve ISI by activating the angiotensin-converting enzyme 2-Ang-(1–7)-Mas axis and inhibiting the mTOR/4E-binding protein 1 (4EBP-1)/S6 kinase 1 (S6K1) signaling pathway (Simanshu et al., 2017; Santos et al., 2018; Ma et al., 2019; Sun et al., 2019); excessive intake of energy or insulin resistance causes overexpression of mTOR, which activates 4EBP-1 and S6K1 phosphorylation. APS promote glucose synthesis by activating GLUT4 and GLUT2 translocation to improve ISI. GLUT4 and GLUT2 are sorted and retained intracellularly, and they dynamically redistribute to the plasma membrane by insulin-regulated vesicular traffic (Thorens, 2015; Jaldin-Fincati et al., 2017). APS could also promote adiponectin secretion to activate the downstream PI3K/Akt/IRS-1 pathway by increasing its receptor AdipoR1 levels (Sun et al., 2019). Changes in morbid adipose tissue in endocrine characteristics could decrease adiponectin secretion, which is an insulin enhancer (Hamid et al., 2017a).

Metabolomics revealed that APS could strengthen ISI by upregulating the mi-RNA transducer of ErbB2.2, TMEM100, and the ubiquitin-specific proteases (USP15) (Liu et al., 2020). There is no direct evidence on IR about the mi-RNAs, but they all affect inflammation, which may influence ISI indirectly (Pan et al., 2019; Jiang et al., 2020; Das et al., 2021). Studies have shown that both the let-7 family and miR-103 can modulate ISI in the liver, and both are the target genes of TMEM100 and USP15, which may explain why APS improve IR (Chakraborty et al., 2014; Liu et al., 2020). However, more experimental validation is required.

2.3 Oxidative Stress, Endoplasmic Reticulum, and Mitochondrial Injury

In NASH patients, studies revealed a positive relationship between OS levels and IR severity, fat degeneration, inflammatory response, and fibrosis (Tariq et al., 2014). ROS are produced primarily by mitochondrial failure, ER stress, particulates, and peroxidase oxidation (Scherz-Shouval and Elazar, 2007; Forrester et al., 2018; Das et al., 2021), all of which are reduced by APS to alleviate liver injury (Wang, 2016). The increased input of fatty acids and oxidation in mitochondria, on the other hand, is a primary source of ROS in NAFLD (Forrester et al., 2018).

2.3.1 Oxidative Stress

OS is a balance between free oxygen radical generation and antioxidant protection (Forrester et al., 2018). Studies have shown APS could regulate the levels of the final products of membrane lipid peroxidation malondialdehyde (MDA), antioxidant metal enzyme superoxide dismutase (SOD), and redox agent glutathione (GSH), which are OS damage indicators and clear the content of hydroxyl free radicals and superoxide anions (Tong et al., 2006; Wang et al., 2015; Wang X. et al., 2016; Yang, 2017; Yuan et al., 2018), both of which are common free oxygen radicals with lipotoxicity (Mota et al., 2016).

APS could activate the nuclear erythroid-derived 2-related factor 2 (NRF2) pathway and its downstream protein glutamate-cysteine ligase and heme oxygenase-1 (HO-1) to anticipate anti-oxidative stress, reversing the marker enzyme of peroxidase catalase, MDA, SOD, and GSH-Px after suffering OS damage (Yan Y. et al., 2020; Qu et al., 2020). NRF2 is a determinant regulating the transcription of antioxidant enzyme lines, which could regulate the expression of more than 100 genes (Wang et al., 2019). Yuan et al. showed that APS regulate the NRF2 pathway, which might be dependent on inhibiting miR-128-3 that can regulate the level of antioxidant enzymes and play a therapeutic role in hyperlipidemia by *in vivo* and *in vitro* experiments (Yuan et al., 2018).

2.3.2 Endoplasmic Reticulum Stress

ER is the main cellular compartment involved in secretory and transmembrane protein productive folding, lipid biogenesis, and calcium homeostasis (Lebeaupin et al., 2018). With the occurrence of abnormal glycolipid metabolism, cells activate unfolded proteins in response to misfolded and unfolded protein aggregation and calcium balance in the ER, and misfolded proteins induce ROS generation while OS disturbs the ER redox state, thereby breaking the correct disulfide bond formation and proper protein foldin (Wang J. et al., 2016).

APS improve ER and the resulting autophagy by inhibiting the ATF6 passage and glucose-regulated protein 78 (GRP78)-related pathways [including IRE-1 α , the c-Jun N-terminal kinase (JNK), and PERK], reducing the apoptosis factors expression of C/EBP-homologous protein and caspase-12 (Wang et al., 2009; Hu et al., 2010; Wei et al., 2018). Under ER stress, partner GRP78 binds to unfolded protein, releasing the following three transmembrane receptors: inositol-requiring enzyme 1 (IRE-1 α), protein kinase-like endoplasmic reticulum kinase (PERK), and activating transcription factor 6 α , allowing their signaling pathways to be activated. The dephosphorylation of PERK and IRE1 could be initiated by APS and suppress p50-ATF6 and activate p90-ATF6 to improve ER and recover glucose homeostasis (Wang et al., 2007; Wang et al., 2009).

2.3.3 Mitochondrial Injury

Increased fatty acid oxidation and lipotoxicity in NASH are principal drivers of mitochondrial deterioration (Schuppan et al., 2018). The liver adapts to the influx of excess fatty acids caused by liver lipid deposition, increasing mitochondrial β oxidation and the number of mitochondria. It is not only a

direct reaction to fatty acids but also an activation of lipid cytokines caused by IR and increasing PPAR- α activation levels, which is inhibited by APS as shown earlier. NAFLD patients show a rise in pro-inflammation cytokine TNF- α levels. Remarkably, APS may reduce TNF- α levels while inhibiting the expression of PPAR- α (Chen et al., 2017).

By stimulating the expression of uncoupling protein 2, APS could improve liver energy metabolism disorders and limit the production of ROS, up-regulating ATP enzyme activity (Gu et al., 2015; Kan, 2018). UCPs are proteins that exist on the inner membrane of mitochondria, limiting the production of ROS by mitochondria, and protecting cells from oxidative damage caused by mitochondrial respiration (Toda and Diano, 2014). High levels of UCPs may lead to high levels of protein leakage and uncoupling of substrate oxidation from ADP phosphorylation, thereby limiting ATP synthesis and energy loss (Demine et al., 2019).

Besides, APS may promote mitochondrial biogenesis through the AMPK-mediated peroxisome proliferator-activated receptor γ coactivator 1 (PGC-1 α)/nuclear factor erythroid 2-like 1 (NRF1) signaling pathway, up-regulating the mitochondrial transcription factor A level to improve mitochondrial oxidative phosphorylation levels and boost mitochondrial function and mitochondrial DNA replication (Cheng et al., 2018; Kan, 2018; Kang et al., 2018).

2.4 Inflammation, Fibrosis, Autophagy, and Apoptosis

Long-term repetitive inflammation irritation is an accomplice to the progression of NAFLD, further leading to sustained hepatic fibrogenesis and, ultimately, cirrhosis (Koyama and Brenner, 2017). Apoptotic hepatocytes activate quiescent hepatic stellate cells (HSCs) and Kupffer cells (KCs) that in turn promote inflammation and fibrosis (Brenner et al., 2013). Inflammation, fibrosis, autophagy, and apoptosis as inter-related pathogenesis deteriorate each other in the progression of NAFLD.

2.4.1 Inflammation

Inflammatory damage as a result of the imbalance between pro-inflammatory cytokines and anti-inflammation is triggered by various endogenous or exogenous factors in adipose tissue or the gut, such as lipotoxicity, cells apoptosis, innate immune responses, OS, mitochondrial dysfunction, and ER (Schuster et al., 2018). APS could down-regulate inflammation-related pathway proteins and cytokines *in vitro* and *in vivo*, such as a series of pro-inflammatory cytokines including tumor necrosis factor- α (TNF- α), interleukin-1 β , interleukin-6, interleukin-18, cyclooxygenase-2, and monocyte chemoattractant protein-1 (MCP-1/CCL2), which up-regulate anti-inflammation cytokine interleukin-10 (Cui et al., 2016; Sun et al., 2019; Cai et al., 2020).

By enhancing the intestinal mucosa, mucosal permeability, and intestinal flora, APS protect against endotoxin generated by intestinal bacteria that enter via the portal circulation to activate toll-like receptor-4 signaling in Kupffer cells (Mollazadeh et al.,

2019; Wang and Sun, 2021). The entry of lipopolysaccharide into the liver via the damaged intestinal mucosal barrier stimulates the release of pro-inflammatory cytokines, and the downstream signaling pathways activation of the adaptor protein myeloid differentiation primary response 88 (MyD88) and nuclear factor- κ B (NF- κ B) have been demonstrated to be inhibited in the APS treatment group to alleviate liver steatosis (Zhang et al., 2012); the associated proteins NF- κ B, NF- κ B p65, and inhibitory kappa B α were lowered, as were the regulatory proteins governing innate and adaptive immune responses (Wang et al., 2013; Hamid et al., 2017b; Freitas and Fraga, 2018).

2.4.2 Fibrosis

Hepatic fibrosis develops as a consequence of a chronic, recurrent wound healing process (Schuppan et al., 2018). Cascade responses (such as OS, necrosis, and apoptosis) induced by liver cell damage are intimately linked to inflammation and can serve as a risk indicator for the development of hepatic fibrosis (Koyama and Brenner, 2017; Schuppan et al., 2018). APS inhibit fibrosis formation by inhibiting oxidative stress, apoptosis, and inflammation; enhancing immunity; and preserving the shape and function of sinusoidal and hepatic cells, as well as reducing extracellular matrix (ECM) deposition (Niu et al., 2012; Xu et al., 2012; Zhang, 2012; Li, 2013; Huang et al., 2015).

Hepatic fibrosis is characterized by the deposition of the ECM, a rise in myofibroblasts, and hyperplasia of fibrous tissue. Additionally, pseudolobules occur, which are reversed by APS (Zhang et al., 2009; Qin, 2012; Huang et al., 2015; Zhang et al., 2015). Collagen, proteoglycan, laminin, fibronectin, and matrix cell proteins are all deposited as ECMs. APS may decrease collagen deposition by inhibiting the activation of Kupffer cells and the hyperplasia of HSCs (Qin, 2012; Huang et al., 2015). The activation indicators of HSCs transforming growth factor- β 1 (TNF- β 1), and α -smooth muscle actin were reduced in the presence of APS (Huang et al., 2015; Zhang et al., 2015; Hamid et al., 2017a; Hamid et al., 2017b). Likewise, APS may decrease MMP9 expression and boost MMP2 to maintain a balance between matrix metalloproteinases (MMPs) and their inhibitors, hence promoting ECM deposition. MMP2 and MMP9 are gelatinases that could also cleave type IV collagen and degrade type V, VII, and X collagen, fibronectin, and elastin (Pittayapruek et al., 2016). ECM deposition in the Disse space results in the establishment of endodermis and the loss of fenestration in hepatic sinusoidal endothelial cells (HSECs). APS may increase defenestration of HSECs, sinusoidal capillaries, and liver cells by increasing Young's modulus, the fenestration area, and several SECs (Li, 2013; Yan F. et al., 2020), as well as the hepatic circulation flow rate and perfusion (Tian and Xu, 2008).

APS may act as a regulator of the TGF- β /small mother against the decapentaplegic (Smad) pathway, thereby preserving the basement membrane-like intercellular material seen in normal liver tissue and preventing the development of scar tissue (Huang et al., 2015; Hu et al., 2018). TGF-1, Smad3, Smad4, and Smad7 expressions were all suppressed while Smad7 increased CCL4-induced fibrosis in rats (Huang et al., 2015).

It has been reported that astragalus has the function of immunity enhancement (Liu CH. et al., 2017; Qi et al., 2017;

Liu and Lv, 2020). Additionally, APS may ameliorate liver damage by boosting immunity, which results in a rise in serum total protein, albumin, and albumin/globulin levels, while decreasing globulin levels (Zou et al., 2002; Niu et al., 2012; Xu et al., 2012).

2.4.3 Autophagy and Apoptosis

Autophagy and apoptosis research in the context of improving NAFLD includes lipid removal and anti-inflammatory and anti-oxidative stress benefits. Hamid et al. observed that APS stimulate KCs by decreasing the amounts of recombinant autophagy-related proteins (ATGs), family members (ATG7, ATG12, and ATG6), and protein II light chain 3 (LC3II), resulting in a decrease in CD68-positive KCs (Hamid et al., 2017b). According to previous studies, ATG7 and LC3II recruited by PI3K further clear hepatocellular lipid droplets, and ATG7 may also control PERK, linking autophagy with ER (Martinez-Lopez and Singh, 2015; Zheng et al., 2019). As shown by the decreased expression of Bcl-2/BAX apoptotic genes, APS may also promote apoptosis in activated HSCs in hepatic fibrosis (Hamid et al., 2017a). The Bcl-2 family of proteins controls and regulates the intrinsic or mitochondrial apoptotic pathway (Peña-Blanco and García-Sáez, 2018). The Bcl-2 protein family regulates and controls the intrinsic or mitochondrial apoptotic process (Mukhopadhyay et al., 2014).

3 CONCLUSION AND FUTURE PERSPECTIVES

As phytotherapy, APS are appropriate for long-term therapeutic options in patients with chronic illness owing to relatively small toxic side effects, which has been the most difficult issue in the study of NAFLD treatments, resulting in a large number of medicines being abandoned in subsequent clinical trials. Increasing data indicate that APS are useful for NAFLD. It may enhance lipid metabolism by reducing the buildup of lipids such as TGs, FFAs, and CHOL (in particular, the production and secretion of CHOL and Bas). FAT/CD36, CPT1B, PCSK9, LDL-R, LOX-1, CYP enzymes, and the SIRT1/PPAR α /FGF21 pathway are the major molecular processes and pathways involved. They have the potential to reverse IR by increasing ISI, restoring islet cell shape and function, controlling insulin secretion, and stimulating glucose absorption, all of which are necessary for proper lipogenesis and glycogen production. APS regulate the PI3K/Akt pathway, phosphorylating IRS-1 and activating the AMPK/ACC pathway to ameliorate inadequate ISI, and down-regulates the mTOR/4EBP-1/S6K1 pathway and the addition of adiponectin. Additionally, the therapeutic impact of APS on NAFLD may be related to its capacity to ameliorate OS, ERS, and mitochondrial damage through regulation of the NRF2/HO-1, GRP78/IRE-1/JNK, and AMPK/PGC-1/NRF1 pathways, as seen in **Figure 3**. APS inhibit inflammation and fibrosis and regulates autophagy and apoptosis in HSCs and Kupffer cells via the TLR4/MyD88/NF- κ B pathway and gut microbiota; ECMs are diminished and proliferation of HSCs and Kupffer cells is inhibited *via* the TGF-

β /Smad pathway; HSEC defenestration and immunity are improved; and autophagy and apoptosis occurs in HSCs. Among them are several small-molecule compounds that have been screened using metabolomics, but their findings have not been confirmed in subsequent research, and many of the current animal and cell experiments have remained in the laboratory. Preliminary verification of pathological improvement needs more systematic and in-depth study; further verification of its mechanism of action requires more systematic and in-depth research. At the moment, no clinical data exist to support the therapeutic efficacy of APS in NAFLD. As a consequence of the progress of so many experiment outcomes, further clinical studies will be required in the future to validate the data.

However, because of the intricacy of its structure and composition, it is difficult to correctly regulate the quality of its compounds, and we must make further efforts toward this end (Zeng et al., 2019). APS have been extensively investigated as an immunostimulant and anti-aging, anti-diabetic, anti-tumor, and antiviral agent (Zheng et al., 2020). Owing to the origin of the raw materials, the medicinal components, the growth years of the medicinal materials, and the extraction technique, the purity, composition (e.g., polysaccharide content), and chemical structure of APS will vary (Li et al., 2015). Huang et al. identified polysaccharides as one of the most essential components of *Astragalus* (Huang et al., 1982). The major components of APS are heteropolysaccharide, neutral polysaccharide, dextran, and acidic polysaccharide, with heteropolysaccharide being the most abundant (Zheng et al., 2020).

As a macromolecular molecule, APS are insoluble in water, have a low oral absorption rate and a low bioavailability, and are quickly affected by stomach acid and other variables, resulting in a highly limited therapeutic effectiveness. In recent years, in conjunction with emerging technologies, a plethora of new preparations aimed at increasing the drug's absorption rate and efficacy have been developed, such as the establishment of APS liposomes and the preparation of APS microcapsules to extend the drug's storage time and enhance its slow-release effect and boost immunological function (Fan et al., 2011). Additionally, APS pellets may be manufactured for use as a colon-targeted formulation, allowing the medicine to bypass the intestinal mucosal barrier and reach the liver (Qin et al., 2016; Lai et al., 2017). Chitosan is used to synthesize APS nanoparticles, which boost the herb's therapeutic efficacy in the treatment of blood disorders (Lai et al., 2017). Additionally, colonized and fermented APS are often employed in anti-liver fibrosis studies (Zhou et al., 2017). In clinical settings, APS injection is used the most. It has been extensively used to increase immune function and aid in the treatment of asthma and hypertension in patients after cancer chemotherapy (Wang et al., 2021). As previously stated, it aims to address the issue of APS's limited oral availability. That said, as we can see, various preparations alter the functional targeting of APS. Is there a better way to handle APS for the treatment of NAFLD? The gut-liver axis is critical in NAFLD, and APS have also been shown to promote intestinal flora. Not only may APS be used as a pharmaceutical, but it can also be utilized as a dietary supplement for metabolic illness nutritional treatment.

Modern experimental technology has made tremendous strides in recent years. High-throughput techniques such as metabolomics, transcriptomics, epigenetics, and gut microbiota analysis may aid in the exploration of drug action mechanisms. APS demand a more thorough examination of the exploration of NAFLD therapeutic mechanisms by those technologies.

AUTHOR CONTRIBUTIONS

JZ is the first author who responsible for conception and design of study, drawing the figures and table, and drafting the manuscript. QF has revised the manuscript for important intellectual context and approved the manuscript to be published.

REFERENCES

- Auyeung, K. K., Han, Q.-B., and Ko, J. K. (2016). Astragalus Membranaceus: A Review of its Protection against Inflammation and Gastrointestinal Cancers. *Am. J. Chin. Med.* 44, 1–22. doi:10.1142/S0192415X16500014
- Brenner, C., Galluzzi, L., Kepp, O., and Kroemer, G. (2013). Decoding Cell Death Signals in Liver Inflammation. *J. Hepatol.* 59, 583–594. doi:10.1016/j.jhep.2013.03.033
- Burri, L., Thoresen, G. H., and Berge, R. K. (2010). The Role of PPAR α Activation in Liver and Muscle. *PPAR Res.* 2010, 542359. doi:10.1155/2010/542359
- Cai, X., Lu, Z., Wang, X., Wang, T., Liu, S., Hao, H., et al. (2020). Effects of Astragalus Polysaccharides on Blood Lipids and Cytokines in Rats with Impaired Glucose Tolerance. *Heilongjiang J. Traditional Chin. Med.* 49, 349–350.
- Chakraborty, C., Doss, C. G., Bandyopadhyay, S., and Agoramoorthy, G. (2014). Influence of miRNA in Insulin Signaling Pathway and Insulin Resistance: Micro-molecules with a Major Role in Type-2 Diabetes. *Wiley Interdiscip. Rev. RNA* 5, 697–712. doi:10.1002/wrna.1240
- Chen, S., Yuan, Q., Wang, Y., and Yang, Z. (2018). Effects of Astragalus Polysaccharides on Glucose and Lipid Metabolism and Pancreatic Tissue Pathological Changes in Hyperlipidemia Rats. *J. Guangdong Pharm. Univ.* 34, 457–461.
- Chen, Z., Liu, L., Gao, C., Chen, W., Vong, C. T., Yao, P., et al. (2020). Astragali Radix (Huangqi): A Promising Edible Immunomodulatory Herbal Medicine. *J. Ethnopharmacol.* 258, 112895. doi:10.1016/j.jep.2020.112895
- Chen, Z., Yu, R., Xiong, Y., Du, F., and Zhu, S. (2017). A Vicious circle between Insulin Resistance and Inflammation in Nonalcoholic Fatty Liver Disease. *Lipids Health Dis.* 16, 203. doi:10.1186/s12944-017-0572-9
- Cheng, C.-F., Ku, H.-C., and Lin, H. (2018). PGC-1 α as a Pivotal Factor in Lipid and Metabolic Regulation. *Int. J. Mol. Sci.* 19, 3447. doi:10.3390/ijms19113447
- Cheng, Y. (2010). *Experimental Study of Astragalus Polysaccharide on Lipid-Lowering Effect and Mechanism of Hyperlipidemia Rats*. Doctoral dissertation. Sun Yat-sen University.
- Cheng, Y., Tang, K., Wu, S., Liu, L., Qiang, C., Lin, X., et al. (2011). Astragalus Polysaccharides Lowers Plasma Cholesterol through Mechanisms Distinct from Statins. *PLoS One* 6, e27437. doi:10.1371/journal.pone.0027437
- Cui, K., Zhang, S., Jiang, X., and Xie, W. (2016). Novel Synergic Antidiabetic Effects of Astragalus Polysaccharides Combined with Crataegus Flavonoids via Improvement of Islet Function and Liver Metabolism. *Mol. Med. Rep.* 13, 4737–4744. doi:10.3892/mmr.2016.5140
- Cui, N., Zhao, W., Ji, X., Han, B., Gao, J., Han, X., et al. (2015a). Effects of Astragalus and its Components on Liver Function of Rats with Spleen Deficiency and Dampness. *Inf. Traditional Chin. Med.* 32, 62–65.
- Cui, N., Zhao, W., Ji, X., Jiang, H., Han, B., Gao, J., et al. (2015b). Study on the Mechanism of the Effect of Astragalus and its Components on Lipid Metabolism in Rats with Spleen Deficiency and Dampness Based on Liver

FUNDING

The research was supported by the National Major Science and Technology Program (Grant No. 2017ZX10205501), the Key research and development program of the Sichuan Science and Technology Department (Grant No. 2020YFS0301), and the Applied Basic Research Project of the Sichuan Provincial Department of Science and Technology (Grant No. 2021YJ0253).

SUPPLEMENTARY MATERIAL

The Supplementary Material for this article can be found online at: <https://www.frontiersin.org/articles/10.3389/fphar.2022.854674/full#supplementary-material>

- Gene Expression Profile Analysis. *World Chin. Med.* 10, 1819–1823. doi:10.3969/j.issn.1673-7202.2015.12.002
- Das, T., Song, E. J., and Kim, E. E. (2021). The Multifaceted Roles of USP15 in Signal Transduction. *Int. J. Mol. Sci.* 22, 4728. doi:10.3390/ijms22094728
- Demine, S., Renard, P., and Arnould, T. (2019). Mitochondrial Uncoupling: A Key Controller of Biological Processes in Physiology and Diseases. *Cells* 8, 795. doi:10.3390/cells8080795
- Ding, R. B., Bao, J., and Deng, C. X. (2017). Emerging Roles of SIRT1 in Fatty Liver Diseases. *Int. J. Biol. Sci.* 13, 852–867. doi:10.7150/ijbs.19370
- Ding, Z., Pothineni, N. V. K., Goel, A., Lüscher, T. F., and Mehta, J. L. (2020). PCSK9 and Inflammation: Role of Shear Stress, Pro-inflammatory Cytokines, and LOX-1. *Cardiovasc. Res.* 116, 908–915. doi:10.1093/cvr/cvz313
- Elfaki, I., Mir, R., Almutairi, F. M., and Duhier, F. M. A. (2018). Cytochrome P450: Polymorphisms and Roles in Cancer, Diabetes and Atherosclerosis. *Asian Pac. J. Cancer Prev.* 19, 2057–2070. doi:10.22034/APJCP.2018.19.8.2057
- Eslam, M., Newsome, P. N., Sarin, S. K., Anstee, Q. M., Targher, G., Romero-Gomez, M., et al. (2020a). A New Definition for Metabolic Dysfunction-Associated Fatty Liver Disease: An International Expert Consensus Statement. *J. Hepatol.* 73, 202–209. doi:10.1016/j.jhep.2020.03.039
- Eslam, M., Sanyal, A. J., and George, J. (2020b). MAFLD: A Consensus-Driven Proposed Nomenclature for Metabolic Associated Fatty Liver Disease. *Gastroenterology* 158, 1999. doi:10.1053/j.gastro.2019.11.312
- Fan, Y., Wang, D., Hu, Y., Liu, J., Gao, H., Wang, Y., et al. (2011). Preparation Condition Optimization of astragalus Polysaccharide Liposome by Orthogonal Test. *Chin. Traditional Herbal Drugs* 42, 470–473.
- Forrester, S. J., Kikuchi, D. S., Hernandez, M. S., Xu, Q., and Griendling, K. K. (2018). Reactive Oxygen Species in Metabolic and Inflammatory Signaling. *Circ. Res.* 122, 877–902. doi:10.1161/CIRCRESAHA.117.311401
- Freitas, R. H. C. N., and Fraga, C. A. M. (2018). NF- κ B- $\text{IKK}\beta$ Pathway as a Target for Drug Development: Realities, Challenges and Perspectives. *Curr. Drug Targets* 19, 1933–1942. doi:10.2174/1389450119666180219120534
- Friedman, S. L., Neuschwander-Tetri, B. A., Rinella, M., and Sanyal, A. J. (2018). Mechanisms of NAFLD Development and Therapeutic Strategies. *Nat. Med.* 24, 908–922. doi:10.1038/s41591-018-0104-9
- Gong, L., Wang, C., Zhou, H., Ma, C., Zhang, Y., Peng, C., et al. (2021). A Review of Pharmacological and Pharmacokinetic Properties of Forsythiaside A. *Pharmacol. Res.* 169, 105690. doi:10.1016/j.phrs.2021.105690
- Gu, C., Zeng, Y., Tang, Z., Wang, C., He, Y., Feng, X., et al. (2015). Astragalus Polysaccharides Affect Insulin Resistance by Regulating the Hepatic SIRT1-PGC-1 α /ppara-FGF21 Signaling Pathway in Male Sprague Dawley Rats Undergoing Catch-Up Growth. *Mol. Med. Rep.* 12, 6451–6460. doi:10.3892/mmr.2015.4245
- Guo, Z., Lou, Y., Kong, M., Luo, Q., Liu, Z., and Wu, J. (2019). A Systematic Review of Phytochemistry, Pharmacology and Pharmacokinetics on Radix: Implications for Radix as a Personalized Medicine. *Int. J. Mol. Sci.* 20, 1463. doi:10.3390/ijms20061463
- Hamid, M., Liu, D., Abdulrahim, Y., Khan, A., Qian, G., and Huang, K. (2017a). Inactivation of Kupffer Cells by Selenizing Astragalus Polysaccharides Prevents

- CCl₄-Induced Hepatocellular Necrosis in the Male Wistar Rat. *Biol. Trace Elem. Res.* 179, 226–236. doi:10.1007/s12011-017-0970-x
- Hamid, M., Liu, D., Abdulrahim, Y., Liu, Y., Qian, G., Khan, A., et al. (2017b). Amelioration of CCl₄-Induced Liver Injury in Rats by Selenizing Astragalus Polysaccharides: Role of Proinflammatory Cytokines, Oxidative Stress and Hepatic Stellate Cells. *Res. Vet. Sci.* 114, 202–211. doi:10.1016/j.rvsc.2017.05.002
- He, X., He, J., Zheng, N., Wang, S., and Li, H. (2016). Study on the Relationship between the Weight Loss Effect of astragalus Polysaccharides on Obese Mice and the Regulation of Intestinal flora. *World Chin. Med.* 11, 2379–2384. doi:10.3969/j.issn.1673-7202.2016.11.046
- Hong, Y., Li, B., Zheng, N., Wu, G., Ma, J., Tao, X., et al. (2020). Integrated Metagenomic and Metabolomic Analyses of the Effect of Astragalus Polysaccharides on Alleviating High-Fat Diet-Induced Metabolic Disorders. *Front. Pharmacol.* 11, 833. doi:10.3389/fphar.2020.00833
- Hu, C., Bi, H., Zhang, Y., and Ouyang, J. (2010). Effects of Astragalus Polysaccharides on the Expression of CHOP in the Liver of Type 2 Diabetic Rats. *Chin. J. Microcirc.* 20, 1–3. doi:10.3969/j.issn.1005-1740.2010.01.001
- Hu, H. H., Chen, D. Q., Wang, Y. N., Feng, Y. L., Cao, G., Vaziri, N. D., et al. (2018). New Insights into TGF- β /Smad Signaling in Tissue Fibrosis. *Chem. Biol. Interact.* 292, 76–83. doi:10.1016/j.cbi.2018.07.008
- Hu, Q., Zhang, W., Wu, Z., Tian, X., Xiang, J., Li, L., et al. (2021). Baicalin and the Liver-Gut System: Pharmacological Bases Explaining its Therapeutic Effects. *Pharmacol. Res.* 165, 105444. doi:10.1016/j.phrs.2021.105444
- Huang, J., Zhang, C., Zhan, F., and Zhang, J. (2015). Effect of Astragalus Polysaccharide on TGF- β /Smads Signal Pathway in Rats with Liver Fibrosis. *China J. Traditional Chin. Med. Pharm.* 30, 2184–2186.
- Huang, Q. S., Lu, G. B., Li, Y. C., Guo, J. H., and Wang, R. X. (1982). Studies on the Polysaccharides of "Huang Qi" (Astragalus Mongolicus Bunge (Author's Transl)). *Yao Xue Xue Bao* 17, 200–206.
- Jaldin-Fincati, J. R., Pavarotti, M., Frendo-Cumbo, S., Bilan, P. J., and Klip, A. (2017). Update on GLUT4 Vesicle Traffic: A Cornerstone of Insulin Action. *Trends Endocrinol. Metab.* 28, 597–611. doi:10.1016/j.tem.2017.05.002
- Jiang, G., Gong, M., Song, H., Sun, W., Zhao, W., and Wang, L. (2020). Tob2 Inhibits TLR-Induced Inflammatory Responses by Association with TRAF6 and MyD88. *J. Immunol.* 205 (205), 981–986. doi:10.4049/jimmunol.2000057
- Kakiyama, G., Marques, D., Martin, R., Takei, H., Rodriguez-Agudo, D., LaSalle, S. A., et al. (2020). Insulin Resistance Dysregulates CYP7B1 Leading to Oxysterol Accumulation: a Pathway for NAFL to NASH Transition. *J. Lipid Res.* 61, 1629–1644. doi:10.1194/jlr.RA120000924
- Kan, D. (2018). *Effects of Astragalus and its Fractions on Energy Metabolism of Rat Liver Cells and its Mechanism*. Doctoral dissertation. Shandong University of Traditional Chinese Medicine.
- Kang, I., Chu, C. T., and Kaufman, B. A. (2018). The Mitochondrial Transcription Factor TFAM in Neurodegeneration: Emerging Evidence and Mechanisms. *FEBS Lett.* 592, 793–811. doi:10.1002/1873-3468.12989
- Koyama, Y., and Brenner, D. A. (2017). Liver Inflammation and Fibrosis. *J. Clin. Invest.* 127, 55–64. doi:10.1172/JCI88881
- Lai, M., Wang, J., Tan, J., Luo, J., Zhang, L. M., Deng, D. Y., et al. (2017). Preparation, Complexation Mechanism and Properties of Nano-Complexes of Astragalus Polysaccharide and Amphiphilic Chitosan Derivatives. *Carbohydr. Polym.* 161, 261–269. doi:10.1016/j.carbpol.2016.12.068
- Lebeaupin, C., Vallée, D., Hazari, Y., Hetz, C., Chevet, E., and Bailly-Maitre, B. (2018). Endoplasmic Reticulum Stress Signalling and the Pathogenesis of Non-alcoholic Fatty Liver Disease. *J. Hepatol.* 69, 927–947. doi:10.1016/j.jhep.2018.06.008
- Leoni, V., and Caccia, C. (2011). Oxysterols as Biomarkers in Neurodegenerative Diseases. *Chem. Phys. Lipids* 164, 515–524. doi:10.1016/j.chemphyslip.2011.04.002
- Li, A. P., Li, Z. Y., Sun, H. F., Li, K., Qin, X. M., and Du, G. H. (2015). Comparison of Two Different Astragalus Radix by a ¹H NMR-Based Metabolomic Approach. *J. Proteome Res.* 14, 2005–2016. doi:10.1021/pr501167u
- Li, D., Liu, J., Wu, Y., Li, H., Wang, Y., Chen, C., et al. (2019). Effects of Astragalus Polysaccharides Combined with Metformin on Glucose and Lipid Metabolism in Liver of Aging Type 2 Diabetic Mice. *Chin. J. Inf. Traditional Chin. Med.* 26, 47–51. doi:10.3969/j.issn.1005-5304.2019.02.011
- Li, J. (2013). *Effect of Astragalus Polysaccharides on the Mechanical Properties of Hepatic Sinusoidal Endothelial Cells*. Doctoral dissertation. China Academy of Chinese Medical Sciences.
- Liu, C. H., Abrams, N. D., Carrick, D. M., Chander, P., Dwyer, J., Hamlet, M. R. J., et al. (2017a). Biomarkers of Chronic Inflammation in Disease Development and Prevention: Challenges and Opportunities. *Nat. Immunol.* 18, 1175–1180. doi:10.1038/ni.3828
- Liu, J., Li, D., Zhao, Y., Wu, Y., and Wang, J. (2020). Effect of Astragalus Polysaccharide Combined with Metformin on Liver mRNA Expression Profile in Aging Diabetic Mice and Functional Analysis. *Lishizhen Med. Materia Med. Res.* 31, 1043–1046. doi:10.3969/j.issn.1008-0805.2020.05.005
- Liu, Q., Zhang, F. G., Zhang, W. S., Pan, A., Yang, Y. L., Liu, J. F., et al. (2017b). Ginsenoside Rg1 Inhibits Glucagon-Induced Hepatic Gluconeogenesis through Akt-FoxO1 Interaction. *Theranostics* 7, 4001–4012. doi:10.7150/thno.18788
- Liu, Y. T., and Lv, W. L. (2020). Research Progress in Astragalus Membranaceus and its Active Components on Immune Responses in Liver Fibrosis. *Chin. J. Integr. Med.* 26, 794–800. doi:10.1007/s11655-019-3039-1
- Lonardo, A., Byrne, C. D., Caldwell, S. H., Cortez-Pinto, H., and Targher, G. (2016). Global Epidemiology of Nonalcoholic Fatty Liver Disease: Meta-Analytic Assessment of Prevalence, Incidence, and Outcomes. *Hepatology* 64, 1388–1389. doi:10.1002/hep.28584
- Ma, Y., Qiu, X., Shi, X., and Yu, C. (2019). Effects of Astragalus Radix Polysaccharides on ACE2-[Ang-(1-7)]-Mas axis and Insulin Resistance in Non-alcoholic Steatohepatitis Rats. *Chin. Traditional Patent Med.* 41, 1012–1017.
- Mao, X., and Ouyang, J. (2007). Preventive Effect of astragalus Polysaccharide on Diet-Induced Liver Insulin Resistance in Mice. *Chin. J. Pathophysiology* 23, 4. doi:10.3321/j.issn:1000-4718.2007.11.031
- Marchesini, G., Petta, S., and Dalle Grave, R. (2016). Diet, Weight Loss, and Liver Health in Nonalcoholic Fatty Liver Disease: Pathophysiology, Evidence, and Practice. *Hepatology* 63, 2032–2043. doi:10.1002/hep.28392
- Marra, F., and Svegliati-Baroni, G. (2018). Lipotoxicity and the Gut-Liver axis in NASH Pathogenesis. *J. Hepatol.* 68, 280–295. doi:10.1016/j.jhep.2017.11.014
- Martinez-Lopez, N., and Singh, R. (2015). Autophagy and Lipid Droplets in the Liver. *Annu. Rev. Nutr.* 35, 215–237. doi:10.1146/annurev-nutr-071813-105336
- Mollazadeh, H., Cicero, A. F. G., Blesso, C. N., Pirro, M., Majeed, M., and Sahebkar, A. (2019). Immune Modulation by Curcumin: The Role of Interleukin-10. *Crit. Rev. Food Sci. Nutr.* 59, 89–101. doi:10.1080/10408398.2017.1358139
- Mota, M., Banini, B. A., Cazanave, S. C., and Sanyal, A. J. (2016). Molecular Mechanisms of Lipotoxicity and Glucotoxicity in Nonalcoholic Fatty Liver Disease. *Metabolism* 65, 1049–1061. doi:10.1016/j.metabol.2016.02.014
- Mukhopadhyay, S., Panda, P. K., Sinha, N., Das, D. N., and Bhutia, S. K. (2014). Autophagy and Apoptosis: where Do They Meet? *Apoptosis* 19, 555–566. doi:10.1007/s10495-014-0967-2
- Niu, C., Liu, B., Xing, Y., Li, L., and Zhao, H. (2012). Effect of Astragalus Polysaccharides on the Protection of Carbon Tetrachloride Liver Injury. *China Med. Eng.* 20, 38–39.
- Pan, L. X., Li, L. Y., Zhou, H., Cheng, S. Q., Liu, Y. M., Lian, P. P., et al. (2019). TMEM100 Mediates Inflammatory Cytokines Secretion in Hepatic Stellate Cells and its Mechanism Research. *Toxicol. Lett.* 317, 82–91. doi:10.1016/j.toxlet.2018.12.010
- Peña-Blanco, A., and García-Sáez, A. J. (2018). Bax, Bak and beyond - Mitochondrial Performance in Apoptosis. *FEBS J.* 285, 416–431. doi:10.1111/febs.14186
- Pierantonelli, I., and Svegliati-Baroni, G. (2019). Nonalcoholic Fatty Liver Disease: Basic Pathogenetic Mechanisms in the Progression from NAFLD to NASH. *Transplantation* 103, e1–e13. doi:10.1097/TP.0000000000002480
- Pittayapruek, P., Meephansan, J., Prapapan, O., Komine, M., and Ohtsuki, M. (2016). Role of Matrix Metalloproteinases in Photoaging and Photocarcinogenesis. *Int. J. Mol. Sci.* 17, 868. doi:10.3390/ijms17060868
- Qi, Y., Gao, F., Hou, L., and Wan, C. (2017). Anti-Inflammatory and Immunostimulatory Activities of Astragalosides. *Am. J. Chin. Med.* 45, 1157–1167. doi:10.1142/S0192415X1750063X
- Qin, Y., Zhang, Y., Yu, L., Wang, Y., Rong, F., and Cong, J. (2016). Preparation of Astragalus Polysaccharide Colon Targeting Pellets. *Chin. Pharm. J.* 51, 35–39.
- Qin, Z. (2012). *Analysis of the Changes of Main Effective Components of Astragalus after Fermentation and the Effect of Polysaccharides on Experimental Liver Fibrosis*. Doctoral dissertation. Gansu Agricultural University.

- Qu, J., Zhang, Y., Su, H., Li, J., Liu, H., Zhang, T., et al. (2020). Astragalus Polysaccharide Attenuates Hepatic Damage by Activating Nrf2/HO-1 Pathway in Diabetic Rats. *Chin. Pharmacol. Bull.* 36, 1422–1427. doi:10.3969/j.issn.1001-1978.2020.10.017
- Ratzliff, V., Bellentani, S., Cortez-Pinto, H., Day, C., and Marchesini, G. (2010). A Position Statement on NAFLD/NASH Based on the EASL 2009 Special Conference. *J. Hepatol.* 53, 372–384. doi:10.1016/j.jhep.2010.04.008
- Régner, M., Polizzi, A., Guillou, H., and Loiseau, N. (2019). Sphingolipid Metabolism in Non-alcoholic Fatty Liver Diseases. *Biochimie* 159, 9–22. doi:10.1016/j.biochi.2018.07.021
- Sabatine, M. S. (2019). PCSK9 Inhibitors: Clinical Evidence and Implementation. *Nat. Rev. Cardiol.* 16, 155–165. doi:10.1038/s41569-018-0107-8
- Santos, R. A. S., Sampaio, W. O., Alzamora, A. C., Motta-Santos, D., Alenina, N., Bader, M., et al. (2018). The ACE2/Angiotensin-(1-7)/MAS Axis of the Renin-Angiotensin System: Focus on Angiotensin-(1-7). *Physiol. Rev.* 98, 505–553. doi:10.1152/physrev.00023.2016
- Scherz-Shouval, R., and Elazar, Z. (2007). ROS, Mitochondria and the Regulation of Autophagy. *Trends Cell Biol.* 17, 422–427. doi:10.1016/j.tcb.2007.07.009
- Schuppman, D., Surabattula, R., and Wang, X. Y. (2018). Determinants of Fibrosis Progression and Regression in NASH. *J. Hepatol.* 68, 238–250. doi:10.1016/j.jhep.2017.11.012
- Schuster, S., Cabrera, D., Arrese, M., and Feldstein, A. E. (2018). Triggering and Resolution of Inflammation in NASH. *Nat. Rev. Gastroenterol. Hepatol.* 15, 349–364. doi:10.1038/s41575-018-0009-6
- Simanshu, D. K., Nissley, D. V., and McCormick, F. (2017). RAS Proteins and Their Regulators in Human Disease. *Cell* 170, 17–33. doi:10.1016/j.cell.2017.06.009
- Smith, B. K., Marcinko, K., Desjardins, E. M., Lally, J. S., Ford, R. J., and Steinberg, G. R. (2016). Treatment of Nonalcoholic Fatty Liver Disease: Role of AMPK. *Am. J. Physiol. Endocrinol. Metab.* 311, E730–E740. doi:10.1152/ajpendo.00225.2016
- Song, J., Hu, Y., Liu, J., Ouyang, J., and Li, J. (2014). Effect of Astragalus Polysaccharides on Blood Free Fatty Acids in Diabetic Rats and its Mechanism. *China Med.* 9, 5. doi:10.3760/cma.j.issn.1673-4777.2014.10.020
- Sun, F. (2012). *Effects of Astragalus Polysaccharides on the Expression of InsR and its Substrate IRS-2 in the Liver of Type 2 Diabetic Rats*. Doctoral dissertation. Xinxiang Medical University.
- Sun, J., Liu, Y., Yu, J., Wu, J., Gao, W., Ran, L., et al. (2019). APS Could Potentially Activate Hepatic Insulin Signaling in HFD-Induced IR Mice. *J. Mol. Endocrinol.* 63, 77–91. doi:10.1530/JME-19-0035
- Tariq, Z., Green, C. J., and Hodson, L. (2014). Are Oxidative Stress Mechanisms the Common Denominator in the Progression from Hepatic Steatosis towards Non-alcoholic Steatohepatitis (NASH)? *Liver Int.* 34, e180–90. doi:10.1111/liv.12523
- Thorens, B. (2015). GLUT2, Glucose Sensing and Glucose Homeostasis. *Diabetologia* 58, 221–232. doi:10.1007/s00125-014-3451-1
- Tian, T., and Xu, L. (2008). “Experimental Study on the Effect of Chinese Medicine for Promoting Blood Circulation and Removing Stasis on Liver Microcirculation,” in The 20th National Academic Conference on Digestive System Diseases of Integrated Traditional Chinese and Western Medicine and Digestive Disease Diagnosis and Treatment Progress Class, Shanghai, China, November 28, 2008.
- Toda, C., and Diano, S. (2014). Mitochondrial UCP2 in the central Regulation of Metabolism. *Best Pract. Res. Clin. Endocrinol. Metab.* 28, 757–764. doi:10.1016/j.beem.2014.02.006
- Tong, H., Tian, Y., Wang, D., Deng, X., and Dong, Z. (2006). Regulation of Astragalus Polysaccharides on Blood Lipid in Rats with Hyperlipidemia. *China Clin. Rehabil.* 10, 68–70. doi:10.3321/j.issn:1673-8225.2006.11.029
- Wang, C., and Sun, X. (2021). The Function of astragalus Polysaccharides in Hepatic Steatosis of Mice. *Hubei Agric. Sci.* 60, 121–125. doi:10.14088/j.cnki.issn0439-8114.2021.08.025
- Wang, J., Yang, X., and Zhang, J. (2016a). Bridges between Mitochondrial Oxidative Stress, ER Stress and mTOR Signaling in Pancreatic β Cells. *Cell Signal* 28, 1099–1104. doi:10.1016/j.cellsig.2016.05.007
- Wang, J., Bi, H., Liu, M., and Qin, J. (2015). Effect of Astragalus Polysaccharide on Blood Sugar and Antioxidant Capacity of Liver in KKAY Mice. *J. Hubei Univ. Chin. Med.* 17, 5–7. doi:10.3969/j.issn.1008-987x.2015.05.01
- Wang, N., Zhang, D., Mao, X., Zou, F., Jin, H., and Ouyang, J. (2009). Astragalus Polysaccharides Decreased the Expression of PTP1B through Relieving ER Stress Induced Activation of ATF6 in a Rat Model of Type 2 Diabetes. *Mol. Cell Endocrinol.* 307, 89–98. doi:10.1016/j.mce.2009.03.001
- Wang, N., Zhang, D., Zou, F., and Ouyang, J. (2007). “Effects of Astragalus Polysaccharides on Relieving Endoplasmic Reticulum Stress in the Liver of STZ-Induced Type 2 Diabetic Rats and Restoring Glucose Homeostasis,” in The 12th Academic Conference of the Microcirculation Professional Committee of the Chinese Pathophysiology Society, Beijing, China, November 9, 2007.
- Wang, T., Chen, C., Yang, L., Zeng, Z., Zeng, M., Jiang, W., et al. (2019). Role of Nrf2/HO-1 Signal axis in the Mechanisms for Oxidative Stress-Relevant Diseases. *Zhong Nan Da Xue Xue Bao Yi Xue Ban* 44, 74–80. doi:10.11817/j.issn.1672-7347.2019.01.012
- Wang, X. (2016). *Experimental Study of Astragalus Polysaccharides on Decreasing Blood Sugar Level in Type 2 Diabetic Rats and Preventing Diabetes Related Complications*. Doctoral dissertation. Xinxiang Medical University.
- Wang, X., Weng, X., Wang, X., Wang, T., and Yin, Q. (2016b). Experimental Study of Astragalus Polysaccharide in Preventing Liver Injury in Type 2 Diabetic Rats. *Prog. Mod. Biomed.* 16, 1846–1849. doi:10.13241/j.cnki.pmb.2016.10.011
- Wang, Y., Zhang, X., Wang, Y., Zhao, W., Li, H., Zhang, L., et al. (2021). Application of Immune Checkpoint Targets in the Anti-tumor Novel Drugs and Traditional Chinese Medicine Development. *Acta Pharm. Sin B* 11, 2957–2972. doi:10.1016/j.apsb.2021.03.004
- Wang, Z., Wang, H., and Lu, M. (2013). Protective Effect of astragalus Polysaccharide on Lipopolysaccharide-Induced Liver Cell Injury. *Pharmacol. Clin. Chin. Materia Med.* 29, 85–88.
- Wei, Z., Weng, S., Wang, L., and Mao, Z. (2018). Mechanism of Astragalus Polysaccharides in Attenuating Insulin Resistance in Rats with Type 2 Diabetes Mellitus via the Regulation of Liver microRNA-203a-3p. *Mol. Med. Rep.* 17, 1617–1624. doi:10.3892/mmr.2017.8084
- Xu, F., Guo, J., Bao, J., Wang, Y., and Xu, Q. (2012). Effect of Astragalus Polysaccharides on TGF- β 1 in Rat Models of Secondary Cholestatic Hepatic Fibrosis. *Chin. Arch. Traditional Chin. Med.* 30, 1026–1029.
- Yan, F., Feng, J., Li, W., Wu, L., and Li, J. (2020a). A Preliminary Study on the Effect and Mechanism of Brevicapsin for Improving Insulin Resistance in HepG2 Cells. *J. Cardiovasc. Pharmacol.* 76, 216–226. doi:10.1097/FJC.0000000000000848
- Yan, Y., Xiao, L., Zhong, M., Huang, J., Li, X., Wu, X., et al. (2020b). Mitigating Effect of Mongolia astragalus Polysaccharide against Dexamethasone-Induced Glucose and Lipid Metabolism Disorder through Regulation on Nrf-2 Signaling Pathway. *Chin. J. Immunol.* 36, 289–293. doi:10.3969/j.issn.1000-484X.2020.03.007
- Yang, L. (2017). *Study on the Antioxidant Effect of Three Kinds of Chinese Medicine Extracted Polysaccharides and Their Compound Polysaccharides*. Doctoral dissertation. Guangdong Pharmaceutical University.
- Yang, L., Wang, X., Hou, A., Zhang, J., Wang, S., Man, W., et al. (2021). A Review of the Botany, Traditional Uses, Phytochemistry, and Pharmacology of the Flos Inulae. *J. Ethnopharmacol.* 276, 114125. doi:10.1016/j.jep.2021.114125
- Ye, Y., Deng, T., Wan, X. Y., Ouyang, J. P., Liu, M., and Mao, X. Q. (2014). The Role of Quantitative Changes in the Expression of Insulin Receptor Substrate-1 and Nuclear Ubiquitin in Abnormal Glycometabolism in the Livers of KKAY Mice and the Relative Therapeutic Mechanisms of Astragalus Polysaccharide. *Int. J. Mol. Med.* 33, 341–350. doi:10.3892/ijmm.2013.1580
- Younossi, Z., Anstee, Q. M., Marietti, M., Hardy, T., Henry, L., Eslam, M., et al. (2018). Global burden of NAFLD and NASH: Trends, Predictions, Risk Factors and Prevention. *Nat. Rev. Gastroenterol. Hepatol.* 15, 11–20. doi:10.1038/nrgastro.2017.109
- Yuan, Q., Tang, S., Chen, S., and Yang, Z. (2018). Effect of astragalus Polysaccharides on Rats with Non-alcoholic Fatty Liver Disease. *Acad. J. Second Mil. Med. Univ.* 39, 573–578. doi:10.16781/j.0258-879x.2018.05.0573
- Zeng, P., Li, J., Chen, Y., and Zhang, L. (2019). The Structures and Biological Functions of Polysaccharides from Traditional Chinese Herbs. *Prog. Mol. Biol. Transl. Sci.* 163, 423–444. doi:10.1016/bs.pmbts.2019.03.003
- Zhang, C., Huang, J., Zhan, F., and Zhang, J. (2015). Protective Effect of astragalus Polysaccharide on Liver Fibrosis Induced by Carbon Tetrachloride in Rats. *World Chin. Med.* 10, 887–890. doi:10.1371/journal.pone.0129621
- Zhang, Q., Wang, C., Liu, Z., Liu, X., Han, C., Cao, X., et al. (2012). Notch Signal Suppresses Toll-like Receptor-Triggered Inflammatory Responses in

- Macrophages by Inhibiting Extracellular Signal-Regulated Kinase 1/2-mediated Nuclear Factor κ B Activation. *J. Biol. Chem.* 287, 6208–6217. doi:10.1074/jbc.M111.310375
- Zhang, S. (2012). *Study on the Effect of Single-Cell Level of astragalus Polysaccharide on the Micro-mechanics of Hepatic Sinusoidal Endothelial Cells*. Doctoral dissertation. China Academy of Chinese Medical Sciences.
- Zhang, X., Dang, S., Cheng, Y., Jia, X., Chen, M., and Liu, E. (2009). Effects of Emodin and astragalus Polysaccharides on Liver Ultrastructure in Rats with Experimental Liver Injury. *J. Xi'an Jiaotong University(Medical Sciences)* 30, 502–505.
- Zheng, W., Xie, W., Yin, D., Luo, R., Liu, M., and Guo, F. (2019). ATG5 and ATG7 Induced Autophagy Interplays with UPR via PERK Signaling. *Cell Commun Signal* 17, 42. doi:10.1186/s12964-019-0353-3
- Zheng, Y., Ren, W., Zhang, L., Zhang, Y., Liu, D., and Liu, Y. (2020). A Review of the Pharmacological Action of Astragalus Polysaccharide. *Front. Pharmacol.* 11, 349. doi:10.3389/fphar.2020.00349
- Zhou, M., Guo, X., Hao, Z., Wang, G., Chang, B., and Liu, J. (2017). The Optimized Preparation Process of Astragalus Polysaccharide Microcapsules. *Feed Res.* 11, 5.
- Zou, F. (2010). *Astragalus Polysaccharides Improve Glucose Metabolism in Type 2 Diabetes and its Effect on AMPK Activity*. Doctoral dissertation. Wuhan University.
- Zou, F., Mao, X. Q., Wang, N., Liu, J., and Ou-Yang, J. P. (2009). Astragalus Polysaccharides Alleviates Glucose Toxicity and Restores Glucose Homeostasis in Diabetic States via Activation of AMPK. *Acta Pharmacol. Sin* 30, 1607–1615. doi:10.1038/aps.2009.168
- Zou, F., Ouyang, J., and Mao, X. (2007). Effect of Astragalus Polysaccharides on the Content of Liver Glycogen in Mice with Hereditary Diabetes. *Chin. J. Microcirc.* 17, 4. doi:10.3969/j.issn.1005-1740.2007.01.004
- Zou, H. (2016). *Effect of Astragalus Polysaccharide on PCSK9 Expression in THP-1 and HepG2 Cells*. Doctoral dissertation. Chongqing Medical University.
- Zou, L., Wu, T., and Cui, L. (2002). Preventive and Therapeutic Effects of astragalus Polysaccharides on Bone Loss in Mice with Liver Fibrosis. *Chin. J. Integrated Traditional West. Med. Liver Dis.* 12, 4. doi:10.3969/j.issn.1005-0264.2002.02.012
- Conflict of Interest:** The authors declare that the research was conducted in the absence of any commercial or financial relationships that could be construed as a potential conflict of interest.
- Publisher's Note:** All claims expressed in this article are solely those of the authors and do not necessarily represent those of their affiliated organizations, or those of the publisher, the editors and the reviewers. Any product that may be evaluated in this article, or claim that may be made by its manufacturer, is not guaranteed or endorsed by the publisher.

Copyright © 2022 Zhang and Feng. This is an open-access article distributed under the terms of the Creative Commons Attribution License (CC BY). The use, distribution or reproduction in other forums is permitted, provided the original author(s) and the copyright owner(s) are credited and that the original publication in this journal is cited, in accordance with accepted academic practice. No use, distribution or reproduction is permitted which does not comply with these terms.



Regression of Liver Steatosis Following Phosphatidylcholine Administration: A Review of Molecular and Metabolic Pathways Involved

D. Osipova¹, K. Kokoreva², L. Lazebnik³, E. Golovanova³, Ch. Pavlov⁴, A. Dukhanin⁵, S. Orlova⁶ and K. Starostin^{7*}

¹Research Centre for Medical Genetics, Moscow, Russia, ²Institute of Pediatric Endocrinology, Endocrinology Research Centre, Moscow, Russia, ³A. I. Evdokimov Moscow State University of Medicine and Dentistry, Ministry of Health of Russia, Moscow, Russia, ⁴I. M. Sechenov First Moscow State Medical University, Ministry of Health of Russia, Moscow, Russia, ⁵Molecular Pharmacology and Radiology Department, Russian National Research Medical University, Moscow, Russia, ⁶Department of Dietetics and Clinical Nutrition of Continuing Medical Education, Medical Institute, RUDN University, Moscow, Russia, ⁷Science Hub, Sanofi, Moscow, Russia

OPEN ACCESS

Edited by:

Ana Blas-García,
University of Valencia, Spain

Reviewed by:

Stefania Di Mauro,
University of Catania, Italy
Giovanni Tarantino,
University of Naples Federico II, Italy

*Correspondence:

K. Starostin
Kirill.Starostin@sanofi.com

Specialty section:

This article was submitted to
Gastrointestinal and Hepatic
Pharmacology,
a section of the journal
Frontiers in Pharmacology

Received: 19 October 2021

Accepted: 08 February 2022

Published: 10 March 2022

Citation:

Osipova D, Kokoreva K, Lazebnik L, Golovanova E, Pavlov C, Dukhanin A, Orlova S and Starostin K (2022) Regression of Liver Steatosis Following Phosphatidylcholine Administration: A Review of Molecular and Metabolic Pathways Involved. *Front. Pharmacol.* 13:797923. doi: 10.3389/fphar.2022.797923

Liver steatosis is a key pathology in non-alcoholic or metabolic associated fatty liver disease. Though largely ignored for decades it is currently becoming the focus of research in hepatology. It is important to consider its origin and current opportunities in terms of pharmacotherapy. Essential phospholipids (EPLs) rich in phosphatidylcholine (PCH) is a widely used treatment option for fatty liver disease, and there is a solid amount of consistent clinical evidence for the regression of steatosis after treatment with EPLs. As knowledge of PCH (a key component of EPLs) pharmacodynamics and mode of action driving this widely observed clinical effect is currently insufficient, we aimed to explore the potential molecular and metabolic pathways involved in the positive effects of PCH on steatosis regression.

Keywords: liver steatosis, essential phospholipids, mode of action, pharmacodynamics, phosphatidylcholine, nonalcoholic fatty liver, review

INTRODUCTION

Non-alcoholic fatty liver disease (NAFLD) is the leading cause of chronic liver disease (CLD), which puts it among the top global health priorities. NAFLD prevalence is increasing dramatically every year. NAFLD was responsible for 46.8% of all chronic liver disease cases in 1994 and 75.1% in 2008 (Younossi et al., 2011). Nowadays it is the second most frequent indication for liver transplantation in the United States (Holmer et al., 2017). NAFLD is expected to be the most common cause of liver transplantation by 2030 (Byrne and Targher, 2015; Tana et al., 2019).

Numerous studies aimed to find the best treatment for NAFLD/NASH (non-alcoholic steatohepatitis). Dozens of clinical trials and studies have been performed recently to assess the efficacy and safety of different candidate molecules. Unfortunately, most of these molecules have fallen short of expectations (cenicriviroc in the CENTAUR study (Friedman et al., 2018), obeticholic acid in the REGENERATE study (Ratziu et al., 2019; Younossi et al., 2019), or elafibranor in the RESOLVE-IT study (NCT02704403)). Vitamin E in high dosage (800 IU) showed some effect in NASH patients, but there was a relapse in inflammation markers after the end of treatment, and authors raised concerns about vitamin E safety profile if taken constantly in such a dosage (Sanyal et al., 2010; Lavine et al., 2011). Most of these new molecules were used to treat NASH and/or

advanced fibrosis, but not the steatosis stage of the disease, for which lifestyle modification has been considered so far as the only treatment option. At the same time, less than 2% of obese patients have reached normal weight in a large real-world data setting (Fildes et al., 2015). So, lifestyle modification, being considered as a key NAFLD treatment (Francque and Vonghia, 2019), is largely useless for 98% of patients (Fildes et al., 2015). Moreover, the concept of steatosis as a physiologically adaptive mechanism is outdated. Nowadays it is challenged, and steatosis is becoming the focus of clinical and scientific interest as a condition increasing cardiovascular risks and mortality and, therefore, requiring pharmacotherapy (Zhou et al., 2012; Adams and Ratziu, 2015; Nassir et al., 2015; Francque and Vonghia, 2019). In this respect, it is also worth mentioning that NAFLD is reconsidered as liver steatosis associated with metabolic disorders and thus may be renamed as MAFLD, i.e., metabolic (disorders) associated fatty liver disease. MAFLD concept cancels NAFLD/NASH dichotomy, with liver steatosis as a key diagnostic criterion along with various metabolic disorders.

Putting this together we suggest that steatosis should be considered not only as a key diagnostic criterion but a target for pharmacotherapy to be combined with lifestyle modification. Simple steatosis is known to be fully reversible and, thus, should be treated before steatohepatitis develops (Choudhary et al., 2015).

Among the existing pharmacotherapeutic options, essential phospholipids (EPLs) containing 72–96% (3-sn-phosphatidyl)choline are of interest as recent randomized controlled trials and meta-analyses showed regression of steatosis associated with EPLs treatment (Gundermann et al., 2016; Popovic and Dajani, 2020). A large observational study showed a similar effect in a real-world setting (Maev et al., 2020b). At the same time, despite abundant evidence of the clinical effect of EPLs, their mode of action is still poorly understood. Our review is aimed to analyze the key potential molecular pathways involved in the clinical effect of PCH, the main component of EPLs.

Essential Phospholipids Source and Chemical Profile

Generally, EPLs are natural phospholipids that can be plant-derived (e.g., from soybeans, rape (canola) seed, wheat germ, sunflower, or flaxseed) or animal-derived (e.g., from egg yolk, milk, or krill). Phospholipids are called essential since they constitute structural and functional components of all cell membranes and, therefore, endogenous substances. The phospholipid content of membranes and the distribution of fatty acid residues vary within a cell and between cell types (Pepeu et al., 1990). The distribution of different types of phospholipids in cells and organs is not yet fully understood, but the interaction of various phospholipids and other membrane components seems to have an important role in signal transduction cascades (Van Hoogevest and Wendel, 2014).

The phospholipid and fatty acid profiles of the EPLs depend on the raw material sources, but for EPLs generally used in liver diseases, most sources use the following well-recognized definition of EPLs. EPLs are a highly purified extract of the semen of soybeans with standardized contents of 72–96% (3-sn-

TABLE 1 | Phospholipid composition of the soybean lecithin extract and chromatography fraction with PC content of 73–79% (Van Hoogevest and Wendel, 2014).

| Component (% w/w) | Fraction with PCH 73–79% |
|-------------------|--------------------------|
| PCH | 79 |
| PE | 3.3 |
| PI | 0.2 |
| PA | 1.6 |
| LPC | 6.1 |
| N-Acyl-PE | 1.7 |

PCH, phosphatidylcholine; PE, phosphatidylethanolamine; PI, phosphatidylinositol; PA, phosphatidic acid; LPC, lysophosphatidylcholine; N-Acyl-PE, phosphatidylethanolamine.

phosphatidyl)choline (PCH) (Gundermann et al., 2011). In most studies in humans EPLs with 76% of PCH were administered (Popovic and Dajani, 2020). The chemical profile of soybean lecithin with 73–79% of PCH is provided in **Table 1**. The process of obtaining EPLs from soybean is well-described elsewhere (Van Hoogevest and Wendel, 2014). The quantitatively and qualitatively dominating molecule is 1,2-Dilinoleoylphosphatidylcholine (DLPC), representing up to 52% of the administered phosphatidylcholine molecules. This high level of DLPC is the primary difference between EPLs and typical unprocessed (natural) phospholipids (e.g., triple lecithin, raw lecithin, and egg lecithin), as well as dietary and endogenous phosphatidylcholines (Gundermann et al., 2011).

Since PCH is a dominating component of EPLs, our review is focused on the analysis of the role of PCH in liver steatosis regression. First of all, we took into consideration liver steatosis pathophysiology and fatty liver modeling approaches to provide an overview of involved metabolic and molecular pathways. Second, we considered it in terms of potential PCH influence on the key processes involved in liver steatosis pathophysiology.

LIVER STEATOSIS PATHOPHYSIOLOGY

Non-alcoholic fatty liver disease (NAFLD), or MAFLD, as it has been renamed in 2020, is a clinical diagnosis involving the presence of at least 5% hepatocytes with lipid droplets observed by microscopy of biopsy material or fatty infiltration revealed by imaging tests and excluding all secondary causes of excessive accumulation of triglycerides (TG) in the liver (Carr et al., 2016).

So, the key pathology is liver steatosis. It is of great interest what the true cause is for *de novo* lipogenesis in hepatocytes. Several models explaining the origins of steatosis exist (Kim et al., 2000; Kotani et al., 2004; Petersen et al., 2007). Of these models, the following are considered most reliable and useful in terms of further research:

1) Metabolic pathway of liver steatosis.

Insulin resistance of peripheral tissues → transient hyperglycemia → glucose uptake by the liver → liponeogenesis

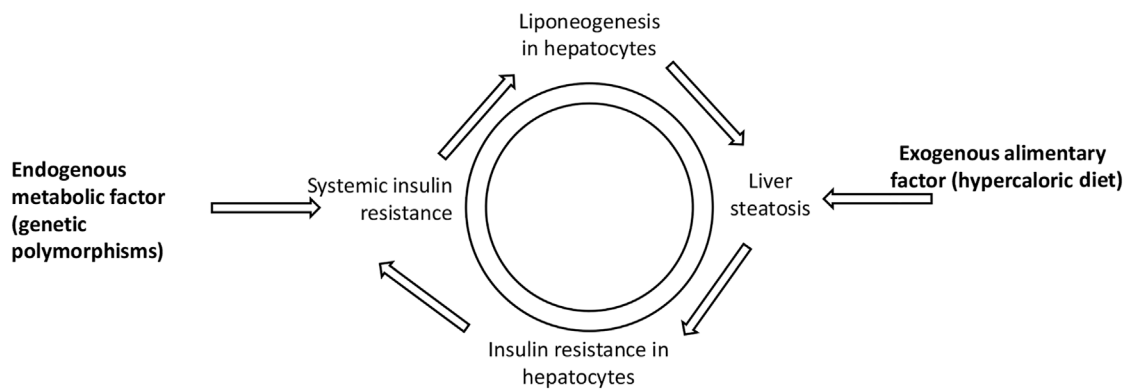


FIGURE 1 | Vicious circle illustrating liver steatosis and prediabetes interconnection. Both exogenous alimentary factor (hypercaloric diet) and endogenous metabolic factor (genetic polymorphisms) may lead to systemic insulin resistance and liver steatosis.

→ accumulation of TG in the liver (Kim et al., 2000; Kotani et al., 2004; Petersen et al., 2007; Liu et al., 2010). In this case, prediabetes is considered the leading cause of NAFLD.

2) Alimentary pathway of liver steatosis.

Kcal overload → lipid transformation and TG accumulation in the liver → insulin resistance of liver cells (Samuel et al., 2004) → systemic insulin resistance (Cai et al., 2005). In this case, NAFLD may be the primary metabolic disorder representing hepatic manifestations of metabolic syndrome leading to prediabetes.

3) Mixed pathway of liver steatosis.

In real-life clinical practice, we believe that both kcal overload and insulin resistance may develop and exist in parallel. In this case, both prediabetes and NAFLD clinical manifestations would be present at the same time. Depending on the dominant pathway in a sample, NAFLD leading to prediabetes or prediabetes leading to NAFLD is observed in different studies which reflects the reciprocal interconnection (Xia et al., 2019).

The pathways of liver steatosis mentioned above may shed light on the correlation between liver steatosis and prediabetes (Chen et al., 2017). Such a vicious circle between fatty liver and prediabetes may be presented as follows (**Figure 1**).

Insulin resistance and liponeogenesis in hepatocyte molecular interconnection are described in detail elsewhere (Chen et al., 2017). For the following review of PCH mode of action, it is worth mentioning that hyperinsulinemia and hyperglycemia in NAFLD induce SREBP-1c (sterol regulatory element-binding protein-1c) and ChREBP (carbohydrate response element-binding protein), respectively, leading to lipogenic pathway activation causing conversion of excess glucose to fatty acids. Improved fatty acids synthesis results in increased levels of malonyl-CoA, which inhibits CPT-1 (carnitine palmitoyltransferase 1), the transporter of fatty acids to mitochondria. These events lead to a shift between free fatty acids beta-oxidation and *de novo* lipogenesis (Di Mauro et al., 2016).

Regardless of the exact pathway of TG accumulation in the liver, it may be characterized by impairment of the following processes:

- 1) Fatty acids and TG utilization in hepatocytes (lipolysis)
- 2) Fatty acids and TG *de novo* synthesis in hepatocytes (liponeogenesis)
- 3) Fatty acids and TG secretion or evacuation
- 4) Fatty acids and TG dietary intake

Therefore, we aimed to explore whether these processes were modified by PCH and may explain its clinical effect observed consistently in randomized controlled trials and observational clinical studies and proven in recent meta-analyses where EPLs were administered (Arvind et al., 2006; Sas et al., 2013; Dajani et al., 2015; Gundermann et al., 2016; Popovic and Dajani, 2020).

FATTY LIVER MODELING STUDIES

In 2005, Buang et al. conducted a perfect *in vivo* study in Sprague-Dawley rats fed a basic diet with TG (control group), TG and orotic acid (fatty liver model group), or orotic acid and phosphatidylcholine (PCH group) for 10 days (Buang et al., 2005). Liver weight was the same across groups at baseline, however, its increase differed at the end of the study in the fatty liver model group vs. the control group. Liver TG increased in the fatty liver model group, but not in the PCH group. Thus, the effect of PCH on steatosis in the liver was reproduced. Moreover, blood cholesterol and TG levels were minimal in the PCH + fatty liver group. Thus, lower levels of liver TG in the PCH group may be explained with fatty acids digestion, synthesis, or oxidation, rather than with excretion from hepatocytes. More importantly, Buang analyzed enzyme activity, which gave us another reason to continue the relevant literature search. The PCH group did show a change in the expression of enzymes involved in fatty acids synthesis and beta-oxidation (fatty acids catabolism). Particularly, in the PCH group, fatty acid synthase (FAS) and glucose-6-phosphate

dehydrogenase (G6PDH) activity and malate dehydrogenase (ME) expression were decreased (involved in fatty acids synthesis), while carnitine palmitoyltransferase (CPT) expression increased (involved in beta-oxidation).

It is known that in the case of choline deficiency triglycerides cannot be removed effectively from the hepatocytes since choline is the precursor of PCH, and PCH is essential for very-low-density lipoproteins (VLDL) synthesis and excretion (Stephenson et al., 2018; Soret et al., 2020; Nababan et al., 2021). That is why fatty liver may be modeled with a choline-deficient diet (Kulinski et al., 2004; Testerink et al., 2009). In a study by Testerink, mutant Chinese hamster ovary cell line MT58 was used containing a thermosensitive mutation in phosphocholine cytidyltransferase (CTP), the regulatory enzyme in the CDP-choline synthesis pathway. MT58 cells had a 50% decrease in PCH level within 24 h when cultured at the nonpermissive temperature, accompanied by an increase in the number of cytosolic lipid droplets (Testerink et al., 2009). In a study by Kulinski, mice were fed a choline-deficient diet (compared with a choline-supplemented diet) for 21 days, and liver triacylglycerol was increased, while plasma apolipoproteins (apo) ¹⁰⁰B and B48 were decreased (Kulinski et al., 2004). There is also evidence that EPLs may influence the intestinal digestion of lipid molecules. For instance, Rampone et al. showed >50% suppression of cholesterol intestinal uptake when incubating it with different dosages of liver lecithin in everted rat gut sacs (Rampone, 1972). Everted rat gut sac model is a standard *in vitro* procedure to study drug absorption (Alam et al., 2012). We investigated these two directions of EPL mode of action as well to develop a unified pharmacodynamic picture.

LIPOLYSIS STIMULATION

PPAR as a Target Molecule for EPLs

Peroxisome proliferator-activated receptors (PPARs) are known to play a huge role in the regulation of energy homeostasis and metabolic functions, including lipid metabolism (Tyagi et al., 2011). These ligand-activated nuclear transcription factors belonging to the large nuclear receptor superfamily are expressed as three isoforms (PPAR α , PPAR β/δ , and PPAR γ). PPAR α is expressed ubiquitously among body tissues with the highest concentration observed in the liver (Liss and Finck, 2017). Its fundamental function is to regulate fatty acids and triglycerides metabolism, beta-oxidation, and ketogenesis (Desvergne and Wahli, 1999). Because of that, PPAR α is of high scientific interest in terms of lipid metabolism correction opportunities (Han et al., 2017a; Han et al., 2017b).

Considering PPAR and fatty liver, Montagner et al., 2016 showed that hepatocyte PPAR α deletion in mice impaired fatty acid catabolism leading to hepatic lipid accumulation even in a fasting state in two steatosis models (Montagner et al., 2016). On the other hand, choline deficiency led to reduced PPAR α expression and consequently to reduced expression of PPAR α -dependent enzymes: ADRP, DGAT2, CPT1a, and FABP4 (Csak et al., 2015). These enzymes are known to be responsible for fatty acid metabolism, VLDL storage, synthesis, and secretion. PPAR α

also regulates beta-oxidation of fatty acids influencing CPT transcription (Mello et al., 2016). In turn, the PCH diet in the fatty liver model led to an increase in CPT activity in rats (Buang et al., 2005). With that in mind, and knowing that PCH may be a potential endogenous ligand for PPAR α (Lamaziere and Wolf, 2010), it is considered a target molecule being affected directly by PCH (Figure 2).

The following studies provided additional data supporting this pathway hypothesis. It was shown that an endogenously synthesized phospholipid can bound to PPAR α isolated from a mouse liver and activate it. Such binding increased under conditions that induce FAS activity and was displaced by systemic injection of a PPAR α agonist. Mass spectrometry identified the species as 1-palmitoyl-2-oleoyl-sn-glycero-3-phosphocholine (16:0/18:1-GPC). Interactions of 16:0/18:1-GPC with the PPAR α ligand-binding domain and co-activator peptide motifs were comparable to those of PPAR α agonists. Portal vein infusion of 16:0/18:1-GPC induced PPAR α -dependent gene expression and decreased hepatic steatosis (Chakravarthy et al., 2009). So, replenishing choline deficiency in the fatty liver with EPLs may stimulate endogenous ligand synthesis to activate PPAR α and, therefore, beta-oxidation of fatty acids in the liver leading to steatosis regression.

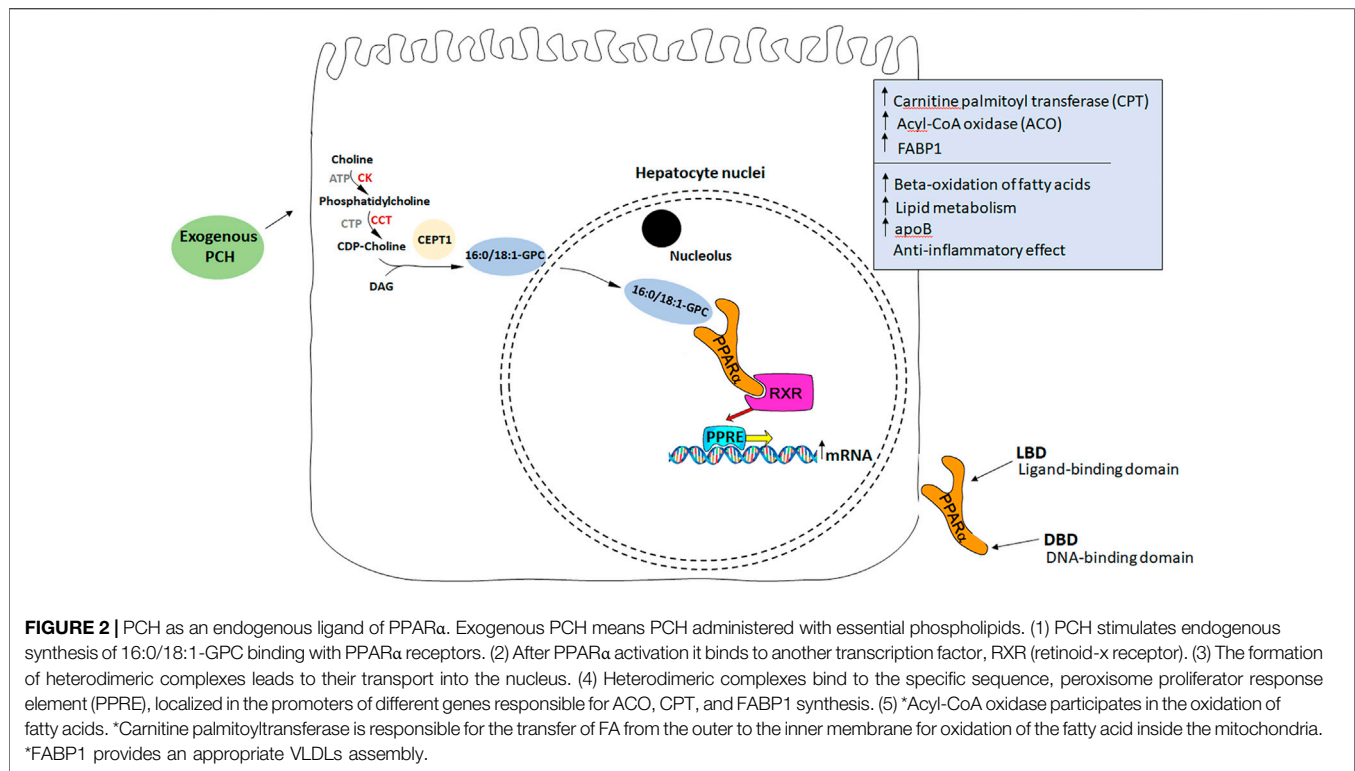
Another interesting observation was made when PCH treatment of myotubes was analyzed. It increased FA uptake and fatty acid-binding protein 3 (FABP3) expression. Remarkably, the effect of PCH on promoting FA utilization in muscles was abolished in PPAR α -null mice and PPAR α -depleted myotubes (Wang et al., 2020).

Thus, improved blood lipid profile in NAFLD patients treated with EPLs may be explained with the effect of PCH not only on the liver PPAR α but also on the muscles PPAR α . We believe that this pharmacodynamic potential requires separate research.

LIPONEOGENESIS INHIBITION

Considering PPAR- δ/γ types, we failed to find consistent data showing that PCH may be an effective agonist of these PPAR subtypes. This is consistent with the data from Chakravarthy et al. (2009). At the same time, it should be mentioned that PCH is not the only molecule potentially influencing PPAR α . The PPAR family is currently one of the key target molecules in terms of NAFLD treatment. For instance, molecules such as lanifibranor and elafibranor are pan-PPAR and PPAR α/δ agonists, respectively. However, a phase III study of elafibranor (RESOLVE-IT, NCT02704403) was terminated due to lack of efficacy, while lanifibranor showed promising results in phase IIb (Francque et al., 2021). There is currently an ongoing phase II lanifibranor study evaluating its effect on liver steatosis (NCT03459079). The results are expected in 2022.

Considering the complexity of PPAR regulation, another promising pathway should be mentioned here, influencing PPAR not directly but via sirtuins: a group of proteins of the silent information regulator two family. Sirtuins are class III histone deacetylases, which is implicated in many cellular and physiological functions, including hepatic glucose and fatty acid



metabolism, mitochondrial function, hepatic gluconeogenesis, insulin secretion, and maturation of fat cells. Seven mammalian sirtuins (SIRT1–SIRT7) have been identified and shown to share the same conserved NAD binding site and catalytic core domain, but with different N and C termini (Nogueiras et al., 2012). SIRT1, 6, and 7 are localized mainly in the nucleus while SIRT3, 4, and 5 are localized in the mitochondrial matrix, and SIRT2 is predominantly cytoplasmic. Decreased expression of SIRT1, SIRT3, SIRT5, and SIRT6 and increased expression of SIRT4 in NAFLD patients compared to the control group was demonstrated. This was associated with increased expression of lipogenic genes including sterol regulatory element-binding protein-1, fatty acid synthase, and acetyl-CoA carboxylase (Wu et al., 2014).

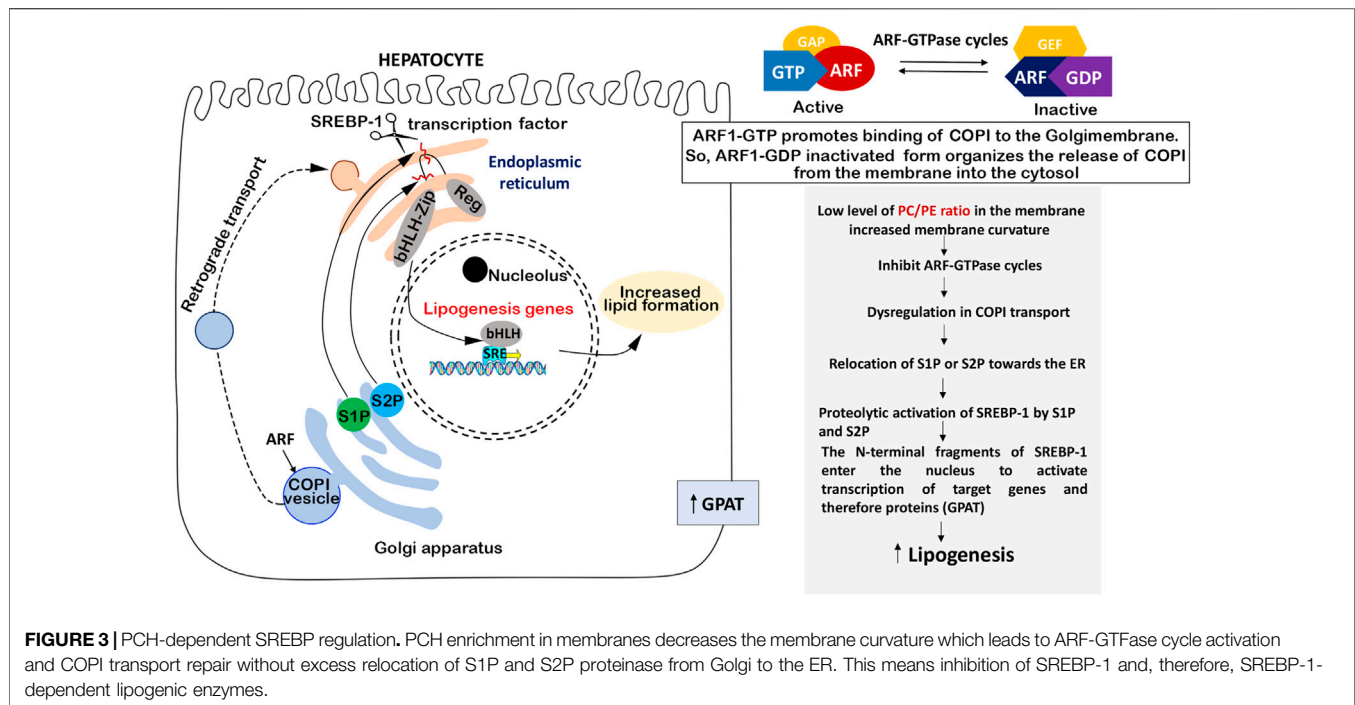
Considering PPAR, it is worth mentioning that SIRT4 modulates the activity of various target substrates involved in fatty acid metabolism and, in particular, suppresses PPAR- α (and beta-oxidation), while SIRT1 and SIRT3 induce fat utilization (Han et al., 2019). SIRT4 also may decrease the amino acid-stimulated insulin secretion by inhibiting the glutamate dehydrogenase activity in pancreatic β -cells (Tarantino et al., 2014). Interestingly, data are suggesting that physical exercises may change the intracellular NAD⁺/NADH ratio and, therefore, alter the activity of some NAD⁺-dependent sirtuins. Considering pharmacotherapeutic agents, current data do not allow us to point at effective agonists/antagonists with the effect supported by clinical findings (Nassir and Ibdah, 2016). This is a new direction of research requiring a better understanding of sirtuin functions, targets, and regulation (Elkhwanky and Hakkola, 2018). We would like to draw the attention of the

readers to some publications in this field, while not intending to cover it comprehensively since it is not the main goal of this review (Xu et al., 2010; Ding et al., 2017).

SREBP-dependent Lipid Accumulation Through the GPAT Activation

Triacylglycerol (TAG) is synthesized in most human cell types through the glycerol phosphate pathway. The first step in this process is the acylation of glycerol-3-phosphate by glycerol-3-phosphate acyltransferase (GPAT). Subsequent steps include fatty acid translocation to lysophosphatidic acid (LPA) by AGPAT (1-acylglycerol-3-phosphate-O-acyltransferase also known as LPA acyltransferase) to form a phosphatide and then diacylglycerol (DAG). The final conversion of DAG into TAG is catalyzed by diacylglycerol acyltransferase (DGAT) (Samuel et al., 2004; Petersen et al., 2007; Liu et al., 2010).

Lipogenesis enzymes regulation is carried out by specific transcription factors. For example, the GPAT enzyme, which plays a primary role in the initiation of TAG synthesis, is regulated at both transcriptional and post-transcriptional levels. Researchers found a 20-fold increase of GPAT1 mRNA in mice liver when resuming a high-carbohydrate diet after fasting (insulin-related stimulation), which was associated with liver lipogenesis activation (Coleman and Lee, 2004). At the same time, SREBP-1c (sterol regulatory element-binding protein 1c) is considered a key transcriptional activation factor of GPAT1. Shown below is how PCH and its membrane concentration may influence SREBP activation and, therefore, GPAT expression and lipogenesis.



SREBPs as a Target for PCH

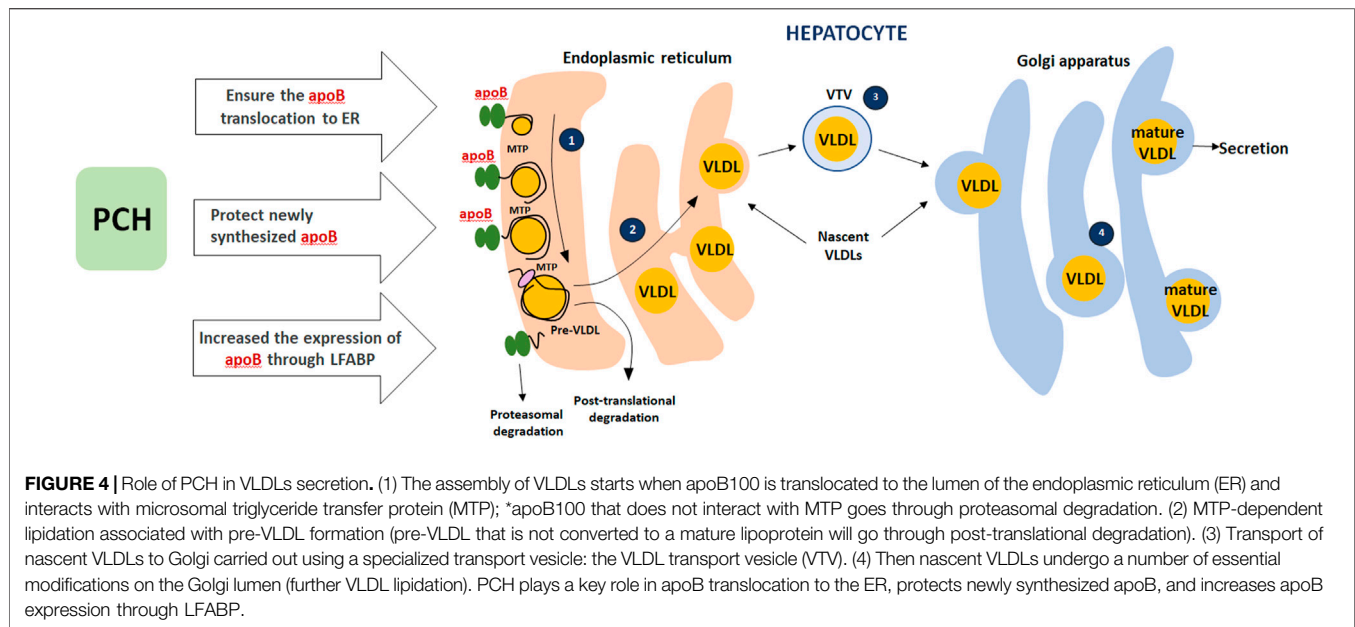
SREBPs (sterol regulatory element-binding proteins) are transcription factors modulating lipid metabolism (Brown and Goldstein, 1997). SREBP-1a and -1c isoforms preferentially regulate genes responsible for the biosynthesis of fatty acids, phospholipids, and TAG, whereas SREBP-2 controls cholesterol metabolism (van der Veen et al., 2017). SREBPs are regulated by digested nutrients: SREBP-2 active form depends on cholesterol levels in the endoplasmic reticulum (Horton et al., 2002), whereas SREBP-1 processing is regulated by the insulin level (Browning and Horton, 2004). Activation of the SREBP-1c isoform leads to the synthesis of enzymes involved in lipogenesis. SREBP-1c overexpression causes FA synthesis, a fourfold increase in fatty acid synthase (FAS) expression, and a 10-fold increase in mtGPAT expression (Shimano et al., 1997; Horton et al., 2002). Thus, SREBPs activate TAG synthesis through the regulation of the GPAT enzyme.

Of note, phospholipids also play an important role in the SREBP-1 regulation of lipogenesis (Dobrosotskaya et al., 2002; Seegmiller et al., 2002; Lim et al., 2011; Walker et al., 2011). Walker et al. found in 2011 that phosphatidylcholine synthesis blocked in *C. elegans*, mouse liver, and human cells led to increased SREBP-1-dependent enzymes transcription and lipid droplet accumulation. In nematode *C. elegans*, reduction of PCH synthesis (via CDP-choline or PEMT pathway inhibition) caused SBP-1 (*C. elegans* ortholog of SREBP) processing and folding enhancement. Increased SREBP-1 processing and enhanced lipogenic genes expression were observed in a mouse model with cytidyltransferase- α (CT α) deficiency and reduced PCH. Thus, we can conclude that SREBP-1 activity depends on PCH level (Walker et al., 2011). Since PCH deficiency models are widely used to induce liver steatosis, this is one of the possible

molecular pathways of its development (Vance et al., 2007; Zeisel, 2008).

The main component of cell membranes is PCH. SREBP-1 activation occurs within the endoplasmic reticulum (ER) and Golgi membranes. It was hypothesized that changes in these membranes could lead to increased SREBP-1 activity (Walker et al., 2011). The PCH/PE ratio is responsible for membrane fluidity and curvature and plays a fundamental role in the regulation of cell metabolism, so depletion of PCH can alter protein transport and lipid accumulation and can be even associated with NAFLD in humans (Testerink et al., 2009; Walker et al., 2011). Thus, changes in PCH levels may alter membrane function leading to SREBP-1 activation (Walker et al., 2011). PCH level can affect the localization of serine protease 1 and 2 (S1P, S2P) localized in the Golgi membrane and necessary to convert the SREBP-1 precursor into an active nuclear transcription factor (Figure 3).

S1P and S2P in Golgi membranes are necessary for SREBP-1 maturing, and its transformation takes place in the ER, so S1P and S2P should be transferred from the Golgi membrane to the ER to activate SREBP-1. S1P and S2P translocation is regulated by COPI-coated transport vesicles, initiated with ADP-ribosylation factor (ARF1). Interestingly, ARF1 is a small GTPase of the Ras superfamily (Kahn and Gilman, 1984) and it may be suppressed by ARF-GTPase repressor (ARF-GAP) in case of the membrane curvature increase caused by a low level of PCH in the membrane (Dobrosotskaya et al., 2002; Seegmiller et al., 2002). In several models, it was shown that blocked ARF1 led to active SREBP-1 nuclear accumulation. So, active SREBP-1 nuclear accumulation takes place in the case of low PCH level through the following mechanism: low PCH level increases the membrane curvature which may affect ARF signaling, deregulate



COPI transport, and shift the distribution of S1P or S2P toward the ER, where they cleave and activate SREBP-1 (Walker et al., 2011). Another important thing is that the PCH-mediated SREBP activation mechanism is not affected by SREBP-2 activation (Walker et al., 2011). This means that PCH does not interfere with cholesterol metabolism and does not block its metabolic pathways.

Considering all the above, we can conclude that replenishing PCH deficiency can normalize the PCH/PE ratio and SREBP-1 activity and, therefore, suppress the synthesis of fatty acids and prevent the accumulation of fat in the liver.

FATTY ACIDS AND TG SECRETION/EVACUATION

PCH appears to ensure the translocation of apoB (apolipoprotein B) from the cytosol to the lumen of the endoplasmic reticulum. This part of the modification is crucial in the early stages of VLDL assembly. Appropriate choline level protects newly synthesized apoB from intracellular degradation during the migration of apoB from the ER to the Golgi apparatus. PCH as an appropriate PPAR α ligand increases the expression and biosynthesis of liver fatty acid-binding protein (LFABP). High expression of FABP1 isoform increases the expression of apoB-100, thus ensuring correct assembly of VLDL in the ER lumen (Olofsson and Borén, 2012; Tiwari and Siddiqi, 2012). This PCH mode of action was not considered the leading one since EPLs lead to steatosis regression in the liver and blood lipid profile improvement with TG, total cholesterol, VLDL, and LDL decrease and HDL increase both in animal models and clinical studies (Gonciarz et al., 1988; Li et al., 2000; Yin, 2000; Wu, 2009; Sas et al., 2013; Maev et al., 2020a, Maev et al., 2020b; Popovic and Dajani, 2020). At the same time, taking into account the PPAR section of our paper, this effect matches PPAR α activation in

muscles and fatty acids uptake. These may work together and contribute to the fatty acids/TG-enriched lipoproteins elimination from the blood and subsequent utilization in tissues (PPARs as metabolic regulators in the liver: Lessons from liver-specific PPAR-null mice). The potential mechanism is presented in **Figure 4**.

DIGESTION OF DIETARY FATTY ACIDS, TG, AND CHOLESTEROL

Rampone et al. showed >50% suppression of cholesterol intestinal digestion when incubating it with lecithin in everted rat gut sacs (Rampone, 1972). Several other studies also add to our understanding of the potential PCH effect on fatty molecules digestion. For instance, it was shown that egg sphingomyelin dose-dependently reduced lymphatic cholesterol concentration in rats (Noh and Koo, 2003; Noh and Koo, 2004). When given orally, it significantly reduced plasma triglyceride and cholesterol levels in mice fed a Western-type diet (Duivenvoorden et al., 2006). Surprisingly, in a study by Noh et al. this effect was more prominent with saturated fatty acids in the PCH tail. Several studies in humans showed a similar effect of phospholipids on cholesterol digestion suppression (Beil and Grundy, 1980; Greten et al., 1980; Kesaniemi and Grundy, 1986). Existing data on the inhibitory effect of phospholipids on cholesterol absorption are well summarized elsewhere (Cohn et al., 2010). However, to reproduce this mechanism of action in clinical practice, a huge dose of PCH (at least 10 g daily) seems to be required. Possible mechanisms for the inhibition of cholesterol absorption by phospholipids have already been presented by Cohn et al. (2008):

- 1) Excess PCH interferes with efficient micellar PL hydrolysis: a prerequisite for mucosal uptake of cholesterol.

- 2) PCH surplus alters the physicochemical properties of mixed micelles (i.e., their size, composition, and/or biological characteristics) resulting in reduced absorption of cholesterol.
- 3) PCH affects the membrane characteristics of enterocytes or has a direct effect on cellular cholesterol transporters that regulate intestinal cholesterol uptake.

CONCLUSION

Four possible mechanisms of PCH-induced steatosis regression showed both *in vivo* (Buang et al., 2005; Lee et al., 2014) and in clinical studies (Gundermann et al., 2016; Maev et al., 2020b; Popovic and Dajani, 2020) are discussed and the following are considered as relevant:

- 1) Stimulation of fatty acids beta-oxidation in hepatocytes (through PPAR α and PPAR-dependent enzymes: acyl-CoA oxidase and carnitine palmitoyltransferase)
- 2) Liponeogenesis inhibition in hepatocytes (through SRBEP-1 and SRBEP-dependent enzymes, mainly glycerol-3-phosphate acyltransferase)
- 3) Fatty acids evacuation followed by their uptake and utilization in muscles (through the role of PCH both in VLDL formation and evacuation and the PPAR α activation in the muscles)

Of course, this concept requires further *in vitro* and *in vivo* testing to obtain a true picture of the PCH mode of action in

clinical practice. We believe that these data contribute to a better understanding of the clinical effect of EPLs and may help design further studies in this field. It is even more important considering the new MAFLD concept and steatosis as a universal phenotypical sign of metabolic disorder in the liver that should be diagnosed and treated.

AUTHOR CONTRIBUTIONS

KS came up with the idea for the paper; DO and KK performed the literature search and primary data analysis and drafted the manuscript; DO was responsible for visualization; KK performed data consolidation; KS critically revised the work for important intellectual content; all the authors substantially contributed to the concept and design of the paper and interpreted the relevant literature; LL, EG, and CP are experts in gastroenterology, a key clinical field of essential phospholipids usage, while AD and SO are experts in molecular pharmacology and nutraceuticals, respectively. All the authors have read and approved the final version of the manuscript.

FUNDING

The medical writing support was provided by Ligand Research LLC, Russia, and was funded by Sanofi-Aventis.

REFERENCES

- Adams, L. A., and Ratziu, V. (2015). Non-Alcoholic Fatty Liver - Perhaps Not So Benign. *J. Hepatol.* 62, 1002–1004. doi:10.1016/j.jhep.2015.02.005
- Alam, M. A., Al-Jenoobi, F. I., and Al-mohizea, A. M. (2012). Everted Gut Sac Model as a Tool in Pharmaceutical Research: Limitations and Applications. *J. Pharm. Pharmacol.* 64, 326–336. doi:10.1111/j.2042-7158.2011.01391.x
- Arvind, N., Savaikar, P., and Rajkumar, J. (2006). Therapy for NAFLD - A Comparative Study of Essential Phospholipids vs. Ursodeoxycholic Acid. *Ind. J. Clin. Pr* 16, 21–24.
- Beil, F. U., and Grundy, S. M. (1980). Studies on Plasma Lipoproteins during Absorption of Exogenous Lecithin in Man. *J. Lipid Res.* 21, 525–536. Available at: <http://www.ncbi.nlm.nih.gov/pubmed/7400685>. doi:10.1016/s0022-2275(20)42223-0
- Brown, M. S., and Goldstein, J. L. (1997). The SREBP Pathway: Regulation of Cholesterol Metabolism by Proteolysis of a Membrane-Bound Transcription Factor. *Cell* 89 (3), 331–340. doi:10.1016/S0092-8674(00)80213-5
- Browning, J. D., and Horton, J. D. (2004). Molecular Mediators of Hepatic Steatosis and Liver Injury. *J. Clin. Invest.* 114 (2), 147–152. doi:10.1172/jci22422
- Buang, Y., Wang, Y.-M., Cha, J.-Y., Nagao, K., and Yanagita, T. (2005). Dietary Phosphatidylcholine Alleviates Fatty Liver Induced by Orotic Acid. *Nutrition* 21, 867–873. doi:10.1016/j.nut.2004.11.019
- Byrne, C. D., and Targher, G. (2015). NAFLD: A Multisystem Disease. *J. Hepatol.* 62, S47–S64. doi:10.1016/j.jhep.2014.12.012
- Cai, D., Yuan, M., Frantz, D. F., Melendez, P. A., Hansen, L., Lee, J., et al. (2005). Local and Systemic Insulin Resistance Resulting from Hepatic Activation of IKK- β and NF-Kb. *Nat. Med.* 11, 183–190. doi:10.1038/nm1166
- Carr, R. M., Oranu, A., and Khungar, V. (2016). Nonalcoholic Fatty Liver Disease: Pathophysiology and Management. *Gastroenterol. Clin. North America* 45, 639–652. doi:10.1016/j.gtc.2016.07.003
- Chakravarthy, M. V., Lodhi, I. J., Yin, L., Malapaka, R. R., Xu, H. E., Turk, J., et al. (2009). Identification of a Physiologically Relevant Endogenous Ligand for PPAR α in Liver. *Cell* 138, 476–488. doi:10.1016/j.cell.2009.05.036
- Chen, Z., Yu, R., Xiong, Y., Du, F., and Zhu, S. (2017). A Vicious circle between Insulin Resistance and Inflammation in Nonalcoholic Fatty Liver Disease. *Lipids Health Dis.* 16, 203. doi:10.1186/s12944-017-0572-9
- Choudhary, N. S., Saraf, N., Saigal, S., Gautam, D., Lipi, L., Rastogi, A., et al. (2015). Rapid Reversal of Liver Steatosis with Life Style Modification in Highly Motivated Liver Donors. *J. Clin. Exp. Hepatol.* 5, 123–126. doi:10.1016/j.jceh.2015.04.002
- Cohn, J. S., Kamili, A., Wat, E., Chung, R. W., and Tandy, S. (2010). Dietary Phospholipids and Intestinal Cholesterol Absorption. *Nutrients* 2, 116–127. doi:10.3390/nu2020116
- Cohn, J. S., Wat, E., Kamili, A., and Tandy, S. (2008). Dietary Phospholipids, Hepatic Lipid Metabolism and Cardiovascular Disease. *Curr. Opin. Lipidol.* 19, 257–262. doi:10.1097/MOL.0b013e3282ffaf96
- Coleman, R. A., and Lee, D. P. (2004). Enzymes of Triacylglycerol Synthesis and Their Regulation. *Prog. Lipid Res.* 43 (2), 134–176. doi:10.1016/S0163-7827(03)00051-1
- Csak, T., Bala, S., Lippai, D., Kodys, K., Catalano, D., Iracheta-Vellve, A., et al. (2015). MicroRNA-155 Deficiency Attenuates Liver Steatosis and Fibrosis without Reducing Inflammation in a Mouse Model of Steatohepatitis. *PLoS One* 10, e0129251. doi:10.1371/journal.pone.0129251
- Dajani, A. I., Abu Hammour, A. M., Zakaria, M. A., Al Jaberi, M. R., Nounou, M. A., and Semrin, A. I. (2015). Essential Phospholipids as a Supportive Adjunct in the Management of Patients with NAFLD. *Arab J. Gastroenterol.* 16, 99–104. doi:10.1016/j.ajg.2015.09.001
- Dajani, A. I., and Popovic, B. (2020). Essential Phospholipids for Nonalcoholic Fatty Liver Disease Associated with Metabolic Syndrome: A Systematic Review and Network Meta-Analysis. *World J. Clin. Cases* 8, 5235–5249. doi:10.12998/wjcc.v8.i21.5235

- Desvergne, B., and Wahli, W. (1999). Peroxisome Proliferator-Activated Receptors: Nuclear Control of Metabolism. *Endocr. Rev.* 20, 649–688. doi:10.1210/er.20.5.649
- Di Mauro, S., Ragusa, M., Urbano, F., Filippello, A., Di Pino, A., Scamporrino, A., et al. (2016). Intracellular and Extracellular miRNome Deregulation in Cellular Models of NAFLD or NASH: Clinical Implications. *Nutr. Metab. Cardiovasc. Dis.* 26, 1129–1139. doi:10.1016/j.numecd.2016.08.004
- Ding, R. B., Bao, J., and Deng, C. X. (2017). Emerging Roles of SIRT1 in Fatty Liver Diseases. *Int. J. Biol. Sci.* 13, 852–867. doi:10.7150/ijbs.19370
- Dobrosotskaya, I. Y., Seegmiller, A. C., Brown, M. S., Goldstein, J. L., and Rawson, R. B. (2002). Regulation of SREBP Processing and Membrane Lipid Production by Phospholipids in *Drosophila*. *Science* 296, 879–883. doi:10.1126/science.1071124
- Duivenvoorden, I., Voshol, P. J., Rensen, P. C., van Duyvenvoorde, W., Romijn, J. A., Emeis, J. J., et al. (2006). Dietary Sphingolipids Lower Plasma Cholesterol and Triacylglycerol and Prevent Liver Steatosis in APOE*3Leiden Mice. *Am. J. Clin. Nutr.* 84, 312–321. doi:10.1093/ajcn/84.1.312
- Elkhwanky, M. S., and Hakkola, J. (2018). Extranuclear Sirtuins and Metabolic Stress. *Antioxid. Redox Signal.* 28, 662–676. doi:10.1089/ars.2017.7270
- Fildes, A., Charlton, J., Rudisill, C., Littlejohns, P., Prevost, A. T., and Gulliford, M. C. (2015). Probability of an Obese Person Attaining normal Body Weight: Cohort Study Using Electronic Health Records. *Am. J. Public Health* 105, e54–e59. doi:10.2105/AJPH.2015.302773
- Francque, S. M., Bedossa, P., Ratzu, V., Anstee, Q. M., Bugianesi, E., Sanyal, A. J., et al. (2021). A Randomized, Controlled Trial of the Pan-PPAR Agonist Lanifibranor in NASH. *N. Engl. J. Med.* 385, 1547–1558. doi:10.1056/NEJMoa2036205
- Francque, S., and Vonghia, L. (2019). Pharmacological Treatment for Non-Alcoholic Fatty Liver Disease. *Adv. Ther.* 36, 1052–1074. doi:10.1007/s12325-019-00898-6
- Friedman, S. L., Ratzu, V., Harrison, S. A., Abdelmalek, M. F., Aithal, G. P., Caballeria, J., et al. (2018). A Randomized, Placebo-Controlled Trial of Cenicriviroc for Treatment of Nonalcoholic Steatohepatitis with Fibrosis. *Hepatology* 67, 1754–1767. doi:10.1002/hep.29477
- Gonciarz, Z., Besser, P., Lelek, E., Gundermann, K. J., and Johannes, K. J. (1988). Randomised Placebo-Controlled Double Blind Trial on “Essential” Phospholipids in the Treatment of Fatty Liver Associated with Diabetes. *Med. Chir. Dig.* 17, 61–65.
- Greten, H., Raetzer, H., Stiehl, A., and Schettler, G. (1980). The Effect of Polyunsaturated Phosphatidylcholine on Plasma Lipids and Fecal Sterol Excretion. *Atherosclerosis* 36, 81–88. doi:10.1016/0021-9150(80)90201-4
- Gundermann, K. J., Kuenker, A., Kuntz, E., and Drożdżik, M. (2011). Activity of Essential Phospholipids (EPL) from Soybean in Liver Diseases. *Pharmacol. Rep.* 63, 643–659. doi:10.1016/S1734-1140(11)70576-X
- Gundermann, K. J., Gundermann, S., Drożdżik, M., and Mohan Prasad, V. G. (2016). Essential Phospholipids in Fatty Liver: A Scientific Update. *Clin. Exp. Gastroenterol.* 9, 105–117. doi:10.2147/CEG.S96362
- Han, L., Shen, W. J., Bittner, S., Kraemer, F. B., and Azhar, S. (2017a). PPARs: Regulators of Metabolism and as Therapeutic Targets in Cardiovascular Disease. Part I: PPAR- α . *Future Cardiol.* 13, 259–278. doi:10.2217/fca-2016-0059
- Han, L., Shen, W.-J., Bittner, S., Kraemer, F. B., and Azhar, S. (2017b). PPARs: Regulators of Metabolism and as Therapeutic Targets in Cardiovascular Disease. Part II: PPAR- β/δ and PPAR- γ . *Future Cardiol.* 13, 279–296. doi:10.2217/fca-2017-0019
- Han, Y., Zhou, S., Coetzee, S., and Chen, A. (2019). SIRT4 and its Roles in Energy and Redox Metabolism in Health, Disease and during Exercise. *Front. Physiol.* 10, 1006. doi:10.3389/fphys.2019.01006
- Holmer, M., Melum, E., Isoniemi, H., Ericzon, B.-G., Castedal, M., Nordin, A., et al. (2017). NAFLD as an Indication for Liver Transplantation in the Nordic Countries - a Cohort Study during 1982–2015. *J. Hepatol.* 66, S421–S422. doi:10.1016/s0168-8278(17)31205-9
- Horton, J. D., Goldstein, J. L., and Brown, M. S. (2002). SREBPs: Activators of the Complete Program of Cholesterol and Fatty Acid Synthesis in the Liver. *J. Clin. Invest.* 109 (9), 1125–1131. doi:10.1172/jci15593
- Kahn, R. A., and Gilman, A. G. (1984). Purification of a Protein Cofactor Required for ADP-Ribosylation of the Stimulatory Regulatory Component of Adenylate Cyclase by Cholera Toxin. *J. Biol. Chem.* 259 (10), 6228–6234.
- Kesaniemi, Y. A., and Grundy, S. M. (1986). Effects of Dietary Polyenylphosphatidylcholine on Metabolism of Cholesterol and Triglycerides in Hypertriglyceridemic Patients. *Am. J. Clin. Nutr.* 43, 98–107. doi:10.1093/ajcn/43.1.98
- Kim, J. K., Michael, M. D., Previs, S. F., Peroni, O. D., Mauvais-Jarvis, F., Neschen, S., et al. (2000). Redistribution of Substrates to Adipose Tissue Promotes Obesity in Mice with Selective Insulin Resistance in Muscle. *J. Clin. Invest.* 105, 1791–1797. doi:10.1172/JCI8305
- Kotani, K., Peroni, O. D., Minokoshi, Y., Boss, O., and Kahn, B. B. (2004). GLUT4 Glucose Transporter Deficiency Increases Hepatic Lipid Production and Peripheral Lipid Utilization. *J. Clin. Invest.* 114, 1666–1675. doi:10.1172/JCI21341
- Kulinski, A., Vance, D. E., and Vance, J. E. (2004). A Choline-Deficient Diet in Mice Inhibits Neither the CDP-Choline Pathway for Phosphatidylcholine Synthesis in Hepatocytes Nor Apolipoprotein B Secretion. *J. Biol. Chem.* 279, 23916–23924. doi:10.1074/jbc.M312676200
- Lamaziere, A., and Wolf, C. (2010). Phosphatidylcholine et PPAR α : une connexion appropriée dans une maladie du foie? *Gastroenterol. Clin. Biol.* 34, 250–251. doi:10.1016/j.gcb.2010.02.005
- Lavine, J. E., Schwimmer, J. B., Van Natta, M. L., Molleston, J. P., Murray, K. F., Rosenthal, P., et al. (2011). Effect of Vitamin E or Metformin for Treatment of Nonalcoholic Fatty Liver Disease in Children and Adolescents: The TONIC Randomized Controlled Trial. *JAMA* 305, 1659–1668. doi:10.1001/jama.2011.520
- Lee, H. S., Nam, Y., Chung, Y. H., Kim, H. R., Park, E. S., Chung, S. J., et al. (2014). Beneficial Effects of Phosphatidylcholine on High-Fat Diet-Induced Obesity, Hyperlipidemia and Fatty Liver in Mice. *Life Sci.* 118, 7–14. doi:10.1016/j.lfs.2014.09.027
- Li, J.-H., Zhong, C.-F., and Min, J. (2000). A Randomized Controlled Study of Essential Phospholipids in the Treatment of Fatty Liver. *Infect. Dis. Inf.* 13, 180–181.
- Lim, H.-Y., Wang, W., Wessells, R. J., Ocorr, K., and Bodmer, R. (2011). Phospholipid Homeostasis Regulates Lipid Metabolism and Cardiac Function through SREBP Signaling in *Drosophila*. *Genes Dev.* 25, 189–200. doi:10.1101/gad.1992411
- Liss, K. H. H., and Finck, B. N. (2017). PPARs and Nonalcoholic Fatty Liver Disease. *Biochimie* 136, 65–74. doi:10.1016/j.biochi.2016.11.009
- Liu, Q., Bengmark, S., and Qu, S. (2010). The Role of Hepatic Fat Accumulation in Pathogenesis of Non-alcoholic Fatty Liver Disease (NAFLD). *Lipids Health Dis.* 9, 42. doi:10.1186/1476-511X-9-42
- Maev, I. V., Samsonov, A. A., Palgova, L. K., Pavlov, C. S., Vovk, E. I., Shirokova, E. N., et al. (2020b). Effectiveness of Phosphatidylcholine in Alleviating Steatosis in Patients with Non-Alcoholic Fatty Liver Disease and Cardiometabolic Comorbidities (MANPOWER Study). *BMJ Open Gastroenterol.* 7, e000341. doi:10.1136/bmjgast-2019-000341
- Maev, I. V., Samsonov, A. A., Palgova, L. K., Pavlov, C. S., Shirokova, E. N., Vovk, E. I., et al. (2020a). Effectiveness of Phosphatidylcholine as Adjunctive Therapy in Improving Liver Function Tests in Patients with Non-alcoholic Fatty Liver Disease and Metabolic Comorbidities: Real-Life Observational Study from Russia. *BMJ Open Gastroenterol.* 7, e000368. doi:10.1136/bmjgast-2019-000368
- Mello, T., Materozzi, M., and Galli, A. (2016). PPARs and Mitochondrial Metabolism: From NAFLD to HCC. *PPAR Res.* 2016, 7403230. doi:10.1155/2016/7403230
- Montagner, A., Polizzi, A., Fouché, E., Ducheix, S., Lippi, Y., Lasserre, F., et al. (2016). Liver PPAR α Is Crucial for Whole-Body Fatty Acid Homeostasis and Is Protective against NAFLD. *Gut* 65, 1202–1214. doi:10.1136/gutjnl-2015-310798
- Nababan, S. H. H., Khairunissa, S. T., Erfan, E., Nafrialdi, N., Krisnuhoni, E., Hasan, I., et al. (2021). Choline-Deficient High-Fat Diet-Induced Steatohepatitis in BALB/c Mice. *Mol. Cel. Biomed. Sci.* 5, 74. doi:10.21705/mcbs.v5i2.193
- Nassir, F., and Ibdah, J. A. (2016). Sirtuins and Nonalcoholic Fatty Liver Disease. *World J. Gastroenterol.* 22, 10084–10092. doi:10.3748/wjg.v22.i46.10084
- Nassir, F., Rector, R. S., Hammoud, G. M., and Ibdah, J. A. (2015). Pathogenesis and Prevention of Hepatic Steatosis. *Gastroenterol. Hepatol. (N Y)* 11, 167–175.
- Nogueiras, R., Habegger, K. M., Chaudhary, N., Finan, B., Banks, A. S., Dietrich, M. O., et al. (2012). Sirtuin 1 and Sirtuin 3: Physiological Modulators of Metabolism. *Physiol. Rev.* 92, 1479–1514. doi:10.1152/physrev.00022.2011
- Noh, S. K., and Koo, S. I. (2003). Egg Sphingomyelin Lowers the Lymphatic Absorption of Cholesterol and Alpha-Tocopherol in Rats. *J. Nutr.* 133, 3571–3576. doi:10.1093/jn/133.11.3571

- Noh, S. K., and Koo, S. I. (2004). Milk Sphingomyelin Is More Effective Than Egg Sphingomyelin in Inhibiting Intestinal Absorption of Cholesterol and Fat in Rats. *J. Nutr.* 134, 2611–2616. doi:10.1093/jn/134.10.2611
- Olofsson, S. O., and Borén, J. (2012). Apolipoprotein B Secretory Regulation by Degradation. *Arterioscler. Thromb. Vasc. Biol.* 32, 1334–1338. doi:10.1161/ATVBAHA.112.251116
- Pepeu, G., Vannucchi, M. G., and Di Patre, P. L. (1990). "Pharmacological Actions of Phospholipids," in *Phospholipids* (Boston, MA: Springer US), 43–50. doi:10.1007/978-1-4757-1364-0_3
- Petersen, K. F., Dufour, S., Savage, D. B., Bilz, S., Solomon, G., Yonemitsu, S., et al. (2007). The Role of Skeletal Muscle Insulin Resistance in the Pathogenesis of the Metabolic Syndrome. *Proc. Natl. Acad. Sci. U S A.* 104, 12587–12594. doi:10.1073/pnas.0705408104
- Rampone, A. J. (1972). The Effects of Bile Salt and Raw Bile on the Intestinal Absorption of Micellar Fatty Acid in the Rat *In Vitro*. *J. Physiol.* 222, 679–690. doi:10.1113/jphysiol.1972.sp009821
- Ratzliff, V., Sanyal, A. J., Loomba, R., Rinella, M., Harrison, S., Anstee, Q. M., et al. (2019). REGENERATE: Design of a Pivotal, Randomised, Phase 3 Study Evaluating the Safety and Efficacy of Obeticholic Acid in Patients with Fibrosis Due to Nonalcoholic Steatohepatitis. *Contemp. Clin. Trials* 84, 105803. doi:10.1016/j.cct.2019.06.017
- Samuel, V. T., Liu, Z. X., Qu, X., Elder, B. D., Bilz, S., Befroy, D., et al. (2004). Mechanism of Hepatic Insulin Resistance in Non-Alcoholic Fatty Liver Disease. *J. Biol. Chem.* 279, 32345–32353. doi:10.1074/jbc.M313478200
- Sanyal, A. J., Chalasani, N., Kowdley, K. V., McCullough, A., Diehl, A. M., Bass, N. M., et al. (2010). Pioglitazone, Vitamin E, or Placebo for Nonalcoholic Steatohepatitis. *N. Engl. J. Med.* 362, 1675–1685. doi:10.1056/NEJMoa0907929
- Sas, E., Grinevich, V., Efimov, O., and Shcherbina, N. (2013). Beneficial Influence of Polyunsaturated Phosphatidylcholine Enhances Functional Liver Condition and Liver Structure in Patients with Nonalcoholic Steatohepatitis. Results of Prolonged Randomized Blinded Prospective Clinical Study. *J. Hepatol.* 58 (Suppl. 1), S549. doi:10.1016/s0168-8278(13)61365-3
- Seegmiller, A. C., Dobrosotskaya, I., Goldstein, J. L., Ho, Y. K., Brown, M. S., and Rawson, R. B. (2002). The SREBP Pathway in *Drosophila*: Regulation by Palmitate, Not Sterols. *Dev. Cell* 2 (2), 229–238. doi:10.1016/S1534-5807(01)00119-8
- Shimano, H., Horton, J. D., Shimomura, I., Hammer, R. E., Brown, M. S., and Goldstein, J. L. (1997). Isoform 1c of Sterol Regulatory Element Binding Protein Is Less Active Than Isoform 1a in Livers of Transgenic Mice and in Cultured Cells. *J. Clin. Invest.* 99, 846–854. doi:10.1172/JCI119248
- Soret, P.-A., Magusto, J., Housset, C., and Gautheron, J. (2020). *In Vitro* and *In Vivo* Models of Non-Alcoholic Fatty Liver Disease: A Critical Appraisal. *J. Clin. Med.* 10, 36. doi:10.3390/jcm10010036
- Stephenson, K., Kennedy, L., Hargrove, L., Demieville, J., Thomson, J., Alpini, G., et al. (2018). Updates on Dietary Models of Nonalcoholic Fatty Liver Disease: Current Studies and Insights. *Gene Expr.* 18, 5–17. doi:10.3727/105221617X15093707969658
- Tana, C., Ballestri, S., Ricci, F., Di Vincenzo, A., Ticinesi, A., Gallina, S., et al. (2019). Cardiovascular Risk in Non-Alcoholic Fatty Liver Disease: Mechanisms and Therapeutic Implications. *Int. J. Environ. Res. Public Health* 16, 3104. doi:10.3390/ijerph16173104
- Tarantino, G., Finelli, C., Scopacasa, F., Pisanisi, F., Contaldo, F., Capone, D., et al. (2014). Circulating Levels of Sirtuin 4, a Potential Marker of Oxidative Metabolism, Related to Coronary Artery Disease in Obese Patients Suffering from NAFLD, with Normal or Slightly Increased Liver Enzymes. *Oxidative Med. Cell Longevity* 2014, 1–10. doi:10.1155/2014/920676
- Testerink, N., van der Sanden, M. H. M., Houweling, M., Helms, J. B., and Vaandrager, A. B. (2009). Depletion of Phosphatidylcholine Affects Endoplasmic Reticulum Morphology and Protein Traffic at the Golgi Complex. *J. Lipid Res.* 50, 2182–2192. doi:10.1194/jlr.M800660-JLR200
- Tiwari, S., and Siddiqi, S. A. (2012). Intracellular Trafficking and Secretion of VLDL. *Arterioscler. Thromb. Vasc. Biol.* 32, 1079–1086. doi:10.1161/ATVBAHA.111.241471
- Tyagi, S., Sharma, S., Gupta, P., Saini, A., and Kaushal, C. (2011). The Peroxisome Proliferator-Activated Receptor: A Family of Nuclear Receptors Role in Various Diseases. *J. Adv. Pharm. Tech. Res.* 2, 236. doi:10.4103/2231-4040.90879
- van der Veen, J. N., Kennelly, J. P., Wan, S., Vance, J. E., Vance, D. E., and Jacobs, R. L. (2017). The Critical Role of Phosphatidylcholine and Phosphatidylethanolamine Metabolism in Health and Disease. *Biochim. Biophys. Acta (Bba) - Biomembranes* 1859, 1558–1572. doi:10.1016/j.bbmem.2017.04.006
- Van Hoogevest, P., and Wendel, A. (2014). The Use of Natural and Synthetic Phospholipids as Pharmaceutical Excipients. *Eur. J. Lipid Sci. Technol.* 116, 1088–1107. doi:10.1002/ejlt.201400219
- Vance, D. E., Li, Z., and Jacobs, R. L. (2007). Hepatic Phosphatidylethanolamine N-Methyltransferase, Unexpected Roles in Animal Biochemistry and Physiology. *J. Biol. Chem.* 282, 33237–33241. doi:10.1074/jbc.R700028200
- Walker, A. K., Jacobs, R. L., Watts, J. L., Rottiers, V., Jiang, K., Finnegan, D. M., et al. (2011). A Conserved SREBP-1/phosphatidylcholine Feedback Circuit Regulates Lipogenesis in Metazoans. *Cell* 147, 840–852. doi:10.1016/j.cell.2011.09.045
- Wang, Y., Nakajima, T., Gonzalez, F. J., and Tanaka, N. (2020). PPARs as Metabolic Regulators in the Liver: Lessons from Liver-specific PPAR-Null Mice. *Int. J. Mol. Sci.* 21 (6), 2061. doi:10.3390/ijms21062061
- Wu, T., Liu, Y. H., Fu, Y. C., Liu, X. M., and Zhou, X. H. (2014). Direct Evidence of Sirtuin Downregulation in the Liver of Non-alcoholic Fatty Liver Disease Patients. *Ann. Clin. Lab. Sci.* 44, 410–418.
- Wu, Y. (2009). Efficacy Analysis of Polyene Phosphatidylcholine for Type 2 Diabetes Complicated with Fatty Liver. *J. TCM Univ. Hunan* 29, 41–42.
- Xia, M. F., Bian, H., and Gao, X. (2019). NAFLD and Diabetes: Two Sides of the Same Coin? Rationale for Gene-Based Personalized NAFLD Treatment. *Front. Pharmacol.* 10, 877. doi:10.3389/fphar.2019.00877
- Xu, F., Gao, Z., Zhang, J., Rivera, C. A., Yin, J., Weng, J., et al. (2010). Lack of SIRT1 (Mammalian Sirtuin 1) Activity Leads to Liver Steatosis in the SIRT1+/- Mice: A Role of Lipid Mobilization and Inflammation. *Endocrinology* 151, 2504–2514. doi:10.1210/en.2009-1013
- Yin, D. K. L. (2000). Observation for Curative Effect of Essentiale in Treatment of Fatty Liver Caused by Diabetes Mellitus. *Med. J. Q. Ilu* 15, 277–278.
- Younossi, Z. M., Ratzliff, V., Loomba, R., Rinella, M., Anstee, Q. M., Goodman, Z., et al. (2019). Obeticholic Acid for the Treatment of Non-alcoholic Steatohepatitis: Interim Analysis from a Multicentre, Randomised, Placebo-Controlled Phase 3 Trial. *Lancet* 394, 2184–2196. doi:10.1016/S0140-6736(19)33041-7
- Younossi, Z. M., Stepanova, M., Afendy, M., Fang, Y., Younossi, Y., Mir, H., et al. (2011). Changes in the Prevalence of the Most Common Causes of Chronic Liver Diseases in the United States from 1988 to 2008. *Clin. Gastroenterol. Hepatol.* 9, 524–e60. doi:10.1016/j.cgh.2011.03.020
- Zeisel, S. H. (2008). Genetic Polymorphisms in Methyl-Group Metabolism and Epigenetics: Lessons from Humans and Mouse Models. *Brain Res.* 1237, 5–11. doi:10.1016/j.brainres.2008.08.059
- Zhou, Y. J., Li, Y. Y., Nie, Y. Q., Huang, C. M., and Cao, C. Y. (2012). Natural Course of Nonalcoholic Fatty Liver Disease in Southern China: A Prospective Cohort Study. *J. Dig. Dis.* 13, 153–160. doi:10.1111/j.1751-2980.2011.00571.x

Conflict of Interest: KS is a Sanofi employee.

The remaining authors declare that the research was conducted in the absence of any commercial or financial relationships that could be construed as a potential conflict of interest.

Publisher's Note: All claims expressed in this article are solely those of the authors and do not necessarily represent those of their affiliated organizations, or those of the publisher, the editors, and the reviewers. Any product that may be evaluated in this article, or claim that may be made by its manufacturer, is not guaranteed or endorsed by the publisher.

Copyright © 2022 Osipova, Kokoreva, Lazebnik, Golovanova, Pavlov, Dukhanin, Orlova and Starostin. This is an open-access article distributed under the terms of the Creative Commons Attribution License (CC BY). The use, distribution or reproduction in other forums is permitted, provided the original author(s) and the copyright owner(s) are credited and that the original publication in this journal is cited, in accordance with accepted academic practice. No use, distribution or reproduction is permitted which does not comply with these terms.



Elevated Serum Regulator of Calcineurin 2 is Associated With an Increased Risk of Non-Alcoholic Fatty Liver Disease

Xia Fang^{1,2,3,4†}, Hongya Wang^{1,2,3,4†}, Xiaozhen Tan^{1,2,3,4}, Ting Ye⁵, Yong Xu^{1,2,3,4*} and Jiahao Fan^{6*†}

¹Department of Endocrinology and Metabolism, The Affiliated Hospital of Southwest Medical University, Luzhou, China, ²Metabolic Vascular Disease Key Laboratory of Sichuan Province, Luzhou, China, ³Sichuan Clinical Research Center for Nephropathy, Luzhou, China, ⁴Cardiovascular and Metabolic Diseases Key Laboratory of Luzhou, Luzhou, China, ⁵Department of Laboratory Medicine, The Affiliated Hospital of Southwest Medical University, Luzhou, China, ⁶Department of Gastroenterology, The Affiliated Hospital of Southwest Medical University, Luzhou, China

OPEN ACCESS

Edited by:

Ana Blas-García,
University of Valencia, Spain

Reviewed by:

Atsushi Umemura,
Kyoto Prefectural University of
Medicine, Japan
JingHong Wan,
INSERM U1149 Centre de Recherche
sur l'Inflammation, France

*Correspondence:

Jiahao Fan
jiahaofan@swmu.edu.cn
Yong Xu
xywyll@swmu.edu.cn

[†]These authors have contributed
equally to this work

Specialty section:

This article was submitted to
Gastrointestinal and Hepatic
Pharmacology,
a section of the journal
Frontiers in Pharmacology

Received: 21 December 2021

Accepted: 24 February 2022

Published: 16 March 2022

Citation:

Fang X, Wang H, Tan X, Ye T, Xu Y and
Fan J (2022) Elevated Serum Regulator
of Calcineurin 2 is Associated With an
Increased Risk of Non-Alcoholic Fatty
Liver Disease.
Front. Pharmacol. 13:840764.
doi: 10.3389/fphar.2022.840764

Background: The promoting effect of the regulator of calcineurin 2 (RCAN2) in hepatic steatosis has been observed in animal studies. However, the association of RCAN2 with non-alcoholic fatty liver disease (NAFLD) in humans remains unclear. This study aimed to evaluate the expression of RCAN2 in the liver of mice with hepatic steatosis and in the serum of NAFLD patients and to explore the relationship between serum RCAN2 levels and NAFLD.

Methods: The mRNA and protein expression of RCAN2 were detected by quantitative real-time PCR (qRT-PCR) and Western blot. NAFLD was diagnosed by abdominal ultrasonography. Circulating RCAN2 levels were measured by ELISA kits. The relationship between serum RCAN2 levels and NAFLD was assessed.

Results: qRT-PCR and Western blot analysis showed that compared with the corresponding controls, the mRNA and protein expression of RCAN2 were significantly increased in the liver tissues of db/db and mice on a high-fat diet. Serum RCAN2 levels were markedly elevated in NAFLD patients compared with non-NAFLD subjects. Binary logistic regression analysis showed that serum RCAN2 levels were significantly associated with NAFLD. Receiver operation characteristic (ROC) curve analysis showed that serum RCAN2 might act as a predictive biomarker for NAFLD [area under the curve (AUC) = 0.663, 95% CI = 0.623–0.702], and the serum RCAN2/(AST/ALT) ratio displayed improved predictive accuracy (AUC = 0.816, 95% CI = 0.785–0.846).

Conclusion: Elevated serum RCAN2 levels were associated with an increased risk of NAFLD. Serum RCAN2, especially the serum RCAN2/(AST/ALT) ratio, might be a candidate diagnostic marker for NAFLD.

Keywords: non-alcoholic fatty liver disease, regulator of calcineurin 2, cross-sectional, biomarker, Chinese

INTRODUCTION

Non-alcoholic fatty liver disease (NAFLD) is defined as the presence of steatosis in more than 5% of the hepatocytes without other clear causes of liver fat accumulation, such as viruses, alcohol, drugs, or genetic factors (Chalasani et al., 2012). NAFLD comprises simple hepatic steatosis (fatty liver) alone and nonalcoholic steatohepatitis (NASH), a more serious process with inflammation, hepatocyte damage, or fibrosis that can eventually progress to liver cirrhosis and hepatocellular carcinoma (HCC) (Chalasani et al., 2018; Parthasarathy et al., 2020). In recent decades, NAFLD has become a major public health concern. The number of NAFLD patients is dramatically increasing worldwide, and the global prevalence of NAFLD has been estimated to be about 25% (Younossi et al., 2016; Negro, 2020). NAFLD has emerged as one of the predominant causes of chronic liver diseases worldwide. Its pathogenesis is complicated, including increased *de novo* synthesis of liver fatty acids, hepatocellular injury, liver insulin resistance, intestinal dysbiosis, and fibrogenesis (Friedman et al., 2018). However, these mechanisms have not been well elucidated, and there are currently no effective drugs for the treatment of NAFLD or approved biomarkers to assess disease progression. Although some studies have evaluated potential biomarkers, they have been rarely verified and seldom used in clinical practice. Therefore, there is still a great need to identify and validate other effective biomarkers to predict NAFLD.

The regulator of calcineurin 2 (RCAN2) [also termed thyroid hormone-responsive protein ZAKI-4, down syndrome candidate region 1-like 1 (DSCR1L1), or myocyte-enriched calcineurin-interacting protein 2 (MCIP2)] (Davies et al., 2007) was initially identified as a thyroid hormone (triiodothyronine, T₃)-responsive gene in human skin fibroblasts (Miyazaki et al., 1996) and then reported to inhibit calcineurin-dependent transcriptional responses by binding to the catalytic subunit A of calcineurin (Fuentes et al., 2000; Kingsbury and Cunningham, 2000). ZAKI-4 has three transcripts, α (also called RCAN2-3), β 1, and β 2, in which β 1 and β 2 encode an identical protein product β (also called RCAN2-1) (Cao et al., 2002). Mouse RCAN2 isoforms are highly homologous with human transcripts. The RCAN2 mouse gene, located on chromosome 17, corresponds exactly to the gene containing the corresponding human homolog on chromosome 6 (Strippoli et al., 2000). The tissue distribution of RCAN2 isoforms in mice is highly consistent with that in humans. RCAN2-3 is expressed only in the brain, while RCAN2-1 is ubiquitously expressed in the brain, heart, muscle, kidney, and liver (Cao et al., 2002; Mizuno et al., 2004). RCAN2 is involved in many pathophysiological processes. In striated muscles, RCAN2 modulates hypertrophic growth and selective programs of gene expression (Rothermel et al., 2000). RCAN2 plays a vital role in the brain development and function by regulating the function of calcineurin (Siddiq et al., 2001). RCAN2 is expressed in endothelial cells and restricts angiogenesis by inhibiting calcineurin activity (Gollogly et al., 2007). RCAN2 is also involved in the development, proliferation, or pro-tumorigenic network of cancers (Niitsu et al., 2016;

Hattori et al., 2019; Mammarella et al., 2021). Interestingly, the knockout of RCAN2 in the whole body can significantly reduce the liver weight of high-fat diet-induced obese mice and did not exhibit liver steatosis (Sun et al., 2011; Zhao et al., 2016). This suggests that RCAN2 plays an important role in NAFLD in mice; however, there is still no evidence that RCAN2 is involved in the development of human NAFLD or that it may be a diagnostic marker for NAFLD.

In the present study, we aimed to conduct the first study to evaluate serum RCAN2 levels in NAFLD patients and non-NAFLD subjects, and the association of serum RCAN2 with NAFLD risk.

MATERIALS AND METHODS

Animal Models and Diet

Six-week-old male C57BL/6 mice, db/db mice, and heterozygous control db/m mice were purchased from SPF Biotechnology Co., Ltd. (Beijing, China). All mice were housed in the IVC system with a 12-h light/dark cycles and ad libitum access to food and water. After a 7-d acclimation, 7-week-old male C57BL/6 mice were fed a high-fat diet (HFD) for 16 weeks (containing 60.0% fat, 20.6% carbohydrate, and 19.4% protein; TP23300) to induce fatty liver or low-fat diet (LFD; TP23302) as controls. HFD and LFD were purchased from Trophic Animal Feed High-Tech Co., Ltd., Nantong, China. The db/db mice served as another fatty liver model and were fed a normal diet for 6 weeks. All animals were sacrificed under anesthesia and the liver tissues were excised and frozen at -80°C for analyzing the mRNA and protein levels. All animal protocols were approved by the Experimental Animal Ethics Committee of Southwest Medical University (Permission no. 2020827).

Liver Histological Analysis, Quantitative Real-Time PCR, and Western Blot Analyses

The liver was fixed overnight with 10% phosphate-buffered formalin acetate at 4°C and embedded in paraffin. The paraffin sections were mounted on glass slides for hematoxylin and eosin (H&E) staining. The total RNA was extracted from the liver tissues using TRIzol reagent (15596026, Thermo Fisher), and then the total RNA was reverse transcribed to cDNA using the first strand cDNA synthesis kit (FSQ-201, Toyobo). qRT-PCR of cDNA was performed using SYBR Green PCR Master Mix (208056, Qiagen) in a StepOnePlus Real-Time PCR System (qTOWER³ G, Germany). The relative mRNA expression levels of the target genes were normalized to GAPDH expression. The primer sequences are shown in **Supplementary Table S1**. Western blots were used for protein expression, as described previously (Gao et al., 2019). Primary antibodies were anti-RCAN2 (1:3,000, Thermo Fisher Scientific, PA5-112914) and anti-tubulin (1:5,000, Beyotime, China, AF5012). Western blots were visualized by a chemiluminescence system (ChemStudio_815, Germany) and quantified by using the ImageJ software (National Institutes of Health, Bethesda, MD).

Study Participants

All participants were recruited from the physical examination center of The Affiliated Hospital of Southwest Medical University. Fatty liver can be diagnosed by abdominal ultrasonography with two of the following three abnormalities: 1) diffusely increased liver tissue near the field ultrasonic echo; 2) kidney echo weaker than liver; and 3) vascular blurring and the gradual attenuation of the far-field ultrasonic echo (Fan et al., 2011). Fatty liver can be divided into mild (ultrasonic echo attenuation does not exceed one-third of the liver), moderate (ultrasonic echo attenuation exceeds one-third and less than two-thirds of the liver), and severe (ultrasonic echo attenuation exceeds two-thirds of the liver). The subjects were excluded if they had any of the following: liver dysfunction caused by other reasons (e.g., alcohol, drugs, toxins, virus, or genetic factors) other than NAFLD, cancer, kidney dysfunction, cardiovascular or cerebrovascular disease, history of thyroid disease, HIV infection, pregnancy or breastfeeding, systemic corticosteroid treatment, anti-inflammatory therapy, and hypoglycemic, lipid-lowering, or antihypertensive treatment. All human investigations followed the ethical guidelines of the 1964 Declaration of Helsinki and were approved by the Human Research Ethics Committee of the Affiliated Hospital of Southwest Medical University (Permission no. KY2021086). Informed consent was obtained from all participants in this study.

Anthropometric and Biochemical Measurements and Serum Sample Collection

After overnight fasting, all anthropometric parameters such as height, body weight (BW), waist circumference (WC), hip circumference (HC), systolic blood pressure (SBP), and diastolic blood pressure (DBP) were measured by professionally trained nurses. The body mass index (BMI) was calculated as BW divided by height squared. The waist-to-hip ratio (WHR) was calculated by WC and HC. Blood indexes such as fasting blood glucose (FBG), alanine aminotransferase (ALT), aspartate aminotransferase (AST), gamma-glutamyl transpeptidase (GGT), alkaline phosphatase (ALP), urea nitrogen (UREA), uric acid (UA), creatinine (CREA), total cholesterol (TC), triglycerides (TG), high-density lipoprotein cholesterol (HDL-C), low-density lipoprotein cholesterol (LDL-C), homocysteine (HCY), and free triiodothyronine (FT3) were tested in the department of laboratory medicine and nuclear medicine of the Affiliated Hospital of Southwest Medical University. The fatty liver index (FLI) was calculated using the following formulae: $FLI = 1/[1 + \exp(-x)] \times 100$, $x = 0.953 \times \ln(\text{triglycerides (mg/dl)} + 0.139 \times \text{BMI (kg/m}^2) + 0.718 \times \ln(\gamma\text{-glutamyl-transferase (U/L)} + 0.053 \times \text{WC (cm)} - 15.745$ (Tan et al., 2021). After overnight fasting, the blood samples from all the participants were collected in the separation gel promoting tubes on the morning of the day of ultrasound examination. The serum was collected after centrifugation at 3,000 rpm at 4°C for

15 min. To avoid repeated freeze-thaw cycles, each sample was divided into several tubes and stored at -80°C until analysis.

Measurements of Serum RCAN2

Serum RCAN2 levels were measured with a commercial enzyme-linked immunosorbent assay (ELISA) kit (Human ELISA kit, AE22621HU; Mouse ELISA Kit, AE22620MO, Abcam, China) according to the manufacturer's protocol. The pilot experiments showed that RCAN2 can be detected in our 10-fold diluted human serum samples and in 100 µL mouse serum samples. Therefore, all human serum samples were diluted 10-fold before detection, while mouse serum samples were tested with 100 µL. The intra- and inter-assay variations were <8% and <12%, respectively.

Statistical Analysis

SPSS 22.0 and GraphPad Prism 8.0 were used for all statistical analysis and graphics. Data were expressed as number (%) for categorical variables or as mean ± standard deviation (SD) for continuous variables. For continuous variables, Student's t-test or the Mann-Whitney U-test was used for the differences between the two groups, and one-way analysis of variance (ANOVA) or the Kruskal-Wallis test was used for the differences among more than two groups. Comparisons of categorical variables were made using the Chi-square test. The correlation between serum RCAN2 and other clinical parameters was determined by partial correlation coefficients. Variables independently associated with serum RCAN2 were analyzed by multiple linear regressions. Binary logistic regression analyses were used to analyze the association between the serum RCAN2 levels and NAFLD risk. The diagnostic value of serum RCAN2 or serum RCAN2/(AST/ALT) ratio for the NAFLD was evaluated by the area under the receiver operating characteristic (ROC) curve (AUC). A *p*-value < 0.05 was considered statistically significant.

RESULTS

Hepatic RCAN2 Expression Was Up-Regulated in Db/db and HFD-induced Hepatic Steatosis Mice

As shown in the **Supplementary Figures S1, S2**, we successfully constructed a mouse model of hepatic steatosis. In order to explore the potential role of RCAN2 in the development of fatty liver, we first analyzed its expression in the liver tissues of mice. Our data showed that compared with db/m mice, the mRNA and protein expression levels were significantly increased in the liver tissues of db/db mice (**Figures 1A,B**). Elevated RCAN2 mRNA and protein expression was also observed in the liver tissues of HFD-induced fatty liver mice (**Figures 1C,D**). We detected the RCAN2 in the serum of NAFLD mice and found a trend of increase but without a statistical difference (**Supplementary Figure S3**). This may be due to the insufficient number of mice.

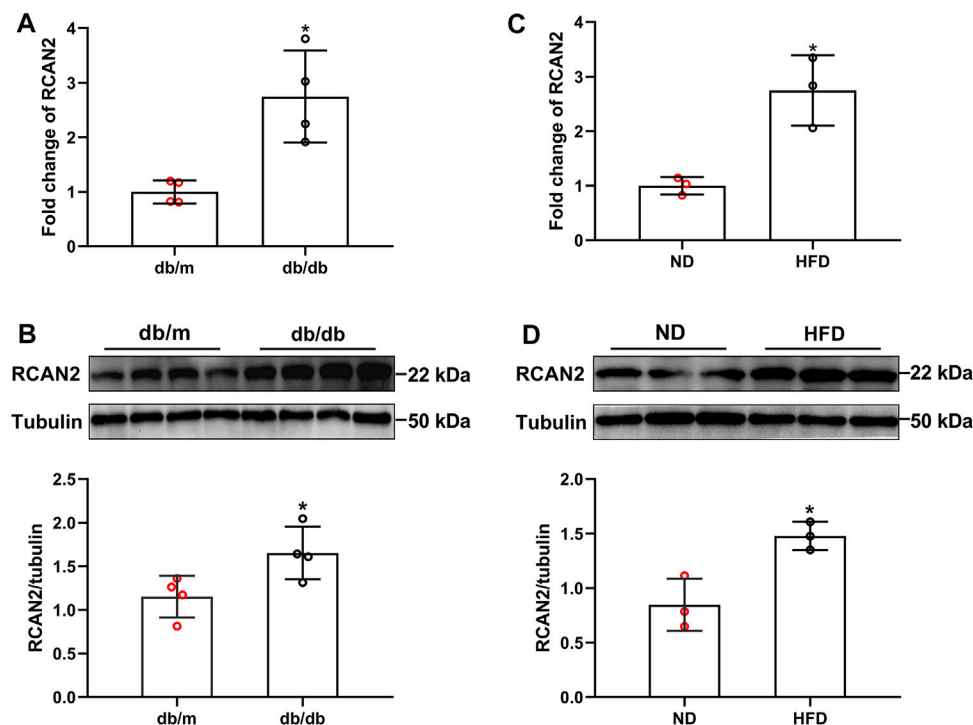


FIGURE 1 | RCAN2 expression was upregulated in livers of db/db mice and HFD-induced mice. The mRNA (**A**) and protein (**B**) expression of RCAN2 in db/db mice vs db/m mice; The mRNA (**C**) and protein (**D**) expression of RCAN2 in HFD mice vs ND mice. ND, normal diet; HFD, high-fat diet. The data was presented as mean \pm SD. * $p < 0.05$ vs ND or db/m.

General Clinical Characteristics and Serum RCAN2 Concentration in the Study Population

In order to investigate the expression of serum RCAN2 in NAFLD patients, 346 non-NAFLD subjects and 369 NAFLD patients were enrolled in this study. The general characteristics of the study subjects are displayed in **Table 1**. The average age of all the subjects was 40.52 ± 10.58 years, including 464 males (64.90%) and 251 females (35.10%). Compared with the non-NAFLD group, the NAFLD group had a higher male/female ratio, BW, BMI, WC, HC, WHR, SBP, DBP, FBG, WBC, NEU, HGB, PLT, ALT, AST, TP, ALB, GGT, ALP, UA, CREA, TC, TG, LDL, HCY, and FLI (all $p < 0.05$) but lower AST/ALT, DBIL, eGFR, and HDL-C (all $p < 0.05$). No significant differences were found in age, GLO, A/G, TBIL, IBIL, and UREA (all $p > 0.05$).

In all study participants, the distribution of serum RCAN2 levels was from 2.44–47.73 ng/mL. As shown in **Table 1** and **Figure 2A**, the serum RCAN2 levels were significantly higher in the NAFLD group than those in the non-NAFLD group (11.47 ± 5.42 ng/ml vs. 8.79 ± 2.85 ng/ml, $p = 0.000$).

Clinical Characteristics and Prevalence of NAFLD by Tertiles of Serum RCAN2 in all Study Subjects

In order to explore the changes of clinical parameters and prevalence of NAFLD under different RCAN2 concentration

gradients in all study subjects, serum RCAN2 levels were divided into tertiles. As shown in **Table 2** and **Figure 2B**, GGT, TC, TG, and the prevalence of NAFLD were gradually increased among the lowest tertile 1, median tertile 2, and the highest tertile 3 groups (all $p < 0.05$). The subjects in the highest tertile 3 had a higher male/female ratio, BW, BMI, WC, WHR, SBP, DBP, FBG, HGB, ALT, AST, TP, ALB, UA, LDL-C, and FLI than the lowest tertile 1 group, and a higher BW, BMI, SBP, and ALB than the median tertile 2 group (all $p < 0.05$).

Correlations and Regression of Serum RCAN2 Levels With Clinical Parameters in the Study Participants

In order to investigate the associations between serum RCAN2 levels and other clinical parameters, partial correlation analysis was performed. As displayed in **Table 3**, after adjustment for age and sex, serum RCAN2 levels were positively associated with BW ($r = 0.157$), BMI ($r = 0.175$), WC ($r = 0.139$), WHR ($r = 0.167$), SBP ($r = 0.143$), DBP ($r = 0.120$), FBG ($r = 0.106$), WBC ($r = 0.096$), ALT ($r = 0.103$), AST ($r = 0.098$), TP ($r = 0.134$), GLO ($r = 0.123$), GGT ($r = 0.088$), ALP ($r = 0.080$), UA ($r = 0.224$), TC ($r = 0.263$), TG ($r = 0.475$), LDL-C ($r = 0.079$), and FLI ($r = 0.304$) but negatively associated with AST/ALT ($r = -0.097$), A/G ($r = -0.084$), DBIL ($r = -0.141$), and HDL-C ($r = -0.158$) in all subjects (all

TABLE 1 | Clinical parameters of all participants in the study.

| Measurements | Total | Non-NAFLD | NAFLD | p-value |
|-------------------------------------|-----------------|----------------|----------------|---------|
| Sample (n) | 715 | 346 | 369 | — |
| Male/Female | 464/251 | 202/144 | 262/107 | 0.000 |
| Age (years) | 40.52 ± 10.58 | 40.14 ± 10.65 | 40.87 ± 10.51 | 0.321 |
| BW (kg) | 68.61 ± 12.84 | 61.94 ± 7.86 | 74.86 ± 13.45 | 0.000 |
| BMI (kg/m ²) | 25.18 ± 3.62 | 23.06 ± 2.29 | 27.16 ± 3.51 | 0.000 |
| WC (cm) | 84.33 ± 9.49 | 79.12 ± 6.56 | 89.22 ± 9.21 | 0.000 |
| HC (cm) | 97.22 ± 6.78 | 94.40 ± 5.10 | 99.86 ± 7.09 | 0.000 |
| WHR (cm/cm) | 0.87 ± 0.06 | 0.84 ± 0.05 | 0.89 ± 0.05 | 0.000 |
| SBP (mmHg) | 122.08 ± 14.21 | 117.64 ± 13.16 | 126.24 ± 13.91 | 0.000 |
| DBP (mmHg) | 73.57 ± 10.10 | 70.65 ± 8.83 | 76.30 ± 10.45 | 0.000 |
| FBG (mmol/L) | 5.26 ± 1.23 | 4.94 ± 0.63 | 5.56 ± 1.54 | 0.000 |
| WBC (*10 ⁹ /L) | 6.37 ± 1.49 | 5.97 ± 1.37 | 6.74 ± 1.50 | 0.000 |
| NEU (*10 ⁹ /L) | 3.70 ± 1.13 | 3.49 ± 1.08 | 3.91 ± 1.14 | 0.000 |
| HGB (g/L) | 149.43 ± 14.44 | 145.51 ± 14.71 | 153.11 ± 13.18 | 0.000 |
| PLT (*10 ⁹ /L) | 234.352 ± 57.03 | 229.04 ± 54.77 | 239.34 ± 58.71 | 0.021 |
| ALT (U/L) | 30.64 ± 25.19 | 20.64 ± 8.77 | 40.01 ± 31.25 | 0.000 |
| AST (U/L) | 24.38 ± 10.70 | 21.35 ± 5.08 | 27.22 ± 13.46 | 0.000 |
| AST/ALT | 0.97 ± 0.39 | 1.15 ± 0.41 | 0.80 ± 0.27 | 0.000 |
| TP (g/L) | 72.33 ± 3.33 | 71.85 ± 3.37 | 72.78 ± 3.24 | 0.001 |
| ALB (g/L) | 46.48 ± 2.28 | 46.18 ± 2.32 | 46.75 ± 2.21 | 0.001 |
| GLO (g/L) | 25.86 ± 2.66 | 25.67 ± 2.50 | 26.04 ± 2.80 | 0.142 |
| A/G | 1.82 ± 0.21 | 1.82 ± 0.20 | 1.82 ± 0.22 | 0.927 |
| TBIL (μmol/L) | 14.73 ± 5.41 | 14.73 ± 4.64 | 14.73 ± 6.05 | 0.137 |
| DBIL (μmol/L) | 4.12 ± 1.54 | 4.23 ± 1.42 | 4.02 ± 1.65 | 0.007 |
| IBIL (μmol/L) | 10.61 ± 4.06 | 10.50 ± 3.41 | 10.72 ± 4.59 | 0.390 |
| GGT (U/L) | 35.87 ± 37.70 | 23.29 ± 20.22 | 47.67 ± 45.67 | 0.000 |
| ALP (U/L) | 73.27 ± 20.16 | 69.99 ± 19.80 | 76.35 ± 20.03 | 0.000 |
| UREA (mol/L) | 5.01 ± 1.09 | 4.94 ± 1.12 | 5.09 ± 1.05 | 0.099 |
| UA (μmol/L) | 351.95 ± 85.69 | 319.24 ± 75.71 | 382.62 ± 83.21 | 0.000 |
| CREA (μmol/L) | 66.70 ± 12.23 | 65.39 ± 12.43 | 67.93 ± 11.92 | 0.006 |
| eGFR [ml/(min*1.73m ²)] | 122.58 ± 20.92 | 124.02 ± 20.74 | 121.22 ± 21.02 | 0.028 |
| TC (mmol/L) | 4.86 ± 0.90 | 4.71 ± 0.83 | 5.00 ± 0.93 | 0.000 |
| TG (mmol/L) | 1.80 ± 1.62 | 1.18 ± 0.59 | 2.38 ± 2.02 | 0.000 |
| HDL-C (mmol/L) | 1.30 ± 0.33 | 1.45 ± 0.35 | 1.16 ± 0.25 | 0.000 |
| LDL-C (mmol/L) | 3.22 ± 0.90 | 3.05 ± 0.83 | 3.37 ± 0.93 | 0.000 |
| HCY (μmol/L) | 12.26 ± 7.86 | 11.92 ± 7.44 | 12.58 ± 8.22 | 0.021 |
| RCAN2 (ng/ml) | 10.18 ± 4.56 | 8.79 ± 2.85 | 11.47 ± 5.42 | 0.000 |
| NAFLD index FLI | 36.27 ± 27.59 | 17.04 ± 13.75 | 54.31 ± 25.02 | 0.000 |

Continuous variables were expressed as mean ± standard deviation. Categorical variables were expressed as n/n. NAFLD, non-alcoholic fatty liver disease; BW, body weight; BMI, body mass index; WC, waist circumference; HC, hip circumference; WHR, waist to hip ratio; SBP, systolic blood pressure; DBP, diastolic blood pressure; FBG, fasting blood glucose; WBC, white blood cells; NEU, neutrophil; ALT, alanine aminotransferase; AST, aspartate aminotransferase; TP, total protein; ALB, albumin; GLO, globulin; A/G, Albumin-globulin-ratio; TBIL, total bilirubin; DBIL, direct bilirubin; IBIL, indirect bilirubin; GGT, gamma-glutamyl transpeptidase; ALP, alkaline phosphatase; UA, uric acid; CREA, creatinine; eGFR, estimated glomerular filtration rate; TC, total cholesterol; TG, triglyceride; HDL-C, high-density lipoprotein cholesterol; LDL-C, low-density lipoprotein cholesterol; HCY, homocysteine; RCAN2, a regulator of calcineurin 2; FLI, fatty liver index. *p < 0.05, **p < 0.01, ***p < 0.001 versus non-NAFLD group.

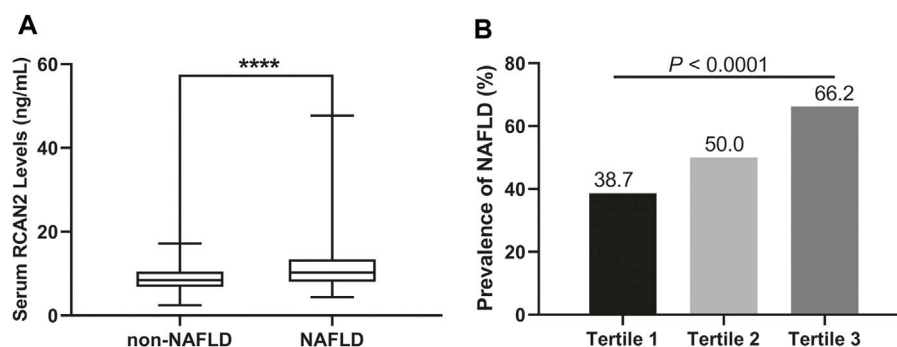


FIGURE 2 | (A) Serum RCAN2 concentration in NAFLD patients and non-NAFLD subjects. **(B)** Prevalence of NAFLD by tertiles of serum RCAN2 levels in all participants. NAFLD, non-alcoholic fatty liver disease; RCAN2, a regulator of calcineurin 2. ****p < 0.0001 compared with non-NAFLD.

TABLE 2 | Clinical and biochemical characteristics by tertiles of serum RCAN2 level in all subjects.

| Measurements | Tertile 1 | Tertile 2 | Tertile 3 | p-value |
|-------------------------------------|----------------|----------------|---------------------|---------|
| Sample (n) | 238 | 240 | 237 | - |
| Male/Female | 140/98 | 153/87 | 171/66** | 0.009 |
| Age (years) | 39.31 ± 10.01 | 40.66 ± 10.89 | 41.59 ± 10.73 | 0.076 |
| BW (kg) | 67.69 ± 13.55 | 67.03 ± 10.91 | 71.13 ± 13.56***# | 0.001 |
| BMI (kg/m ²) | 24.85 ± 3.65 | 24.77 ± 3.11 | 25.92 ± 3.95***# | 0.002 |
| WC (cm) | 83.29 ± 9.12 | 83.88 ± 9.40 | 85.83 ± 9.78* | 0.015 |
| HC (cm) | 97.43 ± 6.50 | 96.56 ± 6.55 | 97.66 ± 7.25 | 0.240 |
| WHR (cm/cm) | 0.85 ± 0.06 | 0.87 ± 0.06 | 0.88 ± 0.05*** | 0.000 |
| SBP (mmHg) | 119.15 ± 13.09 | 121.80 ± 13.53 | 125.30 ± 15.29***# | 0.000 |
| DBP (mmHg) | 71.35 ± 10.03 | 74.10 ± 9.46** | 75.25 ± 10.43*** | 0.000 |
| FBG (mmol/L) | 5.12 ± 0.94 | 5.22 ± 1.00 | 5.45 ± 1.61* | 0.014 |
| WBC (*10 ⁹ /L) | 6.28 ± 1.55 | 6.36 ± 1.46 | 6.46 ± 1.45 | 0.171 |
| NEU (*10 ⁹ /L) | 3.72 ± 1.15 | 3.70 ± 1.14 | 3.68 ± 1.12 | 0.935 |
| HGB (g/L) | 147.35 ± 15.11 | 149.05 ± 13.79 | 151.91 ± 14.09** | 0.004 |
| PLT (*10 ⁹ /L) | 229.99 ± 56.80 | 235.24 ± 50.79 | 237.83 ± 62.89 | 0.524 |
| ALT (U/L) | 26.96 ± 20.02 | 29.70 ± 20.46 | 35.28 ± 32.51** | 0.002 |
| AST (U/L) | 22.67 ± 7.32 | 23.87 ± 9.09 | 26.61 ± 14.17** | 0.004 |
| AST/ALT | 1.03 ± 0.43 | 0.95 ± 0.37 | 0.93 ± 0.35* | 0.015 |
| TP (g/L) | 71.77 ± 3.02 | 72.38 ± 3.36 | 72.84 ± 3.53** | 0.006 |
| ALB (g/L) | 46.24 ± 2.16 | 46.33 ± 2.29 | 46.86 ± 2.35*# | 0.011 |
| GLO (g/L) | 25.54 ± 2.46 | 26.05 ± 2.66 | 25.98 ± 2.84 | 0.143 |
| A/G | 1.83 ± 0.21 | 1.80 ± 0.21 | 1.82 ± 0.22 | 0.106 |
| TBIL (μmol/L) | 14.72 ± 5.57 | 14.60 ± 5.29 | 14.87 ± 5.39 | 0.842 |
| DBIL (μmol/L) | 4.30 ± 1.61 | 4.11 ± 1.47 | 3.95 ± 1.52* | 0.032 |
| IBIL (μmol/L) | 10.43 ± 4.15 | 10.49 ± 3.98 | 10.93 ± 4.06 | 0.242 |
| GGT (U/L) | 30.36 ± 33.50 | 36.03 ± 41.89* | 41.25 ± 36.56***# | 0.000 |
| ALP (U/L) | 71.88 ± 20.02 | 73.32 ± 20.53 | 74.62 ± 19.91 | 0.299 |
| UREA (mol/L) | 4.89 ± 1.09 | 5.05 ± 1.14 | 5.09 ± 1.02 | 0.080 |
| UA (μmol/L) | 339.74 ± 81.43 | 347.82 ± 79.45 | 368.39 ± 93.40** | 0.004 |
| CREA (μmol/L) | 65.67 ± 12.12 | 66.97 ± 12.33 | 67.47 ± 12.22 | 0.218 |
| eGFR [ml/(min*1.73m ²)] | 123.77 ± 21.07 | 121.54 ± 20.37 | 122.42 ± 21.34 | 0.448 |
| TC (mmol/L) | 4.56 ± 0.80 | 4.86 ± 0.87*** | 5.17 ± 0.91***## | 0.000 |
| TG (mmol/L) | 1.34 ± 0.80 | 1.58 ± 0.82** | 2.49 ± 2.43***### | 0.000 |
| HDL-C (mmol/L) | 1.34 ± 0.32 | 1.31 ± 0.35 | 1.26 ± 0.34* | 0.020 |
| LDL-C (mmol/L) | 3.00 ± 0.79 | 3.28 ± 0.84** | 3.38 ± 1.01*** | 0.000 |
| HCY (μmol/L) | 12.02 ± 7.80 | 12.14 ± 6.93 | 12.62 ± 8.77 | 0.450 |
| RCAN2 (ng/ml) | 6.45 ± 1.17 | 9.27 ± 0.80*** | 14.84 ± 4.93***### | 0.000 |
| NAFLD (%) | 38.66 | 50.00* | 66.24***### | 0.000 |
| NAFLD index FLI | 28.70 ± 24.27 | 34.29 ± 25.98 | 45.88 ± 29.57***### | 0.000 |

Continuous variables were expressed as mean ± standard deviation. Categorical variables were expressed as n (%). NAFLD, non-alcoholic fatty liver disease; BW, body weight; BMI, body mass index; WC, waist circumference; HC, hip circumference; WHR, waist to hip ratio; SBP, systolic blood pressure; DBP, diastolic blood pressure; FBG, fasting blood glucose; WBC, white blood cells; NEU, neutrophil; ALT, alanine aminotransferase; AST, aspartate aminotransferase; TP, total protein; ALB, albumin; GLO, globulin; A/G, Albumin-globulin-ratio; TBIL, total bilirubin; DBIL, direct bilirubin; IBIL, indirect bilirubin; GGT, gamma-glutamyl transpeptidase; ALP, alkaline phosphatase; UA, uric acid; CREA, creatinine; eGFR, estimated glomerular filtration rate; TC, total cholesterol; TG, triglyceride; HDL-C, high-density lipoprotein cholesterol; LDL-C, low-density lipoprotein cholesterol; HCY, homocysteine; RCAN2, regulator of calcineurin 2; FLI, fatty liver index. *p < 0.05, **p < 0.01, ***p < 0.001 versus tertile 1 group. #p < 0.05, ##p < 0.01, ###p < 0.001 versus tertile 2 group.

$p < 0.05$). In the non-NAFLD group, serum RCAN2 was found to be positively associated with TP ($r = 0.137$), ALB ($r = 0.129$), TC ($r = 0.191$), TG ($r = 0.182$), and LDL-C ($r = 0.119$), and negatively associated with HC ($r = -0.113$) (all $p < 0.05$). In the NAFLD group, serum RCAN2 levels were positively associated with SBP ($r = 0.105$), GLO ($r = 0.119$), ALP ($r = 0.127$), UA ($r = 0.208$), TC ($r = 0.266$), TG ($r = 0.458$), and FLI ($r = 0.198$) but negatively associated with A/G ($r = -0.110$) and HDL-C ($r = -0.108$) (all $p < 0.05$).

Liner regression analysis was performed to explore variables independently associated with serum RCAN2 levels. As shown in **Figure 3**, all factors enter and stepwise regression analyses showed that group, GGT, and TG were independent factors associated with serum RCAN2 levels.

Association of Serum RCAN2 Levels and Risk of NAFLD

In order to further evaluate the association between serum RCAN2 levels and NAFLD risk, all subjects in the study were divided into three groups according to serum RCAN2 tertiles (lowest: < 8.03 ng/ml; median: 8.03–10.82 ng/ml; highest: ≥10.82 ng/ml). As displayed in **Table 4**, binary logistic regression analysis showed that subjects in the highest tertile of serum RCAN2 levels had a 2.114-fold higher risk of NAFLD than those in the lowest tertile levels (OR = 3.114, 95% CI = 2.141–4.531, $p = 0.000$). After adjusting for age, sex, BMI, SBP, DBP, FBG, WBC, NEU, ALT, AST, GGT, ALP, UA, and eGFR in the Model 2–4, the tendency still existed (OR = 2.912, 95% CI =

TABLE 3 | Partial correlation between serum RCAN2 levels and other parameters.

| Measurements | Serum RCAN2 (age and sex-adjusted) | | | | | |
|-------------------------------------|------------------------------------|--------------|---------------|--------------|---------------|--------------|
| | All subjects | | Non-NAFLD | | NAFLD | |
| — | r | p-value | r | p-value | r | p-value |
| BW (kg) | 0.157 | 0.000 | −0.030 | 0.577 | 0.029 | 0.584 |
| BMI (kg/m ²) | 0.175 | 0.000 | −0.046 | 0.400 | 0.046 | 0.384 |
| WC (cm) | 0.139 | 0.000 | −0.057 | 0.289 | 0.005 | 0.931 |
| HC (cm) | 0.070 | 0.061 | −0.113 | 0.036 | −0.028 | 0.594 |
| WHR (cm/cm) | 0.167 | 0.000 | 0.031 | 0.570 | 0.049 | 0.351 |
| SBP (mmHg) | 0.143 | 0.000 | 0.010 | 0.859 | 0.105 | 0.044 |
| DBP (mmHg) | 0.120 | 0.001 | 0.051 | 0.350 | 0.054 | 0.305 |
| FBG (mmol/L) | 0.106 | 0.005 | 0.049 | 0.363 | 0.034 | 0.518 |
| WBC (*10 ⁹ /L) | 0.096 | 0.010 | 0.002 | 0.963 | 0.044 | 0.403 |
| NEU (*10 ⁹ /L) | 0.032 | 0.377 | −0.092 | 0.089 | 0.014 | 0.785 |
| HGB (g/L) | 0.073 | 0.051 | −0.006 | 0.919 | 0.010 | 0.848 |
| PLT (*10 ⁹ /L) | 0.072 | 0.053 | 0.105 | 0.052 | 0.017 | 0.741 |
| ALT (U/L) | 0.103 | 0.006 | −0.022 | 0.686 | −0.002 | 0.974 |
| AST (U/L) | 0.098 | 0.009 | 0.047 | 0.381 | 0.027 | 0.606 |
| AST/ALT | −0.097 | 0.010 | 0.023 | 0.665 | 0.060 | 0.252 |
| TP (g/L) | 0.134 | 0.000 | 0.137 | 0.011 | 0.086 | 0.099 |
| ALB (g/L) | 0.054 | 0.148 | 0.129 | 0.017 | −0.027 | 0.602 |
| GLO (g/L) | 0.123 | 0.001 | 0.074 | 0.173 | 0.119 | 0.023 |
| A/G | −0.084 | 0.026 | −0.017 | 0.759 | −0.110 | 0.035 |
| TBIL (μmol/L) | −0.027 | 0.467 | 0.003 | 0.955 | −0.036 | 0.492 |
| DBIL (μmol/L) | −0.141 | 0.000 | −0.066 | 0.224 | −0.153 | 0.003 |
| IBIL (μmol/L) | 0.016 | 0.663 | 0.031 | 0.568 | 0.006 | 0.907 |
| GGT (U/L) | 0.088 | 0.019 | −0.035 | 0.517 | 0.006 | 0.912 |
| ALP (U/L) | 0.080 | 0.032 | −0.104 | 0.055 | 0.127 | 0.015 |
| UREA (mol/L) | 0.037 | 0.324 | −0.012 | 0.822 | 0.049 | 0.345 |
| UA (μmol/L) | 0.224 | 0.000 | −0.019 | 0.730 | 0.208 | 0.000 |
| CREA (μmol/L) | −0.009 | 0.804 | −0.061 | 0.261 | 0.010 | 0.844 |
| eGFR [ml/(min*1.73m ²)] | 0.017 | 0.647 | 0.080 | 0.140 | −0.009 | 0.860 |
| TC (mmol/L) | 0.263 | 0.000 | 0.191 | 0.000 | 0.266 | 0.000 |
| TG (mmol/L) | 0.475 | 0.000 | 0.182 | 0.001 | 0.458 | 0.000 |
| HDL-C (mmol/L) | −0.158 | 0.000 | 0.049 | 0.365 | −0.108 | 0.038 |
| LDL-C (mmol/L) | 0.079 | 0.034 | 0.119 | 0.027 | 0.013 | 0.802 |
| HCY (μmol/L) | −0.048 | 0.199 | −0.023 | 0.667 | −0.068 | 0.192 |
| NAFLD index FLI | 0.304 | 0.000 | 0.005 | 0.933 | 0.198 | 0.000 |

Partial correlation coefficients were used for age- and sex-adjusted data. Bold font indicated $p < 0.05$. RCAN2, regulator of calcineurin 2; NAFLD, non-alcoholic fatty liver disease; BW, body weight; BMI, body mass index; WC, waist circumference; HC, hip circumference; WHR, waist to hip ratio; SBP, systolic blood pressure; DBP, diastolic blood pressure; FBG, fasting blood glucose; WBC, white blood cells; NEU, neutrophil; ALT, alanine aminotransferase; AST, aspartate aminotransferase; TP, total protein; ALB, albumin; GLO, globulin; A/G, Albumin-globulin-ratio; TBIL, total bilirubin; DBIL, direct bilirubin; IBIL, indirect bilirubin; GGT, gamma-glutamyl transpeptidase; ALP, alkaline phosphatase; UA, uric acid; CREA, creatinine; eGFR, estimated glomerular filtration rate; TC, total cholesterol; TG, triglyceride; HDL-C, high-density lipoprotein cholesterol; LDL-C, low-density lipoprotein cholesterol; HCY, homocysteine; FLI, fatty liver index.

1.992–4.526, $p = 0.000$), (OR = 2.893, 95% CI = 1.715–4.881, $p = 0.000$), or (OR = 2.406, 95% CI = 1.324–4.373, $p = 0.004$). When further controlling for lipid profiles (TC, TG, LDL-C, and LDL-C) in Model 5, subjects in the highest tertile of serum RCAN2 levels also had a significantly increased risk of NAFLD (OR = 2.081, 95% CI = 1.084–3.995, $p = 0.028$). When considered as continuous variables, every 1-unit increase in serum RCAN2 levels was associated with 20.1, 19.3, 19.9, 18.9, and 17.5% increase, respectively, in risk of NAFLD prevalence in Model 1–5.

Diagnostic Value of Serum RCAN2 Levels and RCAN2/(AST/ALT) Ratio for NAFLD Risk

Finally, ROC curve analysis was performed to investigate the predictive value of serum RCAN2 levels for NAFLD. The results revealed that best cutoff value for serum RCAN2 to predict NAFLD

was 9.11 ng/ml (AUC = 0.663, 95% CI = 0.623–0.702, $p = 0.000$, sensitivity = 63.7%, specificity = 61.3%) (**Figure 4A**). In order to improve the diagnostic value, the factors (AST/ALT, A/G, DBIL, HDL-C) negatively correlated with serum RCAN2 levels in all study subjects were obtained by partial correlation analysis. Then, the ratios of serum RCAN2 levels to AST/ALT, A/G, DBIL, and HDL-C were calculated. ROC curve analysis was performed again to explore the predictive value of these ratios for NAFLD. As displayed in **Figure 4B**, the serum RCAN2/(AST/ALT) ratio showed improved predictive accuracy (AUC = 0.816, 95% CI = 0.785–0.846, $p = 0.000$, sensitivity = 70.2%, specificity = 78.9%).

DISCUSSION

This study was the first to investigate the association between serum RCAN2 levels and NAFLD in humans. The main

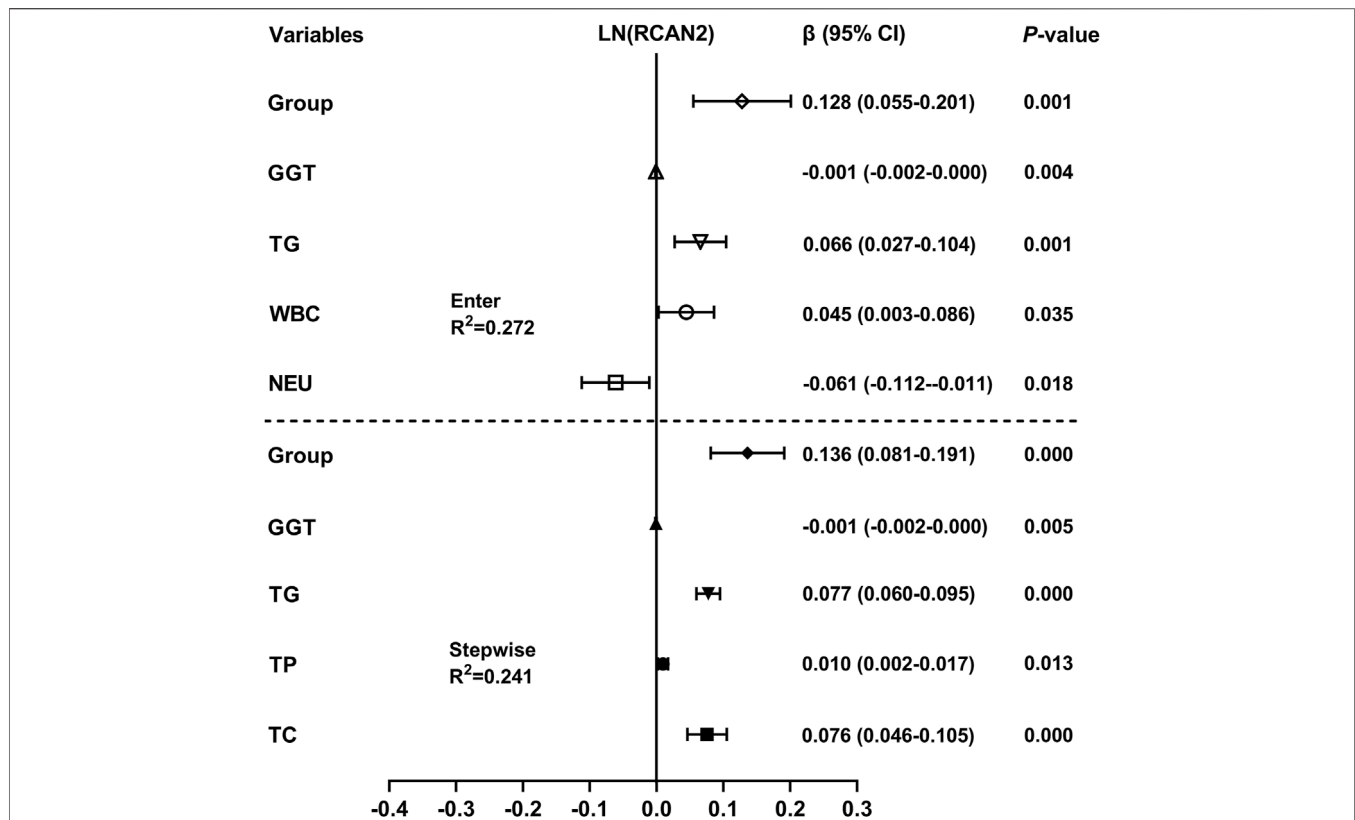


FIGURE 3 | Multiple linear regression analysis of variables independently associated with serum RCAN2 levels in all participants. The regression coefficients (β) and 95% confidence interval (CI) were displayed. Serum RCAN2 levels were naturally logarithmic transformed before analysis. The group of statistic: 1 = non-NAFLD, 2 = NAFLD.

TABLE 4 | Binary logistic regression of NAFLD risks according to tertiles or per 1-unit increases of serum RCAN2 concentrations.

| | RCAN2 tertiles | | | Per 1-unit increase |
|---------------|--------------------|---------------------|---------------------|---------------------|
| | Lowest OR (95% CI) | Median OR (95% CI) | Highest OR (95% CI) | |
| Range (ng/ml) | <8.03 | ≥8.03–10.82 | ≥10.82 | — |
| Model 1 | 1 (reference) | 1.587 (1.103–2.282) | 3.114 (2.141–4.531) | 1.201 (1.145–1.260) |
| p-value | — | 0.013 | 0.000 | 0.000 |
| Model 2 | 1 (reference) | 1.545 (1.071–2.229) | 2.912 (1.992–4.526) | 1.193 (1.136–1.252) |
| p-value | — | 0.020 | 0.000 | 0.000 |
| Model 3 | 1 (reference) | 1.718 (1.045–2.825) | 2.893 (1.715–4.881) | 1.199 (1.121–1.282) |
| p-value | — | 0.033 | 0.000 | 0.000 |
| Model 4 | 1 (reference) | 1.469 (0.842–2.562) | 2.406 (1.324–4.373) | 1.189 (1.102–1.283) |
| p-value | — | 0.176 | 0.004 | 0.000 |
| Model 5 | 1 (reference) | 1.479 (0.825–2.651) | 2.081 (1.084–3.995) | 1.175 (1.083–1.275) |
| p-value | — | 0.188 | 0.028 | 0.000 |

NAFLD, non-alcoholic fatty liver disease; RCAN2, regulator of calcineurin 2; OR, odds ratios; CI, confidence intervals. BMI, body mass index; WC, waist circumference; SBP, systolic blood pressure; DBP, diastolic blood pressure; FBG, fasting blood glucose; WBC, white blood cells; NEU, neutrophil; ALT, alanine aminotransferase; AST, aspartate aminotransferase; GGT, gamma-glutamyl transpeptidase; ALP, alkaline phosphatase; UA, uric acid; eGFR, estimated glomerular filtration rate; TC, total cholesterol; TG, triglyceride; HDL-C, high-density lipoprotein cholesterol; LDL-C, low-density lipoprotein cholesterol. Model 1 was not adjusted. Model 2: adjusted for age and sex. Model 3: adjusted for Model 2 + BMI, WC, SBP, DBP, FBG. Model 4: adjusted for Model 3 + WBC, NEU, ALT, AST, GGT, ALP, UA, eGFR. Model 5: adjusted for Model 4 + TC, TG, HDL-C, LDL-C.

innovation of the current study is that we first demonstrated that RCAN2 was highly expressed in the liver of mice with fatty liver by qRT-PCR and Western blot, and subsequently confirmed that serum RCAN2 levels were also significantly elevated in NAFLD patients. Meanwhile, the results of the present study showed that

serum RCAN2 levels were positively correlated with the prevalence of NAFLD. Systemic knockout of RCAN2 (RCAN2^{-/-}) has been reported to prevent hepatic steatosis in mice fed a high-fat diet (Sun et al., 2011; Zhao et al., 2016). Recently, RCAN2 was found to be a target gene of peroxisome

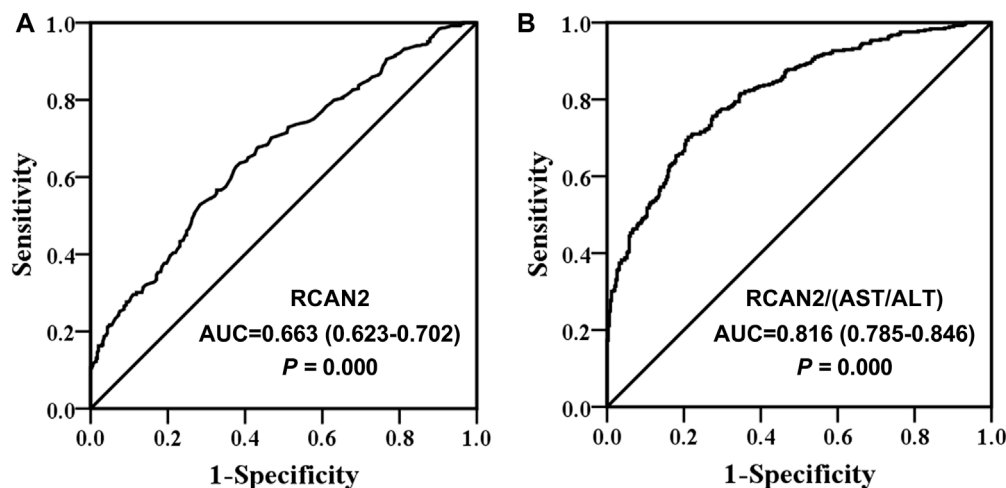


FIGURE 4 | Receiver operating characteristic (ROC) curve analysis of serum RCAN2 levels **(A)** and serum RCAN2/(AST/ALT) ratio **(B)** in NAFLD patients and non-NAFLD subjects. NAFLD, non-alcoholic fatty liver disease; RCAN2, regulator of calcium 2; AUC, area under the curve.

proliferator-activated receptor gamma (PPAR γ) (Yuan et al., 2021), which regulates hepatic lipid deposition in mice with diet-induced obesity (Chen et al., 2022). Taken together, RCAN2 may be a pathogenic driver of NAFLD. It has been reported that the global knockout of RCAN2 can significantly reduce the liver weight in obese mice induced by a high-fat diet by reducing the food intake. This is probably the main reason that RCAN2 $^{-/-}$ mice did not develop typical features of fatty liver on a high-fat diet (Sun et al., 2011; Zhao et al., 2016). Both RCAN2-3 and RCAN2-1 were knocked out in these studies, and it was mainly the downregulation of RCAN2-3 rather than RCAN2-1 that caused the reduction of food intake. RCAN2-3 was expressed only in the brain, while RCAN2-1 was widely expressed in the heart, muscle, kidney, and liver (Cao et al., 2002; Mizuno et al., 2004). Systemic knockout of RCAN2-3 and RCAN2-1 in the whole organism may obscure the role of RCAN2-1 in specific tissues. In the current study, we found that RCAN2-1 was significantly upregulated in the liver tissues of the genetic and HFD-induced steatosis mouse model. Whether liver specific-knockout of RCAN2-1 is involved in the development of NAFLD deserves further study.

RCAN2 was first recognized as a thyroid hormone responsive gene (Miyazaki et al., 1996). In subsequent studies, only RCAN2-3 was regulated by T3 in a human skin fibroblast cell line (Cao et al., 2002). Hypothyroidism significantly decreased the mRNA expression of RCAN2-3 in the brain and had no effect on RCAN2-1, while hyperthyroidism had no influence on RCAN2-1 and RCAN2-3. In the heart, hyperthyroidism upregulated the expression of RCAN2-1, whereas hypothyroidism has no effect on RCAN2-1. However, in the liver, exogenous T3 had no effect on the expression of RCAN2-1 (Mizuno et al., 2004). In animal or cell experiments, T3 was found to reduce hepatocyte lipid storage by promoting fibroblast growth factor 21 (Adams et al., 2010). In the present study, T3 was within the normal range in all the subjects tested for T3 (data not shown). Moreover, partial correlation analysis (age and sex-adjusted) ($r = 0.042$, $p = 0.603$) and

multiple linear regression analysis ($r = 0.768$, 95% CI = $-2.261-3.796$, $p = 0.617$) also showed that serum RCAN2 levels were not correlated with T3. Therefore, these results suggested that elevated serum RCAN2 levels in NAFLD patients may not be associated with T3.

In all study subjects, partial correlation analysis showed that serum RCAN2 levels were positively correlated with BW, BMI, WC, WHR, SBP, DBP, FBG, WC, ALT, AST, TP, GLO, GGT, ALP, UA, TC, TG, and LDL-C, and negatively associated with AST/ALT ratio, A/G ratio, DBIL, and HDL-C. In non-NAFLD participants, the partial correlation analysis showed that serum RCAN2 levels were positively associated with TP, ALB, TC, TG, and LDL-C and negatively associated with HC. In NAFLD patients, after age and sex adjustment, serum RCAN2 was still positively correlated with SBP, GLO, ALP, UA, TC, and TG. Based on these results, we found that RCAN2 was significantly positively correlated with TC and TG in all participants, non-NAFLD subjects, and NAFLD patients, and had a closer correlation with TG, especially in all participants ($r = 0.475$, $p = 0.000$) and NAFLD patients ($r = 0.458$, $p = 0.000$). Additionally, the close relationship between serum RCAN2 and TG was further confirmed by multiple linear regression analysis. It is well known that NAFLD is based on an abnormal increase in the hepatic lipid content (mainly TG), followed by pathological processes such as hepatocellular injury, inflammation, or fibrosis (Donnelly et al., 2005; Friedman et al., 2018). From these findings, we hypothesized that RCAN2 promotes the occurrence of NAFLD by affecting the storage of TG in the liver, but more studies are needed to verify this relationship and clarify the specific mechanism. Given that NASH is a more serious process with inflammation, hepatocyte damage, or fibrosis, it has also been reported that upregulation of RCAN2 promotes inflammation and apoptosis (Luo et al., 2022). Therefore, future studies are necessary to explore the relationship between RCAN2 and fibrosis and inflammatory factors such as C-reactive protein.

Additionally, binary logistic regression analysis showed that subjects in the highest tertile of serum RCAN2 levels had a 2.114-fold higher risk of NAFLD than those in the lowest RCAN2 tertile. The increased risk of NAFLD was also observed at the highest RCAN2 levels after adjusting for age and sex in Model 2, and after further controlling BMI, WC, BP, FBG in Model 3, as well as adjusting for WBC, NEU, ALT, AST, GGT, ALP, UA, and eGFR in Model 4, and even adjusting for TC, TG, HDL-C, and LDL-C in Model 5. Similarly, per 1-unit increase in serum RCAN2 levels was also positively associated with the risk of NAFLD prevalence in Models 1–5. These results increase the possibility that elevated serum RCAN2 levels may serve as a novel biomarker for NAFLD. Further analyses using ROC curves found that serum RCAN2 may be a candidate biomarker for the diagnosis of NAFLD (AUC 0.663, sensitivity 63.7%, and specificity 61.3%). However, the diagnostic role of RCAN2 for NAFLD still needs to be verified in large-scale prospective studies in the future, especially in other ethnic groups and in NAFLD patients diagnosed by liver biopsy. In this study, we also found that serum RCAN2/(AST/ALT) ratio had a better diagnostic accuracy than serum RCAN2 levels, with an AUC of 0.816 and 70.2% sensitivity and 78.9% specificity.

In the present study, there are still some limitations. First, prospective studies are needed to illustrate the causal relationship between the serum RCAN2 levels and NAFLD. In addition, drug-intervention studies may also be used to explore the therapeutic effect of activation or inhibition of RCAN2 on fatty liver in humans or animals. However, there are few studies on RCAN2 at present, we have to start with animal or cell research and explore the role and mechanism of RCAN2 in hepatocyte steatosis model through RNAi, overexpression plasmid, adeno-associated virus, and liver specific knockout. Second, hepatic steatosis was diagnosed by abdominal ultrasound rather than liver biopsy, which can lead to missed or misdiagnosis and cannot determine the severity of NAFLD. Third, animal studies have shown that RCAN2 can increase the food intake. In this clinical study, diet-related information, such as the type and frequency of eating, was not collected. Therefore, the relationship between RCAN2 and food intake was not established. Fourth, the association between serum RCAN2 levels and the progression of the disease cannot be demonstrated due to the lack of data on the diagnosis of NASH/fibrosis. Finally, all subjects were recruited from a physical examination center, which may lead to a selection bias.

In conclusion, the present study found that the serum RCAN2 levels were increased in NAFLD patients and were positively associated with the risk of NAFLD. Serum RCAN2, especially the serum RCAN2/(AST/ALT) ratio might be a novel diagnostic biomarker for NAFLD. In the future, prospective longitudinal studies and basic research, especially tissue-specific knockout

studies of RCAN2, are needed to confirm the role of RCAN2 in the development of NAFLD.

DATA AVAILABILITY STATEMENT

The original contributions presented in the study are included in the article/**Supplementary Material**, further inquiries can be directed to the corresponding authors.

ETHICS STATEMENT

The studies involving human participants were reviewed and approved by the Affiliated Hospital of Southwest Medical University. The patients/participants provided their written informed consent to participate in this study. The animal study was reviewed and approved by the Experimental Animal Ethics Committee of Southwest Medical University.

AUTHOR CONTRIBUTIONS

Guarantors of the article: JF, XF, HW, YX, and JF conceived and designed the study; XF, HW, XT, TY, and JF performed the experiments. XF, HW, and JF analyzed the data. XF, HW, YX, and JF wrote and edited the manuscript. All authors have read and approved the final manuscript.

FUNDING

This work was supported by the Key Project of Natural Science of Southwest Medical University (Grant No. 2020ZRZD003 and 2020ZRZD004), the Doctor Initiation Fund of the Affiliated Hospital of Southwest Medical University (Grant Nos 19064 and 20117), and Natural Science Foundation of China (Grant No. 81970676).

ACKNOWLEDGMENTS

The authors are grateful to all the participants for their participation.

SUPPLEMENTARY MATERIAL

The Supplementary Material for this article can be found online at: <https://www.frontiersin.org/articles/10.3389/fphar.2022.840764/full#supplementary-material>

REFERENCES

Adams, A. C., Astapova, I., Fisher, F. M., Badman, M. K., Kurgansky, K. E., Flier, J. S., et al. (2010). Thyroid Hormone Regulates Hepatic Expression of Fibroblast

Growth Factor 21 in a PPARalpha-dependent Manner. *J. Biol. Chem.* 285 (19), 14078–14082. doi:10.1074/jbc.C110.107375
Cao, X., Kambe, F., Miyazaki, T., Sarkar, D., Ohmori, S., and Seo, H. (2002). Novel Human ZAKI-4 Isoforms: Hormonal and Tissue-specific Regulation and Function as Calcineurin Inhibitors. *Biochem. J.* 367 (Pt 2), 459–466. doi:10.1042/BJ20011797

- Chalasani, N., Younossi, Z., Lavine, J. E., Diehl, A. M., Brunt, E. M., Cusi, K., et al. (2012). The Diagnosis and Management of Non-alcoholic Fatty Liver Disease: Practice Guideline by the American Association for the Study of Liver Diseases, American College of Gastroenterology, and the American Gastroenterological Association. *Hepatology* 55 (6), 2005–2023. doi:10.1002/hep.25762
- Chalasani, N., Younossi, Z., Lavine, J. E., Charlton, M., Cusi, K., Rinella, M., et al. (2018). The Diagnosis and Management of Nonalcoholic Fatty Liver Disease: Practice Guidance from the American Association for the Study of Liver Diseases. *Hepatology* 67 (1), 328–357. doi:10.1002/hep.29367
- Chen, Z. Y., Sun, Y. T., Wang, Z. M., Hong, J., Xu, M., Zhang, F. T., et al. (2022). Rab2A Regulates the Progression of Nonalcoholic Fatty Liver Disease Downstream of AMPK-TBC1D1 axis by Stabilizing PPAR γ . *Plos Biol.* 20 (1), e3001522. doi:10.1371/journal.pbio.3001522
- Davies, K. J., Ermak, G., Rothermel, B. A., Pritchard, M., Heitman, J., Ahnn, J., et al. (2007). Renaming the DSCR1/Adapt78 Gene Family as RCAN: Regulators of Calcineurin. *FASEB J.* 21 (12), 3023–3028. doi:10.1096/fj.06-7246com
- Donnelly, K. L., Smith, C. I., Schwarzenberg, S. J., Jessurun, J., Boldt, M. D., and Parks, E. J. (2005). Sources of Fatty Acids Stored in Liver and Secreted via Lipoproteins in Patients with Nonalcoholic Fatty Liver Disease. *J. Clin. Invest.* 115 (5), 1343–1351. doi:10.1172/JCI23621
- Fan, J. G., Jia, J. D., Li, Y. M., Wang, B. Y., Lu, L. G., Shi, J. P., et al. (2011). Guidelines for the Diagnosis and Management of Nonalcoholic Fatty Liver Disease: Update 2010: (Published in Chinese on Chinese Journal of Hepatology 2010; 18:163-166). *J. Dig. Dis.* 12 (1), 38–44. doi:10.1111/j.1751-2980.2010.00476.x
- Friedman, S. L., Neuschwander-Tetri, B. A., Rinella, M., and Sanyal, A. J. (2018). Mechanisms of NAFLD Development and Therapeutic Strategies. *Nat. Med.* 24 (7), 908–922. doi:10.1038/s41591-018-0104-9
- Fuentes, J. J., Genescà, L., Kingsbury, T. J., Cunningham, K. W., Pérez-Riba, M., Estivill, X., et al. (2000). DSCR1, Overexpressed in Down Syndrome, Is an Inhibitor of Calcineurin-Mediated Signaling Pathways. *Hum. Mol. Genet.* 9 (11), 1681–1690. doi:10.1093/hmg/9.11.1681
- Gao, P., Zhang, H., Zhang, Q., Fang, X., Wu, H., Wang, M., et al. (2019). Caloric Restriction Exacerbates Angiotensin II-Induced Abdominal Aortic Aneurysm in the Absence of P53. *Hypertension* 73 (3), 547–560. doi:10.1161/HYPERTENSIONAHA.118.12086
- Gollogly, L. K., Ryeom, S. W., and Yoon, S. S. (2007). Down Syndrome Candidate Region 1-like 1 (DSCR1-L1) Mimics the Inhibitory Effects of DSCR1 on Calcineurin Signaling in Endothelial Cells and Inhibits Angiogenesis. *J. Surg. Res.* 142 (1), 129–136. doi:10.1016/j.jss.2006.10.011
- Hattori, Y., Sentani, K., Shinmei, S., Oo, H. Z., Hattori, T., Imai, T., et al. (2019). Clinicopathological Significance of RCAN2 Production in Gastric Carcinoma. *Histopathology* 74 (3), 430–442. doi:10.1111/his.13764
- Kingsbury, T. J., and Cunningham, K. W. (2000). A Conserved Family of Calcineurin Regulators. *Genes Dev.* 14 (13), 1595–1604. doi:10.1101/gad.14.13.1595
- Luo, Y. Y., Xu, H. T., Yang, Z. Q., Lin, X. F., Zhao, F. L., Huang, Y. S., et al. (2022). Long Non-coding RNA MALAT1 Silencing Elevates microRNA-26a-5p to Ameliorate Myocardial Injury in Sepsis by Reducing Regulator of Calcineurin 2. *Arch. Biochem. Biophys.* 15, 715. doi:10.1016/j.abb.2021.109047
- Mammarella, E., Zampieri, C., Panatta, E., Melino, G., and Amelio, I. (2021). NUAKE2 and RCAN2 Participate in the P53 Mutant Pro-tumorigenic Network. *Biol. Direct* 16 (1), 11. doi:10.1186/s13062-021-00296-5
- Miyazaki, T., Kanou, Y., Murata, Y., Ohmori, S., Niwa, T., Maeda, K., et al. (1996). Molecular Cloning of a Novel Thyroid Hormone-Responsive Gene, ZAKI-4, in Human Skin Fibroblasts. *J. Biol. Chem.* 271 (24), 14567–14571. doi:10.1074/jbc.271.24.14567
- Mizuno, Y., Kanou, Y., Rogatcheva, M., Imai, T., Refetoff, S., Seo, H., et al. (2004). Genomic Organization of Mouse ZAKI-4 Gene that Encodes ZAKI-4 Alpha and Beta Isoforms, Endogenous Calcineurin Inhibitors, and Changes in the Expression of These Isoforms by Thyroid Hormone in Adult Mouse Brain and Heart. *Eur. J. Endocrinol.* 150 (3), 371–380. doi:10.1530/eje.0.1500371
- Negro, F. (2020). Natural History of NASH and HCC. *Liver Int.* 40 (Suppl. 1), 72–76. doi:10.1111/liv.14362
- Niitsu, H., Hinoi, T., Kawaguchi, Y., Sentani, K., Yuge, R., Kitadai, Y., et al. (2016). KRAS Mutation Leads to Decreased Expression of Regulator of Calcineurin 2, Resulting in Tumor Proliferation in Colorectal Cancer. *Oncogenesis* 5 (8), e253. doi:10.1038/oncsis.2016.47
- Parthasarathy, G., Revelo, X., and Malhi, H. (2020). Pathogenesis of Nonalcoholic Steatohepatitis: An Overview. *Hepatol. Commun.* 4 (4), 478–492. doi:10.1002/hep4.1479
- Rothermel, B., Vega, R. B., Yang, J., Wu, H., Bassel-Duby, R., and Williams, R. S. (2000). A Protein Encoded within the Down Syndrome Critical Region Is Enriched in Striated Muscles and Inhibits Calcineurin Signaling. *J. Biol. Chem.* 275 (12), 8719–8725. doi:10.1074/jbc.275.12.8719
- Siddiqi, A., Miyazaki, T., Takagishi, Y., Kanou, Y., Hayasaka, S., Inouye, M., et al. (2001). Expression of ZAKI-4 Messenger Ribonucleic Acid in the Brain during Rat Development and the Effect of Hypothyroidism. *Endocrinology* 142 (5), 1752–1759. doi:10.1210/endo.142.5.8156
- Strippoli, P., Petrini, M., Lenzi, L., Carinci, P., and Zannotti, M. (2000). The Murine DSCR1-like (Down Syndrome Candidate Region 1) Gene Family: Conserved Synteny with the Human Orthologous Genes. *Gene* 257 (2), 223–232. doi:10.1016/s0378-1119(00)00407-8
- Sun, X. Y., Hayashi, Y., Xu, S., Kanou, Y., Takagishi, Y., Tang, Y. P., et al. (2011). Inactivation of the Rcan2 Gene in Mice Ameliorates the Age- and Diet-Induced Obesity by Causing a Reduction in Food Intake. *PLoS One* 6 (1), e14605. doi:10.1371/journal.pone.0014605
- Tan, L. J., Jung, H., Kim, S. A., and Shin, S. (2021). The Association between Coffee Consumption and Nonalcoholic Fatty Liver Disease in the South Korean General Population. *Mol. Nutr. Food Res.* 65 (18), e2100356. doi:10.1002/mnfr.202100356
- Younossi, Z. M., Koenig, A. B., Abdelatif, D., Fazel, Y., Henry, L., and Wymer, M. (2016). Global Epidemiology of Nonalcoholic Fatty Liver Disease-Meta-Analytic Assessment of Prevalence, Incidence, and Outcomes. *Hepatology* 64 (1), 73–84. doi:10.1002/hep.28431
- Yuan, H., Suzuki, S., Hirata-Tsuchiya, S., Sato, A., Nemoto, E., Saito, M., et al. (2021). PPAR γ -Induced Global H3K27 Acetylation Maintains Osteo/Cementogenic Abilities of Periodontal Ligament Fibroblasts. *Int. J. Mol. Sci.* 22 (16), 8646. doi:10.3390/ijms22168646
- Zhao, J., Li, S. W., Gong, Q. Q., Ding, L. C., Jin, Y. C., Zhang, J., et al. (2016). A Disputed Evidence on Obesity: Comparison of the Effects of Rcan2(-/-) and Rps6kb1(-/-) Mutations on Growth and Body Weight in C57BL/6J Mice. *J. Zhejiang Univ. Sci. B* 17 (9), 657–671. doi:10.1631/jzus.B1600276

Conflict of Interest: The authors declare that the research was conducted in the absence of any commercial or financial relationships that could be construed as a potential conflict of interest.

Publisher's Note: All claims expressed in this article are solely those of the authors and do not necessarily represent those of their affiliated organizations, or those of the publisher, the editors, and the reviewers. Any product that may be evaluated in this article, or claim that may be made by its manufacturer, is not guaranteed or endorsed by the publisher.

Copyright © 2022 Fang, Wang, Tan, Ye, Xu and Fan. This is an open-access article distributed under the terms of the Creative Commons Attribution License (CC BY). The use, distribution or reproduction in other forums is permitted, provided the original author(s) and the copyright owner(s) are credited and that the original publication in this journal is cited, in accordance with accepted academic practice. No use, distribution or reproduction is permitted which does not comply with these terms.

GLOSSARY

A/G Albumin-globulin-ratio

ALB Albumin

ALP Alkaline phosphatase

ALT Alanine aminotransferase

AST Aspartate aminotransferase

AUC Area under the curve

BMI Body mass index

Crea Creatinine

DBP Diastolic blood pressure

FBG Fasting blood glucose

FLI Fatty liver index

GGT Gamma-glutamyl transpeptidase

GLO Globulin

HC Hip circumference

HCY Homocysteine

HDL-C High-density lipoprotein cholesterol

LDL-C Low-density lipoprotein cholesterol

NAFLD Non-alcoholic fatty liver disease

NASH Non-alcoholic steatohepatitis

NEU Neutrophil

qRT-PCR Quantitative real-time PCR

SBP Systolic blood pressure

TC Total cholesterol

TG Triglyceride

TP Total protein

UA Uric acid

WBC White blood cells

WC Waist circumference

WHR Waist to hip ratio

RCAN2 Regulator of calcineurin 2



NUSAP1 Could be a Potential Target for Preventing NAFLD Progression to Liver Cancer

Tao-fei Zeng^{1†}, Guang-lei Chen^{2†}, Xin-bo Qiao², Hui Chen³, Lisha Sun², Qing-tian Ma², Na Li^{4,5}, Jun-qi Wang¹, Chao-liu Dai¹ and Feng Xu^{1*}

¹Department of General Surgery, Hepatobiliary and Splenic Surgery Ward, Shengjing Hospital of China Medical University, Shenyang, China, ²Department of Oncology, Shengjing Hospital of China Medical University, Shenyang, China, ³Department of General Surgery, Pancreatic and Thyroid Surgery Ward, Shengjing Hospital of China Medical University, Shenyang, China, ⁴Department of Pediatrics, Shengjing Hospital of China Medical University, Shenyang, China, ⁵Department of Pediatrics, The Second Affiliated Hospital of Dalian Medical University, Dalian, China

OPEN ACCESS

Edited by:

Francisco Javier Cubero,
Complutense University of Madrid,
Spain

Reviewed by:

Prasanna K. Santhekadur,
JSS Academy of Higher Education
and Research, India
Arantza Lamas Paz,
Universidad Complutense de Madrid,
Spain

*Correspondence:

Feng Xu
xuf@sj-hospital.org
fxu@cmu.edu.cn

[†]These authors have contributed
equally to this work

Specialty section:

This article was submitted to
Gastrointestinal and Hepatic
Pharmacology,
a section of the journal
Frontiers in Pharmacology

Received: 26 November 2021

Accepted: 11 March 2022

Published: 01 April 2022

Citation:

Zeng T, Chen G, Qiao X, Chen H,
Sun L, Ma Q, Li N, Wang J, Dai C and
Xu F (2022) NUSAP1 Could be a
Potential Target for Preventing NAFLD
Progression to Liver Cancer.
Front. Pharmacol. 13:823140.
doi: 10.3389/fphar.2022.823140

Background: Non-alcoholic fatty liver disease (NAFLD) has gradually emerged as the most prevalent cause of chronic liver diseases. However, specific changes during the progression of NAFLD from non-fibrosis to advanced fibrosis and then hepatocellular carcinoma (HCC) are unresolved. Here, we firstly identify the key gene linking NAFLD fibrosis and HCC through analysis and experimental verification.

Methods: Two GEO datasets (GSE89632, GSE49541) were performed for identifying differentially expressed genes (DEGs) associated with NAFLD progression from non-fibrosis to early fibrosis and eventually to advanced fibrosis. Subsequently, Gene Ontology (GO), Kyoto Encyclopedia of Genes and Genomes (KEGG) pathways enrichment analysis, protein-protein interaction (PPI) network were integrated to explore the potential function of the DEGs and hub genes. The expression of NUSAP1 was confirmed *in vivo* and *in vitro* NAFLD models at mRNA and protein level. Then, cell proliferation and migration under high fat conditions were verified by cell counting kit-8 (CCK-8) and wound-healing assays. The lipid content was measured with Oil Red O staining. Finally, the analysis of clinical survival curves was performed to reveal the prognostic value of the crucial genes among HCC patients via the online web-tool GEPIA2 and KM plotter.

Results: 5510 DEGs associated with non-fibrosis NAFLD, 3913 DEGs about NAFLD fibrosis, and 739 DEGs related to NAFLD progression from mild fibrosis to advanced fibrosis were identified. Then, a total of 112 common DEGs were found. The result of enrichment analyses suggested that common DEGs were strongly associated with the glucocorticoid receptor pathway, regulation of transmembrane transporter activity, peroxisome, and proteoglycan biosynthetic process. Six genes, including KIAA0101,

Abbreviations: DEGs, differentially expressed genes; DFS, distance free survival; GO, gene ontology; GEPIA2, gene expression profiling interactive analysis; HCC, hepatocellular carcinoma; KEGG, kyoto encyclopedia of genes and genomes; KIF22, kinesin family member 22; KIAA0101, proliferating cell nuclear antigen-binding factor; NUSAP1, nucleolar and spindle associated protein 1; NAFLD, non-alcoholic fatty liver disease; NASH, non-alcoholic steatohepatitis; OS, overall survival; PPI, protein-protein interaction; RAD51AP1, RAD51-associated protein 1; PPARs, peroxisome proliferator-activated receptors; RFS, relapse free survival; PFS, progression free survival; UHRF1, ubiquitin-like with PHD and ring finger domains 1; ZWINT, ZW10 interacting kinetochore protein.

NUSAP1, UHRF1, RAD51AP1, KIF22, and ZWINT, were identified as crucial candidate genes via the PPI network. The expression of NUSAP1 was validated highly expressed *in vitro* and *vivo* NAFLD models at mRNA and protein level. NUSAP1 silence could inhibit the ability of cell proliferation, migration and lipid accumulation *in vitro*. Finally, we also found that NUSAP1 was significantly up-regulated at transcriptional and protein levels, and associated with poor survival and advanced tumor stage among HCC patients.

Conclusion: NUSAP1 may be a potential therapeutic target for preventing NAFLD progression to liver cancer.

Keywords: non-alcoholic fatty liver disease, liver fibrosis, hepatocellular carcinoma, bioinformatics analysis, drug targets

INTRODUCTION

Nonalcoholic fatty liver disease (NAFLD) is one of the most widespread chronic liver diseases globally, affecting 25% of the general population and 85%–98% of morbidly obese patients worldwide (Friedman et al., 2018; Berardo et al., 2020). The disease progression of NAFLD is a dynamic process. In the early stage of NAFLD, hepatocytes begin to experience lipid deposition. As lipid deposition increases, lipotoxicity damages of hepatocytes aggravate, which in turn induces oxidative stress, leads to damage to cell mitochondria, triggers inflammatory factors release, and exacerbates hepatocyte damage (Schuster et al., 2018). With the aggravation of lipid deposition in hepatocytes and the occurrence of inflammation, about 20% of NAFLD patients can progress to non-alcoholic steatohepatitis (NASH) (Eslam et al., 2018; Younossi et al., 2018). Some patients with NASH progressively developed liver cirrhosis, hepatocellular carcinoma (HCC), and eventually liver disease-related death (Anstee et al., 2019). Therefore, the increasing prevalence of NAFLD worldwide is entirely worthy of clinical attention.

Until now, no specific pharmacological therapies are attainable for the treatment of NAFLD (Rinella and Sanyal, 2016). The physical therapy treatments for patients suffering from NAFLD and NASH was recommended to change lifestyle and balance nutrition, in addition to control weight loss and physical exercise. Contrary to expectations, the majority of patients fail to lose weight (Vilar-Gomez et al., 2015; Marchesini et al., 2016). Therefore, it is worth elucidating the intrinsic molecular pathogenesis of NAFLD, and more exhaustive and detailed research is needed to explore the molecular mechanism and obtain new specific therapeutic targets.

We conducted a more comprehensive bioinformatics analysis between normal liver tissues and non-fibrosis/fibrosis NAFLD tissues, advanced fibrosis and mild fibrosis NAFLD tissues in the present study. Based on comprehensive bioinformatics analyses, hub genes identification, biological processes and pathways were also determined. Finally, we also demonstrated that these genes were highly expressed in NAFLD-associated HCC patients and strongly associated with poor prognosis and more advanced tumor stages. Our realization will provide meaningful clues for the treatment of NAFLD and NAFLD-associated HCC.

METHODS

Acquisition of Datasets

Three NAFLD-related datasets GSE89632 (Arendt et al., 2015), GSE49541 (Moylan et al., 2014) and GSE164441 (Yang et al., 2021) were downloaded from the Gene Expression Omnibus (GEO) database (<https://www.ncbi.nlm.nih.gov/geo/>) including the gene expression profile data and related annotation file. The search keywords used were “Nonalcoholic fatty liver disease” AND “*Homo sapiens*.” The inclusion criteria for the dataset are as follows: (1) Each dataset included contained at least 10 samples; (2) Each sample contained pathological information; (3) The raw data or gene expression profiling from these datasets are accessible at the GEO.

The details of these datasets were shown in **Table 1**. The platform for GSE89632 was Illumina HumanHT-12 WG-DASL V4.0 R2 expression beadchip, for GSE49541 was Affymetrix Human Genome U133 Plus 2.0 Array (HG-U133_Plus_2), and for GSE164441 was GPL20301, Illumina HiSeq 4000 (*Homo sapiens*). It is important to note that samples with no specific pathologic information were not analyzed.

DEGs Identification

The “limma” software package in R software was used to screen out DEGs based on the cut-off criteria (Ritchie et al., 2015). The conditions of $|\log_2 FC| \geq 0.5$, adjust p -value < 0.05 (corrected by B and H method) was used for NAFLD without fibrosis vs. healthy liver sample and NAFLD with fibrosis vs. healthy liver sample group to obtain DEGs associated with NAFLD fibrosis. GSE49541 included 40 mild NAFLD liver tissue samples and 32 advanced NAFLD liver tissue samples. The cut-off criterion of adjust p -value < 0.05 (corrected by B and H method) was used to obtain DEGs associated with NAFLD fibrosis progression. The heatmap for the DEGs was created using the “ggplot2” package (<https://ggplot2.tidyverse.org>), and the Venn plot for co-expressed DEGs was integrated using the “ggvenn” (<https://github.com/yanlinlin82/ggvenn>) packages, and utilized for the following analysis.

Functional and Pathway Enrichment Analysis

To investigate the functional biological roles of the co-expressed DEGs, Gene Ontology (GO) terms and Kyoto Encyclopedia of

TABLE 1 | Characteristics of the included microarray datasets.

| GSE ID | Participants Included | Tissues | Analysis | Platform | Year |
|-----------|--|---------|----------|----------|------|
| GSE89632 | 21 cases with no fibrosis, 18 cases with fibrosis and 11 healthy controls | Liver | Array | GPL14951 | 2016 |
| GSE49541 | 40 cases with mild fibrosis and 32 cases with advanced fibrosis | Liver | Array | GPL570 | 2013 |
| GSE164441 | 10 cases with (NAFLD)- associated HCC tumor ($n = 10$) and adjacent non-tumor liver tissues ($n = 10$) | Liver | RNA-seq | GPL20301 | 2021 |

TABLE 2 | Hub genes with a high degree of connectivity.

| Gene | MCODE Score | MCODE Cluster |
|----------|-------------|---------------|
| KIF22 | 4.0 | 1 |
| ZWINT | 4.0 | 1 |
| KIAA0101 | 3.73 | 1 |
| UHRF1 | 3.73 | 1 |
| NUSAP1 | 3.73 | 1 |
| RAD51AP1 | 3.73 | 1 |

Genes and Genomes (KEGG) pathways were automatically completed and visualized by the Metascape (Zhou et al., 2019). p -value < 0.05 was set as the significance threshold.

Protein-Protein Interaction Network Construction

The common significant DEGs were mapped to the STRING database (<http://www.string-db.org/>), then set confidence >0.4 to conduct the PPI network analysis (Szklarczyk et al., 2019), which were visualized by Cytoscape software (v3.8.1) (Shannon et al., 2003). Module analysis was performed to identify significant modules and explore the hub genes using the Molecular Complex Detection (MCODE V2.0.0) (Bader and Hogue, 2003), which is a plug-in of Cytoscape (MCODE score ≥ 3.5).

Expression Levels and Prognostic Value of Hub Genes in HCC

First, we downloaded the gene expression matrix from GSE164441, composed of 10 cases with (NAFLD)-associated HCC tumor and paired adjacent non-tumor liver tissues. The “ggolot2” package visualized the expression of key genes in NAFLD-induced tumor tissues and adjacent non-tumor liver tissues. Clinical survival analyses were retrieved online using the online tools, Gene Expression Profiling Interactive Analysis (GEPIA2) (<http://gepia.cancer-pku.cn/>) and Kaplan-Meier Plotter (<http://kmplot.com/analysis/>). p -value = 0.05 and $|\log_2FC| = 1$ and were defined as the threshold for statistical significance (Tang et al., 2017). Finally, the HPA database (<https://www.proteinatlas.org/>) provides tissue and cellular distribution information of various human proteins using immunoassay technology (Uhlén et al., 2005; Berglund et al., 2008; Pontén et al., 2008; Uhlén et al., 2015; Thul et al., 2017; Uhlen et al., 2017).

Cell Culture and Treatment

The human hepatocyte cell lines HL-7702 and hepatoma cell line MHCC-97H (iCell Bioscience Inc., Shanghai, China) were

cultured in a humidified incubator at 37°C with 5% CO₂ using RPMI-1640 with 10% FBS and 1% P/S solution (Procell). To establish the *in vitro* NAFLD cell model, HL-7702 and MHCC-97H cells were cultured in the presence or absence of 1 mmol/L free fatty acids (FFA, containing oleic acid and palmitic acid at a 2:1 volume ratio) for 24 h and then used for the indicated assays (Long et al., 2019).

Construction of NAFLD Model Mice

Ten male C57/BL6 mice (7–8 weeks old) were randomly divided into two groups, one was administrated with a 60% high-fat diet (HFD) (New Brunswick, NJ08901, United States) ($n = 5$) and the other with a control diet (CD, 10% fat) for 12 weeks ($n = 5$) (Jiang et al., 2019). The animals were housed in a temperature-controlled environment, with a 12-h light/dark cycle and received food and water ad libitum, at the center of experimental animals of Benxi Laboratory, Shengjing Hospital of China Medical University. The animal experiments received ethical clearance from the Ethics Committee of Shengjing Hospital of China Medical University (2021PS570K).

Sample Collection

After 12 weeks' treatment, the mice were sacrificed under deeply anesthesia. The livers were then perfused with PBS via the portal vein to remove the blood and divided into two pieces. One was preserved in 10% neutral-buffered formalin, while the other was immediately frozen in liquid N₂ and stored at -80°C.

RT-PCR

Trizol reagent (Invitrogen, CA, United States) was utilized to extract total RNA according to the manufacturer's protocol. Total RNA was then reverse-transcribed into the complementary DNAs (cDNAs) with the PrimeScript RT Reagent Kit with gDNA Eraser (TaKaRa, Dalian, China) and amplified by GoTaq qPCR Master Mix (Promega, Madison, WI, United States) using the ABI ViiA 7 Real-time PCR system (Applied Biosystems, United States). The relative mRNA levels were normalized to those of the housekeeping gene GAPDH. All samples were determined by the $2^{-\Delta\Delta CT}$ method. The primer pairs used in this study are listed in **Supplementary Table S1**.

Cell Transfection

The NUSAP1 siRNA and negative controls were purchased from HANBIO (HANBIO, Shanghai, China). The transfection of HL-7702 and MHCC-97H cells was conducted in accordance with manufacturer's guidance.

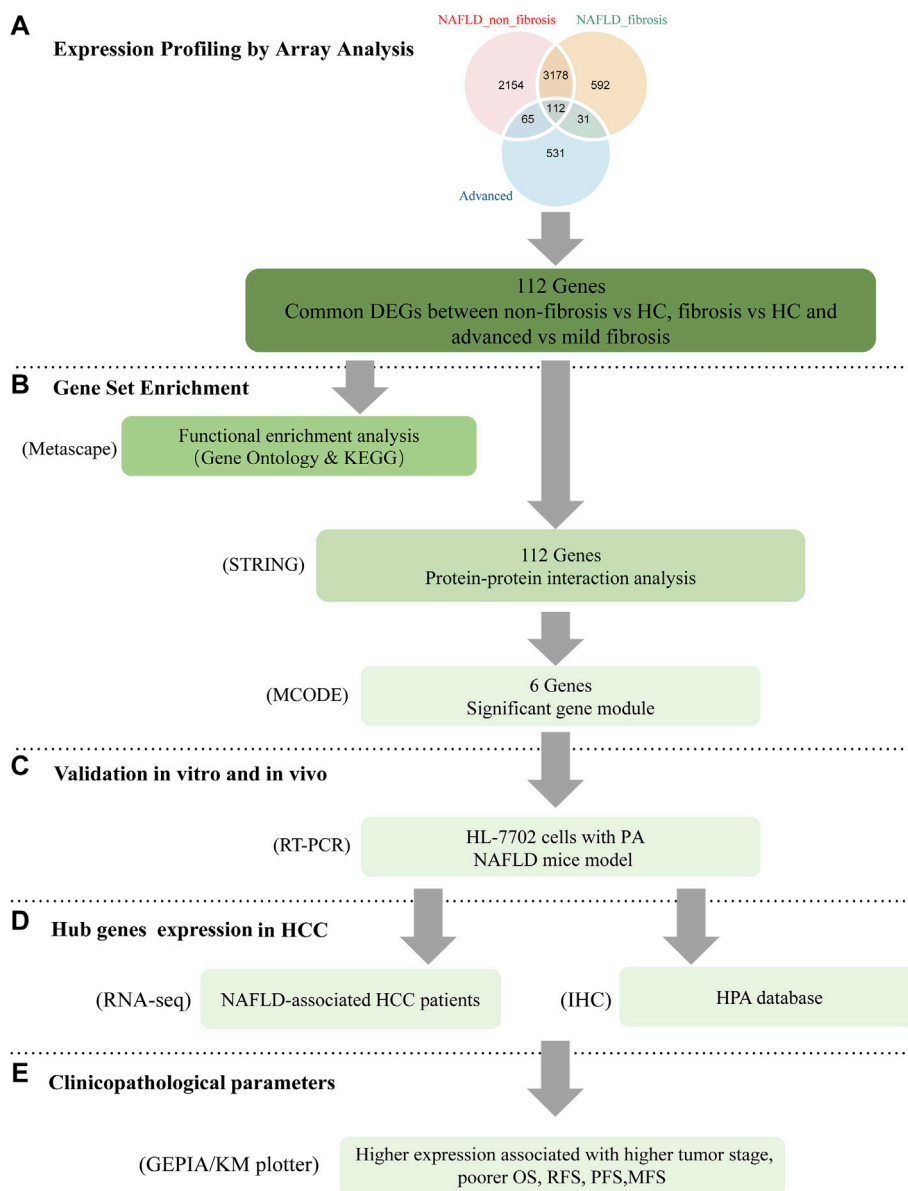


FIGURE 1 | Workflow of the present study. **(A)** common DEGs between non-fibrosis vs HC, fibrosis vs HC and advanced vs mild fibrosis were identified by integrated bioinformatics analysis. **(B)** Enrichment analysis was carried by the Metascape online database. The hub genes were attained by PPI with STRING and MCODE with cytoscape. **(C)** The expression of key genes was verified by *in vitro* and *in vivo* experiments. The function of NUSAP1 was confirmed by silencing assay. **(D,E)** The expression of NUSAP1 in hepatocellular carcinoma and its relationship with prognosis were explored. DEGs, differentially expressed genes; HC, Healthy Control; FFA, free fatty acids; IHC, immunohistochemistry; HPA, The Human Protein Atlas.

Cell Counting Kit-8 Assay

Cells transfected with si-NUSAP1 were plated in 96-well plates and cultured for 24 h. Then, the transfected cells were add with 10 μ L CCK-8 reagent. After 2 h incubation, the well's absorbance at 450 nm was measured by microplate reader. Each group set was repeated for five times and each measurement was performed three times repeatedly.

Oil Red O Staining

Fresh or frozen tissues were fixed with 4% paraformaldehyde for 1 h at room temperature, and cell samples were washed with PBS and then fixed with 4% paraformaldehyde for 20min. Oil red O stain (Servicebio, G1015-100ML, Yikeshengwu, China) were operated in accordance with the manufacturer's instructions.

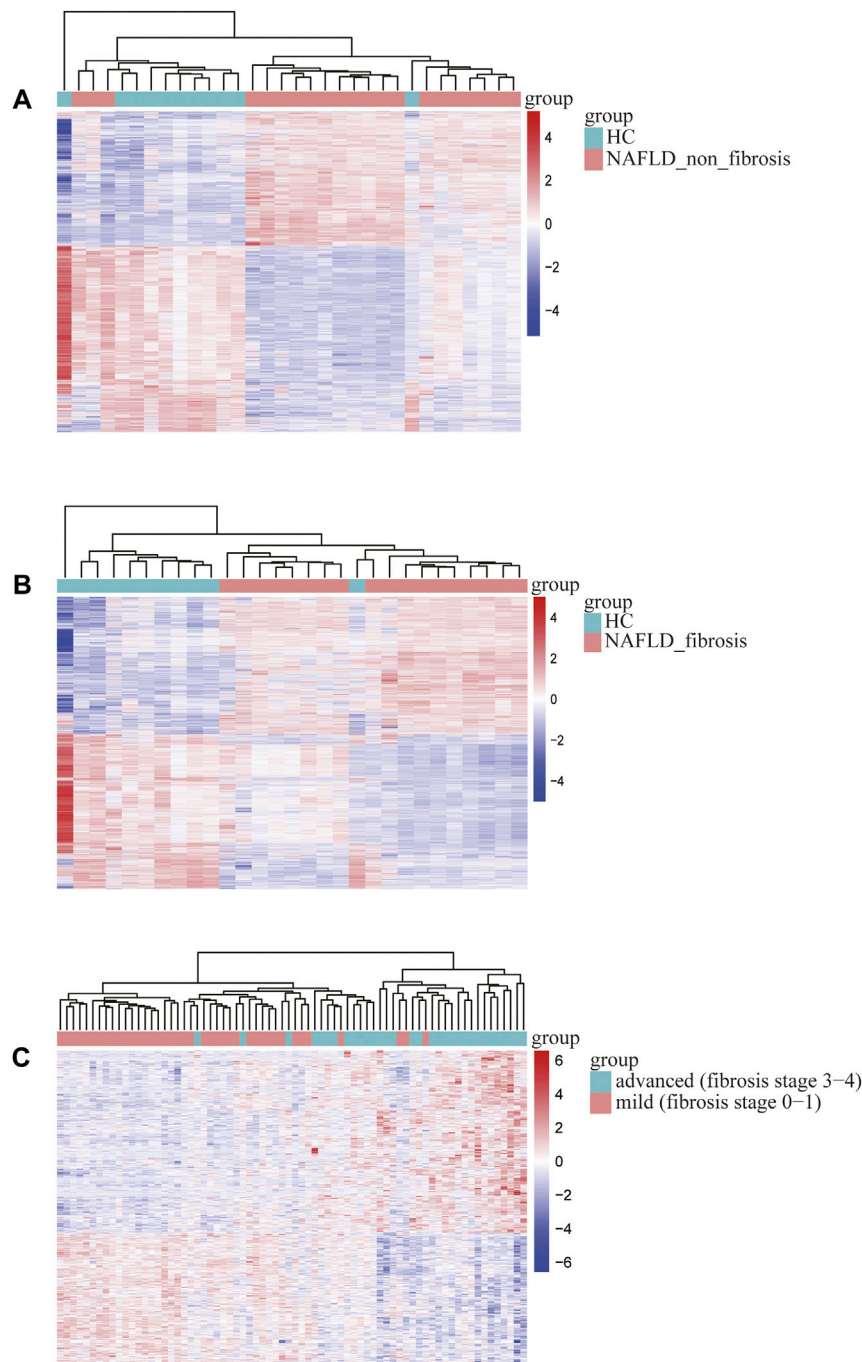


FIGURE 2 | Heatmap of differentially expressed genes identified in **(A)** non-fibrosis vs. HC group in GSE89632, **(B)** fibrosis vs. HC group in GSE89632, **(C)** advanced vs. mild fibrosis in GSE49541. Legend on the top right indicates the relative expression levels of the genes.

Western Blotting

Detailed steps of Western blotting are described (Zhou et al., 2010). Primary antibodies was NUSAP1 polyclonal antibody (ProteinTech, 12024-1-AP, United States) and GAPDH (ProteinTech Group, Rosemont, IL, United States) epitopes monoclonal antibodies. Then, the secondary antibody for Western blotting was the

horseradish-peroxidase-labeled secondary antibody (ProteinTech Group, Rosemont, IL, United States).

Statistical Analysis

All the contents of bioinformatics analysis were analyzed with R version 4.0.5 (<https://www.r-project.org/>). Student's t-test was used to

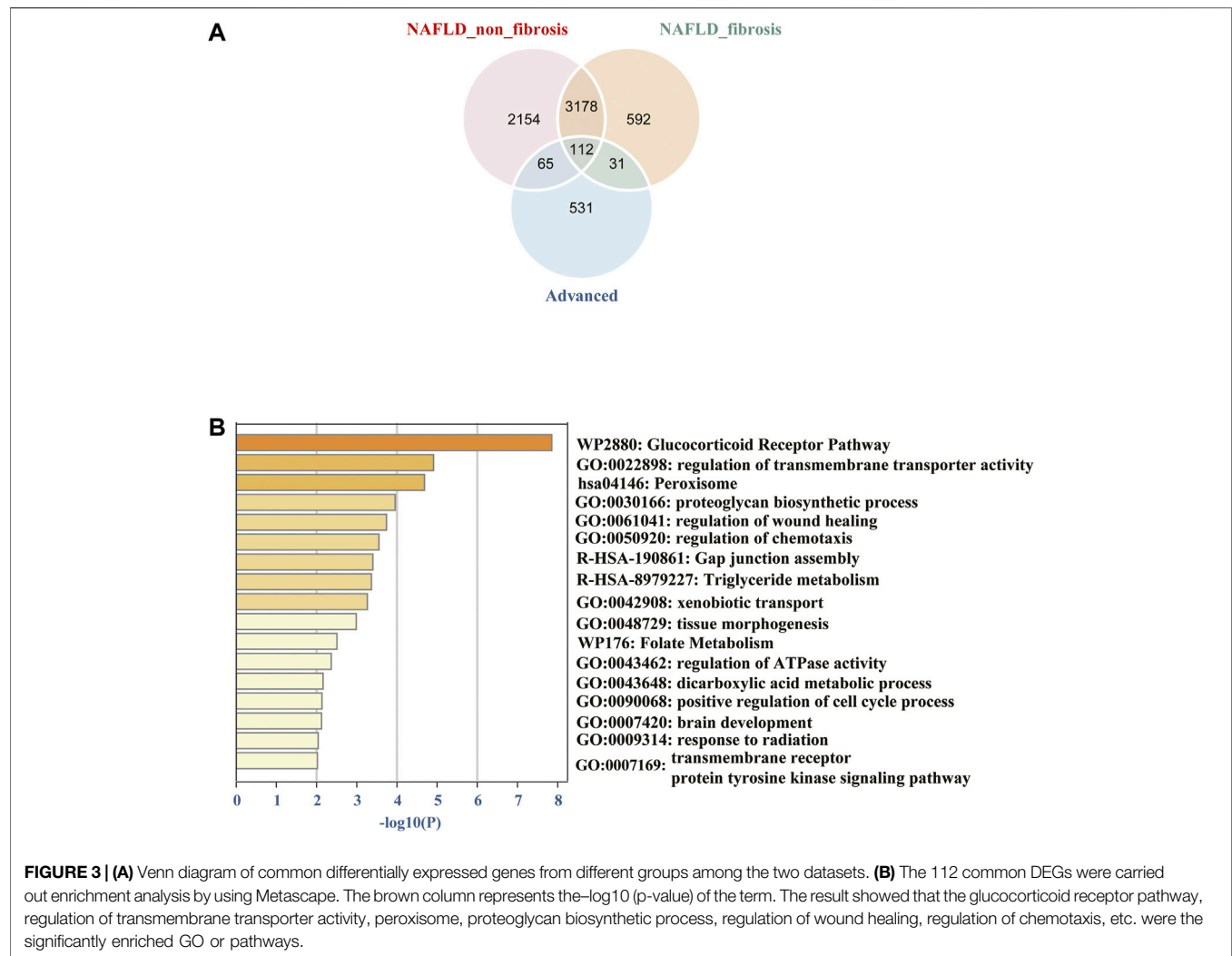


FIGURE 3 | (A) Venn diagram of common differentially expressed genes from different groups among the two datasets. **(B)** The 112 common DEGs were carried out enrichment analysis by using Metascape. The brown column represents the $-\log_{10}$ (p-value) of the term. The result showed that the glucocorticoid receptor pathway, regulation of transmembrane transporter activity, peroxisome, proteoglycan biosynthetic process, regulation of wound healing, regulation of chemotaxis, etc. were the significantly enriched GO or pathways.

analyze the relative expression levels of hub genes. The $p < 0.05$ was considered statistically significant. * $p < 0.05$, ** $p < 0.01$; *** $p < 0.001$; ns, not significant.

RESULTS

Identification of DEGs Throughout NAFLD Progression

The bioinformatics analysis workflow is summarized in **Figure 1**. DEGs related to fibrosis, and advanced fibrosis were identified by integrated bioinformatics analysis. We first determined the DEGs among different groups of GSE89632, which consisted of 18 cases with fibrosis, 21 cases with non-fibrosis and 11 healthy controls (HC). Total number of 5510 DEGs were determined for the non-fibrosis vs. HC group and a total of 3913 DEGs were identified from the fibrosis vs. HC group. Then, we analyzed the datasets GSE49541 (32 cases with advanced fibrosis and 40 cases with mild fibrosis) and identified 739 DEGs associated with advanced fibrosis. The list of differential genes in each group were visualized by the heatmaps whose hierarchical clustering was based on Euclidean distance (**Figure 2**).

GO and KEGG Pathway Analysis of Common DEGs

The common DEGs were showed using the “ggvenn” R package, which were significantly associated with progression of NAFLD from non-fibrosis to advanced fibrosis (**Figure 3A**). More specific information about the DEGs was shown in the additional file (**Supplementary Table S2**). To gain insight into biological significance of these genes, we carried out enrichment analysis by using the Metascape online database. The results showed that pathways such as glucocorticoid receptor pathway, regulation of transmembrane transporter activity, peroxisome, proteoglycan biosynthetic process, regulation of wound healing, regulation of chemotaxis, etc., were the significantly enriched GO or pathways (**Figure 3B**).

PPI Network Analysis and Core Genes Selection

To uncover the potential relationship between 112 common DEGs, a PPI network that included 112 nodes and 65 edges

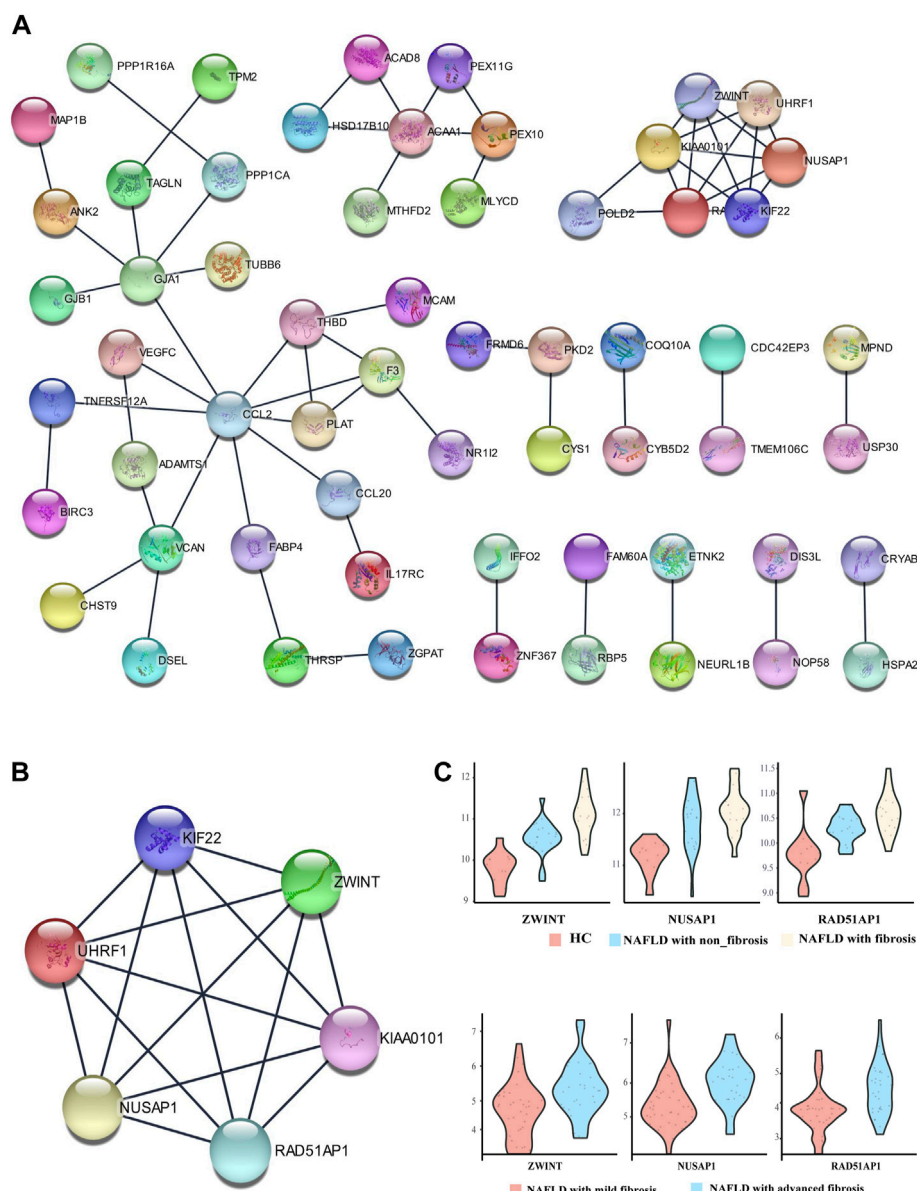


FIGURE 4 | Protein-protein interaction (PPI) network. **(A)** PPI network of differentially expressed genes (DEGs), **(B)** subnetwork of top-six hub genes from the PPI network, **(C)** The expression pattern of ZWINT, NUSAP1 and RAD51AP1 in the different stage of NAFLD.

were constructed using the STRING tool (Figure 4A). Then, the most significant modules were recognized by the MCODE plug-in of cytoscape. The top six hub genes in the MCODE cluster1 were selected (Table 2), including Kinesin Family Member 22 (KIF22), ZW10 interacting kinetochore protein (ZWINT), nucleolar and spindle associated protein 1 (NUSAP1), proliferating cell nuclear antigen-binding factor (KIAA0101), ubiquitin-like with PHD and ring finger domains 1 (UHRF1), RAD51-associated protein 1 (RAD51AP1) (Figure 4B). ZWINT, NUSAP1 and RAD51AP1 expression showed an increasing trend in the progression of NAFLD (Figure 4C), but KIF22, KIAA0101 and UHRF1 exhibits a different expression profile in different stages of the NAFLD (Supplementary Figure S1).

Validation of Hub Genes Expression *in Vitro* and *Vivo*

To further confirm the role of the hub genes in the progression of NAFLD, experimental validation was conducted *in vitro* and *vivo*. The expression of ZWINT, NUSAP1, RAD51AP1 were highly expressed in HL-7702 cells treated with FFA for 24 h as mentioned above by RT-PCR screening (Figures 5A,B). Due to a high homology between mouse and human genes, we also used mouse models of NAFLD established by HFD feeding for 12 weeks to further examine the hub gene expression levels. H&E and Oil red O staining of liver tissues exhibited compressed liver sinusoids, more dispersed lipid vacuoles

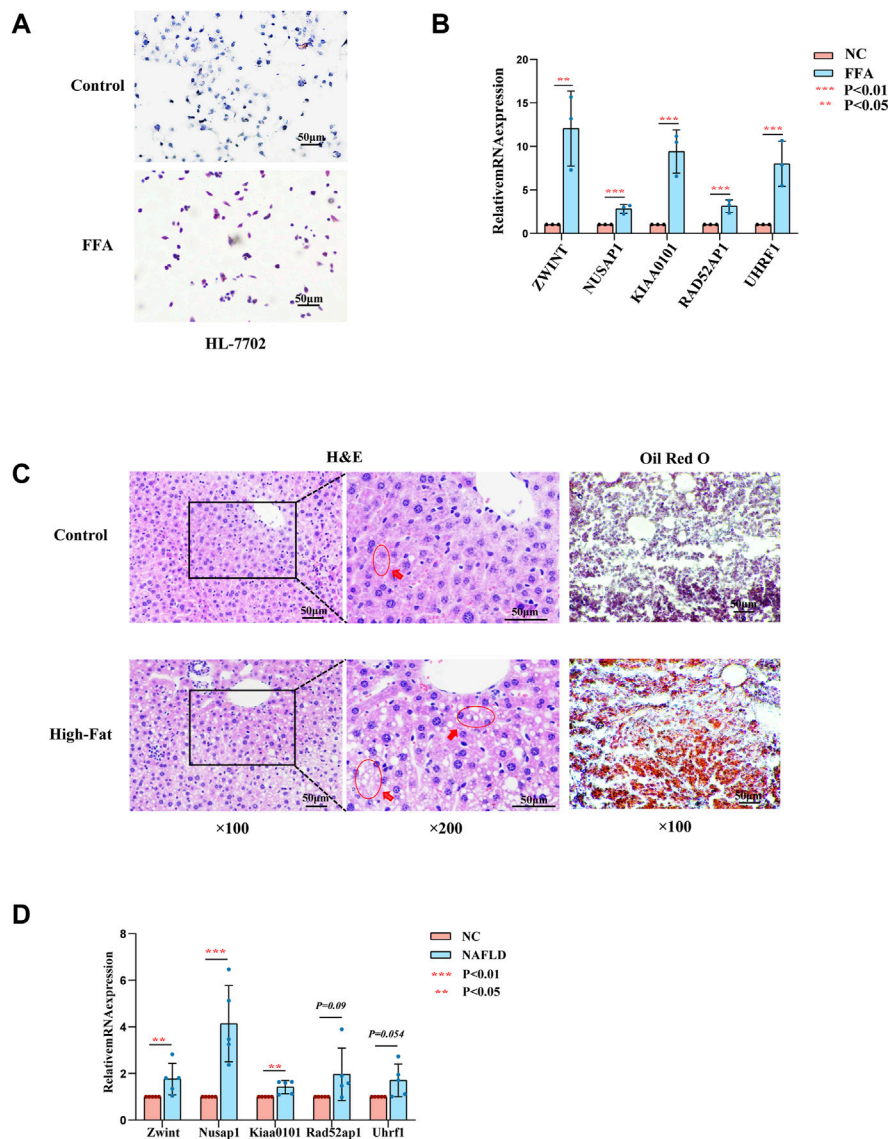


FIGURE 5 | Experiments *in vitro* and *in vivo*. **(A)** Represent Oil Red O staining of HL-7702 cells treated with or without FFA for 24 h. **(B)** Expression levels of hub genes in HL-7702 cells treated with FFA for 24 h was assessed by RT-PCR ($n = 3$). **(C)** Represent HE (left, middle) and Oil Red O staining (right) of showing hepatic steatosis in liver tissues. 100x for the HE images (left), 200x for the HE images (middle) and Oil red O images (right). **(D)** Expression levels of hub genes in NAFLD mice was assessed by RT-PCR ($n = 3-5$).

and increased hepatocyte volumes in NAFLD mice than those in control mice (**Figure 5C**). The expression of *Zwint*, and *Nusap1* were significantly upregulated in NAFLD mice compared to the control group by RT-PCR, which was consistent with the results of our previous analysis. In contrast to our previous results, *Kiaa0101* was significantly increased in NAFLD mouse. The expression levels of *Rad51ap1* and *Uhrf1* tended to increase in NAFLD mice but the difference was not statistically significant ($p = 0.09$ and $p = 0.054$) (**Figure 5D**). Therefore, NUSAP1 and ZWINT may be the key genes in the progression of NAFLD.

NUSAP1 was Highly Expressed in NAFLD-Associated HCC was Associated With Cell Migration Cell Proliferation, Migration and Fat Accumulation Under High Fat Condition

To further inquire the expression of NUSAP1 and ZWINT in the (NAFLD)-associated HCC patients, we downloaded the data set GSE164441 including 10 paired NAFLD-associated HCC tumor and adjacent normal tissues. It was found that the expression of NUSAP1 and ZWINT was significant higher ($p < 0.05$) in tumours specimens compared with para-cancer tissues

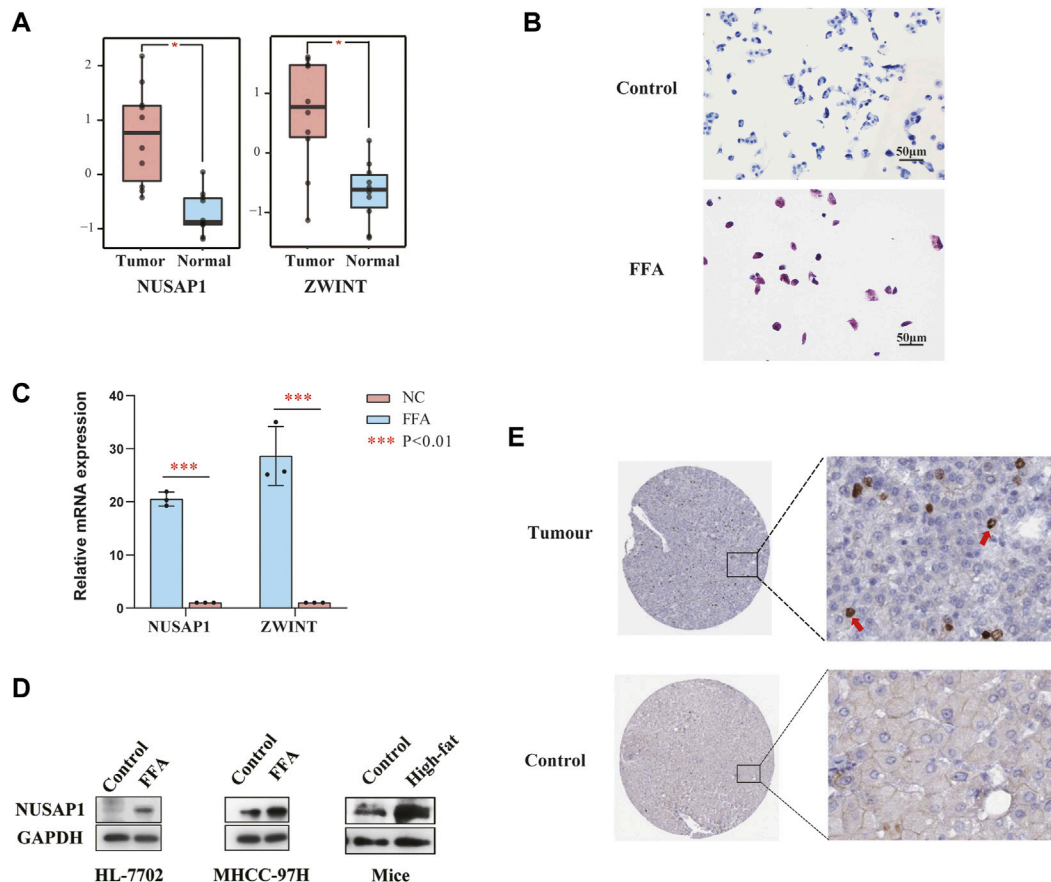


FIGURE 6 | (A) Relative mRNA expression of NUSAP1 and ZWINT in NAFLD-related cancer tissues and paired paracancer tissue (** $p < 0.001$). **(B)** Represent Oil Red O staining of MHCC-97H cells treated with or without FFA for 24 h. **(C)** Expression levels of NUSAP1 and ZWINT in MHCC-97H cell lines treated with FFA for 24 h was assessed by RT-PCR ($n = 3$). The data were presented as mean \pm SEM, $n = 3$ each group. * $p < 0.05$, *** $p < 0.001$. **(D)** The protein levels of NUSAP1 in HL-7702, MHCC-97H cell lines and NAFLD mice liver. *In vitro* $n = 3$ for each group, *in vivo*, $n = 3$ –5 for each group. **(E)** The IHC-based protein expression of NUSAP1 in HCC tissues and normal liver tissues. All the IHC staining images were obtained from the HPA database (<https://www.proteinatlas.org/ENSG00000137804-NUSAP1/pathology/liver+cancer#img>).

(Figure 6A). We then confirmed this result in *in vitro* cell line studies. NUSAP1 was highly expressed in MHCC-97H cell lines treated with 1 mmol/L of FFA for 24 h (Figures 6B,C). Then, we also investigated the protein expression of NUSAP1. Similarly, protein levels of NUSAP1 in liver normal cell HL-7702, liver cancer cell MHCC-97H and NAFLD mice liver significantly elevated (Figure 6D). What's more, IHC results about the NUSAP1 expression, obtained from the HPA database, showed that NUSAP1 had a higher intensity in HCC tissues than that in normal liver tissues (Figure 6E). In order to further verify the functional characteristics of NUSAP1, we conducted the NUSAP1 silencing assay. We firstly confirmed the efficiency of si-NUSAP1 (Figure 7A). Then CCK-8 analysis and Wound healing assays indicated that knockdown of the NUSAP1 gene could result in a significant reduction in migration of MHCC-97H cell under high fat condition (Figures 7B,C). In addition, the lipid content of the cells reduced significantly after NUSAP1 silence (Figure 7D), suggesting that NUSAP1 may be associated with lipid accumulation in this study.

NUSAP1 Correlated With Poorer Prognosis in Liver Cancer

To further understand the role of NUSAP1 expression in HCC patients, the prognostic value of NUSAP1 was analyzed on the GEPIA and Kaplan-Meier Plotter website. The expression of NUSAP1 was significantly higher in liver cancer tissues than that in normal tissues (Figure 8A) and associated with tumor staging I-III but not stage IV (Figure 8B). In addition, the Kaplan-Meier curve and log-rank test analyses revealed that the increased NUSAP1 mRNA levels corresponded to the shortened OS (overall survival), RFS (relapse free survival), PFS (progression free survival) and DFS (distance free survival) in HCC ($p < 0.05$) (Figures 8C–G).

DISCUSSION

NAFLD is one of the most frequent metabolic diseases worldwide at present. It encompasses a wide spectrum of

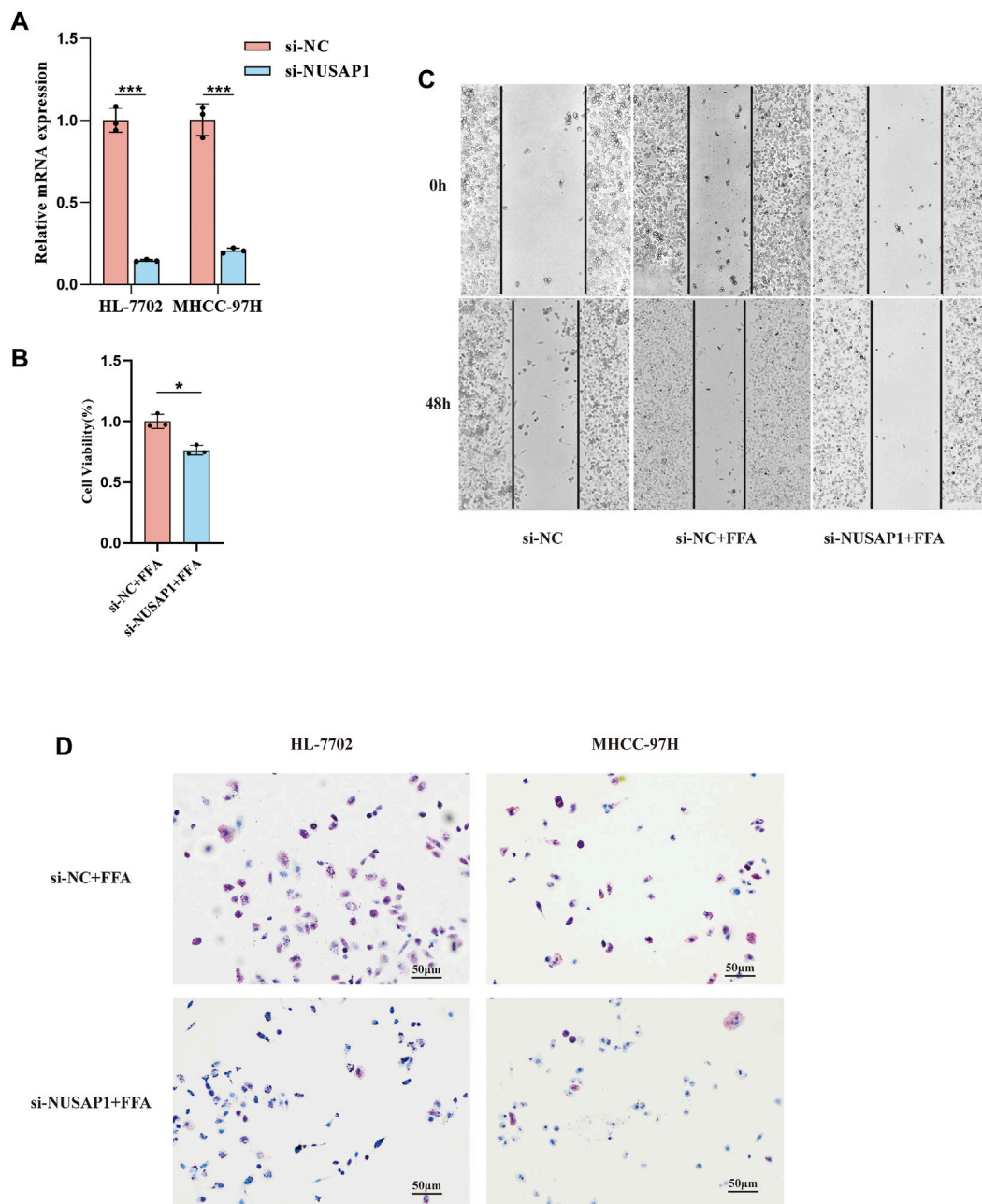


FIGURE 7 | Validation of the function of NUSAP1 via the silencing assay. **(A)** Confirmation of NUSAP1 silence efficiency in HL-7702 and MHCC-97H cell lines by RT-PCR. **(B)** CCK-8 analysis of cell growth in MHCC97H ($n = 3$). **(C)** Wound-healing assays for MHCC-97H. **(D)** Oil Red O staining of the NUSAP1 silence in HL-7702 and MHCC-97H cell treated with FFA for 24 h, 100X for the images. The data were presented as mean \pm SEM, $n = 3$ each group. * $p < 0.05$, *** $p < 0.001$.

disorders including simple steatosis or nonalcoholic fatty liver (NAFL) and nonalcoholic steatohepatitis (NASH), which may progress to liver fibrosis, hepatic cirrhosis or even hepatocellular carcinoma (Pierantonelli and Svegliati-Baroni, 2019). A variable extent of fibrosis occurs in approximately 20–30% of patients with chronically NAFLD and the mortality rate attributable to NAFLD-related cirrhosis is around 12–25% (Massoud and Charlton, 2018). Another characteristic feature of NAFLD progression is HCC (Bessone

et al., 2019). NAFLD-related cirrhosis accounts for 10–34% of the known causative factor of HCC, while patients with noncirrhotic NASH comprising 13–49% of all HCCs. At present, diabetes mellitus and obesity are considered as the major risk factors for the pathogenesis of NAFLD (Huang et al., 2021). The metabolic disorder of diabetes could promote the release of free fatty acids, which triggers the generation of pro-inflammatory cytokines and ROS (reactive oxygen species), and obesity could further stimulate the

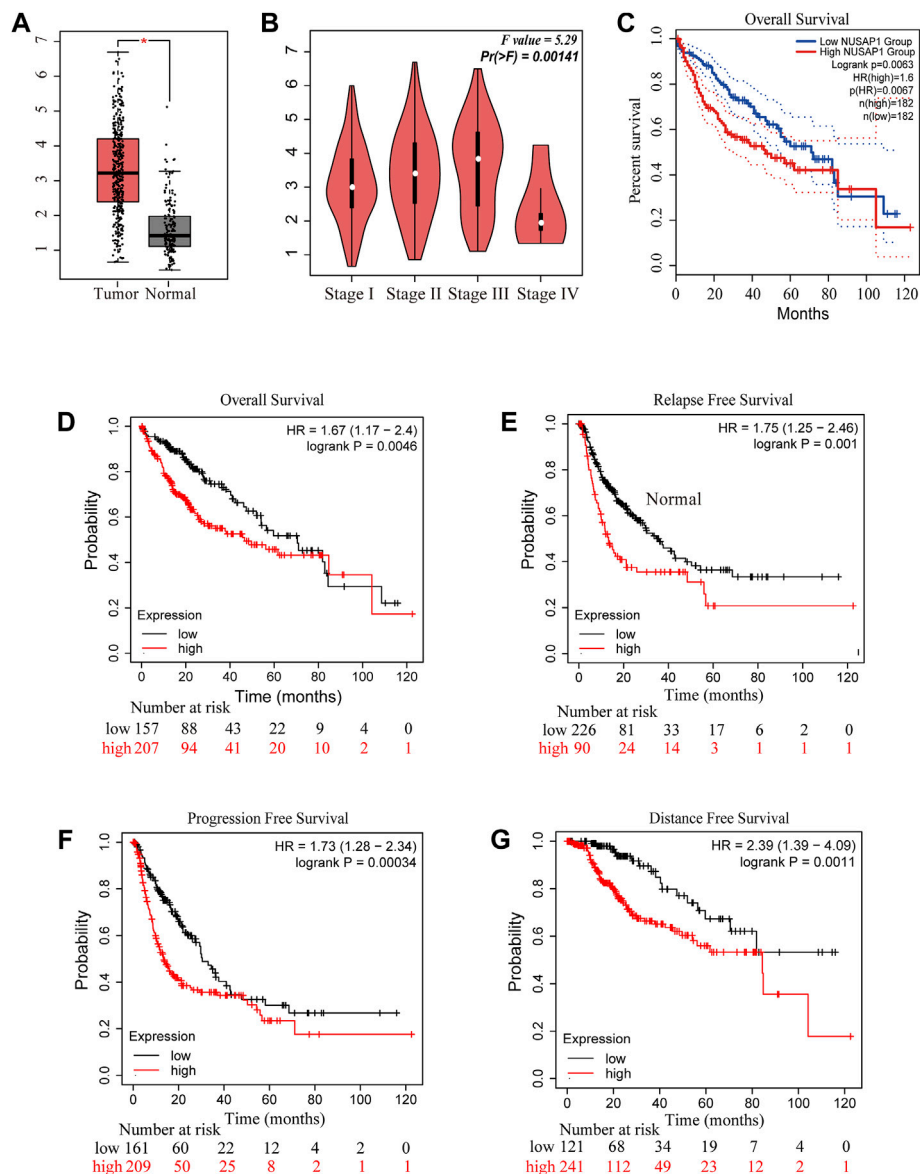


FIGURE 8 | NUSAP1 was highly expressed in HCC and correlated with poorer prognosis. **(A)** The expression of NUSAP1 in liver cancer (GEPIA), **(B)** Correlation between the expression of NUSAP1 and tumor stage in liver cancer patients (GEPIA). Correlation between the expression of NUSAP1 and OS **(C,D)**, RFS **(E)**, PFS **(F)** and DFS **(G)** in liver cancer patients **(C)** from GEPIA: <http://gepia.cancer-pku.cn/>; **(D-G)** from KM plotter: <http://kmplot.com/analysis/>.

development of chronic liver inflammation. Hepatic accumulation of free fatty acids impairs mitochondrial functions and mediates death of $CD4^+$ T lymphocytes selectively mediated by ROS, and reducing immune surveillance (Ma et al., 2016). In addition, it has been demonstrated that IgA^+ cells accumulated in nonalcoholic steatohepatitis (NASH) and accelerated hepatocarcinogenesis via suppressing $CD8^+$ T cells (Shalapour et al., 2017). Thus, the progression of NAFLD could contribute to the prevalence of cirrhosis and HCC worldwide. However, the molecular mechanisms on how NAFLD progresses from non-fibrosis to advanced fibrosis, which ultimately lead to HCC, are yet to be excavated.

In this current study, we extracted gene expression matrix of non-fibrosis NAFLD and fibrosis NAFLD tissue comparing to normal liver tissue or advanced fibrosis NAFLD tissue comparing to mild fibrosis from the two GEO datasets and screened out 112 co-expressed DEGs that could affect NAFLD progression. To further gain insight into the potential functions of these target genes, standard biological processes and pathways analysis of the common DEGs indicated that NAFLD progression from non-fibrosis to advanced fibrosis was inseparable from the glucocorticoid receptor pathway, regulation of transmembrane transporter activity, peroxisome and proteoglycan biosynthetic process. Studies has shown that the glucocorticoid receptor pathway

was crucial for the progression of NAFLD. Glucocorticoid receptor β could induce hepatic steatosis via inflammation activation (Marino et al., 2016), and selective regulation on glucocorticoid receptor could reverse and prevent nonalcoholic fatty liver disease in mice models (Koorneef et al., 2018). Regulation of transmembrane transporter activity was proved to retard NAFLD progression by ameliorating hepatic glucose metabolic disorder (Guo et al., 2020). Peroxisome was also involved in multiple perturbed biological processes in NAFLD, including glucose and lipid metabolism, inflammation, and overall energy homeostasis (Francque et al., 2021). Peroxisome proliferator-activated receptors (PPARs) are a series of nuclear regulatory factors which regulate the activation of inflammatory cells and the fibrogenic process. It has been demonstrated that PPARs agonism shown favorable effect on liver morphology in phase IIb clinical trials (Ratzliff et al., 2016; Francque et al., 2021). What is more, proteoglycan biosynthetic process was activated during the progression of NAFLD. For instance, TSK, a member of proteoglycan family that could link NAFLD to the development of atherogenic dyslipidemia and atherosclerosis (Mouchiroud et al., 2019). Therefore, we thought that these genes were strongly associated with NAFLD progression and worth further study.

Subsequently, 6 hub genes were identified following construction of the PPI network, which were considered as potential markers during the process of NAFLD progression. Through both *in vivo* and *in vitro* experiments, we demonstrated that ZWINT and NUSAP1 were up-regulated under high fat conditions and consistent with sequencing results. To identify genes linking NAFLD progression and HCC, we further explored the expression pattern and prognostic value of these two genes in NAFLD related HCC through public databases. NUSAP1 was not only up-regulated in NAFLD liver cancer but also associated with shorter OS ($p < 0.05$), RFS ($p < 0.05$), PFS ($p < 0.05$) and DFS ($p < 0.05$). In summary, NUSAP1 was identified as a target which could mediate NAFLD progression from no-fibrosis to advanced fibrosis which contributed to the NAFLD-HCC eventually.

NUSAP1 was a 55-kD nucleolar-spindle-associated protein expressed in proliferating cells preferentially (Raemaekers et al., 2003), which was involved in many biological processes such as mitosis, cytokinesis, kinetochore microtubule dynamics and chromosomal segregation (Li et al., 2016a; Li et al., 2016b). In addition, NUSAP1 also played essential roles in tumor progression. Michael et al. has demonstrated that NUSAP1 could serve as SCFcyclin F substrate that took part in the process of ubiquitin-dependent proteolysis during S and G2 phases of the cell cycle (Emanuele et al., 2011) and the presence of NUSAP1 was associated with more resistance formation upon chemotherapy agents (Emanuele et al., 2011). In liver cancer, knockdown of NUSAP1 could inhibit HCC cell proliferation, migration, and invasion *in vitro* and reduce its growth *in vivo* (Roy et al., 2018). In our study, we also demonstrated that NUSAP1 was high up-regulated in NAFLD patients and

liver cancer cells under high fat conditions. NUSAP1 was also associated with cell proliferation and migration under high fat conditions and may promote lipid accumulation. That may be why NUSAP1 was elevated in NAFLD patients with liver fibrosis, where the capacity of regeneration of the liver by compensatory proliferation is dramatically reduced. More importantly, pro-inflammatory cytokines and ROS played an important role in the progress of NAFLD to HCC. Lipid accumulation results in chronic low-grade inflammation, triggering production of the cytokines IL-6 and TNF (Park et al., 2010), which induced cell proliferation and antiapoptotic pathways, and was found to be important for NASH-related HCC development (Kutlu et al., 2018). Therefore, cell proliferation might be an important NAFLD progression signatures, and NUSAP1 could serve as a prospective therapeutic target for NAFLD.

To conclude, 112 prospective candidate genes associated with NAFLD progression were screened out, which are involved in many pathways related to pathogenesis. All of these DEG should be further validated by experimental validation. Moreover, NUSAP1, ZWINT, KIAA0101, UHRF1, RAD51AP1, as prospective markers for NAFLD progression, they have not been linked previously, either in diagnosis or in research. Finally, we demonstrated that NUSAP1 had great potential as a drug target for preventing based on *in vitro* and *in vivo* experiments.

However, some limitations in this study also should be recognized. First of all, given the complexity of datasets included in this study, it is difficult to assess some confounding covariates when analyzing the DEGs, such as different ages, races, regions, and classification of patients. Secondly, the hub genes were all strongly linked to the disease progression of NAFLD, but the mechanism of regulation was not precise.

CONCLUSION

Our study confirmed that the abnormally elevated expression of NUSAP1 was closely related to the progression of NAFLD patients from no-fibrosis to fibrosis, and even to HCC, indicating that their antagonism may inhibit or delay the process of NAFLD to HCC.

DATA AVAILABILITY STATEMENT

The datasets presented in this study can be found in online repositories. The names of the repository/repositories and accession number(s) can be found in the article/Supplementary Material.

ETHICS STATEMENT

The animal study was reviewed and approved by Ethics Committee of Shengjing Hospital of China Medical University.

AUTHOR CONTRIBUTIONS

FX and CD conceived the study and revised the manuscript; TZ is completely responsible for data analysis and manuscript writing; GC proofread the manuscript and prepared the figures and tables; XQ performed real-time PCR experiments; QM and LS assisted in cell culture. HC and NL helped with the construction of NAFLD mouse model. All authors have read and approved the final manuscript.

FUNDING

This study was supported in part by the grants from Natural Science Fund of Liaoning Province (20180551193 and 2020-MS-181 to FX), and the 345 Talent Project of Shengjing Hospital (40B to FX).

REFERENCES

- Anstee, Q. M., Reeves, H. L., Kotsiliti, E., Govaere, O., and Heikenwalder, M. (2019). From NASH to HCC: Current Concepts and Future Challenges. *Nat. Rev. Gastroenterol. Hepatol.* 16, 411–428. doi:10.1038/s41575-019-0145-7
- Arendt, B. M., Comelli, E. M., Ma, D. W., Lou, W., Teterina, A., Kim, T., et al. (2015). Altered Hepatic Gene Expression in Nonalcoholic Fatty Liver Disease Is Associated with Lower Hepatic N-3 and N-6 Polyunsaturated Fatty Acids. *Hepatology* 61, 1565–1578. doi:10.1002/hep.27695
- Bader, G. D., and Hogue, C. W. (2003). An Automated Method for Finding Molecular Complexes in Large Protein Interaction Networks. *BMC Bioinformatics* 4, 2. doi:10.1186/1471-2105-4-2
- Berardo, C., Di Pasqua, L. G., Cagna, M., Richelmi, P., Vairetti, M., and Ferrigno, A. (2020). Nonalcoholic Fatty Liver Disease and Non-alcoholic Steatohepatitis: Current Issues and Future Perspectives in Preclinical and Clinical Research. *Int. J. Mol. Sci.* 21, 21. doi:10.3390/ijms21249646
- Berglund, L., Björling, E., Oksvold, P., Fagerberg, L., Asplund, A., Szgyarto, C. A., et al. (2008). A Genecentric Human Protein Atlas for Expression Profiles Based on Antibodies. *Mol. Cel. Proteomics* 7, 2019–2027. doi:10.1074/mcp.R800013-MCP200
- Bessone, F., Razori, M. V., and Roma, M. G. (2019). Molecular Pathways of Nonalcoholic Fatty Liver Disease Development and Progression. *Cell Mol Life Sci* 76, 99–128. doi:10.1007/s00018-018-2947-0
- Emanuele, M. J., Elia, A. E., Xu, Q., Thoma, C. R., Izhar, L., Leng, Y., et al. (2011). Global Identification of Modular Cullin-RING Ligase Substrates. *Cell* 147, 459–474. doi:10.1016/j.cell.2011.09.019
- Eslam, M., Valenti, L., and Romeo, S. (2018). Genetics and Epigenetics of NAFLD and NASH: Clinical Impact. *J. Hepatol.* 68, 268–279. doi:10.1016/j.jhep.2017.09.003
- Francque, S., Szabo, G., Abdelmalek, M. F., Byrne, C. D., Cusi, K., Dufour, J. F., et al. (2021). Nonalcoholic Steatohepatitis: the Role of Peroxisome Proliferator-Activated Receptors. *Nat. Rev. Gastroenterol. Hepatol.* 18, 24–39. doi:10.1038/s41575-020-00366-5
- Friedman, S. L., Neuschwander-Tetri, B. A., Rinella, M., and Sanyal, A. J. (2018). Mechanisms of NAFLD Development and Therapeutic Strategies. *Nat. Med.* 24, 908–922. doi:10.1038/s41591-018-0104-9
- Guo, J. W., Liu, X., Zhang, T. T., Lin, X. C., Hong, Y., Yu, J., et al. (2020). Hepatocyte TMEM16A Deletion Retards NAFLD Progression by Ameliorating Hepatic Glucose Metabolic Disorder. *Adv. Sci. (Weinh)* 7, 1903657. doi:10.1002/advs.201903657
- Huang, D. Q., El-Serag, H. B., and Loomba, R. (2021). Global Epidemiology of NAFLD-Related HCC: Trends, Predictions, Risk Factors and Prevention. *Nat. Rev. Gastroenterol. Hepatol.* 18, 223–238. doi:10.1038/s41575-020-00381-6
- Jiang, M., Wu, N., Chen, X., Wang, W., Chu, Y., Liu, H., et al. (2019). Pathogenesis of and Major Animal Models Used for Nonalcoholic Fatty Liver Disease. *J. Int. Med. Res.* 47, 1453–1466.

ACKNOWLEDGMENTS

The authors are deeply grateful to Zhijing Na, from the Shengjing Hospital, China Medical University, and Bin Zhao in Medical College, Xiamen University for their critical reading and editing of this manuscript.

SUPPLEMENTARY MATERIAL

The Supplementary Material for this article can be found online at: <https://www.frontiersin.org/articles/10.3389/fphar.2022.823140/full#supplementary-material>

Supplementary Figure S1 | The expression pattern of UHRF1, KIF22 and ZWINT in the different stage of NAFLD.

- Koorneef, L. L., van den Heuvel, J. K., Kroon, J., Boon, M. R., 't Hoen, P. A. C., Hettne, K. M., et al. (2018). Selective Glucocorticoid Receptor Modulation Prevents and Reverses Nonalcoholic Fatty Liver Disease in Male Mice. *Endocrinology* 159, 3925–3936. doi:10.1210/en.2018-00671
- Kutlu, O., Kaleli, H. N., and Ozer, E. (2018). Molecular Pathogenesis of Nonalcoholic Steatohepatitis- (NASH-) Related Hepatocellular Carcinoma. *Can. J. Gastroenterol. Hepatol.* 2018, 8543763. doi:10.1155/2018/8543763
- Li, C., Xue, C., Yang, Q., Low, B. C., and Liou, Y. C. (2016). NuSAP Governs Chromosome Oscillation by Facilitating the Kid-Generated Polar Ejection Force. *Nat. Commun.* 7, 10597. doi:10.1038/ncomms10597
- Li, C., Zhang, Y., Yang, Q., Ye, F., Sun, S. Y., Chen, E. S., et al. (2016). NuSAP Modulates the Dynamics of Kinetochore Microtubules by Attenuating MCAK Depolymerisation Activity. *Sci. Rep.* 6, 18773. doi:10.1038/srep18773
- Long, J. K., Dai, W., Zheng, Y. W., and Zhao, S. P. (2019). miR-122 Promotes Hepatic Lipogenesis via Inhibiting the LKB1/AMPK Pathway by Targeting Sirt1 in Non-alcoholic Fatty Liver Disease. *Mol. Med.* 25, 26. doi:10.1186/s10020-019-0085-2
- Ma, C., Kesarwala, A. H., Eggert, T., Medina-Echeverez, J., Kleiner, D. E., Jin, P., et al. (2016). NAFLD Causes Selective CD4(+) T Lymphocyte Loss and Promotes Hepatocarcinogenesis. *Nature* 531, 253–257. doi:10.1038/nature16969
- Marchesini, G., Petta, S., and Dalle Grave, R. (2016). Diet, Weight Loss, and Liver Health in Nonalcoholic Fatty Liver Disease: Pathophysiology, Evidence, and Practice. *Hepatology* 63, 2032–2043. doi:10.1002/hep.28392
- Marino, J. S., Stechschulte, L. A., Stec, D. E., Nestor-Kalinowski, A., Coleman, S., and Hinds, T. D., Jr. (2016). Glucocorticoid Receptor β Induces Hepatic Steatosis by Augmenting Inflammation and Inhibition of the Peroxisome Proliferator-Activated Receptor (PPAR) α . *J. Biol. Chem.* 291, 25776–25788. doi:10.1074/jbc.M116.752311
- Massoud, O., and Charlton, M. (2018). Nonalcoholic Fatty Liver Disease/Nonalcoholic Steatohepatitis and Hepatocellular Carcinoma. *Clin. Liver Dis.* 22, 201–211. doi:10.1016/j.cld.2017.08.014
- Mouchiroud, M., Camiré, É., Aldow, M., Caron, A., Jubinville, É., Turcotte, L., et al. (2019). The Hepatokine Tsukushi Is Released in Response to NAFLD and Impacts Cholesterol Homeostasis. *JCI Insight* 4, e129492. doi:10.1172/jci.insight.129492
- Moylan, C. A., Pang, H., Dellinger, A., Suzuki, A., Garrett, M. E., Guy, C. D., et al. (2014). Hepatic Gene Expression Profiles Differentiate Presymptomatic Patients with Mild versus Severe Nonalcoholic Fatty Liver Disease. *Hepatology* 59, 471–482. doi:10.1002/hep.26661
- Park, E. J., Lee, J. H., Yu, G. Y., He, G., Ali, S. R., Holzer, R. G., et al. (2010). Dietary and Genetic Obesity Promote Liver Inflammation and Tumorigenesis by Enhancing IL-6 and TNF Expression. *Cell* 140, 197–208. doi:10.1016/j.cell.2009.12.052
- Pierantonelli, I., and Svegliati-Baroni, G. (2019). Nonalcoholic Fatty Liver Disease: Basic Pathogenetic Mechanisms in the Progression from NAFLD to NASH. *Transplantation* 103, e1–e13. doi:10.1097/TP.0000000000002480

- Pontén, F., Jirstrom, K., and Uhlen, M. (2008). The Human Protein Atlas-Aa Tool for Pathology. *J. Pathol.* 216, 387–393. doi:10.1002/path.2440
- Raemaekers, T., Ribbeck, K., Beaudouin, J., Annaert, W., Van Camp, M., Stockmans, I., et al. (2003). NuSAP, a Novel Microtubule-Associated Protein Involved in Mitotic Spindle Organization. *J. Cel. Biol.* 162, 1017–1029. doi:10.1083/jcb.200302129
- Ratzliff, V., Harrison, S. A., Francque, S., Bedossa, P., Leher, P., Serfaty, L., et al. (2016). Elafibranor, an Agonist of the Peroxisome Proliferator-Activated Receptor- α And - δ , Induces Resolution of Nonalcoholic Steatohepatitis without Fibrosis Worsening. *Gastroenterology* 150, 1147–1159.e5. doi:10.1053/j.gastro.2016.01.038
- Rinella, M. E., and Sanyal, A. J. (2016). Management of NAFLD: a Stage-Based Approach. *Nat. Rev. Gastroenterol. Hepatol.* 13, 196–205. doi:10.1038/nrgastro.2016.3
- Ritchie, M. E., Phipson, B., Wu, D., Hu, Y., Law, C. W., Shi, W., et al. (2015). Limma powers Differential Expression Analyses for RNA-Sequencing and Microarray Studies. *Nucleic Acids Res.* 43, e47. doi:10.1093/nar/gkv007
- Roy, S., Hooiveld, G. J., Seehawer, M., Caruso, S., Heinzmann, F., Schneider, A. T., et al. (2018). microRNA 193a-5p Regulates Levels of Nucleolar- and Spindle-Associated Protein 1 to Suppress Hepatocarcinogenesis. *Gastroenterology* 155, 1951–1966.e26. doi:10.1053/j.gastro.2018.08.032
- Schuster, S., Cabrera, D., Arrese, M., and Feldstein, A. E. (2018). Triggering and Resolution of Inflammation in NASH. *Nat. Rev. Gastroenterol. Hepatol.* 15, 349–364. doi:10.1038/s41575-018-0009-6
- Shalapour, S., Lin, X. J., Bastian, I. N., Brain, J., Burt, A. D., Aksenov, A. A., et al. (2017). Erratum: Inflammation-Induced IgA+ Cells Dismantle Anti-Liver Cancer Immunity. *Nature* 552, 430–435. doi:10.1038/nature25028
- Shannon, P., Markiel, A., Ozier, O., Baliga, N. S., Wang, J. T., Ramage, D., et al. (2003). Cytoscape: a Software Environment for Integrated Models of Biomolecular Interaction Networks. *Genome Res.* 13, 2498–2504. doi:10.1101/gr.1239303
- Szklarczyk, D., Gable, A. L., Lyon, D., Junge, A., Wyder, S., Huerta-Cepas, J., et al. (2019). STRING V11: Protein-Protein Association Networks with Increased Coverage, Supporting Functional Discovery in Genome-wide Experimental Datasets. *Nucleic Acids Res.* 47, D607–d613. doi:10.1093/nar/gky1131
- Tang, Z., Li, C., Kang, B., Gao, G., Li, C., and Zhang, Z. (2017). GEPIA: a Web Server for Cancer and normal Gene Expression Profiling and Interactive Analyses. *Nucleic Acids Res.* 45, W98–w102. doi:10.1093/nar/gkx247
- Thul, P. J., Åkesson, L., Wiking, M., Mahdessian, D., Geladaki, A., Ait Blal, H., et al. (2017). A Subcellular Map of the Human Proteome. *Science* 356, eaal3321. doi:10.1126/science.aal3321
- Uhlén, M., Björling, E., Agaton, C., Szigartyo, C. A., Amini, B., Andersen, E., et al. (2005). A Human Protein Atlas for normal and Cancer Tissues Based on Antibody Proteomics. *Mol. Cel Proteomics* 4, 1920–1932. doi:10.1074/mcp.M500279-MCP200
- Uhlén, M., Fagerberg, L., Hallström, B. M., Lindskog, C., Oksvold, P., Mardinoglu, A., et al. (2015). Proteomics. Tissue-Based Map of the Human Proteome. *Science* 347, 1260419. doi:10.1126/science.1260419
- Uhlen, M., Zhang, C., Lee, S., Sjostedt, E., Fagerberg, L., Bidkhori, G., et al. (2017). A Pathology Atlas of the Human Cancer Transcriptome. *Science* 357, eaan2507. doi:10.1126/science.aan2507
- Vilar-Gomez, E., Martinez-Perez, Y., Calzadilla-Bertot, L., Torres-Gonzalez, A., Gra-Oramas, B., Gonzalez-Fabian, L., et al. (2015). Weight Loss through Lifestyle Modification Significantly Reduces Features of Nonalcoholic Steatohepatitis. *Gastroenterology* 149, 367–378.e5; quiz e14–5. doi:10.1053/j.gastro.2015.04.005
- Yang, W., Feng, Y., Zhou, J., Cheung, O. K., Cao, J., Wang, J., et al. (2021). A Selective HDAC8 Inhibitor Potentiates Antitumor Immunity and Efficacy of Immune Checkpoint Blockade in Hepatocellular Carcinoma. *Sci. Transl. Med.* 13, 13. doi:10.1126/scitranslmed.aaz6804
- Younossi, Z., Anstee, Q. M., Marietti, M., Hardy, T., Henry, L., Eslam, M., et al. (2018). Global burden of NAFLD and NASH: Trends, Predictions, Risk Factors and Prevention. *Nat. Rev. Gastroenterol. Hepatol.* 15, 11–20. doi:10.1038/nrgastro.2017.109
- Zhou, L., Tan, X., Kamohara, H., Wang, W., Wang, B., Liu, J., et al. (2010). MEK1 and MEK2 Isoforms Regulate Distinct Functions in Pancreatic Cancer Cells. *Oncol. Rep.* 24, 251–255. doi:10.3892/or_00000853
- Zhou, Y., Zhou, B., Pache, L., Chang, M., Khodabakhshi, A. H., Tanaseichuk, O., et al. (2019). Metascape Provides a Biologist-Oriented Resource for the Analysis of Systems-Level Datasets. *Nat. Commun.* 10, 1523. doi:10.1038/s41467-019-09234-6

Conflict of Interest: The authors declare that the research was conducted in the absence of any commercial or financial relationships that could be construed as a potential conflict of interest.

Publisher's Note: All claims expressed in this article are solely those of the authors and do not necessarily represent those of their affiliated organizations, or those of the publisher, the editors, and the reviewers. Any product that may be evaluated in this article, or claim that may be made by its manufacturer, is not guaranteed or endorsed by the publisher.

Copyright © 2022 Zeng, Chen, Qiao, Chen, Sun, Ma, Li, Wang, Dai and Xu. This is an open-access article distributed under the terms of the Creative Commons Attribution License (CC BY). The use, distribution or reproduction in other forums is permitted, provided the original author(s) and the copyright owner(s) are credited and that the original publication in this journal is cited, in accordance with accepted academic practice. No use, distribution or reproduction is permitted which does not comply with these terms.



Rifaximin Ameliorates Non-alcoholic Steatohepatitis in Mice Through Regulating gut Microbiome-Related Bile Acids

OPEN ACCESS

Edited by:

Ana Blas-García,
University of Valencia, Spain

Reviewed by:

Robert N. Helsley,
University of Kentucky, United States
Esther Caparrós,
Miguel Hernández University of Elche,
Spain

*Correspondence:

Menghui Zhang
mhzhzhang@sjtu.edu.cn
Xuan Zhu
jyyfyzx@163.com
Wei-Fen Xie
weifexie@medmail.com.cn

[†]These authors have contributed
equally to this work and share first
authorship

Specialty section:

This article was submitted to
Gastrointestinal and Hepatic
Pharmacology,
a section of the journal
Frontiers in Pharmacology

Received: 22 December 2021

Accepted: 14 March 2022

Published: 04 April 2022

Citation:

Jian J, Nie M-T, Xiang B, Qian H, Yin C,
Zhang X, Zhang M, Zhu X and Xie W-F
(2022) Rifaximin Ameliorates Non-
alcoholic Steatohepatitis in Mice
Through Regulating gut Microbiome-
Related Bile Acids.
Front. Pharmacol. 13:841132.
doi: 10.3389/fphar.2022.841132

Jie Jian^{1†}, Mei-Tong Nie^{2,3†}, Baoyu Xiang⁴, Hui Qian⁵, Chuan Yin⁵, Xin Zhang⁵,
Menghui Zhang^{4*}, Xuan Zhu^{1*} and Wei-Fen Xie^{5*}

¹Department of Gastroenterology, First Affiliated Hospital of Nanchang University, Nanchang, China, ²Department of Gastroenterology, Shanghai East Hospital, Tongji University School of Medicine, Shanghai, China, ³Shanghai Institute of Stem Cell Research and Clinical Translation, Shanghai, China, ⁴State Key Laboratory of Microbial Metabolism, Joint International Research Laboratory of Metabolic and Developmental Sciences, and School of Life Sciences and Biotechnology, Shanghai Jiao Tong University, Shanghai, China, ⁵Department of Gastroenterology, Changzheng Hospital, Naval Medical University, Shanghai, China

Non-alcoholic steatohepatitis (NASH) is the progressive stage of non-alcoholic fatty liver disease (NAFLD). The non-absorbable antibiotic rifaximin has been used for treatment of irritable bowel syndrome, traveling diarrhea, and hepatic encephalopathy, but the efficacy of rifaximin in NASH patients remains controversial. This study investigated the effects and underlying mechanisms of rifaximin treatment in mice with methionine and choline deficient (MCD) diet-induced NASH. We found that rifaximin greatly ameliorated hepatic steatosis, lobular inflammation, and fibrogenesis in MCD-fed mice. Bacterial 16S rRNA sequencing revealed that the gut microbiome was significantly altered in MCD-fed mice. Rifaximin treatment enriched 13 amplicon sequence variants (ASVs) belonging to the groups *Muribaculaceae*, *Parabacteroides*, *Coriobacteriaceae_UCG-002*, *uncultured Oscillospiraceae*, *Dubosiella*, *Rikenellaceae_RC9_gut_group*, *Mucispirillum*, and *uncultured Desulfovibrionaceae*. However, rifaximin treatment also reduced seven ASVs in the groups *Aerococcus*, *Oscillospiraceae*, *uncultured Ruminococcaceae*, *Bilophila*, *Muribaculaceae*, *Helicobacter*, and *Alistipes* in MCD-fed mice. Bile acid-targeted metabolomic analysis indicated that the MCD diet resulted in accumulation of primary bile acids and deoxycholic acid (DCA) in the ileum. Rifaximin delivery reduced DCA levels in MCD-fed mice. Correlation analysis further showed that DCA levels were associated with differentially abundant ASVs modulated by rifaximin. In conclusion, rifaximin may ameliorate NASH by decreasing ileal DCA through alteration of the gut microbiome in MCD-fed mice. Rifaximin treatment may therefore be a promising approach for NASH therapy in humans.

Keywords: rifaximin, non-alcoholic steatohepatitis, gut microbiome, bile acids, deoxycholic acid, farnesoid X receptor

INTRODUCTION

Non-alcoholic fatty liver disease (NAFLD) is one of the most common chronic liver diseases worldwide. Approximately 20–30% of the generally Western population and 25% of Chinese people are estimated to suffer from NAFLD (Younossi et al., 2019; Lin et al., 2020). The early stage of NAFLD primarily manifests as hepatic steatosis with increased serum cholesterol and triglyceride levels. Non-alcoholic steatohepatitis (NASH), the progressive subtype of NAFLD, is characterized by liver steatosis, hepatocellular injury, inflammation, and different degrees of fibrosis (Ni et al., 2017; Friedman et al., 2018). NASH is a pathogenic factor for end-stage liver diseases such as cirrhosis and hepatocellular carcinoma (HCC) (Kim et al., 2018; Zhang et al., 2021). Although the high prevalence of NAFLD and related chronic liver diseases is a great public health concern, many clinical trials for NAFLD treatments have failed, and there is still no approved effective medicine to treat NASH (Haas et al., 2016; Francque, 2021; Francque et al., 2021).

It is well recognized that gut microbiome composition is essential for the progression of NAFLD. Bacterial fermentation metabolites, including short-chain fatty acids (SCFAs), succinate, ethanol, and bile acids, have been reported to affect the occurrence and progression of NAFLD (Gil-Gomez et al., 2021). Primary bile acids, are synthesized in the liver, followed by conjugation and transported to the intestine. Such primary bile acids include chenodeoxycholic acid (CDCA) and cholic acid (CA) in humans, and CA, muricholic acids (MCAs), and ursodeoxycholic acid (UDCA) in rodents (Wahlstrom et al., 2016). Intestinal bacteria convert primary bile acids into secondary bile acids, such as deoxycholic acid (DCA), tauroursodeoxycholic acid (TUDCA) and lithocholic acid (LCA) (Wahlstrom, et al., 2016). One of the most essential functions of these bile acids is to regulate farnesoid X receptor (FXR), which influences lipid metabolism (Fiorucci et al., 2021). A semisynthetic derivative of CDCA named obeticholic acid (OCA) is an agonist of FXR (Pellicciari et al., 2002). In Phase II and III trials, OCA reduced NASH-induced fibrosis (Fiorucci et al., 2019). A previous study revealed that the inhibition of intestinal FXR signaling by glyoursodeoxycholic acid (GUDCA) reduces the expression of fibroblast growth factor 15 (FGF15) and subsequently reverses lipid metabolic dysregulation in obese mice (Sun et al., 2018). Moreover, blocking bile acid transportation in the intestine was associated with decreased lipid accumulation in the liver of high fat diet (HFD)-fed mice (Rao et al., 2016; Arab et al., 2017). Thus, gut microbiome-related bile acid metabolic disorders may play important roles in NAFLD.

Rifaximin is a non-systemic antibiotic targeting a broad range of bacteria in the gastrointestinal tunnel with minimal absorption. It has been used clinically for the treatment of irritable bowel syndrome, traveling diarrhea and hepatic encephalopathy (Bass et al., 2010; Caraceni et al., 2021). Rifaximin is also used for the treatment of NASH in rats and humans, but the efficacy of this treatment remains controversial. A study by Cheng et al., in 2012 revealed that chronic exposure to rifaximin (6 months) led to hepatic steatosis in pregnant X

receptor-humanized mice, demonstrating this is a potential side effect of rifaximin (Cheng et al., 2012). A recent report by Yukihiya et al. indicated that rifaximin combined with angiotensin-II receptor blocker attenuated choline-deficient/l-amino acid-defined (CDAA) diet-induced NASH fibrosis in rat (Fujinaga et al., 2020). Clinically, Gangarapu et al. found that short-term rifaximin treatment (1,200 mg/day) for 28 days decreased the level of serum endotoxemia and increased liver function in NASH patients (Gangarapu et al., 2015). Abdel-Razik et al. also reported that rifaximin administration (1,100 mg/day) for 6 months reduced NAFLD liver fat scores and improved serum endotoxemia, insulin resistance, and proinflammatory cytokine levels (Abdel-Razik et al., 2018). However, Cobbold et al. showed that a 6-week treatment with rifaximin (800 mg/day) had no beneficial effect on NASH (Cobbold et al., 2018). Therefore, the role of rifaximin in NASH treatment requires further clarification.

In the present study, we aimed to investigate the potential benefits of rifaximin in treating methionine and choline deficient (MCD) diet-induced NASH in mice (Zhu et al., 2019). We also analyzed the effect of rifaximin on the gut microbiome and bile acids profile. Our results provide new insights into potential clinical treatment of NAFLD by using rifaximin to alter the gut microbiome and associated metabolites.

METHODS AND MATERIALS

Animals and Treatments

Male C57BL/6 wild-type littermates (6 weeks old, weighing nearly 20 g, obtained from the Shanghai Experimental Center of Chinese Academy of Sciences) were fed with an MCD diet (TP 3005M, Trophic Animal Feed High-tech Company, China) or standard methionine- and choline-sufficient (MCS) diet (TP 3005 GS, Trophic Animal Feed High-tech Company, China) ad libitum for 6 weeks. To evaluate the effects of rifaximin, a dose of 100 mg/kg/day rifaximin was administered by gavage to eight mice 2 weeks after beginning the MCD diet and continuing for 4 weeks. The control mice were gavage by saline. All mice were housed at the experimental animal center of Second Military Medical University in a specific pathogen-free environment at 24°C temperature under a 12/12 h light/dark cycle. At experimental end points, mice were euthanized and samples were harvested. Body and liver weight were recorded.

Histological Studies

Mouse liver sections fixed with 10% formalin were embedded in paraffin, then sliced into 4 µm-thick sections and stained with hematoxylin and eosin (H&E) for histopathological examination. Two investigators blinded to the treatments independently assigned a Non-alcoholic Fatty Liver Disease Activity Score (NAS) for each sample. NAS is a composite score including steatosis, lobular inflammation, and cytological ballooning (Puri and Sanyal 2012). Steatosis was scored on a scale of 0–3 based on low to medium power evaluation of parenchymal involvement according to the following criteria: 0 (<5%), 1 (5–33%), 2 (33–66%), or 3 (>66%). Inflammation was scored on a scale of

0–3 by overall assessment of all inflammatory foci according to the following criteria: 0 (No foci), 1 (<2 foci per 20x optical field), 2 (2–4 foci per 20x optical field), or 3 (>4 foci per 20x optical field). Hepatocellular ballooning was scored on a scale of 0–2 based on evaluation of enlarged vacuolated cells proportion according to the following criteria: 0 (none), 1 (mild, few), or 2 (moderate, many) (Puri and Sanyal 2012). Oil Red O staining was performed on liver sections fixed in 4% paraformaldehyde or frozen samples embedded in optimal cutting temperature compound (OCT). Samples were cut with a cryostat into 8- μ m sections to evaluate the degree of hepatocyte steatosis. Fibrosis was assessed in liver sections embedded in paraffin and stained with Sirius Red. The intensity of steatosis and fibrogenesis were measured based on the percentage of tissue area stained with Oil Red O staining or Sirius Red using the image analysis software IMAGE-PRO Plus 6.0 (Media Cybernetics, United States).

Immunohistochemistry

Immunohistochemical staining was performed on the paraffin-embedded liver sections according to standard procedures. Liver sections were deparaffinized with 100% xylene, rehydrated with an ethanol gradient followed by 100% ethanol, 95% ethanol, 85% ethanol, and 75% ethanol, and immersed in 3% H₂O₂ to remove endogenous peroxidase. After antigen retrieval, slides were incubated with the primary antibodies α -SMA (ab5694, Abcam, Cambridge, United Kingdom) and Col1a1 (BA0325, Boster, Wuhan, China) overnight at 4°C. Samples were then incubated with horseradish peroxidase-linked immunoglobulin G secondary antibody (GK500710, Gene Tech, Shanghai, China) at room temperature for 1 h. Staining was performed using an Envision Detection Rabbit/Mouse Kit (GK500710, Gene Tech).

Quantitative Real-Time PCR Analysis

Total RNA was extracted from liver and terminal ileum tissues using TRIzol Reagent (Invitrogen, Carlsbad, CA, United States). The 20 μ l first-strand cDNA synthesis consists with 2 μ g of total RNA resolved in RNase free water and retrotranscribed with 4 μ l PrimeScript RT Master Mix (Takara, Kyoto, Japan). For quantitative PCR, cDNA was reverse-transcribed and then amplified with SYBR Green PCR Kit (Life Technologies, Carlsbad, CA, United States). PCR conditions were as follows: 95°C 10 min, then 40 cycles at 95°C for 30 s and 60°C for 1 min mRNA levels were normalized to those of Gapdh mRNA. Primers for Acta2, Col1a1, Cyp7a1, Cyp7b1, Cyp8b1, Cyp27a1, Fxr, Fgf15, and Shp are shown in **Supplementary Table S1**.

Western Blot Analysis of Hepatic Proteins

Western blot was performed on liver protein extracts using RIPA buffer as previously described, including Srebp1, Ppar γ , α -SMA, Col1a1, and Gapdh (Qian et al., 2015). Gapdh was used as the loading control for total protein. Primary antibodies are listed in **Supplementary Table S2**.

Lipopolysaccharide Measurement

Serum LPS was quantified using a commercial enzyme-linked immunosorbent assay (ELISA) kit for Mouse LPS (F11123, Xi Tang, Shanghai, China). In short, serum samples were first

diluted into 1:10 and added per well for 100 μ l incubating 40 min at 37°C. The board was washed with washing solution 6 times before adding biotinylated antibody. Next, after enzyme conjugated with biotinylated antibody, 100 μ l coloring solution and 100 μ l stop solution per well were added subsequently. Microplate reader was used to measure the absorbance at 450 nm.

Measurement of Hepatic Hydroxyproline Content

Total hepatic hydroxyproline levels were assayed to quantify liver collagen content using a commercial hydroxyproline assay kit (A030-2, Jiancheng, Nanjing, China). Briefly, 100 mg of wet liver samples was hydrolyzed for 20 min at 95°C. Next, samples were adjusted to neutrality and reacted with the corresponding detected resolution. The absorbance at 550 nm was recorded using microplate reader, and the concentration were calculated based on a standard product.

Determination of Bile Acids

One hundred mg terminal ileum samples were mixed with NaOH and acetonitrile and centrifugated. After centrifugation, supernatants were placed in a chromatographic bottle for detection of bile acid levels (Majorbio Bio-Pharm Biotechnology, Shanghai, China). Chlorpropamide was used as an internal standard for bile acid levels. Bile acid concentrations of terminal ileum samples were qualitatively and quantitatively determined by LC-ESI-MS/MS analysis method (Waters Corp., Milford, MA). Mass spectrometry system included air curtain gas 40, ion spray voltage –4500 V, temperature 550°C, ion source GAS1:50, and ion source GAS2:50. Chromatographic separation was performed on a BEH C18 liquid chromatography column (100 \times 2.1 mm, 1.8 μ m, Waters Corp.). The injection quantity is 5 μ l and mobile phase included phase A (0.1% formic acid in water) and phase B (0.1% formic acid in acetonitrile). Bile acids standards were used to identify different bile acids metabolites detected by LC-MS. Finally, the mass spectral peak area of the sample analyte was substituted into linear equation to calculate the concentration of bile acids levels.

Stool Sample Collection, Microbial DNA Extraction and Sequencing

Fresh fecal samples were collected from the 24 mice on the day of sacrifice and immediately frozen at –80°C. DNA extraction and purification were performed with the QIAamp DNA Stool Minikit (Qiagen Ltd., Strasse, Germany) according to the manufacturer's instructions. Briefly, weighing 150 mg wet stool were added to microcentrifuge tube containing lysis buffer and 25 μ l Proteinase K, and vortexed to begin homogenization. Buffer AL (200 μ l) was added to the sample and mixed. The QIAamp spin column labeled 1.5 ml microcentrifuge tube was placed for collecting DNA extraction. The quality of the extracted DNA was visualized on a 1% agarose gel. The V3–V4 hypervariable regions of the 16S rRNA genes were amplified using primers 338F (5'-ACTCCTACGGGAGGCAGCAG-3') and 806R (5'-GGACTACHVGGGTWTCTAAT-3'). Paired end sequencing

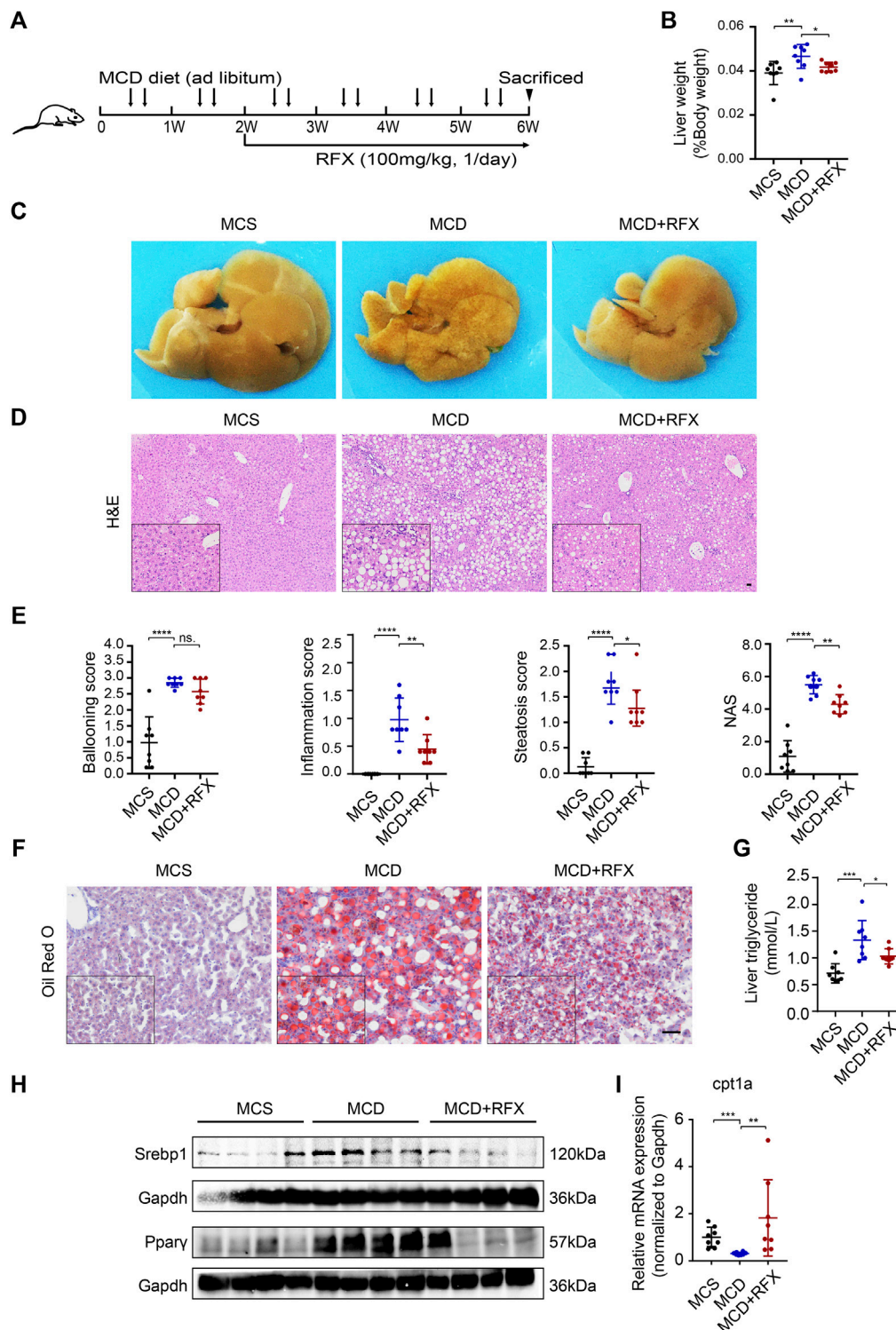


FIGURE 1 | Administration of rifaximin ameliorates experimental non-alcoholic steatohepatitis (NASH) in MCD-fed mice. **(A)** Schematic illustration of the experimental design. **(B)** Liver to body weight ratio of C57BL/6 mice. **(C)** Representative macroscopic photographs of livers for mice fed with control diet (MCS) or MCD and with rifaximin gavage. **(D)** Representative images of paraffin-embedded liver sections stained with hematoxylin and eosin (H&E). Scale bars = 200 μ m. **(E)** Histological scores of hepatic ballooning, inflammation, steatosis and total NAS based on H&E staining. **(F)** Representative histological staining for neutral lipid (Oil Red O) in mouse livers. Scale bars = 100 μ m. **(G)** Hepatic triglyceride levels in mice. **(H)** Srebp1 and Ppar α expression in mouse liver. **(I)** Cpt1a mRNA levels in mouse livers. Gapdh is for normalization. Data are expressed as mean \pm standard deviation. For B, E, G and I: * p < 0.05, ** p < 0.01, *** p < 0.001, **** p < 0.0001 (p value was determined by one-way ANOVA). n = 8 mice per group.

was performed on the Illumina MiSeq PE300 platform (Illumina, San Diego, CA, United States) using standard protocols by Majorbio Bio-Pharm Technology Co. Ltd. (shanghai, China).

Bioinformatic Analysis

The original data pre-processing and downstream bioinformatic analysis were primary conducted using Quantitative Insights into Microbial Ecology 2 (QIIME2, version 2021.04). Unless otherwise stated, default parameters for all programs and analyzes were used. Briefly, adapter sequences were trimmed with the script “qiime cutadapt trim-paired”. The DADA2 pipeline (with parameters “-p-trunc-len-f 269 -p-trunc-len-r 204”) was used for sequence filtering, dereplication, chimera identification and clustering high-quality reads into amplicon sequence variants (ASVs). The SILVA reference database (version 138) was used to annotate the ASVs (Quast et al., 2013). To correct for bias derived from sampling depth, subsampling was performed to 23,680 reads per biological sample. The alpha and beta diversity were calculated with “qiime diversity core-metrics-phylogenetic”. PICRUST (version 2.4.1) was applied to predict functional genes and pathways.

Data Visualization

GraphPad 7.0 (GraphPad Software, San Diego, CA, United States) was used to visualize data for mice features, qRT-PCR, histological data and bile acid contents. The gut microbiome analysis was visualized using Origin Pro 2021 (OriginLab, Northampton, MA, United States).

Statistical Analysis

Statistical analyze were performed in GraphPad Prism 7.0. Comparisons made between multiple treatment groups were conducted with one-way analysis of variance (ANOVA) or Kruskal-Wallis test. Principal coordinate analysis (PCoA) was performed using the Unweighted Unifrac method. The linear discriminant analysis (LDA) effect size (LEfSe) method was implemented using LEfSe v1.0. ASV clustering was performed using the between-groups linkage method, and Pearson correlation calculation was conducted with SPSS Statistics 26 (SPSS Inc., Chicago, IL, United States). Correlation analysis of gut microbiome with bile acids in the terminal ileum was conducted using the nonparametric Spearman's rank test with Origin Pro 2021. $p < 0.05$ was considered statistically significant.

RESULTS

Rifaximin Alleviates Steatohepatitis in MCD Diet-Induced NASH Mice

To evaluate the effect of Rifaximin on non-alcoholic steatohepatitis (NASH) in mice, C57BL/6 mice were fed with a methionine- and choline-deficient (MCD) diet for 6 weeks to induce NASH. Rifaximin treatment was started after 2 weeks of the MCD diet and continued for 4 weeks (Figure 1A). As expected, MCD-fed mice had a significant decrease in body weight and increase in liver/body weight ratio compared with the control methionine and choline-sufficient (MCS)-fed mice

(Figure 1B, Supplementary Figure S1A). Interestingly, rifaximin markedly reduced the liver/body weight ratio but did not alter body weight in MCD-induced NASH mice (Figure 1B, Supplementary Figure S1A). Macroscopic observation showed much more severe hepatic lipid deposition in MCD-fed mice compared with MCS-fed mice, whereas rifaximin treatment reduced liver lipid deposition in MCD-fed mice (Figure 1C). The Non-alcoholic Fatty Liver Disease Activity Score (NAS) incorporates hepatocellular ballooning, interlobular inflammation and steatosis scores, and has been used to evaluate the severity of NASH (Puri and Sanyal 2012). Rifaximin treatment decreased the interlobular inflammation and steatosis scores and NAS in MCD-fed mice. The ballooning score was numerically improved but with no significant difference in rifaximin-treated mice compared with untreated MCD-fed mice (Figures 1D,E). Consistent with the steatosis scores, Oil Red O staining and hepatic triglyceride level confirmed that elevated lipid deposition in the liver of MCD-fed mice was reduced by rifaximin treatment (Figures 1F,G and Supplementary Figure S1C). Srebp1 and Ppar γ , which are essential regulators of lipid synthesis (Lee et al., 2018; Romano et al., 2021), were increased in MCD-fed mice and downregulated by rifaximin treatment (Figure 1H). To evaluate the activation of Srebp1, we investigated the location of Srebp1 expression using IHC. The data showed that the levels of Srebp1 in nuclear and cytoplasm were increased in the liver of MCD-fed NASH mice and reduced by rifaximin treatment (Supplementary Figure S1D). We also detected the expression of lipogenic genes regulated by Srebp1 using real-time qPCR and found that rifaximin treatment significantly reduced the expression of acetyl-CoA carboxylase-1 (ACC) in the mouse liver (Supplementary Figure S1E). Moreover, fatty oxidation related genes like carnitine palmitoyl transferase 1A (Cpt1a) mRNA was decreased in MCD-diet mice and rifaximin treatment reversed its transcriptional expression, indicating that rifaximin may also contribute to increasing hepatic lipid oxidation (Figure 1I). The MCD diet also increased plasma levels of alanine aminotransferase (ALT) and aspartate aminotransferase (AST), which were suppressed by rifaximin treatment (Supplementary Figure S1B). These data demonstrate a preventive effect of rifaximin on MCD diet-induced NASH in mice.

Rifaximin Treatment Attenuates MCD Diet-Induced Hepatic Inflammation and Fibrosis in NASH Mice

Previous studies have revealed that the MCD diet induces hepatic inflammation (Li et al., 2020; Zhang et al., 2018). Serum lipopolysaccharide (LPS) serves as a trigger of hepatic inflammation (Okubo et al., 2016); we therefore measured LPS levels. The MCD diet resulted in a significant increase in serum LPS content, which was reduced by rifaximin treatment (Supplementary Figure S2A). The elevation of serum LPS levels caused increased expression of proinflammatory cytokines (Peng et al., 2021). Consistent with these results,

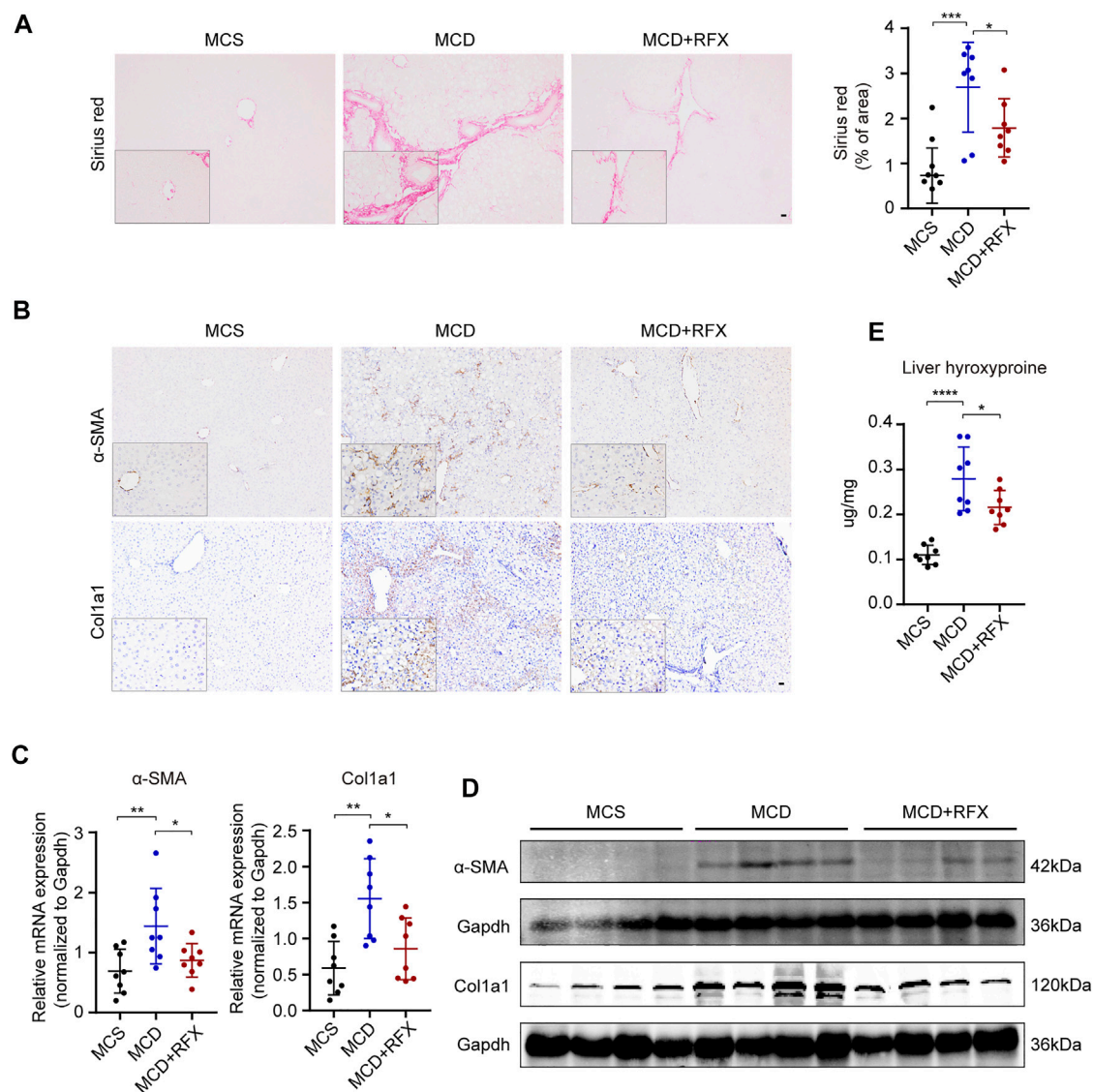


FIGURE 2 | Rifaximin treatment alleviates MCD diet-induced hepatic fibrosis in mice. **(A)** Representative images of paraffin-embedded liver sections stained with Sirius Red (left panel) and semiquantitative analysis of Sirius Red staining positive area in mouse liver tissues (right panel). Scale bars = 200 μ m. **(B)** Representative images of α -SMA and Col1a1 immunostaining. Scale bars = 200 μ m. **(C)** qRT-PCR analysis of Acta2 and Col1a1 mRNA levels in mouse livers. Gapdh is for normalization. **(D)** Representative western blot analysis of α -SMA and Col1a1 in mouse livers. **(E)** Hydroxyproline content in mouse livers. Data are expressed as mean \pm standard deviation. For A, C, E: * $p < 0.05$, ** $p < 0.01$, *** $p < 0.001$, **** $p < 0.0001$ (p value was determined by one-way ANOVA). $n = 8$ mice per group.

qRT-PCR revealed increased expression of proinflammatory cytokine genes, including *Tnfa* and *Mcp1* in the liver of the NASH mice (Supplementary Figure S2B). Expression of *Tnfa* was decreased significantly after rifaximin treatment, indicating that rifaximin attenuated the lobular inflammation of MCD-fed mice (Supplementary Figure S2B).

Liver fibrosis is one of the most essential determinants to assess the stage and progression of NASH (Puri and Sanyal 2012). We found that collagen deposition and expression of collagen alpha 1 (Col1a1) and alpha smooth muscle actin (α -SMA) were increased in the livers of MCD-fed mice (Figures 2A–D). Rifaximin treatment significantly decreased collagen deposition

and the expression of Col1a1 and α -SMA (Figures 2A–D). Liver hydroxyproline content was also enhanced in MCD-fed mice compared with MCS-fed mice (Figure 2E). However, after rifaximin treatment, hydroxyproline content in the liver was markedly reduced. These data indicate that rifaximin alleviates hepatic inflammation and fibrosis in NASH mice.

Rifaximin Administration Alters the gut Microbiome in NASH Mice

As a non-systemic antibiotic, rifaximin targets the intestinal microbiome with minimal absorption. To evaluate the effect of

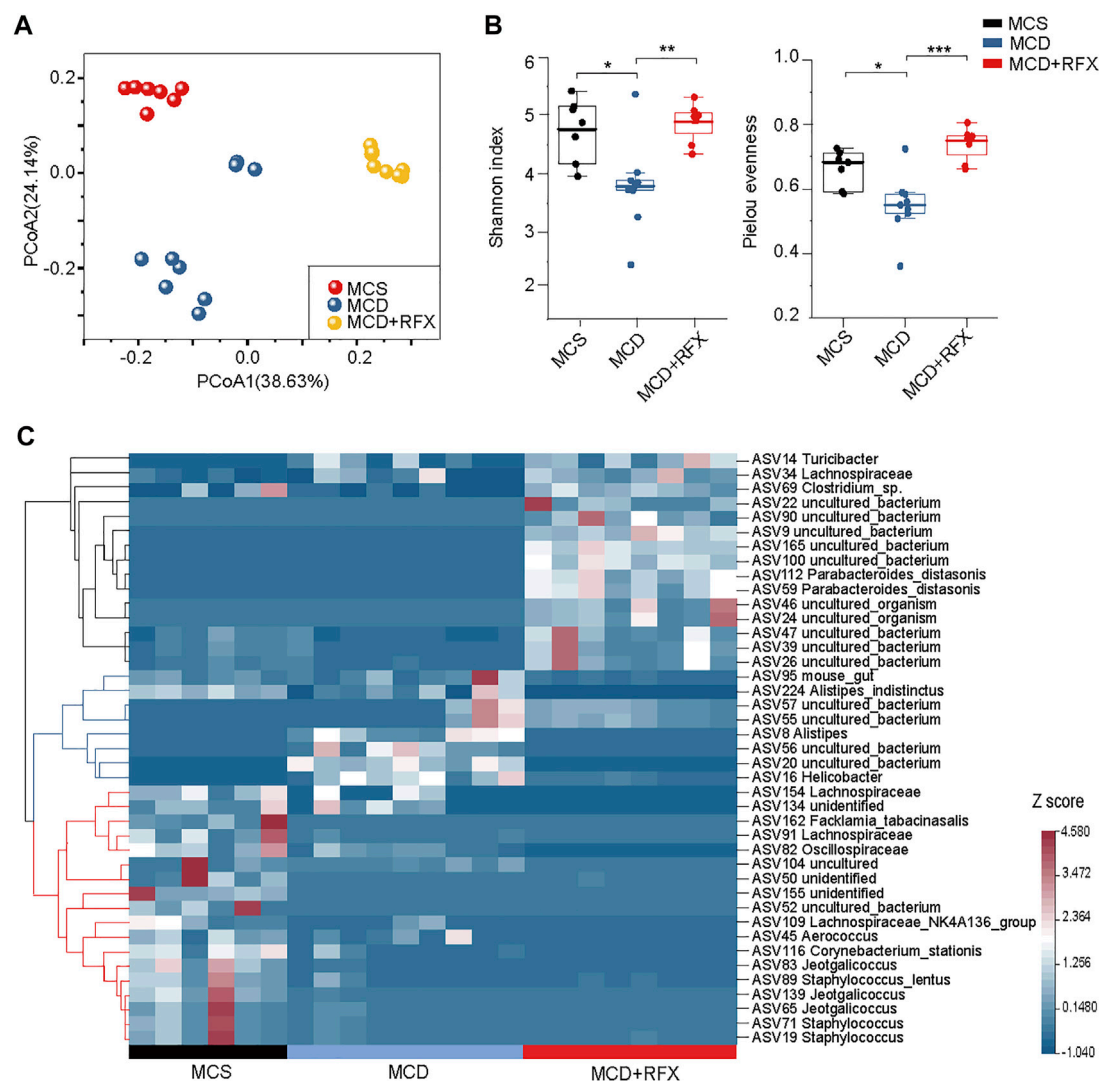


FIGURE 3 | Effects of rifaximin on the gut microbiome in the MCD diet induced NASH mice. **(A)** Clear separation of samples by diets and rifaximin treatment was observed via Principal coordinate analysis (PCoA) of the Unweighted UniFrac distance based on ASVs. **(B)** Alpha diversity of three cohorts based on ASVs, measured in terms of the Shannon index and Pielou's evenness. **(C)** The relative abundance of 41 differentially abundant ASVs identified by linear discriminant analysis effect size (LEfSe) ($\log(\text{LDA}) > 2$ and $p < 0.05$) among the MCS diet, MCD diet, and rifaximin treatment groups through pairwise comparison between multiple groups. Clustering was performed using the Pearson measurement. * $p < 0.05$, ** $p < 0.01$, *** $p < 0.001$.

rifaximin on the intestinal microbiome, we performed 16S rRNA amplicon sequencing of microbial DNA. Unweighted UniFrac principal coordinate analysis (PCoA) based on amplicon sequence variant (ASV) distributions revealed that the overall composition of the intestinal microbiome was significantly altered by the MCD diet ($p = 0.001$) and by rifaximin treatment ($p = 0.001$) (**Figure 3A**). The MCD diet significantly reduced alpha diversity indexes, such as Shannon diversity and Pielou's evenness (**Figure 3B**). However, this effect was significantly reversed by rifaximin treatment.

A total of 41 ASVs were increased or decreased between samples, as identified by LEfSe analysis through pairwise comparison between multiple groups ($\log(\text{LDA}) > 2$, $p < 0.05$)

(**Figure 3C**). The 41 ASVs formed three main clusters when using the Pearson measurement (**Figure 3C**). A total of six ASVs including ASV162 (*Facklamia tabacinasalis*) were enriched in the control diet group and decreased in the MCD diet-induced NASH mice. ASV8 (*Alistipes*), ASV16 (*Helicobacter*), ASV56 (*uncultured_bacterium*), and ASV20 (*uncultured_bacterium*) were significantly increased in the MCD-fed mice, but rifaximin treatment nearly depleted these ASVs. Moreover, rifaximin treatment increased abundant of 13 ASVs, including ASV69 (*Clostridium_sp.*) and ASV112 (*Parabacteroides distasonis*) (**Figure 3C**). These results indicate that rifaximin further changes the MCD diet-induced alteration of the gut microbiome in NASH mice.

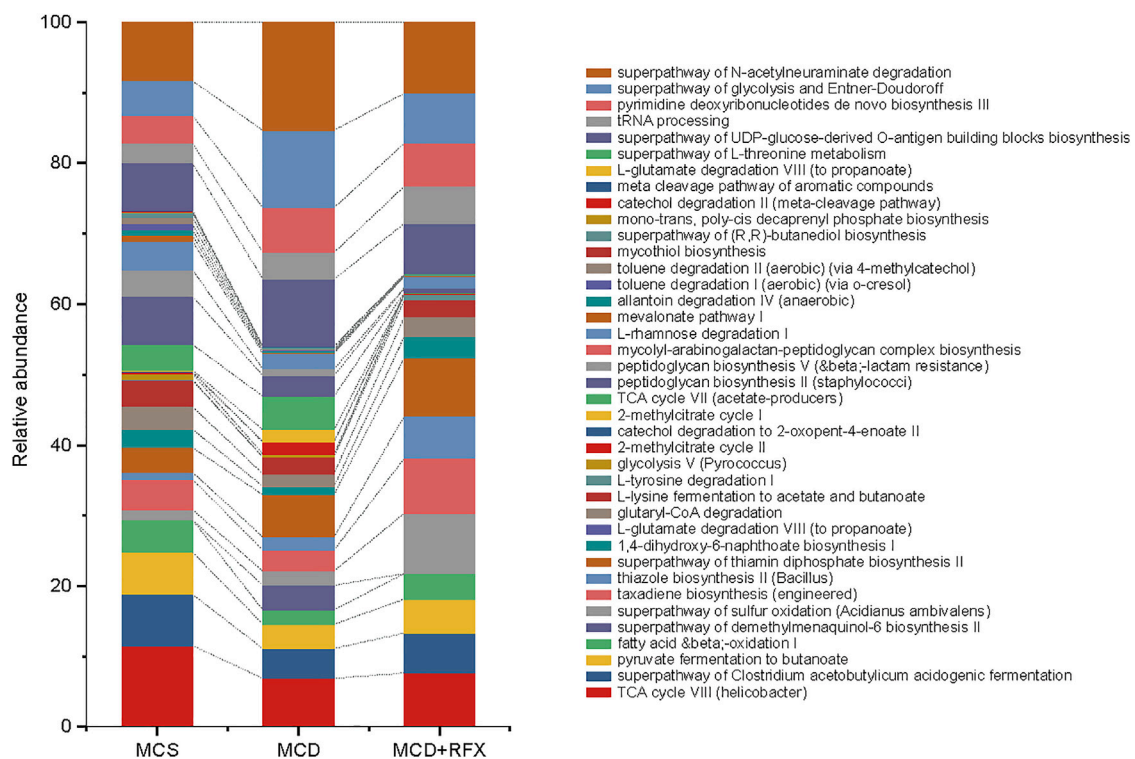


FIGURE 4 | Functional pathways of the gut microbiome were altered by MCD diet and rifaximin treatment. KEGG pathways that were enriched or depleted in different treatment groups were identified by PICRUSt analysis and selected using linear discriminant analysis through pairwise comparison between multiple groups ($\log(\text{LDA}) > 2$ and $p < 0.05$). Stacked bars display the relative abundance of different KEGG biological pathways.

Rifaximin Shifts the Metagenomic Function of the Intestinal Microbiome in the MCD Diet-Induced NASH Mice

The function of gut microbiome was predicted with PICRUSt (Langille et al., 2013). Biochemical pathways that were enriched or decreased by MCD diet and rifaximin treatment were assessed by LEfSe based on pathways from the Kyoto Encyclopedia of Genes and Genomes (KEGG) (Kanehisa et al., 2008). The MCD diet decreased four KEGG pathways: TCA cycle VIII (helicobacter), superpathway of *Clostridium acetobutylicum* acidogenic fermentation, pyruvate fermentation to butanoate, and fatty acid and beta oxidation I, whereas the superpathway of demethylmenaquinol-6 biosynthesis II was increased (Figure 4). Rifaximin administration enriched eleven KEGG pathways: superpathway of sulfur oxidation, taxadiene biosynthesis, thiazole biosynthesis II, superpathway of thiamin diphosphate biosynthesis II, 1, 4-dihydroxy-6-naphthoate biosynthesis I, L-glutamate degradation VIII, glutaryl-CoA degradation, L-lysine fermentation to acetate and butanoate, L-tyrosine degradation I, TCA cycle VIII, and fatty acid and beta oxidation I (Figure 4). Rifaximin decreased six KEGG pathways: which were related to the glycolysis V, 2-methylcitrate cycle II, catechol degradation to 2-oxopent-4-enoate II, 2-methylcitrate cycle I, TCA cycle VII (acetate-producers), and superpathway of demethylmenaquinol-6

biosynthesis II (Figure 4). Among these predicted pathways data using PICRUSt, we found rifaximin treatment altered microorganisms' functional pathways in the MCD diet induced NASH mice, including fatty acid and beta oxidation I pathway et al. Therefore, we proposed that rifaximin treatment may be related to microorganisms' lipid metabolism.

Rifaximin Regulates the Level of DCA in the Ileum in the MCD Diet Induced NASH Mice

Disorders in the intestinal bile acids profile are associated with the development of Non-alcoholic fatty liver disease (NAFLD) (Hu et al., 2020). In this study, we investigated metabolic profiles of bile acids in the mouse ileum. The MCD diet induced notable upregulation of primary bile acids including cholic acid (CA), chenodeoxycholic acid (CDCA), muricholic acids (MCAs), ursodeoxycholic acid (UDCA), and glycine cholic acid (GCA) in mice. This suggested that the MCD diet may alter synthesis of primary bile acids in the liver (Figure 5A). Furthermore, the secondary bile acid deoxycholic acid (DCA) was also substantially higher in the MCD diet induced NASH mice (Figure 5A). Notably, rifaximin administration significantly suppressed the DCA content while the other bile acid levels remained statistically unchanged (Figure 5A). Because DCA is a natural agonist of farnesoid X receptor, we performed qRT-PCR to measure expression of genes related to Fxr-Fgf15 signaling in the

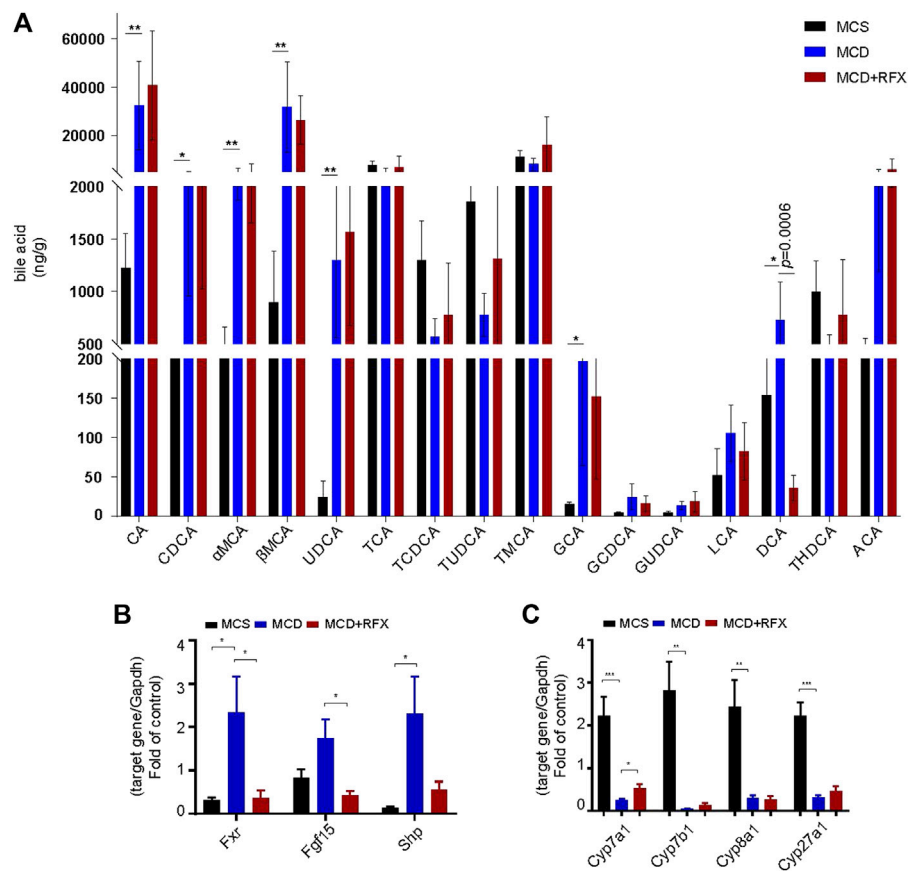


FIGURE 5 | Impact of rifaximin on bile acid levels in the ileum and on the Fxr signaling pathway. **(A)** Bile acid levels in the distal ileum. Levels of DCA decreased significantly after rifaximin treatment in MCD-fed mice $n = 7$ mice in each group. **(B)** Relative expression of Fxr and its target genes Fgf15 and Shp in the mouse intestine. **(C)** Relative expression of Cyp7a1, Cyp7b1, Cyp8a1, and Cyp27a1 mRNAs. Gapdh is for normalization. * $p < 0.05$, ** $p < 0.01$, *** $p < 0.001$ (Kruskal-Wallis test). $n = 8$ mice in each group.

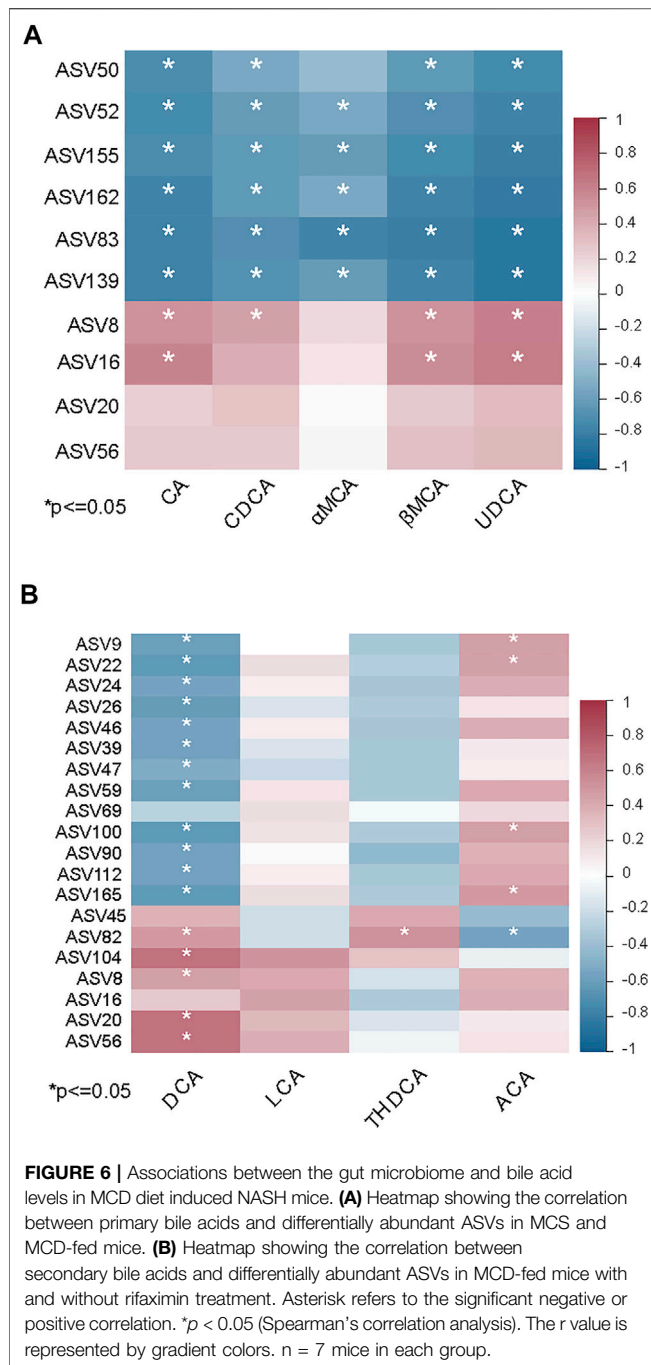
intestine and its negative feedback loop in the liver (Makishima et al., 1999). Consistent with the increase in DCA levels associated with the MCD diet, Fxr, Shp1, and Fgf15 were upregulated in the intestine while Cyp7a1, Cyp7b1, Cyp8a1 and Cyp27a1 were significantly downregulated in the liver (Figures 5B,C). Moreover, rifaximin reversed the activation of Fxr-Fgf15 signaling in the ileum and promoted expression of Cyp7a1 in the liver (Figures 5B,C). These data suggest that rifaximin may attenuate MCD-induced NASH by modulating the DCA profile and downstream signaling in the intestine.

Many studies have revealed that the gut microbiome has an impact on the synthesis of bile acids (Sayin et al., 2013; Wahlstrom, et al., 2016). To further identify interactions between the gut microbiome and levels of bile acids in the ileum, Spearman correlation analysis was performed to determine if there was an association between differentially abundant ASVs and bile acid levels. Eight ASVs were associated with the significant increase of primary bile acids in the MCD-fed mice compared with MCS-fed mice. The primary bile acids in mice, namely CA, CDCA, MCAs, UDCA, and GCA, were negatively correlated with six ASVs and positively correlated with two ASVs (Figure 6A). In contrast, DCA showed a negative

correlation with rifaximin-elevated ASVs (belonging to uncultured *Desulfovibrionaceae*, *Mucispirillum*, *Rikenellaceae_RC9_gut_group*, *Dubosiella*, *Parabacteroides*, *Coriobacteriaceae_UCG-002*, *Muribaculaceae*) (Figure 6B). Notably, ASV8, ASV20 and ASV56 (belonging to the groups *Alistipes*, *Muribaculaceae*, *Bilophila*, respectively), which were enriched by the MCD diet but decreased by rifaximin treatment, exhibited a positive correlation with DCA (Figure 6B). These data indicate that rifaximin may decrease the DCA content by altering the gut microbiome in NASH mice.

DISCUSSION

To our knowledge, there has been no prior report investigating the preventive effect of rifaximin for NASH mice. There are three published studies that evaluate the efficacy of rifaximin in human NASH therapy, but with contradictory conclusions (Abdel-Razik, et al., 2018; Cobbolt, et al., 2018; Gangarapu, et al., 2015). The discrepancies may be due to differing treatment parameters (dosage and duration). For example, in the open-label pilot study that revealed no therapeutic benefit of rifaximin for



NASH patients, the rifaximin dosage was relatively low (800 mg/day) and the duration was relatively short (6 weeks) (Cobbald, et al., 2018). In this study, we found that rifaximin delivery markedly inhibited MCD diet-induced liver steatosis and deposition, and reduced NAS in mice. Thus, we speculate that rifaximin may exert beneficial effects on NASH at a more standard dosage (1,100 or 1,200 mg/day). Interestingly, Cheng et al. reported that low dose (1 mg/kg) rifaximin treated to the PXR-humanized healthy mice for 6 months significantly up-regulated triglyceride synthesis genes in liver. However,

feeding diet and rifaximin dosage may all have impact on the hepatic lipid metabolism. Moreover, the relation between PXR and rifaximin in NASH requires further investigation.

Many clinical trials have shown that rifaximin can decrease serum LPS and its downstream proinflammatory cytokines (Abdel-Razik, et al., 2018; Gangarapu, et al., 2015). In the present study, we also found that rifaximin decreased hepatic inflammation, serum LPS, and Tnfa and Mcp1 expression in MCD-fed mice. Additionally, the effect of rifaximin in inhibiting NASH-fibrosis has been reported in a previous study in rats (Fujinaga, et al., 2020). Consistent with those prior results, we found that rifaximin ameliorated MCD diet-induced fibrosis in the NASH mouse liver. Consequently, we inferred that the reduction of hepatic inflammation may contribute to relief of hepatic fibrosis in NASH mice.

Rifaximin suppresses the activity of pathogens such as enterotoxigenic *Escherichia coli* and *Shigella* by altering microbial virulence (DuPont, 2011). One study showed that the clinical improvement of patients with ulcerative colitis or irritable bowel syndrome undergoing rifaximin treatment was associated with an increase in *Faecalibacterium* abundance (Ponziani et al., 2020). In a visceral hyperalgesia rat model, rifaximin reduced the overall small bowel bacterial burden but increased the abundance of *Lactobacillus* species (Xu et al., 2014; Bloom et al., 2021). These results implied that rifaximin treatment results in alteration of gut bacterial composition. In this study, rifaximin was also found to have a great capacity to regulate the gut microbial composition. Rifaximin treatment decreased the abundance of seven ASVs, such as ASV8 (*Alistipes*) and ASV16 (*Helicobacter*) while increasing several ASVs such as ASV112 (*Parabacteroides distasonis*). Additionally, we determined that rifaximin enriched or depleted cohorts of new uncultured bacteria. The function and the impact of these new uncultured bacteria on humans was required to be defined. These data suggest that the effect of rifaximin on MCD diet-induced NASH may be partly attributed to modulation of the gut microbiome.

Studies have revealed that intestinal flora are closely associated with bile acid metabolism (Hutka et al., 2021). Intestinal bacteria convert primary bile acids into secondary bile acids by microbial biotransformation, including deconjugation and oxidation of hydroxyl groups (Wahlstrom, et al., 2016). Previous studies had identified *Clostridium* and *Eubacterium* belonging to the *Firmicutes* phylum are associated with secondary bile acids (Kitahara et al., 2001). In the present study, we investigated the ileal bile acid profiles and discovered that DCA was significantly decreased by rifaximin treatment. We also found that DCA levels were negatively correlated with several ASVs belonging to the *Firmicutes* phylum, including ASV26, ASV39, ASV47, which were increased after rifaximin treatment. Bile acids regulate metabolism in the host mainly through the bile acid receptor Fxr (Wahlstrom, et al., 2016). As a natural intestinal Fxr agonist, DCA activates the intestinal Fxr-Fgf15 signaling pathway to inhibit hepatic expression of *Cyp7a1* and *Cyp7b1*, which regulate lipid metabolism (de Aguiar Vallim et al., 2013; Kang et al., 2021). Our data show that rifaximin treatment significantly downregulated *Fxr* and *Fgf15* in the terminal ileum while upregulating *Cyp7a1* and *Cyp7b1* in the liver. Based on these

results, we inferred that rifaximin may alter the gut microbiome and reduce DCA in the terminal ileum to attenuate MCD diet-induced NASH in mice. However, additional studies are needed to confirm this conclusion and explore the exact mechanism. Taken together, we found that rifaximin treatment relieved the MCD-induced NASH by modulating gut microbiome and decreasing DCA-Fxr signaling in the ileum. This study may serve as the basis for the development of promising treatment of NAFLD by administering rifaximin in the future.

DATA AVAILABILITY STATEMENT

The datasets presented in this study can be found in online repositories. The names of the repository/repositories and accession number(s) can be found below: <https://www.ncbi.nlm.nih.gov/>, PRJNA771219.

ETHICS STATEMENT

All animal experiments were in accordance with the National Institute of Health Guide for the Care and Use of Laboratory Animals, and were approved by the Scientific Investigation Board of Naval Medical University.

REFERENCES

- Abdel-Razik, A., Mousa, N., Shabana, W., Refaey, M., Elzehery, R., Elhelaly, R., et al. (2018). Rifaximin in Nonalcoholic Fatty Liver Disease: Hit Multiple Targets with a Single Shot. *Eur. J. Gastroenterol. Hepatol.* 30 (10), 1237–1246. doi:10.1097/MEG.0000000000001232
- Arab, J. P., Karpen, S. J., Dawson, P. A., Arrese, M., and Trauner, M. (2017). Bile Acids and Nonalcoholic Fatty Liver Disease: Molecular Insights and Therapeutic Perspectives. *Hepatology* 65 (1), 350–362. doi:10.1002/hep.28709
- Bass, N. M., Mullen, K. D., Sanyal, A., Poordad, F., Neff, G., Leevy, C. B., et al. (2010). Rifaximin Treatment in Hepatic Encephalopathy. *N. Engl. J. Med.* 362 (12), 1071–1081. doi:10.1056/NEJMoa0907893
- Bloom, P. P., Tapper, E. B., Young, V. B., and Lok, A. S. (2021). Microbiome Therapeutics for Hepatic Encephalopathy. *J. Hepatol.* 75, 1452–1464. doi:10.1016/j.jhep.2021.08.004
- Caraceni, P., Vargas, V., Solà, E., Alessandria, C., Wit, K., Trebicka, J., et al. (2021). The Use of Rifaximin in Patients with Cirrhosis. *Hepatology* 74, 1660–1673. doi:10.1002/hep.31708
- Cheng, J., Krausz, K. W., Tanaka, N., and Gonzalez, F. J. (2012). Chronic Exposure to Rifaximin Causes Hepatic Steatosis in Pregnane X Receptor-Humanized Mice. *Toxicol. Sci.* 129 (2), 456–468. doi:10.1093/toxsci/kfs211
- Cobbald, J. F. L., Atkinson, S., Marchesi, J. R., Smith, A., Wai, S. N., Stove, J., et al. (2018). Rifaximin in Non-alcoholic Steatohepatitis: An Open-Label Pilot Study. *Hepatol. Res.* 48 (1), 69–77. doi:10.1111/hepr.12904
- de Aguiar Vallim, T. Q., Tarling, E. J., and Edwards, P. A. (2013). Pleiotropic Roles of Bile Acids in Metabolism. *Cell Metab.* 17 (5), 657–669. doi:10.1016/j.cmet.2013.03.013
- DuPont, H. L. (2011). Biologic Properties and Clinical Uses of Rifaximin. *Expert Opin. Pharmacother.* 12 (2), 293–302. doi:10.1517/14656566.2011.546347
- Fiorucci, S., Di Giorgio, C., and Distrutti, E. (2019). Obeticholic Acid: An Update of its Pharmacological Activities in Liver Disorders. *Handb. Exp. Pharmacol.* 256, 283–295. doi:10.1007/164_2019_227
- Fiorucci, S., Distrutti, E., Carino, A., Zampella, A., and Biagioli, M. (2021). Bile Acids and Their Receptors in Metabolic Disorders. *Prog. Lipid Res.* 82, 101094. doi:10.1016/j.plipres.2021.101094

AUTHOR CONTRIBUTIONS

W-FX conceived and designed the experiments; XZ reviewed the article; MZ assisted with the bioinformatic analysis; JJ and M-TN performed animal experiments and wrote the original draft; M-TN edited article, analyzed, and visualized results; BX analyzed the gut microbiome data; XZ critically revised the manuscript; HQ, CY, and XZ contributed expert advice; All authors corrected and approved the final manuscript.

FUNDING

This work was supported by funding from the national natural science foundation of China under grants 82030021 and 81960120; The Shanghai Natural Science Fund under grants 22ZR1477400; Peak Disciplines (Type IV) of Institutions of Higher Learning in Shanghai.

SUPPLEMENTARY MATERIAL

The Supplementary Material for this article can be found online at: <https://www.frontiersin.org/articles/10.3389/fphar.2022.841132/full#supplementary-material>

- Francque, S., Szabo, G., Abdelmalek, M. F., Byrne, C. D., Cusi, K., Dufour, J. F., et al. (2021). Nonalcoholic Steatohepatitis: the Role of Peroxisome Proliferator-Activated Receptors. *Nat. Rev. Gastroenterol. Hepatol.* 18 (1), 24–39. doi:10.1038/s41575-020-00366-5
- Francque, S. (2021). Saroglitazar for the Treatment of NASH: The Peroxisome Proliferator-Activated Receptor Story Goes on! *Hepatology* 74, 1730–1733. doi:10.1002/hep.32024
- Friedman, S. L., Neuschwander-Tetri, B. A., Rinella, M., and Sanyal, A. J. (2018). Mechanisms of NAFLD Development and Therapeutic Strategies. *Nat. Med.* 24 (7), 908–922. doi:10.1038/s41591-018-0104-9
- Fujinaga, Y., Kawaratani, H., Kaya, D., Tsuji, Y., Ozutsumi, T., Furukawa, M., et al. (2020). Effective Combination Therapy of Angiotensin-II Receptor Blocker and Rifaximin for Hepatic Fibrosis in Rat Model of Nonalcoholic Steatohepatitis. *Int. J. Mol. Sci.* 21 (15), 5589. doi:10.3390/ijms21155589
- Gangarapu, V., Ince, A. T., Baysal, B., Kayar, Y., Kılıç, U., Gök, Ö., et al. (2015). Efficacy of Rifaximin on Circulating Endotoxins and Cytokines in Patients with Nonalcoholic Fatty Liver Disease. *Eur. J. Gastroenterol. Hepatol.* 27 (7), 840–845. doi:10.1097/MEG.0000000000000348
- Gil-Gómez, A., Brescia, P., Rescigno, M., and Romero-Gómez, M. (2021). Gut-Liver Axis in Nonalcoholic Fatty Liver Disease: the Impact of the Metagenome, End Products, and the Epithelial and Vascular Barriers. *Semin. Liver Dis.* 41 (2), 191–205. doi:10.1055/s-0041-1723752
- Haas, J. T., Francque, S., and Stals, B. (2016). Pathophysiology and Mechanisms of Nonalcoholic Fatty Liver Disease. *Annu. Rev. Physiol.* 78, 181–205. doi:10.1146/annurev-physiol-021115-105331
- Hu, H., Lin, A., Kong, M., Yao, X., Yin, M., Xia, H., et al. (2020). Intestinal Microbiome and NAFLD: Molecular Insights and Therapeutic Perspectives. *J. Gastroenterol.* 55 (2), 142–158. doi:10.1007/s00535-019-01649-8
- Hutka, B., Lázár, B., Tóth, A. S., Ágg, B., László, S. B., Makra, N., et al. (2021). The Nonsteroidal Anti-inflammatory Drug Ketorolac Alters the Small Intestinal Microbiota and Bile Acids without Inducing Intestinal Damage or Delaying Peristalsis in the Rat. *Front. Pharmacol.* 12, 664177. doi:10.3389/fphar.2021.664177
- Kanehisa, M., Araki, M., Goto, S., Hattori, M., Hirakawa, M., Itoh, M., et al. (2008). KEGG for Linking Genomes to Life and the Environment. *Nucleic Acids Res.* 36, D480–D484. doi:10.1093/nar/gkm882

- Kang, M., Kim, E. H., Jeong, J., and Ha, H. (2021). Heukcha, Naturally post-fermented green tea Extract, Ameliorates Diet-induced Hypercholesterolemia and NAFLD in Hamster. *J. Food Sci.* 86, 5016–5025. doi:10.1111/1750-3841.15929
- Kim, D., Touro, A., and Kim, W. R. (2018). Nonalcoholic Fatty Liver Disease and Metabolic Syndrome. *Clin. Liver Dis.* 22 (1), 133–140. doi:10.1016/j.cld.2017.08.010
- Kitahara, M., Takamine, F., Imamura, T., and Benno, Y. (2001). Clostridium Hiranonis Sp. nov., a Human Intestinal Bacterium with Bile Acid 7 α -Dehydroxylating Activity. *Int. J. Syst. Evol. Microbiol.* 51 (Pt 1), 39–44. doi:10.1099/00207713-51-1-39
- Langille, M. G., Zaneveld, J., Caporaso, J. G., McDonald, D., Knights, D., Reyes, J. A., et al. (2013). Predictive Functional Profiling of Microbial Communities Using 16S rRNA Marker Gene Sequences. *Nat. Biotechnol.* 31 (9), 814–821. doi:10.1038/nbt.2676
- Lee, Y. K., Park, J. E., Lee, M., and Hardwick, J. P. (2018). Hepatic Lipid Homeostasis by Peroxisome Proliferator-Activated Receptor Gamma 2. *Liver Res.* 2 (4), 209–215. doi:10.1016/j.livres.2018.12.001
- Li, W., Zhou, C., Fu, Y., Chen, T., Liu, X., Zhang, Z., et al. (2020). Targeted Delivery of Hyaluronic Acid Nanomicelles to Hepatic Stellate Cells in Hepatic Fibrosis Rats. *Acta Pharm. Sin B* 10 (4), 693–710. doi:10.1016/j.apsb.2019.07.003
- Lin, L., Jian, J., Song, C. Y., Chen, F., Ding, K., Xie, W. F., et al. (2020). SHP-1 Ameliorates Nonalcoholic Steatohepatitis by Inhibiting Proinflammatory Cytokine Production. *FEBS Lett.* 594 (18), 2965–2974. doi:10.1002/1873-3468.13879
- Makishima, M., Okamoto, A. Y., Repa, J. J., Tu, H., Learned, R. M., Luk, A., et al. (1999). Identification of a Nuclear Receptor for Bile Acids. *Science* 284 (5418), 1362–1365. doi:10.1126/science.284.5418.1362
- Ni, Q., Ding, K., Wang, K. Q., He, J., Yin, C., Shi, J., et al. (2017). Deletion of HNF1 α in Hepatocytes Results in Fatty Liver-Related Hepatocellular Carcinoma in Mice. *FEBS Lett.* 591 (13), 1947–1957. doi:10.1002/1873-3468.12689
- Okubo, H., Kushiya, A., Sakoda, H., Nakatsu, Y., Iizuka, M., Taki, N., et al. (2016). Involvement of Resistin-like Molecule β in the Development of Methionine-Choline Deficient Diet-Induced Non-alcoholic Steatohepatitis in Mice. *Sci. Rep.* 6, 20157. doi:10.1038/srep20157
- Pellicciari, R., Fiorucci, S., Camaioni, E., Clerici, C., Costantino, G., Maloney, P. R., et al. (2002). 6 α -ethyl-chenodeoxycholic Acid (6-ECDCA), a Potent and Selective FXR Agonist Endowed with Anticholestatic Activity. *J. Med. Chem.* 45 (17), 3569–3572. doi:10.1021/jm025529g
- Peng, H., Harvey, B. T., Richards, C. I., and Nixon, K. (2021). Neuron-Derived Extracellular Vesicles Modulate Microglia Activation and Function. *Biology* 10 (10), 948. doi:10.3390/biology10100948
- Ponziani, F. R., Scaldaferri, F., De Siena, M., Mangiola, F., Matteo, M. V., Pecere, S., et al. (2020). Increased Faecalibacterium Abundance Is Associated with Clinical Improvement in Patients Receiving Rifaximin Treatment. *Benef. Microbes* 11 (6), 519–525. doi:10.3920/BM2019.0171
- Puri, P., and Sanyal, A. J. (2012). Nonalcoholic Fatty Liver Disease: Definitions, Risk Factors, and Workup. *Clin. Liver Dis. (Hoboken)* 1 (4), 99–103. doi:10.1002/cld.81
- Qian, H., Deng, X., Huang, Z. W., Wei, J., Ding, C. H., Feng, R. X., et al. (2015). An HNF1 α -Regulated Feedback Circuit Modulates Hepatic Fibrogenesis via the Crosstalk between Hepatocytes and Hepatic Stellate Cells. *Cell Res* 25 (8), 930–945. doi:10.1038/cr.2015.84
- Quast, C., Pruesse, E., Yilmaz, P., Gerken, J., Schweer, T., Yarza, P., et al. (2013). The SILVA Ribosomal RNA Gene Database Project: Improved Data Processing and Web-Based Tools. *Nucleic Acids Res.* 41 (Database issue), D590–D596. doi:10.1093/nar/gks1219
- Rao, A., Kusters, A., Mells, J. E., Zhang, W., Setchell, K. D., Amanso, A. M., et al. (2016). Inhibition of Ileal Bile Acid Uptake Protects against Nonalcoholic Fatty Liver Disease in High-Fat Diet-Fed Mice. *Sci. Transl. Med.* 8 (357), 357ra122. doi:10.1126/scitranslmed.aaf4823
- Romano, A., Friuli, M., Del Coco, L., Longo, S., Vergara, D., Del Boccio, P., et al. (2021). Chronic Oleoylethanolamide Treatment Decreases Hepatic Triacylglycerol Level in Rat Liver by a PPAR γ /SREBP-Mediated Suppression of Fatty Acid and Triacylglycerol Synthesis. *Nutrients* 13 (2), 394. doi:10.3390/nu13020394
- Sayin, S. I., Wahlström, A., Felin, J., Jäntti, S., Marschall, H. U., Bamberg, K., et al. (2013). Gut Microbiota Regulates Bile Acid Metabolism by Reducing the Levels of Tauro-Beta-Muricholic Acid, a Naturally Occurring FXR Antagonist. *Cel. Metab.* 17 (2), 225–235. doi:10.1016/j.cmet.2013.01.003
- Sun, L., Xie, C., Wang, G., Wu, Y., Wu, Q., Wang, X., et al. (2018). Gut Microbiota and Intestinal FXR Mediate the Clinical Benefits of Metformin. *Nat. Med.* 24 (12), 1919–1929. doi:10.1038/s41591-018-0222-4
- Wahlström, A., Sayin, S. I., Marschall, H. U., and Bäckhed, F. (2016). Intestinal Crosstalk between Bile Acids and Microbiota and its Impact on Host Metabolism. *Cel. Metab.* 24 (1), 41–50. doi:10.1016/j.cmet.2016.05.005
- Xu, D., Gao, J., Gilliland, M., 3rd, Wu, X., Song, I., Kao, J. Y., et al. (2014). Rifaximin Alters Intestinal Bacteria and Prevents Stress-Induced Gut Inflammation and Visceral Hyperalgesia in Rats. *Gastroenterology* 146 (2), 484–e4. doi:10.1053/j.gastro.2013.10.026
- Younossi, Z., Tacke, F., Arrese, M., Chander Sharma, B., Mostafa, I., Bugianesi, E., et al. (2019). Global Perspectives on Nonalcoholic Fatty Liver Disease and Nonalcoholic Steatohepatitis. *Hepatology* 69 (6), 2672–2682. doi:10.1002/hep.30251
- Zhang, J., Zhang, H., Deng, X., Zhang, N., Liu, B., Xin, S., et al. (2018). Baicalin Attenuates Non-alcoholic Steatohepatitis by Suppressing Key Regulators of Lipid Metabolism, Inflammation and Fibrosis in Mice. *Life Sci.* 192, 46–54. doi:10.1016/j.lfs.2017.11.027
- Zhang, X., Coker, O. O., Chu, E. S., Fu, K., Lau, H. C. H., Wang, Y. X., et al. (2021). Dietary Cholesterol Drives Fatty Liver-Associated Liver Cancer by Modulating Gut Microbiota and Metabolites. *Gut* 70 (4), 761–774. doi:10.1136/gutjnl-2019-319664
- Zhu, X., Gan-Schreier, H., Otto, A. C., Cheng, Y., Staffer, S., Tuma-Kellner, S., et al. (2019). iPLA2 β Deficiency in Mice Fed with MCD Diet Does Not Correct the Defect of Phospholipid Remodeling but Attenuates Hepatocellular Injury via an Inhibition of Lipid Uptake Genes. *Biochim. Biophys. Acta Mol. Cel Biol Lipids* 1864 (5), 677–687. doi:10.1016/j.bbalip.2019.02.003

Conflict of Interest: The authors declare that the research was conducted in the absence of any commercial or financial relationships that could be construed as a potential conflict of interest.

Publisher's Note: All claims expressed in this article are solely those of the authors and do not necessarily represent those of their affiliated organizations, or those of the publisher, the editors and the reviewers. Any product that may be evaluated in this article, or claim that may be made by its manufacturer, is not guaranteed or endorsed by the publisher.

Copyright © 2022 Jian, Nie, Xiang, Qian, Yin, Zhang, Zhang, Zhu and Xie. This is an open-access article distributed under the terms of the Creative Commons Attribution License (CC BY). The use, distribution or reproduction in other forums is permitted, provided the original author(s) and the copyright owner(s) are credited and that the original publication in this journal is cited, in accordance with accepted academic practice. No use, distribution or reproduction is permitted which does not comply with these terms.



Celastrol: An Update on Its Hepatoprotective Properties and the Linked Molecular Mechanisms

Mengzhen Li¹, Faren Xie², Lu Wang², Guoxue Zhu², Lian-Wen Qi^{1*} and Shujun Jiang^{2*}

¹Clinical Metabolomics Center, China Pharmaceutical University, Nanjing, China, ²Nanjing Hospital of Chinese Medicine Affiliated to Nanjing University of Chinese Medicine, Nanjing, China

OPEN ACCESS

Edited by:

Francisco Javier Cubero,
Complutense University of Madrid,
Spain

Reviewed by:

Lili Ding,
Shanghai University of Traditional
Chinese Medicine, China
Raquel Benedé-Ubieto,
Complutense University of Madrid,
Spain
Olga Estévez Vázquez,
Complutense University of Madrid,
Spain

*Correspondence:

Lian-Wen Qi
qilw@cpu.edu.cn
Shujun Jiang
fairyjsj@163.com

Specialty section:

This article was submitted to
Gastrointestinal and Hepatic
Pharmacology,
a section of the journal
Frontiers in Pharmacology

Received: 19 January 2022

Accepted: 21 February 2022

Published: 04 April 2022

Citation:

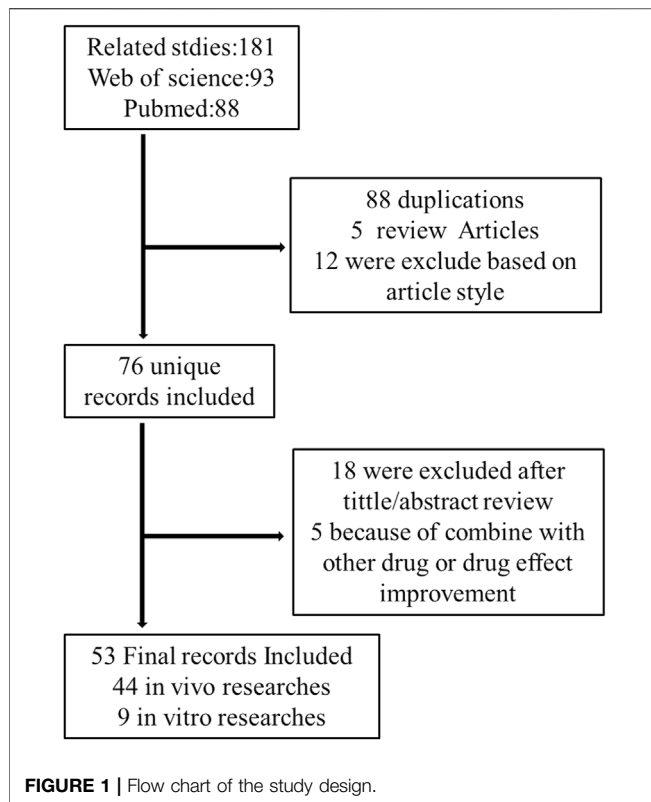
Li M, Xie F, Wang L, Zhu G,
Qi L-W and Jiang S (2022) Celastrol:
An Update on Its Hepatoprotective
Properties and the Linked
Molecular Mechanisms.
Front. Pharmacol. 13:857956.
doi: 10.3389/fphar.2022.857956

The liver plays an important role in glucose and lipid homeostasis, drug metabolism, and bile synthesis. Metabolic disorder and inflammation synergistically contribute to the pathogenesis of numerous liver diseases, such as metabolic-associated fatty liver disease (MAFLD), liver injury, and liver cancer. Celastrol, a triterpene derived from *Tripterygium wilfordii* Hook.f., has been extensively studied in metabolic and inflammatory diseases during the last several decades. Here we comprehensively review the pharmacological activities and the underlying mechanisms of celastrol in the prevention and treatment of liver diseases including MAFLD, liver injury, and liver cancer. In addition, we also discuss the importance of novel methodologies and perspectives for the drug development of celastrol. Although celastrol has been claimed as a promising agent against several metabolic diseases, both preclinical and clinical studies are highly required to accelerate the clinical transformation of celastrol in treating different liver illness. It is foreseeable that celastrol-derived therapeutics is evolving in the field of liver ailments.

Keywords: celastrol, liver diseases, liver injury, liver cancer, MAFLD

INTRODUCTION

The liver is a metabolic organ that is responsible for glucose and lipid homeostasis, drug metabolism, and bile synthesis (Diehl-Jones and Askin, 2002; Almazroo et al., 2017; Tappy, 2021). Liver diseases contain non-alcoholic fatty liver disease (NAFLD) and its related diseases, drugs or infections induced liver injury, liver cancer, and among others. With the aging of the population and the prevalence of obesity, NAFLD, known as metabolic-associated fatty liver disease (MAFLD), is becoming a threat to human health in the world, (Eslam et al., 2020). MAFLD begins with the accumulation of hepatic lipid, metabolic syndrome (central adiposity, hyperglycemia, dyslipidemia, and hypertension) (Mundi et al., 2020). Environment factors like dietary habits and the genetic factors such as *PNPLA3* (encoding patatin-like phospholipase domain-containing protein3), *TM6SF2* (encoding transmembrane 6 superfamily member 2), and epigenetic factors are the risk factors of MAFLD (Younossi et al., 2018). The current global prevalence of MAFLD is approximately 25%, which may develop into non-alcoholic steatohepatitis, eventually leading to liver fibrosis, cirrhosis, and even liver cancer if not treated in a timely fashion (Ye et al., 2020). Except for the liver damage, MAFLD and non-alcoholic steatohepatitis can also aggravate or induce insulin resistance, which are closely related to the high incidence of type 2 diabetes and cardiovascular disease (Liang et al., 2022). Liver injury as a loss of liver function is mainly caused by drug, infections, and intrahepatic cholestasis (Thawley, 2017). The drug-induced liver injury (DILI) is one of the most common and serious adverse drug reactions, which can lead to acute liver failure and even death in severe cases (Licata, 2016). With 831,000 death cases and 905,000 new cases in 2020, liver cancer



with high mortality and incidence remains a global menace (Sung et al., 2021). Although many patients are diagnosed and treated at an early stage of the disease, the recurrence rate is still high. For middle and late-stage hepatic carcinoma, the prognosis is even less optimistic. Therefore, new therapy or drugs with better efficacy and lower toxicity are of great importance.

Traditional Chinese Medicine (TCM) was used to treat various diseases such as metabolic diseases, liver diseases, inflammation, and cancers for many years. In light of their numerous pharmacological activities, low toxicity, and low side effects, nature compounds from TCM are widely used to protect against liver diseases, such as berberine, curcumin, ginsenoside, celastrol, to name a few (Xu et al., 2018a). In Europe and America, up to 65% of patients choose herbal medicines to treat liver diseases (Zhang et al., 2013; Madrigal-Santillán et al., 2014; Bagherniya et al., 2018). Celastrol, a pharmacologically active compound from *Tripterygium wilfordii* Hook.f., possesses therapeutic properties for multiple diseases, such as rheumatoid arthritis, inflammatory bowel diseases, hepatitis, as well as anti-cancer, anti-obesity, and metabolic modulating (Feng et al., 2013; Lin et al., 2015; Liu et al., 2015; Tseng et al., 2017; Saito et al., 2019; Song et al., 2019). In recent years, celastrol has attracted the attention of researchers and the pharmaceutical industry due to its benefits on human health. Here, we summarized the studies exploring the pharmacological properties of celastrol in liver protection during 15 years from 2007 to 2021, and made a general statement about its mechanisms in liver-related diseases.

STUDY DESIGN

The PubMed and Web of Science databases were used to search related articles from 2007 to 2021. Cellular, animal, or human studies were searched with the keywords (celastrol) and (liver). Papers were extracted using the following inclusion criteria: (1) these studies should be research articles to estimate the hepatoprotective effects of celastrol; (2) only articles written in English were included. All titles and abstracts of publications retrieved were reviewed to select potentially eligible studies. Full texts of literatures potentially eligible were reviewed by two independent investigators. From a total of 181 results, 76 unique studies were identified, 88 duplication, 5 reviews, and 12 other article styles were excluded. After carefully reviewing the title and/or abstract, 18 were excluded 5 publications are irrelevant. A total of 53 articles were included in this review. A flowchart of this is illustrated in **Figure 1**.

CELASTROL AND LIVER DISEASES

Celastrol and MAFLD

MAFLD, characterized by the hepatic fat accumulation, is usually correlated with the metabolic disorder related obesity (Samuel and Shulman, 2018; Jarvis et al., 2020), hepatic inflammation (Kazankov et al., 2019), oxidative stress (Ore and Akinloye, 2019; Świdarska et al., 2019), and intestinal microbiome dysbiosis (Caussy and Loomba, 2018). Lipotoxicity induced by abnormal hepatic fat deposition activated Kuepfer cell (KC) to promote inflammation in MAFLD patients (Lanthier, 2015). Oxidative stress and endoplasmic reticulum (ER) stress resulted in mitochondrial reactive oxygen species (ROS) accumulation in hepatocytes, which in turn impaired glycolipid metabolism, accelerated inflammatory response, and introduced cell death in MAFLD (Ore and Akinloye, 2019; Świdarska et al., 2019; Chen et al., 2020a). The reasonable management of body weight and dietary habits should be given a high priority in MAFLD patients. Although the antidiabetic and lipid-lowering drugs may help to reduce hepatic lipid accumulation (Mundi et al., 2020), there are no specific drugs for MAFLD approved in Europe and the United States. Recent research mainly focused on the metabolic targets, immune targets, fibrosis, cell stress, and apoptosis (Friedman et al., 2018). Celastrol as a promising compound exhibits good anti-obesity and anti-inflammatory effect on treating MAFLD.

Anti-Obesity Effects

The liver is vital for lipid and glucose metabolism and homeostasis, protein, and amino acid metabolism, where bile acids produce and flux to the digestive system. Numerous evidences supported that obesity is strongly associated with MAFLD development (Fabbrini et al., 2010). The liver protective effect and molecular mechanism of celastrol on high fat diet (HFD) induced MAFLD animal models have been well-investigated (Wang et al., 2014; Ma et al., 2015; Zhang et al., 2017a; Hu et al., 2017; Luo et al., 2017; Kyriakou et al., 2018; Pfuhmann et al., 2018; Zhang et al., 2018; Feng et al., 2019a; Zhao

TABLE 1 | The summary of preclinical studies of celastrol in HFD induced MAFLD models.

| Experimental model used | Model inducer | Dosage and drug-delivery way | Drug treatment period | Phenotype and mechanism | Reference |
|--------------------------|------------------------|--|-----------------------|--|-------------------------|
| Wild type animal models | | | | | |
| Male Sprague–Dawley rats | HFD | 1 mg/kg/day, 3 mg/kg/day, and 9 mg/kg/day by oral administration | 6 weeks | Promoted weight loss and lipid metabolism, attenuated oxidative injury through improving ABCA1 and antioxidant enzymes activities, reducing NADPH oxidase activity | Wang et al. (2014) |
| | HFD for 11 weeks | 500 µg/kg/day by oral administration | 3 weeks | Decreased body weight and lipid accumulation in liver, promoted energy expenditure by increasing ratio of <i>Bacteroidetes</i> to <i>Firmicutes</i> rather than food intake, leptin signaling pathway, gut microbiota homeostasis | Hu et al. (2020) |
| | HFD for 17 weeks | 1 mg/kg/day, 3 mg/kg/day mixed with drinking water | 8 weeks | Reduced body weight, alleviated inflammatory response in adipose tissue and enhanced mitochondrial functions in skeletal muscle by upregulation of AMPK/SIRT1 signaling pathways | Abu Bakar et al. (2020) |
| Male C57BL/6J mice | HFD for 16–20 weeks | 100 µg/kg/day by i.p injection, or 10 mg/kg/day by oral administration | 3 weeks | Improved weight loss and glucose homeostasis by reducing food consumption and ER stress in hypothalamus | Liu et al. (2015) |
| | NCD or HFD for 9 weeks | 100 µg/kg/day or 500 µg/kg/day by i.p injection | 24 days | Reduced body weight and fat mass by decreased food intake, improved metabolism by increased homeostatic regulation of energy balance related gene expressions in the hypothalamus | Saito et al. (2019) |
| | HFD for 8 weeks | 1 mg/kg/day, 3 mg/kg/day mixed with food | 3 weeks | Enhanced energy expenditure, and mitochondrial function in fat and muscle by activated HSF1-PGC1α axis | Ma et al. (2015) |
| | HFD for 14 weeks | 200 µg/kg/every 2 days by i.p injection | 4 weeks | Inhibited lipid synthesis by downregulation of Srebp-1c expression, reduced oxidative stress and inflammation by enhanced the phosphorylation of hepatic AMPKα and Sirt1 | Zhang et al. (2017a) |
| | HFD for 12 weeks | 100 µg/kg/day by i.p injection | 2 weeks | Suppressed hepatic inflammation and immune cell accumulation by reducing expression and production of IL-1β and IL-6 | Hu et al. (2017) |
| | HFD for 16 weeks | 100 µg/kg/day by i.p injection | 8 weeks | Attenuated inflammation and insulin resistance by inhibition of TLR4/NF-κB | Zhang et al. (2018) |
| | HFD for 32 weeks | 100 µg/kg/day by i.p injection | 6 days | Promoted weight loss through hypoplasia and activation of leptin-STAT3 signaling in elder mice | Pfuhlmann et al. (2018) |
| | HFD for 8–12 weeks | 100 µg/kg/day by i.p injection | 10 days | Lowered body weight by inhibition of PTP1B and TCPTP in hypothalamus | Kyriakou et al. (2018) |
| | HFD for 16–20 weeks | 100 µg/kg/day by i.p injection | 4 days | Celastrol's anti-obesity effects was not dependent on LCN2 | Feng et al. (2019a) |
| | HFD for 16 weeks | 0.1 mg/kg/day by i.p injection | 21 days | Suppressed gluconeogenesis by activating CREB/PGC-1α pathway | Fang et al. (2019) |
| | HFD for 12 weeks | 150 µg/kg, 300 µg/kg by i.p injection | 3 weeks | Reduced weight gain without affecting food intake, ameliorated metabolic disorder and hepatic inflammation by inhibition of TLR3/NLRP3 inflammasome | Yang et al. (2021) |
| | HFD for 6 weeks | 3 mg/kg/day was mixed with food | 24 days | Prevented intestinal lipid absorption by downregulation of CD36, FATP2, FATP4 | Hua et al. (2021) |
| | HFD for 12 weeks | 50 µg/kg/day, 100 µg/kg/day, 200 µg/kg/day by i.p injection | 12 weeks | Attenuated inflammation through the suppression of MMP-2 and MMP-9 | Ouyang et al. (2021) |
| Male C57BL/6 N mice | HFD for 12 weeks | 5 mg/kg/day and 7.5 mg/kg/day mixed with food | 3 weeks | Reduced body weight gain, insulin resistance, hepatic steatosis, and inflammation by inhibition of CAP1–resistin interaction, PKA–NF-κB pathway | Zhu Y. et al. (2021) |
| | HFD for 12 weeks | 5 mg/kg/day or 7.5 mg/kg/day by oral administration | 3 weeks | Prevented M1 macrophage polarization, inflammation, and insulin resistance via regulating Nrf2/HO-1, MAPK signal, and NF-κB pathway | Luo et al. (2017) |
| | | | | Reduced body weight and fat mass inhibited inflammatory response by downregulation of expression of macrophage M1 biomarkers (e.g., IL-6, IL-1β, TNF-α, iNOS) and enhanced expression of macrophage M2 biomarkers (e.g., Arg-1, IL-10) | Zhao et al. (2019a) |

(Continued on following page)

TABLE 1 | (Continued) The summary of preclinical studies of celastrol in HFD induced MAFLD models.

| Experimental model used | Model inducer | Dosage and drug-delivery way | Drug treatment period | Phenotype and mechanism | Reference |
|---|----------------------------|---|-----------------------|--|-------------------------|
| Genetic deficiency animal models | | | | | |
| Lep ^{ob} mice | NCD | 100 µg/kg/day by i.p. injection, or 10 mg/kg/day by oral administration | 3 weeks | No significant change of body weight | Liu et al. (2015) |
| | | 100 µg/kg/day by subcutaneous injection | 6 days | | Pfuhlmann et al. (2018) |
| | | 100 µg/kg by i.p. injection | 3 weeks | | Feng et al. (2019b) |
| | | 100 µg/kg by i.p. injection | 4 days | | Feng et al. (2019a) |
| | | 0.1 mg/kg/day by i.p. injection for 10 days, then 0.5 mg/kg by i.p.injection for 15 days | 25 days | Body weight slightly reduced | (Saito et al., 2019)] |
| Lep ^{+/-} rats and Lep ^{-/-} rats | HFD for 17 weeks | 0.5 mg/kg/day or 1 mg/kg/day by oral administration | 3 weeks | 1,000 µg/kg celastrol decreased the BW of Lep ^{+/-} rats not Lep ^{-/-} rats | Hu et al. (2020) |
| Lep ^{ob} mice | NCD for 6 or 14 weeks | 100 µg/kg/day by subcutaneous injection | 6 days | Promoted weight loss in young Lep ^{ob} mice not old Lep ^{ob} mice | Liu et al. (2015) |
| HSF1 ^{-/-} Mice | HFD for 4 weeks | 3 mg/kg/day mixed with powdered chow | 4 weeks | Had no effects on body weight and energy consumption | Ma et al. (2015) |
| Liver specific Sirt1 KO mice | HFD for 14 weeks | 200 µg/kg/every 2 days by i.p.injection | 4 weeks | Reduced food intake and increased the hepatic lipid accumulation by inhibited phosphorylation of AMPKα and hepatic LKB1 expression | Zhang et al. (2017a) |
| Nur77 ^{-/-} mice | HFD for 17 weeks | 0.1 mg/kg/day by i.p injection | 2 weeks | Mild reduced the body weight and anti-inflammation effects attenuated | Hu et al. (2017) |
| Global PTP1B KO mice | NCD or HFD for 10 weeks | 0.1 mg/kg/day by i.p injection | 7 days | Induced weight loss both in NCD and HFD PTP1B mice, reduction of fat and lean mass is owing to weight loss of HFD PTP1B mice not for NCD mice | Pfuhlmann et al. (2018) |
| UCP1 KO mice | HFD for 20 weeks | 100 µg/kg/day by subcutaneous injection | 6 days | Decreased body weight and food intake by fat mass loss | Pfuhlmann et al. (2018) |
| IL1R1 ^{-/-} mice | HFD for 20 weeks | 100 µg/kg/day by i.p. injection | 3 weeks | No change of body weight, fat mass, and food intake | Zhao et al. (2019a) |
| Lcn2 ^{-/-} mice | NCD or HFD for 16-20 weeks | 100 µg/kg/day by i.p. injection | 3 weeks | Reduced body weight and fat mass without affected food intake in NCD Lcn2 ^{-/-} mice, inhibited hepatosteatosis, and metabolic disorder induce by HFD in Lcn2 ^{-/-} mice | Feng et al. (2019a) |
| ApoE ^{-/-} mice | NCD or HFD for 12 weeks | 100 µg/kg/day by oral administration | 12 weeks | Alleviated inflammatory reaction in apoE ^{-/-} mice fed with HFD | Zhu Y. et al. (2021) |
| Melanocortin 4 receptor (MC4R)-null mice | NCD | 0.1 mg/kg/day by i.p injection for 10 days, then 0.5 mg/kg/day by i.p injection for 15 days | 25 days | Reduced body weight, food intake, fat and lean mass, enhanced energy expenditure by upregulation of adrenergic receptor and PRDM16 without affecting UCP-1 and PGC-1α | Saito et al. (2019) |
| HnRNPA1 deficiency/overexpression mice | NCD | 2 mg/kg/day by gavage administration | 12 days | Inhibited energy expenditure and abrogated weight loss effects in HnRNPA1 overexpression mice | Zhu C. et al. (2021) |
| Other model | | | | | |
| Young (4–6 month) and Old (18–22 month) male mice | NCD | 100–200 µg/kg/day by i.p. injection | 4–6 days | Promoted weight and lean mass loss by lowering food intake in aged mice, but not in young controls | Chellappa et al. (2019) |

HFE, high fat emulsion; NCD, normal chow diet; HFD, high fat diet; ABCA1, ATP-binding cassette transporter A1; NADPH, nicotinamide adenine dinucleotide phosphate; AMPK, Adenosine 5'-monophosphate (AMP)-activated protein kinase; SIRT1, sirtuin1; ER, endoplasmic reticulum; HSF1, heat shock factor 1; PGC-1α, Peroxisome proliferator-activated receptor γ coactivator 1α; Srebp-1c, sterol regulatory element binding protein-1c; IL-1β, interleukin-1β; IL-6, interleukin-6; TLR4, Toll-like receptor 4; NF-κB, nuclear factor kappa-B; STAT3, signal transducer and activator of transcription 3; LCN2, lipocalin-2; PTP1B, protein tyrosine phosphatase (PTP) 1B; TCTP, T-cell PTP; TLR3, Toll-like receptor 3; NLRP3, NOD-like receptor protein 3; CD36, cluster of differentiation 36; FATP2, very-long-chain acyl-CoA, synthetase; FATP4, fatty acid transport protein 4; MMP-2, Matrix metalloproteinase-2; MMP-9, Matrix metalloproteinase-9; CAP1, adenylate cyclase-associated protein 1; PKA, Protein kinase A; NF-κB, nuclear factor kappa B; Nrf2, nuclear respiratory factor 1; HO-1, Heme oxygenase 1; MAPK, mitogen-activated protein kinase; TNF-α, tumor necrosis factor α; iNOS, inducible nitric oxide synthase; Arg-1, arginase-1; IL-10, interleukin-10; Lep, leptin; BW, body weight; LKB1, liver kinase B1; PTP1B, Protein tyrosine phosphatase 1; ApoE, apolipoproteinE; PRDM16, PR, domain-containing 16; UCP-1, Uncoupling protein 1; HnRNPA1, heterogeneous nuclear ribonucleoprotein A1.

et al., 2019a; Feng et al., 2019b; Chellappa et al., 2019; Fang et al., 2019; Abu Bakar et al., 2020; Hu et al., 2020; Zhu C. et al., 2021; Zhu Y. et al., 2021; Hua et al., 2021; Ouyang et al., 2021; Yang et al., 2021).

As a typical feature of obesity, leptin resistance was involved in the hepatic steatosis during the development of MAFLD (Myers et al., 2010; Boutari and Mantzoros, 2020). Leptin, a hormone secreted by adipose tissue, directly interacted with the leptin receptor in the brain and mediated food intake, energy metabolism, body weight, and other physiological processes (Xu et al., 2018b; Caron et al., 2018; Pan and Myers, 2018). Brain leptin promoted hepatic lipid flux and reduced lipogenesis in the liver (Hackl et al., 2019). Celastrol as a leptin sensitizer exhibited significant weight loss and food consumption reduction in HFD-obesity animals (Wang et al., 2014; Liu et al., 2015; Ma et al., 2015; Zhang et al., 2017a; Hu et al., 2017; Luo et al., 2017; Kyriakou et al., 2018; Pfuhlmann et al., 2018; Zhang et al., 2018; Feng et al., 2019a; Zhao et al., 2019a; Feng et al., 2019b; Chellappa et al., 2019; Fang et al., 2019; Saito et al., 2019; Abu Bakar et al., 2020; Hu et al., 2020; Zhu C. et al., 2021; Zhu Y. et al., 2021; Hua et al., 2021; Ouyang et al., 2021; Yang et al., 2021) (**Table 1**).

Celastrol (100 µg/kg by intraperitoneally injection [i.p], or 10 mg/kg by oral administration [OA]) increased the leptin sensitivity to suppress food intake and reduce body weight in HFD induced C57BL/6J mice and was firstly reported in 2015 by Ozcan's group (Liu et al., 2015), while the benefits of celastrol on obesity were abrogated in lean mice, leptin receptor-deficient (*db/db*), or leptin-deficient (*ob/ob*) mice/rats (Liu et al., 2015; Pfuhlmann et al., 2018; Feng et al., 2019a; Feng et al., 2019b; Saito et al., 2019; Hu et al., 2020). Compared with leptin or celastrol alone, the combined use of leptin and celastrol could significantly inhibit appetite and weight gain of different mice, even for *ob/ob* mice (Liu et al., 2015). Numerous studies verified the effect of leptin sensitizer celastrol on appetite as showing in **Table 1**.

The underlying molecular mechanism of celastrol anti-obesity and increase the leptin sensitivity can be attributed to Sirtuin 1 (Sirt1) (Zhang et al., 2017a; Abu Bakar et al., 2020), interleukin-1 receptor 1 (IL1R1) (Feng et al., 2019b), protein tyrosine phosphatase (PTP) 1B (PTP1B), and T-cell PTP (TCPTP) (Kyriakou et al., 2018). SIRT1 as a deacetylase activated by energy deprivation was involved in glucose, lipid, and bile acid metabolism regulation (Purushotham et al., 2009; García-Rodríguez et al., 2014). It has been reported that celastrol exacerbated liver metabolic disorder by suppressing the phosphorylation of AMP-activated protein kinase α (AMPK α) in liver specific Sirt1 knock out mice fed with HFD (Zhang et al., 2017a). In line with that, celastrol (3 mg/kg/day for 8 weeks) significantly increased insulin sensitivity and weight loss through enhancing AMPK/SIRT1 signaling in HFD-induced rats (Abu Bakar et al., 2020). IL1R1, a cytokine receptor, was associated with cell death and inflammation. IL1R1 deficient mice showed the phenotype of mature-onset obesity and leptin resistance (García et al., 2006). Feng and his colleagues demonstrated that the protective property of celastrol on obesity reversed by IL1R1 deficiency, which indicated that IL1R1 is essential for celastrol to reduce food consumption and body weight, alleviate glucose

intolerance and insulin tolerance, as well as hepatic steatosis in HFD mice (Feng et al., 2019). However, these studies were only performed in genetic deficient animals, and whether the hepatoprotective effects of celastrol depended on its direct interaction with Sirt1 or IL1R1 need further studies. The surface plasmon resonance (SPR) assay, circular dichroism (CD) spectroscopy, and other methods might be effective methods to verify the above hypothesis. PTP1B and TCPTP negatively regulate leptin signaling in the hypothalamus (Dodd et al., 2019). Eleni et al. demonstrated that celastrol-induced weight loss was attributed to the suppression of PTP1B and TCPTP, and inhibition of PTP1B and TCPTP is mediated by reversible noncompetitive binding to an allosteric pocket close to the active site (Kyriakou et al., 2018). In addition, different studies demonstrated the anti-obesity effect of celastrol was independent on melanocortin 4 receptor (MC4R), and lipocalin 2 (Lcn2) (Feng et al., 2019a; Saito et al., 2019), because the deletion of these genes did not weaken the weight-loss and liver-protecting effect of celastrol in mice.

Obesity related MAFLD was triggered by energy imbalance, with features of excessive lipid deposition. Peroxisome proliferator-activated receptor γ coactivator 1 α (PGC-1 α), a nuclear transcriptional coactivator factor, increased energy expenditure by regulating mitochondrial function and biogenesis (Vega et al., 2000; Rodgers et al., 2005; Minsky and Roeder, 2015). Liver-specific deficient PGC-1 α mice exhibit hepatic steatosis (Rodgers et al., 2005). Accumulating evidences uncovered that celastrol promotes the white adipose tissue (iWAT) browning and brown adipose tissue (BAT) activation by upregulating PGC-1 α and uncoupling protein 1 (UCP1, a downstream effector of PGC-1 α , is responsible for electron transport of mitochondrial oxidative phosphorylation) expression (**Table 2**). A total of 3 mg/kg/day celastrol (OA) significantly increased the HSF1 (Heat Shock Transcription Factor 1)/PGC-1 α axis activity and protected against obesity in HFD mice by increasing energy expenditure, including iWAT browning, BAT activation, and mitochondrial gene transcription, while such benefit was abrogated by HSF1 depletion (Ma et al., 2015). In agreement with this result, several reports also clarified that celastrol increased the energy expenditure by activating iWAT browning through upregulation of PGC-1 α and UCP1 (Fang et al., 2019; Yang et al., 2021). However, these studies were challenged by Katrin's group, and they showed that celastrol intervention only upregulated the UCP1, while the expression of PGC-1 α in BAT of HFD mice was not altered, and UCP1 deletion in HFD mice did not abolish food consumption and body weight reduction effects of celastrol (Pfuhlmann et al., 2018). This indicated that weight loss effect of celastrol was not dependent on UCP1-mediated thermogenesis under nutrient stress. In accordance with Katrin's study, other researchers did not observe that the upregulation of UCP1 and PGC-1 α expression in iWAT and BAT of HFD induced mice and rats with celastrol administration (Saito et al., 2019; Hu et al., 2020; Hua et al., 2021). The disparity of above observations of celastrol's hepatoprotective effects might be caused by different celastrol-delivery way (OA vs. i.p), dosage, and intervention time period (**Table 2**). All above results indicated that iWAT browning

TABLE 2 | The regulation of celastrol on iWAT browning and BAT thermogenesis gene.

| Animal model | Model inducer | Dosage | Intervention time | Gene | | Reference |
|--------------------------|------------------------|---|-------------------|-------------|----------------|------------------------|
| | | | | UCP-1 | PGC-1 α | |
| Male Sprague–Dawley rats | HFD for 11 weeks | 0.5 mg/kg/day by oral administration | 3 weeks | no change | no change | Hu et al. (2020) |
| C57BL/6J | NCD or HFD for 9 weeks | 0.1 mg/kg/day or 0.5 mg/kg/day by i.p injection | 24 days | no change | no change | Saito et al. (2019) |
| | HFD for 6 weeks | 3 mg/kg/day celastrol was mixed with food | 24 days | no change | no change | Hua et al. (2021) |
| | HFD for 8 weeks | 1 mg/kg/day, 3 mg/kg/day mixed with food | 3 weeks | upregulated | upregulated | Ma et al. (2015) |
| | HFD for 12 weeks | 0.1 mg/kg/day, 0.3 mg/kg/day by i.p injection | 3 weeks | upregulated | upregulated | Yang et al. (2021) |
| | HFD for 16 weeks | 0.1 mg/kg/day by i.p injection | 21 days | upregulated | upregulated | Fang et al. (2019) |
| | HFD for 32 weeks | 0.1 mg/kg/day by i.p injection | 6 days | upregulated | no change | Pfuhmann et al. (2018) |
| MC4R-null mice | NCD | 0.1 mg/kg/d by i.p injection for 10 days, then 0.5 mg/kg/d by i.p injection for 15 days | 25 days | no change | no change | Saito et al. (2019) |
| HSF1 ^{-/-} mice | NCD for 8 weeks | 3 mg/kg/day mixed with food | 4 weeks | no change | no change | Ma et al. (2015) |

iWAT, inguinal white adipose tissue; BAT, brown adipose tissue; SD, Sprague–Dawley; UCP-1, Uncoupling protein 1; PGC-1 α , Peroxisome proliferator-activated receptor γ coactivator 1 α ; MC4R, melanocortin 4 receptor; HSF1, heat shock factor 1; NCD, normal chow diet; HFD, high fat diet.

happened at a specific time after celastrol treatment, and celastrol improved energy expenditure through other pathways not only depending on browning of iWAT.

Numerous studies proved that gut microbiota dysbiosis can also be attributed to fatty liver disease development (Le Roy et al., 2013; Canfora et al., 2019; Frazier and Chang, 2020). Oral administration of 500 μ g/kg/day celastrol markedly enhanced energy expenditure and enhanced liver lipid metabolism in HFD rats by improving the gut microbiota homeostasis and activating the hypothalamic leptin signaling pathway rather than affecting food intake (Hu et al., 2020). *Firmicutes* promoted lipid absorption not fatty acid oxidation (Murphy et al., 2013). Increased ratio of *Bacteroidetes* to *Firmicutes* played a critical role in improvement of lipid consumption in celastrol-treated HFD rats (Murphy et al., 2013). Consistent with this, oral administration of celastrol (3 mg/kg/d) inhibited intestinal lipid absorption to ameliorate metabolic disturbance by reconstructing the gut microbiota profile in HFD mice (Hua et al., 2021). Although it has been reported that celastrol improved lipid metabolism by modulating gut microbiota, its specific mechanism of gut microbiota involved in MAFLD still needs to be explored. In addition, recent study demonstrated that age-associated obesity mice injected with celastrol (100–200 μ g/kg) exhibited reduction body weight and fasting glucose level owing to fat loss and circadian rhythms restored without impact on lean mass (Chellappa et al., 2019), and whether gut microbiota act as an actuator of host circadian rhythms involved in the procedure remains to be studied (Frazier and Chang, 2020; Saran et al., 2020).

In summary, celastrol reduced body weight and hepatic fat accumulation mainly by increasing leptin sensitivity, enhancing energy metabolism, and modulating gut microbiota. Above all, Sirt1, IL1R1, PTP1B, and TCPTP might be the potential targets of celastrol, but whether celastrol directly interacted with these targets should be deeply explored. Moreover, the effect of celastrol on PGC-1 α and UCP1 is controversial, and further

studies should be performed to verify this effect. Gut microbiota have been extensively studied in recent years, but the molecular mechanism of celastrol on anti-obesity through gut microbiota is still unclear.

Anti-Inflammatory Response Activity

Macrophage infiltration and inflammation caused by dyslipidemia is associated with progression of MAFLD (Kazankov et al., 2019; Katsiki et al., 2016; Luo et al., 2018). Different animal experiments have elucidated that the inflammation in fatty liver mice treated with celastrol are remarkably attenuated (Table 1). Macrophage infiltration and inflammatory factors (IL-1 β , IL-18, MCP-1 α , and TNF- α) were reduced in liver of HFD induced C57BL/6J or C57BL/6N mice by celastrol treated for 3 weeks (Hu et al., 2017; Luo et al., 2017; Zhang et al., 2018; Ouyang et al., 2021; Zhu Y. et al., 2021). In addition, adipose tissue inflammation and mitochondrial dysfunction in skeletal muscle ameliorated in HFD-induced SD rats treated with 3 mg/kg/day celastrol for 8 weeks (Abu Bakar et al., 2020). The mechanism exhibited that celastrol can activate AMPK/SIRT1 signaling pathways for mitochondrial function improvement and attenuate inflammatory responses via decreasing nuclear factor kappa-B (NF- κ B) activity (Abu Bakar et al., 2020). Celastrol-mediated hepatoprotective effects in C57BL/6J mice fed with HFD abolished in liver specific Sirt1-deficient mice fed HFD (Zhang et al., 2017a). Celastrol directly interacted with adenylyl cyclase associated protein 1 (CAP1) in macrophages contributed to improvement of metabolism and attenuation of inflammatory response through NF- κ B signaling pathway in HFD-induced mice (Zhu Y. et al., 2021). Apart from that, LPS induced acute liver inflammation and HFD induced chronic inflammation are both inhibited by celastrol through binding Nur77 and promoting Nur77 interact with TRAF2 inducing autophagy (Hu et al., 2017). Deletion of Nur77 or Sirt1 impaired the anti-inflammation ability of celastrol, but LCN2 or ApoE deficiency did not influence the anti-

hepatosteatosis of celastrol (Hu et al., 2017; Zhang et al., 2017a; Feng et al., 2019b; Ouyang et al., 2021). In general, the protective effects of celastrol against inflammation might be attributed to suppression of NF- κ B involved signaling pathway.

In summary, different animal experiments confirmed that celastrol had metabolic improvement effect on HFD induced SD rats/mice or aged-obesity mice, but has no effect on gene deficiency mice such as HSF1 deletion mice, IL1R1 null mice, Sirt1 deficient mice, etc. (Ma et al., 2015; Zhang et al., 2017a; Feng et al., 2019b). This indicated that HSF1, IL1R1, and Sirt1 might act as the target of celastrol. In addition, oral administration of celastrol hardly affects food intake but has the same benefit on metabolic compared to intraperitoneal injection. Therefore, it is better to use oral administration to explore the pharmacological mechanism of celastrol. The effects of celastrol on MAFLD are summarized in **Figure 2**.

Celastrol and Liver Injury

Liver injury characterized by a loss of hepatocyte function in patients resulted from mitochondrial oxidative stress, endoplasmic reticulum stress, inflammation, and autophagy in hepatocyte (Vento and Cainelli, 2020). Drugs, infections, and intrahepatic cholestasis can all lead to liver injury (Fontana et al., 2014). Celastrol, an anti-inflammatory drug, ameliorated the damage in hepatocyte or liver injury (Abdelaziz et al., 2017; El-Tanbouly et al., 2017; Jannuzzi et al., 2018; Wu et al., 2018; Zhao et al., 2019b; Guo et al., 2019; Wang et al., 2020; Zhao et al., 2020; Yan et al., 2021) (**Table 3**).

As the number and variety of drug applications grow rapidly, drug-induced liver injury (DILI), especially acetaminophen (APAP) overdose, is becoming the most common cause of acute liver failure (ALF) in America and Europe (Shehu et al., 2017). A series of studies demonstrated that pretreatment with celastrol attenuated the APAP-induced oxidative stress and inflammation by raising antioxidant enzyme activities such as glutathione peroxidase (GPx), glutathione reductase (GR), catalase, and superoxide dismutase (SOD) activities both *in vitro* and *in vivo* (Abdelaziz et al., 2017; Jannuzzi et al., 2018). CCl₄ as another hepatotoxic chemical could induce liver injury by inflammatory activation and antioxidant enzymes inhibition (Zhang et al., 2017b). Celastrol might also suppress inflammation in CCl₄ induced liver injury rat by activating AMPK-SIRT3 signaling (Wang et al., 2020). In the latest research, Li and his colleagues found that celastrol could eliminate oxidative stress and reduce the release of proinflammatory cytokines by activating PPAR α signaling pathway in CCl₄ intoxicant mice (Zhao et al., 2020). However, celastrol itself as a drug also has toxicity, the balance between the liver protection and liver injury needs to be further studied, and new structure modification and formulation should be developed to reduce toxicity and enhance efficacy.

Cholestasis is a pathophysiological process caused by bile secretion and excretion disorders. It is manifested as excessive accumulation of bile components such as bile acid, cholesterol, and bilirubin in the liver and systemic circulation, causing damage to liver cells and whole body. Long-term continuous cholestasis will progress to liver fibrosis and even cirrhosis

(Zollner and Trauner, 2008; Padda et al., 2011). Li and his colleagues demonstrated that celastrol ameliorated cholestatic liver injury induced by α -naphthyl isothiocyanate (ANIT) and thioacetamide (TAA) through activation of SIRT1-FXR signaling pathway, while the hepatoprotective effects of celastrol were abrogated in FXR deficiency or SIRT1 inhibition mice (Zhao et al., 2019b). In addition to that, 5 mg/kg/day celastrol remarkably alleviated intrahepatic cholestasis of pregnancy via downregulating matrix metalloproteinase (MMP-2 and MMP-9) and total bile acid in pregnant rats (Guo et al., 2019).

Sepsis is a serious clinical syndrome caused by many organisms including bacteria, viruses, and fungi, which might lead to liver injury (Strnad et al., 2017). Cecal ligation and puncture (CLP) model and lipopolysaccharide (LPS) inducement is often used to mimics sepsis (Zhang et al., 2014; Xiong et al., 2017; Li et al., 2020). Celastrol attenuated CLP induced hepatic dysfunction in rats by inhibiting toll-like receptor-4 (TLR-4)/NF- κ B (El-Tanbouly et al., 2017). In addition, celastrol pretreatment was found to attenuate propionibacterium acnes/lipopolysaccharides induced liver damage via NLRP3 inflammasome suppression and inflammatory inhibition (Yan et al., 2021). On the contrary, celastrol aggravated liver injury by exacerbation of inflammatory and elevation of oxidative stress in LPS intoxicant mice (Wu et al., 2018). The contradictory results were attributed to the different dosage of LPS and celastrol, and it is hard for high dosage of celastrol to reverse the severe liver failure that resulted from high dose of LPS, and the toxicity of celastrol should be taken into consideration in treating sepsis.

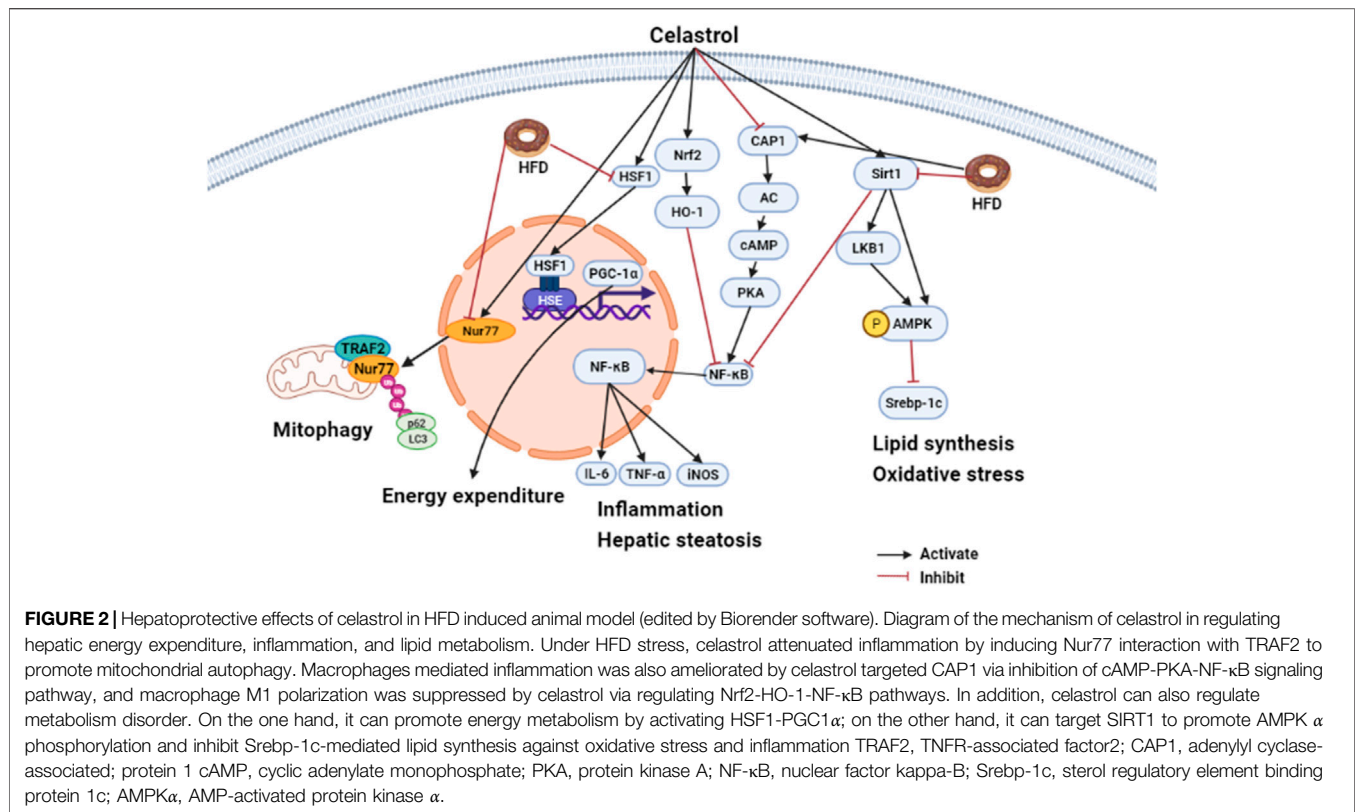
In short, these data suggested that celastrol is a potential candidate for treatment of hepatic injury, mainly owing to its ability to inhibit inflammation and oxidative stress and recover bile acid homeostasis. While protecting the liver injury, the toxicity of celastrol should be also taken into consideration to avoid side effects.

Celastrol and Liver Cancer

Hepatocellular carcinoma (HCC) as one highly malignant cancer remains a global menace. Effective systemic treatment of HCC is impeded by its complicated molecular pathogenesis, high rate of metastasis, recurrence, and chemo-resistance. It is imperative to explore effective therapy strategies for liver cancer. Natural medicine with long history of clinical use exhibited great potential in anti-cancer due to its high efficiency and availability, as well as low side effects (Hu et al., 2013). Numerous studies have shown that celastrol exerts anticancer effects by inhibiting their proliferation, metastasis, and inflammatory properties depending on modulating a variety of signaling pathways (Kashyap et al., 2018).

Anti-Proliferation and Pro-Apoptotic Effects *In Vitro*

Celastrol arrested cell cycle and promoted apoptosis through suppression of STAT3/JAK2 signaling, PI3 K/Akt signaling, and ER-stress/UPR signaling in different hepatocellular cell lines (**Table 4**) (Chen et al., 2011; Rajendran et al., 2012; Li et al., 2013; Wei et al., 2014; Li et al., 2015; Ma et al., 2017; Ren et al., 2017; Du et al., 2020; Kun-Ming et al., 2020). In addition,



celastrol inhibited hepatoma cell line growth and proliferation via arresting cell cycle in sub-G1 (Rajendran et al., 2012) and G2/M phase (Chen et al., 2011; Ren et al., 2017). Further studies showed that celastrol reduced the expression of c-myc and cyclin D1 which was closely related to cell cycle arrest of tumor cells *in vivo* on a time- and dose-dependent manner (Rajendran et al., 2012; Ma et al., 2017). Mechanistic studies revealed that celastrol could impede liver cancer through downregulation of HSP90 proteins, activation of c-Jun NH2 terminal kinase (JNK), and weakened MRC complex I activity (Chen et al., 2011). Apart from that, celastrol could also inhibit the migration, invasion, and metastasis of liver cancer by inhibiting the ROCK2-mediated phosphorylation of ezrin at Thr567 (Du et al., 2020), suppressing NF-κB and Akt activity, and downregulating miR-224, MMP-2, and MMP-9 (Li et al., 2013).

Tumor Suppression Effects *In Vivo*

As show in **Table 5** (Chen et al., 2011; Rajendran et al., 2012; Wei et al., 2014; Chang et al., 2016; Kun-Ming et al., 2020; Saber et al., 2020; Si et al., 2021), studies have manifested that celastrol exhibits anticancer activity against a variety of liver cancer animal models such as HCC patient-derived xenografts BALB/cJ mice (Wei et al., 2014), different hepatocellular carcinoma cells derived xenografts mouse models (Rajendran et al., 2012; Ma et al., 2014; Ren et al., 2017; Si et al., 2021), and DEN induced HCC rats/mice (Chang et al., 2016; Saber et al., 2020) with dosage of 1–10 mg/kg for 3–10 weeks. Celastrol (4 mg/kg) prevented tumor proliferation and increased apoptosis via inhibition of

STAT3/JAK2 signaling pathway in PLC/PRF5 cells derived xenografts HCC mice (Rajendran et al., 2012). Recently, different studies validated that inhibition of circ_SLIT3/miR-223-3p/CXCR4 signaling is involved in the anti-HCC activity of celastrol both *in vitro* and *in vivo* (Kun-Ming et al., 2020; Si et al., 2021). Meanwhile, celastrol has been demonstrated to decrease the hepatic lesions and elevation of serum alanine aminotransferase (ALT), glutamic oxalacetic transaminase (AST), alkaline phosphatase (ALP), and alpha fetoprotein (AFP) in diethylnitrosamine (DEN)-induced hepatocellular carcinoma (HCC) rats, due to activation of mitochondrial apoptosis induced by p53 (Chang et al., 2016; Saber et al., 2020). Consistent with this, combination therapy with celastrol (2 mg/kg) and metformin (200 mg/kg) not only attenuated hepatic injury with elevated liver enzymes but also decreased NLRP3 mediated NF-κB signaling to suppress anti-apoptotic processes in mice with DEN-induced HCC (Saber et al., 2020). Meanwhile, Jiang and his colleagues found that synergistic use of celastrol and PHA665752 (a c-Met inhibitor) significantly inhibited cell growth, migration in c-met deficient Huh7 cells, and Huh7 xenografts nude mice (Jiang et al., 2013). Besides that, celastrol could enhance the activity of anti-liver cancer drugs including sorafenib, lapatinib, and ABT-737 by cell growth inhibition and apoptosis induction (Zhu et al., 2012; Yan et al., 2014; Zhang et al., 2019). These results indicated that celastrol not only has good efficiency on killing cancer cells but also can improve the anti-cancer ability of first-line drugs for tumor therapy.

TABLE 3 | Pharmacological activities of celastrol in the treatment of liver injury.

| Model style | Cell/animal | Inducer | Dosage of celastrol | Treatment time | Phenotype/mechanism | Reference |
|--------------------------------|---|----------------------|--|--|---|---------------------------|
| Chemicals induced liver injury | HepG2 cells | APAP | 50, 100, and 200 nM | 24 h | Ameliorated oxidative stress and cytotoxicity caused by APAP | Jannuzzi et al. (2018) |
| Chemicals induced liver injury | Male BALB/c mice | APAP | 2 mg/kg by i.p injection | 2 h prior APAP-induction | Prevented oxidative stress and inflammation by attenuating inflammatory cells accumulation and reducing inflammation factors | Abdelaziz et al. (2017) |
| Chemicals induced liver injury | Male WT mice and Ppara ^{-/-} mice on the 129/Sv genetic background | CCl ₄ | 10 mg/kg by oral treatment | 5 days | Inhibited inflammatory cytokine and oxidative stress by suppressing PPAR α signaling pathway, the effects of celastrol attenuated DCA-EGR1-inflammatory factor signaling in CCl ₄ -induced PPAR α deleted mice | Zhao et al. (2020) |
| Chemicals induced liver injury | Male Sprague Dawley rats | CCl ₄ | 0.25 mg/kg/day, 0.5 mg/kg/day, 1 mg/kg/day by i.p injection | 4 weeks | Suppressed inflammation in liver fibrosis by activating AMPK-SIRT3 signaling | Wang et al. (2020) |
| Cholestatic liver injury | Male C57BL/6J mice | ANIT | 10 mg/kg/day by oral administration | 5 days | Alleviated cholestatic liver injury by activation SIRT1-FXR signaling pathway | Zhao et al. (2019b) |
| | Male C57BL/6J mice and Fxr-null mice | TAA | | | FXR disruption attenuated protection effects of celastrol on cholestatic liver injury | |
| Cholestatic liver injury | Female Sprague-Dawley rats | EE | 5 mg/kg/day by an oral administration | 5 days | Alleviated phenotype of ICP by inhibited MMP-2 and MMP-9 | Guo et al. (2019) |
| Sepsis induced liver injury | Male Sprague Dawley rats | CLP | 1 mg/kg by i.p injection | 60 min before CLP | Attenuated inflammation by suppressing NF- κ B, reduced TLR-4 and 5-LOX expression, downregulated the expression of IL-6 | El-Tanbouly et al. (2017) |
| Sepsis induced liver injury | Male C57BL/6 mice | LPS | 1.5 mg/kg/day by i.p injection | 24 h before LPS induction, after LPS intoxicant for another 24 h | Aggravated liver injury through activating inflammation and deteriorating oxidative stress | Wu et al. (2018) |
| Sepsis induced liver injury | Male C57BL/6J mice and NLRP3 ^{-/-} mice | <i>P. acnes</i> /LPS | 0.5 or 0.25 mg/kg by i.p injection on every other day after <i>P. acnes</i> induction for 3 days | 3 days | Suppressed NLRP3 inflammasome formation by blocking deubiquitylation of NLRP3 | Yan et al. (2021) |

APAP, acetaminophen; CCl₄, carbon tetrachloride; AMPK, Adenosine 5'-monophosphate (AMP)-activated protein kinase; SIRT3, sirtuin3; PPAR α , Peroxisome Proliferator Activated Receptor α ; DCA, deoxycholic acid; EGR1, Early Growth Response 1; ANIT, α -naphthyl isothio-cyanate; TAA, thioacetamide; SIRT1, sirtuin1; FXR, Farnesoid X receptor; EE, 17 β -estradiol; ICP, intrahepatic cholestasis of pregnancy; MMP-2, Matrix metalloproteinase-2; MMP-9, Matrix metalloproteinase-9; CLP, cecal ligation and puncture; NF- κ B, nuclear factor kappa-B; TLR4, Toll-like receptor 4; 5-LOX, 5-Lipoxygenase; IL-6, Interleukin-6; LPS, lipopolysaccharides; *P. acnes*/LPS, *Propionibacterium acnes*/lipopolysaccharides; NLRP3, NOD-like receptor protein 3.

The Role of Hypoxia-Inducible Factor in Anti-Tumor Activity of Celastrol

Hypoxia was one of most important regulators in liver cancer progression. Hypoxia-inducible factor (HIF-1), a nuclear transcription factor, might be activated under hypoxia and specifically regulated oxygen and metabolic homeostasis (Balamurugan, 2016). HIF-1/2 α protein is highly expressed in human HCC tissues, and correlates with tumor invasion and metastasis in HCC patients (Bangoura et al., 2004; Wong et al., 2014). In addition to antiproliferative and proapoptotic effects, celastrol repressed tumor growth, angiogenesis, invasion, and metastasis through reduced hypoxia-induced accumulation of HIF-1 α protein (Ma et al., 2014). Ma et al. demonstrated that celastrol inhibited the hypoxia-induced accumulation of HIF-1 α protein due to the downregulation of mTOR/p70S6K/EIF4E and

ERK1/2 phosphorylation in Hep3B cells derived xenografts nude female mice, and the expression of angiogenesis related factors-vascular endothelial growth factor (VEGF) and erythropoietin (EPO) are both prevented (Ma et al., 2014). However, this result was challenged by Han and his co-workers, who found that celastrol promoted HIF-1 α protein accumulation by inducing ROS and activating Akt/p70S6K signaling in HepG2 cells under hypoxia, and celastrol suppressed cancer cell growth by promoting mitochondrial autophagy and apoptosis *in vitro* (Han et al., 2014). The difference in hypoxia exposure time (16 h in Han et al.'s work vs. 6 h in Ma et al.'s study) of HepG2 cells might contribute to the discrepant results on HIF-1 α expression for celastrol in the above studies.

Summarily, celastrol might be a potential therapeutic candidate for the treatment of liver cancer due to reduction of the oxidative

TABLE 4 | Anti-cancer effects of celastrol *in vitro*.

| Cell line | Effect of celastrol | Mechanism | Doses | Time | Reference |
|-----------------|--|---|---------------------------------|------------------|--|
| HepG2, Bel-7402 | Anti-proliferation, induce apoptosis | Downregulated the expression of E2F1 | 2.5 and 5 μ M | 24 h, 48 h | Ma et al. (2017) |
| HepG2, Bel-7402 | Anti-proliferation, induce apoptosis | Induced autophagy and ER stress, lead to G2/M phase arrested | 1.25, 2.5, and 5 μ M | 24 h | Ren et al. (2017) |
| Bel-7402 | Anti-proliferation, induce apoptosis | Promoted cytochrome c release, increase the expression of cleaved caspase-9, caspase 3 and the ratio of Bax/Bcl-2 | 0.78, 1.56, and 3.12 μ g/ml | 24, 48, and 72 h | Li et al. (2015) |
| HepG2 | Anti-proliferation, anti-migration | Inhibited the CXCR4 mediated PI3K/Akt pathway, lead to sub-G0 phase arrested | 0.1, 0.3, 0.625, and 1 μ M | 24 h | Kun-Ming et al. (2020) |
| HepG2 | Anti-proliferation, induce apoptosis | Induced ROS accumulation and G2-M phase blockage | 2, 4, and 6 μ M | 24 h | Chen et al. (2011) |
| HepG2 | Anti-metastasis | Repressed NF- κ B and Akt activity, downregulate the expression of miR-224, MMP2, and MMP9 | 0.1, 0.5, 1 μ M | 18 h | Li et al. (2013) |
| Huh7, Hep3B | Anti-proliferation, Anti-migration, Anti-invasion and Enhanced Apoptosis | Repressed circ_SLIT3 and Bcl-2, raised the Bax expression, impeded circ_SLIT3/miR-223-3p/CXCR4 signaling | 0.5, 1 μ M | 48 h | (Si et al., 2013; Kun-Ming et al., 2020) |
| C3A | Anti-proliferation, induce apoptosis, anti-metastasis | Modulated STAT3 activation with the inhibition of c-Src, JAK1, and JAK2 activation; downregulate the expression of cyclin D1, Bcl-2, Bcl-xL, survivin, Mcl-1, and VEG, caused sub-G1 phase arrested | 2.5, 5, and 10 μ M | 24, 48, and 72 h | Rajendran et al. (2012) |
| MHCC97H | Anti-migration | Inhibited the ROCK2 mediated phosphorylation of ezrin at Thr567 | 0.5 μ M | 4 and 8 h | Du et al. (2020) |

E2F1, E2F transcription factor 1; *ER*, endoplasmic reticulum; *Bcl-2*, B-cell lymphoma-2; *Bax*, BCL2-Associated X; *CXCR4*, C-X-C motif chemokine receptor 4; *PI3K*, phosphatidylinositol-3-kinase; *AKT*, protein kinase B; *ROS*, reactive oxygen species; *NF- κ B*, nuclear factor kappa B; *MMP2*, Matrix metalloproteinase 2; *MMP9*, Matrix metalloproteinase 9; *circ_SLIT3*, circRNA, slit guidance ligand 3; *JAK1*, Janus kinase1; *JAK2*, Janus kinase2; *Mcl-1*, Myeloid Cell Leukemia Sequence 1; *VEGF*, vascular endothelial growth factor; *ROCK2*, Rho Associated Coiled-Coil Containing Protein kinase 2.

TABLE 5 | The anti-tumor effects of celastrol *in vivo*.

| Cancer model (animal) | Dose and formulation | Treatment period | Tumor volume | Mechanism | Reference |
|---|--|------------------|---------------------|--|--|
| HCC patient-derived xenografts (BALB/cJ mice) | 4 mg/kg/day by intravenous injection | 3 weeks | Reduce 2–5 fold | Pro-apoptosis, anti-proliferation through inhibited phosphorylation of protein kinases in the Raf/MEK/ERK and PI3K/AKT/mTOR signaling pathways | Wei et al. (2014) |
| H22 cells derived xenografts (female BALB/c mice) | 1 and 2 mg/kg/day by i.p injection | 3 weeks | Reduce 2–4 fold | Induced of ER stress and apoptosis | Ren et al. (2017) |
| Hep3B cells derived xenografts (athymic nu/nu female mice) | 3 and 10 mg/kg/day by oral administration three times a week | 5 weeks | Reduce 2–2.5 fold | Reduced the hypoxia-induced accumulation of HIF-1 α protein, inhibited angiogenesis, invasion, and metastasis | Ma et al. (2014) |
| PLC/PRF5 cells derived xenografts (athymic nu/nu female mice) | 1 and 2 mg/kg/day by i.p injection | 3 weeks | Reduce 1.5–2.5 fold | Antiproliferative and proapoptotic effects through suppression of STAT3 signaling | Rajendran et al. (2012) |
| Hep3B cells derived xenografts (athymic nu/nu female mice) | 2 mg/kg/day by i.p injection every 5 days | 30 days | Reduce 2–2.5 fold | Inhibited circ_SLIT3/miR-223-3p/CXCR4 signaling | Si et al. (2021) |
| DEN induced HCC in rats | 2, 4, and 8 mg/kg/day by oral administration | 10 weeks | Reduce 1.5–3 fold | Activated mitochondrial apoptosis pathway | (Chang et al., 2016; Saber et al., 2020) |

i.p., intraperitoneal; *Raf*, rapidly accelerated fibrosarcoma; *ERK*, Extracellular-signal-regulated kinases; *MEK*, Mitogen-activated protein kinase/ERK kinase; *PI3K*, phosphatidylinositol-3-kinase; *AKT*, protein kinase B; *mTOR*, mammalian target of rapamycin; *STAT3*, signal transducer and activator of transcription 3; *HIF-1 α* , hypoxia-inducible factor, *circ_SLIT3*, circRNA slit guidance ligand 3; *CXCR4*, C-X-C motif chemokine receptor.

stress, inhibition of inflammatory response, and activation of mitochondrial autophagy. Although the studies were performed both *in vitro* and *in vivo*, the clinical research still should be performed to evaluate whether celastrol could apply as effective drug or adjuvant drug to further improve clinical outcomes. The mechanisms of celastrol on anti-cancer are summarized in **Figure 3**.

LIMITATIONS AND STRATEGIES FOR THE USE OF CELASTROL

Although celastrol exhibited many benefits on various liver diseases, the shortcomings of celastrol limited its clinical transformation. On the one hand, the poor water solubility of

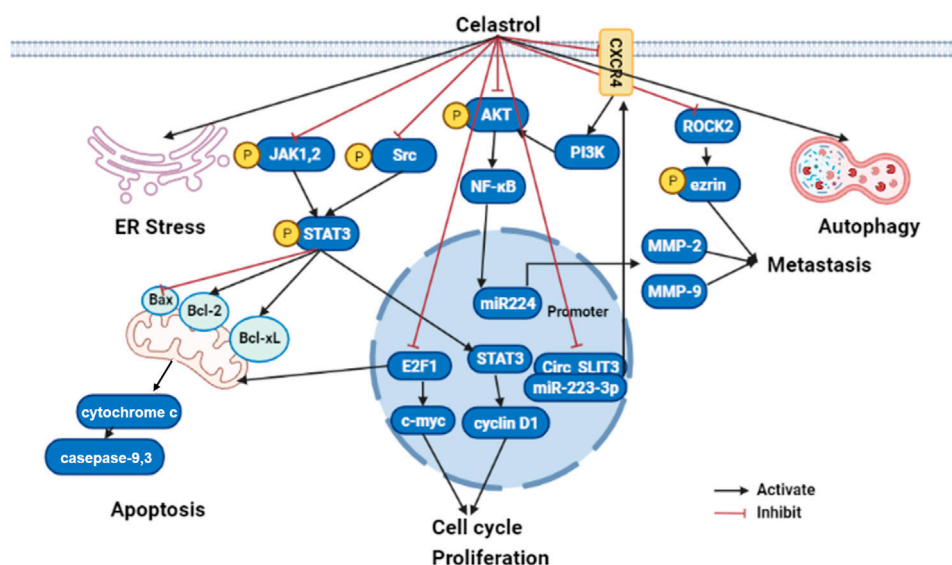


FIGURE 3 | The molecular mechanisms of celastrol in liver cancer (edited by Biorender software). Celastrol exert anticancer effect by restraining their cell growth, metastasis, and inflammatory response, while boosting ER stress, apoptosis, and autophagy depending on modulated different signaling pathways. Firstly, celastrol can activate cancer cell apoptosis through inhibiting JAK2 and STAT3 phosphorylation, then downregulated BCL-2 family proteins (Bcl-2 and Bcl-xL) and upregulated caspase family proteins (caspase 3 and caspase 9). Secondly, celastrol repressed tumor cell proliferation by suppressing cyclin D1 and c-myc through E2F1 and STAT3; Lastly, celastrol prohibited tumor metastasis by NF-κB signaling pathway modulated MMP-2 and MMP-9 through the CXCR4-related signaling pathway, as well as the ROCK2-mediated phosphorylation of ezrin at Thr567. ER, endoplasmic reticulum; JAK1, Janus kinase1; JAK2, Janus kinase2; STAT3, signal transducer and activator of transcription 3; Bcl-2, B-cell lymphoma-2; PI3K, phosphatidylinositol-3-kinase; AKT, protein kinase B; NF-κB, nuclear factor kappa B; MMP2, Matrix metalloproteinase 2; MMP9, Matrix metalloproteinase 9; circ_SLIT3, circRNA slit guidance ligand 3; ROCK2, Rho Associated Coiled-Coil Containing Protein kinase 2.

celastrol ($13.25 \pm 0.83 \mu\text{g/ml}$ at 37°C) results in low oral bioavailability (17.06% in rat) (Qi et al., 2014), and more researches should be conducted on improving its water solubility and oral bioavailability. On the other hand, the side effects of celastrol and narrow therapeutic window of dose also could be a big problem for its clinical use. While 0.25 mg or 0.5 mg/kg/d, celastrol (i.p.) attenuated the LPS induced inflammation (Yan et al., 2021), 1.5 mg/kg/d, celastrol (i.p.) (Wu et al., 2018) aggravated the liver injury induced by celastrol. Beyond that, it was insufficient for CYP450s to metabolize celastrol, which led to the hepatotoxicity. In addition to damaging the liver, celastrol also has side effects on kidney (Wu et al., 2018), cardiovascular system, and hematopoietic system (Zhang et al., 2012). New modification and formulation are urgently needed to overcome the shortcomings and improve its efficacy.

Hopefully, new approaches have been reported to improve the water solubility and bioavailability of celastrol. Lipid-based nanocarriers (including the self-microemulsifying drug delivery system [SMEDDS] [Chen et al., 2012], nanostructured lipid carrier [NLC], and phytosomes) (Freag et al., 2018), polymer-based nanocarriers like PEG-PCL (poly(ethylene glycol)-poly(ϵ -caprolactone) copolymers) nanoparticles (Zhao et al., 2019a), and galactosylated liposomes (Chen et al., 2020b) markedly enhanced the water solubility and oral bioavailability of celastrol. Combination with other drugs can be an effective approach to reduce the toxicity and enhance the efficacy of celastrol. Currently, celastrol combined with chemotherapeutic agents,

tumor necrosis factor superfamily, active ingredients of TCM, ionizing radiation, nucleic acid, and other therapies have been applied to the treatment of various cancers *in vitro* (Shi et al., 2020). The combined therapy reduced the dosage of celastrol and the related adverse effect, while the efficacy of celastrol improved. In addition, structural modifications will be a promising way to reduce the toxicity and improve the water bioavailability of celastrol, and the correlation between structure and toxicity have been well studied (Hou et al., 2020). Chemical modifications of celastrol mainly focused on the A/B ring and C-20 carboxyl group. In addition to chemical modifications, Chang et al. demonstrated that the glycosylation of celastrol formed by biotransformation showed over 53-fold higher water solubility and exhibited 50-fold less toxicity than celastrol *in vivo* (Chang et al., 2021), which indicated that biotransformation or biosynthesis might be a useful strategy for the clinical use of celastrol.

CONCLUSION AND PERSPECTIVES

A large number of studies have shown that celastrol might be a potential drug for different liver diseases treatment. In this review, we summarized the recent studies about the protective effects and mechanisms of celastrol in several liver diseases, including MAFLD, and it caused liver injury, or liver cancer. The liver protection effect could be attributed to modulating metabolic balance, inhibiting inflammatory response, and activating autophagy by altering different cellular pathways (Tables 1–5).

Although many researchers elucidated the molecular mechanisms of celastrol in liver diseases, the direct targets of celastrol are unknown. The SPR assay, affinity chromatographic methods, and other methods might be used to explore the direct interaction between celastrol and the potential targets. At the same time, with the development of omics, celastrol regulates gut microbes and liver metabolism to exert hepatoprotective effects required further investigated.

Moreover, although accumulating evidence demonstrated that celastrol grants tremendous potential in liver diseases at cellular or animal levels, the clinical studies of celastrol in liver diseases are very rare. Comprehensive studies on efficacy, safety, and toxicity in humans urgently need to be carried out. Besides, the poor water solubility, low bioavailability, and narrow therapeutic window of dose also limited the clinical application of celastrol. New modifications and formulations are needed to overcome the shortcomings and improve its efficacy. It is foreseeable that celastrol and its derivatives will be a promising drug for the treatment of liver diseases.

REFERENCES

- Abdelaziz, H. A., Shaker, M. E., Hamed, M. F., and Gameil, N. M. (2017). Repression of Acetaminophen-Induced Hepatotoxicity by a Combination of Celastrol and Brilliant Blue G. *Toxicol. Lett.* 275, 6–18. doi:10.1016/j.toxlet.2017.04.012
- Abu Bakar, M. H., Shariff, K. A., Tan, J. S., and Lee, L. K. (2020). Celastrol Attenuates Inflammatory Responses in Adipose Tissues and Improves Skeletal Muscle Mitochondrial Functions in High Fat Diet-Induced Obese Rats via Upregulation of AMPK/SIRT1 Signaling Pathways. *Eur. J. Pharmacol.* 883, 173371. doi:10.1016/j.ejphar.2020.173371
- Almazroo, O. A., Miah, M. K., and Venkataramanan, R. (2017). Drug Metabolism in the Liver. *Clin. Liver Dis.* 21, 1–20. doi:10.1016/j.cld.2016.08.001
- Bagherniya, M., Nobili, V., Blesso, C. N., and Sahebkar, A. (2018). Medicinal Plants and Bioactive Natural Compounds in the Treatment of Non-alcoholic Fatty Liver Disease: A Clinical Review. *Pharmacol. Res.* 130, 213–240. doi:10.1016/j.phrs.2017.12.020
- Balamurugan, K. (2016). HIF-1 at the Crossroads of Hypoxia, Inflammation, and Cancer. *Int. J. Cancer* 138, 1058–1066. doi:10.1002/ijc.29519
- Bangoura, G., Yang, L. Y., Huang, G. W., and Wang, W. (2004). Expression of HIF-2 α /EPAS1 in Hepatocellular Carcinoma. *World J. Gastroenterol.* 10, 525–530. doi:10.3748/wjg.v10.i4.525
- Boutari, C., and Mantzoros, C. S. (2020). Adiponectin and Leptin in the Diagnosis and Therapy of NAFLD. *Metabolism* 103, 154028. doi:10.1016/j.metabol.2019.154028
- Canfora, E. E., Meex, R. C. R., Venema, K., and Blaak, E. E. (2019). Gut Microbial Metabolites in Obesity, NAFLD and T2DM. *Nat. Rev. Endocrinol.* 15 (5), 261–273. doi:10.1038/s41574-019-0156-z
- Caron, A., Lee, S., Elmquist, J. K., and Gautron, L. (2018). Leptin and Brain-Adipose Crosstalks. *Nat. Rev. Neurosci.* 19, 153–165. doi:10.1038/nrn.2018.7
- Caussy, C., and Loomba, R. (2018). Gut Microbiome, Microbial Metabolites and the Development of NAFLD. *Nat. Rev. Gastroenterol. Hepatol.* 15, 719–720. doi:10.1038/s41575-018-0058-x
- Chang, T. S., Wang, T. Y., Chiang, C. M., Lin, Y. J., Chen, H. L., Wu, Y. W., et al. (2021). Biotransformation of Celastrol to a Novel, Well-Soluble, Low-Toxic and Anti-oxidative Celastrol-29-O- β -Glucoside by Bacillus Glycosyltransferases. *J. Biosci. Bioeng.* 131, 176–182. doi:10.1016/j.jbiosc.2020.09.017
- Chang, W., He, W., Li, P. P., Song, S. S., Yuan, P. F., Lu, J. T., et al. (2016). Protective Effects of Celastrol on Diethylnitrosamine-Induced Hepatocellular Carcinoma in Rats and its Mechanisms. *Eur. J. Pharmacol.* 784, 173–180. doi:10.1016/j.ejphar.2016.04.045
- Chellappa, K., Perron, I. J., Naidoo, N., and Baur, J. A. (2019). The Leptin Sensitizer Celastrol Reduces Age-Associated Obesity and Modulates Behavioral Rhythms. *Aging cell* 18, e12874. doi:10.1111/acer.12874
- Chen, G., Zhang, X., Zhao, M., Wang, Y., Cheng, X., Wang, D., et al. (2011). Celastrol Targets Mitochondrial Respiratory Chain Complex I to Induce Reactive Oxygen Species-dependent Cytotoxicity in Tumor Cells. *BMC cancer* 11, 170. doi:10.1186/1471-2407-11-170
- Chen, X., Hu, X., Hu, J., Qiu, Z., Yuan, M., and Zheng, G. (2020). Celastrol-Loaded Galactosylated Liposomes Effectively Inhibit AKT/c-Met-Triggered Rapid Hepatocarcinogenesis in Mice. *Mol. Pharm.* 17, 738–747. doi:10.1021/acs.molpharmaceut.9b00428
- Chen, Y., Yuan, L., Zhou, L., Zhang, Z. H., Cao, W., and Wu, Q. (2012). Effect of Cell-Penetrating Peptide-Coated Nanostructured Lipid Carriers on the Oral Absorption of Tripterine. *Int. J. Nanomedicine* 7, 4581–4591. doi:10.2147/IJN.S34991
- Chen, Z., Tian, R., She, Z., Cai, J., and Li, H. (2020). Role of Oxidative Stress in the Pathogenesis of Nonalcoholic Fatty Liver Disease. *Free Radic. Biol. Med.* 152, 116–141. doi:10.1016/j.freeradbiomed.2020.02.025
- Diehl-Jones, W. L., and Askin, D. F. (2002). The Neonatal Liver, Part 1: Embryology, Anatomy, and Physiology. *Neonatal. Netw.* 21, 5–12. doi:10.1891/0730-0832.21.2.5
- Dodd, G. T., Xirouchaki, C. E., Eramo, M., Mitchell, C. A., Andrews, Z. B., Henry, B. A., et al. (2019). Intranasal Targeting of Hypothalamic PTP1B and TCPTP Reinstates Leptin and Insulin Sensitivity and Promotes Weight Loss in Obesity. *Cell Rep* 28, 2905–e5. doi:10.1016/j.celrep.2019.08.019
- Du, S., Song, X., Li, Y., Cao, Y., Chu, F., Durojaye, O. A., et al. (2020). Celastrol Inhibits Ezrin-Mediated Migration of Hepatocellular Carcinoma Cells. *Sci. Rep.* 10, 11273. doi:10.1038/s41598-020-68238-1
- El-Tanbouly, G. S., El-Awady, M. S., Megahed, N. A., Salem, H. A., and El-Kashef, H. A. (2017). The NF-Kb Inhibitor Celastrol Attenuates Acute Hepatic Dysfunction Induced by Cecal Ligation and Puncture in Rats. *Environ. Toxicol. Pharmacol.* 50, 175–182. doi:10.1016/j.etap.2017.02.002
- Eslam, M., Sanyal, A. J., George, J., and International Consensus, P. (2020). MAFLD: A Consensus-Driven Proposed Nomenclature for Metabolic Associated Fatty Liver Disease. *Gastroenterology* 158, 1999–2014. doi:10.1053/j.gastro.2019.11.312
- Fabbri, E., Sullivan, S., and Klein, S. (2010). Obesity and Nonalcoholic Fatty Liver Disease: Biochemical, Metabolic, and Clinical Implications. *Hepatology* 51, 679–689. doi:10.1002/hep.23280
- Fang, P., He, B., Yu, M., Shi, M., Zhu, Y., Zhang, Z., et al. (2019). Treatment with Celastrol Protects against Obesity through Suppression of Galanin-Induced Fat Intake and Activation of PGC-1 α /GLUT4 axis-mediated Glucose Consumption. *Biochim. Biophys. Acta Mol. Basis Dis.* 1865, 1341–1350. doi:10.1016/j.bbdis.2019.02.002
- Feng, L., Zhang, D., Fan, C., Ma, C., Yang, W., Meng, Y., et al. (2013). ER Stress-Mediated Apoptosis Induced by Celastrol in Cancer Cells and Important Role

AUTHOR CONTRIBUTIONS

SJ, ML, and L-WQ conceived the study, SJ and ML wrote the manuscript, FX and LW drew the figure, ML, SJ, and GZ performed tables analysis. All authors contributed to the article and approved the submitted version.

FUNDING

This research funded by the National Natural Science Foundation of China (Grant No. 81900780 and Grant No. 82003933).

ACKNOWLEDGMENTS

The author acknowledges and thanks Dr. Haijian Sun and Dr. Raphael N. Alolga for editing our article.

- of Glycogen Synthase Kinase-3 β in the Signal Network. *Cell Death Dis* 4, e715. doi:10.1038/cddis.2013.222
- Feng, X., Guan, D., Auen, T., Choi, J. W., Salazar Hernández, M. A., Lee, J., et al. (2019). IL1RI Is Required for Celastrol's Leptin-Sensitization and Antiobesity Effects. *Nat. Med.* 25, 575–582. doi:10.1038/s41591-019-0358-x
- Feng, X., Guan, D., Auen, T., Choi, J. W., Salazar-Hernandez, M. A., Faruk, F., et al. (2019). Lipocalin 2 Does Not Play A Role in Celastrol-Mediated Reduction in Food Intake and Body Weight. *Sci. Rep.* 9, 12809. doi:10.1038/s41598-019-49151-8
- Fontana, R. J., Hayashi, P. H., Gu, J., Reddy, K. R., Barnhart, H., Watkins, P. B., et al. (2014). Idiosyncratic Drug-Induced Liver Injury Is Associated with Substantial Morbidity and Mortality within 6 Months from Onset. *Gastroenterology* 147, 96–e4. doi:10.1053/j.gastro.2014.03.045
- Frazier, K., and Chang, E. B. (2020). Intersection of the Gut Microbiome and Circadian Rhythms in Metabolism. *Trends Endocrinol. Metab.* 31, 25–36. doi:10.1016/j.tem.2019.08.013
- Freag, M. S., Saleh, W. M., and Abdallah, O. Y. (2018). Self-assembled Phospholipid-Based Phytosomal Nanocarriers as Promising Platforms for Improving Oral Bioavailability of the Anticancer Celastrol. *Int. J. Pharm.* 535, 18–26. doi:10.1016/j.ijpharm.2017.10.053
- Friedman, S. L., Neuschwander-Tetri, B. A., Rinella, M., and Sanyal, A. J. (2018). Mechanisms of NAFLD Development and Therapeutic Strategies. *Nat. Med.* 24, 908–922. doi:10.1038/s41591-018-0104-9
- García, M. C., Wernstedt, I., Berndtsson, A., Enge, M., Bell, M., Hultgren, O., et al. (2006). Mature-onset Obesity in Interleukin-1 Receptor I Knockout Mice. *Diabetes* 55, 1205–1213. doi:10.2337/db05-1304
- García-Rodríguez, J. L., Barbier-Torres, L., Fernández-Álvarez, S., Gutiérrez-de Juan, V., Monte, M. J., Halilbasic, E., et al. (2014). SIRT1 Controls Liver Regeneration by Regulating Bile Acid Metabolism through Farnesoid X Receptor and Mammalian Target of Rapamycin Signaling. *Hepatology* 59, 1972–1983. doi:10.1002/hep.26971
- Guo, J., Wang, Y., Wang, N., Bai, Y., and Shi, D. (2019). Celastrol Attenuates Intrahepatic Cholestasis of Pregnancy by Inhibiting Matrix Metalloproteinases-2 and 9. *Ann. Hepatol.* 18, 40–47. doi:10.5604/01.3001.0012.7860
- Hackl, M. T., Fürnsinn, C., Schuh, C. M., Krssak, M., Carli, F., Guerra, S., et al. (2019). Brain Leptin Reduces Liver Lipids by Increasing Hepatic Triglyceride Secretion and Lowering Lipogenesis. *Nat. Commun.* 10, 2717. doi:10.1038/s41467-019-10684-1
- Han, X., Sun, S., Zhao, M., Cheng, X., Chen, G., Lin, S., et al. (2014). Celastrol Stimulates Hypoxia-Inducible Factor-1 Activity in Tumor Cells by Initiating the ROS/Akt/p70S6K Signaling Pathway and Enhancing Hypoxia-Inducible Factor-1 α Protein Synthesis. *PloS one* 9, e112470. doi:10.1371/journal.pone.0112470
- Hou, W., Liu, B., and Xu, H. (2020). Celastrol: Progresses in Structure-Modifications, Structure-Activity Relationships, Pharmacology and Toxicology. *Eur. J. Med. Chem.* 189, 112081. doi:10.1016/j.ejmech.2020.112081
- Hu, M., Luo, Q., Alitongbieke, G., Chong, S., Xu, C., Xie, L., et al. (2017). Celastrol-Induced Nur77 Interaction with TRAF2 Alleviates Inflammation by Promoting Mitochondrial Ubiquitination and Autophagy. *Mol. Cell* 66, 141–e6. doi:10.1016/j.molcel.2017.03.008
- Hu, W., Wang, L., Du, G., Guan, Q., Dong, T., Song, L., et al. (2020). Effects of Microbiota on the Treatment of Obesity with the Natural Product Celastrol in Rats. *Diabetes Metab. J.* 44, 747–763. doi:10.4093/dmj.2019.0124
- Hu, Y., Wang, S., Wu, X., Zhang, J., Chen, R., Chen, M., et al. (2013). Chinese Herbal Medicine-Derived Compounds for Cancer Therapy: a Focus on Hepatocellular Carcinoma. *J. Ethnopharmacol* 149, 601–612. doi:10.1016/j.jep.2013.07.030
- Hua, H., Zhang, Y., Zhao, F., Chen, K., Wu, T., Liu, Q., et al. (2021). Celastrol Inhibits Intestinal Lipid Absorption by Reproiling the Gut Microbiota to Attenuate High-Fat Diet-Induced Obesity. *iScience* 24, 102077. doi:10.1016/j.isci.2021.102077
- Jannuzzi, A. T., Kara, M., and Alpertunga, B. (2018). Celastrol Ameliorates Acetaminophen-Induced Oxidative Stress and Cytotoxicity in HepG2 Cells. *Hum. Exp. Toxicol.* 37, 742–751. doi:10.1177/0960327117734622
- Jarvis, H., Craig, D., Barker, R., Spiers, G., Stow, D., Anstee, Q. M., et al. (2020). Metabolic Risk Factors and Incident Advanced Liver Disease in Non-alcoholic Fatty Liver Disease (NAFLD): A Systematic Review and Meta-Analysis of Population-Based Observational Studies. *Plos Med.* 17, e1003100. doi:10.1371/journal.pmed.1003100
- Jiang, H. L., Jin, J. Z., Wu, D., Xu, D., Lin, G. F., Yu, H., et al. (2013). Celastrol Exerts Synergistic Effects with PHA-665752 and Inhibits Tumor Growth of C-Met-Deficient Hepatocellular Carcinoma *In Vivo*. *Mol. Biol. Rep.* 40, 4203–4209. doi:10.1007/s11033-013-2501-y
- Kashyap, D., Sharma, A., Tuli, H. S., Sak, K., Mukherjee, T., and Bishayee, A. (2018). Molecular Targets of Celastrol in Cancer: Recent Trends and Advancements. *Crit. Rev. Oncol. Hematol.* 128, 70–81. doi:10.1016/j.critrevonc.2018.05.019
- Katsiki, N., Mikhailidis, D. P., and Mantzoros, C. S. (2016). Non-alcoholic Fatty Liver Disease and Dyslipidemia: An Update. *Metabolism* 65, 1109–1123. doi:10.1016/j.metabol.2016.05.003
- Kazankov, K., Jørgensen, S. M. D., Thomsen, K. L., Møller, H. J., Vilstrup, H., George, J., et al. (2019). The Role of Macrophages in Nonalcoholic Fatty Liver Disease and Nonalcoholic Steatohepatitis. *Nat. Rev. Gastroenterol. Hepatol.* 16, 145–159. doi:10.1038/s41575-018-0082-x
- Kun-Ming, C., Chih-Hsien, C., Chen-Fang, L., Ting-Jung, W., Hong-Shiue, C., and Wei-Chen, L. (2020). Potential Anticancer Effect of Celastrol on Hepatocellular Carcinoma by Suppressing CXCR4-Related Signal and Impeding Tumor Growth *In Vivo*. *Arch. Med. Res.* 51, 297–302. doi:10.1016/j.arcmed.2020.03.001
- Kyriakou, E., Schmidt, S., Dodd, G. T., Pfuhlmann, K., Simonds, S. E., Lenhart, D., et al. (2018). Celastrol Promotes Weight Loss in Diet-Induced Obesity by Inhibiting the Protein Tyrosine Phosphatases PTP1B and TCPTP in the Hypothalamus. *J. Med. Chem.* 61, 11144–11157. doi:10.1021/acs.jmedchem.8b01224
- Lanthier, N. (2015). Targeting Kupffer Cells in Non-alcoholic Fatty Liver Disease/non-Alcoholic Steatohepatitis: Why and How? *World J. Hepatol.* 7, 2184–2188. doi:10.4254/wjh.v7.i19.2184
- Le Roy, T., Llopis, M., Lepage, P., Bruneau, A., Rabot, S., Bevilacqua, C., et al. (2013). Intestinal Microbiota Determines Development of Non-Alcoholic Fatty Liver Disease in Mice. *Gut* 62 (12), 1787–1794. doi:10.1136/gutjnl-2012-303816
- Li, H., Li, Y., Liu, D., Sun, H., and Liu, J. (2013). miR-224 Is Critical for Celastrol-Induced Inhibition of Migration and Invasion of Hepatocellular Carcinoma Cells. *Cell Physiol Biochem* 32, 448–458. doi:10.1159/000354450
- Li, P. P., He, W., Yuan, P. F., Song, S. S., Lu, J. T., and Wei, W. (2015). Celastrol Induces Mitochondria-Mediated Apoptosis in Hepatocellular Carcinoma Bel-7402 Cells. *Am. J. Chin. Med.* 43, 137–148. doi:10.1142/S0192415X15500093
- Li, Z., Feng, H., Han, L., Ding, L., Shen, B., Tian, Y., et al. (2020). Chicoric Acid Ameliorate Inflammation and Oxidative Stress in Lipopolysaccharide and D-Galactosamine Induced Acute Liver Injury. *J. Cell Mol Med* 24, 3022–3033. doi:10.1111/jcmm.14935
- Liang, Y., Chen, H., Liu, Y., Hou, X., Wei, L., Bao, Y., et al. (2022). Association of MAFLD with Diabetes, Chronic Kidney Disease, and Cardiovascular Disease: A 4.6-Year Cohort Study in China. *J. Clin. Endocrinol. Metab.* 107, 88–97. doi:10.1210/clinem/dgab641
- Licata, A. (2016). Adverse Drug Reactions and Organ Damage: The Liver. *Eur. J. Intern. Med.* 28, 9–16. doi:10.1016/j.ejim.2015.12.017
- Lin, L., Sun, Y., Wang, D., Zheng, S., Zhang, J., and Zheng, C. (2015). Celastrol Ameliorates Ulcerative Colitis-Related Colorectal Cancer in Mice via Suppressing Inflammatory Responses and Epithelial-Mesenchymal Transition. *Front. Pharmacol.* 6, 320. doi:10.3389/fphar.2015.00320
- Liu, J., Lee, J., Salazar Hernandez, M. A., Mazitschek, R., and Ozcan, U. (2015). Treatment of Obesity with Celastrol. *Cell* 161, 999–1011. doi:10.1016/j.cell.2015.05.011
- Luo, D., Guo, Y., Cheng, Y., Zhao, J., Wang, Y., and Rong, J. (2017). Natural Product Celastrol Suppressed Macrophage M1 Polarization against Inflammation in Diet-Induced Obese Mice via Regulating Nrf2/HO-1, MAP Kinase and NF-Kb Pathways. *Aging (Albany NY)* 9, 2069–2082. doi:10.18632/aging.101302
- Luo, X., Li, H., Ma, L., Zhou, J., Guo, X., Woo, S. L., et al. (2018). Expression of STING Is Increased in Liver Tissues from Patients with NAFLD and Promotes Macrophage-Mediated Hepatic Inflammation and Fibrosis in Mice. *Gastroenterology* 155, 1971–e4. doi:10.1053/j.gastro.2018.09.010
- Ma, J., Han, L. Z., Liang, H., Mi, C., Shi, H., Lee, J. J., et al. (2014). Celastrol Inhibits the HIF-1 α Pathway by Inhibition of mTOR/p70S6K/eIF4E and ERK1/2

- Phosphorylation in Human Hepatoma Cells. *Oncol. Rep.* 32, 235–242. doi:10.3892/or.2014.3211
- Ma, L., Peng, L., Fang, S., He, B., and Liu, Z. (2017). Celastrol Downregulates E2F1 to Induce Growth Inhibitory Effects in Hepatocellular Carcinoma HepG2 Cells. *Oncol. Rep.* 38, 2951–2958. doi:10.3892/or.2017.5971
- Ma, X., Xu, L., Alberobello, A. T., Gavrilova, O., Bagattin, A., Skarulis, M., et al. (2015). Celastrol Protects against Obesity and Metabolic Dysfunction through Activation of a HSF1-Pgc1 α Transcriptional Axis. *Cell Metab* 22, 695–708. doi:10.1016/j.cmet.2015.08.005
- Madrigal-Santillán, E., Madrigal-Bujaidar, E., Álvarez-González, I., Sumaya-Martínez, M. T., Gutiérrez-Salinas, J., Bautista, M., et al. (2014). Review of Natural Products with Hepatoprotective Effects. *World J. Gastroenterol.* 20, 14787–14804. doi:10.3748/wjg.v20.i40.14787
- Minsky, N., and Roeder, R. G. (2015). Direct Link between Metabolic Regulation and the Heat-Shock Response through the Transcriptional Regulator PGC-1 α . *Proc. Natl. Acad. Sci. U S A.* 112, E5669–E5678. doi:10.1073/pnas.1516219112
- Mundi, M. S., Velapati, S., Patel, J., Kellogg, T. A., Abu Dayyeh, B. K., and Hurt, R. T. (2020). Evolution of NAFLD and its Management. *Nutr. Clin. Pract.* 35, 72–84. doi:10.1002/ncp.10449
- Murphy, E. F., Cotter, P. D., Hogan, A., O'Sullivan, O., Joyce, A., Fouhy, F., et al. (2013). Divergent Metabolic Outcomes Arising from Targeted Manipulation of the Gut Microbiota in Diet-Induced Obesity. *Gut* 62, 220–226. doi:10.1136/gutjnl-2011-300705
- Myers, M. G., Jr., Leibel, R. L., Seeley, R. J., and Schwartz, M. W. (2010). Obesity and Leptin Resistance: Distinguishing Cause from Effect. *Trends Endocrinol. Metab.* 21, 643–651. doi:10.1016/j.tem.2010.08.002
- Ore, A., and Akinloye, O. A. (2019). Oxidative Stress and Antioxidant Biomarkers in Clinical and Experimental Models of Non-alcoholic Fatty Liver Disease. *Medicina (Kaunas)* 55. doi:10.3390/medicina55020026
- Ouyang, M., Qin, T., Liu, H., Lu, J., Peng, C., and Guo, Q. (2021). Enhanced Inflammatory Reaction and Thrombosis in High-Fat Diet-Fed ApoE $^{-/-}$ Mice Are Attenuated by Celastrol. *Exp. Clin. Endocrinol. Diabetes* 129, 339–348. doi:10.1055/a-1010-5543
- Padda, M. S., Sanchez, M., Akhtar, A. J., and Boyer, J. L. (2011). Drug-induced Cholestasis. *Hepatology* 53, 1377–1387. doi:10.1002/hep.24229
- Pan, W. W., and Myers, M. G., Jr. (2018). Leptin and the Maintenance of Elevated Body Weight. *Nat. Rev. Neurosci.* 19, 95–105. doi:10.1038/nrn.2017.168
- Pfuhmann, K., Schriever, S. C., Baumann, P., Kabra, D. G., Harrison, L., Mazibuko-Mbeje, S. E., et al. (2018). Celastrol-Induced Weight Loss Is Driven by Hypophagia and Independent from UCP1. *Diabetes* 67, 2456–2465. doi:10.2337/db18-0146
- Purushotham, A., Schug, T. T., Xu, Q., Surapureddi, S., Guo, X., and Li, X. (2009). Hepatocyte-specific Deletion of SIRT1 Alters Fatty Acid Metabolism and Results in Hepatic Steatosis and Inflammation. *Cell Metab* 9, 327–338. doi:10.1016/j.cmet.2009.02.006
- Qi, X., Qin, J., Ma, N., Chou, X., and Wu, Z. (2014). Solid Self-Microemulsifying Dispersible Tablets of Celastrol: Formulation Development, Characterization and Bioavailability Evaluation. *Int. J. Pharm.* 472, 40–47. doi:10.1016/j.ijpharm.2014.06.019
- Rajendran, P., Li, F., Shanmugam, M. K., Kannaiyan, R., Goh, J. N., Wong, K. F., et al. (2012). Celastrol Suppresses Growth and Induces Apoptosis of Human Hepatocellular Carcinoma through the Modulation of STAT3/JAK2 Signaling cascade *In Vitro* and *In Vivo*. *Cancer Prev. Res. (Phila)* 5, 631–643. doi:10.1158/1940-6207.CAPR-11-0420
- Ren, B., Liu, H., Gao, H., Liu, S., Zhang, Z., Fribley, A. M., et al. (2017). Celastrol Induces Apoptosis in Hepatocellular Carcinoma Cells via Targeting ER-Stress/UPR. *Oncotarget* 8, 93039–93050. doi:10.18632/oncotarget.21750
- Rodgers, J. T., Lerin, C., Haas, W., Gygi, S. P., Spiegelman, B. M., and Puigserver, P. (2005). Nutrient Control of Glucose Homeostasis through a Complex of PGC-1 α and SIRT1. *Nature* 434, 113–118. doi:10.1038/nature03354
- Saber, S., Ghanim, A. M. H., El-Ahwany, E., and El-Kader, E. M. A. (2020). Novel Complementary Antitumor Effects of Celastrol and Metformin by Targeting I κ B β , Apoptosis and NLRP3 Inflammasome Activation in Diethylnitrosamine-Induced Murine Hepatocarcinogenesis. *Cancer Chemother. Pharmacol.* 85, 331–343. doi:10.1007/s00280-020-04033-z
- Saito, K., Davis, K. C., Morgan, D. A., Toth, B. A., Jiang, J., Singh, U., et al. (2019). Celastrol Reduces Obesity in MC4R Deficiency and Stimulates Sympathetic Nerve Activity Affecting Metabolic and Cardiovascular Functions. *Diabetes* 68, 1210–1220. doi:10.2337/db18-1167
- Samuel, V. T., and Shulman, G. I. (2018). Nonalcoholic Fatty Liver Disease as a Nexus of Metabolic and Hepatic Diseases. *Cell Metab* 27, 22–41. doi:10.1016/j.cmet.2017.08.002
- Saran, A. R., Dave, S., and Zarrinpar, A. (2020). Circadian Rhythms in the Pathogenesis and Treatment of Fatty Liver Disease. *Gastroenterology* 158, 1948–1966. doi:10.1053/j.gastro.2020.01.050
- Shehu, A. I., Ma, X., and Venkataraman, R. (2017). Mechanisms of Drug-Induced Hepatotoxicity. *Clin. Liver Dis.* 21, 35–54. doi:10.1016/j.cld.2016.08.002
- Shi, J., Li, J., Xu, Z., Chen, L., Luo, R., Zhang, C., et al. (2020). Celastrol: A Review of Useful Strategies Overcoming its Limitation in Anticancer Application. *Front. Pharmacol.* 11, 558741. doi:10.3389/fphar.2020.558741
- Si, H., Wang, H., Xiao, H., Fang, Y., and Wu, Z. (2021). Anti-Tumor Effect of Celastrol on Hepatocellular Carcinoma by the circ_SLIT3/miR-223-3p/CXCR4 Axis. *Cancer Manag. Res.* 13, 1099–1111. doi:10.2147/CMAR.S278023
- Song, X., Zhang, Y., Dai, E., Du, H., and Wang, L. (2019). Mechanism of Action of Celastrol against Rheumatoid Arthritis: A Network Pharmacology Analysis. *Int. Immunopharmacol.* 74, 105725. doi:10.1016/j.intimp.2019.105725
- Strnad, P., Tacke, F., Koch, A., and Trautwein, C. (2017). Liver - Guardian, Modifier and Target of Sepsis. *Nat. Rev. Gastroenterol. Hepatol.* 14, 55–66. doi:10.1038/nrgastro.2016.168
- Sung, H., Ferlay, J., Siegel, R. L., Laversanne, M., Soerjomataram, I., Jemal, A., et al. (2021). Global Cancer Statistics 2020: GLOBOCAN Estimates of Incidence and Mortality Worldwide for 36 Cancers in 185 Countries. *CA A. Cancer J. Clin.* 71, 209–249. doi:10.3322/caac.21660
- Świdarska, M., Maciejczyk, M., Zalewska, A., Pogorzelska, J., Flisiak, R., and Chabowski, A. (2019). Oxidative Stress Biomarkers in the Serum and Plasma of Patients with Non-alcoholic Fatty Liver Disease (NAFLD). Can Plasma AGE Be a Marker of NAFLD? Oxidative Stress Biomarkers in NAFLD Patients. *Free Radic. Res.* 53, 841–850. doi:10.1080/10715762.2019.1635691
- Tappy, L. (2021). Metabolism of Sugars: A Window to the Regulation of Glucose and Lipid Homeostasis by Splanchnic Organs. *Clin. Nutr.* 40, 1691–1698. doi:10.1016/j.clnu.2020.12.022
- Thawley, V. (2017). Acute Liver Injury and Failure. *Vet. Clin. North America: Small Anim. Pract.* 47, 617–630. doi:10.1016/j.cvsm.2016.11.010
- Tseng, C. K., Hsu, S. P., Lin, C. K., Wu, Y. H., Lee, J. C., and Young, K. C. (2017). Celastrol Inhibits Hepatitis C Virus Replication by Upregulating Heme Oxygenase-1 via the JNK MAPK/Nrf2 Pathway in Human Hepatoma Cells. *Antivir. Res.* 146, 191–200. doi:10.1016/j.antiviral.2017.09.010
- Vega, R. B., Huss, J. M., and Kelly, D. P. (2000). The Coactivator PGC-1 Cooperates with Peroxisome Proliferator-Activated Receptor Alpha in Transcriptional Control of Nuclear Genes Encoding Mitochondrial Fatty Acid Oxidation Enzymes. *Mol. Cell Biol* 20, 1868–1876. doi:10.1128/mcb.20.5.1868-1876.2000
- Vento, S., and Cainelli, F. (2020). Acute Liver Failure. *Lancet* 395, 1833. doi:10.1016/S0140-6736(20)30046-5
- Wang, C., Shi, C., Yang, X., Yang, M., Sun, H., and Wang, C. (2014). Celastrol Suppresses Obesity Process via Increasing Antioxidant Capacity and Improving Lipid Metabolism. *Eur. J. Pharmacol.* 744, 52–58. doi:10.1016/j.ejphar.2014.09.043
- Wang, Y., Li, C., Gu, J., Chen, C., Duanmu, J., Miao, J., et al. (2020). Celastrol Exerts Anti-inflammatory Effect in Liver Fibrosis via Activation of AMPK-SIRT3 Signalling. *J. Cell Mol Med* 24, 941–953. doi:10.1111/jcmm.14805
- Wei, W., Wu, S., Wang, X., Sun, C. K., Yang, X., Yan, X., et al. (2014). Novel Celastrol Derivatives Inhibit the Growth of Hepatocellular Carcinoma Patient-Derived Xenografts. *Oncotarget* 5, 5819–5831. doi:10.18632/oncotarget.2171
- Wong, C. C., Kai, A. K., and Ng, I. O. (2014). The Impact of Hypoxia in Hepatocellular Carcinoma Metastasis. *Front. Med.* 8, 33–41. doi:10.1007/s11684-013-0301-3
- Wu, M., Chen, W., Yu, X., Ding, D., Zhang, W., Hua, H., et al. (2018). Celastrol Aggravates LPS-Induced Inflammation and Injuries of Liver and Kidney in Mice. *Am. J. Transl. Res.* 10, 2078–2086.
- Xiong, X., Ren, Y., Cui, Y., Li, R., Wang, C., and Zhang, Y. (2017). Obeticholic Acid Protects Mice against Lipopolysaccharide-Induced Liver Injury and Inflammation. *Biomed. Pharmacother.* 96, 1292–1298. doi:10.1016/j.biopha.2017.11.083

- Xu, J., Bartolome, C. L., Low, C. S., Yi, X., Chien, C. H., Wang, P., et al. (2018). Genetic Identification of Leptin Neural Circuits in Energy and Glucose Homeostases. *Nature* 556, 505–509. doi:10.1038/s41586-018-0049-7
- Xu, L., Zhao, W., Wang, D., and Ma, X. (2018). Chinese Medicine in the Battle against Obesity and Metabolic Diseases. *Front. Physiol.* 9, 850. doi:10.3389/fphys.2018.00850
- Yan, C. Y., Ouyang, S. H., Wang, X., Wu, Y. P., Sun, W. Y., Duan, W. J., et al. (2021). Celastrol Ameliorates Propionibacterium acnes/LPS-Induced Liver Damage and MSU-Induced Gouty Arthritis via Inhibiting K63 Deubiquitination of NLRP3. *Phytomedicine* 80, 153398. doi:10.1016/j.phymed.2020.153398
- Yan, Y. Y., Guo, Y., Zhang, W., Ma, C. G., Zhang, Y. X., Wang, C., et al. (2014). Celastrol Enhanced the Anticancer Effect of Lapatinib in Human Hepatocellular Carcinoma Cells *In Vitro*. *J. BUON* 19, 412–418.
- Yang, X., Wu, F., Li, L., Lynch, E. C., Xie, L., Zhao, Y., et al. (2021). Celastrol Alleviates Metabolic Disturbance in High-Fat Diet-Induced Obese Mice through Increasing Energy Expenditure by Ameliorating Metabolic Inflammation. *Phytother. Res.* 35, 297–310. doi:10.1002/ptr.6800
- Ye, Q., Zou, B., Yeo, Y. H., Li, J., Huang, D. Q., Wu, Y., et al. (2020). Global Prevalence, Incidence, and Outcomes of Non-obese or Lean Non-alcoholic Fatty Liver Disease: a Systematic Review and Meta-Analysis. *Lancet Gastroenterol. Hepatol.* 5, 739–752. doi:10.1016/S2468-1253(20)30077-7
- Younossi, Z., Anstee, Q. M., Marietti, M., Hardy, T., Henry, L., Eslam, M., et al. (2018). Global burden of NAFLD and NASH: Trends, Predictions, Risk Factors and Prevention. *Nat. Rev. Gastroenterol. Hepatol.* 15, 11–20. doi:10.1038/nrgastro.2017.109
- Zhang, A., Sun, H., and Wang, X. (2013). Recent Advances in Natural Products from Plants for Treatment of Liver Diseases. *Eur. J. Med. Chem.* 63, 570–577. doi:10.1016/j.ejmech.2012.12.062
- Zhang, D. G., Zhang, C., Wang, J. X., Wang, B. W., Wang, H., Zhang, Z. H., et al. (2017). Obeticholic Acid Protects against Carbon Tetrachloride-Induced Acute Liver Injury and Inflammation. *Toxicol. Appl. Pharmacol.* 314, 39–47. doi:10.1016/j.taap.2016.11.006
- Zhang, J., Li, C. Y., Xu, M. J., Wu, T., Chu, J. H., Liu, S. J., et al. (2012). Oral Bioavailability and Gender-Related Pharmacokinetics of Celastrol Following Administration of Pure Celastrol and its Related Tablets in Rats. *J. Ethnopharmacol.* 144, 195–200. doi:10.1016/j.jep.2012.09.005
- Zhang, R., Chen, Z., Wu, S. S., Xu, J., Kong, L. C., and Wei, P. (2019). Celastrol Enhances the Anti-liver Cancer Activity of Sorafenib. *Med. Sci. Monit.* 25, 4068–4075. doi:10.12659/MSM.914060
- Zhang, S., Yang, N., Ni, S., Li, W., Xu, L., Dong, P., et al. (2014). Pretreatment of Lipopolysaccharide (LPS) Ameliorates D-GalN/LPS Induced Acute Liver Failure through TLR4 Signaling Pathway. *Int. J. Clin. Exp. Pathol.* 7, 6626–6634.
- Zhang, X., Wang, Y., Ge, H. Y., Gu, Y. J., Cao, F. F., Yang, C. X., et al. (2018). Celastrol Reverses Palmitic Acid (PA)-caused TLR4-MD2 Activation-dependent Insulin Resistance via Disrupting MD2-related Cellular Binding to PA. *J. Cell Physiol.* 233, 6814–6824. doi:10.1002/jcp.26547
- Zhang, Y., Geng, C., Liu, X., Li, M., Gao, M., Liu, X., et al. (2017). Celastrol Ameliorates Liver Metabolic Damage Caused by a High-Fat Diet through Sirt1. *Mol. Metab.* 6, 138–147. doi:10.1016/j.molmet.2016.11.002
- Zhao, J., Luo, D., Zhang, Z., Fan, N., Wang, Y., Nie, H., et al. (2019). Celastrol-loaded PEG-PCL Nanomicelles Ameliorate Inflammation, Lipid Accumulation, Insulin Resistance and Gastrointestinal Injury in Diet-Induced Obese Mice. *J. Control. Release* 310, 188–197. doi:10.1016/j.jconrel.2019.08.026
- Zhao, Q., Liu, F., Cheng, Y., Xiao, X. R., Hu, D. D., Tang, Y. M., et al. (2019). Celastrol Protects from Cholestatic Liver Injury through Modulation of SIRT1-FXR Signaling. *Mol. Cell Proteomics* 18, 520–533. doi:10.1074/mcp.RA118.000817
- Zhao, Q., Tang, P., Zhang, T., Huang, J. F., Xiao, X. R., Zhu, W. F., et al. (2020). Celastrol Ameliorates Acute Liver Injury through Modulation of PPARα. *Biochem. Pharmacol.* 178, 114058. doi:10.1016/j.bcp.2020.114058
- Zhu, C., Yang, J., Zhu, Y., Li, J., Chi, H., Tian, C., et al. (2021). Celastrol Alleviates Comorbid Obesity and Depression by Directly Binding Amygdala HnRNPA1 in a Mouse Model. *Clin. Transl. Med.* 11, e394. doi:10.1002/ctm2.394
- Zhu, H., Yang, W., He, L. J., Ding, W. J., Zheng, L., Liao, S. D., et al. (2012). Upregulating Noxa by ER Stress, Celastrol Exerts Synergistic Anti-cancer Activity in Combination with ABT-737 in Human Hepatocellular Carcinoma Cells. *PloS one* 7, e23333. doi:10.1371/journal.pone.0052333
- Zhu, Y., Wan, N., Shan, X., Deng, G., Xu, Q., Ye, H., et al. (2021). Celastrol Targets Adenylyl Cyclase-Associated Protein 1 to Reduce Macrophages-Mediated Inflammation and Ameliorates High Fat Diet-Induced Metabolic Syndrome in Mice. *Acta Pharm. Sin B* 11, 1200–1212. doi:10.1016/j.apsb.2020.12.008
- Zollner, G., and Trauner, M. (2008). Mechanisms of Cholestasis. *Clin. Liver Dis.* 12, 1–26. doi:10.1016/j.cld.2007.11.010

Conflict of Interest: The authors declare that the research was conducted in the absence of any commercial or financial relationships that could be construed as a potential conflict of interest.

Publisher's Note: All claims expressed in this article are solely those of the authors and do not necessarily represent those of their affiliated organizations, or those of the publisher, the editors, and the reviewers. Any product that may be evaluated in this article, or claim that may be made by its manufacturer, is not guaranteed or endorsed by the publisher.

Copyright © 2022 Li, Xie, Wang, Zhu, Qi and Jiang. This is an open-access article distributed under the terms of the Creative Commons Attribution License (CC BY). The use, distribution or reproduction in other forums is permitted, provided the original author(s) and the copyright owner(s) are credited and that the original publication in this journal is cited, in accordance with accepted academic practice. No use, distribution or reproduction is permitted which does not comply with these terms.



FGF9 Alleviates the Fatty Liver Phenotype by Regulating Hepatic Lipid Metabolism

Fanrong Zhao^{1†}, Lei Zhang^{1†}, Menglin Zhang¹, Jincan Huang¹, Jun Zhang^{2*} and Yongsheng Chang^{1*}

¹Key Laboratory of Immune Microenvironment and Disease (Ministry of Education), Tianjin Key of Cellular Homeostasis and Disease, Department of Physiology and Pathophysiology, Tianjin Medical University, Tianjin, China, ²Department of Basic Medicine, School of Medicine, Shihezi University, Shihezi, China

OPEN ACCESS

Edited by:

Ana Blas-García,
University of Valencia, Spain

Reviewed by:

Fadila Benhamed,
INSERM U1016 Institut Cochin,
France
Zhuoxian Meng,
Zhejiang University, China

*Correspondence:

Jun Zhang
zhangjunyc@163.com
Yongsheng Chang
changys@tmu.edu.cn

[†]These authors have contributed
equally to this work

Specialty section:

This article was submitted to
Gastrointestinal and Hepatic
Pharmacology,
a section of the journal
Frontiers in Pharmacology

Received: 07 January 2022

Accepted: 16 March 2022

Published: 20 April 2022

Citation:

Zhao F, Zhang L, Zhang M, Huang J,
Zhang J and Chang Y (2022) FGF9
Alleviates the Fatty Liver Phenotype by
Regulating Hepatic Lipid Metabolism.
Front. Pharmacol. 13:850128.
doi: 10.3389/fphar.2022.850128

Although the fatty liver has been linked to numerous impairments of energy homeostasis, the molecular mechanism responsible for fatty liver development remains largely unknown. In the present study, we show that fibroblast growth factors 9 (FGF9) expression is increased in the liver of diet-induced obese (DIO), db/db, and ob/ob mice relative to their respective controls. The long-term knockdown of hepatic FGF9 expression mediated by adeno-associated virus expressing FGF9-specific short hairpin RNA (AAV-shFGF9) aggravated the fatty liver phenotype of DIO mice. Consistently, downregulation of FGF9 expression mediated by adenovirus expressing FGF9-specific shRNA (Ad-shFGF9) in the primary hepatocyte promoted the cellular lipid accumulation, suggesting that FGF9 exerts its effects in an autocrine manner. In contrast, adenoviruses expressing FGF9 (Ad-FGF9) mediated FGF9 overexpression in the liver of DIO mice alleviated hepatic steatosis and improved the insulin sensitivity and glucose intolerance. Moreover, the liver-specific FGF9 transgenic mice phenocopied the Ad-FGF9-infected mice. Mechanistically, FGF9 inhibited the expression of genes involved in lipogenesis and increased the expression of genes involved in fatty acid oxidation, thereby reducing cellular lipid accumulation. Thus, targeting FGF9 might be exploited to treat nonalcoholic fatty liver disease (NAFLD) and metabolic syndrome.

Keywords: lipid synthesis, fatty acid oxidation, lipogenesis, fatty liver, FGF9

INTRODUCTION

The liver is a central metabolic organ that regulates hepatic lipid metabolism, including lipogenesis, fatty acid oxidation, and lipoprotein uptake and secretion (Browning and Horton, 2004). The excessive accumulation of triglycerides (TGs) in hepatocytes is the hallmark of NAFLD. The spectrum of NAFLD ranges from simple fatty liver (hepatic steatosis) to nonalcoholic steatohepatitis (NASH), which may lead to liver fibrosis and cirrhosis, resulting in increased morbidity and mortality (Brunt, 2010). NAFLD is closely associated with insulin resistance, obesity, and other metabolic diseases (Browning and Horton, 2004). Although the fatty liver has been attributed to abnormal energy metabolism, the molecular mechanisms underlying fatty liver development remain largely unknown.

De novo lipogenesis is remarkably induced in NAFLD patients, contributing to the excessive TG accumulation in the liver. Moreover, hepatic lipogenesis, which is normally inhibited in the fasting

state, is relatively high under fasting conditions and fails to further increase after feeding in NAFLD patients (Diraison et al., 2003; Donnelly et al., 2005). Carbohydrate response element-binding protein (ChREBP) is a basic helix-loop-helix leucine-zipper transcription factor, which is highly expressed in the liver and has been shown to regulate hepatic lipogenesis *via* activating its target genes, including fatty acid synthase (FAS), acetyl-CoA carboxylase 1 (ACCC1), and stearoyl CoA desaturase 1 (SCD1) (Jois and Sleeman, 2017). The liver-specific knockout of ChREBP in ob/ob mice improved hepatic steatosis and insulin resistance (Dentin et al., 2006). In contrast, overexpression of ChREBP in the liver of mice resulted in worsening of hepatic steatosis (Benhamed et al., 2012). These studies clearly suggest that ChREBP is a key mediator of hepatic steatosis.

Peroxisome proliferator-activated receptor γ (PPAR γ) belongs to the nuclear receptor superfamily, which is highly expressed in adipose and required for the differentiation of preadipocytes to mature adipocytes. PPAR γ is typically expressed in the liver at only 20% of the levels found in adipose tissue (Tontonoz et al., 1994). However, PPAR γ expression is markedly induced in the severe fatty liver. Hepatic PPAR γ deficiency remarkably alleviates the fatty liver phenotype (Matsusue et al., 2003), clearly indicating that PPAR γ is capable of activating the expression of genes involved in TG accumulation in hepatocytes and promoting the development of fatty liver. However, PPAR α , another member of the PPAR subfamily, stimulates fatty acid oxidation and improves lipoprotein metabolism by regulating the expression of genes involved in peroxisomal and mitochondrial β -oxidation pathways, fatty acid uptake, and triglyceride catabolism. Mice lacking PPAR α accumulate a copious amount of hepatic TG and become hypoketonemic and hypoglycemic during fasting (Leone et al., 1999). Fibrates, the synthetic PPAR α agonists, have been used to treat dyslipidemia (Lefebvre et al., 2006).

The family of fibroblast growth factors (FGFs) regulates a plethora of developmental processes and physiological functions (Beenken and Mohammadi, 2009). In mammals, 18 members of the FGF family are divided into two categories, namely, endocrine and paracrine. The FGF19, FGF21, and FGF23 subfamilies have been shown to function in an endocrine manner, dependent on the presence of Klotho proteins in their target tissues, to regulate glucose, bile acid, vitamin D, and phosphate homeostasis, while other members of the FGF family are considered paracrine factors and are known for their roles in tissue patterning and organogenesis during embryogenesis (Degirolamo et al., 2016). Previous studies suggest that FGF9 participates in palate formation, sex determination, and lung development (Colvin et al., 2001; Yin et al., 2011; Iwata et al., 2012). Interestingly, recently two studies showed that FGF9 regulates browning of white adipocytes and is associated with human obesity (Sun et al., 2019; Shamsi et al., 2020). However, the physiological role of FGF9 in other metabolically active tissues remains unexplored. In the present study, we show that fasting-induced FGF9 in the liver regulates hepatic lipid metabolism in a cell-autonomous manner. Targeting FGF9 signaling might be exploited to treat NAFLD and other metabolic diseases.

RESULTS

The Expression of FGF9 is Dysregulated in the Liver of Mice With Hepatic Steatosis

FGF21 is a peptide hormone, secreted predominantly from the liver, and its expression is increased in the fasting state (Badman et al., 2007; Inagaki et al., 2007). FGF21 has been shown to regulate the metabolism of lipids and glucose, and FGF21 agonism holds significant potential for treatment of NASH (Ritchie et al., 2020).

To identify a novel secreted protein regulating systemic glucose and lipid metabolism, we have previously performed microarray analysis of livers of mice with hepatic steatosis (Shen et al., 2014). Preliminary data suggest that mRNA levels of FGF9, another member of FGF family, are also increased in the liver of ob/ob mice. Our real-time PCR and Western blotting data confirmed the microarray analysis (**Figures 1A,B**). We obtained similar results in DIO mice (**Figures 1C,D**). Interestingly, similar to FGF21, fasting-induced hepatic FGF9 expression, while refeeding, reversed this effect (**Figures 1E,F**).

These results indicate that FGF9 expression is regulated by different nutritional statuses, and FGF9 might have an important effect on hepatic glucose and lipid metabolism.

Knockdown of FGF9 by AAV-shFGF9 in the Liver of DIO Mice Aggravated Hepatic Steatosis

Given that FGF9 expression is induced in the liver of DIO mice, we explored the effects of long-term hepatic FGF9 deficiency on systemic metabolism. We first generated an adeno-associated virus expressing FGF9-specific short hairpin RNA (AAV-shFGF9) and infused AAV-shFGF9 into mice *via* the tail vein. Feeding a chow diet or high-fat diet after eight weeks, the mice were sacrificed for further studies. As a result, the knockdown of FGF9 did not affect hepatic lipid metabolism or systemic glucose metabolism in mice fed with a chow diet (**Supplementary Figures S1B–E**). However, an increased liver-to-body weight ratio was observed in mice injected with AAV-shFGF9 (**Figure 2A**). Moreover, AAV-shFGF9 treatment further aggravated glucose intolerance and insulin resistance induced by HFD (**Figures 2B,C**), and impaired hepatic insulin signaling (**Figure 2D**). Furthermore, H&E and Oil Red O staining revealed lipid accumulation in the liver (**Figure 2E**). The biochemical analysis also confirmed the significant increase in hepatic TG levels in AAV-shFGF9-injected mice (**Figure 2F**).

We also explored the molecular mechanism for the aggravated fatty liver phenotype in AAV-shFGF9-injected mice. We found that FGF9 knockdown in the liver increased the expression of genes involved in lipid synthesis (ChREBP, Fasn, and PPAR γ) and fatty acid transport (Fabp1, Fabp4, and CD36). Meanwhile, AAV-shFGF9 treatment also decreased the expression of genes involved in lipid oxidation (Cpt1a, Cyp4a10, and Cyp4a14),

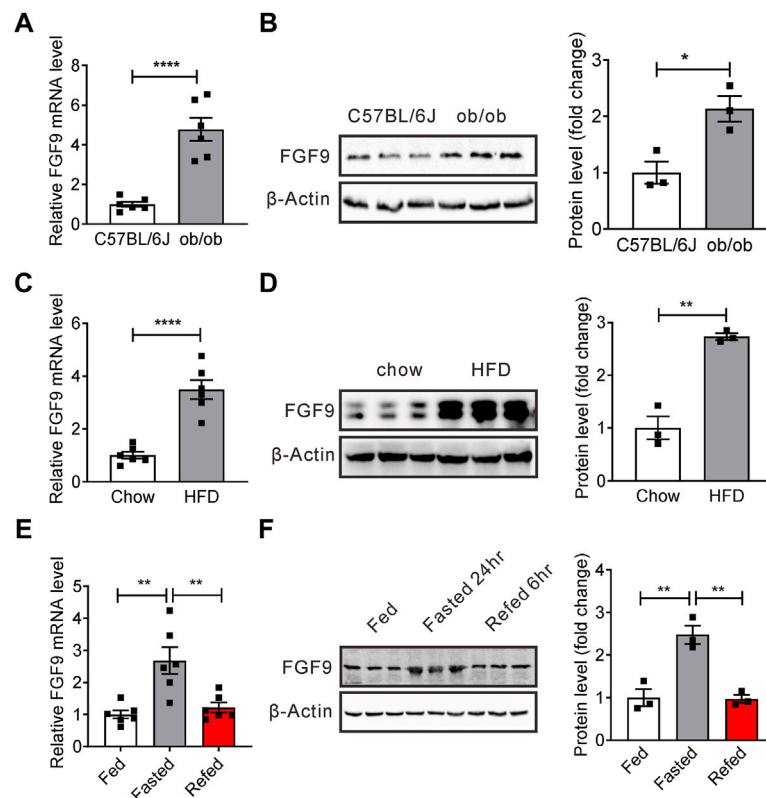


FIGURE 1 | Expression of hepatic FGF9 is dysregulated in mice with fatty liver. **(A)** Quantitative PCR analysis of hepatic FGF9 in ob/ob mice ($n = 6/\text{group}$). **(B)** Representative Western blotting analysis of hepatic FGF9 in ob/ob mice. **(C)** Quantitative PCR analysis of hepatic FGF9 in C57BL/6J mice fed with a chow diet or high-fat diet for 3 months (DIO mice) ($n = 6/\text{group}$). **(D)** Representative Western blotting analysis of hepatic FGF9 in mice in **(C)**. **(E)** Quantitative PCR analysis of hepatic FGF9 in mice under *ad libitum*-fed, 24 hour-fasted, or 6 hour re-fed conditions ($n = 6/\text{group}$). **(F)** Representative Western blotting analysis of hepatic FGF9 in mice in **(E)**. All the data are presented as mean \pm SEM, * $p < 0.05$, ** $p < 0.01$, **** $p < 0.0001$, 2-tailed Student's t-test **(A–D)**, 1-way ANOVA **(E,F)**.

as shown in **Figures 2G,H**. The results suggest that FGF9 plays an important role in the hepatic lipid metabolism.

Knockdown of FGF9 Expression in Primary Hepatocyte Increased Cellular Triglyceride Contents

We next studied whether the effect of FGF9 deficiency on hepatic lipid metabolism is cell autonomous. We generated an adenovirus expressing FGF9-specific shRNA (Ad-shFGF9) and controlled adenovirus Ad-shCon. Primary hepatocytes treated with OA&PA, which stimulates cellular lipid synthesis, were infected with Ad-shFGF9 to observe the short-term effects of FGF9 deficiency on cellular lipid metabolism. As a result, the knockdown of FGF9 expression in primary hepatocytes increased lipid accumulation, as shown in **Figures 3A,B**.

Consistent with the aforementioned data obtained in DIO mice, we found that Ad-shFGF9 treatment increased the expression of several genes involved in lipogenesis such as ChREBP, Fasn, and PPAR γ in primary hepatocytes. The expression of lipid-coated proteins such as cidea and plin2 was also increased. However, the expression of genes related to fatty acid oxidation such as Cpt1a, CYP4a10, and Cyp4a14 was down-

regulated in primary hepatocytes infected with Ad-shFGF9. The Western blotting analysis confirmed real-time PCR results, as shown in **Figures 3C,D**. These results suggested that FGF9 regulating hepatic lipid metabolism is a cell-autonomous effect and FGF9 acts as an autocrine factor.

Overexpression of FGF9 Mediated by Adenovirus in Primary Hepatocyte Reduced Cellular Lipid Contents

Given that FGF9 knockdown increased cellular lipid accumulation, we next explored whether an increased expression of FGF9 in hepatocytes can reduce cellular lipid contents. To this end, the primary hepatocytes were infected with either Ad-FGF9 or Ad-GFP and followed by treatment with palmitic acid and oleic acid (OA&PA). As expected, cellular lipid accumulation induced by OA&PA was suppressed by Ad-FGF9 treatment (**Figures 4A,B**).

Correspondingly, Ad-FGF9 treatment decreased the expression of several genes involved in lipogenesis such as ChREBP, Fasn, and PPAR γ , and fatty acid transport, including CD36, in primary hepatocytes, whereas it increased the expression of genes related to fatty acid oxidation such as Cpt1a, CYP4A10, and Cyp4a14

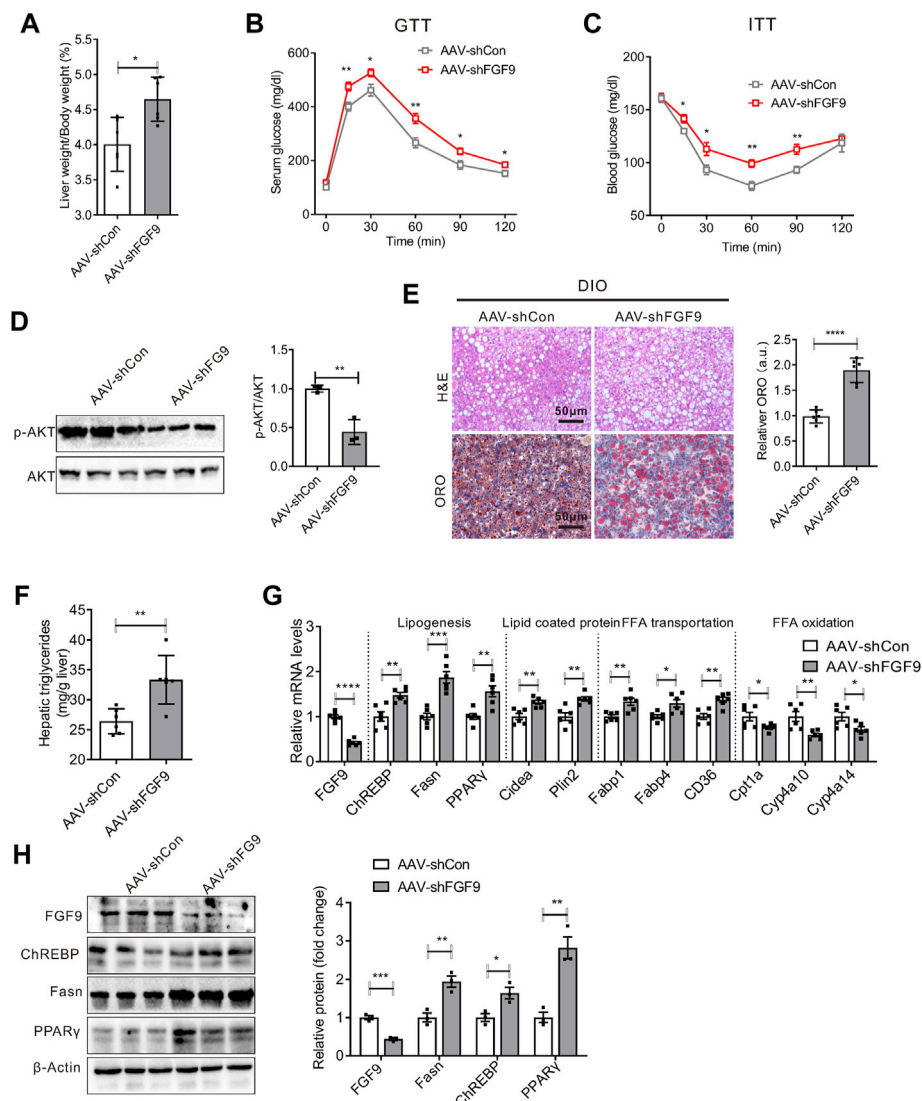


FIGURE 2 | Knockdown of FGF9 in the liver of DIO mice exacerbated fatty liver phenotype. **(A)** Ratio of liver weight to body weight in C57BL/6J mice injected with AAV-shCon or AAV-shFGF9. AAV-infected mice were then fed with a high-fat diet (HFD) for 8 weeks ($n = 6/\text{group}$). **(B,C)** Blood glucose levels during GTTs **(B)** and ITTs **(C)** performed in mice in **(A)** ($n = 6/\text{group}$). **(D)** Representative Western blotting analysis of phosphorylated and total AKT in the liver of mice in **(A)** 20 min after intraperitoneal injection of insulin (0.75 U/kg). **(E)** Representative H&E (top panel) and Oil Red O staining (bottom panel) of livers from mice in **(A)**. **(F)** Hepatic TG levels in mice **(A)** ($n = 6/\text{group}$). **(G)**, Quantitative PCR analysis of genes involved in lipid metabolism in the liver of mice in **(A)** ($n = 6/\text{group}$). **(H)** Representative Western blotting analysis of genes involved in lipid synthesis in mice as described in **(A)**. All the data are presented as mean \pm SEM, * $p < 0.05$, ** $p < 0.01$, *** $p < 0.001$, **** $p < 0.0001$, 2-way ANOVA **(B,C)**, 2-tailed Student's t -test **(A,D-H)**.

(Figure 4C). Meanwhile, the Western blotting analysis further confirmed these results (Figure 4D). The results suggested that the overexpression of FGF9 in primary hepatocyte reduced cellular lipid accumulation induced by OA&PA.

Adenovirus-Mediated FGF9 Overexpression in the Liver of Diet-Induced Obese Mice Alleviates Hepatic Steatosis

To further explore the effect of FGF9 overexpression on hepatic lipid metabolism, we injected Ad-FGF9 or Ad-GFP

(as a control) into chow or high-fat diet-fed C57BL/6J mice *via* the tail vein. As shown in **Supplementary Figure S2**, FGF9 overexpression in chow diet-fed mice did not significantly influence the systemic glucose metabolism or hepatic lipid metabolism.

However, the injection of Ad-FGF9 into DIO mice decreased the ratio of liver weight to body weight (Figure 5A). In contrast to the results obtained in AAV-shFGF9-infected DIO mice, Ad-FGF9 injection improves glucose intolerance as revealed by GTT experiments (Figure 5B), and enhanced insulin sensitivity, as revealed by

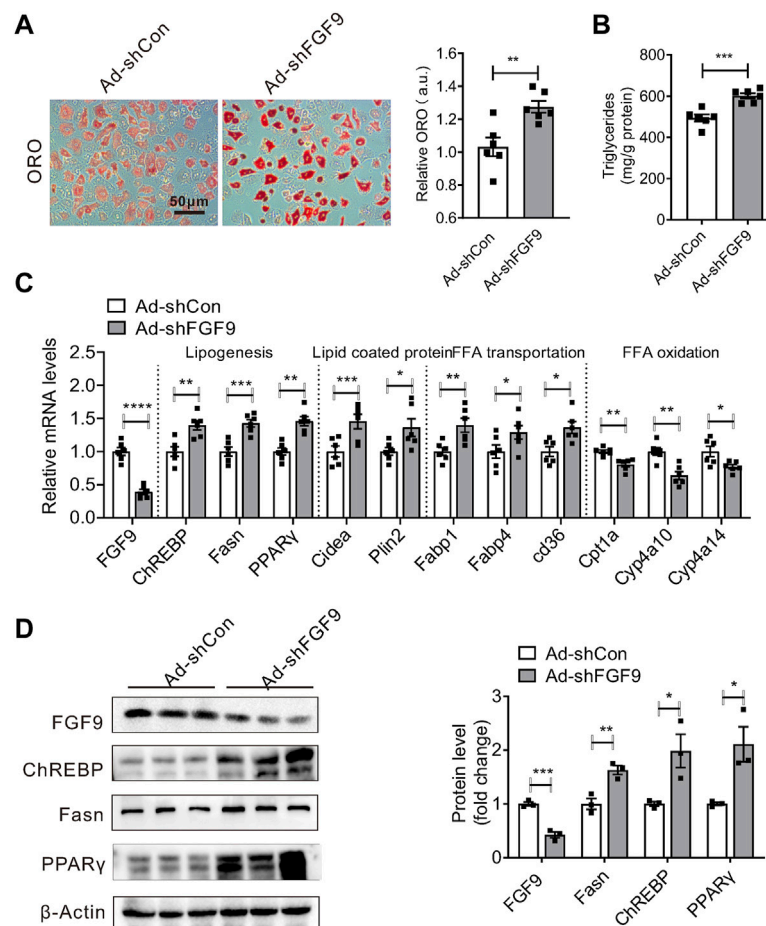


FIGURE 3 | Knockdown of FGF9 in primary hepatocyte increased cellular TG content. **(A)** Representative Oil Red O staining of primary hepatocyte treatment with OA & PA for 24 h, followed by infecting with Ad-shCon or Ad-shFGF9 for 12 h prior to harvest for further analysis. **(B)** TG levels in primary hepatocyte in **(A)**. **(C)** Quantitative PCR analysis of genes involved in lipid metabolism in primary hepatocytes in **(A)**. **(D)** Representative Western blotting analysis of genes involved in lipid synthesis in primary hepatocytes in **(A)**. All the data are represented as mean \pm SEM, * p < 0.05, ** p < 0.01, *** p < 0.001, **** p < 0.0001, 2-tailed Student's t-test **(A–D)**.

ITT experiments (**Figure 5C**), and enhanced hepatic insulin signaling (**Figure 5D**). Notably, histological analysis of liver sections (H&E and Oil Red O staining) indicated that the fatty liver phenotype was markedly alleviated in DIO mice injected with Ad-FGF9 (**Figure 5E**). The biochemical analysis confirmed the reduced hepatic triglyceride content in Ad-FGF9-treated DIO mice (**Figure 5F**). At the same time, the decreased ALT and AST levels in DIO mice injected with Ad-FGF9 indicate that the overexpression of FGF9 alleviated the liver injury induced by HFD (**Figures 5G,H**).

Consistent with the results obtained *in vitro*, Western blotting and real-time PCR analysis confirmed that FGF9 overexpression in the liver of DIO mice inhibited the expression of genes involved in lipogenesis and increased the expression of genes related to fatty acid oxidation (**Figures 5I,J**). These results clearly suggest that FGF9 regulates the hepatic lipid metabolisms in DIO mice.

Liver-Specific FGF9 Transgenic Mice Protected Against Hepatic Steatosis and Insulin Resistance Induced by HFD

To further confirm whether the overexpression of FGF9 inhibits NAFLD development induced by HFD, we generated liver-specific FGF9 transgenic mice (FGF9^{alb-cre}) by crossing Alb-Cre mice and FGF9 Rosa26 knockin mice. Alb-Cre mice express the Cre-recombinant gene under the control of the albumin gene promoter. The FGF9 Rosa26 knockin mice were generated by the insertion of FGF9 cDNA downstream of the Rosa26 promoter and a loxP-stop-loxP cassette. The Western blotting analysis confirmed the FGF9 overexpression in the liver of FGF9^{alb-cre} (**Figure 6A**). FGF9 Rosa26 knockin mice were used as control mice. Again, when mice were fed a chow diet, FGF9 transgene in the liver did not affect markedly the systemic glucose metabolism and hepatic lipid metabolism (**Supplementary Figure S3**). However, when mice were fed

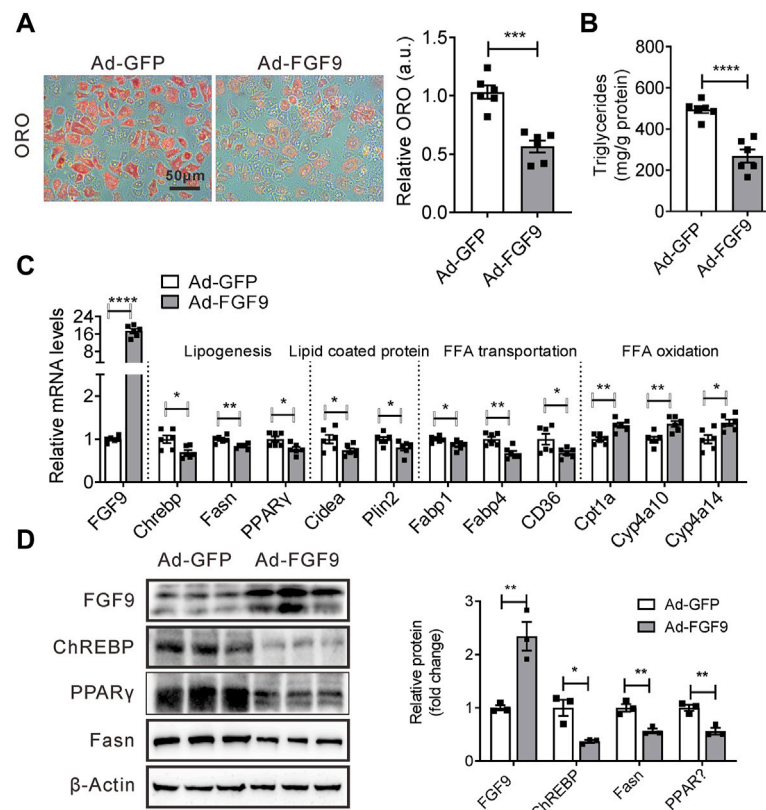


FIGURE 4 | Overexpression of FGF9 in primary hepatocyte reduced cellular TG contents. **(A)** Representative Oil Red O staining of primary hepatocyte infected with Ad-GFP or Ad-FGF9 for 12 h, followed by treatment with OA & PA for 24 h prior to harvest for further analysis. **(B)** TG levels in primary hepatocyte in **(A)**. **(C)** Quantitative PCR analysis of genes involved in lipid metabolism in primary hepatocytes in **(A)**. **(D)** Representative Western blotting analysis of genes involved in lipid synthesis in primary hepatocytes in **(A)**. All the data are represented as mean \pm SEM, * p < 0.05, ** p < 0.01, *** p < 0.001, **** p < 0.0001, 2-tailed Student's t-test **(A–D)**.

a high-fat diet, we observed that the ratio of liver weight to body weight in FGF9^{alb-cre} mice was lower than that of control mice (**Figure 6B**). Moreover, FGF9 transgene enhanced the insulin sensitivity and improved glucose intolerance in diet-induced obese FGF9^{alb-cre} mice when compared to the control mice (**Figures 6C–E**). Furthermore, lipid accumulation in the liver was reduced from FGF9^{alb-cre} mice, as revealed by H&E and Oil Red O staining analysis (**Figure 6F**), and biochemical analysis (**Figure 6G**). Consistently, FGF9 transgene decreased the levels of serum ALT and AST, further confirming that the overexpression of FGF9 can alleviate the liver injury induced by HFD (**Figure 6H**).

We also examined the expression of genes involved in lipid metabolism in the liver of FGF9 transgenic mice. Western blotting and real-time PCR data further confirmed that FGF9 transgene inhibited the expression of lipogenic genes, while it enhanced the expression of genes related to fatty acid oxidation (**Figures 6I,J**). Collectively, these results clearly suggested that liver-specific FGF9 transgenic mice were resistant to HFD-induced NAFLD.

DISCUSSION

Given the rising incidence and high prevalence of NAFLD, the absence of approved therapies is striking. Currently, lifestyle changes, weight loss, and exercise are the main treatments available to modify the disease process. Thus, there is an urgent need of new drugs for treatment of NAFLD and NASH (Tiniakos et al., 2010; Rotman and Sanyal, 2017).

Previous studies indicated that FGF9 is involved in multiple developmental processes (Colvin et al., 2001; Yin et al., 2011; Iwata et al., 2012). Recently two studies showed that FGF9 regulates browning of white adipocytes and is associated with human obesity (Sun et al., 2019; Shamsi et al., 2020). Sun et al. (2019) reported that FGF9 expression in adipose tissue is reduced upon cold exposure and FGF9 treatment inhibited browning of white adipocytes. However, Shamsi et al. reported that cold exposure induces FGF9 expression in adipose tissues and FGF9 strongly induced UCP1 expression in adipocytes and preadipocytes, which is independent of adipogenesis and involves the FGFR3-PGE2-EP2/4 signaling pathway. Thus, it appears that FGF9 exerts its metabolic effects in an autocrine manner.

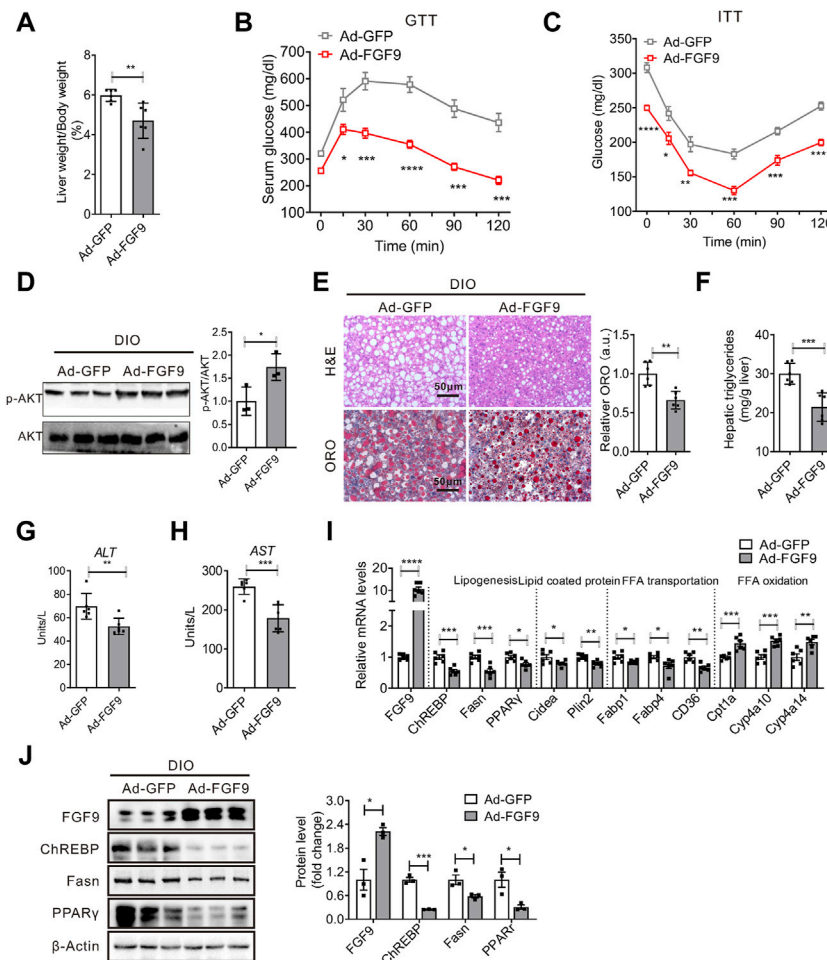


FIGURE 5 | Adenovirus-mediated FGF9 overexpression in the liver of DIO mice alleviated NAFLD. **(A)** Ratio of liver weight to body weight in DIO mice infected with Ad-GFP or Ad-FGF9 for 15 days ($n = 6/\text{group}$). **(B,C)** Blood glucose levels during GTTs and ITTs performed in **(A)** ($n = 6/\text{group}$). **(D)** Representative Western blotting analysis of phosphorylated and total AKT in the liver of mice in **(A)** 20 min after intraperitoneal injection of insulin (0.75 U/kg). **(E)** Representative H&E staining (top panel) and Oil Red O staining (bottom panel) of liver sections from the mice in **(A)**. **(F)** Hepatic TG levels in mice in **(A)** ($n = 6/\text{group}$). **(G,H)** Plasma ALT and AST levels in mice in **(A)** ($n = 6/\text{group}$). **(I)** Quantitative PCR analysis of genes involved in lipid metabolism in the liver of mice in **(A)** ($n = 6/\text{group}$). **(J)** Representative Western blotting analysis of genes involved in lipid synthesis in mice in **(A)**. All the data are represented as mean \pm SEM, $^*p < 0.05$, $^{**}p < 0.01$, $^{***}p < 0.001$, 2-way ANOVA **(B,C)**, 2-tailed Student's *t*-test **(A,D–J)**.

In the present study, we showed that hepatic FGF9 expression is upregulated in mice with the fatty liver, including HFD-induced obese and ob/ob mice relative to their respective control mice. Of note, we detected the two bands of FGF9 protein in livers of DIO mice, as revealed by Western blotting analysis, possibly due to the alternate splicing of FGF9 mRNA in DIO mice or different antibodies we used to detect an unspecific protein. Currently, two bands of FGF9 in nature remain unclear. Moreover, fasting also induces FGF9 expression in the mouse liver. Furthermore, FGF9 knockdown in the primary hepatocyte treated with OA and PA increased cellular lipid accumulation. Consistently, FGF9 knockdown in the liver of HFD-induced obese mice aggravated the symptoms of hepatic steatosis. These data suggest that FGF9 regulates hepatic lipid metabolism in an autocrine manner, as that observed in adipose tissues (Sun et al., 2019; Shamsi et al., 2020). Notably,

FGF9 knockdown in the liver of chow diet-fed mice did not significantly change hepatic TG contents, indicating FGF9 exerts its effects in the context of high-fat stress. FGF9 expression is induced in the liver of both DIO mice and ob/ob mice. The overexpression of FGF9 in the liver of DIO mice improved insulin sensitivity and fatty liver phenotype. Whether FGF9 has same effects in ob/ob mice remains unexplored. Additionally, although our study shows that FGF9 regulates hepatic triglycerides contents in DIO mice, we did not characterize the lipid species influenced by FGF9. Ceramides are the best studied sphingolipids in relation to insulin resistance (Meikle and Summers, 2017). Thus, whether and how FGF9 influences ceramides contents deserve further study.

Multiple factors contribute to fatty liver development. Increased TG accumulation in the liver reflects an input/output imbalance of hepatic FFA metabolism. An increase in

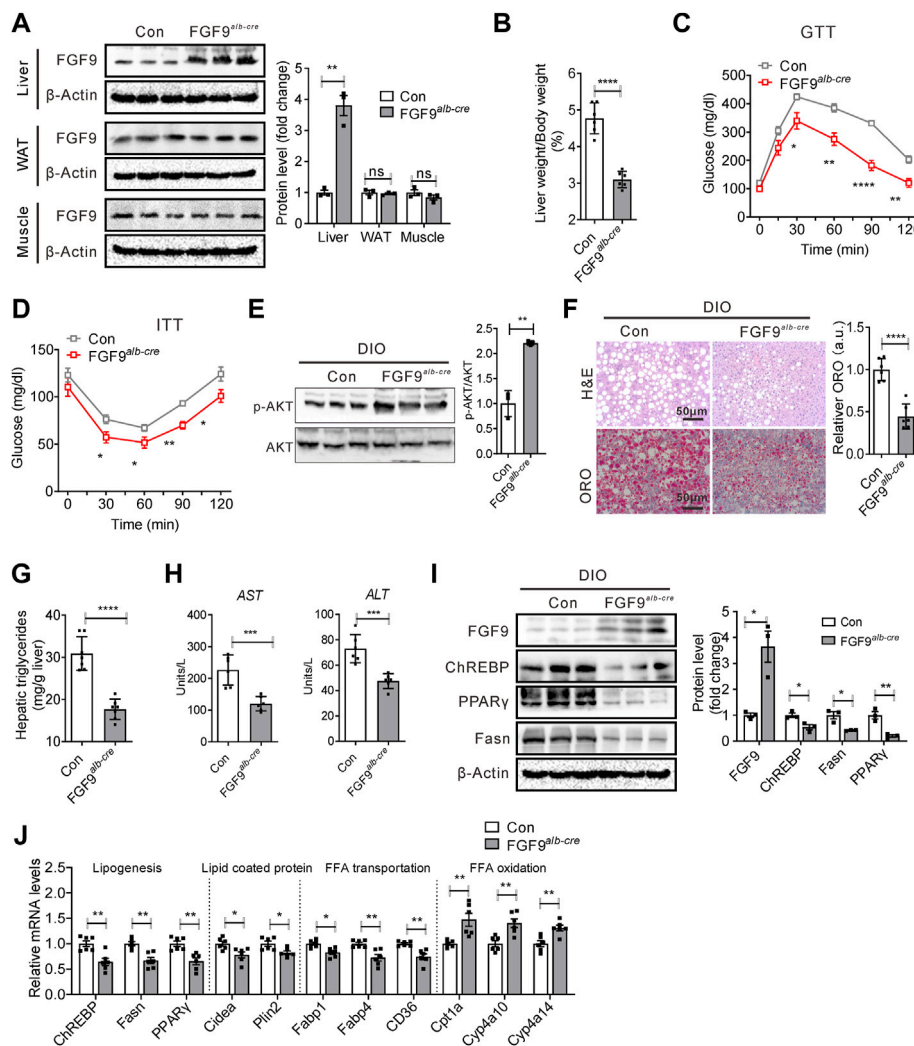


FIGURE 6 | Liver-specific FGF9 transgene protected mice against NAFLD induced by HFD. **(A)** Representative Western blotting analysis of FGF9 protein levels in the liver, white adipose tissue (WAT), and muscle of FGF9 Rosa26 knockin mice (control) and liver-specific FGF9 transgenic mice (FGF9^{alb-cre}). Data were normalized to β -actin. **(B)** Ratio of liver weight to body weight in control and FGF9^{alb-cre} mice fed with a HFD for 3 months ($n = 6$ /group). **(C,D)** Blood glucose levels during GTTs and ITTs performed in mice in **(B)** ($n = 6$ /group). **(E)** Representative Western blotting analysis of phosphorylated and total AKT in the liver of mice in **(B)** 20 min after intraperitoneal injection of insulin (0.75 U/kg). **(F)** Representative H&E staining and Oil Red O staining of livers from the mice in **(B)**. **(G)** Hepatic TG levels in mice in **(B)** ($n = 6$ /group). **(H)** Plasma ALT and AST levels in mice in **(B)** ($n = 6$ /group). **(I)** Representative Western blotting analysis of genes involved in lipid synthesis in the liver of mice in **(B)**. **(J)** Quantitative PCR analysis of genes involved in lipid metabolism in the liver of mice in **(B)** ($n = 6$ /group). All the data are represented as mean \pm SEM. * $p < 0.05$, ** $p < 0.01$, *** $p < 0.001$, **** $p < 0.0001$, 2-way ANOVA **(C,D)**, 2-tailed Student's t -test **(A,B,E-J)**.

FFA delivery to the liver due to adipose tissue insulin resistance, and *de novo* lipogenesis driven by the hyperinsulinemia might cause fatty liver disease (Rotman and Sanyal, 2017). In contrast, the decrease in VLDL secretion or fatty acid β -oxidation also induces the fatty liver phenotype (Fabbrini et al., 2008; Zhang et al., 2013). In the present study, we found that FGF9 regulates hepatic lipid metabolism with several distinct mechanisms. FGF9 inhibits cellular lipid synthesis by repressing the expression of ChREBP, Fasn, and PPAR γ , while it enhances fatty acid oxidation by inducing target genes of PPAR α , including Cpt1a, Cyp4a11, and Cyp4a14. Of note, FGF9 did not influence the protein levels of PPAR α (data not shown). We speculated that FGF9 might enhance PPAR α transcriptional activity via posttranslational

modification (Hinds et al., 2016) or increase the contents of its endogenous ligands. In addition, how FGF9 represses the expression of ChREBP and PPAR γ remains unclear. Further studies are required to clarify this question.

FGF21, another member of FGF family, acting as an endocrine factor, is also induced directly by PPAR α in the mouse liver in response to fasting and PPAR α agonists. Induced FGF21, in turn, stimulates fatty acid oxidation and ketogenesis in the liver (Badman et al., 2007; Inagaki et al., 2007). Moreover, the adenoviral knockdown of FGF21 in the liver of mice fed a high-fat, low carbohydrate ketogenic diet (KD) caused the fatty liver and reduced serum ketones (Badman et al., 2007). Furthermore, injection of recombinant FGF21 proteins into DIO

mice reversed hepatic steatosis due to FGF21 inhibition of hepatic lipogenesis (Xu et al., 2009). Our study indicates that FGF9 regulates hepatic lipid metabolism in an autocrine manner. Thus, FGF9 regulates hepatic lipid metabolism with similar mechanisms as FGF21. Fasting-induced FGF9 promotes hepatic fatty acid oxidation; meanwhile, it also inhibits hepatic lipogenesis, thereby improving the fatty liver phenotype.

NAFLD is the hepatic manifestation of the metabolic syndrome and becoming increasingly common with the rising incidence of obesity, diabetes, hyperlipidemia, and cardiovascular disease worldwide. Thus, the treatment of fatty liver should exhibit wider systemic effects and fit into a larger treatment of the syndrome (Ritchie et al., 2020). Our results suggest the beneficial effect of FGF9 on NAFLD, and targeting the FGF9 signaling pathway might be exploited to treat NAFLD or NASH. Of note, FGF9 has potential mitogenic activity (Tsai et al., 2002), which may lead to safety concerns. Fortunately, Shamsi et al. (2020) generated a modified FGF9 protein carrying K168Q/R173V/R177Q triple mutations in its HS-binding sites. This mutant reduced the molecule's mitogenic potential without impacting its metabolic function. Thus, this FGF9 mutant might have potential for treatment of NAFLD.

MATERIALS AND METHODS

Animal Treatment

Male C57BL/6J, ob/ob, db/db, and db/m mice at 8 weeks of age were purchased from the Model Animal Research Center of Nanjing University (Nanjing, China) and housed and maintained in 12 h light and dark photoperiods with a regular unrestricted diet.

For adenovirus infection, 8-week-old male C57BL/6J mice were fed a chow diet or HFD (D12492, Jiangsu Xietong Bio-engineering Co., Ltd., China) for 3 months, followed by injection with $1-2 \times 10^9$ PFU per recombinant virus (Ad-GFP or Ad-FGF9) via the tail vein. Mice were fasted for 6 h and sacrificed for further analysis, 15 days after infection.

For AAV infection, mice were injected with 5×10^{11} vg of the AAV-shFGF9 or AAV-shCon via the tail vein, followed by feeding a chow diet or HFD for 8 weeks. Then, mice were sacrificed for further analysis.

FGF9 Rosa26 knockin mice were generated by the insertion of FGF9 cDNA downstream of the Rosa26 promoter and a loxP-stop-loxP cassette at Beijing Biocytogen Co., Ltd., and Alb-Cre mice (express the Cre-recombinant gene under the control of the albumin gene promoter) were provided by Hongbing Zhang (Institute of Basic Medical Sciences, Peking Union Medical College), and then liver-specific FGF9 transgenic mice were obtained by crossing Alb-Cre mice to FGF9 Rosa26 knockin mice. FGF9 Rosa26 knockin mice were used as controls. All the mice were fed on a chow diet or HFD for 3 months.

All the protocol related with animals was approved by the Animal Care and Use Committee of Tianjin Medical University (TMUaMEC) and conformed to criteria outlined in the National Institutes of Health (NIH; Bethesda, MD) Guide for the Care and Use of Laboratory Animals.

Culture of Mouse Primary Hepatocyte and Adenoviral Infections

Briefly, 8-week-old male mice were anesthetized with bromethol and perfused with 0.5 mg/ml type II collagenase (Sigma-Aldrich) via the inferior vena cava to obtain hepatocytes as previously described (Wang et al., 2010). The cells were seeded at 6 well collagen-coated plates, and cultured with RPMI 1640 medium (H10394; Invitrogen) containing 10% (v/v) FBS (ExCell Bio, Shanghai, China), 50 units/ml penicillin and 50 µg/ml streptomycin (Penicillin-Streptomycin Solution, 100X, Solarbio Life Sciences, Beijing, China). After cell attachment for 4 h, a fresh medium was added after the unattached cells were washed away with PBS. For the adenovirus infection, primary hepatocytes were treated with 0.5 mM OA (CAS No. 112-80-1, Selleck) and 0.25 mM PA (CAS No. 57-10-3, Selleck) for 24 h before (Ad-shCon and Ad-shFGF9, MOI = 100) or after (Ad-GFP and Ad-FGF9, MOI = 100) adenovirus particle infection for 12 h.

Triglyceride Content

Liver tissue of 100 mg was homogenized in 1 ml of 5% Nonidet P-40 dissolved in water, heated to 95°C for 5 min, centrifuged for 2 min at 13,000×g. A fluorometric assay kit was used to measure triglyceride levels according to the manufacturer's guidelines (Applygen Technologies, Inc., Beijing, China). Finally, the levels of triglyceride levels were normalized to the weight of liver and expressed as mg of triglyceride/g of tissue weight.

AAV-shRNA Viral Production and Purification

For the FGF9 knockdown studies, AAV gene delivery vectors were constructed by cloning FGF9 shRNA sequences into an AAV-shRNA-Ctrl plasmid (Addgene #85741, Watertown, MA), and AAV-shRNA-Ctrl encoding a nontargeting shRNA, was used as a control virus (AAV-shCon). For AAV-shFGF9, we generated the shRNA that would target FGF9 by using the Dharmacon siDESIGN center (<http://www.dharmacon.com>) as described (Yu et al., 2002), the antisense-loop-sense oligonucleotides synthesized, annealed, and subcloned into the Bbs1 and Xba1 sites of the AAV-shRNA-Ctrl plasmid. The AAV2/8 virus was generated by transfecting HEK-293T cells with pAAV2 insert containing either shRNA control or shRNA-FGF9 under the control of the mouse U6 promoter, pAAV2/8 (Addgene #112864, Watertown, MA) packaging plasmid expressing Rep/Cap genes, and pAdDeltaF6 (#112867).

The three plasmids were used for viral production with a triple-transfection, and the virus was purified according to the modified published methods (Challis et al., 2019). Briefly, triple plasmids were co-transfected to HEK-293T cells, and the cell culture medium was harvested at 72, 96, and 120 h. After purification by an iodixanol step gradient, the fraction containing the virus was desalted on 100 K concentrators with PBS as the diluent. AAV titers were determined by qPCR using primers targeting CMV. Each virus titer was calculated in genomes/ml with AAV-shRNA-Ctrl Luciferase at 2.4×10^{13} vg/

ml, AAV-shFGF9 at 2.6×10^{13} vg/ml. The viruses were aliquoted into siliconized tubes and stored at -80°C .

The primers used for constructing AAV-shFGF9 are as follows:

shRNA FGF9 F: 5'-GATCCGCAGGACTGGATTTCATTTAGTTCAAGAGACTAAATGAAATCCAGTCTGCTTTTTC TCGAGG-3';

shRNA FGF9 R: 5'-AATTCCTCGAGAAAAAGCAGGACTGGATTTCATTTAGTCTCTTGAATAAATGAAATCCAGTCTGCG-3'.

Recombinant Adenovirus Production and Purification

Adenoviruses expressing FGF9 was prepared as previously described (Luo et al., 2007). Briefly, the full-length mouse FGF9 gene was first cloned into the pAd-Track-CMV shuttle vector. The resultant plasmid was linearized by digesting with restriction endonuclease PmeI and subsequently transformed into competent cells, which were BJ5183 derivatives containing the adenoviral backbone plasmid pAdEasy-1. Recombinants were selected for kanamycin resistance, and recombination was confirmed by restriction endonuclease analyses. Overall, the confirmed recombinant adenovirus plasmids were digested with PacI to liberate both inverted terminal repeats and transfected into HEK-293A cells. Recombinant adenoviruses were typically generated within 14–20 days. Ad-shCon and Ad-shFGF9 were purchased from Hanbio Biotechnology Co., Ltd.

Glucose Tolerance Tests and Insulin Tolerance Tests

For the GTTs, mice were injected with glucose (25% glucose, 1 g/kg) intraperitoneally after a 16-h fasting. For the ITTs, mice were fasted for 6 h and injected with insulin (0.75 U/kg; Novolinhuman insulin) intraperitoneally. Blood glucose levels were recorded using a glucose monitor (OneTouch; LifeScan, Inc., Milpitas, CA) at 0, 15, 30, 60, 90 and 120 min after glucose or insulin injection.

Analysis of Hepatic Insulin Signaling

Mice were fasted for 16 h and intraperitoneally injected with insulin (0.75 U/kg). After twenty minutes, mice were euthanized, and the liver tissues were quickly excised, snap-frozen in liquid nitrogen, and stored at -80°C until use. For the evaluation of insulin signaling, primary antibodies against Ser-473-AKT (Cat No. AP0655, ABclonal) and total AKT (Cat No. A3145, ABclonal) were used for Western blotting analysis.

Oil Red O Staining

The livers were mounted and frozen in Tissue-Tek O.C.T and sectioned at $5\ \mu\text{m}$. The frozen sections were air-dried, fixed in 10% neutral-buffered formalin, rinsed in tap water followed by 60% isopropanol, and stained in Oil Red O solution for 15 min. Then, the sections were further rinsed in 60% isopropanol, and the nuclei were stained with hematoxylin followed by aqueous mounting and cover slipping. For primary hepatocytes, the cells were fixed in 10% neutral-buffered formalin, rinsed in tap water

followed by 60% isopropanol, and stained in the Oil Red O solution for 15 min.

All the sections were imaged using a color Axiocam105 camera with Zen 2 software attached to a Zeiss Axioplan microscope. The images were analyzed using ImageJ software.

Hematoxylin-Eosin Staining

For H&E staining, liver tissues were fixed in 10% neutral-buffered formalin, embedded in paraffin, and cut into $5\ \mu\text{m}$ sections. The sections were stained with hematoxylin and eosin followed by the manufacturer's instructions (Polysciences, #24901). Briefly, the sections were deparaffinized and rehydrated in distilled water, followed by staining. Finally, the samples were dehydrated, cleared, and mounted, followed by imaging using light microscopy.

Western Blotting Analysis

The homogenate of liver tissue or cells was prepared in lysis buffer (20 mM Tris-Cl pH7.5, 140 mM NaCl, 1 mM CaCl_2 and MgCl_2 , 10 mM NaF, 1% NP-40, 10% glycerol, 2 mM Na-Vanadate, and 1 mM PMSF) supplemented with complete Protease Inhibitor Cocktail (cOmplete™, Sigma-Aldrich, Dallas, TX) for 30 min, centrifuged at 12,000 rpm at 4°C for 15 min. The protein samples were resolved by SDS-polyacrylamide gel electrophoresis and electrophoretically transferred to PVDF membranes. The membranes were blocked at room temperature for 2 h in 5% defatted milk dissolved in TBST (10 mM Tris-HCl, pH 7.4, and 150 mM NaCl), incubated at 4°C for overnight with the following antibodies: PPAR γ (#AF6284, Affinity, 1:1000), FGF9 (#A6374, ABclonal, 1:500 and #ab206408, Abcam, 1:500), ChREBP (#A7630, ABclonal, 1:1000), Fasn (#DF6106, Affinity, 1:1000), or β -Actin (#AF7018, 1:10000), washed in TBST (0.1% Tween 20) for 15 min (repeated three times) and incubated with a goat anti-mouse (# S0002, Affinity) or goat anti-rabbit (# S0001, Affinity) IgG (H + L) HRP secondary antibody (1:5000 dilution in TBS) for 1 h at RT. Immunoreactivity was visualized and quantified by infrared scanning using the Odyssey system (LI-COR Biosciences).

Quantitative PCR

Total RNA from either the mouse livers or the primary hepatocytes were extracted using the TRIzol-based method (Invitrogen). cDNA was prepared using the Applied Biosystems' High-Capacity cDNA Reverse-Transcription Kit. Quantitative real-time reverse-transcriptase PCR (qRT-PCR) was performed using the SYBR Green I Q-PCR kit (TransGen) on a Bio-Rad IQ5 system. All gene expression data were normalized to 36B4 expression levels. All primer sequences are shown in **Supplementary Table S1**.

STATISTICAL ANALYSIS

The quantitative data are represented as the mean \pm SEM. A two-tailed, unpaired Student's t-test was used for the pairwise comparison of genotypes or treatments. 1-way ANOVA and 2-

way ANOVA were used when comparing 3 or more groups, as indicated in the figure legends. The graphs and analysis were performed using GraphPad Prism 7.0 software. $p < 0.05$ was considered statistically significant.

DATA AVAILABILITY STATEMENT

The original contributions presented in the study are included in the article/**Supplementary Material**, further inquiries can be directed to the corresponding authors.

ETHICS STATEMENT

The animal study was reviewed and approved by the Animal Care and Use Committee of Tianjin Medical University.

AUTHOR CONTRIBUTIONS

YC and JZ designed research studies. FZ, LZ and JH conducted experiments; FZ and MZ analyzed data; and YC wrote the manuscript. YC is the guarantor of this work and

had full access to all of the data in the study and takes responsibility for the integrity of the data and the accuracy of the data analysis.

FUNDING

This work was supported by the National Natural Science Foundation of China (Grants 81825004 and 81730024), the National Key Research and Development Program of China (2018YFA0800601), and the Scientific and Technological Research Project of Xinjiang Production and Construction Corps (Grant 2021AB028).

SUPPLEMENTARY MATERIAL

The Supplementary Material for this article can be found online at: <https://www.frontiersin.org/articles/10.3389/fphar.2022.850128/full#supplementary-material>

Supplementary Table S1 | List of specific primers used for real-time quantitative PCR gene expression analysis.

REFERENCES

- Badman, M. K., Pissios, P., Kennedy, A. R., Koukos, G., Flier, J. S., and Maratos-Flier, E. (2007). Hepatic Fibroblast Growth Factor 21 Is Regulated by PPARalpha and Is a Key Mediator of Hepatic Lipid Metabolism in Ketotic States. *Cell Metab* 5 (6), 426–437. doi:10.1016/j.cmet.2007.05.002
- Beenken, A., and Mohammadi, M. (2009). The FGF Family: Biology, Pathophysiology and Therapy. *Nat. Rev. Drug Discov.* 8 (3), 235–253. doi:10.1038/nrd2792
- Benhamed, F., Denechaud, P. D., Lemoine, M., Robichon, C., Moldes, M., Bertrand-Michel, J., et al. (2012). The Lipogenic Transcription Factor ChREBP Dissociates Hepatic Steatosis from Insulin Resistance in Mice and Humans. *J. Clin. Invest.* 122 (6), 2176–2194. doi:10.1172/jci41636
- Browning, J. D., and Horton, J. D. (2004). Molecular Mediators of Hepatic Steatosis and Liver Injury. *J. Clin. Invest.* 114 (2), 147–152. doi:10.1172/jci22422
- Brunt, E. M. (2010). Pathology of Nonalcoholic Fatty Liver Disease. *Nat. Rev. Gastroenterol. Hepatol.* 7 (4), 195–203. doi:10.1038/nrgastro.2010.21
- Challis, R. C., Ravindra Kumar, S., Chan, K. Y., Challis, C., Beadle, K., Jang, M. J., et al. (2019). Systemic AAV Vectors for Widespread and Targeted Gene Delivery in Rodents. *Nat. Protoc.* 14 (2), 379–414. doi:10.1038/s41596-018-0097-3
- Colvin, J. S., Green, R. P., Schmahl, J., Capel, B., and Ornitz, D. M. (2001). Male-to-female Sex Reversal in Mice Lacking Fibroblast Growth Factor 9. *Cell* 104 (6), 875–889. doi:10.1016/s0092-8674(01)00284-7
- Degrolamo, C., Sabbà, C., and Moschetta, A. (2016). Therapeutic Potential of the Endocrine Fibroblast Growth Factors FGF19, FGF21 and FGF23. *Nat. Rev. Drug Discov.* 15 (1), 51–69. doi:10.1038/nrd.2015.9
- Dentin, R., Benhamed, F., Hainault, I., Fauveau, V., Foulle, F., Dyck, J. R., et al. (2006). Liver-specific Inhibition of ChREBP Improves Hepatic Steatosis and Insulin Resistance in Ob/ob Mice. *Diabetes* 55 (8), 2159–2170. doi:10.2337/db06-0200
- Diraion, F., Moulin, P., and Beylot, M. (2003). Contribution of Hepatic De Novo Lipogenesis and Reesterification of Plasma Non Esterified Fatty Acids to Plasma Triglyceride Synthesis during Non-alcoholic Fatty Liver Disease. *Diabetes Metab.* 29 (5), 478–485. doi:10.1016/s1262-3636(07)70061-7
- Donnelly, K. L., Smith, C. I., Schwarzenberg, S. J., Jessurun, J., Boldt, M. D., and Parks, E. J. (2005). Sources of Fatty Acids Stored in Liver and Secreted via Lipoproteins in Patients with Nonalcoholic Fatty Liver Disease. *J. Clin. Invest.* 115 (5), 1343–1351. doi:10.1172/jci23621
- Fabbri, E., Mohammed, B. S., Magkos, F., Korenblat, K. M., Patterson, B. W., and Klein, S. (2008). Alterations in Adipose Tissue and Hepatic Lipid Kinetics in Obese Men and Women with Nonalcoholic Fatty Liver Disease. *Gastroenterology* 134 (2), 424–431. doi:10.1053/j.gastro.2007.11.038
- Hinds, T. D., Jr., Burns, K. A., Hosick, P. A., McBeth, L., Nestor-Kalinowski, A., Drummond, H. A., et al. (2016). Biliverdin Reductase A Attenuates Hepatic Steatosis by Inhibition of Glycogen Synthase Kinase (GSK) 3β Phosphorylation of Serine 73 of Peroxisome Proliferator-Activated Receptor (PPAR) α. *J. Biol. Chem.* 291 (48), 25179–25191. doi:10.1074/jbc.M116.731703
- Inagaki, T., Dutchak, P., Zhao, G., Ding, X., Gautron, L., Parameswara, V., et al. (2007). Endocrine Regulation of the Fasting Response by PPARalpha-Mediated Induction of Fibroblast Growth Factor 21. *Cell Metab* 5 (6), 415–425. doi:10.1016/j.cmet.2007.05.003
- Iwata, J., Tung, L., Urata, M., Hacia, J. G., Pelikan, R., Suzuki, A., et al. (2012). Fibroblast Growth Factor 9 (FGF9)-Pituitary Homeobox 2 (PITX2) Pathway Mediates Transforming Growth Factor β (TGFβ) Signaling to Regulate Cell Proliferation in Palatal Mesenchyme during Mouse Palatogenesis. *J. Biol. Chem.* 287 (4), 2353–2363. doi:10.1074/jbc.M111.280974
- Jois, T., and Sleeman, M. W. (2017). The Regulation and Role of Carbohydrate Response Element-Binding Protein in Metabolic Homeostasis and Disease. *J. Neuroendocrinol.* 29 (10). doi:10.1111/jne.12473
- Lefebvre, P., Chinetti, G., Fruchart, J. C., and Staels, B. (2006). Sorting Out the Roles of PPAR Alpha in Energy Metabolism and Vascular Homeostasis. *J. Clin. Invest.* 116 (3), 571–580. doi:10.1172/jci27989
- Leone, T. C., Weinheimer, C. J., and Kelly, D. P. (1999). A Critical Role for the Peroxisome Proliferator-Activated Receptor Alpha (PPARalpha) in the Cellular Fasting Response: the PPARalpha-Null Mouse as a Model of Fatty Acid Oxidation Disorders. *Proc. Natl. Acad. Sci. U S A.* 96 (13), 7473–7478. doi:10.1073/pnas.96.13.7473
- Luo, J., Deng, Z. L., Luo, X., Tang, N., Song, W. X., Chen, J., et al. (2007). A Protocol for Rapid Generation of Recombinant Adenoviruses Using the AdEasy System. *Nat. Protoc.* 2 (5), 1236–1247. doi:10.1038/nprot.2007.135
- Matsusue, K., Haluzik, M., Lambert, G., Yim, S. H., Gavrilova, O., Ward, J. M., et al. (2003). Liver-specific Disruption of PPARgamma in Leptin-Deficient Mice Improves Fatty Liver but Aggravates Diabetic Phenotypes. *J. Clin. Invest.* 111 (5), 737–747. doi:10.1172/jci17223
- Meikle, P. J., and Summers, S. A. (2017). Sphingolipids and Phospholipids in Insulin Resistance and Related Metabolic Disorders. *Nat. Rev. Endocrinol.* 13 (2), 79–91. doi:10.1038/nrendo.2016.169

- Ritchie, M., Hanounieh, I. A., Nouredin, M., Rolph, T., and Alkhouri, N. (2020). Fibroblast Growth Factor (FGF)-21 Based Therapies: A Magic Bullet for Nonalcoholic Fatty Liver Disease (NAFLD)? *Expert Opin. Investig. Drugs* 29 (2), 197–204. doi:10.1080/13543784.2020.1718104
- Rotman, Y., and Sanyal, A. J. (2017). Current and Upcoming Pharmacotherapy for Non-alcoholic Fatty Liver Disease. *Gut* 66 (1), 180–190. doi:10.1136/gutjnl-2016-312431
- Shamsi, F., Xue, R., Huang, T. L., Lundh, M., Liu, Y., Leiria, L. O., et al. (2020). FGF6 and FGF9 Regulate UCP1 Expression Independent of Brown Adipogenesis. *Nat. Commun.* 11 (1), 1421. doi:10.1038/s41467-020-15055-9
- Shen, L., Cui, A., Xue, Y., Cui, Y., Dong, X., Gao, Y., et al. (2014). Hepatic Differentiated Embryo-Chondrocyte-Expressed Gene 1 (Dec1) Inhibits Sterol Regulatory Element-Binding Protein-1c (Srebp-1c) Expression and Alleviates Fatty Liver Phenotype. *J. Biol. Chem.* 289 (34), 23332–23342. doi:10.1074/jbc.M113.526343
- Sun, Y., Wang, R., Zhao, S., Li, W., Liu, W., Tang, L., et al. (2019). FGF9 Inhibits Browning Program of white Adipocytes and Associates with Human Obesity. *J. Mol. Endocrinol.* 62 (2), 79–90. doi:10.1530/JME-18-0151
- Tiniakos, D. G., Vos, M. B., and Brunt, E. M. (2010). Nonalcoholic Fatty Liver Disease: Pathology and Pathogenesis. *Annu. Rev. Pathol.* 5, 145–171. doi:10.1146/annurev-pathol-121808-102132
- Tontonoz, P., Hu, E., Graves, R. A., Budavari, A. I., and Spiegelman, B. M. (1994). mPPAR Gamma 2: Tissue-specific Regulator of an Adipocyte Enhancer. *Genes Dev.* 8 (10), 1224–1234. doi:10.1101/gad.8.10.1224
- Tsai, S. J., Wu, M. H., Chen, H. M., Chuang, P. C., and Wing, L. Y. (2002). Fibroblast Growth Factor-9 Is an Endometrial Stromal Growth Factor. *Endocrinology* 143 (7), 2715–2721. doi:10.1210/endo.143.7.8900
- Wang, R., Kong, X., Cui, A., Liu, X., Xiang, R., Yang, Y., et al. (2010). Sterol-regulatory-element-binding Protein 1c Mediates the Effect of Insulin on the Expression of Cidea in Mouse Hepatocytes. *Biochem. J.* 430 (2), 245–254. doi:10.1042/bj20100701
- Xu, J., Lloyd, D. J., Hale, C., Stanislaus, S., Chen, M., Sivits, G., et al. (2009). Fibroblast Growth Factor 21 Reverses Hepatic Steatosis, Increases Energy Expenditure, and Improves Insulin Sensitivity in Diet-Induced Obese Mice. *Diabetes* 58 (1), 250–259. doi:10.2337/db08-0392
- Yin, Y., Wang, F., and Ornitz, D. M. (2011). Mesothelial- and Epithelial-Derived FGF9 Have Distinct Functions in the Regulation of Lung Development. *Development* 138 (15), 3169–3177. doi:10.1242/dev.065110
- Yu, J. Y., DeRuiter, S. L., and Turner, D. L. (2002). RNA Interference by Expression of Short-Interfering RNAs and Hairpin RNAs in Mammalian Cells. *Proc. Natl. Acad. Sci. U S A.* 99 (9), 6047–6052. doi:10.1073/pnas.092143499
- Zhang, H., Chen, Q., Yang, M., Zhu, B., Cui, Y., Xue, Y., et al. (2013). Mouse KLF11 Regulates Hepatic Lipid Metabolism. *J. Hepatol.* 58 (4), 763–770. doi:10.1016/j.jhep.2012.11.024

Conflict of Interest: The authors declare that the research was conducted in the absence of any commercial or financial relationships that could be construed as a potential conflict of interest.

Publisher's Note: All claims expressed in this article are solely those of the authors and do not necessarily represent those of their affiliated organizations, or those of the publisher, the editors, and the reviewers. Any product that may be evaluated in this article, or claim that may be made by its manufacturer, is not guaranteed or endorsed by the publisher.

Copyright © 2022 Zhao, Zhang, Zhang, Huang, Zhang and Chang. This is an open-access article distributed under the terms of the Creative Commons Attribution License (CC BY). The use, distribution or reproduction in other forums is permitted, provided the original author(s) and the copyright owner(s) are credited and that the original publication in this journal is cited, in accordance with accepted academic practice. No use, distribution or reproduction is permitted which does not comply with these terms.



Revealing the Mechanism of Huazhi Rougan Granule in the Treatment of Nonalcoholic Fatty Liver Through Intestinal Flora Based on 16S rRNA, Metagenomic Sequencing and Network Pharmacology

OPEN ACCESS

Edited by:

Ana Blas-García,
University of Valencia, Spain

Reviewed by:

Yu Zhao,
Shanghai University of Traditional
Chinese Medicine, China
Wei Zhong,
University of North Carolina at
Greensboro, United States

*Correspondence:

Guoliang Cheng
cgl.yb@163.com
Yanfang Mou
Incattleya@163.com
Jiarui Wu
exogamy@163.com

Specialty section:

This article was submitted to
Gastrointestinal and Hepatic
Pharmacology,
a section of the journal
Frontiers in Pharmacology

Received: 14 February 2022

Accepted: 16 March 2022

Published: 26 April 2022

Citation:

Liu Y, Tan Y, Huang J, Wu C, Fan X,
Stalin A, Lu S, Wang H, Zhang J,
Zhang F, Wu Z, Li B, Huang Z, Chen M,
Cheng G, Mou Y and Wu J (2022)
Revealing the Mechanism of Huazhi
Rougan Granule in the Treatment of
Nonalcoholic Fatty Liver Through
Intestinal Flora Based on 16S rRNA,
Metagenomic Sequencing and
Network Pharmacology.
Front. Pharmacol. 13:875700.
doi: 10.3389/fphar.2022.875700

Yingying Liu¹, Yingying Tan¹, Jiaqi Huang¹, Chao Wu¹, Xiaotian Fan¹, Antony Stalin²,
Shan Lu¹, Haojia Wang¹, Jingyuan Zhang¹, Fanqin Zhang¹, Zhishan Wu¹, Bing Li³,
Zhihong Huang¹, Meilin Chen¹, Guoliang Cheng^{3*}, Yanfang Mou^{3*} and Jiarui Wu^{1*}

¹Department of Clinical Chinese Pharmacy, School of Chinese Materia Medica, Beijing University of Chinese Medicine, Beijing, China, ²Institute of Fundamental and Frontier Sciences, University of Electronic Science and Technology of China, Chengdu, China, ³State Key Laboratory of Generic Manufacture Technology of Chinese Traditional Medicine, Linyi, China

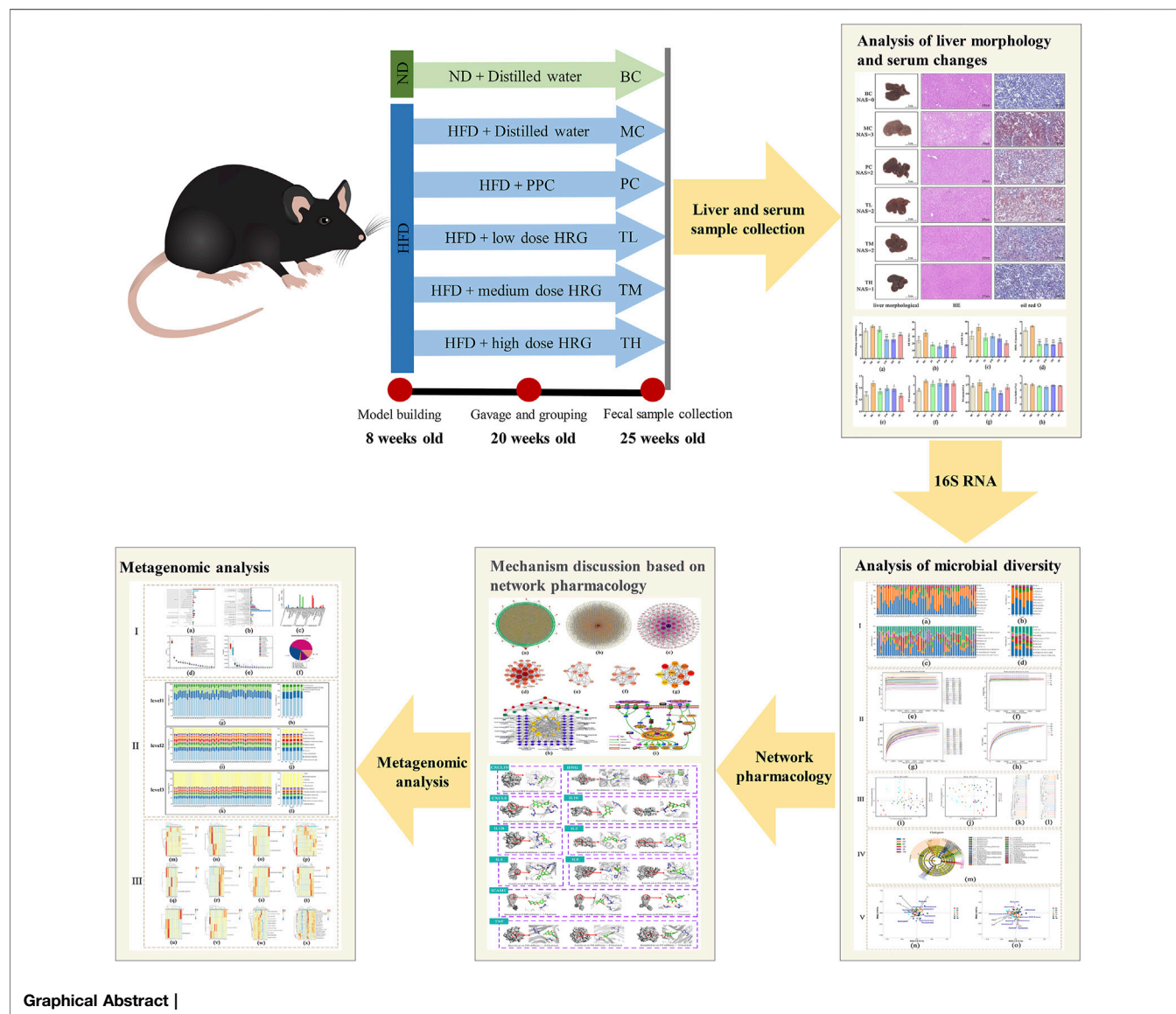
Background: The incidence of Nonalcoholic Fatty Liver (NAFL) is increasing year by year, growing evidence suggests that the intestinal flora plays a causative role in NAFL. Huazhi Rougan Granule (HRG) is commonly used in the clinical treatment of NAFL. It is reported that it can reduce lipids and protect the liver, but no research has confirmed whether the drug's effect is related to the intestinal flora. Therefore, we investigated whether the effect of HRG is related to the regulation of intestinal flora to further explore the mechanism of HRG in the treatment of NAFL through intestinal flora.

Methods: In this study, C57BL/6J mice were fed a high-fat diet for 8 weeks, and the high-fat diet plus HRG or polyene phosphatidylcholine capsules were each administered by gavage for 4 weeks. High-throughput sequencing, network pharmacology, and molecular docking were used to explore the mechanism of HRG in the treatment of NAFL through intestinal flora.

Results: HRG treatment can reduce body weight gain, lipid accumulation in liver and lipogenesis and reduce serum biochemical indexes in high-fat-fed mice. Analysis of intestinal flora showed that HRG changed the composition of intestinal flora, which was characterized by a decrease in the Firmicutes/Bacteroidetes ratio. Moreover, the species distribution was significantly correlated with AKP, HDL-C, and TG. Metagenetic analysis showed that HRG altered the functional composition and functional diversity of microorganisms, which was mainly characterized by an increase in the abundance of metabolic pathways. The network pharmacology results show that the mechanism of HRG in the treatment of NAFL through intestinal flora is mainly reflected in the biological process of gene function and related to infectious diseases, immune systems, and signal transduction pathways, such as cytokine-cytokine receptor interaction, Chagas disease, IL-17 signaling pathway and other signaling pathways.

Conclusion: These results strongly suggest that HRG may alleviate NAFL by preventing IFD.

Keywords: nonalcoholic simple fatty liver, high-fat diet, intestinal flora disorder, 16s sequencing, network pharmacology



BACKGROUND

Nonalcoholic Fatty Liver (NAFL) is a common, multifactorial, and less significant liver disease whose incidence is increasing worldwide. The occurrence of NAFL is mainly related to unhealthy dietary habits and lifestyles. This leads to pathological accumulation of fat droplets in hepatocytes (Cobbina and Akhlaghi, 2017; Romero-Gómez et al., 2017). There is increasing evidence that obesity, cardiovascular disease, and type 2 diabetes are closely related to the

progression of NAFL and represent an increasing burden to society (Eckel et al., 2010; Yang et al., 2015; Graffy and Pickhardt, 2016; Younossi et al., 2019; de Vries et al., 2020; Deprince et al., 2020). Although NAFL is usually clinically asymptomatic, it can progress over time to non-alcoholic steatohepatitis, cirrhosis, and end-stage liver disease (Papatheodoridi and Cholongitas, 2018; Zhou et al., 2020). Currently, lifestyle changes are the mainstay of treatment, including dietary changes and exercise (Younossi et al., 2018; Kořínková et al., 2020). Therefore, the development of drugs and

nutraceuticals for NAFL remains a challenge for all scientists (Targher et al., 2020).

In recent years, intestinal flora has gradually attracted the attention of scientists. A growing number of studies show that intestinal flora is closely related to human health homeostasis, which opens a new direction for us to understand the occurrence and progression of NAFL (Milani et al., 2017; Mohajeri et al., 2018; Gomaa, 2020; Kim et al., 2020; Manor et al., 2020). Studies have shown that intestinal flora can affect lipid metabolism and lipid levels in blood and tissues in mice and humans (Zhou et al., 2017; Wang et al., 2018; Kong et al., 2019; Yuan et al., 2019; Hong et al., 2020; Yiu et al., 2020). In addition, animal and clinical studies have shown that regulation of intestinal flora and its metabolites can influence the degree of a high-fat diet-induced hepatic steatosis in NAFL mice and NAFL patients, thereby interfering with the occurrence and development of NAFL (Jiang et al., 2015; Moreira et al., 2018; Wu et al., 2019; Nakano et al., 2020; Zhang et al., 2021). Therefore, there are good reasons to believe that the composition of intestinal flora may help predict the severity of NAFL and may be a new therapeutic target for NAFL.

Huazhi Rougan Granule (HRG) is widely used to treat dampness-heat obstruction of NAFL. It has the function of clearing heat and detoxifying, eliminating blood stasis, and softening the liver. The composition of HRG is Yinchen (YC), Juemingzi (JMZ), Dahuang (DH), Zexie (ZX), Zhuling (ZL), Shanzha (SZ), Cangzhu (CZ), Baizhu (BZ), Chenpi (CP), Gualou (GL), Nvzhenzi (NZZ), Mohanlian (MHL), Gouqizi (GQZ), Xiaoji (XJ), Chaihu (CH), Gancao (GC). Studies have shown that this formula can not only improve lipid deposition in the liver, protect liver cell membranes and reduce liver damage but also protect the intestinal barrier and regulate intestinal flora (Niu et al., 2011; Chen et al., 2015; Gao et al., 2021; Zhang et al., 2021; Zhang et al., 2021).

Since intestinal flora disorder is the breakthrough point in network pharmacology, the treatment of NAFL-related intestinal flora disorder by HRG was investigated to explore the mechanism of HRG in the treatment of NAFL by intestinal flora in multiple dimensions. Therefore, this study not only explored the mechanism of HRG in the treatment of NAFL by intestinal flora using network pharmacology but also established a NAFL model for experiments. The intervention effect in NAFL mice was analyzed by the high-throughput sequencing method to analyze the diversity of intestinal flora in mice to provide a better basis for further exploration of the mechanism of HRG in the treatment of NAFL through intestinal flora.

MATERIALS AND METHODS

Experimental Animals

Seventy-two 6-week-old SPF-grade male C57BL/6J mice, weighing between 20–22 g, were purchased from Beijing Speifu Biotechnology Co., Ltd. They were housed in the ICV cage of the Experimental Animal Center of Beijing University of Traditional Chinese Medicine ($n = 5/\text{cage}$). Animals were housed at $20 \pm 2^\circ\text{C}$ in a 12-h light/12-h dark cycle and had free access to food and water.

Main Reagents in the Experiment

Reagents: Huazhi Rougan Granule (Lunan Pharmaceutical Co., Ltd.); Polyene Phosphatidylcholine Capsule (Yishanfu); high-fat diet [78.8% basic feed +10% lard +10% egg yolk powder +1% cholesterol +0.2% sodium cholate, product number is SCXK (Jing) 2019-0010, Beijing Speifu Biotechnology Co., Ltd.]; normal diet [corn, soybean meal, fish meal, flour, bran, salt calcium ammonium phosphate, stone powder, a variety of vitamins, a variety of trace elements, amino acids, etc, product number is SCXK (Jing) 2019-0010, Beijing Speifu Biotechnology Co., Ltd.]; 4% tissue cell fixative (Beijing Bairuiji Biotechnology Co., Ltd.); AKP, ALT, AST, TG, TC, HDLC, LDLC assay kit (Nanjing Jiancheng).

Animal Grouping and Model Establishment

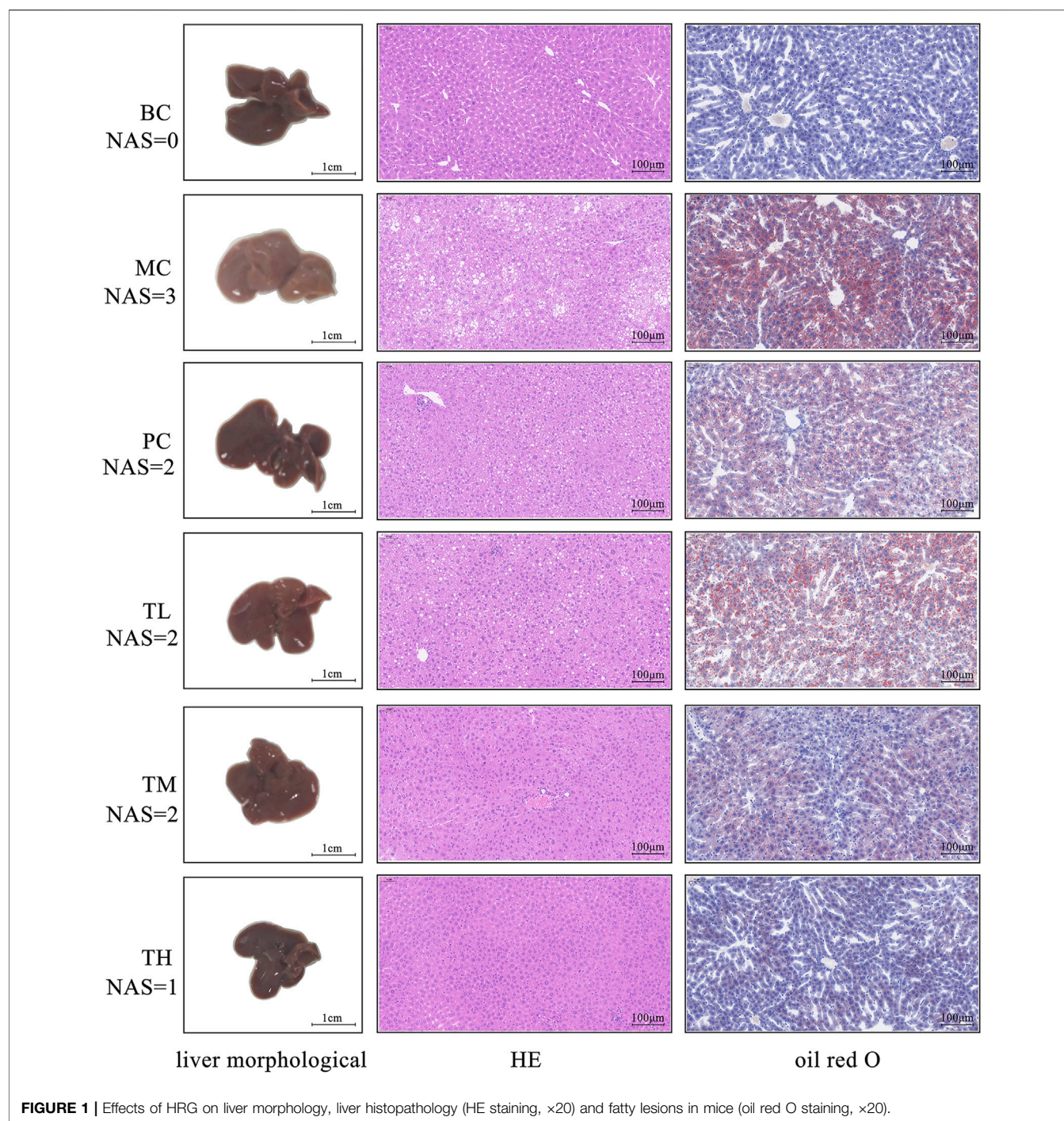
After 1 week of adaptive feeding of male C57 mice, 12 mice were randomly selected as a blank control group (BC) and fed with a normal diet (ND); the remaining mice were fed with high-fat diet (HFD) to replicate the NAFL model. After 12 consecutive weeks, relevant indicators were evaluated. Mice that passed the evaluation could be considered successful modeling, gavage at week 13, and sampled at week 17. Gavage continued for 5 weeks. The successfully established mice were randomly divided into a model control group (MC), a positive drug control group (PC), and a high-medium-low-dose HRG group (TH/TM/TL), with 10 mice in each group. Finally, there were nine mice in each group after sampling. HRG and Polyene Phosphatidylcholine Capsule (PPC) were administered at equivalent doses converted from the upper clinical limits of the human body, with doses of 3.12 g/kg and 0.18 g/kg respectively. The high, medium and low doses of HRG were 4, 2, and 1 times, respectively, the equivalent dose after conversion.

Collection and Preparation of Samples

After collection of mouse feces, the feces were placed in sterile cryopreservation tubes, quickly frozen in liquid nitrogen, and stored in an ultra-low temperature refrigerator at -80°C for subsequent analysis of intestinal flora diversity. After the mice fasted for 12 h, the eyeballs were removed, and the blood was collected in a 2 ml sterile centrifuge tube, centrifuged at 3,000 r/min for 15 min at 4°C . The supernatant was stored in a centrifuge tube for subsequent biochemical index analysis. One-third of mouse liver lobes were fixed in 4% paraformaldehyde fixative, routinely processed, embedded in paraffin, 3 μm sections were stained with hematoxylin and eosin (HE) for histological analysis, and frozen sections (8 μm) were stained with oil red O. The fat accumulation and inflammatory response of liver tissue were observed under the microscope.

16S rRNA and Metagenomic Sequencing

16S rRNA sequencing: After extraction of the total DNA from the sample, all primers were designed according to the conserved region. 338F (5'-ACTCCTACGGGAGGCAGCA-3') and 806R (5'-GGACTACHVGGGTWTCTAAT-3') were used for PCR amplification of the V3-V4 region of the 16S rDNA gene to perform the Illumina deep sequencing. PCR products were detected by 1.8% agarose gel electrophoresis. Metagenome



sequencing: extract DNA from fecal samples, detect the DNA of the sample, and fragment the DNA with ultrasonic waves after passing the test. Then, the fragmented DNA is purified, the end repaired, A is added to the three ends, and the sequencing adapter is ligated. Fragment size selection was performed by agarose gel electrophoresis, and PCR amplification was performed to form a sequencing library. The constructed libraries are first checked for quality, and qualified libraries are sequenced on the Illumina sequencing platform. Beijing BioMarker Technologies Co., Ltd.

provided library construction and sequencing Beijing BioMarker Technologies Co., Ltd. (Beijing, China).

Network Pharmacology Analysis

Through the Traditional Chinese Medicine Systems Pharmacology Platform (TCMSP, <https://tcmsp.com/tcmsp.php>) (Ru et al., 2014; Zhang et al., 2020) and the Integrative Pharmacology-based Research Platform of Traditional Chinese Medicine (TCMIP v2.0, <http://www.tcmip.cn/TCMIP/index>).

TABLE 1 | Comparison of serum biochemical indexes of mice in each group after 5 weeks of gavage ($\bar{x} \pm se$, $n = 9$).

| Group | HDLC (mmol/L) | LDLC (mmol/L) | TG (mmol/L) | TC (mmol/L) | AST (U/L) | ALT (U/L) | AKP(King unit/100 ml) |
|-------|---------------------------------|--------------------------------|-----------------------------------|-------------------------------|-------------------------------|-------------------|--------------------------------------|
| BC | 4.48 \pm 0.15* | 0.71 \pm 0.07**** | 1.41 \pm 0.06 | 4.69 \pm 0.21*** | 35.31 \pm 5.27 | 24.11 \pm 3.40 | 11.55 \pm 0.39* |
| MC | 5.22 \pm 0.13 | 1.19 \pm 0.11 | 1.62 \pm 0.15 | 6.87 \pm 0.35 | 50.25 \pm 5.15 | 34.61 \pm 4.08 | 13.56 \pm 0.53 [#] |
| TL | 2.13 \pm 0.17 ^{*,##} | 0.84 \pm 0.08** | 1.10 \pm 0.05 ^{*,##,▲} | 6.17 \pm 0.45 ^{##} | 32.38 \pm 3.91 | 17.57 \pm 1.06* | 11.96 \pm 0.70 [▲] |
| TM | 2.20 \pm 0.23 ^{*,##} | 0.96 \pm 0.07 ^{*,▲} | 1.34 \pm 0.12 | 6.40 \pm 0.57 ^{##} | 34.35 \pm 2.19 [▲] | 15.39 \pm 2.43* | 7.80 \pm 0.65 ^{***,###,▲} |
| TH | 2.10 \pm 0.15 ^{*,##} | 0.95 \pm 0.11 [▲] | 1.02 \pm 0.05 ^{*,▲} | 6.24 \pm 0.50 ^{##} | 31.02 \pm 4.48 | 18.25 \pm 3.07 | 8.03 \pm 0.87 ^{***,###,▲} |
| PC | 2.43 \pm 0.08 ^{*,##} | 0.66 \pm 0.06** | 1.34 \pm 0.10 | 6.23 \pm 0.39 ^{##} | 22.67 \pm 1.99** | 15.58 \pm 1.49* | 9.97 \pm 0.34 ^{***} |

Compared with the model group, * $p < 0.05$, ** $p < 0.01$, *** $p < 0.001$.

Compared with the blank group, # $p < 0.05$, ## $p < 0.01$, ### $p < 0.001$.

Compared with the PC, group, ▲ $p < 0.05$, ▲▲ $p < 0.01$, ▲▲▲ $p < 0.001$.

php/Home/) (Wang et al., 2021), the active ingredients of HRG were screened. The TCMSP database and the Swiss Target Prediction platform (<http://www.swisstargetprediction.ch/>) (Daina et al., 2019) were used to identify the targets of the main active ingredients. The Uniprot database (<https://www.uniprot.org/>) (UniProt Consortium, 2021) is used to find the gene information corresponding to the targets. After integration, the active components and related target information of HRG were obtained. The Gene Cards database (<https://www.genecards.org>) (Stelzer et al., 2016), DigSee database (<http://210.107.182.61/geneSearch/>) (Kim et al., 2013) and NCBI Gene (<https://www.ncbi.nlm.nih.gov/gene/>) (NCBI Resource Coordinators, 2018) were used to search for targets related to NAFL and IFD. The above targets were respectively integrated and duplicate genes were removed. A total of 198 targets related to IFD and 1,395 targets related to NAFL were obtained.

Herb-compound-target network, PPI network and multi-element network of “herb-key compound-key target-disease-KEGG pathway” of HRG were constructed by Cytoscape 3.7.2. (Otasek et al., 2019). Comprehensive modular analysis and cytoHubba analysis were used to screen the key targets of HRG in the treatment of NAFL through the intestinal flora. GO enrichment analysis and KEGG pathway enrichment analysis were performed on the targets in the intersection network using R 4.0.3 (Layeghifard et al., 2018; The Gene Ontology Consortium, 2019; Kanehisa and Sato, 2020). The potential active ingredients obtained by the analysis were docked onto the potential targets. Autodock Tools 1.5.6 was used to perform preprocessing such as water removal, hydrogenation, and atom typesetting for proteins and small molecule compounds, Autodock Vina 1.1.2 was used to perform molecular docking calculations, and Pymol 2.3.2 (<https://pymol.org/2/>) was used to visualize the result (Trott and Olson, 2010; Mooers, 2020; Eberhardt et al., 2021).

Bioinformatics Analysis

Microbial diversity analysis: FLASH v1.2.11 was used to stitch the original data. The spliced sequences were quality filtered and chimeras were removed to obtain high-quality Tags sequences. Sequences were clustered at a similarity level of 97%, and OTUs were filtered with a threshold of 0.005% of all sequenced sequences. Alpha diversity and beta diversity were analyzed using the BMK Cloud platform (www.biocloud.net).

Metagenome analysis: use of Trimmomatic (version 0.33) software to filter raw data (Raw Tags); use of bowtie2 (version

2.2.4) to align with host genome sequence to remove host contamination; MEGAHIT (Version 1.1.2) was used for metagenomic assembly to filter contig sequences shorter than 300 bp; MetaGeneMark (Version 3.26) was used for gene prediction; cd-hit (Version 4.6.6) was used to remove redundancy. The similarity threshold was set a 95%, and the coverage threshold was set at 90%. Both functional diversity analysis and species diversity analysis are analyzed on the BMK Cloud platform (www.biocloud.net).

Statistical Analysis

The relevant results are expressed as mean \pm SE. SPSS software was used for data analysis and GraphPad Prism was used for visualization. p values of less than 0.05 were considered statistically significant.

RESULTS

Lipid Accumulation in Mice Induced by HFD

As shown in **Figure 1**, in the model group compared with the BC group, the fat accumulation in the liver increased, the liver volume increased, white color, and the edge became blunt. After administration, the degree of redness of the liver improved in each group, especially in the group TH. The results of HE and oil red O staining showed more balloon denatured hepatocytes and more red lipids in the liver tissue of the model group but less in the administration group. The pathological degree of the MC group was the most severe, that of the TH group was the mildest, and there was no significant difference between the TL group and the PC group. Therefore, HRG ameliorates HFD-induced hepatic fat accumulation and weight gain, and HRG may improve liver lesions in a dose-dependent manner.

Serum Analysis

Compared with the blank group, the indexes of liver enzymes and blood lipids were higher in the model group, among which there were significant differences in TC, HDL-C, LDL-C, AKP, ALT, and AST. However, there was no significant difference in TG. After administration, liver enzymes and blood lipids were lower than in the model group. There were significant differences in ALT, AST and HDL-C between the MC and administration groups. There were no significant differences in TC, ALT and

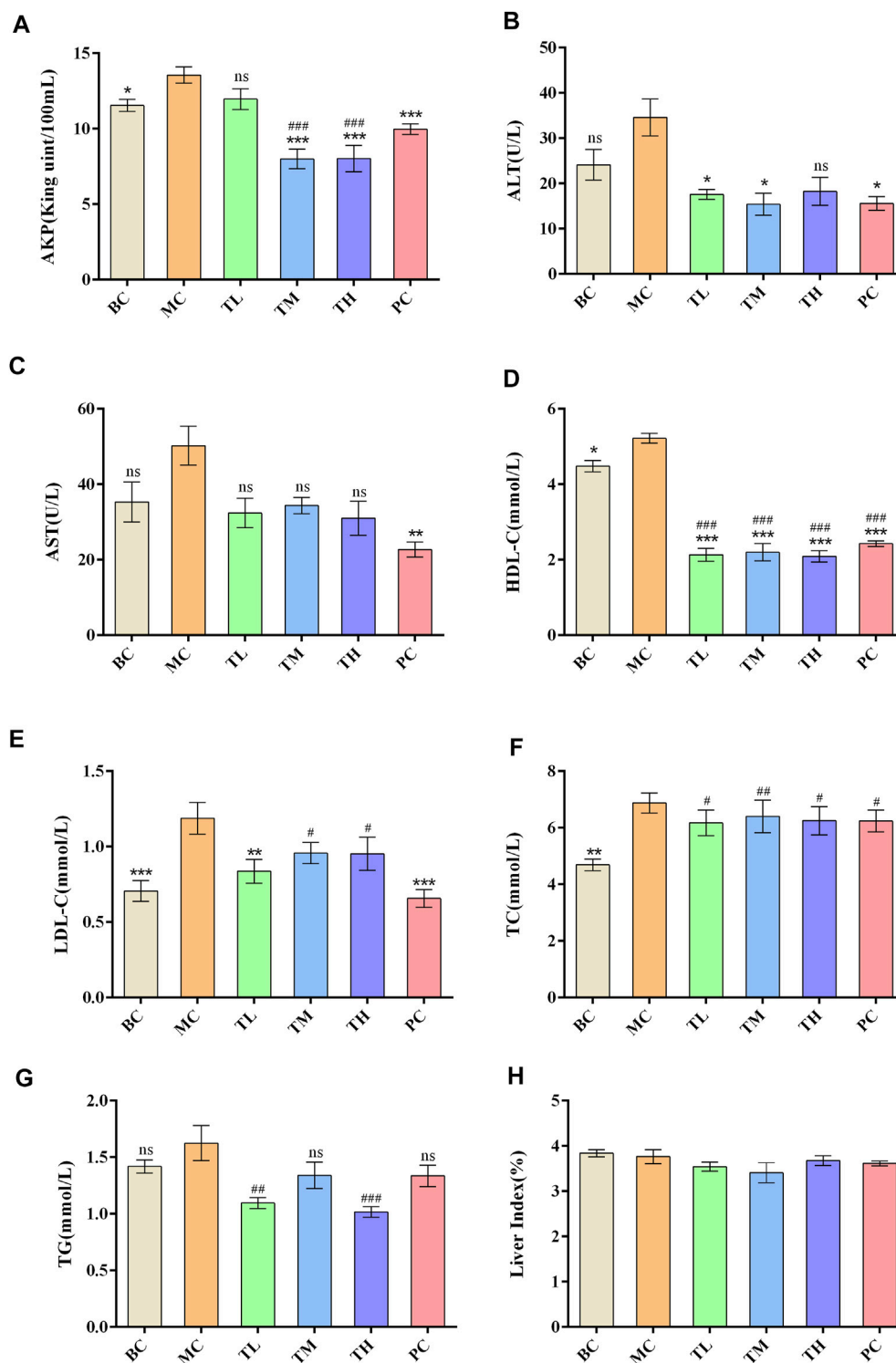
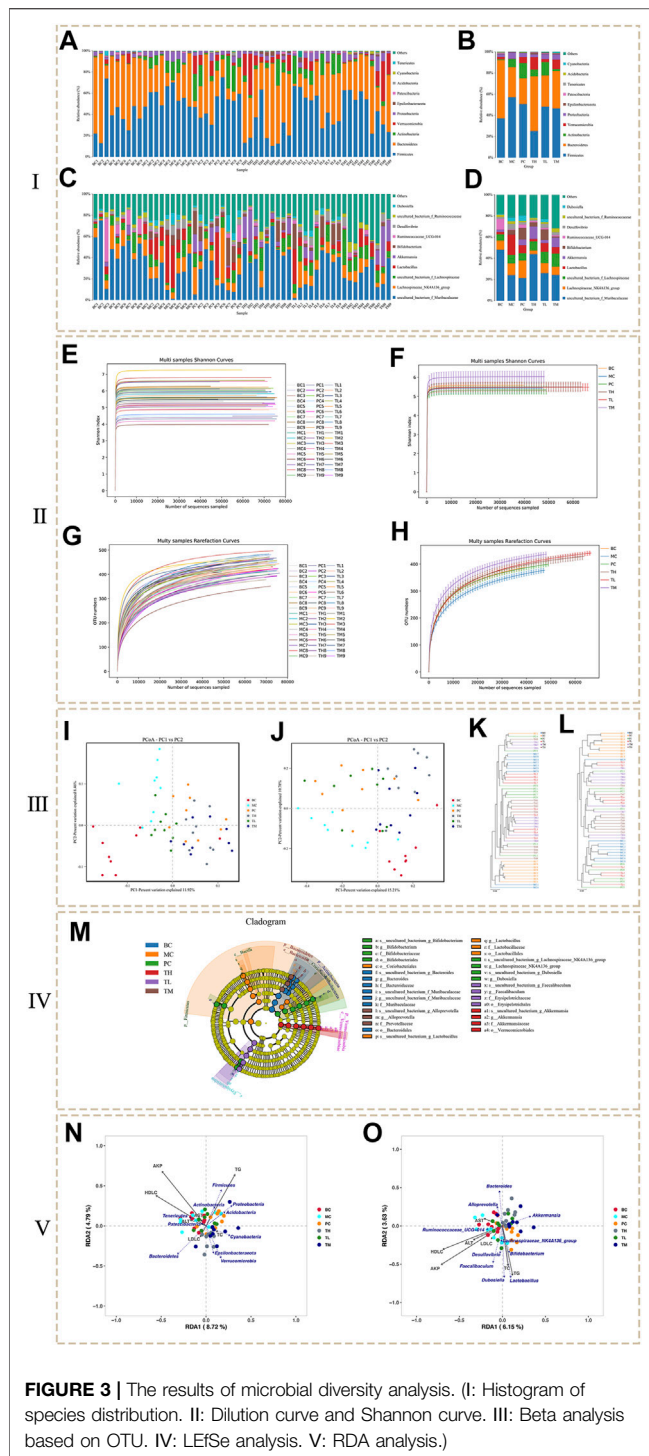


FIGURE 2 | Effect of HRG on biochemical indexes and statistical histogram of organ index in mice. **(A)** Effects of HRG on serum AKP level in mice. **(B)** Effects of HRG on serum ALT level in mice. **(C)** Effects of HRG on serum AST level in mice. **(D)** Effects of HRG on serum HDL-C level in mice. **(E)** Effects of HRG on serum LDL-C level in mice. **(F)** Effects of HRG on serum TC level in mice. **(G)** Effects of HRG on serum TG level in mice. **(H)** Effects of HRG on liver index in mice. Compared with the model group, * $p < 0.05$, ** $p < 0.01$, *** $p < 0.001$; compared with the blank group, # $p < 0.05$, ## $p < 0.01$, ### $p < 0.001$).



HDL-C between the administration groups. There were differences in AKP, AST, TG and LDL-C between the HRG group and the PC group.

The effect of reducing AKP in the TM and TH group was better than in the TL group, and the effect of lowering in the TG group was better than in the TM group. The effect of lowering AKP in the PC group was better than in the TL group but worse

than in the TM and TH groups. In addition, the effect of LDL-C lowering in the PC group was better than in the TM and TH groups. The above differences were statistically significant. This suggest that HFD can lead to abnormal metabolism of blood lipids and liver enzymes, and that HRG can improve this. Compared with positive drugs, HRG has advantages in improving HDL-C, TG, and AKP, and the degree of improvement may be dose-dependent. There was no significant difference in organ index between groups. The comparison of the different indexes of each group is shown in **Table 1**, and the effects of HRG on the biochemical indexes and organ index of mice are shown in **Figure 2**.

Microbial Diversity Analysis

The intestinal flora is considered to play a causal role in the pathogenesis of NAFL. We evaluated the effects of administration on intestinal flora composition by high-throughput sequencing of the bacterial 16S rRNA V3 + V4 region. High-throughput sequencing generated a total of 4,191,545 raw reads from 54 samples. After screening, a total of 4,178,702 high-quality reads were obtained. Based on a similarity level of 97%, all effective reads were clustered into OTUs for OTU cluster analysis and species taxonomy analysis. The quality evaluation of the sequencing data is shown in **Supplementary Table S1**.

In this study, the flora was identified and analyzed at the phylum, class, order, family, and genus levels. Finally, a total of 17 phyla, 26 classes, 56 orders, 86 families and 187 genera were identified. The figure shows the annotation of species and the taxonomic analysis. The histogram of species distribution (**Figures 3A–D**) shows that species are mainly distributed in Firmicutes and Bacteroidetes, followed by Actinobacteria, Verrucomicrobia and Proteobacteria. In addition, is they are mainly distributed in the genera of uncultured_bacterium_f_Muribaculacea and lachnospiraceae NK4A136 group, followed by uncultured_bacterium_f_Lachnospirae, *Lactobacillus* and Akkermansia.

At the phylum level (**Figures 3A,B**), the levels of Firmicutes, Proteobacteria and Actinobacteria were higher in the MC group than in the BC group, whereas the levels of Bacteroidetes and Verrucomicrobia were lower. Compared to the BC group, the levels of Firmicutes and Proteobacteria decreased in the administration group, especially in the TH group; Actinobacteria decreased in the TH and TM groups, most significantly in the TM group, but increased in the PC and TL groups. Bacteroidetes were significantly higher in the TH and TM groups than in the MC group, and Verrucomicrobia increased most significantly in the TH and TM groups. Compared with the BC group, the proportion of *Lactobacillus* and *Desulfovibrio* was higher in the MC group at the genus level (**Figures 3C,D**). In comparison, Akkermansia and Ruminococcaceae UGG-014 accounted for a lower proportion. After administration, *Lactobacillus* (decreased the most in TH group) and *Desulfovibrio* (decreased the most in TH group) decreased, Akkermansia (increased the most in TH group) and ruminococcaceae UGG-014 (increased the most in PC group) increased. After administration, *Lactobacillus* and *Desulfovibrio*

TABLE 2 | Alpha diversity statistics ($\bar{x} \pm se$, $n = 9$).

| Group | BC | MC | PC | TH | TL | TM |
|---------------------|------------------------|-----------------------|-----------------------------------|------------------------------------|---------------------------------------|---|
| Shannon index | 5.5847 \pm 0.1425 | 5.4356 \pm 0.2673 | 5.3317 \pm 0.2126 | 5.4967 \pm 0.2489 | 5.4752 \pm 0.187 | 6.0296 \pm 0.2885 [▲] |
| Simpson index | 0.9445 \pm 0.0089 | 0.9311 \pm 0.0208 | 0.9228 \pm 0.0157 | 0.9346 \pm 0.0158 | 0.9412 \pm 0.0115 | 0.9509 \pm 0.0147 |
| ACE index | 464.1403 \pm 7.6454 | 452.5716 \pm 6.7194 | 457.6025 \pm 5.263 | 472.0735 \pm 9.1531 | 492.6638 \pm 7.061 ^{*,#} | 496.8799 \pm 9.3045 ^{***,##} |
| Chao1 index | 472.0195 \pm 10.5494 | 457.5262 \pm 8.1369 | 464.9995 \pm 5.4769 | 477.7676 \pm 9.7134 | 492.5886 \pm 7.293 ^{**} | 505.3993 \pm 9.6354 ^{***,##} |
| PD whole tree index | 25.1176 \pm 0.3986 | 24.8614 \pm 0.3622 | 25.3351 \pm 0.2404 | 26.193 \pm 0.4081 ^{*,#} | 26.721 \pm 0.3868 ^{***,##} | 26.9273 \pm 0.2881 ^{***,##} |
| OTU | 414.56 \pm 8.056 | 402.89 \pm 9.137 | 420.11 \pm 5.397 | 434.44 \pm 11.973 [*] | 446.22 \pm 7.240 ^{**} | 457.11 \pm 8.389 ^{***,##} |
| Coverage (%) | 99.8878 \pm 0.0128 | 99.9056 \pm 0.0112 | 99.9167 \pm 0.0058 [#] | 99.9167 \pm 0.0071 [#] | 99.9078 \pm 0.0040 | 99.9111 \pm 0.0102 |

Compared with the model group, * $p < 0.05$, ** $p < 0.01$, *** $p < 0.001$.

Compared with the blank group, # $p < 0.05$, ## $p < 0.01$, ### $p < 0.001$.

Compared with the PC, group, ▲ $p < 0.05$, ▲▲ $p < 0.01$, ▲▲▲ $p < 0.001$.

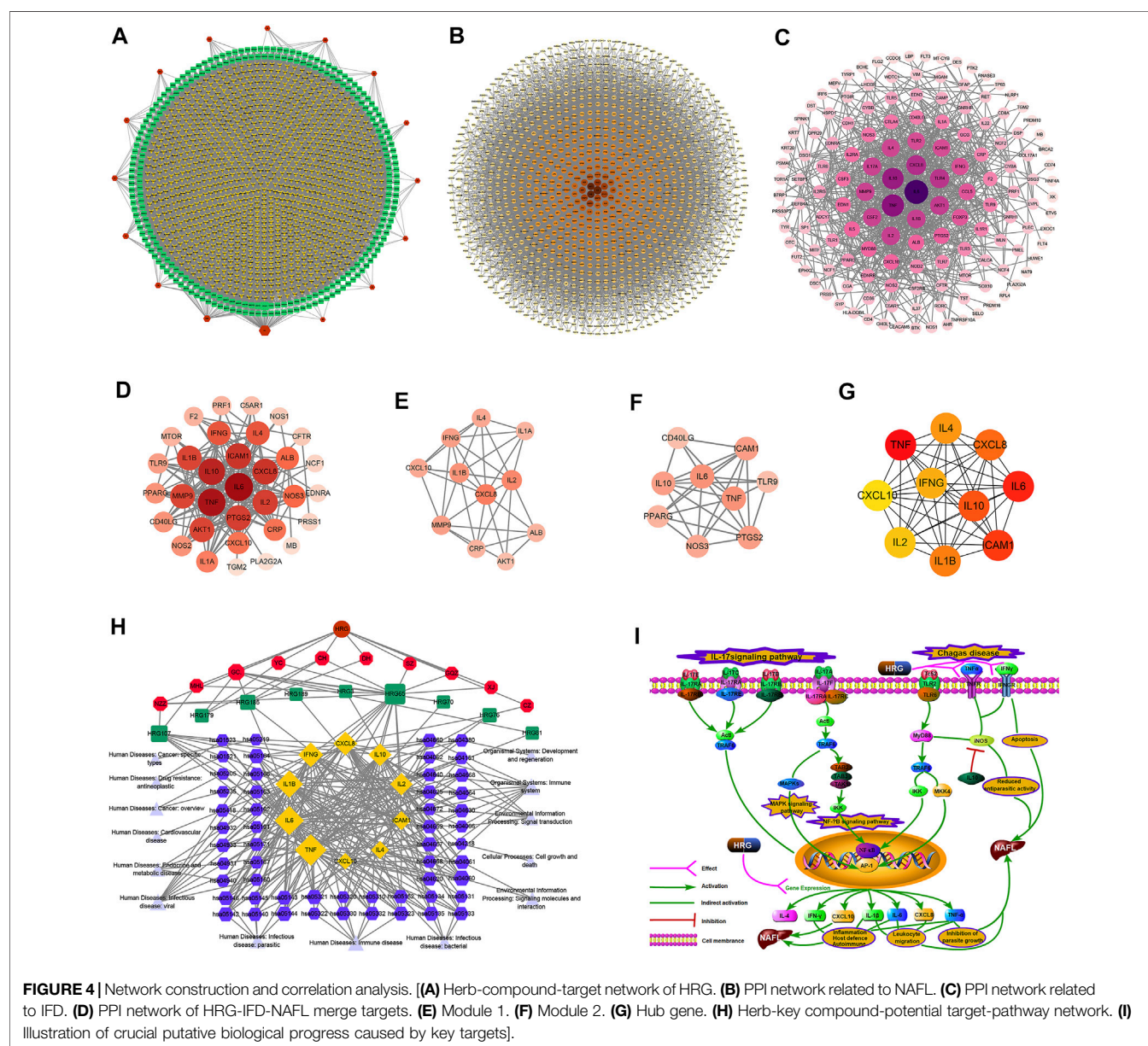


TABLE 3 | Compound information in the top 20 nodes in the “herb-compound-target” network of HRG.

| Number | Compound | TCMSP ID | Pubchem ID | Degree | OB(%) | DL | Herb source |
|--------|-------------------------------|-----------|------------|--------|-------|------|-----------------------------------|
| HRG65 | Quercetin | MOL000098 | 5280343 | 238 | 46.43 | 0.28 | YC, SZ, NZZ, MHL, GOZ, CH, XJ, GC |
| HRG185 | Kaempferol | MOL000422 | 5280863 | 158 | 41.88 | 0.24 | DH, NZZ, CH, GC |
| HRG107 | Luteolin | MOL000006 | 5280445 | 150 | 36.16 | 0.25 | MHL, NZZ |
| HRG3 | 7-Methoxy-2-methyl isoflavone | MOL003896 | 354368 | 144 | 42.56 | 0.2 | GC |
| HRG76 | wogonin | MOL000173 | 5281703 | 142 | 30.68 | 0.23 | CZ |
| HRG53 | Glabridin | MOL004908 | 124052 | 138 | 53.25 | 0.47 | GC |
| HRG81 | 7-Acetoxy-2-methylisoflavone | MOL004991 | 268208 | 136 | 38.92 | 0.26 | GC |
| HRG189 | Licochalcone a | MOL000497 | 5318998 | 135 | 40.79 | 0.29 | GC |
| HRG88 | Glyasperins M | MOL005007 | NA | 134 | 72.67 | 0.59 | GC |
| HRG74 | 4'-O-Methylglabridin | MOL004978 | 9927807 | 134 | 36.21 | 0.52 | GC |
| HRG70 | 1-Methoxyphaseollidin | MOL004959 | 480873 | 134 | 69.98 | 0.64 | GC |
| HRG86 | Licoagrocarpin | MOL005003 | 15840593 | 133 | 58.81 | 0.58 | GC |
| HRG239 | Medicarpin | MOL002565 | 336327 | 133 | 49.22 | 0.34 | GC |
| HRG179 | isorhamnetin | MOL000354 | 5281654 | 133 | 49.6 | 0.31 | YC, CH, GC |

decreased and Akkermansia increased, especially in the TH group; Ruminococcaceae UGG-014 increased, especially in the PC group. Therefore, it is tentatively suggested that HRG can increase Bacteroidetes, Verrucomicrobia, uncultured bacterium f Lachnospiceae and Akkermansia, and reduce Firmicutes and Proteobacteria, *Lactobacillus* and *Desulfovibrio*. HRG can improve NAFL by changing the structure of intestinal flora of NAFL mice.

The analysis of alpha diversity can be represented by the index in **Table 2**. The larger the index, the higher the diversity of the sample. The results showed no significant difference between the Shannon index and the Simpson index in the community diversity evaluation. The ACE index and the Chao index in community richness evaluation showed that the richness of the TL and TM groups was significantly higher than that of the BC group, the MC group and the PC group. Shannon index from large to small TM > BC > TH > TL > MC > PC, Simpson index from large to small TM > BC > TL > TH > MC > PC, ACE index from large to small TM > TL > TH > BC > PC > MC, PD whole tree index from large to small TM > TL > TH > PC > BC > MC, Chao1 index from large to small TM > TL > TH > BC > PC > MC. Various indexes of alpha diversity showed that HRG could improve the diversity of NAFL mice, and the curative effect was better than that of the PC group. At the same time, the coverage rate of each group of samples is greater than 99%, indicating that the probability of undetected sequences in the samples is very low, and the sequencing depth can accurately reflect the composition diversity of the flora. The dilution curve shows that when the curve becomes gradually flat, increasing the sequencing depth has no significant impact on alpha diversity, as shown in **Figures 3E,F**. The Shannon index curve shows that when the curve tends to become flat, the characteristic species do not increase with the increase of sequencing quantity, as shown in **Figures 3G,H**.



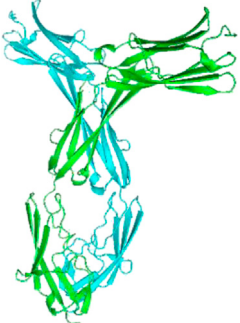
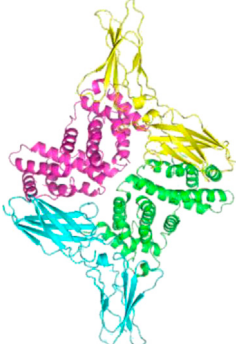
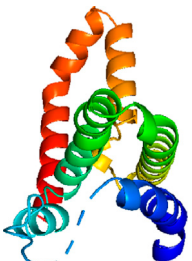
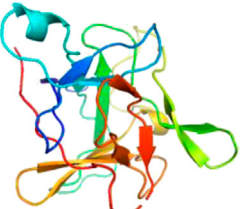
The comparison of the changing trend of β diversity of intestinal flora in each group is based on visual analysis of ecological differences by the Jaccard and Bray-Curtis PCoA algorithm based on independent OTU. As shown in the Jaccard PCoA in **Figure 3I**, the contribution of principal coordinates 1 (PC1) and PC2 to the distribution of samples is 11.92 and 8.46%, respectively. The clustering of the intestinal

flora shows that there are obvious differences in the microbial community between the samples of BC and MC groups, and there are obvious differences in the microbial community between the administration group, BC group and MC group. In addition, the Bray-Curtis PCoA confirms these findings (**Figure 3J**). PC1 (15.21%) can better distinguish the microecology of BC and MC group, MC and TM, TH group. When PC2 (10.78%) was introduced, PC and BC, PC and MC, TH and BC, and TH and MC could also be significantly separated (**Figure 3J**). Community similarity analysis is another method that uses hierarchical clustering of the distance matrix to represent β diversity. The similarity and differences between samples can be described by the dendritic structure (**Figures 3K,L**). These data further indicated that the BC and MC groups had large differences in microbial community structure and that the HRG administration group and the control group had large differences in microbial community structure.

In order to find the biomarker flora with statistical abundance differences between the different groups, LEfSe analysis of the samples between the groups was performed. **Figure 3M** shows the evolutionary branch diagram of LEfSe analysis. The results showed that Bacteroidetes, Actinobacteria, Firmicutes, and Verrucomicrobia were significantly different species at the phylum level. At the genus level, *Bifidobacterium*, *Bacteroides*, *Alloprevotella*, *Lactobacillus*, *Lachnospiraceae*_NK4A136_group, *Dubosiella*, *Faecalibaculum* and *Akkermansia* were significantly different species. *t*-test at the phylum and genus levels between the groups showed (**Supplementary Tables S2, S3**) that the dominant bacterial groups of NAFL mice and HRG group were mainly Firmicutes, Proteobacteria, Actinobacteria, and Bacteroidetes. At the genus levels, they were mainly *Adlercreutzia* and *Ruminococcaceae*_UCG-013, *Sphingomonas*, etc. It is suggested that HRG may improve NAFL by changing the flora of Firmicutes, Proteobacteria, Actinobacteria and Bacteroidetes.




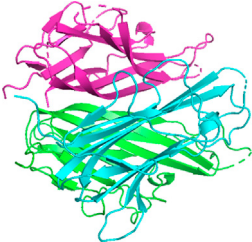
RDA analysis was performed for intestinal flora abundance and serum index parameters (**Figure 3N**: phylum level, **Figure 3O**: genus level). The results showed that AKP, HDLC, TC, and TG were highly correlated with species distribution, and they were distributed in the same direction. At the genus level,

TABLE 4 | Information of molecular docking.

| Structure | PDB ID | Target | Compound ID | Compound name | Affinity (kcal/mol) |
|---|--------|--------|-------------|---------------|---------------------|
|  | 1O80 | CXCL10 | HRG65 | Quercetin | −6.5 |
|  | 3IL8 | CXCL8 | HRG65 | Quercetin | −6.8 |
|  | 1P53 | ICAM1 | HRG107 | Luteolin | −7.3 |
| | 1P53 | ICAM1 | HRG185 | Kaempferol | −7 |
| | 1P53 | ICAM1 | HRG65 | Quercetin | −7.3 |
|  | 1FYH | IFNG | HRG107 | Luteolin | −8.1 |
| | 1FYH | IFNG | HRG65 | Quercetin | −8 |
|  | 2H24 | IL10 | HRG107 | Luteolin | −6.6 |
| | 2H24 | IL10 | HRG65 | Quercetin | −6.5 |
|  | 5R86 | IL1B | HRG65 | Quercetin | −6.8 |

(Continued on following page)

TABLE 4 | (Continued) Information of molecular docking.

| Structure | PDB ID | Target | Compound ID | Compound name | Affinity (kcal/mol) |
|---|--------|--------|-------------|---------------|---------------------|
|  | 4NEM | IL2 | HRG107 | Luteolin | -7 |
| | 4NEM | IL2 | HRG65 | Quercetin | -6.8 |
|  | 5FHX | IL4 | HRG107 | Luteolin | -7.9 |
|  | 5FUC | IL6 | HRG107 | Luteolin | -8.9 |
| | 5FUC | IL6 | HRG65 | Quercetin | -9 |
|  | 7KPA | TNF | HRG107 | Luteolin | -8.3 |
| | 7KPA | TNF | HRG185 | Kaempferol | -9.5 |
| | 7KPA | TNF | HRG65 | Quercetin | -10 |

they were positively correlated with *Faecalibaculum*, *Desulfovibrio*, *Dubosiella* and *Lactobacillus*, and negatively correlated with *Bacteroides*, *Akkermansia* and *Alloprevotella*. At the phylum level, AKP, HDL-C and TG were highly correlated with species distribution, positively correlated with Firmicutes and Actinobacteria, and negatively correlated with Epsilonbacteraeota and Verrucomicrobia. Acidobacteria and Proteobacteria were negatively correlated with AKP and HDL-C and positively correlated with TG. Bacteroidetes were positively correlated with HDL-C and negatively correlated with AKP and TG. The results showed that these changes in colony abundance were closely related to the structural changes of intestinal flora in NAFL mice before and after administration.

Network Pharmacology

249 effective compounds were obtained by screening and removing the repetitive compounds among the herbs. The above compounds were used for target prediction, correction,

and deletion of duplicate targets, and a total of 1,186 standard gene names for the targets were obtained. The “herb-compound-target” network of HRG is shown in **Figure 4A** (the yellow nodes represent drug targets, the green nodes represent compounds, and the red nodes represent herb), and 14 compounds in the 20 nodes with the highest degree value were selected as key compounds (**Table 3**). The PPI network of NAFL is shown in **Figure 4B** and the PPI network of IFD is shown in **Figure 4C**. The targets related to NAFL, the targets related to IFD, and the targets corresponding to the compounds were merged simultaneously, and the targets of HRG to treat NAFL through intestinal flora were obtained (**Figure 4D**). Module analysis and cytoHubba analysis were performed with this merged network. Module analysis shows module one (**Figure 4E**, score = 7.2) and module two (**Figure 4F**, score = 7.0), and cytoHubba analysis shows the top 10 targets (**Figure 4G**). Finally, 10 key potential therapeutic targets were obtained: CXCL10, CXCL8, ICAM1, IFNG, IL10, IL1B, IL2, IL4,

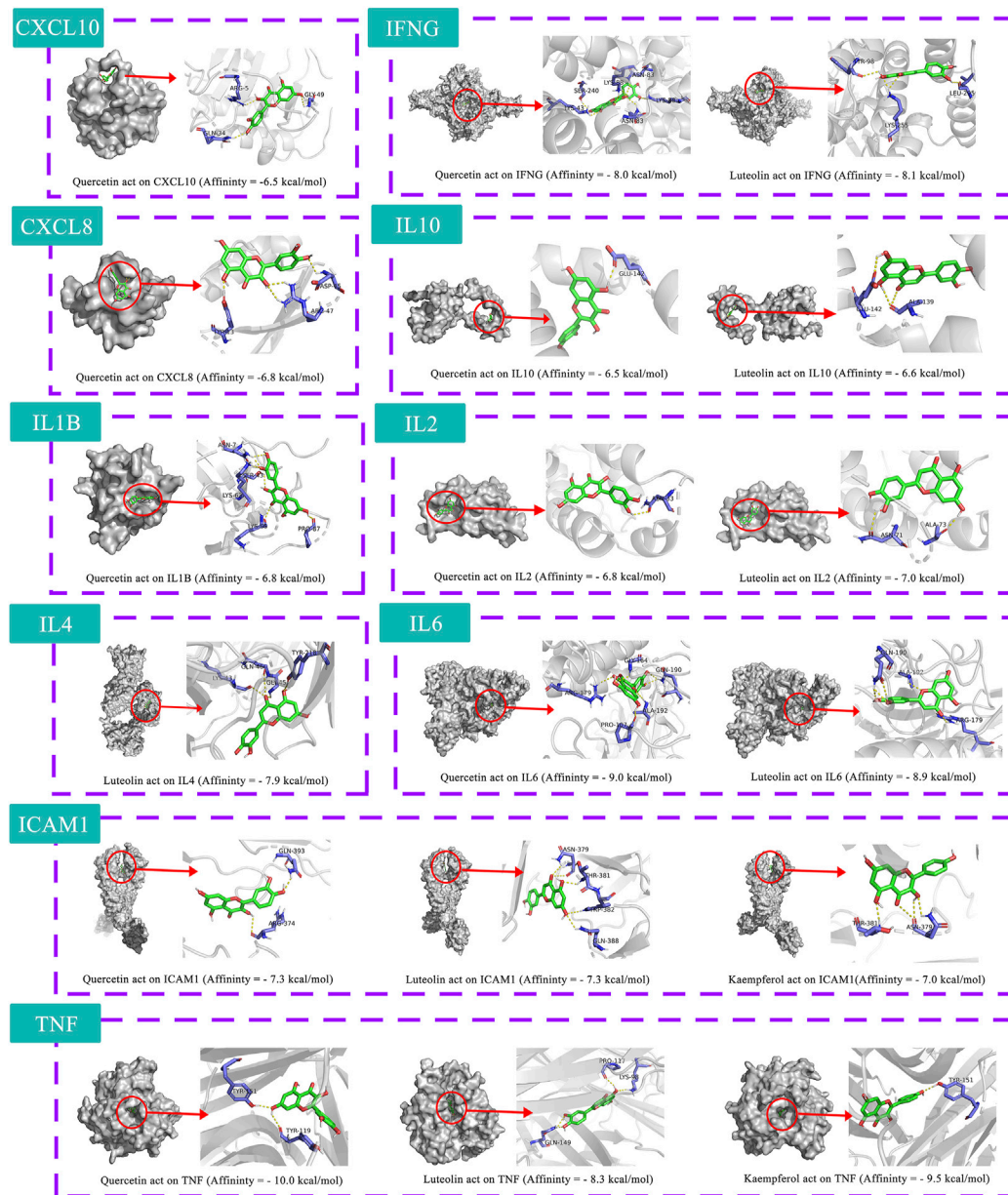


FIGURE 5 | Molecular docking simulation.

IL6, TNF. The node size in **Figures 4A–F** is positively correlated with the degree value. Node colors in **Figures 4B–F** are positively correlated with degree values.

GO and KEGG enrichment analysis were performed for the intersection targets, and a total of 184 pathways (**Supplementary Table S4**) and 980 GO entries (**Supplementary Table S5**) were enriched. The KEGG enrichment results showed that there were 59 pathways related to Organic Systems, eight pathways related to Metabolism, 80 pathways related to Human Diseases, one pathway related to Genetic Information Processing, and 25 pathways related to Environmental Information Processing

and 11 pathways related to Cellular Processes. The enrichment results showed that Cytokine-cytokine receptor interaction, Chagas disease, Influenza A and other pathways had better enrichment results. The GO enrichment results showed that the BP entries accounted for 97.04%, the MF entries accounted for 2.65%, and the CC entries accounted for 0.31%. BP mainly related to metabolic process of reactive oxygen species, response to molecules of bacterial origin, regulation of inflammatory response, etc. MF mainly related to Receptor ligand activity, signaling receptor activator activity, cytokine receptor binding, etc. CC mainly related to membrane raft, membrane microdomain and membrane region.

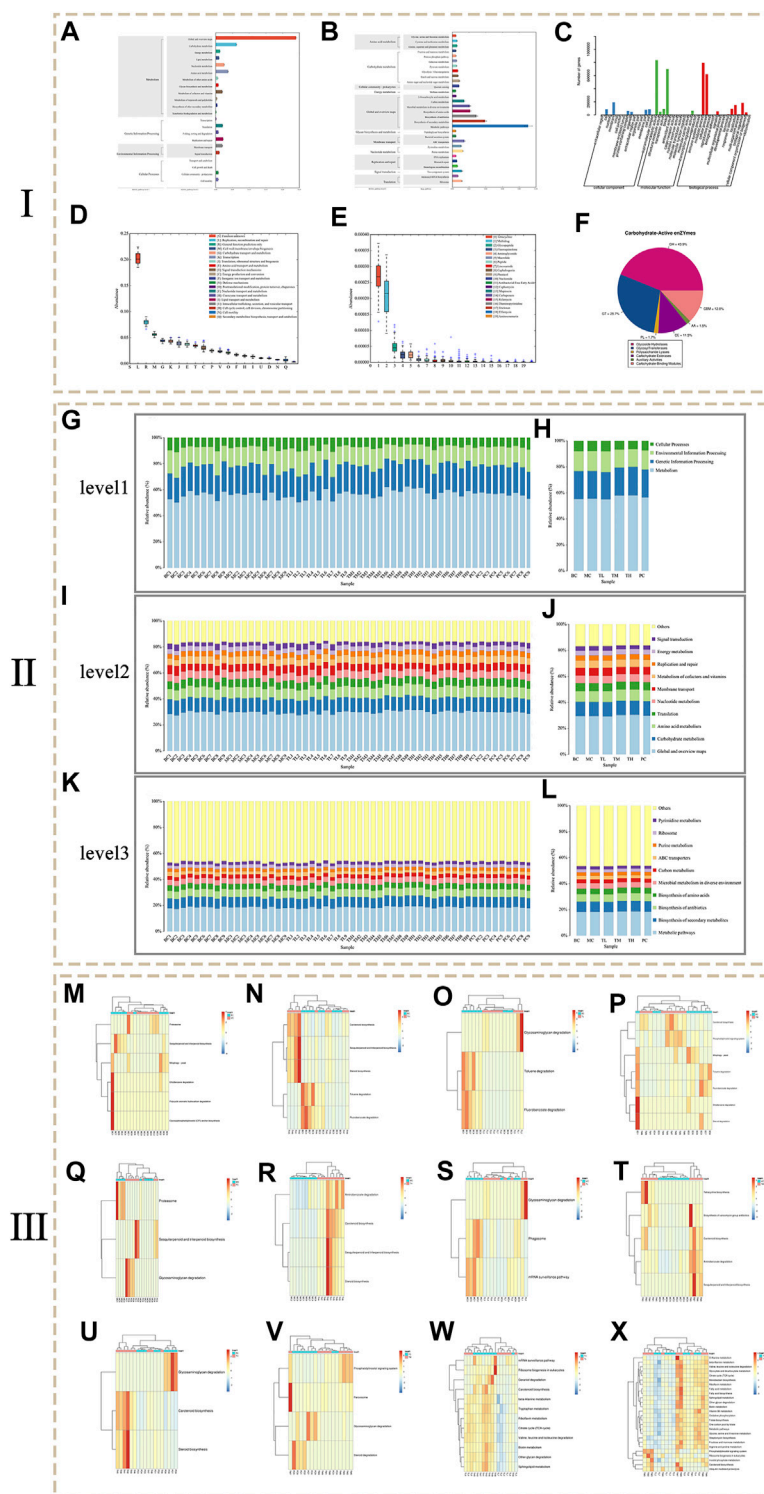


FIGURE 6 | The results of metagenomics sequencing. (I: Functional annotation analysis. II: Histogram of KEGG pathway composition and abundance. III: Heat map of metagenomeSeq differential pathway abundance).

The 10 key therapeutic targets, 14 key compounds, and related pathways were used to construct a network diagram of “herb-key compound-potential target-pathway” through Cytoscape

(Figure 4H). The top three compounds were selected as potential compounds (quercetin, Luteolin, Kaempferol). The top three signaling pathways were selected as key pathways

(Cytokine-cytokine receptor interaction, Chagas disease, IL-17 signaling pathway). Pathway Builder Tool 2.0 was used to draw the cartoon pathway mechanism of HRG in the treatment of NAFL through the intestinal flora (**Figure 4I**). The 10 key targets were molecularly docked with three potential compounds, and a total of 18 pairs of docking results were obtained (**Table 4**). The results were visualized using Pymol (**Figure 5**).

Metagenomics Sequencing

The functional diversity of the environmental samples is analyzed from the perspective of gene function, and the species diversity contained in the environmental samples is analyzed from the perspective of species. The original sequence was filtered by fastp software to obtain high-quality sequencing data. Bowtie2 was used to align with the host genome sequence to remove host contamination. MEGAHIT software was used for macrogenome assembly, and contig sequences shorter than 300 bp were filtered. QUASt software was used to evaluate the assembly results. A total of 360,000,366,878 bp of clean reads were obtained through quality control, and the final number of effective reads was 914,019,667 bp. 15,830,378 contigs were obtained with a total length of 16,591,141,994 bp. MMseqs2 software was used to remove redundancy. The similarity threshold was set at 95% and the coverage threshold was set at 90%. The statistical results of the quality control of the sequencing data of each group can be found in **Supplementary Table S6**, and the statistical information of the assembly results can be found in **Supplementary Table S7**.

Function annotation is based on the KEGG (**Figures 6A,B**), GO (**Figure 6C**), eggNOG (**Figure 6D**), CARD (**Figure 6E**), and CAZy (**Figure 6F**) databases. A total of 6055 KO (KEGG Ontology) and 2104 EC (enzyme) were annotated. Function was enriched in the pathways, resulting in four pathways at level 1, 22 pathways at level 2 and 167 pathways at level 3. The KEGG functional genes are closely related to metabolism related pathways, and the abundance of global and overview maps is highest for secondary pathways. Go annotated three categories, 42 secondary classifications, and 1,558 entries. EggNOG was annotated in four categories, 25 secondary classifications and 31039 eggNOG. The results showed that the number of corresponding functional genes of Replication, recommendation and repair and General function prediction only accounted for a relatively high proportion. Cell wall/membrane/envelope biogenesis and Carbohydrate transport and metabolism ranked second. The annotation results of the CARD database showed that the relative content of resistance genes corresponding to Tetracycline and Multidrug of antibiotic resistance is high, followed by Fluoroquinolone and Aminoglycoside. The annotation results of the CAZy database show that the top three carbohydrate enzymes are glycoside hydrolase (GH), glycosyltransferase (GT) and non-catalytic carbohydrate binding module (CBM).

Figures 6G–L shows the composition of the KEGG pathways at different levels of each group and sample. At level 1 of each group, the abundance of Metabolic was the highest and the abundance of Cellular processes was the lowest. At level 2 of each group, the abundance of Global and overview maps is the highest, followed by Carbohydrate metabolism and Amino acid

metabolism. The abundances of Translation, Nucleoside metabolism, Membrane transport and Metabolism of cofactors and vitamins are similar. Among the levels 3 of each group, the abundance of metabolic pathways was the highest, followed by biosynthesis of secondary metals, and third was Biosynthesis of antibiotics. Biosynthesis of amino acids and Microbial metabolism in diverse environments have little difference in abundance. In contrast, Carbon metabolism, ABC transporters, Purine metabolism, Ribosome and Pyrimidine metabolism have little difference in abundance. The results showed that compared with the blank group and the model group, the abundance of Metabolism at level 1, Global and overview maps at level 2 and Metabolic pathways at level 3 increases to some extent in the HRG group. It is speculated that HRG can improve NAFL by increasing metabolic pathways associated with metabolic regulation.

MetagenomeSeq was used to test the difference in abundance of KEGG at level 3 ($p < 0.05$), and the analyzed difference was plotted according to abundance, as shown in **Figures 6M–X**. The results showed that the abundance of Proteasome in the MC group was significantly higher than that in the BC group, and the Sesquiterpenoid and triterpenoid biosynthesis in the MC group was significantly lower than that in the BC group. Compared with the MC group, the PC group changed this trend. Compared with the BC group, the abundance of Fluorobenzoate degradation and Toluene degradation was higher in the HRG group. Compared with the MC group, the metabolic pathways with higher abundance in the HRG group include Aminobenzoate degradation, Carotenoid biosynthesis, Sesquiterpenoid and triterpenoid biosynthesis, Steroid biosynthesis, Glycosaminoglycan degradation, Phagosome, mRNA surveillance pathway, Tetracycline biosynthesis, Biosynthesis of vancomycin group antibiotics, Carotenoid biosynthesis, Aminobenzoate degradation, Sesquiterpenoid and triterpenoid biosynthesis. Therefore, HRG may improve NAFL through Metabolism and Cellular processes in which metabolism related pathways play an important role. Aminobenzoate degradation, Steroid biosynthesis, and Sesquiterpenoid and triterpenoid biosynthesis are important metabolic pathways.

DISCUSSION

Nonalcoholic Fatty Liver (NAFL), a common chronic disease in the clinic, can develop into nonalcoholic steatohepatitis, which can progress to cirrhosis or even liver cancer and is also related with the occurrence and development of other chronic diseases (Wang and Malhi, 2018; Aron-Wisniewsky et al., 2020). When liver tissue is diseased or liver cells are damaged, the activity of related liver enzymes and serum concentrations, such as AKP, ALT and AST, is increased (Zhou et al., 2017; Eshraghian et al., 2020; Choudhary et al., 2021; Nielsen et al., 2021). NAFL itself is also a metabolic disease that may be manifested by abnormal lipid metabolism and a significant or insignificant increase in blood lipids, such as HDLC, LDL-C, TC and TG (Jimenez-Rivera et al., 2017; Chen et al., 2020; Liu et al., 2020; Mohammadi et al., 2020). In our study, serum HDL-C in model mice increased and

decreased after administration, which was similar to the results of Sheng et al. (Sheng et al., 2019). Changes in serum levels may be related to the degree of NAFLD, species and individual differences. A number of studies have shown that adjuvant therapy regulated by intestinal flora can effectively improve liver function, blood lipids, BMI and other levels of NAFL patients, suggesting that intestinal flora plays an important role in NAFL treatment (Tsai et al., 2020; Burz et al., 2021; Fernandez-Botran et al., 2021; Pan et al., 2021; Yang et al., 2021). The results of this study showed that Huazhi Rougan granules (HRG) could improve liver enzymes and lipid indexes of NAFL mice. The improvement effect of HDL-C, TG and AKP was better than that of the positive control group, and the therapeutic effect was related to the concentration. In addition, HRG can improve the accumulation of liver lipids in NAFL model mice, and the improvement of liver lesions may be dose-dependent.

The results of microbial diversity analysis showed that HRG could increase microbial diversity, increase species richness, and affect the microbial structure of NAFL mice. At the phylum level, HRG increased *Bacteroides* and Verrucomicrobia and decreased Firmicutes and Proteobacteria in NAFL mice. At the genus level, Akkermansia increased, and *Lactobacillus* and *Desulfovibrio* reduced. RDA analysis showed that species distribution was significantly correlated with AKP, HDL-C and TG. Bacteroidetes were negatively correlated with AKP, AST, TG and TC, while Firmicutes were negatively correlated with ALT, LDL-C and TC. Other studies have also found that the intestinal flora composition affects NAFL (Rau et al., 2018; Demir et al., 2020). Studies have shown that the Firmicutes/Bacteroidetes (F/B) ratio is related not only to intestinal homeostasis but also related to NAFL (Porras et al., 2017; Lee et al., 2020; Stojanov et al., 2020; Jasirwan et al., 2021). The results of the animal experiment by Bao et al. were similar to ours, and the reduction of F/B ratio could improve NAFL-related indicators (Bao et al., 2020). Huang et al.'s experiment also showed that the reduction of F/B ratio could alleviate NAFL in mice (Huang et al., 2019). Metagenomic sequencing analysis is mainly concerned with functional information. The results showed that metabolism-related functions, such as metabolism-related pathways, including metabolic pathways, secondary metabolites, antibiotics and amino acid biosynthesis, were increased in the treatment group compared with the model group. The results showed that metabolism-related functions increased in the treatment group compared with the model group, and there were significant differences in metabolism-related pathways. Analysis of the differences in metabolic pathways showed that metabolism-related pathways differed significantly between groups, indicating that the metabolic activities of bacteria were vigorous. The application of HRG increased Aminobenzoate degradation, Steroid biosynthesis, Sesquiterpenoid and triterpenoid biosynthesis. Many sesquiterpenoids have been isolated from plants, fungi, marine organisms, and *Streptomyces* species (Bertea et al., 2006; Nagegowda et al., 2008; Field et al., 2011). Furthermore, sesquiterpene pyridine alkaloids from *Tripterygium* were predicted to target several proteins and signaling pathways and may play an important role in curing Alzheimer's disease, Chagas disease, and NAFL

(Long et al., 2021). The aminobenzoate degradation pathway could promote tryptophan metabolism and benzoate degradation (Naidu and Ragsdale, 2001; McLeish et al., 2003; Toraya et al., 2004). The animal studies by Zhang et al. showed that the main changes in fecal metabolites of high-fat fed mice included metabolites related to tryptophan metabolism (Zhang et al., 2021). Steroid biosynthesis is associated with lipid metabolism and may increase primary bile acid biosynthesis (Lange and Ghassemian, 2003; Morikawa et al., 2006). Studies have shown that key pathways of lipid metabolisms, such as steroid biosynthesis, fatty acid synthesis, and oxidation, are involved in the progression of non-alcoholic fatty liver disease (Huang et al., 2020). A number of studies have also shown that primary bile acid biosynthesis is closely related to the occurrence and development of non-alcoholic fatty liver disease, and inhibition of this metabolic pathway can improve lipid accumulation in NAFL (Zhong et al., 2018; Na et al., 2019; Zhang et al., 2020). Therefore, NAFL can be alleviated by decreasing the F/B ratio and increasing the corresponding metabolic pathways. These results suggest that HRG may regulate intestinal flora and improve lipid metabolism in NAFL mice through the above channels.

Three potential compounds (Quercetin, Luteolin, Kaempferol), 10 core targets (CXCL10, CXCL8, ICAM1, IFNG, IL10, IL1B, IL2, IL4, IL6, TNF) and three key pathways (Cytokine–cytokine receptor interaction, Chagas disease, IL-17 signaling pathway) were identified based on the network pharmacology results. The 10 identified core targets are mainly related to inflammation, and these cytokines play an important role in the inflammatory response and immune regulation (Ouyang and O'Garra, 2019; Torretta et al., 2020; Jurdziński et al., 2020; Bui et al., 2020; Zhong et al., 2020). A number of studies have shown that the occurrence and progression of NAFL are closely related to the increased expression level of inflammatory factors (Chakraborty et al., 2019; Her et al., 2020; Moreno-Fernandez et al., 2021). The rat experiments by Ogunlana et al. showed that inhibition of oxidative stress, increase in antioxidant enzyme levels, and decrease in pro-inflammatory markers (IL-2, IL-6, TNF- α) could reverse NAFL-induced histological changes in the liver in rats (Ogunlana et al., 2020). Other studies have reported that these cytokines are associated with intestinal microflora disorder, intestinal immunity and intestinal inflammation (Sun et al., 2020). For example, Hui et al. found that alterations in the bacterial flora of neonatal necrotizing enterocolitis patients resulted in overt intestinal inflammation and increased expression of IL-1, IL-2, IL-4, IL-6, IL-8, IL-10, TNF- α , IFN- γ and IL-17 in the samples (Hui et al., 2017). Other experiments have also proved that inflammatory factors have an important relationship with intestinal flora disorder in NAFL mice, and improving intestinal flora disorder may intervene in the occurrence and progression of NAFL (Zhang et al., 2018; Li et al., 2020; Kang et al., 2021; Li et al., 2021; Shi et al., 2021). Studies have shown that Chagas disease is related to the changes and dysfunction of intestinal microbiota, which may be an important mechanism for the occurrence of intestinal flora disorder (de Souza-Basqueira et al., 2020; Duarte-Silva et al., 2020; Schaub, 2021). The study by Wang et al. suggests that the

differentiation of cytokines related to the IL-17 signaling pathway is related to the colonization of intestinal flora and may be involved in intestinal immune homeostasis (Wang et al., 2019). The animal experiments of Xin et al. and the mass spectrometry analysis Du et al. showed that both the enterohepatic circulation and the intestinal flora are involved in the absorption process of quercetin and kaempferol and that isorhamnetin 3-O-glucoside could be successively decomposed into quercetin and kaempferol under bacterial action (Du et al., 2014; Du et al., 2017; Xin et al., 2019). A number of animal experiments have shown that quercetin can improve hepatic steatosis and prevent hepatic lipid accumulation, thereby treating NAFL (Esrefoglu et al., 2017; Donaldson et al., 2019). Therefore, we believe that HRG may improve intestinal inflammation, intestinal immunity, and lipid synthesis through relevant pathways, thereby improving NAFL by regulating intestinal flora. However, our study has some limitations, and more studies are needed for further verification.

CONCLUSION

In conclusion, HRG may alter microbial diversity, structure, and function to improve NAFL induced by high-fat diets. It is also possible to improve NAFL-related lipid accumulation and liver lesions by regulating intestinal related metabolic pathways, inflammatory responses, and immune responses. These results strongly suggest that HRG may alleviate NAFL by preventing intestinal flora disorder. Moreover, HRG can treat NAFL with multiple components, multiple metabolic pathways, and multiple targets through intestinal flora. This study provides a new idea for the treatment of NAFL, proves the relationship between intestinal flora and NAFL, and suggests that HRG has a good therapeutic effect.

DATA AVAILABILITY STATEMENT

The datasets presented in this study can be found in online repositories. The names of the repository/repositories and accession number(s) can be found below: <https://www.ncbi.nlm.nih.gov/>

REFERENCES

- Aron-Wisniewsky, J., Warmbrunn, M. V., and Nieuwdorp, M. (2020). Nonalcoholic Fatty Liver Disease: Modulating Gut Microbiota to Improve Severity? *Gastroenterology* 158 (7), 1881–1898. doi:10.1053/j.gastro.2020.01.049
- Bao, T., He, F., and Zhang, X. (2020). Inulin Exerts Beneficial Effects on Non-alcoholic Fatty Liver Disease via Modulating Gut Microbiome and Suppressing the Lipopolysaccharide-toll-like Receptor 4-M Ψ -Nuclear Factor- κ B-nod-like Receptor Protein 3 Pathway via Gut-Liver Axis in Mice. *Front. Pharmacol.* 11, 558525. doi:10.3389/fphar.2020.558525
- Bertea, C. M., Voster, A., and Verstappen, F. W. (2006). Isoprenoid Biosynthesis in *Artemisia Annua*: Cloning and Heterologous Expression of a Germacrene A Synthase from a Glandular Trichome cDNA Library. *Arch. Biochem. Biophys.* 448 (1–2), 3–12. doi:10.1016/j.abb.2006.02.026

[nlm.nih.gov/](https://www.ncbi.nlm.nih.gov/); 16S rRNA sequencing data is available via BioProject PRJNA807481, metagenomic sequencing data is available via BioProject PRJNA807437.

ETHICS STATEMENT

The animal study was reviewed and approved by the animals were raised in ICV cages of experimental Animal Center of Beijing University of Chinese Medicine. Ethical Code: BUCM-4-2021032003-1090.

AUTHOR CONTRIBUTIONS

YL and JW conceived and designed the study; YT and CW provided significative suggestions on the methodology; JH and XF modeled the animals; JH, SL, HW, JZ, FZ, ZW, and ZH collected the experimental animal samples; BL, MC, GC, and YM performed the network pharmacology analysis; AS polished the manuscript. YL was a major contributor in writing the manuscript. All authors read and approved the final of the manuscript. Thanks to all authors for their contribution to this manuscript.

FUNDING

This work was supported by grants from the Young Scientists Training Program of Beijing University of Chinese Medicine (Grant nos. BUCM-201901001), National Nature Science Foundation of China (Grant nos.82074284) and the Project of Cooperation between Beijing University of Chinese Medicine and Lunan Pharmaceutical (Grant nos. BUCM-2021-JS-FW-028).

SUPPLEMENTARY MATERIAL

The Supplementary Material for this article can be found online at: <https://www.frontiersin.org/articles/10.3389/fphar.2022.875700/full#supplementary-material>

- Bui, T. M., Wiesolek, H. L., and Sumagin, R. (2020). ICAM-1: A Master Regulator of Cellular Responses in Inflammation, Injury Resolution, and Tumorigenesis. *J. Leukoc. Biol.* 108 (3), 787–799. doi:10.1002/JLB.2MR0220-549R
- Burz, S. D., Monnoye, M., and Philippe, C. (2021). Fecal Microbiota Transplant from Human to Mice Gives Insights into the Role of the Gut Microbiota in Non-alcoholic Fatty Liver Disease (NAFLD). *Microorganisms* 9 (1), 199. doi:10.3390/microorganisms9010199
- Chakraborty, A., Choudhury, A., and Saha, A. (2019). Development of Non-alcoholic Fatty Liver Disease (NAFLD) in Young Obese Tribal Subjects of Tripura: Link between Low 25 (OH) Vitamin-D Levels and Immune Modulators. *J. Assoc. Physicians India* 67 (8), 52–56.
- Chen, K. L., Bi, K. S., and Han, F. (2015). Evaluation of the Protective Effect of Zhi-Zi-Da-Huang Decoction on Acute Liver Injury with Cholestasis Induced by α -naphthylisothiocyanate in Rats. *J. Ethnopharmacol.* 172, 402–409. doi:10.1016/j.jep.2015.06.043

- Chen, M., Guo, W. L., and Li, Q. Y. (2020). The Protective Mechanism of *Lactobacillus Plantarum* FZU3013 against Non-alcoholic Fatty Liver Associated with Hyperlipidemia in Mice Fed a High-Fat Diet. *Food Funct.* 11 (4), 3316–3331. doi:10.1039/c9fo03003d
- Choudhary, N. S., Saraf, N., and Saigal, S. (2021). Nonalcoholic Fatty Liver in Lean Individuals: Clinicobiochemical Correlates of Histopathology in 157 Liver Biopsies from Healthy Liver Donors. *J. Clin. Exp. Hepatol.* 11 (5), 544–549. doi:10.1016/j.jceh.2021.01.004
- Cobbina, E., and Akhlaghi, F. (2017). Non-alcoholic Fatty Liver Disease (NAFLD) - Pathogenesis, Classification, and Effect on Drug Metabolizing Enzymes and Transporters. *Drug Metab. Rev.* 49 (2), 197–211. doi:10.1080/03602532.2017.1293683
- Daina, A., Michielin, O., and Zoete, V. (2019). SwissTargetPrediction: Updated Data and New Features for Efficient Prediction of Protein Targets of Small Molecules. *Nucleic Acids Res.* 47 (W1), W357–W364. doi:10.1093/nar/gkz382
- de Souza-Basqueira, M., Ribeiro, R. M., and de Oliveira, L. C. (2020). Gut Dysbiosis in Chagas Disease. A Possible Link to the Pathogenesis. *Front. Cel. Infect. Microbiol.* 10, 402. doi:10.3389/fcimb.2020.00402
- de Vries, M., Westerink, J., and Kaasjager, K. H. A. H. (2020). Prevalence of Nonalcoholic Fatty Liver Disease (NAFLD) in Patients with Type 1 Diabetes Mellitus: A Systematic Review and Meta-Analysis. *J. Clin. Endocrinol. Metab.* 105 (12), 3842–3853. doi:10.1210/clinem/dgaa575
- Demir, M., Lang, S., and Martin, A. (2020). Phenotyping Non-alcoholic Fatty Liver Disease by the Gut Microbiota: Ready for Prime Time? *J. Gastroenterol. Hepatol.* 35 (11), 1969–1977. doi:10.1111/jgh.15071
- Deprince, A., Haas, J. T., and Stals, B. (2020). Dysregulated Lipid Metabolism Links NAFLD to Cardiovascular Disease. *Mol. Metab.* 42, 101092. doi:10.1016/j.molmet.2020.101092
- Donaldson, J., Ngema, M., and Nkomozepi, P. (2019). Quercetin Administration post-weaning Attenuates High-Fructose, High-Cholesterol Diet-Induced Hepatic Steatosis in Growing, Female, Sprague Dawley Rat Pups. *J. Sci. Food Agric.* 99 (15), 6954–6961. doi:10.1002/jsfa.9984
- Du, L. Y., Zhao, M., and Tao, J. H. (2017). The Metabolic Profiling of Isorhamnetin-3-O-Neohesperidoside Produced by Human Intestinal Flora Employing UPLC-Q-TOF/MS. *J. Chromatogr. Sci.* 55 (3), 243–250. doi:10.1093/chromsci/bmw176
- Du, L. Y., Zhao, M., and Xu, J. (2014). Analysis of the Metabolites of Isorhamnetin 3-O-Glucoside Produced by Human Intestinal flora *In Vitro* by Applying Ultraperformance Liquid Chromatography/quadrupole Time-Of-Flight Mass Spectrometry. *J. Agric. Food Chem.* 62 (12), 2489–2495. doi:10.1021/jf405261a
- Duarte-Silva, E., Morais, L. H., and Clarke, G. (2020). Targeting the Gut Microbiota in Chagas Disease: What Do We Know So Far? *Front. Microbiol.* 11, 585857. doi:10.3389/fmicb.2020.585857
- Eberhardt, J., Santos-Martins, D., and Tillack, A. F. (2021). AutoDock Vina 1.2.0: New Docking Methods, Expanded Force Field, and Python Bindings. *J. Chem. Inf. Model.* 61 (8), 3891–3898. doi:10.1021/acs.jcim.1c00203
- Eckel, R. H., Alberti, K. G., and Grundy, S. M. (2010). The Metabolic Syndrome. *Lancet* 375 (9710), 181–183. doi:10.1016/S0140-6736(09)61794-3
- Eshraghian, A., Nikeghbalian, S., and Geramizadeh, B. (2020). Characterization of Biopsy Proven Non-alcoholic Fatty Liver Disease in Healthy Non-obese and Lean Population of Living Liver Donors: The Impact of Urlic Acid. *Clin. Res. Hepatol. Gastroenterol.* 44 (4), 572–578. doi:10.1016/j.clinre.2019.09.002
- Esrefoglu, M., Cetin, A., and Taslidere, E. (2017). Therapeutic Effects of Melatonin and Quercetin in Improvement of Hepatic Steatosis in Rats through Suppression of Oxidative Damage. *Bratisl. Lek. Listy.* 118 (6), 347–354. doi:10.4149/BLL_2017_066
- Fernandez-Botran, R., Plankey, M. W., and Ware, D. (2021). Changes in Liver Steatosis in HIV-Positive Women Are Associated with the BMI, but Not with Biomarkers. *Cytokine* 144, 155573. doi:10.1016/j.cyto.2021.155573
- Field, B., Fiston-Lavier, A. S., and Kemen, A. (2011). Formation of Plant Metabolic Gene Clusters within Dynamic Chromosomal Regions. *Proc. Natl. Acad. Sci. USA.* 108 (38), 16116–16121. doi:10.1073/pnas.1109273108
- Gao, G. Y., Xue, J. D., Bai, Y. Y., Kang, Y., and Bai, X. (2021). Research Progress on Effects of Single Chinese Medicine and its Active Components on Animal Model of Nonalcoholic Fatty Liver Disease. *Mod. J. Integrated Traditional Chin. West. Med.* 30 (15), 1702–1706.
- Gomaa, E. Z. (2020). Human Gut Microbiota/microbiome in Health and Diseases: a Review. *Antonie Van. Leeuwenhoek.* 113 (12), 2019–2040. doi:10.1007/s10482-020-01474-7
- Graffy, P. M., and Pickhardt, P. J. (2016). Quantification of Hepatic and Visceral Fat by CT and MR Imaging: Relevance to the Obesity Epidemic, Metabolic Syndrome and NAFLD. *Br. J. Radiol.* 89 (1062), 20151024. doi:10.1259/bjr.20151024
- Her, Z., Tan, J. H. L., and Lim, Y. S. (2020). CD4+ T Cells Mediate the Development of Liver Fibrosis in High Fat Diet-Induced NAFLD in Humanized Mice. *Front. Immunol.* 11, 580968. doi:10.3389/fimmu.2020.580968
- Hong, Y., Li, B., and Zheng, N. (2020). Integrated Metagenomic and Metabolomic Analyses of the Effect of Astragalus Polysaccharides on Alleviating High-Fat Diet-Induced Metabolic Disorders. *Front. Pharmacol.* 11, 833. doi:10.3389/fphar.2020.00833
- Huang, X., Chen, W., and Yan, C. (2019). Gypenosides Improve the Intestinal Microbiota of Non-alcoholic Fatty Liver in Mice and Alleviate its Progression. *Biomed. Pharmacother.* 118, 109258. doi:10.1016/j.biopha.2019.109258
- Huang, Z. R., Chen, M., and Guo, W. L. (2020). Monascus Purpureus-Fermented Common Buckwheat Protects against Dyslipidemia and Non-alcoholic Fatty Liver Disease through the Regulation of Liver Metabolome and Intestinal Microbiome. *Food Res. Int.* 136, 109511. doi:10.1016/j.foodres.2020.109511
- Hui, L., Dai, Y., and Guo, Z. (2017). Immunoregulation Effects of Different $\gamma\delta$ T Cells and Toll-like Receptor Signaling Pathways in Neonatal Necrotizing Enterocolitis. *Medicine (Baltimore)* 96 (8), e6077. doi:10.1097/MD.0000000000006077
- Jasirwan, C. O. M., Muradi, A., and Hasan, I. (2021). Correlation of Gut Firmicutes/Bacteroidetes Ratio with Fibrosis and Steatosis Stratified by Body Mass Index in Patients with Non-alcoholic Fatty Liver Disease. *Biosci. Microbiota Food Health* 40 (1), 50–58. doi:10.12938/bmfh.2020-046
- Jiang, C., Xie, C., and Li, F. (2015). Intestinal Farnesoid X Receptor Signaling Promotes Nonalcoholic Fatty Liver Disease. *J. Clin. Invest.* 125 (1), 386–402. doi:10.1172/JCI76738
- Jimenez-Rivera, C., Hadjiyannakis, S., Davila, J., and Hurteau, J. (2017). Prevalence and Risk Factors for Non-alcoholic Fatty Liver in Children and Youth with Obesity. *BMC Pediatr.* 17 (1), 113. doi:10.1186/s12887-017-0867-z
- Jurdziński, K. T., Potempa, J., and Grabiec, A. M. (2020). Epigenetic Regulation of Inflammation in Periodontitis: Cellular Mechanisms and Therapeutic Potential. *Clin. Epigenetics.* 12 (1), 186. doi:10.1186/s13148-020-00982-7
- Kanehisa, M., and Sato, Y. (2020). KEGG Mapper for Inferring Cellular Functions from Protein Sequences. *Protein Sci.* 29 (1), 28–35. doi:10.1002/pro.3711
- Kang, Y., Yang, Y., and Wang, J. (2021). Correlation between Intestinal Flora and Serum Inflammatory Factors in Post-stroke Depression in Ischemic Stroke. *J. Coll. Physicians Surg. Pak.* 31 (10), 1224–1227. doi:10.29271/jcpsp.2021.10.1224
- Kim, J., So, S., and Lee, H. J. (2013). DigSee: Disease Gene Search Engine with Evidence Sentences (Version Cancer). *Nucleic Acids Res.* 41, W510–W517. doi:10.1093/nar/gkt531
- Kim, M. H., Yun, K. E., and Kim, J. (2020). Gut Microbiota and Metabolic Health Among Overweight and Obese Individuals. *Sci. Rep.* 10 (1), 19417. doi:10.1038/s41598-020-76474-8
- Kong, C., Gao, R., and Yan, X. (2019). Probiotics Improve Gut Microbiota Dysbiosis in Obese Mice Fed a High-Fat or High-Sucrose Diet. *Nutrition* 60, 175–184. doi:10.1016/j.nut.2018.10.002
- Kořínková, L., Pražienková, V., and Černá, L. (2020). Pathophysiology of NAFLD and NASH in Experimental Models: The Role of Food Intake Regulating Peptides. *Front. Endocrinol. (Lausanne)* 11, 597583. doi:10.3389/fendo.2020.597583
- Lange, B. M., and Ghassemian, M. (2003). Genome Organization in *Arabidopsis thaliana*: a Survey for Genes Involved in Isoprenoid and Chlorophyll Metabolism. *Plant Mol. Biol.* 51 (6), 925–948. doi:10.1023/a:1023005504702
- Layeghifard, M., Hwang, D. M., and Guttman, D. S. (2018). Constructing and Analyzing Microbiome Networks in R. *Methods Mol. Biol.* 1849, 243–266. doi:10.1007/978-1-4939-8728-3_16
- Lee, N. Y., Yoon, S. J., and Han, D. H. (2020). *Lactobacillus* and *Pediococcus* Ameliorate Progression of Non-alcoholic Fatty Liver Disease through Modulation of the Gut Microbiome. *Gut Microbes* 11 (4), 882–899. doi:10.1080/19490976.2020.1712984

- Li, J., Hu, Q., and Xiao-Yu, D. (2020). Effect of Sheng-Jiang Powder on Gut Microbiota in High-Fat Diet-Induced NAFLD. *Evid. Based Complement. Alternat. Med.* 2020, 6697638. doi:10.1155/2020/6697638
- Li, L., Yan, Q., and Ma, N. (2021). Analysis of Intestinal flora and Inflammatory Cytokine Levels in Children with Non-infectious Diarrhea. *Transl. Pediatr.* 10 (5), 1340–1345. doi:10.21037/tp-21-168
- Liu, Q., Cai, B. Y., and Zhu, L. X. (2020). Liraglutide Modulates Gut Microbiome and Attenuates Nonalcoholic Fatty Liver in Db/db Mice. *Life Sci.* 261, 118457. doi:10.1016/j.lfs.2020.118457
- Long, C., Yang, Y., and Yang, Y. (2021). The Exploration of Novel Pharmacophore Characteristics and Multidirectional Elucidation of Structure-Activity Relationship and Mechanism of Sesquiterpene Pyridine Alkaloids from Tripterygium Based on Computational Approaches. *Evid. Based Complement. Alternat. Med.* 2021, 6676470. doi:10.1155/2021/6676470
- Manor, O., Dai, C. L., and Kornilov, S. A. (2020). Health and Disease Markers Correlate with Gut Microbiome Composition across Thousands of People. *Nat. Commun.* 11 (1), 5206. doi:10.1038/s41467-020-18871-1
- McLeish, M. J., Kneen, M. M., and Gopalakrishna, K. N. (2003). Identification and Characterization of a Mandelamide Hydrolase and an NAD(P)⁺-dependent Benzaldehyde Dehydrogenase from *Pseudomonas Putida* ATCC 12633. *J. Bacteriol.* 185 (8), 2451–2456. doi:10.1128/JB.185.8.2451-2456.2003
- Milani, C., Duranti, S., and Bottacini, F. (2017). The First Microbial Colonizers of the Human Gut: Composition, Activities, and Health Implications of the Infant Gut Microbiota. *Microbiol. Mol. Biol. Rev.* 81 (4), e00036–17. doi:10.1128/MMBR.00036-17
- Mohajeri, M. H., Brummer, R. J. M., and Rastall, R. A. (2018). The Role of the Microbiome for Human Health: from Basic Science to Clinical Applications. *Eur. J. Nutr.* 57 (Suppl. 1), 1–14. doi:10.1007/s00394-018-1703-4
- Mohammadi, S., Farajnia, S., and Shadmand, M. (2020). Association of Rs780094 Polymorphism of Glucokinase Regulatory Protein with Non-alcoholic Fatty Liver Disease. *BMC Res. Notes* 13 (1), 26. doi:10.1186/s13104-020-4891-y
- Moers, B. H. M. (2020). Shortcuts for Faster Image Creation in PyMOL. *Protein Sci.* 29 (1), 268–276. doi:10.1002/pro.3781
- Moreira, G. V., Azevedo, F. F., and Ribeiro, L. M. (2018). Liraglutide Modulates Gut Microbiota and Reduces NAFLD in Obese Mice. *J. Nutr. Biochem.* 62, 143–154. doi:10.1016/j.jnutbio.2018.07.009
- Moreno-Fernandez, M. E., Giles, D. A., and Oates, J. R. (2021). PKM2-dependent Metabolic Skewing of Hepatic Th17 Cells Regulates Pathogenesis of Non-alcoholic Fatty Liver Disease. *Cell Metab.* 33 (6), 1187–1204.e9. doi:10.1016/j.cmet.2021.04.018
- Morikawa, T., Mizutani, M., and Aoki, N. (2006). Cytochrome P450 CYP710A Encodes the Sterol C-22 Desaturase in Arabidopsis and Tomato. *Plant Cell* 18 (4), 1008–1022. doi:10.1105/tpc.105.036012
- Na, J., Choi, S. A., and Khan, A. (2019). Integrative Omics Reveals Metabolic and Transcriptomic Alteration of Nonalcoholic Fatty Liver Disease in Catalase Knockout Mice. *Biomol. Ther. (Seoul)* 27 (2), 134–144. doi:10.4062/biomolther.2018.175
- Nagegowda, D. A., Gutensohn, M., and Wilkerson, C. G. (2008). Two Nearly Identical Terpene Synthases Catalyze the Formation of Nerolidol and Linalool in Snapdragon Flowers. *Plant J.* 55 (2), 224–239. doi:10.1111/j.1365-3113X.2008.03496.x
- Naidu, D., and Ragsdale, S. W. (2001). Characterization of a Three-Component Vanillate O-Demethylase from *Moorella thermoacetica*. *J. Bacteriol.* 183 (11), 3276–3281. doi:10.1128/JB.183.11.3276-3281.2001
- Nakano, H., Wu, S., and Sakao, K. (2020). Bilberry Anthocyanins Ameliorate NAFLD by Improving Dyslipidemia and Gut Microbiome Dysbiosis. *Nutrients* 12 (11), 3252. doi:10.3390/nu12113252
- NCBI Resource Coordinators (2018). Database Resources of the National Center for Biotechnology Information. *Nucleic Acids Res.* 46 (D1), D8–D13. doi:10.1093/nar/gkx1095
- Nielsen, M. J., Leeming, D. J., and Goodman, Z. (2021). Comparison of ADAPT, FIB-4 and APRI as Non-invasive Predictors of Liver Fibrosis and NASH within the CENTAUR Screening Population. *J. Hepatol.* 75 (6), 1292–1300. doi:10.1016/j.jhep.2021.08.016
- Niu, C., Chen, C., and Chen, L. (2011). Decrease of Blood Lipids Induced by Shan-Zha (Fruit of *Crataegus Pinnatifida*) Is Mainly Related to an Increase of PPARα in Liver of Mice Fed High-Fat Diet. *Horm. Metab. Res.* 43 (9), 625–630. doi:10.1055/s-0031-1283147
- Ogunlana, O. O., Ogunlana, O. E., and Adekunbi, T. S. (2020). Anti-inflammatory Mechanism of Ruzu Bitters on Diet-Induced Nonalcoholic Fatty Liver Disease in Male Wistar Rats. *Evid. Based Complement. Alternat. Med.* 2020, 5246725. doi:10.1155/2020/5246725
- Otasek, D., Morris, J. H., and Bouças, J. (2019). Cytoscape Automation: Empowering Workflow-Based Network Analysis. *Genome Biol.* 20 (1), 185. doi:10.1186/s13059-019-1758-4
- Ouyang, W., and O'Garra, A. (2019). IL-10 Family Cytokines IL-10 and IL-22: from Basic Science to Clinical Translation. *Immunity* 50 (4), 871–891. doi:10.1016/j.immuni.2019.03.020
- Pan, X., Kaminga, A. C., and Liu, A. (2021). Gut Microbiota, Glucose, Lipid, and Water-Electrolyte Metabolism in Children with Nonalcoholic Fatty Liver Disease. *Front. Cell Infect. Microbiol.* 11, 683743. doi:10.3389/fcimb.2021.683743
- Papathodoridi, M., and Cholongitas, E. (2018). Diagnosis of Non-alcoholic Fatty Liver Disease (NAFLD): Current Concepts. *Curr. Pharm. Des.* 24 (38), 4574–4586. doi:10.2174/1381612825666190117102111
- Porras, D., Nistal, E., and Martínez-Flórez, S. (2017). Protective Effect of Quercetin on High-Fat Diet-Induced Non-alcoholic Fatty Liver Disease in Mice Is Mediated by Modulating Intestinal Microbiota Imbalance and Related Gut-Liver axis Activation. *Free Radic. Biol. Med.* 102, 188–202. doi:10.1016/j.freeradbiomed.2016.11.037
- Rau, M., Rehman, A., and Dittrich, M. (2018). Fecal SCFAs and SCFA-Producing Bacteria in Gut Microbiome of Human NAFLD as a Putative Link to Systemic T-Cell Activation and Advanced Disease. *United Eur. Gastroenterol. J* 6 (10), 1496–1507. doi:10.1177/2050640618804444
- Romero-Gómez, M., Zelber-Sagi, S., and Trenell, M. (2017). Treatment of NAFLD with Diet, Physical Activity and Exercise. *J. Hepatol.* 67 (4), 829–846. doi:10.1016/j.jhep.2017.05.016
- Ru, J., Li, P., Wang, J., and Zhou, W. (2014). TCMSP: a Database of Systems Pharmacology for Drug Discovery from Herbal Medicines. *J. Cheminform.* 6, 13. doi:10.1186/1758-2946-6-13
- Schaub, G. A. (2021). An Update on the Knowledge of Parasite-Vector Interactions of Chagas Disease. *Res. Rep. Trop. Med.* 12, 63–76. doi:10.2147/RRM.S274681
- Sheng, D., Zhao, S., and Gao, L. (2019). BabaoDan Attenuates High-Fat Diet-Induced Non-alcoholic Fatty Liver Disease via Activation of AMPK Signaling. *Cell Biosci.* 9, 77. doi:10.1186/s13578-019-0339-2
- Shi, A., Li, T., and Zheng, Y. (2021). Chlorogenic Acid Improves NAFLD by Regulating Gut Microbiota and GLP-1. *Front. Pharmacol.* 12, 693048. doi:10.3389/fphar.2021.693048
- Stelzer, G., Rosen, N., and Plaschkes, I. (2016). The GeneCards Suite: From Gene Data Mining to Disease Genome Sequence Analyses. *Curr. Protoc. Bioinformatics* 54, 1. doi:10.1002/cpbi.510.1002/cpbi.5
- Stojanov, S., Berlec, A., and Štrukelj, B. (2020). The Influence of Probiotics on the Firmicutes/Bacteroidetes Ratio in the Treatment of Obesity and Inflammatory Bowel Disease. *Microorganisms* 8 (11), 1715. doi:10.3390/microorganisms8111715
- Sun, Z., Hu, Y., and Wang, Y. (2020). Bupi Hewei Decoction Ameliorates 5-Fluorouracil-Induced Intestinal Dysbiosis in Rats through T Helper 17/T Regulatory Cell Signaling Pathway. *J. Tradit. Chin. Med.* 40 (1), 38–48.
- Targher, G., Byrne, C. D., and Tilg, H. (2020). NAFLD and Increased Risk of Cardiovascular Disease: Clinical Associations, Pathophysiological Mechanisms and Pharmacological Implications. *Gut* 69 (9), 1691–1705. doi:10.1136/gutjnl-2020-320622
- The Gene Ontology Consortium (2019). The Gene Ontology Resource: 20 Years and Still GOing strong. *Nucleic Acids Res.* 47 (D1), D330–D338. doi:10.1093/nar/gky1055
- Toraya, T., Oka, T., and Ando, M. (2004). Novel Pathway for Utilization of Cyclopropanecarboxylate by *Rhodococcus Rhodochrous*. *Appl. Environ. Microbiol.* 70 (1), 224–228. doi:10.1128/AEM.70.1.224-228.2004
- Torretta, S., Scagliola, A., and Ricci, L. (2020). D-mannose Suppresses Macrophage IL-1β Production. *Nat. Commun.* 11 (1), 6343. doi:10.1038/s41467-020-20164-6
- Trott, O., and Olson, A. J. (2010). AutoDock Vina: Improving the Speed and Accuracy of Docking with a New Scoring Function, Efficient Optimization, and Multithreading. *J. Comput. Chem.* 31 (2), 455–461. doi:10.1002/jcc.21334
- Tsai, M. C., Liu, Y. Y., and Lin, C. C. (2020). Gut Microbiota Dysbiosis in Patients with Biopsy-Proven Nonalcoholic Fatty Liver Disease: A Cross-Sectional Study in Taiwan. *Nutrients* 12 (3), 820. doi:10.3390/nu12030820

- UniProt Consortium (2021). UniProt: the Universal Protein Knowledgebase in 2021. *Nucleic Acids Res.* 49 (D1), D480–D489. doi:10.1093/nar/gkaa1100
- Wang, P., Wang, S., and Chen, H. (2021). TCMIP v2.0 Powers the Identification of Chemical Constituents Available in Xinglou Chengqi Decoction and the Exploration of Pharmacological Mechanisms Acting on Stroke Complicated with Tanre Fushi Syndrome. *Front. Pharmacol.* 12, 598200. doi:10.3389/fphar.2021.598200
- Wang, W., Zhao, J., and Gui, W. (2018). Tauroursodeoxycholic Acid Inhibits Intestinal Inflammation and Barrier Disruption in Mice with Non-alcoholic Fatty Liver Disease. *Br. J. Pharmacol.* 175 (3), 469–484. doi:10.1111/bph.14095
- Wang, X. J., and Malhi, H. (2018). Nonalcoholic Fatty Liver Disease. *Ann. Intern. Med.* 169 (9), ITC65–ITC80. doi:10.7326/AITC201811060
- Wang, Y., Yin, Y., and Chen, X. (2019). Induction of Intestinal Th17 Cells by Flagellins from Segmented Filamentous Bacteria. *Front. Immunol.* 10, 2750. doi:10.3389/fimmu.2019.02750
- Wu, T. R., Lin, C. S., and Chang, C. J. (2019). Gut Commensal Parabacteroides Goldsteinii Plays a Predominant Role in the Anti-obesity Effects of Polysaccharides Isolated from *Hirsutella Sinensis*. *Gut* 68 (2), 248–262. doi:10.1136/gutjnl-2017-315458
- Xin, L., Liu, X. H., and Yang, J. (2019). The Intestinal Absorption Properties of Flavonoids in Hippophaë Rhamnoides Extracts by an *In Situ* Single-Pass Intestinal Perfusion Model. *J. Asian Nat. Prod. Res.* 21 (1), 62–75. doi:10.1080/10286020.2017.1396976
- Yang, C., Wan, M., and Xu, D. (2021). Flaxseed Powder Attenuates Non-alcoholic Steatohepatitis via Modulation of Gut Microbiota and Bile Acid Metabolism through Gut-Liver Axis. *Int. J. Mol. Sci.* 22 (19), 10858. doi:10.3390/ijms221910858
- Yang, W., Xu, H., and Yu, X. (2015). Association between Retinal Artery Lesions and Nonalcoholic Fatty Liver Disease. *Hepatol. Int.* 9 (2), 278–282. doi:10.1007/s12072-015-9607-3
- Yiu, J. H. C., Chan, K. S., and Cheung, J. (2020). Gut Microbiota-Associated Activation of TLR5 Induces Apolipoprotein A1 Production in the Liver. *Circ. Res.* 127 (10), 1236–1252. doi:10.1161/CIRCRESAHA.120.317362
- Younossi, Z., Anstee, Q. M., and Marietti, M. (2018). Global burden of NAFLD and NASH: Trends, Predictions, Risk Factors and Prevention. *Nat. Rev. Gastroenterol. Hepatol.* 15 (1), 11–20. doi:10.1038/nrgastro.2017.109
- Younossi, Z. M., Golabi, P., and de Avila, L. (2019). The Global Epidemiology of NAFLD and NASH in Patients with Type 2 Diabetes: A Systematic Review and Meta-Analysis. *J. Hepatol.* 71 (4), 793–801. doi:10.1016/j.jhep.2019.06.021
- Yuan, J., Chen, C., and Cui, J. (2019). Fatty Liver Disease Caused by High-Alcohol-Producing *Klebsiella pneumoniae*. *Cell. Metab.* 30 (4), 675–688.e7. doi:10.1016/j.cmet.2019.08.01810.1016/j.cmet.2019.11.006
- Zhang, D., Zhang, Y., and Gao, Y. (2020). Translating Traditional Herbal Formulas into Modern Drugs: a Network-Based Analysis of Xiaoyao Decoction. *Chin. Med.* 15, 25. doi:10.1186/s13020-020-00302-4
- Zhang, J., Wang, C., and Wang, J. (2018). Relationship between Intestinal flora and Inflammatory Factors in Patients with Nonalcoholic Steatohepatitis. *Exp. Ther. Med.* 15 (1), 723–726. doi:10.3892/etm.2017.5490
- Zhang, Q., Fan, X. Y., and Guo, W. L. (2020). The Protective Mechanisms of Macroalgae *Laminaria Japonica* Consumption against Lipid Metabolism Disorders in High-Fat Diet-Induced Hyperlipidemic Rats. *Food Funct.* 11 (4), 3256–3270. doi:10.1039/d0fo00065e
- Zhang, X., Coker, O. O., and Chu, E. S. (2021). Dietary Cholesterol Drives Fatty Liver-Associated Liver Cancer by Modulating Gut Microbiota and Metabolites. *Gut* 70 (4), 761–774. doi:10.1136/gutjnl-2019-319664
- Zhang, Y., Zhao, M., and Jiang, X. (2021). Comprehensive Analysis of Fecal Microbiome and Metabolomics in Hepatic Fibrosis Rats Reveal Hepatoprotective Effects of Yinchen Wuling Powder from the Host-Microbial Metabolic Axis. *Front. Pharmacol.* 12, 713197. doi:10.3389/fphar.2021.713197
- Zhang, Y., Zhao, M., and Liu, Y. (2021). Investigation of the Therapeutic Effect of Yinchen Wuling Powder on CCl4-Induced Hepatic Fibrosis in Rats by 1H NMR and MS-based Metabolomics Analysis. *J. Pharm. Biomed. Anal.* 200, 114073. doi:10.1016/j.jpba.2021.114073
- Zhang, Z., Chen, X., and Cui, B. (2021). Modulation of the Fecal Microbiome and Metabolome by Resistant Dextrin Ameliorates Hepatic Steatosis and Mitochondrial Abnormalities in Mice. *Food Funct.* 12 (10), 4504–4518. doi:10.1039/d1fo00249j
- Zhong, D., Xie, Z., and Huang, B. (2018). Ganoderma Lucidum Polysaccharide Peptide Alleviates Hepatosteatosis via Modulating Bile Acid Metabolism Dependent on FXR-SHP/FGF. *Cell Physiol Biochem* 49 (3), 1163–1179. doi:10.1159/000493297
- Zhong, Y., He, S., and Huang, K. (2020). Neferine Suppresses Vascular Endothelial Inflammation by Inhibiting the NF-Kb Signaling Pathway. *Arch. Biochem. Biophys.* 696, 108595. doi:10.1016/j.abb.2020.108595
- Zhou, D., Pan, Q., and Xin, F. Z. (2017). Sodium Butyrate Attenuates High-Fat Diet-Induced Steatohepatitis in Mice by Improving Gut Microbiota and Gastrointestinal Barrier. *World J. Gastroenterol.* 23 (1), 60–75. doi:10.3748/wjg.v23.i1.60
- Zhou, J., Zhou, F., and Wang, W. (2020). Epidemiological Features of NAFLD from 1999 to 2018 in China. *Hepatology* 71 (5), 1851–1864. doi:10.1002/hep.31150
- Zhou, Y. J., Zou, H., and Zheng, J. N. (2017). Serum Alkaline Phosphatase, a Risk Factor for Non-alcoholic Fatty Liver, but Only for Women in Their 30s and 40s: Evidence from a Large Cohort Study. *Expert Rev. Gastroenterol. Hepatol.* 11 (3), 269–276. doi:10.1080/17474124.2017.1283984

Conflict of Interest: BL, GC, and YM were employed by the company Lunan Pharmaceutical Group Co. Ltd.

The remaining authors declare that the research was conducted in the absence of any commercial or financial relationships that could be construed as a potential conflict of interest.

Publisher's Note: All claims expressed in this article are solely those of the authors and do not necessarily represent those of their affiliated organizations, or those of the publisher, the editors and the reviewers. Any product that may be evaluated in this article, or claim that may be made by its manufacturer, is not guaranteed or endorsed by the publisher.

Copyright © 2022 Liu, Tan, Huang, Wu, Fan, Stalin, Lu, Wang, Zhang, Zhang, Wu, Li, Huang, Chen, Cheng, Mou and Wu. This is an open-access article distributed under the terms of the Creative Commons Attribution License (CC BY). The use, distribution or reproduction in other forums is permitted, provided the original author(s) and the copyright owner(s) are credited and that the original publication in this journal is cited, in accordance with accepted academic practice. No use, distribution or reproduction is permitted which does not comply with these terms.



Obeticholic Acid Induces Hepatotoxicity Via FXR in the NAFLD Mice

Chuangzhen Lin^{1†}, Bingqing Yu^{1†}, Lixin Chen¹, Zhaohui Zhang¹, Weixiang Ye², Hui Zhong³, Wenke Bai¹, Yuping Yang¹ and Biao Nie^{1*}

¹Department of Gastroenterology, The First Affiliated Hospital of Jinan University, Jinan University, Guangzhou, China,

²Department of Gastrointestinal Endoscopy of Dongpu Branch, The First Affiliated Hospital of Jinan University, Jinan University, Guangzhou, China, ³Department of Gastroenterology, Nanfang Hospital, Southern Medical University, Guangzhou, China

Objective: Obeticholic acid (OCA), a potent farnesoid X receptor (FXR) agonist, is a promising drug for nonalcoholic fatty liver disease (NAFLD); however, it can cause liver injury, especially at high doses. Here, we investigated the role of FXR in the high-dose OCA-induced hepatotoxicity in the condition of the NAFLD mouse model.

Methods: Wild-type (WT) mice and FXR^{-/-} mice were administered with over-dose OCA (0.40%) and high-dose OCA (0.16%), in a high-fat diet. RNA-seq on liver samples of mice fed with high-dose OCA was performed to dig out the prominent biological events contributing to hepatic fibrosis.

Results: Over-dose OCA induced liver injury and shortened survival in WT mice, but not FXR^{-/-} mice. High-dose OCA caused hepatic stellate cell activation and liver fibrosis in the presence of FXR. Furthermore, high-dose OCA induced cholesterol accumulation in livers via the upregulation of genes involved in cholesterol acquisition and downregulation of genes regulating cholesterol degradation in liver, leading to the production of interleukin -1 β and an FXR-mediated inflammatory response.

Conclusion: The high-dose OCA induced FXR-dependent hepatic injury via cholesterol accumulation and interleukin -1 β pathway in the NAFLD mice.

Keywords: nonalcoholic fatty liver disease (NAFLD), obeticholic acid (OCA), farnesoid X receptor (FXR), hepatic fibrosis, interleukin -1 β

OPEN ACCESS

Edited by:

Francisco Javier Cubero,
Complutense University of Madrid,
Spain

Reviewed by:

Matthew McMillin,
University of Texas at Austin,
United States
Sara De Martin,
University of Padua, Italy

*Correspondence:

Biao Nie
biaonie@jnu.edu.cn

[†]These authors have contributed
equally to this work

Specialty section:

This article was submitted to
Gastrointestinal and Hepatic
Pharmacology,
a section of the journal
Frontiers in Pharmacology

Received: 21 February 2022

Accepted: 25 April 2022

Published: 09 May 2022

Citation:

Lin C, Yu B, Chen L, Zhang Z, Ye W,
Zhong H, Bai W, Yang Y and Nie B
(2022) Obeticholic Acid Induces
Hepatotoxicity Via FXR in the
NAFLD Mice.
Front. Pharmacol. 13:880508.
doi: 10.3389/fphar.2022.880508

INTRODUCTION

Nonalcoholic fatty liver disease (NAFLD) is the most common chronic liver disease worldwide (Fan et al., 2017; Younossi et al., 2018), and becoming a major cause of liver transplantation (Eslam and George, 2020). However, there are no medical treatment available for NAFLD. Farnesoid X receptor (FXR) is a novel therapeutic target for liver diseases. Activation of FXR suppresses hepatic *de novo* fatty acid synthesis (Watanabe et al., 2004), negatively regulates inflammatory response (Wang et al., 2008; Mencarelli et al., 2009; Armstrong and Guo, 2017; Hao et al., 2017), and protects against cholestatic liver damage (Liu et al., 2003). Obeticholic acid (OCA), a potent and selective FXR agonist (Pellicciari et al., 2002), is a Food and Drug Administration-approved therapy for primary biliary cholangitis and is a promising drug for NAFLD (Chapman and Lynch, 2020). Nonetheless, it has been reported that OCA resulted in side effects, including pro-atherogenic lipoprotein profile changes (Neuschwander-Tetri et al., 2015), pruritus (Neuschwander-Tetri et al., 2015; Younossi et al., 2019), liver injury especially in patients exposed to high-dose OCA (Chapman and Lynch,

2020). Recently, the U.S. Food and Drug Administration restricted the use of OCA in patients with primary biliary cholangitis and advanced cirrhosis because it may cause liver failure, which sometimes requires liver transplantation (Eaton et al., 2020). Plasma OCA concentrations were markedly elevated (13-fold) in patients with severe hepatic impairment compared with healthy volunteers (Edwards et al., 2016). Thus, OCA caused deterioration of hepatic decompensation in patients with advanced cirrhosis might due to high concentration of OCA. However, the mechanisms underlying high-dose OCA-induced hepatotoxicity and the role of FXR in the high-dose OCA-induced hepatic injury are unclear. The purpose of this study was to explore the mechanisms of high-dose OCA-induced hepatotoxicity in the context of FXR activity.

MATERIALS AND METHODS

Animal Experiments

All animal experiments were approved by the Laboratory Animal Ethics Committee of Jinan University. Wild-type (WT) mice and whole body FXR knock out (FXR^{-/-}) mice were purchased from Cyagen Biosciences (China). All mice were on a C57BL/6 background. Animals were maintained under specific pathogen-free conditions and had free access to water and food. Eight-week-old male mice were fed a high-fat diet (HFD; 60% kcal from fat) mixed with different doses of OCA (0.04%, normal-dose; 0.16%, high-dose; 0.40%, over-dose; HFD + OCA group) or without OCA (HFD group). Body weight and food consumption were recorded weekly.

Serum Biochemical Analysis and Hepatic Cholesterol Content Measurements

Serum total cholesterol, alanine aminotransferase (ALT), and aspartate aminotransferase (AST), were determined using enzymatic methods kits (Nanjing Jiancheng, China). To measure liver total cholesterol content, 0.1 g of each liver was lysed and measured by a cholesterol kit (Nanjing Jiancheng, China) according to the manufacturer's protocol.

Hepatic Hydroxyproline Content

Liver tissue (70 mg) was hydrolyzed in HCl (6N) as previously described (Trebicka et al., 2007). Hepatic hydroxyproline levels were determined using a hydroxyproline assay kit (Nanjing Jiancheng, China) in accordance with the manufacturer's protocol.

Western Blots

An equal amount of denatured protein was separated by SDS-PAGE gel and transferred to a PVDF membrane (Millipore, United States). The membranes were blocked and incubated with anti-IL-1 β (abcam, ab9722), anti-NLRP3 (ABclonal, A12694) or anti-GAPDH (Proteintech, 60,004-1-Ig) overnight. After an incubation with horseradish peroxidase-conjugated antibodies, protein bands were visualized using chemiluminescence kit (Millipore, United States) and LAS

Chemiluminescent Imaging System (LAS500, United States). The bands were quantified by ImageJ.

RNA Sequencing (RNA-Seq) Analysis

Total RNA from liver was extracted for complementary DNA (cDNA) library construction. Single-end libraries were sequenced by BGISEQ-500, and Bowtie2 software (version 2.2.5) was used to align clean reads to mouse genes and genomes. Gene expression levels (fragments per kilo base of exon per million fragments mapped) were quantified by RSEM (version 1.2.8). Read counts were inputted to DESeq2 to calculate differential gene expression and statistical significance. Differentially expressed genes (DEGs) (HFD + OCA group vs HFD group) were identified as 1) a fold change larger than 2, and 2) Q-value (adjusted *p*-value) less than 0.001. Pathways overrepresented by DEGs were annotated in the Kyoto Encyclopedia of Genes and Genomes (KEGG) database. Pathways with a Q-value (corrected *p*-value) less than 0.05 was considered significantly enriched. Gene Set Enrichment Analysis (GSEA) software (version 4.1) was utilized to identify enriched signaling pathways. Annotated gene sets of gene ontology (GO) biological processes were used as enrichment inputs. The mouse version of MSigDB gene sets were obtained from Walter and Eliza Hall Institute website (<https://bioinf.wehi.edu.au/MSigDB/v7.1/>). Enriched pathways were identified as a *p*-value < 0.05 and a false discovery rate (FDR) Q-value < 0.25.

Real-Time Quantitative PCR

Total RNA was extracted from liver using TRIzol (Thermo Fisher, United States) and reverse transcribed using a reverse transcriptase kit (TAKARA, China). The cDNA and SYBR GREEN Premix EXtaq (TAKARA, China) were used for real-time quantitative PCR in a CFX96 Real-Time PCR Detection System. Primer sequences are listed in **Supplementary Table S1**.

Statistical Analysis

Data are displayed as mean \pm standard error. Comparisons between two groups were evaluated by a two-tailed unpaired Student's *t*-test. *p* < 0.05 was considered statistically significant.

RESULTS

Over-Dose OCA Caused Hepatic Injury and Impaired Mice Survival in an FXR-dependent Manner

To explore whether FXR is involved in OCA-induced hepatotoxicity, wild-type (WT) mice and FXR^{-/-} mice were administered with an over-dose OCA (0.40% incorporated into an HFD) for 5 days. Mice were humanely euthanatized when they were unable to ambulate. During the 5-days period, over-dose OCA caused all of WT mice died, but none of FXR^{-/-} mice died (**Figure 1A**). Liver slices of WT mice showed disordered and necrotic hepatocytes, as well as infiltrated inflammatory cells (**Figure 1B**). Furthermore, compared to the

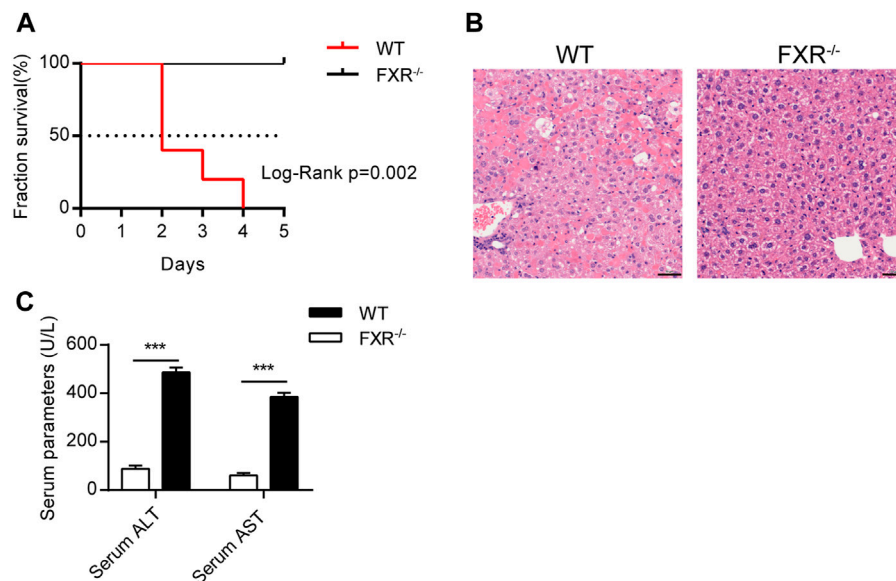


FIGURE 1 | Over-dose OCA reduced survival and promoted hepatic injury in an FXR-dependent manner. Wild-type (WT) and FXR^{-/-} mice were given a high dose of OCA (0.40% OCA incorporated into a high-fat diet) for 5 days (n = 5). **(A)** Survival of WT and FXR^{-/-} mice; Log-Rank $p = 0.002$; HR = 26.85, 95% CI (3.50, 205.70). **(B)** HE staining of liver sections from WT mice and FXR^{-/-} mice. **(C)** Serum alanine aminotransferase (ALT) and serum aspartate aminotransferase (AST) of WT mice and FXR^{-/-} mice. ns, not significant; *, $p < 0.05$; **, $p < 0.01$; ***, $p < 0.001$.

FXR^{-/-} mice, WT mice displayed a marked elevation in both serum ALT and serum AST on an over-dose OCA (**Figure 1C**).

High-Dose OCA Induced Hepatic Stellate Cell Activation and Liver Fibrosis in the Presence of FXR

Over-dose OCA (0.4% OCA) is lethal, therefore, a non-lethal but toxic dose was used for exploring the mechanisms leading to hepatotoxicity. WT mice and FXR^{-/-} mice were fed with 0.04% (normal dose) OCA for 14 weeks, after which the dose of OCA was increased to 0.16% (high dose) for 8 weeks. During the 22-week period, none of the mice died. However, the body weight of WT mice dropped sharply after the dosage increase (**Figure 2A**, left panel), while the decrease in body weight of FXR^{-/-} mice was mild (**Figure 2A**, right panel). Furthermore, high-dose OCA led to increased serum AST levels (**Figure 2B**, right panel) in WT mice, which are indicative of liver injury. The high-dose OCA induced hepatic fibrosis in WT mice but not in FXR^{-/-} mice, as shown by Masson's staining liver slices (**Figure 2C**) and increased hepatic hydroxyproline content (**Figure 2D**). The mRNA expression of tissue inhibitor of matrix metalloproteinase 1 (*Timp1*) and connective tissue growth factor (*Ctgf*), markers of hepatic stellate cell activation, were markedly upregulated in the livers of WT mice (**Figure 2E**, left panel). FXR deficiency abolished the effect of high-dose OCA on hepatic stellate cell activation (**Supplementary Figure S1A**). Hence, FXR was essential for high-dose OCA-induced hepatic stellate cell activation and liver fibrosis. Furthermore,

high-dose OCA decreased the hepatic TG content in WT mice and FXR^{-/-} mice (**Supplementary Figures S2A,B**).

High-Dose OCA Caused an FXR-Mediated Inflammatory Response

To explore the mechanism underlying high-dose OCA-induced hepatic fibrosis, RNA-seq was performed on the livers of WT mice (WT group) and FXR^{-/-} mice (FXR^{-/-} group) fed high-dose OCA, and WT mice fed normal-dose OCA (WT-N group). A total of 5,509 DEGs were found in WT group, while 468 DEGs in FXR^{-/-} group and 918 DEGs in WT-N group (**Figure 3A**). KEGG enrichment analysis of DEGs highlighted six enriched pathways in WT group (compared to FXR^{-/-} group) that were related to 1) inflammasome activation and inflammatory responses (cytokine-cytokine receptor interaction, NOD-like receptor signaling pathway, c-type lectin receptor signaling pathway), and 2) fibrogenic responses (osteoclast differentiation, MAPK signaling pathway, and Ras signaling pathway) (**Figure 3B**). The enrichment of these pathways was almost consistent in the WT-N group and the FXR^{-/-} group (**Figure 3B**). Furthermore, high-dose OCA upregulated proinflammatory mediators and fibrosis gene expression in livers of WT mice, but not in FXR^{-/-} mice (**Figure 3C**). However, normal-dose OCA did not induce the expression of these genes in WT mice (**Figure 3C**). The evidence demonstrated that OCA caused an FXR-mediated inflammatory and fibrogenic response in a dose-dependent manner. GSEA analysis of WT group indicated that the most significantly enriched pathway was positive regulation of IL-1 β production (**Figure 3D**, left panel). Notably, the majority (6

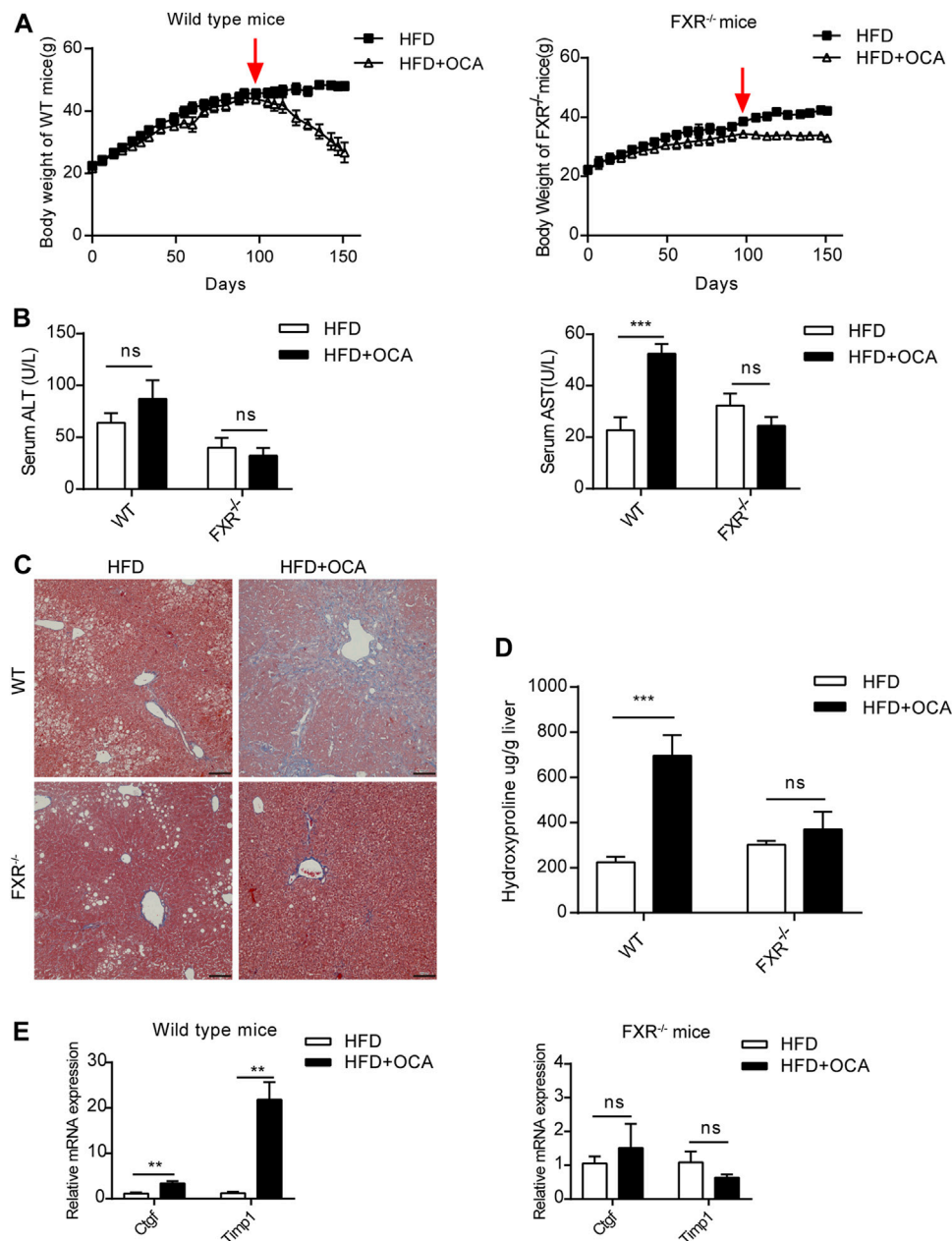


FIGURE 2 | High-dose OCA caused hepatic fibrosis and hepatic stellate cell activation in the presence of FXR. Mice were administered with a high-fat diet supplemented with 0.04% OCA for 14 weeks, after which mice received a high-fat diet containing a high dose of OCA (0.16%, red arrows) for 8 weeks ($n = 3-6$). **(A)** Left panel, body weight of WT mice; right panel, body weight of FXR^{-/-} mice. **(B)** Serum parameters of WT mice and FXR^{-/-} mice. **(C)** Masson's staining of liver sections from WT mice and FXR^{-/-} mice. **(D)** Hepatic hydroxyproline content. **(E)** Ctgf and Timp1 was determined by quantitative real-time PCR in WT mice and FXR^{-/-} mice. ALT, alanine aminotransferase; AST, aspartate aminotransferase; FXR, farnesoid X receptor; OCA, obeticholic acid; WT, wild-type; ns, not significant; *, $p < 0.05$; **, $p < 0.01$; ***, $p < 0.001$.

out of 10, 60%) of the most significant pathways in WT group were involved in the IL-1 β pathway (Figure 3D, right panel). The mRNA and protein expression of IL-1 β were upregulated in livers of WT group (Figures 4A,E,G), but not in FXR^{-/-} group (Figures 4B,F,G). In addition, the expression of *Nlrp3* and *Tnfa* also upregulated in the presence of FXR (Figures 4A-D).

High-Dose OCA Disrupted Liver Cholesterol Metabolism

FXR plays a crucial role in cholesterol homeostasis (Chavez-Talavera et al., 2017). We found that the high-dose OCA decreased serum cholesterol and caused cholesterol accumulation in the livers of WT mice (Figure 5A). The mRNA expression of 3-hydroxy-3-

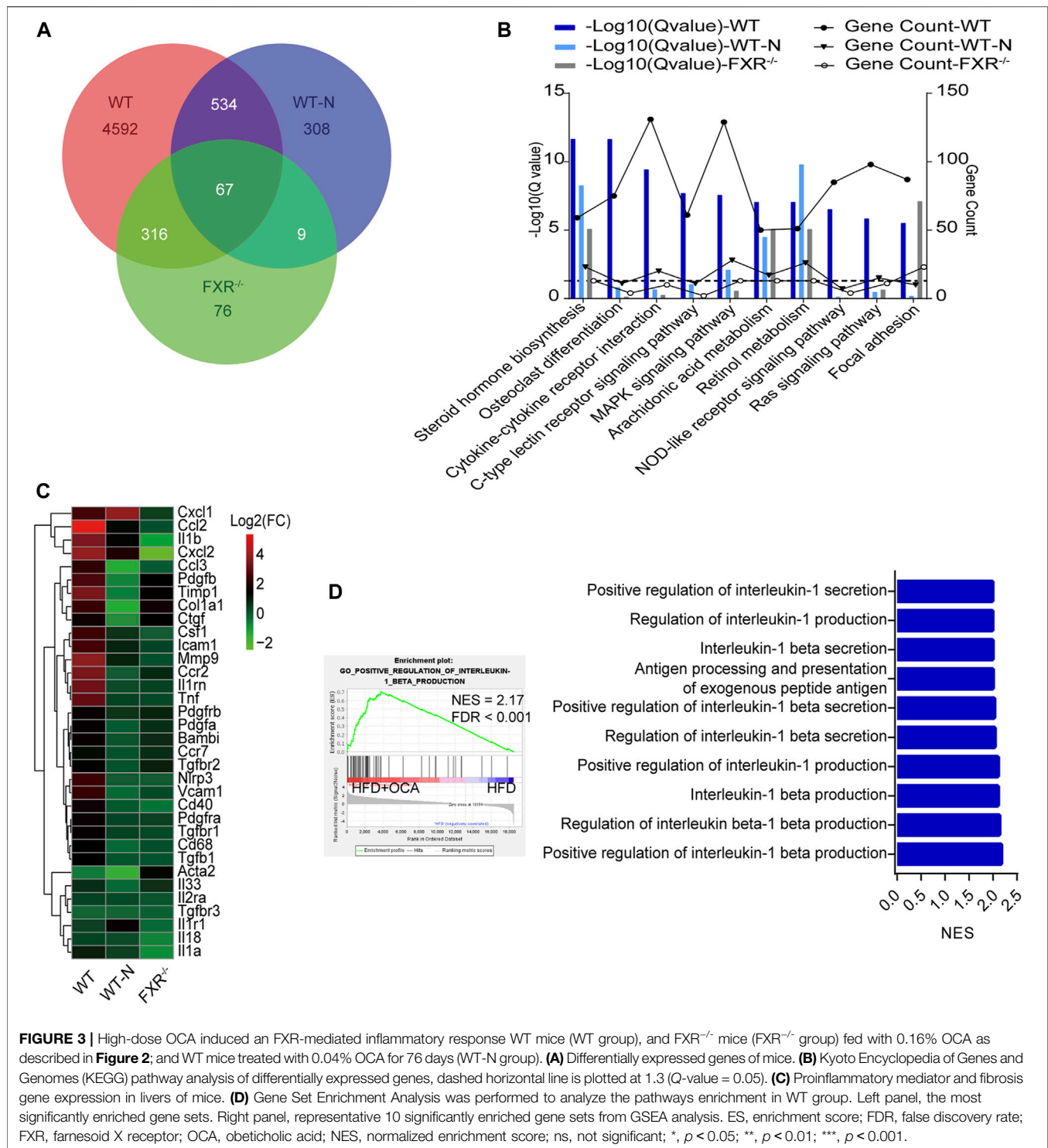


FIGURE 3 | High-dose OCA induced an FXR-mediated inflammatory response WT mice (WT group), and FXR^{-/-} mice (FXR^{-/-} group) fed with 0.16% OCA as described in **Figure 2**; and WT mice treated with 0.04% OCA for 76 days (WT-N group). **(A)** Differentially expressed genes of mice. **(B)** Kyoto Encyclopedia of Genes and Genomes (KEGG) pathway analysis of differentially expressed genes, dashed horizontal line is plotted at 1.3 (Q-value = 0.05). **(C)** Proinflammatory mediator and fibrosis gene expression in livers of mice. **(D)** Gene Set Enrichment Analysis was performed to analyze the pathways enrichment in WT group. Left panel, the most significantly enriched gene sets. Right panel, representative 10 significantly enriched gene sets from GSEA analysis. ES, enrichment score; FDR, false discovery rate; FXR, farnesoid X receptor; OCA, obeticholic acid; NES, normalized enrichment score; ns, not significant; *, $p < 0.05$; **, $p < 0.01$; ***, $p < 0.001$.

methylglutaryl-CoA reductase (*Hmgcr*), the rate-limiting enzyme for cholesterol synthesis, was upregulated by high-dose OCA in the livers of WT mice (**Figures 5B,C**). High-dose OCA also upregulated the expression of *Srb1*, which is responsible for hepatic uptake high-density lipoprotein (HDL) cholesterol from circulation. Moreover, high-dose OCA markedly suppressed the expression of enzymes

involved in cholesterol conversion to bile acids, such as *Cyp7a1*, *Cyp8b1*, and *Cyp27a1* (**Figures 5B,C**) in the livers of WT mice. Conversely, the expression of these genes in the livers of FXR^{-/-} mice had no such differences with high-dose OCA treatment (**Figures 5B,D**). The results revealed that in the presence of FXR, high-dose OCA upregulated genes involved in cholesterol acquisition and

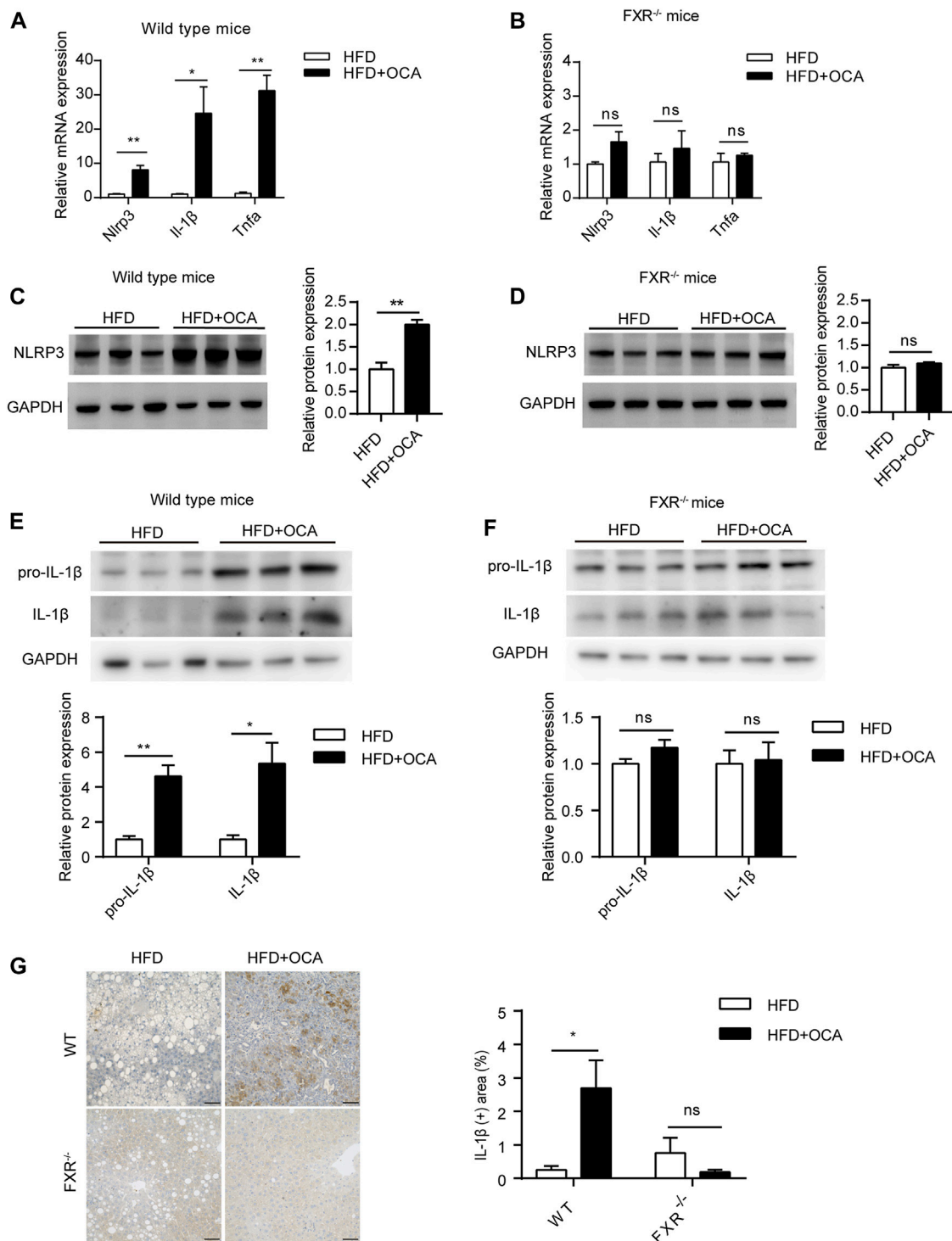


FIGURE 4 | High-dose OCA upregulated IL-1 β dependent of FXR. **(A)** Relative mRNA expression of *Nlrp3*, *Il-1 β* , and *Tnfa* was determined by quantitative real-time PCR (qPCR) in wild type mice. **(B)** Relative mRNA expression was determined by qPCR in FXR^{-/-} mice. **(C)** Protein expression of NLRP3 in WT group. **(D)** Protein expression of NLRP3 in FXR^{-/-} mice. **(E)** Protein expression of IL-1 β in WT group. **(F)** Protein expression of IL-1 β in FXR^{-/-} mice. **(G)** Immunohistochemistry for IL-1 β in the liver of the mice. (Scale bars, 50 μ m). OCA, obeticholic acid; ns, not significant; *, $p < 0.05$; **, $p < 0.01$; ***, $p < 0.001$.

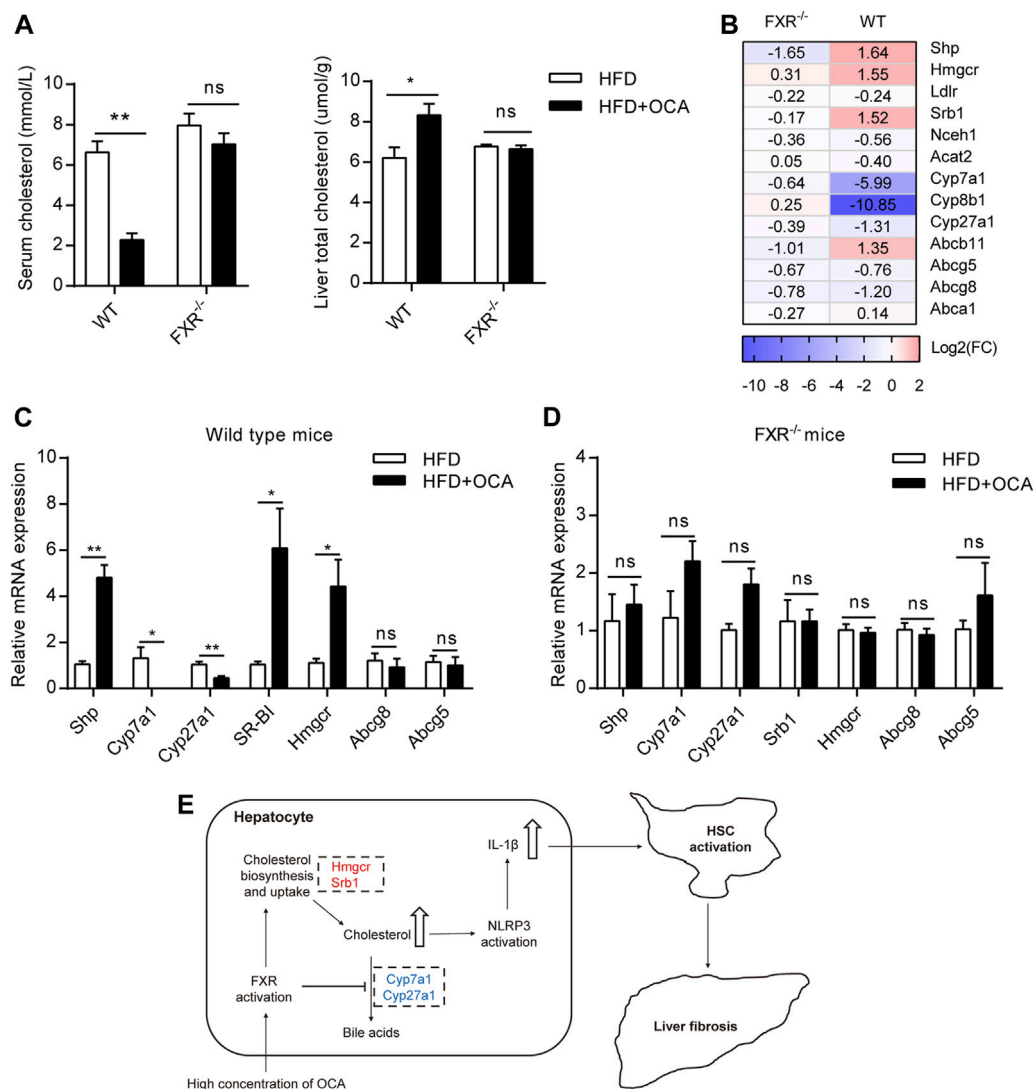


FIGURE 5 | High-dose OCA disrupted liver cholesterol metabolism via FXR activation. Mice were administered with OCA as described in **Figure 2**. **(A)** Left panel, serum cholesterol; right panel, liver total cholesterol. **(B)** Fold change (FC) of FXR-target genes and cholesterol metabolism genes, as determined by RNA-seq. **(C)** Relative mRNA expression of genes involved in cholesterol metabolism in WT mice, as determined by real-time quantitative PCR (qPCR). **(D)** Relative mRNA expression determined by qPCR in $FXR^{-/-}$ mice. **(E)** Molecular pathways of high-dose OCA-induced hepatic fibrosis (upregulated genes are shown in red; downregulated genes are shown in blue). ns, not significant; *, $p < 0.05$; **, $p < 0.01$; ***, $p < 0.001$.

downregulated those involved in secretion of cholesterol in the livers. Together, these changes contributed to the cholesterol accumulation in livers. Cholesterol trigger NLRP3 activation, leading to the production of IL-1 β , which triggers an inflammatory response, and promotes hepatic stellate cell proliferation (Ioannou, 2016). Therefore, high-dose OCA may have resulted in hepatic fibrosis via cholesterol accumulation and increased the production of IL-1 β in an FXR-mediated manner (**Figure 5E**).

DISCUSSION

This study revealed that high-dose OCA induced liver injury in an FXR-dependent manner.

OCA was designed as a potent FXR agonist, it alleviates bile acids-induced hepatotoxicity (Trivedi et al., 2016) and NAFLD via FXR activation (Watanabe et al., 2004). However, FXR activation elevated plasma total cholesterol and LDL-c cholesterol levels, and decreased plasma HDL cholesterol levels in human (Neuschwander-Tetri et al., 2015; Pencek et al., 2016; Chavez-Talavera et al., 2017). Thus, FXR activation induces a higher cardiovascular risk lipoprotein profile in human. Interestingly, it is different in mice. FXR activation reduced circulating cholesterol in mice by inhibiting intestinal cholesterol absorption, promoting reverse cholesterol transport in macrophage (Xu et al., 2016), and increasing the expression of hepatic low-density lipoprotein receptor (Singh et al., 2018). In our study, high-dose OCA also reduced serum cholesterol levels in mice.

Even though FXR activation inhibited hepatic cholesterol converted to bile acid and promoted HDL-c uptakes from circulation (Chavez-Talavera et al., 2017), several studies indicated that a therapeutic concentration of OCA decreased hepatic cholesterol content (Cipriani et al., 2010; Dong et al., 2017; Goto et al., 2018; Morrison et al., 2018). Conversely, in this study, a supratherapeutic concentration of OCA induced hepatic cholesterol accumulation dependent of FXR, which leading to inflammatory response. Previous study shown that activation of FXR suppressed the expression of *Cyp7a1*, *Cyp8b1*, and *Cyp27a1*, and induced the expression of *Srb1* (Li and Chiang, 2014). Importantly, activation of FXR decreased hepatic cholesterol synthesis by suppressing the expression of *Hmgcr* (Hubbert et al., 2007), and promoted cholesterol secretion from hepatocytes by inducing *Abcg8* and *Abcg5* expression (Li et al., 2011). These changes caused by FXR activation were responsible for hepatic cholesterol reduction. However, in the present study, high-dose OCA increased the expression of *Hmgcr* without the upregulation of *Abcg8* or *Abcg5*. Therefore, high-dose OCA disturbed the hepatic cholesterol homeostasis and induced hepatic cholesterol accumulation.

Cholesterol activated NLRP3 inflammasomes in macrophages contributing to atherogenesis was reported (Duewell et al., 2010; Rajamaki et al., 2010). Accumulating evidence demonstrated that hepatic free cholesterol is a molecular mediator of lipotoxicity (Ioannou, 2016), which activated NLRP3 inflammasomes and upregulated IL-1 β , promoting liver inflammation (Mridha et al., 2017). Additionally, blocking NLRP3 activation alleviated hepatic inflammation induced by a methionine/choline-deficient diet and atherogenic diet (Mridha et al., 2017). Hepatic cholesterol accumulation also upregulated expression of TAZ, a profibrotic transcriptional regulator, and leading to liver fibrosis (Wang et al., 2020). Dysregulated cholesterol metabolism results in cholesterol accumulation in the liver of NAFLD patients (Puri et al., 2007; Caballero et al., 2009; Min et al., 2012), which can lead to NLRP3 inflammasome activation (Mridha et al., 2017), hepatic inflammation, and fibrosis (Ioannou, 2016).

Toxicity studies of OCA indicated that the toxicity of OCA to mice fed with a standard diet is primarily on the liver (EUROPEAN MEDICINES AGENCY, 2016). In this study, we explored the mechanism of high-dose OCA-induced hepatotoxicity in the condition of the NAFLD mouse model. The result showed that high-dose OCA resulted in hepatotoxicity in the presence of FXR. The high-dose OCA upregulated the expression of genes involved in the deposition of hepatic cholesterol and decreased the expression of genes involved in cholesterol secretion in livers. This led to an accumulation of cholesterol in liver, which triggered an inflammatory response in the liver, as demonstrated by the increased expression of IL-1 β only in the presence of FXR. IL-1 β , a potent inflammatory cytokine, promotes hepatic stellate cell proliferation (Reiter et al., 2016) and is involved in the pathogenesis of hepatic fibrosis, the latter of which can be induced by several factors, such as toxins, ethanol, and NASH (Seki and Schwabe, 2015). We demonstrated that FXR plays an important role in OCA-induced

liver fibrosis when OCA is administered at high dose or in conditions of advanced cirrhosis, the latter of which resulted in a sharp increase in OCA plasma concentrations (Edwards et al., 2016).

There two limitations of this study. One is that the preclinical toxicology study was performed in mice but not in rats. As we know, the translational value of mice is limited in toxicological studies. Another is that the effect of high-dose OCA on bile acid metabolism was unknown for the measure of hepatic total bile acids was not performed.

In summary, the current study revealed that FXR is essential for high-dose OCA-induced hepatotoxicity.

DATA AVAILABILITY STATEMENT

The datasets presented in this study can be found in online repositories. The names of the repository/repositories and accession number(s) can be found below: <https://www.ncbi.nlm.nih.gov/search/all/?term=PRJNA701084>.

ETHICS STATEMENT

The animal study was reviewed and approved by the Laboratory Animal Ethics Committee of Jinan University.

AUTHOR CONTRIBUTIONS

BN designed the experiments. BN, CL, and YY interpreted the data; CL, BY, BN, LC, and ZZ performed the experiments. WY, HZ, and WB helped with experiments. CL wrote the manuscript. BN revised the manuscript. All authors approved the final manuscript.

FUNDING

This work was supported by Scientific Research Foundation for Returned Scholars of the Ministry of Education of China and the National Natural Science Foundation of China (81471080) for BN.

ACKNOWLEDGMENTS

We thank Georgia Lenihan-Geels (Edanz) for editing a draft of this manuscript.

SUPPLEMENTARY MATERIAL

The Supplementary Material for this article can be found online at: <https://www.frontiersin.org/articles/10.3389/fphar.2022.880508/full#supplementary-material>

REFERENCES

- Armstrong, L. E., and Guo, G. L. (2017). Role of FXR in Liver Inflammation during Nonalcoholic Steatohepatitis. *Curr. Pharmacol. Rep.* 3, 92–100. doi:10.1007/s40495-017-0085-2
- Caballero, F., Fernández, A., De Lacy, A. M., Fernández-Checa, J. C., Caballería, J., and García-Ruiz, C. (2009). Enhanced Free Cholesterol, SREBP-2 and StAR Expression in Human NASH. *J. Hepatol.* 50, 789–796. doi:10.1016/j.jhep.2008.12.016
- Chapman, R. W., and Lynch, K. D. (2020). Obeticholic Acid-A New Therapy in PBC and NASH. *Br. Med. Bull.* 133, 95–104. doi:10.1093/bmb/ldaa006
- Chávez-Talavera, O., Tailleux, A., Lefebvre, P., and Staels, B. (2017). Bile Acid Control of Metabolism and Inflammation in Obesity, Type 2 Diabetes, Dyslipidemia, and Nonalcoholic Fatty Liver Disease. *Gastroenterology* 152, 1679–e3. doi:10.1053/j.gastro.2017.01.055
- Cipriani, S., Mencarelli, A., Palladino, G., and Fiorucci, S. (2010). FXR Activation Reverses Insulin Resistance and Lipid Abnormalities and Protects against Liver Steatosis in Zucker (Fa/fa) Obese Rats. *J. Lipid Res.* 51, 771–784. doi:10.1194/jlr.M001602
- Dong, B., Young, M., Liu, X., Singh, A. B., and Liu, J. (2017). Regulation of Lipid Metabolism by Obeticholic Acid in Hyperlipidemic Hamsters. *J. Lipid Res.* 58, 350–363. doi:10.1194/jlr.M070888
- Duewell, P., Kono, H., Rayner, K. J., Sirois, C. M., Vladimer, G., Bauernfeind, F. G., et al. (2010). NLRP3 Inflammasomes Are Required for Atherogenesis and Activated by Cholesterol Crystals. *Nature* 464, 1357–1361. doi:10.1038/nature08938
- Eaton, J. E., Vuppalanchi, R., Reddy, R., Sathapathy, S., Ali, B., and Kamath, P. S. (2020). Liver Injury in Patients with Cholestatic Liver Disease Treated with Obeticholic Acid. *Hepatology* 71, 1511–1514. doi:10.1002/hep.31017
- Edwards, J. E., LaCerte, C., Peyret, T., Gosselin, N. H., Marier, J. F., Hofmann, A. F., et al. (2016). Modeling and Experimental Studies of Obeticholic Acid Exposure and the Impact of Cirrhosis Stage. *Clin. Transl. Sci.* 9, 328–336. doi:10.1111/cts.12421
- Eslam, M., and George, J. (2020). Genetic Contributions to NAFLD: Leveraging Shared Genetics to Uncover Systems Biology. *Nat. Rev. Gastroenterol. Hepatol.* 17, 40–52. doi:10.1038/s41575-019-0212-0
- EUROPEAN MEDICINES AGENCY (2016). Ocaliva Assessment Report. https://www.ema.europa.eu/en/documents/assessment-report/ocaliva-epar-public-assessment-report_en.pdf (Accessed March 15, 2021).
- Fan, J. G., Kim, S. U., and Wong, V. W. (2017). New Trends on Obesity and NAFLD in Asia. *J. Hepatol.* 67, 862–873. doi:10.1016/j.jhep.2017.06.003
- Goto, T., Itoh, M., Suganami, T., Kanai, S., Shirakawa, I., Sakai, T., et al. (2018). Obeticholic Acid Protects against Hepatocyte Death and Liver Fibrosis in a Murine Model of Nonalcoholic Steatohepatitis. *Sci. Rep.* 8, 8157. doi:10.1038/s41598-018-26383-8
- Hao, H., Cao, L., Jiang, C., Che, Y., Zhang, S., Takahashi, S., et al. (2017). Farnesoid X Receptor Regulation of the NLRP3 Inflammasome Underlies Cholestasis-Associated Sepsis. *Cell Metab.* 25, 856–e5. doi:10.1016/j.cmet.2017.03.007
- Hubbert, M. L., Zhang, Y., Lee, F. Y., and Edwards, P. A. (2007). Regulation of Hepatic Insig-2 by the Farnesoid X Receptor. *Mol. Endocrinol.* 21, 1359–1369. doi:10.1210/me.2007-0089
- Ioannou, G. N. (2016). The Role of Cholesterol in the Pathogenesis of NASH. *Trends Endocrinol. Metab.* 27, 84–95. doi:10.1016/j.tem.2015.11.008
- Li, T., and Chiang, J. Y. (2014). Bile Acid Signaling in Metabolic Disease and Drug Therapy. *Pharmacol. Rev.* 66, 948–983. doi:10.1124/pr.113.008201
- Li, T., Matozel, M., Boehme, S., Kong, B., Nilsson, L. M., Guo, G., et al. (2011). Overexpression of Cholesterol 7 α -Hydroxylase Promotes Hepatic Bile Acid Synthesis and Secretion and Maintains Cholesterol Homeostasis. *Hepatology* 53, 996–1006. doi:10.1002/hep.24107
- Liu, Y., Binz, J., Numerick, M. J., Dennis, S., Luo, G., Desai, B., et al. (2003). Hepatoprotection by the Farnesoid X Receptor Agonist GW4064 in Rat Models of Intra- and Extrahepatic Cholestasis. *J. Clin. Invest.* 112, 1678–1687. doi:10.1172/JCI18945
- Mencarelli, A., Renga, B., Migliorati, M., Cipriani, S., Distrutti, E., Santucci, L., et al. (2009). The Bile Acid Sensor Farnesoid X Receptor Is a Modulator of Liver Immunity in a Rodent Model of Acute Hepatitis. *J. Immunol.* 183, 6657–6666. doi:10.4049/jimmunol.0901347
- Min, H. K., Kapoor, A., Fuchs, M., Mirshahi, F., Zhou, H., Maher, J., et al. (2012). Increased Hepatic Synthesis and Dysregulation of Cholesterol Metabolism Is Associated with the Severity of Nonalcoholic Fatty Liver Disease. *Cell Metab.* 15, 665–674. doi:10.1016/j.cmet.2012.04.004
- Morrison, M. C., Verschuren, L., Salic, K., Verheij, J., Menke, A., Wielinga, P. Y., et al. (2018). Obeticholic Acid Modulates Serum Metabolites and Gene Signatures Characteristic of Human NASH and Attenuates Inflammation and Fibrosis Progression in Ldlr^{-/-} Leiden Mice. *Hepatol. Commun.* 2, 1513–1532. doi:10.1002/hep4.1270
- Mridha, A. R., Wree, A., Robertson, A. A. B., Yeh, M. M., Johnson, C. D., Van Rooyen, D. M., et al. (2017). NLRP3 Inflammasome Blockade Reduces Liver Inflammation and Fibrosis in Experimental NASH in Mice. *J. Hepatol.* 66, 1037–1046. doi:10.1016/j.jhep.2017.01.022
- Neuschwander-Tetri, B. A., Loomba, R., Sanyal, A. J., Lavine, J. E., Van Natta, M. L., Abdelmalek, M. F., et al. (2015). Farnesoid X Nuclear Receptor Ligand Obeticholic Acid for Non-cirrhotic, Non-alcoholic Steatohepatitis (FLINT): a Multicentre, Randomised, Placebo-Controlled Trial. *Lancet* 385, 956–965. doi:10.1016/s0140-6736(14)61933-4
- Pellicciari, R., Fiorucci, S., Camaioni, E., Clerici, C., Costantino, G., Maloney, P. R., et al. (2002). 6 α -ethyl-chenodeoxycholic Acid (6-ECDCA), a Potent and Selective FXR Agonist Endowed with Anticholestatic Activity. *J. Med. Chem.* 45, 3569–3572. doi:10.1021/jm025529g
- Pencek, R., Marmon, T., Roth, J. D., Liberman, A., Hooshmand-Rad, R., and Young, M. A. (2016). Effects of Obeticholic Acid on Lipoprotein Metabolism in Healthy Volunteers. *Diabetes Obes. Metab.* 18, 936–940. doi:10.1111/dom.12681
- Puri, P., Baillie, R. A., Wiest, M. M., Mirshahi, F., Choudhury, J., Cheung, O., et al. (2007). A Lipidomic Analysis of Nonalcoholic Fatty Liver Disease. *Hepatology* 46, 1081–1090. doi:10.1002/hep.21763
- Rajamäki, K., Lappalainen, J., Öörni, K., Välimäki, E., Matikainen, S., Kovanen, P. T., et al. (2010). Cholesterol Crystals Activate the NLRP3 Inflammasome in Human Macrophages: a Novel Link between Cholesterol Metabolism and Inflammation. *PLoS One* 5, e11765. doi:10.1371/journal.pone.0011765
- Reiter, F. P., Wimmer, R., Wottke, L., Artmann, R., Nagel, J. M., Carranza, M. O., et al. (2016). Role of Interleukin-1 and its Antagonism of Hepatic Stellate Cell Proliferation and Liver Fibrosis in the Abcb4^{-/-} Mouse Model. *World J. Hepatol.* 8, 401–410. doi:10.4254/wjh.v8.i8.401
- Seki, E., and Schwabe, R. F. (2015). Hepatic Inflammation and Fibrosis: Functional Links and Key Pathways. *Hepatology* 61, 1066–1079. doi:10.1002/hep.27332
- Singh, A. B., Dong, B., Kraemer, F. B., Xu, Y., Zhang, Y., and Liu, J. (2018). Farnesoid X Receptor Activation by Obeticholic Acid Elevates Liver Low-Density Lipoprotein Receptor Expression by mRNA Stabilization and Reduces Plasma Low-Density Lipoprotein Cholesterol in Mice. *Arterioscler. Thromb. Vasc. Biol.* 38, 2448–2459. doi:10.1161/atvbaha.118.311122
- Trebicka, J., Hennenberg, M., Laleman, W., Shelest, N., Biecker, E., Schepke, M., et al. (2007). Atorvastatin Lowers Portal Pressure in Cirrhotic Rats by Inhibition of RhoA/Rho-Kinase and Activation of Endothelial Nitric Oxide Synthase. *Hepatology* 46, 242–253. doi:10.1002/hep.21673
- Trivedi, P. J., Hirschfield, G. M., and Gershwin, M. E. (2016). Obeticholic Acid for the Treatment of Primary Biliary Cirrhosis. *Expert Rev. Clin. Pharmacol.* 9, 13–26. doi:10.1586/17512433.2015.1092381
- Wang, X., Cai, B., Yang, X., Sonubi, O. O., Zheng, Z., Ramakrishnan, R., et al. (2020). Cholesterol Stabilizes TAZ in Hepatocytes to Promote Experimental Non-alcoholic Steatohepatitis. *Cell Metab.* 31, 969–e7. doi:10.1016/j.cmet.2020.03.010
- Wang, Y. D., Chen, W. D., Wang, M., Yu, D., Forman, B. M., and Huang, W. (2008). Farnesoid X Receptor Antagonizes Nuclear Factor κ B in Hepatic Inflammatory Response. *Hepatology* 48, 1632–1643. doi:10.1002/hep.22519
- Watanabe, M., Houten, S. M., Wang, L., Moschetta, A., Mangelsdorf, D. J., Heyman, R. A., et al. (2004). Bile Acids Lower Triglyceride Levels via a Pathway Involving FXR, SHP, and SREBP-1c. *J. Clin. Invest.* 113, 1408–1418. doi:10.1172/JCI21025
- Xu, Y., Li, F., Zalzal, M., Xu, J., Gonzalez, F. J., Adorini, L., et al. (2016). Farnesoid X Receptor Activation Increases Reverse Cholesterol Transport by Modulating Bile Acid Composition and Cholesterol Absorption in Mice. *Hepatology* 64, 1072–1085. doi:10.1002/hep.28712

- Younossi, Z., Anstee, Q. M., Marietti, M., Hardy, T., Henry, L., Eslam, M., et al. (2018). Global Burden of NAFLD and NASH: Trends, Predictions, Risk Factors and Prevention. *Nat. Rev. Gastroenterol. Hepatol.* 15, 11–20. doi:10.1038/nrgastro.2017.109
- Younossi, Z. M., Ratziu, V., Loomba, R., Rinella, M., Anstee, Q. M., Goodman, Z., et al. (2019). Obeticholic Acid for the Treatment of Non-alcoholic Steatohepatitis: Interim Analysis from a Multicentre, Randomised, Placebo-Controlled Phase 3 Trial. *Lancet* 394, 2184–2196. doi:10.1016/S0140-6736(19)33041-7

Conflict of Interest: The authors declare that the research was conducted in the absence of any commercial or financial relationships that could be construed as a potential conflict of interest.

Publisher's Note: All claims expressed in this article are solely those of the authors and do not necessarily represent those of their affiliated organizations, or those of the publisher, the editors and the reviewers. Any product that may be evaluated in this article, or claim that may be made by its manufacturer, is not guaranteed or endorsed by the publisher.

Copyright © 2022 Lin, Yu, Chen, Zhang, Ye, Zhong, Bai, Yang and Nie. This is an open-access article distributed under the terms of the Creative Commons Attribution License (CC BY). The use, distribution or reproduction in other forums is permitted, provided the original author(s) and the copyright owner(s) are credited and that the original publication in this journal is cited, in accordance with accepted academic practice. No use, distribution or reproduction is permitted which does not comply with these terms.



Mendelian Randomization Rules Out Causation Between Inflammatory Bowel Disease and Non-Alcoholic Fatty Liver Disease

Lanlan Chen[†], Zhongqi Fan[†], Xiaodong Sun, Wei Qiu, Yuguo Chen, Jianpeng Zhou and Guoyue Lv^{*}

Department of Hepatobiliary and Pancreatic Surgery, The First Hospital of Jilin University, Changchun, China

Background: Inflammatory bowel disease (IBD) and non-alcoholic fatty liver disease (NAFLD) usually co-exist clinically. However, whether such association is causal is still unknown.

Methods: Genetic variants were extracted as instrumental variables from the largest genome-wide association study (GWAS) of IBD, Crohn's disease (CD) and ulcerative colitis (UC) with 25,042 cases and 34,915 controls (GWAS p -value $< 5 \times 10^{-8}$). Information of genetic variants in NAFLD was extracted from a GWAS with 1,483 cases and 17,781 controls. Also, liver fat content (LFC) was included as the outcome. Then, a bi-direction Mendelian randomization (MR) was carried out to appraise the causal relationship between NAFLD on IBD. Besides, a multivariable MR (MVMR) design was carried to adjust for body mass index (BMI) and type 2 diabetes (T2D) as well.

Results: Generally, IBD might not affect the risk of NAFLD (OR = 0.994 [0.970, 1.019]), together with its subtypes including UC and CD. However, genetically-elevated risk of IBD might cause liver fat accumulation (beta = 0.019, p -value = 0.016) while turning insignificant at Bonferroni correction. Besides, no causal effect of NAFLD on IBD was observed (OR = 0.968 [0.928, 1.009]), together with UC and CD. Also, genetically-elevated LFC could not impact IBD, UC and CD either. The MR CAUSE analysis supported these null associations and MVMR analysis also supported such null associations even after adjusting for BMI and T2D.

Conclusion: This MR study ruled out the causal relationship between IBD and NAFLD, suggesting therapeutics targeting NAFLD might not work for IBD and vice versa.

Keywords: null association, causal inference, genetic epidemiology, mendelian randomization, NAFLD (non alcoholic fatty liver disease), IBD— inflammatory bowel disease

INTRODUCTION

Non-alcoholic fatty liver disease (NAFLD), a disease characterized with liver steatosis and determined by liver fat content (LFC), is amongst the most important causes of liver diseases even in lean patients and its global prevalence is estimated to reach over 24% (Younossi et al., 2018). Inflammatory bowel disease (IBD), including ulcerative colitis (UC) and Crohn's disease (CD), is a chronic intestinal inflammation

OPEN ACCESS

Edited by:

Ana Blas-García,
University of Valencia, Spain

Reviewed by:

Lorena Ortega Moreno,
Autonomous University of Madrid,
Spain
Güray Can,
Abant İzzet Baysal University, Turkey

*Correspondence:

Guoyue Lv
lvgy@jlu.edu.cn

[†]These authors have contributed
equally to this work

Specialty section:

This article was submitted to
Gastrointestinal and Hepatic
Pharmacology,
a section of the journal
Frontiers in Pharmacology

Received: 07 March 2022

Accepted: 05 April 2022

Published: 19 May 2022

Citation:

Chen L, Fan Z, Sun X, Qiu W, Chen Y,
Zhou J and Lv G (2022) Mendelian
Randomization Rules Out Causation
Between Inflammatory Bowel Disease
and Non-Alcoholic Fatty Liver Disease.
Front. Pharmacol. 13:891410.
doi: 10.3389/fphar.2022.891410

which can reduce patient's life expectancy from age-related comorbidities like cardiovascular diseases, and its global prevalence will be as high as 1% by 2030 in many regions (Kaplan and Windsor, 2021). Considerable epidemiological evidence has linked these two diseases together where IBD was associated with increased risk of NAFLD and they usually coexist (McHenry et al., 2019; Zou et al., 2019; Lin et al., 2021). However, an observational study suggested there were no significant differences in terms of IBD characteristics between IBD patients with and without NAFLD, indicating the interplay between NAFLD and IBD is no easy (Magri et al., 2019). Besides, it should be noted that all the available evidence is based on observational studies, which might be biased by unavoidable potential confounders and reverse causation (Piovani et al., 2021). There is a paucity of evidence illustrating whether the observed association is causal.

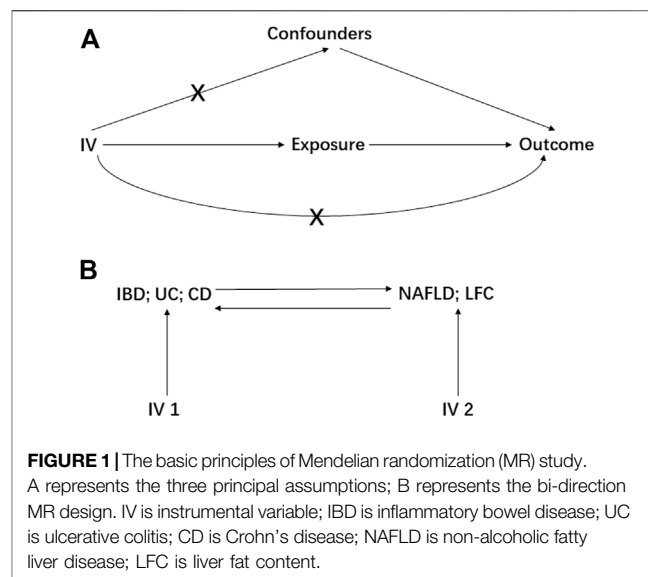
Mendelian randomization (MR) is an emerging epidemiological method of causal inference and has made great contribution to detection of causal risk factors for diseases. For instance, Voight et al. ruled out the possibility that high-density lipoprotein cholesterol (HDL-C) could lower risk of myocardial infarction using MR design, challenging the traditional concept (Voight et al., 2012). MR design utilizes genetic variants as instrument variables (IVs), usually single nucleotide polymorphisms (SNPs) and can largely evade bias caused by potential confounders as SNPs are allocated randomly at conception and free from influence of confounders (Davey Smith and Hemani, 2014). Thanks to the rapid development of genome-wide association study (GWAS) and accumulation of publicly available GWAS summary statistics, MR design based on two-sample setting is becoming more flexible and accessible. Several MR studies have identified causal risk factors of IBD, such as body fat percentage (Carreras-Torres et al., 2020) and ankylosing spondylitis (Cui et al., 2020). Also, a MR study clarified the causal relationship between NAFLD, type 2 diabetes (T2D) and obesity (Liu et al., 2020).

However, there is no MR study exploring the causal relationship between NAFLD and IBD. In this study, we aim to explore the causal relationship between NAFLD and IBD, hoping to disentangle their complex interplay and provide useful advice in clinical practice.

MATERIALS AND METHODS

GWAS Summary Statistics of NAFLD and IBD

The GWAS summary statistics of NAFLD were obtained from a recent published GWAS, with 1,483 European NAFLD cases and 17,781 genetically matched controls, and this study included the first five principal components as covariates (Anstee et al., 2020). Considering NAFLD is closely associated with LFC, we also selected a recent LFC GWAS which included 32,858 European participants from United Kingdom Biobank and adjusted for age at imaging visit, age squared, sex, imaging center, scan date, scan time, genotyping batch, and genetic relatedness (Liu et al., 2021). The IBD data were downloaded from an IBD meta-GWAS which



included a total of 59,957 subjects, with 12,194 Crohn's disease and 12,366 ulcerative colitis, and this study adjusted for the first ten principal components for each cohort (de Lange et al., 2017). As for the IBD GWAS, there were 25,042 European and unknown ancestry cases, together with 34,915 European and unknown ancestry controls (de Lange et al., 2017). Genomic control has been applied to all these studies. Each GWAS has been approved by corresponding Ethics Committees.

Mendelian Randomization Design

MR study should be carried out under three principal assumptions: (Younossi et al., 2018): the genetic variants should be closely associated with the exposure; (Kaplan and Windsor, 2021) the genetic variants should not be associated with any potential confounders that might mediate the way from exposure to outcome; (McHenry et al., 2019) the genetic variants should not be associated with outcome if conditioned on exposure (Emdin et al., 2017) (Figure 1). Besides, additional assumptions should be satisfied as well, such as linearity and no interaction between mediator and outcome.

Genetic variants were selected as IVs if reaching the genome-wide significance (GWAS p -value $< 5 \times 10^{-8}$) and were further clumped based on linkage disequilibrium (LD, $r^2 = 0.01$) and genomic region (clump window 1,000 kilobases). Also, SNP with lower minor allele frequency (MAF < 0.01) would be removed in the following analysis. In the two-sample setting, we harmonized summary statistic data to ensure each IV was aligned with the same effect allele.

Preliminarily, the IBD, UC and CD were treated as the exposures to estimate their causal effect on NAFLD and LFC, resulting in six pairs of causal relationships including IBD-NAFLD, IBD-LFC, UC-NAFLD, UC-LFC, CD-NAFLD and CD-LFC. Then, a bi-directional MR analysis was performed where the NAFLD and LFC were set to be the exposures, generating another six pairs of causal relationship namely NAFLD-IBD, NAFLD-UC, NAFLD-CD, LFC-IBD, LFC-UC and LFC-CD (Figure 1). Furthermore, a multivariable MR (MVMR)

design was elaborated with adjusting for body mass index (BMI) and type 2 diabetes (T2D), two potential confounders according to a recent meta-analysis (Lin et al., 2021). Therein, the GWAS summary statistics of BMI was from the Genetic Investigation of ANthropometric Traits (GIANT) consortium (Locke et al., 2015) and these of T2D was from the DIABetes Genetics Replication And Meta-analysis (DIAGRAM) consortium (Mahajan et al., 2014).

Statistical Analysis and Data Visualization

Initially, Wald ratio estimation was utilized to obtain the effect size of exposure on outcome for each IV and then each IV's causal effect size was combined using an inverse-variance weighted (IVW) method. F statistics were calculated for each IV to ensure a sufficient power. The Cochran's Q value was calculated to appraise heterogeneity and the multiplicative random effect model would be adopted if there exists heterogeneity. The MR Steiger test has been performed to judge whether the IVs affect exposure more than outcome and we would eliminate the IV if it explained outcome more than exposure (Hemani et al., 2017).

Considering the horizontal pleiotropy can largely mislead the MR estimation, various methods have been utilized to minimize the bias caused by it, including both correlated and uncorrelated horizontal pleiotropy. For correlated horizontal pleiotropy, MR-Egger regression (Bowden et al., 2015) and MR-PRESSO (Verbanck et al., 2018) were utilized. The MR-Egger regression uses the intercept obtained from regression analysis to judge the correlated horizontal pleiotropy and we assume there is no correlated horizontal pleiotropy if the intercept equals to zero (Bowden et al., 2015). The MR-PRESSO uses distortion test to detect outliers that might manifest horizontal pleiotropy and further corrects the IVW estimation with removal of outliers (Verbanck et al., 2018). For uncorrelated horizontal pleiotropy, another two methods were adopted, including weighted median (Bowden et al., 2016) and CAUSE (Morrison et al., 2020). Therein, CAUSE can allow for both correlated and uncorrelated horizontal pleiotropy, and it was functioned based on full summary statistics (Morrison et al., 2020). In CAUSE analysis, the threshold of SNP-exposure p -value was 1×10^{-3} , ensuring enough IVs to estimate nuisance parameters.

All statistical analyses were performed using R packages, including "TwoSampleMR" (Hemani et al., 2018), "MRPRESSO" (Verbanck et al., 2018) and "cause" (Morrison et al., 2020) in R software 3.6.0 (<https://www.r-project.org/>). The data visualization was conducted using R packages, including "TwoSampleMR" (Hemani et al., 2018) and "forestplot".

Sensitivity Analysis

The leave-on-out sensitivity analysis was performed to find the IV that might drive the main results, guaranteeing the MR results were robust.

RESULTS

Generally, our MR study indicated there might be no causal relationship between NAFLD and IBD although the

genetic liability to IBD might elevate the LFC slightly. The number of IVs for each phenotype varied from 4 to 145 and each F statistic was greater than the empirical threshold 10, indicating less bias caused by weak instruments (Table 1).

Preliminarily, genetic predisposition to IBD could not elevate the risk of NAFLD (OR = 0.994 [0.970, 1.019], IVW p -value = 0.645), including two subtypes of IBD as UC (OR = 1.007 [0.952, 1.066], IVW p -value = 0.800) and CD (OR = 0.996 [0.986, 1.007], IVW p -value = 0.491) (Figure 2). After adjusting for BMI and T2D, the genetic predisposition to IBD could not affect the risk of NAFLD (OR = 1.057 [0.993, 1.125], IVW p -value = 0.082). Similar results were obtained for UC and CD in MVMR analysis as well (IVW p -value > 0.05). However, we observed a slight causal effect of IBD on LFC where genetically-elevated risk of IBD could lead to liver fat accumulation (β = 0.019, se = 0.008, IVW p -value = 0.016). Considering LFC is a continuous variable, we used β value to represent the effect size. It should be noted that the causal effect of IBD on LFC turned insignificant after Bonferroni correction (Bonferroni-corrected IVW p -value = 0.096). Besides, genetically-driven UC (β = 0.010, se = 0.007, IVW p -value = 0.164) and CD (β = 0.006, se = 0.007, IVW p -value = 0.363) could not alter LFC either (Figure 2). The impact of genetic predisposition to IBD on LFC was insignificant after adjusting for BMI and T2D (β = -0.018, se = 0.010, p -value = 0.065). The MVMR results were similar in UC-LFC and CD-LFC associations (IVW p -value > 0.05). All pairs of causal association were insignificant in the MR-Egger regression and weighted-median method (Table 2). Although slight heterogeneity was detected for CD-NAFLD, CD-LFC and IBD-LFC pairs, the conclusions still held after removal of outliers. Also, genetic liability to CD could not affect the risk of NAFLD yet after correcting horizontal pleiotropy (OR = 0.024 [0.792, 1.008], MR-Egger p -value = 0.070).

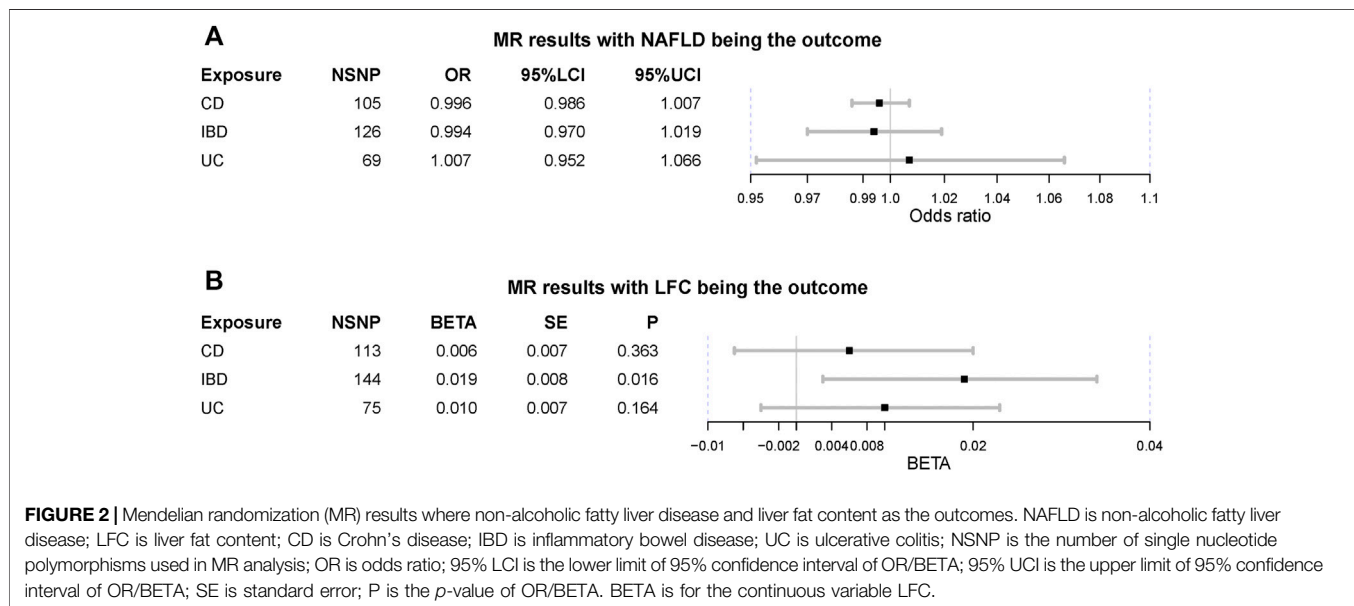
When treating NAFLD as the exposure, no causal association was detected, including IBD (OR = 0.968 [0.928, 1.009], IVW p -value = 0.123), UC (OR = 0.953 [0.878, 1.034], IVW p -value = 0.247) and CD (OR = 0.983 [0.935, 1.034], IVW p -value = 0.516) (Figure 3). The MVMR suggested there was no causation between NAFLD and IBD (UC and CD) after adjusting for BMI and T2D (IBD OR = 1.024 [0.983, 1.066], IVW p -value = 0.255). Also, the liver fat accumulation appeared not to affect the risk of IBD (OR = 0.954 [0.861, 1.058], IVW p -value = 0.373), UC (OR = 0.961 [0.855, 1.081], IVW p -value = 0.511) or CD (OR = 0.932 [0.784, 1.109], IVW p -value = 0.426). The MVMR suggested genetically-predicted LFC could not alter the risk of IBD, UC or CD after adjusting for BMI and T2D (IVW p -value > 0.05). No significant association was observed in MR-Egger regression and weighted-median method (Table 2). No horizontal pleiotropy was detected and there existed heterogeneity in NAFLD-UC and LFC-CD pairs. Also, the conclusions still held after removing outliers.

The MR CAUSE analysis indicated the causal model did not hold in estimating the causal associations abovementioned as all p -values of causal model were greater than 0.05 (Table 3). However, it should be paid attention to that the direction of gamma values from CASUE were all positive in estimating causal associations if treating NAFLD

TABLE 1 | A brief description of each GWAS summary statistics.

| Phenotype | Ancestry | Sample Size | Unit | NSNP | R ² (%) | F | PMID |
|----------------------------------|----------|----------------------------------|-----------------|------|--------------------|--------|------------|
| Inflammatory bowel disease | Mixed | 25,042 cases and 34,915 controls | 1-unit of logOR | 145 | 15.37 | 74.91 | 28,067,908 |
| Ulcerative disease | Mixed | 12,366 cases and 33,609 controls | 1-unit of logOR | 75 | 8.53 | 57.07 | 28,067,908 |
| Crohn's disease | Mixed | 12,194 cases and 28,072 controls | 1-unit of logOR | 113 | 12.97 | 52.95 | 28,067,908 |
| Nonalcoholic fatty liver disease | European | 1,483 cases and 17,781 controls | 1-unit of logOR | 4 | 1.59 | 77.79 | 32,298,765 |
| Liver fat content | European | 32,858 participants | SD | 13 | 4.32 | 114.07 | 34,128,465 |

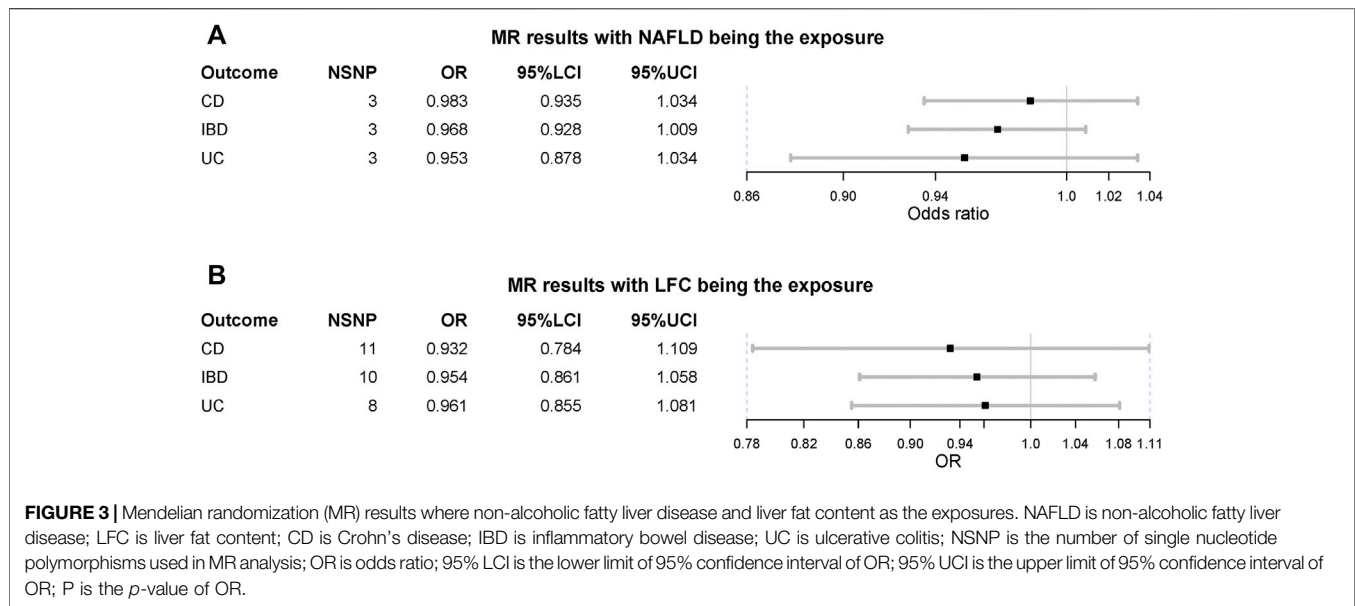
NSNP, the number of single nucleotide polymorphism; R², variance of phenotype explained by SNPs; logOR, logarithm of odds ratio; SD, standard deviation; F, F statistics; PMID, ID of publication in the PubMed.

**TABLE 2** | MR results of MR-Egger regression and weighted-median method.

| Exposure | Outcome | NSNP | MR-Egger | | | | Weighted-Median | | | | P _{heterogeneity} | P _{pleiotropy} |
|----------|---------|------|-----------|--------|--------|-------|-----------------|--------|--------|-------|----------------------------|-------------------------|
| | | | OR (BETA) | 95%LCI | 95%UCI | P | OR (BETA) | 95%LCI | 95%UCI | P | | |
| UC | NAFLD | 69 | 0.922 | 0.770 | 1.105 | 0.383 | 0.992 | 0.925 | 1.064 | 0.817 | 0.188 | 0.481 |
| CD | NAFLD | 105 | 0.024 | 0.792 | 1.008 | 0.070 | 0.020 | 0.990 | 1.006 | 0.655 | 0.016 | 0.038 |
| IBD | NAFLD | 126 | 0.947 | 0.822 | 1.091 | 0.455 | 1.004 | 0.978 | 1.030 | 0.785 | 0.063 | 0.499 |
| UC | LFC | 75 | 0.013 | -0.023 | 0.049 | 0.487 | 0.012 | -0.008 | 0.032 | 0.224 | 0.308 | 0.847 |
| CD | LFC | 113 | 0.032 | -0.003 | 0.067 | 0.077 | 0.009 | -0.009 | 0.026 | 0.327 | 0.015 | 0.253 |
| IBD | LFC | 144 | 0.024 | -0.017 | 0.064 | 0.251 | 0.020 | -0.002 | 0.042 | 0.080 | 0.000 | 0.797 |
| NAFLD | UC | 3 | 1.108 | 0.865 | 1.421 | 0.566 | 0.966 | 0.912 | 1.023 | 0.236 | 0.065 | 0.430 |
| NAFLD | CD | 3 | 1.039 | 0.872 | 1.238 | 0.741 | 0.987 | 0.936 | 1.041 | 0.635 | 0.483 | 0.635 |
| NAFLD | IBD | 3 | 1.067 | 0.934 | 1.220 | 0.513 | 0.979 | 0.938 | 1.021 | 0.321 | 0.318 | 0.373 |
| LFC | UC | 8 | 1.046* | 0.883 | 1.239 | 0.622 | 0.976* | 0.841 | 1.133 | 0.751 | 0.313 | 0.240 |
| LFC | CD | 11 | 1.118* | 0.885 | 1.412 | 0.375 | 0.977* | 0.861 | 1.109 | 0.718 | 0.002 | 0.076 |
| LFC | IBD | 10 | 1.055* | 0.914 | 1.216 | 0.486 | 0.961* | 0.875 | 1.057 | 0.415 | 0.103 | 0.110 |

UC, ulcerative colitis; CD, Crohn's disease; IBD, inflammatory bowel disease; NAFLD, non-alcoholic fatty liver disease; LFC, liver fat content; NSNP, the number of single nucleotide polymorphism; OR, odds ratio; 95%LCI, lower limit of 95% confidence interval; 95%UCI, upper limit of 95% confidence interval; P, *p*-value of OR(BETA); P_{heterogeneity}, *p*-value of heterogeneity test from Cochrane's Q value; P_{pleiotropy}, *p*-value of pleiotropy test from MR-Egger intercept.

Please note "*" represent the BETA, for the continuous variable LFC.

**TABLE 3 |** Results of MR CAUSE analysis.

| Exposure | Outcome | Model | Gamma | Eta | Q | P |
|----------|---------|---------|---------------------|---------------------|-------------------|-------|
| UC | NAFLD | Sharing | 0 (−0.01, 0.01) | −0.58 (−1.51, 0.43) | 0.02 (0, 0.12) | 0.937 |
| | | Causal | | −0.54 (−1.64, 0.61) | 0.02 (0, 0.15) | |
| CD | NAFLD | Sharing | 0 (−0.01, 0.01) | −1.33 (−2, 0.02) | 0.02 (0, 0.08) | 0.842 |
| | | Causal | | −1.3 (−2, 0.11) | 0.02 (0, 0.09) | |
| IBD | NAFLD | Sharing | 0 (−0.01, 0.01) | −1 (−1.55, −0.42) | 0.06 (0.01, 0.12) | 0.922 |
| | | Causal | | −0.99 (−1.57, −0.2) | 0.06 (0.01, 0.13) | |
| UC | LFC | Sharing | 0.01 (0, 0.02) | 0.03 (−0.22, 0.33) | 0.03 (0, 0.24) | 0.523 |
| | | Causal | | 0 (−0.24, 0.31) | 0.03 (0, 0.24) | |
| CD | LFC | Sharing | 0.01 (0, 0.02) | 0.02 (−0.45, 0.2) | 0.03 (0, 0.23) | 0.543 |
| | | Causal | | −0.02 (−0.4, 0.18) | 0.02 (0, 0.23) | |
| IBD | LFC | Sharing | 0.01 (−0.01, 0.02) | 0.03 (−0.31, 0.27) | 0.03 (0, 0.23) | 0.598 |
| | | Causal | | −0.01 (−0.34, 0.23) | 0.03 (0, 0.24) | |
| NAFLD | UC | Sharing | −0.03 (−0.06, 0) | −0.07 (−0.35, 0.32) | 0.06 (0, 0.32) | 0.168 |
| | | Causal | | 0.01 (−0.34, 0.42) | 0.04 (0, 0.25) | |
| NAFLD | CD | Sharing | −0.02 (−0.06, 0.01) | −0.1 (−0.59, 0.34) | 0.04 (0, 0.24) | 0.543 |
| | | Causal | | −0.05 (−0.57, 0.38) | 0.04 (0, 0.24) | |
| NAFLD | IBD | Sharing | −0.03 (−0.05, 0) | −0.07 (−0.4, 0.3) | 0.05 (0, 0.29) | 0.127 |
| | | Causal | | −0.01 (−0.42, 0.39) | 0.03 (0, 0.24) | |
| LFC | UC | Sharing | −0.03 (−0.16, 0.09) | 0.29 (−1.69, 3.81) | 0.03 (0, 0.21) | 0.880 |
| | | Causal | | 0.4 (−1.47, 3.74) | 0.04 (0, 0.23) | |
| LFC | CD | Sharing | −0.02 (−0.14, 0.1) | −0.09 (−1.99, 2.14) | 0.04 (0, 0.22) | 0.985 |
| | | Causal | | −0.04 (−1.88, 2.03) | 0.04 (0, 0.23) | |
| LFC | IBD | Sharing | −0.04 (−0.12, 0.05) | −0.11 (−1.81, 2.77) | 0.04 (0, 0.22) | 0.823 |
| | | Causal | | 0 (−1.69, 2.75) | 0.04 (0, 0.22) | |

UC, ulcerative colitis; CD, Crohn's disease; IBD, inflammatory bowel disease; NAFLD, non-alcoholic fatty liver disease; LFC, liver fat content. Model represents the type of two traits where "Sharing" means two traits have shared genetics and "Causal" means the exposure can causally affect the outcome. Gamma is the effect size of exposure on outcome; Eta is the effect size of correlated pleiotropy; Q represents the proportion of variants exhibiting correlated pleiotropy; P is the probability of accepting a sharing model.

and LFC as the outcomes ($\gamma > 0$) while these gamma values turned negative if treating IBD, UC and CD as the outcomes ($\gamma < 0$). These results suggested the order of disease initiation might lead to opposite outcomes unexpectedly.

After removal of outliers detected in MR-PRESSO, no SNP that might drive the results was identified in leave-one-out sensitivity analysis.

DISCUSSION

Although genetic liability to IBD might contribute to liver fat accumulation slightly, this MR study indicated there might be no causal link between NAFLD and IBD and it should be noted that the direction of NAFLD's effect on IBD is negative, contrary to previous findings where NAFLD and IBD usually co-existed.

The observed causal effect of IBD on LFC might be a false positive one as this result was insignificant in both MR-Egger regression and weighted-median method. Besides, it was still insignificant in MR CAUSE analysis, a suitable method that can control false positive rate in MR analysis with consideration of both correlated and uncorrelated horizontal pleiotropy. However, we cannot completely rule out such causation as high-fat diet has impact on the quality of the intestinal barrier and the composition of the intestinal microbiome, influencing the pathogenesis of IBD (Ruemmele, 2016) and another study suggested LFC might be associated with UC as well (Jamali et al., 2017). Thus, further investigations should be carried out to elucidate such association.

As for the null associations, several reasons can be utilized to explain them. Metabolic syndrome, usually characterized by obesity, hyperglycemia, dyslipidemia and systemic hypertension, is currently the strongest risk factor of NAFLD (Friedman et al., 2018). Over 70% NAFLD patients are usually presented with high triglycerides (TG), high total cholesterol (TC), high low density lipoprotein cholesterol (LDL-C) and low high density lipoprotein cholesterol (HDL-C), most of which are primarily synthesized in liver, indicating dysregulated lipid metabolism in these patients, while the serum lipid profile is remarkably different in terms of serum TC and LDL-C in IBD patients at active stage, which can be rescued after intestinal surgery. Another study supported that less than 5% IBD patients are presented with dyslipidemia (Hoffmann et al., 2020), meanwhile, 25.0%–69.7% IBD patients at active stage developed malnutrition rather than obesity (Mijac et al., 2010). Therefore, we speculate that IBD brings out a specific metabolic state that might not be suitable for NAFLD.

Lean NAFLD is a special obesity resistant classification of NAFLD and believed to be with a distinct pathophysiological feature, characterized by higher serum secondary bile acid, increased expression of FGF19 and a shifted gut microbiota profile compared with non-lean NAFLD (Chen et al., 2020). IBD patients with NAFLD are often in absence of metabolic syndrome (Carr et al., 2017). There is still no report identifying the association between IBD and lean NAFLD. We cannot exclude that IBD and lean NAFLD have causal relationship, for no publicly available GWAS database can be utilized to address this problem until now.

Intriguingly, there was direct evidence illustrating that glucocorticoid for IBD could promote the initiation and progression of NAFLD instead of inhibiting NAFLD, and the use of azathioprine for CD was also determined as one risk factor for NAFLD (Woods et al., 2015). Similarly, bowel resection, a therapeutic strategy for severe IBD, was regarded as the risk factor for NAFLD in CD (Hoffmann et al., 2020), seemingly indicating inhibition of IBD could precipitate NAFLD. However, it is worthwhile to note that glucocorticoid as well as bowel surgery per se have the potential to result in liver steatosis or cholestasis, even without IBD history (Sasdeli et al., 2019). Thus, the observed co-existence of NAFLD and IBD might result from the effect of treatments, especially for the impact of IBD therapies on NAFLD (Restellini et al., 2017). Furthermore, Magri et al. reported there are no significant associations between NAFLD and IBD-related factors in IBD patients (Magri et al., 2019). In a word, it is very difficult to

demonstrate that IBD can contribute to the development of NAFLD based on previous studies.

On the other hand, accumulating evidence pointed to it that alteration of gut microbiota should have potential influence on the various risk factors of metabolic syndrome (Dabke et al., 2019). IBD is a chronic immunologically-mediated disease at the intersection of complex interactions between genetics, environment and gut microbiota (Ananthakrishnan, 2015), and gut microbiota have been reported to play an important role in pathogenesis of IBD (Franzosa et al., 2019). Metformin therapy for NAFLD could interact with gut microbiota (Vallianou et al., 2019) and so did the glucocorticoid therapy for IBD (Wu et al., 2018). Therefore, we postulate that gut microbiota may exert their effects on NAFLD and IBD concomitantly, and it can be comprehended as the pleiotropy of gut microbiota. As a result, NAFLD and IBD usually co-exist in clinical observation although there should be no causal relationship between them. Further investigations are needed to elucidate this hypothesis and corroborate our findings.

As no causal relationship was observed between NAFLD and IBD, it is still possible the underlying causal effect might be cancelled out due to opposite direct and indirect effects as omega 3 (ω 3) fatty acids could alleviate intestinal inflammation (Marton et al., 2019). Therefore, it should be possible that the effects of “bad” lipids and “good” lipids can cancel out each other. Additionally, the negative results of MR study cannot completely rule out the causal relationship as the genetically-driven exposure cannot equals to the exposure and the negative results usually happen as the strict selection of IV.

As abovementioned, the pleiotropic effect of gut microbiota, impact of therapeutic treatments and opposite direct and indirect effects might help to explain the null causal relationship between NAFLD and IBD.

Our study has several strengths as follows: (Younossi et al., 2018) MR design was used to detect the causal relationship between and it could free this study from potential bias and reverse causation; (McHenry et al., 2019) both correlated and uncorrelated horizontal pleiotropy were controlled in this MR study; (McHenry et al., 2019) a bi-directional MR analysis was carried out to clarify the causation. However, some limitations should also be pointed out: (Younossi et al., 2018) horizontal pleiotropy should also be a major concern in MR study as various statistical methods fail to rule out horizontal pleiotropy caused by undetected biological mechanism; (Kaplan and Windsor, 2021) the proportion of NAFLD cases is relatively slow which might reduce the statistical power; (McHenry et al., 2019) the exclusion-restriction the selection might be violated as the binary phenotype was treated as the exposure due to data limitation; (Zou et al., 2019) the selection bias caused by competing risk factors could not be assessed as individual-level data was unavailable.

CONCLUSION

This MR study ruled out the causal relationship between IBD and NAFLD, suggesting therapeutics targeting NAFLD might not work for IBD and vice versa.

DATA AVAILABILITY STATEMENT

Publicly available datasets were analyzed in this study. This data can be found here: <https://www.ebi.ac.uk/gwas/>.

ETHICS STATEMENT

All analyses were based on summary-level GWAS statistics and all subjects are de-identified. Each GWAS was approved by its corresponding ethical committee and the summary statistics can be freely used without restriction. The patients/participants provided their written informed consent to participate in this study.

AUTHOR CONTRIBUTIONS

GL proposed the conception, designed the study and supervised the whole analysis. LC acquired the data and performed statistical analysis. LC drafted the article. ZF checked the statistical analysis

REFERENCES

- Ananthakrishnan, A. N. (2015). Epidemiology and Risk Factors for IBD. *Nat. Rev. Gastroenterol. Hepatol.* 12, 205–217. doi:10.1038/nrgastro.2015.34
- Anstee, Q. M., Darlay, R., Cockell, S., Meroni, M., Govaere, O., Tiniakos, D., et al. (2020). Genome-wide Association Study of Non-alcoholic Fatty Liver and Steatohepatitis in a Histologically Characterised Cohort☆. *J. Hepatol.* 73, 505–515. doi:10.1016/j.jhep.2020.04.003
- Bowden, J., Davey Smith, G., and Burgess, S. (2015). Mendelian Randomization with Invalid Instruments: Effect Estimation and Bias Detection through Egger Regression. *Int. J. Epidemiol.* 44, 512–525. doi:10.1093/ije/dyv080
- Bowden, J., Davey Smith, G., Haycock, P. C., and Burgess, S. (2016). Consistent Estimation in Mendelian Randomization with Some Invalid Instruments Using a Weighted Median Estimator. *Genet. Epidemiol.* 40, 304–314. doi:10.1002/gepi.21965
- Carr, R. M., Patel, A., Bownik, H., Oranu, A., Kerner, C., Praestgaard, A., et al. (2017). Intestinal Inflammation Does Not Predict Nonalcoholic Fatty Liver Disease Severity in Inflammatory Bowel Disease Patients. *Dig. Dis. Sci.* 62, 1354–1361. doi:10.1007/s10620-017-4495-0
- Carreras-Torres, R., Ibáñez-Sanz, G., Obón-Santacana, M., Duell, E. J., and Moreno, V. (2020). Identifying Environmental Risk Factors for Inflammatory Bowel Diseases: a Mendelian Randomization Study. *Sci. Rep.* 10, 19273. doi:10.1038/s41598-020-76361-2
- Chen, F., Esmaili, S., Rogers, G. B., Bugianesi, E., Petta, S., Marchesini, G., et al. (2020). Lean NAFLD: A Distinct Entity Shaped by Differential Metabolic Adaptation. *Hepatology* 71, 1213–1227. doi:10.1002/hep.30908
- Cui, Z., Hou, G., Meng, X., Feng, H., He, B., and Tian, Y. (2020). Bidirectional Causal Associations between Inflammatory Bowel Disease and Ankylosing Spondylitis: A Two-Sample Mendelian Randomization Analysis. *Front. Genet.* 11, 587876. doi:10.3389/fgene.2020.587876
- Dabke, K., Hendrick, G., and Devkota, S. (2019). The Gut Microbiome and Metabolic Syndrome. *J. Clin. Invest.* 129, 4050–4057. doi:10.1172/JCI129194
- Davey Smith, G., and Hemani, G. (2014). Mendelian Randomization: Genetic Anchors for Causal Inference in Epidemiological Studies. *Hum. Mol. Genet.* 23, R89–R98. doi:10.1093/hmg/ddu328
- de Lange, K. M., Moutsianas, L., Lee, J. C., Lamb, C. A., Luo, Y., Kennedy, N. A., et al. (2017). Genome-wide Association Study Implicates Immune Activation of Multiple Integrin Genes in Inflammatory Bowel Disease. *Nat. Genet.* 49, 256–261. doi:10.1038/ng.3760
- Emdin, C. A., Khera, A. V., and Kathiresan, S. (2017). Mendelian Randomization. *Jama* 318, 1925–1926. doi:10.1001/jama.2017.17219

and substantially revised the draft. XS and WQ read the whole manuscript and revised it. YC and JZ provided some necessary statistical suggestions and improved the English writing. All authors gave final approval of the version to be submitted.

FUNDING

The work is supported by National Natural Science Foundation of China (Grant No. 81602059) and Jilin Provincial Finance Department (Grant No. 2018SCZWSZX-042, 2018SCZWSZX-033).

ACKNOWLEDGMENTS

We would like to thank all investigators who made these GWAS summary statistics publicly available.

- Franzosa, E. A., Sirota-Madi, A., Avila-Pacheco, J., Fornelos, N., Haiser, H. J., Reinker, S., et al. (2019). Gut Microbiome Structure and Metabolic Activity in Inflammatory Bowel Disease. *Nat. Microbiol.* 4, 293–305. doi:10.1038/s41564-018-0306-4
- Friedman, S. L., Neuschwander-Tetri, B. A., Rinella, M., and Sanyal, A. J. (2018). Mechanisms of NAFLD Development and Therapeutic Strategies. *Nat. Med.* 24, 908–922. doi:10.1038/s41591-018-0104-9
- Hemani, G., Zheng, J., Elsworth, B., Wade, K. H., Haberland, V., Baird, D., et al. (2018). The MR-Base Platform Supports Systematic Causal Inference across the Human Phenome. *Elife* 7. doi:10.7554/eLife.34408
- Hemani, G., Tilling, K., and Davey Smith, G. (2017). Orienting the Causal Relationship between Imprecisely Measured Traits Using GWAS Summary Data. *Plos Genet.* 13, e1007081. doi:10.1371/journal.pgen.1007081
- Hoffmann, P., Jung, V., Behnisch, R., and Gauss, A. (2020). Prevalence and Risk Factors of Nonalcoholic Fatty Liver Disease in Patients with Inflammatory Bowel Diseases: A Cross-Sectional and Longitudinal Analysis. *World J. Gastroenterol.* 26, 7367–7381. doi:10.3748/wjg.v26.i46.7367
- Jamali, R., Biglari, M., Seyyed Hosseini, S. V., Shakouri Rad, A., and Kosari, F. (2017). The Correlation between Liver Fat Content and Ulcerative Colitis Disease Severity. *Acta Med. Iran* 55, 333–339.
- Kaplan, G. G., and Windsor, J. W. (2021). The Four Epidemiological Stages in the Global Evolution of Inflammatory Bowel Disease. *Nat. Rev. Gastroenterol. Hepatol.* 18, 56–66. doi:10.1038/s41575-020-00360-x
- Lin, A., Roth, H., Anyane-Yeboah, A., Rubin, D. T., and Paul, S. (2021). Prevalence of Nonalcoholic Fatty Liver Disease in Patients with Inflammatory Bowel Disease: A Systematic Review and Meta-Analysis. *Inflamm. Bowel Dis.* 27, 947–955. doi:10.1093/ibd/izaa189
- Liu, Y., Basti, N., Whitcher, B., Bell, J. D., Sorokin, E. P., van Bruggen, N., et al. (2021). Genetic Architecture of 11 Organ Traits Derived from Abdominal MRI Using Deep Learning. *Elife*, 10. doi:10.7554/elifelife.65554
- Liu, Z., Zhang, Y., Graham, S., Wang, X., Cai, D., Huang, M., et al. (2020). Causal Relationships between NAFLD, T2D and Obesity Have Implications for Disease Subphenotyping. *J. Hepatol.* 73, 263–276. doi:10.1016/j.jhep.2020.03.006
- Locke, A. E., Kahali, B., Berndt, S. I., Justice, A. E., Pers, T. H., Day, F. R., et al. (2015). Genetic Studies of Body Mass Index Yield New Insights for Obesity Biology. *Nature* 518, 197–206. doi:10.1038/nature14177
- Magri, S., Paduano, D., Chicco, F., Cingolani, A., Farris, C., Delogio, G., et al. (2019). Nonalcoholic Fatty Liver Disease in Patients with Inflammatory Bowel Disease: Beyond the Natural History. *World J. Gastroenterol.* 25, 5676–5686. doi:10.3748/wjg.v25.i37.5676
- Mahajan, A., Go, M. J., Zhang, W., Below, J. E., Gaulton, K. J., Mahajan, A., et al. (2014). Genome-wide Trans-ancestry Meta-Analysis Provides Insight into the

- Genetic Architecture of Type 2 Diabetes Susceptibility. *Nat. Genet.* 46, 234–244. doi:10.1038/ng.2897
- Marton, L. T., Goulart, R. A., Carvalho, A. C. A., and Barbalho, S. M. (2019). Omega Fatty Acids and Inflammatory Bowel Diseases: An Overview. *Int. J. Mol. Sci.* 20. doi:10.3390/ijms20194851
- McHenry, S., Sharma, Y., Tirath, A., Tsai, R., Mintz, A., Fraum, T. J., et al. (2019). Crohn's Disease Is Associated with an Increased Prevalence of Nonalcoholic Fatty Liver Disease: A Cross-Sectional Study Using Magnetic Resonance Proton Density Fat Fraction Mapping. *Clin. Gastroenterol. Hepatol.* 17, 2816–2818. doi:10.1016/j.cgh.2019.02.045
- Mijac, D. D., Janković, G. L., Jorga, J., and Krstić, M. N. (2010). Nutritional Status in Patients with Active Inflammatory Bowel Disease: Prevalence of Malnutrition and Methods for Routine Nutritional Assessment. *Eur. J. Intern. Med.* 21, 315–319. doi:10.1016/j.ejim.2010.04.012
- Morrison, J., Knoblauch, N., Marcus, J. H., Stephens, M., and He, X. (2020). Mendelian Randomization Accounting for Correlated and Uncorrelated Pleiotropic Effects Using Genome-wide Summary Statistics. *Nat. Genet.* 52, 740–747. doi:10.1038/s41588-020-0631-4
- Piovani, D., Pansieri, C., Peyrin-Biroulet, L., Danese, S., and Bonovas, S. (2021). Confounding and Bias in Observational Studies in Inflammatory Bowel Disease: a Meta-Epidemiological Study. *Aliment. Pharmacol. Ther.* 53, 712–721. doi:10.1111/apt.16222
- Restellini, S., Chazouillères, O., and Frossard, J. L. (2017). Hepatic Manifestations of Inflammatory Bowel Diseases. *Liver Int.* 37, 475–489. doi:10.1111/liv.13265
- Ruemmele, F. M. (2016). Role of Diet in Inflammatory Bowel Disease. *Ann. Nutr. Metab.* 68 Suppl 1 (Suppl. 1), 33–41. doi:10.1159/000445392
- Sasdeli, A. S., Agostini, F., Pazzeschi, C., Guidetti, M., Lal, S., and Pironi, L. (2019). Assessment of Intestinal Failure Associated Liver Disease According to Different Diagnostic Criteria. *Clin. Nutr.* 38, 1198–1205. doi:10.1016/j.clnu.2018.04.019
- Vallianou, N. G., Stratigou, T., and Tsagarakis, S. (2019). Metformin and Gut Microbiota: Their Interactions and Their Impact on Diabetes. *Hormones (Athens)* 18, 141–144. doi:10.1007/s42000-019-00093-w
- Verbanck, M., Chen, C. Y., Neale, B., and Do, R. (2018). Detection of Widespread Horizontal Pleiotropy in Causal Relationships Inferred from Mendelian Randomization between Complex Traits and Diseases. *Nat. Genet.* 50, 693–698. doi:10.1038/s41588-018-0099-7
- Voight, B. F., Peloso, G. M., Orho-Melander, M., Frikke-Schmidt, R., Barbalic, M., Jensen, M. K., et al. (2012). Plasma HDL Cholesterol and Risk of Myocardial Infarction: a Mendelian Randomisation Study. *Lancet* 380, 572–580. doi:10.1016/S0140-6736(12)60312-2
- Woods, C. P., Hazlehurst, J. M., and Tomlinson, J. W. (2015). Glucocorticoids and Non-alcoholic Fatty Liver Disease. *J. Steroid Biochem. Mol. Biol.* 154, 94–103. doi:10.1016/j.jsbmb.2015.07.020
- Wu, T., Yang, L., Jiang, J., Ni, Y., Zhu, J., Zheng, X., et al. (2018). Chronic Glucocorticoid Treatment Induced Circadian Clock Disorder Leads to Lipid Metabolism and Gut Microbiota Alterations in Rats. *Life Sci.* 192, 173–182. doi:10.1016/j.lfs.2017.11.049
- Younossi, Z., Anstee, Q. M., Marietti, M., Hardy, T., Henry, L., Eslam, M., et al. (2018). Global burden of NAFLD and NASH: Trends, Predictions, Risk Factors and Prevention. *Nat. Rev. Gastroenterol. Hepatol.* 15, 11–20. doi:10.1038/nrgastro.2017.109
- Zou, Z. Y., Shen, B., and Fan, J. G. (2019). Systematic Review with Meta-Analysis: Epidemiology of Nonalcoholic Fatty Liver Disease in Patients with Inflammatory Bowel Disease. *Inflamm. Bowel Dis.* 25, 1764–1772. doi:10.1093/ibd/izz043

Conflict of Interest: The authors declare that the research was conducted in the absence of any commercial or financial relationships that could be construed as a potential conflict of interest.

Publisher's Note: All claims expressed in this article are solely those of the authors and do not necessarily represent those of their affiliated organizations, or those of the publisher, the editors and the reviewers. Any product that may be evaluated in this article, or claim that may be made by its manufacturer, is not guaranteed or endorsed by the publisher.

Copyright © 2022 Chen, Fan, Sun, Qiu, Chen, Zhou and Lv. This is an open-access article distributed under the terms of the Creative Commons Attribution License (CC BY). The use, distribution or reproduction in other forums is permitted, provided the original author(s) and the copyright owner(s) are credited and that the original publication in this journal is cited, in accordance with accepted academic practice. No use, distribution or reproduction is permitted which does not comply with these terms.



Targeting Thyroid Hormone/Thyroid Hormone Receptor Axis: An Attractive Therapy Strategy in Liver Diseases

Qianyu Tang^{1†}, Min Zeng^{2†}, Linxi Chen^{3*} and Nian Fu^{1,4*}

¹Department of Gastroenterology, The Affiliated Nanhua Hospital, Hunan Provincial Clinical Research Center of Metabolic Associated Fatty Liver Disease, Hengyang Medical School, University of South China, Hengyang, China, ²Department of Gastroenterology, Liuyang Hospital of Chinese Medicine, Changsha, China, ³Department of Pharmacy and Pharmacology, Hunan Provincial Key Laboratory of Tumor Microenvironment Responsive Drug Research, Hunan Province Cooperative Innovation Center for Molecular Target New Drug Study, School of Basic Medical Science, Hengyang Medical School, University of South China, Hengyang, China, ⁴The Affiliated Nanhua Hospital, Laboratory of Liver Disease, Institute of Clinical Research, Hengyang Medical School, University of South China, Hengyang, China

OPEN ACCESS

Edited by:

Francisco Javier Cubero,
Complutense University of Madrid,
Spain

Reviewed by:

Simone Wajner,
Federal University of Rio Grande do
Sul, Brazil
Hang Hang Wu,
Complutense University of Madrid,
Spain

*Correspondence:

Linxi Chen
1995001765@usc.edu.cn
Nian Fu
2002funian@163.com

[†]These authors have contributed
equally to this work

Specialty section:

This article was submitted to
Gastrointestinal and Hepatic
Pharmacology,
a section of the journal
Frontiers in Pharmacology

Received: 07 February 2022

Accepted: 19 April 2022

Published: 02 June 2022

Citation:

Tang Q, Zeng M, Chen L and Fu N
(2022) Targeting Thyroid Hormone/
Thyroid Hormone Receptor Axis: An
Attractive Therapy Strategy in
Liver Diseases.
Front. Pharmacol. 13:871100.
doi: 10.3389/fphar.2022.871100

Thyroid hormone/thyroid hormone receptor (TH/TR) axis is characterized by TH with the assistance of plasma membrane transporters to combine with TR and mediate biological activities. Growing evidence suggests that TH/TR participates in plenty of hepatic metabolism. Thus, this review focuses on the role of the TH/TR axis in the liver diseases. To be specific, the TH/TR axis may improve metabolic-associated fatty liver disease, hepatitis, liver fibrosis, and liver injury while exacerbating the progression of acute liver failure and alcoholic liver disease. Also, the TH/TR axis has paradoxical roles in hepatocellular carcinoma. The TH/TR axis may be a prospecting target to cure hepatic diseases.

Keywords: TH/TR axis, thyroid hormone receptor, thyroid hormone, metabolic-associated fatty liver disease, hepatocellular carcinoma

INTRODUCTION

Thyroid hormones (THs), including thyroid hormones 3,5,3',5'- tetraiodothyronine or thyroxine (T₄) and 3,5,3'-triiodothyronine (T₃), are secreted by the thyroid gland to mediate homeostasis of biological growth, development, and metabolism (Senese et al., 2019; Turan and Turksoy, 2021). Thyroid hormone receptor (TR), a member of the nuclear receptor superfamily, is a ligand-dependent transcriptional factor. TR isoforms include TRα1, TRα2, TRβ1, TRβ2, and v-erbA (Ventura-Holman et al., 2011; Knabl et al., 2020). TRα and TRβ are encoded by chromosome 17 and chromosome 3, respectively (Onigata and Szinnai, 2014). V-erbA, acting like a transcriptional suppressor, is a derivant after TRα1 is affected by the avian erythroblastosis virus (AEV) (Ciana et al., 1998). TRα1 is mainly expressed in most peripheral organs except the liver, while TRβ1 is highly expressed in the liver. Although the TRα1 and TRβ1 mRNA levels are similar in metabolically active fats and muscles, protein levels are quite different (TRβ: TRα = 1:10). Moreover, TRβ2 is highly expressed in the pituitary gland, and gender differences in the expression have been found (Minakhina et al., 2020). The active form of TH, T₃, and its nuclear receptor assembles ligand-dependent TH/TR complexes, thus regulating gene expression and directing downstream transcriptional activities (Lin et al., 2020a). In addition, thyroid hormone-response element (TRE) is located on the promoters of T₃ target genes and affects the activity of the TR transcription response (Cheng, 2005). In pituitary gland, thyroid-stimulating hormone (TSH) is responsible for synthesis and secretion

of TH while the encoding genes of TSH are also regulated by TH in a negative way (Bargi-Souza et al., 2017).

Dysfunction of the TH/TR axis leads to numerous pathologies, especially including growth, skeletal development, heart diseases, cognitive dissonance, gastrointestinal function, obesity, dysmetabolism, and cancers (Brent, 2012; Ortega-Carvalho et al., 2014; Ajdukovic et al., 2021; Moutzouri et al., 2021; Niedowicz et al., 2021; Salman et al., 2021). Therefore, the abnormality of the TH/TR axis elicits a series of diseases, the most common of which is metabolic disease (Malm, 2004). The correlation between the TH/TR axis and many metabolism-associated diseases has been well-elucidated. For example, the TH/TR axis plays a protective role in hyperlipidemia, obesity, and type 2 diabetes (Grover et al., 2007). Intriguingly, the TH/TR axis is intimately associated with the development of the brain and the cerebellar both in fetal and adults (Ishii et al., 2021). Also, the TH/TR axis acts as a promoter in arrhythmia, gastric tumors, and alcoholic-related liver injury (Puhr et al., 2020; Deng et al., 2021). Considering the aforementioned facts, the TH/TR axis may be an indispensable part in maintaining hepatic metabolism.

Indeed, accumulating evidence has demonstrated that the TH/TR axis plays an important role in liver diseases. For instance, TR β 1, a subtype of TH, is highly expressed in the liver, regulating the metabolism of cholesterol and carbohydrates (Dawson and Parini, 2018; Gautherot et al., 2018). Additionally, the TH/TR axis, a strong inducer of hepatic autophagy contributing to lipid droplet degradation, as well as maintaining mitochondrial biogenesis and turnover, causes the removal of damaged mitochondria and ROS, ultimately preventing hepatic injury (Chi et al., 2019). As the TH/TR axis is correlated with various hepatic physiological alterations, more emphasis should be placed on the mechanism of the TH/TR axis in liver diseases. This review summarizes the regulatory mechanism of the TH/TR axis in the liver and focuses on the role of the TH/TR axis in hepatic diseases.

TH/TR AXIS PROMOTES HEPATOCYTE PROLIFERATION AND LIVER REGENERATION

TH has proven to be a hepatic mitogen, thus eliciting hepatocyte proliferating and liver repopulation. López-Fontal et al. (2010) also discovered that hypothyroidism and TR-deficient mice showed delayed recovery of liver mass. Interestingly, hypothyroidism can induce moderate non-alcoholic steatohepatitis, thereby promoting liver regeneration (Rodríguez-Castelán et al., 2017). A large number of studies reported that TR β is involved in liver regeneration by the TH/TR axis (Sun et al., 2007). For instance, two TR β agonists, TG68 and IS25, promote hepatocyte proliferation without TH/TR axis-dependent side effects (Perra et al., 2020). This aforementioned finding hints that the regulation of hepatocyte proliferation by the TH/TR axis is of great importance. Accordingly, studies have suggested the effect of the TH/TR axis on hepatocyte proliferation that TH promotes liver regeneration after 50% liver transplantation in mice *via* elevating histone 3 mRNA, proliferating cell nuclear antigen (PCNA), cyclin-dependent kinase 2 (cdk2),

cyclin A, and cyclin D1 levels (Oren et al., 1999; Columbano et al., 2008; Taki-Eldin et al., 2011). The TH/TR axis activates β -catenin to induce hepatocyte proliferation through PKA and Wnt-dependent pathways (Fanti et al., 2014; Alvarado et al., 2016). Moreover, poly (ADP-ribose) polymerase (PARP), a nuclear enzyme involved in cell replication, is involved in the early steps of liver regeneration induced by TH after partial hepatectomy (PH) (Cesarone et al., 2000). The decrease of Dio3 elicits TH-dependent hepatocyte proliferation and liver regeneration (Kester et al., 2009). In addition, T3 binds to nucleoprotein and then changes the interaction between nucleoprotein and TRE during liver regeneration (Hirose-Kumagai et al., 1995). These studies show that the regulation of hepatocyte proliferation by the TH/TR axis has been gradually demonstrated. Otherwise, the TH/TR axis is also involved in some specific regulation mechanisms of liver regeneration. For instance, Anan et al. (Abu Rmilah et al., 2020) summarized that TH mediates cell cycle regulators and apoptosis in liver regeneration. In addition, T3 improves liver regeneration by promoting the expression of VEGF and its receptor Flt-1 (Bockhorn et al., 2007). These studies suggest that the TH/TR axis may protect hepatocyte proliferation and liver regeneration (Figure 1).

INTERPLAY BETWEEN TH/TR AXIS AND LIVER DISEASES

Hepatocyte proliferation, regeneration, and lipid homeostasis in the liver are involved in many hepatic diseases. Significantly, numerous studies have shown that the prevalence and development of hepatic diseases are related to TH/TR axis abnormality (Mishkin et al., 1981). The interplay between the TH/TR axis and liver diseases are summarized. These diseases mainly include metabolic-associated fatty liver disease (MAFLD), hepatocellular carcinoma (HCC), hepatitis of hepatitis B virus (HBV) and hepatitis C virus (HCV) infection, acute liver failure (ALF), liver fibrosis, alcoholic liver disease, and liver injury.

TH/TR Axis Might Improve MAFLD

MAFLD, formerly named as non-alcoholic fatty liver disease, is a serious liver issue worldwide and will be the leading cause of liver transplantation in the forthcoming decades (Méndez-Sánchez and Díaz-Orozco, 2021). A large number of studies reported that TH regulates hepatic triglyceride and cholesterol metabolism (Zhao et al., 2020). Accordingly, TH increases the activity of hepatic lipase, thus enhancing lipid mobilization from fat droplets. Moreover, TR activation triggers free fatty acid transporting into the hepatocytes (Tanase et al., 2020). Considering the aforementioned facts, the TH/TR axis is likely to be intimately correlated with hepatic diseases such as MAFLD. Accumulating evidence has demonstrated that the TH/TR axis is involved in MAFLD. To be specific, MAFLD is positively related with hypothyroidism, elevated TSH, T3, and thyroid peroxidase antibody (TPOAb), and suppressed T4 (Gor et al., 2021; D'Ambrosio et al., 2021).

The fact that whether the TH/TR axis can be a risk factor in MAFLD is not clear. Martínez-Escudé A et al. (2021) reported

TABLE 1 | Comparison of different effects on selective TR β receptor agonists.

| Drug category (or categories) | Type of agonist/affinity | Effects on | | | Supplement | Reference |
|---------------------------------------|---|---|--|---|--|---|
| | | Heart | Thyroid hormone axis (THA) | Lipid metabolism | | |
| MGL- 3,196 (Resmetirom) | TR β -selective agonist (28-fold over TR α) | Non-cardiac electrocardiogram change | At the highest dose, reversible free T4 was reduced by 20%. No significant change in TSH, free T3, and thyroid axis dysfunction | LDL-cholesterol, non-HDL-cholesterol, apolipoprotein B, and triglycerides were reduced. Liver weight, hepatic steatosis, plasma alanine aminotransferase activity, and blood glucose were reduced. The dose of 80 mg has the greatest effect on lipid metabolism. | No effect on body weight. No dose- related adverse events, no changes in liver enzymes, and vital signs. Phase 2–3 clinical trials are under way. Effects on insulin resistance and dog cartilage abnormality are dispute. | Sinha et al. (2012); Kagawa et al. (2018); Ritter et al. (2020) |
| MB07811 (vk2809; precursor of KB-141) | TR β agonists | No significant change | Total and free T4 levels were decreased by day 7, with both doses of MB07811 and remaining constant over the subsequent 6 weeks of treatment. Levels of TSH and TSH mRNA were reduced. | Decreased serum TGs, liver TGs, and liver weight | No effect on body weight, fasting blood glucose, plasma insulin and plasma FFA, SREBP-2, and HMG- CoA reductase or phosphoenolpyruvate carboxykinase in the liver | Kowalik et al. (2018) |
| KB-141 | TR β agonists | Increased heart rate, the first derivative of left ventricular pressure, and systolic aortic pressure, followed by reduced weight | Decreased total 3,5,3, 5-tetraiodo- L-thyronine (T4) and free T4, total T3, and free T3 | Not liver TGs but lower serum TGs and liver weight | No difference in the maximum cholesterol lowering effect between KB-141 and MB07811. | Kowalik et al. (2018) |
| Sobetirome (GC- 1) | GC-1 binds TR β higher than that of TR α | No undesirable effects | TRH suppression:T3>Sob-AM2>sobetirome, decreased or depleted circulating T4 and T3 levels without altered serum TSH levels | Reduced serum cholesterol triglyceride and lipoprotein (a) levels. Reverse very high-fat diet (VHFD)-induced fat accumulation in the liver and induced weight loss. Reverse cholesterol transport pathway | Hyperglycemia and insulin resistance. The drug was stopped after the first phase of clinical trial. | Taub et al. (2013), Fanti et al. (2014), Raza et al. (2021) |
| DITPA | Similar affinity to both TR isoforms with relatively low affinity | Increased cardiac index and decreased systemic vascular resistance | Lowered serum TSH levels, to a lesser extent, serum T3 and T4, and no differences in clinical manifestations of thyrotoxicosis or hypothyroidism | Decreased serum cholesterol, low-density lipoprotein cholesterol and body weight, and a transient decrease in triglycerides and no change in high-density lipoprotein cholesterol | Reduced body weight and dangerous skeletal actions | Erion et al. (2007), Senese et al. (2019) |
| KB2115 (Eprotriome) | KB2115 has modestly higher affinity for TR β than for TR α | No undesirable effects | No adverse extrahepatic thyromimetic effects | Reduced serum total and LDL-cholesterol, apolipoprotein B, triglycerides, and Lp (a) lipoprotein, prevents hepatic steatosis | Increase in transaminase and conjugated bilirubin concentrations; clinical trials were discontinued because long-term studies in dogs resulted in cartilage damage. | Senese et al. (2019), Kannt et al. (2021) |

that TSH, regarded as a risk factor of MAFLD, is involved in obesity, atherogenic dyslipidemia, metabolic syndrome (MetS), hypertransaminasemia, and altered cholesterol and triglycerides levels. Then, a recent research hint that TSH is a MAFLD risk factor but excludes the FT3 and FT4 levels (Tan et al., 2021). Intriguingly, the result in a middle-aged and elderly euthyroid subjects showed that high-normal FT3 and low-normal TSH independently predict the high incidence of MAFLD (Gu et al.,

2021). In addition, Chao et al. thought that FT3 and FT4 are independent risk factors to MAFLD. Conversely, although the level of TSH in non-MAFLD and MAFLD subjects who are undergoing health examinations are significantly different, TSH is excluded as an independent risk factor of MAFLD (Zhang X. et al., 2020; Chao and Chen, 2021). As described earlier, there is still controversy to identify TSH and TH as independent risk factors of MAFLD.

Importantly, the TH/TR axis regulate hepatic lipid metabolism such as mitochondrial fatty acid β -oxidation, lipid autophagy, and expression of lipid-related genes (Sinha et al., 2012; Kagawa et al., 2018). Thus, selective TR β agonists may improve hepatic lipid disorders and MAFLD (Kowalik et al., 2018; Senese et al., 2019; Ritter et al., 2020). These agonists include MGL-3196 (Taub et al., 2013; Raza et al., 2021; Kannt et al., 2021), MB07811 (Erion et al., 2007), KB-141 (Erion et al., 2007), sobetisome (GC-1) (Huang Y. Y. et al., 2013; Ferrara et al., 2018; Saponaro et al., 2020), KB2115 (Eprotirome) (Ladenson et al., 2010a; Senese et al., 2019), and DITPA (Ladenson et al., 2010b; Senese et al., 2019) (Table 1). The side effects of selective TR β agonists mostly result from TR α -induced dose-dependent cardiac effects, muscle metabolism, and bone turnover (Erion et al., 2007; Kelly et al., 2014). In short, the TH/TR axis may act as a promising treatment method for MAFLD.

TH/TR Axis Is Involved in HCC Growth, Proliferation, Invasion, and Metastasis

HCC is one of the most common malignant tumors. The TH/TR axis is involved in HCC. Some studies have demonstrated that mutations of TR genes are associated with human carcinoma (Anyetel-Anum et al., 2018; Piqué et al., 2020). A clinical study exhibited that hypothyroidism delays hepatocyte growth while hyperthyroidism promotes HCC (Mishkin et al., 1981). Additionally, the level of TR expression in adenomas (83%) and cancer (68%) is significantly lower than that in normal epithelium (96%) (Liu et al., 2019). Moreover, TH-related mitochondrial turnover protects hepatocytes from HBV hepatocarcinogenesis (Chi et al., 2017; Hossain et al., 2020). In addition, the TH/TR axis regulates proliferation, differentiation, metastasis, and drug resistance, autophagy in HCC (Jazdzewski et al., 2011; Rosen and Privalsky, 2011; Jerzak et al., 2015; Liu et al., 2019; Lin et al., 2020a).

TH/TR Axis May Be Involved in Hepatitis of Hepatitis B Virus and Hepatitis C Virus Infection

Hepatitis of HBV and HCV infection are global issues, which have a risk to develop severe liver disease such as liver cirrhosis and HCC (Jing et al., 2020; Zhang et al., 2021). A study hinted that the FT3 level decreases in HBV patients, while the FT3 and FT4 levels increase in HCV patients (Orságová et al., 2014). More specifically is that along with the increasing inflammatory grade, the level of TT3 primary increased and then decreased, but only the increased level was significantly statistic (Hu et al., 2020). Interestingly, HBV/HCV coinfection elevates the probability of thyroid dysfunction (Ji et al., 2016). Meanwhile, one of the major problems with interferon therapy in hepatitis is the occurrence of aberrant TSH, T3, and T4 values, as well as autoantibodies and thyroid diseases (Ignatova et al., 1998; Orságová et al., 2014; Karwowska et al., 2018). Nevertheless, Huang MJ et al. (1999) indicated that seropositivity of thyroid autoantibodies should not be a contraindication to IFN therapy in HCV-infected patients. Similarly, a recent research reported that the antithyroid

antibodies do not cause severe autoimmune disorders in children with chronic HBV infection and merely associated with subclinical hypothyroidism (Kansu et al., 2004).

Downregulated TH/TR Function Ameliorates Acute Liver Failure

Acute liver failure (ALF), characterized by elevated liver biochemistry, coagulopathy, and hepatic encephalopathy (HE) but with no underlying chronic liver disease (CLF), is a severe and complex clinical syndrome (Lopes and Samant, 2021). The TH/TR axis may be involved in ALF. On the one hand, type A HE is strongly related to low TSH in ALF patients with a concerning poor survival rate (Anastasiou et al., 2015; Wang et al., 2017). HINAT ACLF has proposed liver failure incorporating TSH into the standard (Feng and Shi, 2018; Wu et al., 2018). Interestingly, type C HE often happens to patients with cirrhosis and lower T3 and T4 levels (Wang et al., 2017). In addition, ALF induced by surgical liver devascularization in female pigs observed a decrease in serum-free T3 and T4 as well as TR α protein levels (Kostopanagiotou et al., 2009). Intriguingly, thioacetamide-induced ALF promotes hepatocyte proliferation in response to T3 in the rat (Malik et al., 2006). On the other hand, hypothyroidism prevents immune-mediated acute liver injury in mice, subsequently elevating TSH levels and survival rates and declining serum liver enzymes, blood ammonia, and prothrombin time. It has been reported that a patient with ALF results from non-controlled hyperthyroidism (Sousa Domínguez, 2015). Clinically, plasma exchange is an effective method to eliminate TH in acute liver failure with thyroid storm (Zeng et al., 2017). Mechanistically, low T3 and T4 levels in hypometabolism-associated hypothyroidism link to inflammation and oxidative stress (Bruck et al., 1998). In general, high TSH levels and low TH/TR functions manifest a protector in ALF.

TH/TR Axis Improves Liver Fibrosis

Liver fibrosis is characterized by chronic inflammation and fibrous scar formation in the liver, finally resulting in hepatocyte deficiency and loss of hepatic function (Erhardttsen et al., 2021). Advanced fibrosis is associated with decreased serum FT3 levels (Du et al., 2021). As an independent risk factor, an elevated TSH level is significantly correlated with the risk of fibrosis (Martínez-Escudé et al., 2021). In a recent study, compared with 12.19% in chronic hepatitis C (CHC) patients without thyroid disease (TD), severe fibrosis is found at 92.85% among CHC patients with TD (Biciusca et al., 2020). However, studies have suggested that hypothyroidism was not highly associated with fibrosis (D'Ambrosio et al., 2021). Treating with TR β agonist resmetirom in advanced NASH with fibrosis mice have lower α -smooth muscle actin, fibrogenesis-involved genes, and markers of fibrosis, especially including liver stiffness and N-terminal type III collagen pro-peptide (PRO-C3), which indicate that resmetirom can improve fibrosis (Harrison et al., 2021; Kannt et al., 2021). As a result, the TH/TR axis ameliorates liver fibrosis, although the deeper connection between hepatic fibrosis and the TH/TR axis needs more exploration.

TABLE 2 | Regulatory mechanism of the TH/TR axis alleviates acute liver injury. The regulatory mechanisms are clarified into three categories, including the effects of protection or exacerbation, treating factors, and changed factors. TH downregulates 8-OHdG, PCO, and AOPP levels. TH can also synergize with MP to improve oxidative stress and liver damage and realize anti-inflammatory and antioxidant effects. T3 scavenges lipid peroxyl free radicals and improves cell. The combined supplementation of T3 and n-3 PUFA was given to rats to decrease IR liver injury and oxidative stress. T3 treatment recovers NF- κ B activity, STAT3, TNF- α , and haptoglobin and increases liver GSH depletion and protein oxidation protection against IR. T3 upregulates the liver redox-sensitive nuclear transcription factor Nrf2 DNA, detoxification, and drug transport proteins expression, especially including protein levels of Eh1, NQO1, GST Ya, GST Yp, MRP-2, MRP-3, and MRP-4. The inactivation of Kupffer cell by GdCl₃ can suppress T3-induced oxidative stress, thus ameliorating the development of liver injury. T3 induces liver PC against IR supported by triggering AMPK, ultimately accelerating the depletion of inflammatory factors such as hepatic NLRP3 and IL-1 β . T3 induces hepatocyte proliferation in toxic liver injury. T3 injection protects liver IR damage by enhancing MEK/ERK/mTORC1 mediated autophagy. TH-induced MAO inhibitors inhibit the activity of MAO protecting against liver injury. The accumulation of TR mRNA may remove negative influences in fluoride-related liver injury *via* preventing disruption of lipid metabolism, oxidative damage, and apoptosis. Hyperthyroidism promotes liver injury. Thionamides, methimazole, and propylthiouracil are associated with drug-induced liver injury. The Yinning Tablet restores the expression of antiapoptotic Bcl-2 cytosol cytochrome c protein overexpression and downregulates the expression of L-thyroxine-induced overexpressed caspase-9, -8, -3, proapoptotic BAX and Dio1, thus ameliorating TH-induced liver injury in rats through regulating mitochondria-mediated apoptotic signals. (The arrows indicate factors are unregulated or downregulated.)

| Effects of protection | Treating factor | Changed factor |
|----------------------------|--------------------------------|---|
| Oxidative stress | T3 + insulin GdCl ₃ | 8-OHdG, PCO, and AOPPs ↓ Inactivation of Kupffer cells |
| Cell ferroptosis | T3 | Lipid peroxyl free radicals ↓ |
| Detoxification | T3 | Nrf2, Eh1, NQO1, GST Ya, and GST Yp MRP-2, -3, -4 ↑ |
| Inflammation | TH + MP | — |
| Autophagy | T3 | MEK/ERK/mTORC1 ↑ |
| Lipid metabolism apoptosis | Yinning Tablet | TR ↑ TR ↑ Bcl-2 and cytochrome c protein ↑ caspase-9, -8, -3, proapoptotic BAX, and Dio1 ↓ |
| DNA and protein damage | T3 + insulin | — |
| IR | TH + nPUFA | NF- κ B, STAT3, THF- α , and haptoglobin ↓ |
| | — | GSH depletion and protein oxidation ↑ |
| | T3 | AMPK ↑ NLRP3 and IL-1 β ↓ |
| Other mechanisms | T3 | MAO ↓ |

TH May Accelerate Alcoholic Liver Disease

Alcoholic liver disease is caused by long-term heavy drinking, initially manifesting as fatty liver, and hepatocyte necrosis, then developing into alcoholic hepatitis, liver fibrosis, cirrhosis, and liver failure (Wang and Mu, 2021). Papineni et al. (2017) indicated that TH-free T3 (fT3) decreases in alcoholic hepatitis and cirrhosis while fT3 and fT4 increase in chronic alcoholic liver disease patients after treatment. More specifically speaking, low fT3 not only probably reflects the severity of liver disease, the degree of liver damage but may also increase the withdrawal effects and craving for alcohol (Nomura et al., 1975; Israel et al., 1979; Burra et al., 1992). However, it has been reported that alcohol and TH also might cause a hypermetabolic state of the liver and liver cell damage. Accordingly, antithyroid drugs can cure alcoholic fatty liver *via* inhibiting ethanol metabolic rate (EMR) in chronic ethanol-consuming patients (Szilagyi et al., 1983). Overall, the TH/TR axis may aggravate alcoholic liver disease.

TH/TR Axis Ameliorates Liver Injury

Liver injury is caused by multiple factors mainly including some drugs, poisons, or chronic liver, and extrahepatic diseases (Yamamoto, 1995). In CCl₄-induced liver injury in rats, the serum T3 level is reduced due to the decreased release of T3 from liver cells rather than a decreased conversion of T4 to T3

(Ikeda et al., 1986). In general, the TH/TR axis protects against liver damage, and thyroid disorder aggravates the development of liver injury. From the protective aspect, T3 replenishment protects against liver injury *via* improving oxidative stress, cell ferroptosis, detoxification, and increasing drug transport proteins expression, inflammatory factors, autophagy, and lipid metabolism. DNA damage generated by reactive oxygen species upregulates 8-hydroxy-2-deoxyguanosine (8-OHdG) levels. During diabetes, hypothyroidism, and hypothyroidism with diabetes, the use of TH downregulates the level of 8-OHdG, protein carbonyl content (PCO), protein oxidation, and advanced oxidation protein products (AOPPs) (Altan et al., 2010). In addition, TH synergizes with methylprednisolone (MP) to improve oxidative stress and liver damage and then realizing anti-inflammatory and antioxidant effects (D'Espessailles et al., 2013). Intriguingly, T3 scavenges lipid peroxyl free radicals and improves cell ferroptosis in the LPS/galactosamine-induced liver injury mouse model (Mishima et al., 2020). Moreover, the combined supplementation of T3 and n-3 polyunsaturated fatty acid (n-3 PUFA) in rat decreases ischemia-reperfusion (IR) liver injury and oxidative stress. From the aggravating aspect, hyperthyroidism promotes liver injury. Otherwise, thionamides, methimazole, and propylthiouracil are associated with drug-induced liver injury (LiverTox, 2012; Yan et al., 2017) (Table 2). In a word, the activation of the TH/TR axis can ameliorate liver injury.

THE REGULATORY MECHANISMS UNDERLYING TH/TR AXIS MAY SUPPLY NOVEL TREATMENT METHODS FOR LIVER DISEASES

The regulatory mechanism of the TH/TR axis in liver diseases has been gradually elucidated. However, the understanding of the regulatory mechanism of the TH/TR axis in liver diseases is not entirely clear, which is still being explored. The study on the regulatory mechanism of the TH/TR axis in hepatic diseases is helpful to reveal the importance in liver diseases.

MAFLD

In MAFLD, the deiodinase family members, especially including types 1, 2, and 3 iodothyronine deiodinases (Dio1, 2, and 3) and responsible for the activation and inactivation of TH, can modulate the TH/TR axis. As hepatic enzymes, Dio1 and Dio2 convert T4 to T3 and increase T3/T4 levels. Conversely, Dio3 inactivates TH. To be specific, the activation of Dio3 activates hypoxia-inducible factor 1 α (HIF-1 α), thus inhibiting T3 signaling and the metabolic rate (Bianco and da Conceição, 2018; Luongo et al., 2019; Russo et al., 2021). Increased Dio1 level promotes β -oxidation of fatty acid and oxidative phosphorylation, then preventing hepatocyte steatosis. Moreover, the level of Dio1 mRNA depends on the dietary conditions. When fed a normal chow diet (NCD), Leprdb mice grows up with severe steatosis with only mild inflammation. The depletion of Dio1 in Leprdb mice upregulates hepatic Tnfa and Co1a1 mRNA levels, which are inflammation and fibrosis biomarkers, respectively (Bruinstroop et al., 2021). Genes related to reverse cholesterol transport and lipase activity decrease with the downregulation of Dio2 in rats (Russo et al., 2021). The sites of *de novo* DNA hypermethylation (H sites) disrupt long-distant chromatin interactions, looping enhancers, and promoters in hepatocytes. TH produced from Dio2 activation depletes H3K9me3 and interferes with the formation of more than a thousand H sites, subsequently maintaining the liver development and function (Fonseca et al., 2021). In general, the TH/TR axis modulated by the deiodinases may delay MAFLD progression. Nevertheless, the regulatory mechanism of the TH/TR axis in MAFLD remains to be further studied (Figure 1).

HCC

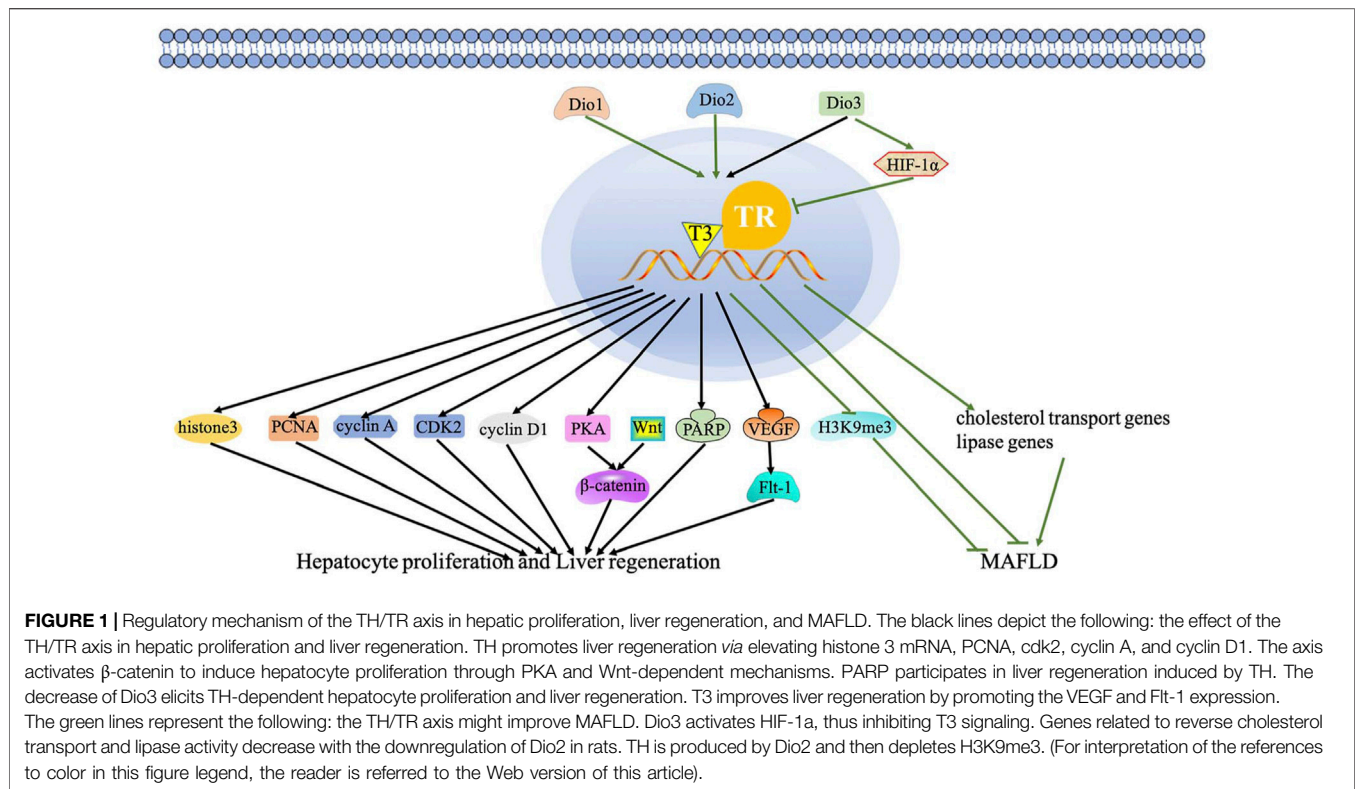
The TH/TR axis modulates cyclin-dependent kinase (CDK) and cyclins, MicroRNAs (miRNAs), long non-coding RNA (lncRNA), TGF- β signaling, hedgehog (Hh) (relying on the local deiodinase expression), and other tumor-related genes and -proteins to be involved in the growth, proliferation, and metastasis of HCC (Manka et al., 2018).

In addition, CDKs and regulatory subunits cyclins regulate the cell cycle in mammalian. P21, as a CDK inhibitor, halts G1/S and G2/M transitions of cell cycle progression by inhibiting CDK4,6/cyclin-D and CDK2/cyclin-E, respectively (Karimian et al., 2016). The inhibition of HCC cells growth and proliferation is dependent upon the activation of P21 by the TH/TR axis. A recent study reported that the activation of the TH/TR axis upregulates endoglin in HCC cells, thus restraining P21 polyubiquitination-induced cell

proliferation (Lin et al., 2013a). In addition, the TH/TR axis inhibits hepatoma cell growth *via* repressing UHRF1 and relieves UHRF1-mediated P21 silence (Wu et al., 2015). Furthermore, TH induces the miR-214-3p expression, followed by interfering with the proto-oncogene serine/threonine-protein kinase (PIM-1) and activating P21, thus blocking cell proliferation (Huang et al., 2017). Other CDKs and cyclins also involve in the regulatory mechanism in HCC in a TH/TR axis-dependent fashion. Ezequiel et al. (Ridruejo et al., 2021) suggested that hexachlorobenzene (HCB) is an endocrine disruptor and a liver tumor promoter. In the HepG2 cell line, the depletion of HCB by TH leads to the downregulation of the TGF- β 1/pSMAD-2/3 signaling pathway, thus increasing Dio1 levels and decreasing p21 and P27, ultimately suppressing cell proliferation. Beyond that, the silence of TGF- β mice promote the proliferation by increasing the expressions of CDK2, cyclin E, and cyclin A, as well as decreasing the expression of CDKn1a/p21 (Baek et al., 2010). It has been reported that depleting forkhead box M1 (FOXO1) by TH interferes with oncogenic expression of cyclin D1, cyclin E, and CDK2, thereby inhibits HCC cells proliferation (Barrera-Hernandez et al., 1999; Wu et al., 2020). These pathways all manifest that the TH/TR axis closely interacts with p21, CDKs, and its regulatory subunits cyclins to affect cell proliferation in HCC.

Moreover, miRNAs, a class of evolutionarily conserved non-protein-coding small RNA, are responsible for regulating gene expression at the translation level (Oura et al., 2020). The TH/TR axis regulates miRNAs, thereby producing various effects in HCC. For example, the downregulation of the TH/TR axis induces nodule regression and the increased expression of targeted microRNA, miR-27a, miR-181a, miR-204a, and miR-181a in the resistance-hepatocyte rat model (R-H model) and human cirrhotic peritumoral tissue (Frau et al., 2015). Beyond that, miR-214-3p, miR-130b, miR-17, miR-21, miR-424, and miR-503 also participate in the regulation of the TH/TR axis-mediated liver cancer (Huang Y. H. et al., 2013; Lin et al., 2013b; Ruiz-Llorente et al., 2014; Lin et al., 2015). Thus, miRNAs have the potential to be targets in TH/TR-involved HCC.

Furthermore, lncRNA, the human major transcriptional genome, is a length greater than 200 nucleotides, which is a non-coding protein (Dang et al., 2015). A recent study has reported that compared to the non-tumor samples, the expression of lncRNA related genes including MSC-AS1, POLR2J4, EIF3J-AS1, SERHL, RMST, and PVT1 are upregulated in tumor samples. Beyond that, lncRNA genes mostly cluster in the TGF- β signaling pathway, internal ribosome entry pathway, granzyme A mediated apoptosis, FAS signaling pathway, calcium signaling by HBx, and p38/MAPK signaling pathway (Gu et al., 2019). It has been reported that lncRNA CRNDE and lncRNA SNHG7 are independent risk factors of synchronous colorectal liver metastasis (SCLM), which also predict a high tumor recurrence rate (Zhang P. et al., 2020). Since lncRNA is associated with the occurrence of tumor, it is plausible that lncRNA may intimately be regulated by the TH/TR axis. Indeed, the TH/TR axis is related to lncRNA in HCC. For instance, brain cytoplasmic RNA 1 (BCYRN1 or BC200) is widely expressed in tumors. BC200 is also inhibited by T3/TR, then downregulating the expressions of CDK2, cyclin E1, and



cyclin E2 and upregulating P21, thereby repressing cell growth and tumor sphere formation and preventing the evolvement of HCC (Lin et al., 2018). Otherwise, the downregulation of taurine upregulated gene 1 (TUG1) by the TH/TR axis also cause AFP mRNA, cyclin E, and H3K27me3 silence and cell growth inhibition (Lin et al., 2020b).

Finally, other TH/TR-related genes and -proteins are involved in HCC. Thyroid hormone receptor-interacting proteins (TRIP), the Zyxin family of LIM proteins, is responsible for regulating transcription of TR. Significantly, the transcriptional activation of the TH/TR axis in HCC may depend on TRIP. Specifically, when TRIP6 activates FOXC1, migration, invasion, and proliferation are strongly promoted. It is also found that TRIP6 induces cyclin D1 expression, decreases p21 and p27 activation, and HCC cell proliferation arrest (Lee et al., 1995; Zhao et al., 2017; Wang et al., 2020). Moreover, the downregulation of TRIP13 impairs the NHEJ repair process, increased apoptosis, and cell cycle arrest at the S-phase, ultimately inhibiting the proliferation, migration, and invasion of HCC cells (Ju et al., 2018). In addition, pituitary tumor transforming gene 1 (PTTG1) is silenced by Sp2, which is negatively mediated by T3/TR in Hep3B hepatoma cells (Chen et al., 2008). Ndr2 is a Myc suppressor gene. The activation of V-erbA leads to the depletion of Ndr2, thus exacerbating tumor invasion and metastasis (Ventura-Holman et al., 2011). As a tumor-associated protein, lipocalin 2 (Lcn2) can activate the Met/FAK pathway in a TH/TR axis-dependent manner, thus enhancing tumor cell migration and invasion (Chung et al., 2015). Intriguingly, T3/TR/MEK/ERK/NUPR1/PDGFA cascade may play a vital role in hepatocarcinogenesis. Consistently, T3/

TR positively regulates nuclear protein 1(NUPR1) *via* binding to the NUPR1 promoter regions, therefore promoting vascular invasion (Chen et al., 2019). Recently, it has been found that increasing thyroid hormone responsive (THRSP) prevents the silence of the ERK/ZEB1 signaling pathway and inhibits the process of epithelial-to-mesenchymal transition, subsequently preventing hepatocellular carcinogenesis (Hu et al., 2021). A secreted protein named Dickkopf 4 (DKK 4) antagonizes the Wnt signal pathway and inhibits tumor metastasis, which is dependent upon the activation of the T3/TR axis (Chi et al., 2013).

In short, the TH/TR axis have paradoxical role in the growth, proliferation, invasion, metastasis, and migration of HCC. A relevant regulatory mechanism of the TH/TR axis in HCC remains to be further explored (Figures 2, 3).

Liver Injury

In liver injury, the studies show that T3 treatment recovers NF- κ B activity, signal transducer, and activator of transcription 3 (STAT3), TNF- α and haptoglobin and increases liver GSH depletion and protein oxidation protecting against IR (Fernández et al., 2007; Mardones et al., 2012). A study exhibited that T3 upregulates the liver redox-sensitive nuclear transcription factor erythroid 2-related factor 2 (Nrf2) DNA, detoxification, and drug transport proteins expression, mainly including protein levels of epoxide hydrolase 1 (Eh1), NADPH-quinone oxidoreductase 1 (NQO1), glutathione-S-transferases Ya (GST Ya), GST Yp, multidrug resistance-associated proteins 2 (MRP-2), mrp-3, and MRP-4 in male Sprague-Dawley rats,

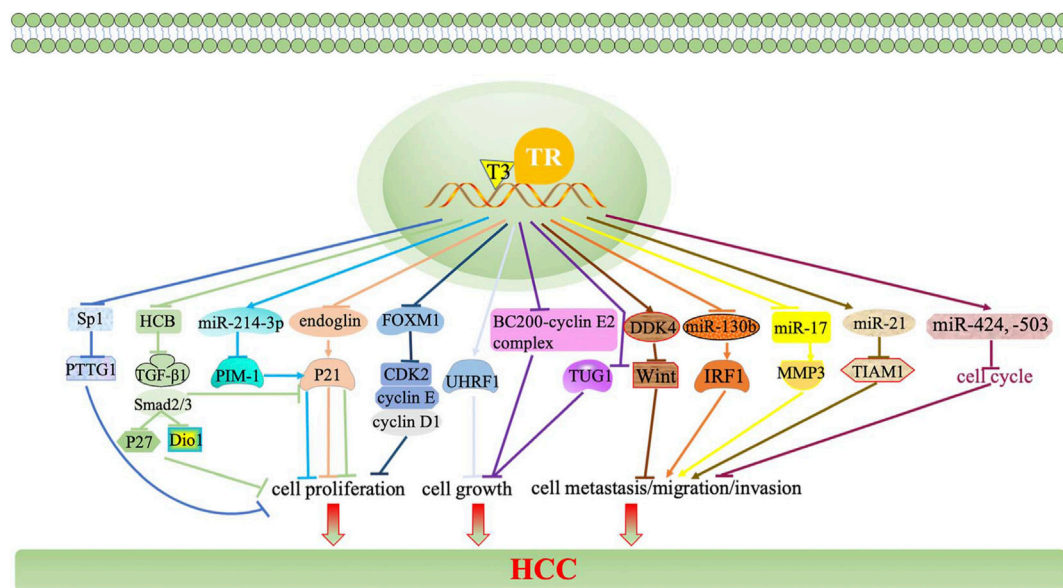


FIGURE 2 | TH/TR axis is involved in HCC growth, proliferation, invasion, and metastasis. The TH/TR axis upregulates endoglin, thus restraining P21 polyubiquitination-induced cell proliferation. The TH/TR axis inhibits hepatoma cell growth *via* repressing UHRF1 and relieves UHRF1-mediated P21 silence. TH induces the miR-214-3p expression, followed by interfering with PIM-1 and activating P21, thus blocking cell proliferation. The depletion of HCB by TH downregulates the TGF- β 1/pSMAD-2/3 signaling pathway, thus increasing Dio1 levels and decreasing p21 and P27, ultimately suppressing cell proliferation. The silence of TGF- β mice promote the proliferation by increasing the expressions of CDK2, cyclin E, and cyclin A, as well as decreasing the expression of CDKn1a/p21. Depleting FOXM1 by TH interferes with cyclin D1, cyclin E, and CDK2, thereby inhibiting HCC cell proliferation.

which may indicate the hepatocyte protective mechanism in liver injury attributed to ROS and chemical toxicity (Cornejo et al., 2013). In addition, the inactivation of Kupffer cell by gadolinium chloride (GdCl₃) can suppress T3-induced oxidative stress, thus ameliorating the development of liver injury characterized by neutrophil infiltration and necrosis (Simon-Giavarotti et al., 2002). Accumulating evidence has demonstrated that T3 induces liver preconditioning (PC) against IR supported by triggering AMP-activated protein kinase (AMPK), ultimately accelerating the depletion of inflammatory factors such as hepatic NLRP3 and IL-1 β (Fernández et al., 2009; Vargas and Videla, 2017). T3 induces hepatocyte proliferation in toxic liver injury (Malik et al., 2006). T3 injection protects liver IR damage by enhancing MEK/ERK/mTORC1-mediated autophagy in male C57BL/6 mice (Yang et al., 2015). In addition, TH-induced monoamine oxidase (MAO) inhibitors inhibit the activity of MAO protecting against liver injury in rats (Obata and Aomine, 2009). In addition to the TH/TR axis also prevents liver damage. It has been discovered that the accumulation of TR mRNA may remove negative influences in fluoride-related liver injury *via* preventing disruption of lipid metabolism, oxidative damage, and apoptosis (Bo et al., 2018). Particularly, traditional Chinese medicine is also involved in improving the TH/TR axis-induced liver injury. To be specific, the Yinning Tablet restores the expression of antiapoptotic Bcl-2 cytosol cytochrome c protein and downregulates the expression of L-thyroxine-induced overexpressed caspase-9, -8, -3, proapoptotic BAX and Dio1, thus ameliorating TH-induced liver injury in rats

via regulating mitochondria-mediated apoptotic signals (Yang et al., 2020).

Other Liver Diseases

The TH/TR axis may be correlated with hepatitis. Some studies have demonstrated that ubiquitin-specific protease 18 (USP18), known as UBP43, participates in gene regulations of the TH signaling pathway. Li et al, (2017) discovered that USP18 regulates the signaling of antivirus by the TH signaling pathway, prolactin signaling pathway, insulin resistance and complement, and have crosstalk among them. Also, the thyroid hormone-uncoupling protein (TRUP) gene and thyroid hormone receptor-associated protein 150 alpha gene are associated to the integration of HBV DNA into liver cell DNA, which are the key regulators of cell proliferation and viability (Gozuacik et al., 2001; Paterlini-Br  chot et al., 2003). In recent years, the relationship between the TH/TR axis and hepatitis of HBV and HCV infection has been gradually elucidated. However, understanding of the antiviral mechanism of the TH/TR axis is not entirely clear, which is still being explored.

Furthermore, the TH/TR axis is associated with alcohol-related hepatic alterations. For example, TH has been proven to increase the level of Dio2, thereby elevating susceptibility to hepatic steatosis in a model of alcoholism (Fonseca et al., 2019; Hernandez, 2019). In addition, the mRNA level of TRIP12 is significantly different in alcohol-feed (AF) and control pair-feed (PF) mice (Zhang et al., 2018) (**Figure 4**).

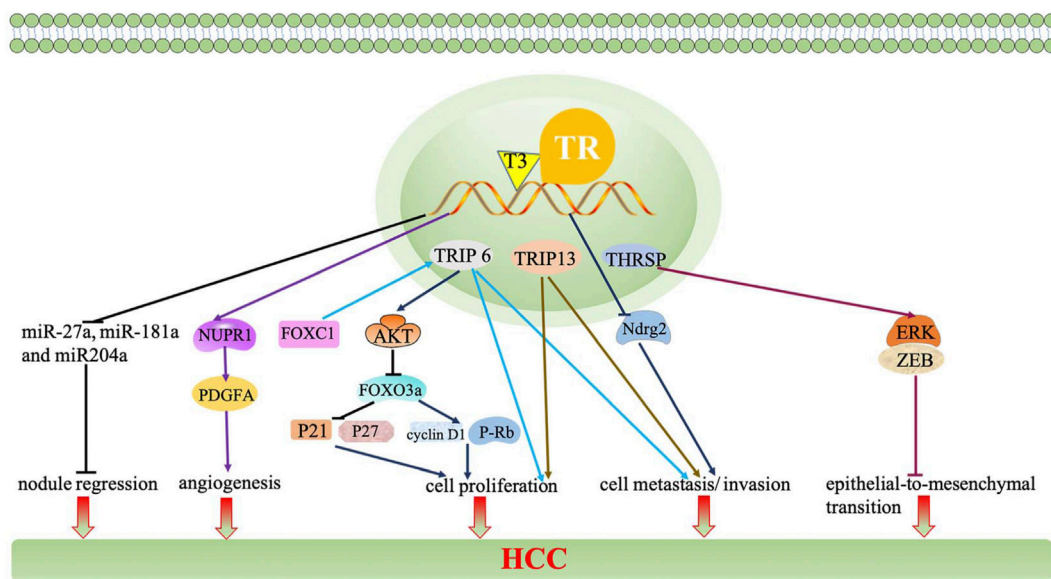


FIGURE 3 | The TH/TR axis inhibits nodule regression and decreases the expressions of miR-27a, miR-181a, and miR-204a. BC200 is inhibited by T3/TR and downregulates the expressions of CDK2, cyclin E1, and cyclin E2 and upregulates P21, thereby repressing cell growth. The downregulation of TUG1 by the TH/TR axis causes AFP mRNA, cyclin E, and H3K27me3 silence and cell growth inhibition. When TRIP is activated by FOXC1, migration, invasion, and proliferation are strongly promoted. TRIP6 induces the AKT signaling pathway, thereby preventing FOXO3a overexpression-induced cyclin D1 interference, p21 and p27 activation, and HCC cell proliferation arrest. The downregulation of PTTG1 is silenced by Sp2, which is negatively mediated by T3/TR. The activation of V-erbA leads to the depletion of Ndr2, thus exacerbating tumor invasion and metastasis. Lcn2 can activate the Met/FAK pathway in a TH/TR axis-dependent manner, thus enhancing cell migration and invasion. T3/TR/MEK/ERK/NUPR1/PDGFA cascade may play a vital role in hepatocarcinogenesis. T3/TR upregulates NUPR1 via binding to the NUPR1 promoter regions, therefore promoting vascular invasion. THRSP prevents silence of the ERK/ZEB1 signaling pathway and inhibits the process of epithelial-to-mesenchymal transition. DKK 4 antagonizes the Wnt signal pathway and inhibits tumor metastasis, which depends upon the activation of the T3/TR axis.

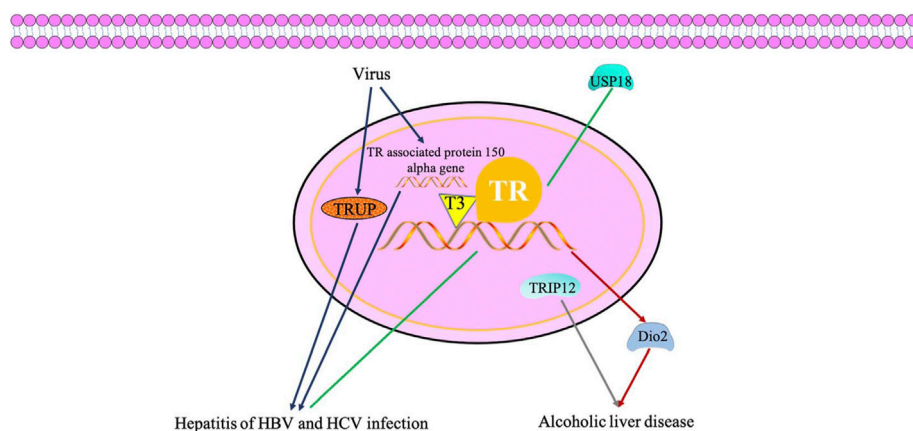


FIGURE 4 | TH/TR axis may be involved in hepatitis of hepatitis B virus and hepatitis C virus infection and accelerates alcoholic liver disease. USP18 regulates the signaling of antiviral by the thyroid hormone signaling pathway. TRUP gene and thyroid hormone receptor associated protein 150 alpha gene are associated to the integration of HBV DNA into the liver cell DNA, which are key regulators of cell proliferation and viability. TH has been proven to increase the level of Dio2, thereby elevating susceptibility to hepatic steatosis in a model of alcoholism. The mRNA level of TRIP12 is significantly different in alcohol liver disease.

CONCLUSION

Here, we amply reviewed the function of the TH/TR axis in hepatic diseases. The TH/TR axis may protect against metabolic-associated fatty liver disease, hepatitis B virus and

hepatitis C virus infection, liver fibrosis, and drug-induced and extrahepatic liver injury but may accelerate the development of acute liver failure and alcoholic liver disease. Meanwhile, the axis has a dual role in hepatocellular carcinoma. As a result, targeting the TH/TR axis should be considered for treating

liver disease, which may be a promising disease-reversing strategy for patients.

PROSPECTIONS

The total T3 in different stages of inflammation exhibits a trend of first increasing and then decreasing (Hu et al., 2020). Although there is no statistical significance of the total T3 decreases, it is still trustworthy, owing to the fact that the initial stage of TH also occurs booming in acute liver failure. Subsequently, the later declination may be due to the adjustment and balance of the body in different periods. In this retrospective study, the patient's aggravation is not serious, and the samples are not large enough ($n = 6$), thus leading to an insignificant decrease.

TH protects liver cells from damage by mediating the HBV/HCV infectious signaling pathway and then improves hepatitis-related carcinogenic transformation. TSH and TT3 are promising aspects to be included in the evaluation criteria for inflammatory activities and served as biological markers to reduce the proportion of liver biopsy and the medical burden. Moreover, the treatment of interferon is not strongly related to autoimmune diseases except for thyroid. However, virus infection and antiviral endeavors lead to format a certain proportion of thyroid autoantibodies and related thyroid diseases such as hypothyroidism, and this cannot be ignored.

To date, it is reported that the mutation of the TR β gene in thyroid hormone resistance patients leads to the impairment of TR β signals in the hepatic steatosis. The mutation type of the TR β gene is the substitution of glycine by arginine at position 243 (R243Q) of TR β . Compared with patients with WT relatives, serum T3 and T4 of RTH β patients are higher than the upper limit of a reference range. However, there is no significant difference in TSH. They also found that the liver fat content, serum free fatty acids, and HDL cholesterol were higher (Chaves et al., 2021). At present, the fragments related to lipid metabolism are all located in the hinge region of TR. In the future, gene mutations may be used to discover the region that regulates TR lipid metabolism in the hinge region, as well as other regions and their functions, and this pathway exactly can become the therapy targets of NASH/NAFLD and HCC.

Post-translational modifications participate in the occurrence and development of liver disease. Both TR α and TR β are

regulated by the level of PTM, including SUMOylation (Liu and Brent, 2018). The small ubiquitin-like modifier (SUMO) family, existing widely in eukaryotes, is a highly conserved post-translational modification protein that regulate lipid metabolism, inflammatory response, bile acid homeostasis, autophagy, and other related biological functions in nuclear receptors (Zeng et al., 2020; Liu et al., 2021). The research team found that the sumo-3 protein (mainly expressed in the nucleus) and TR receptor have significantly upregulated in oleic acid (OA)-induced NAFLD in WRL68 cells and human liver tissue models (published in Chinese journals). TR can be SUMOylated (Anyetei-Anum et al., 2019). At the same time, nuclear autophagy can improve metabolic disorders (Fu et al., 2018). TR SUMOylation may associate with nuclear autophagy to improve metabolic disorders and prospectively become a therapeutic target in NAFLD.

In summary, the TH/TR axis provides effective insights into the treatment of hepatic diseases. The research and application prospects for the TH/TR axis in liver diseases are promising. TH/TR may provide new potential therapeutic targets

AUTHOR CONTRIBUTIONS

QT wrote the manuscript, and MZ searched for references. NF and LC were responsible for revising the manuscript.

FUNDING

This work was jointly supported by the National Natural Science Foundation of China (81973326), the Hunan Provincial Natural Science Foundation (2019JJ40255; 2021JJ30628), the Innovative Province Construction Special Project of Hunan Province (2021SK4031), the Clinical Medical Technology Innovation Guidance Project of Hunan Province (2020SK51904), the Postgraduate Scientific Research Innovation Project of Hunan Province (CX20210979), the Scientific Research Fund Project of Hunan Provincial Health Commission (20201901), the Scientific Research Project of University of South China [Documents of the University of South China (2019)02], and the Guiding Planning Project of Hengyang [Documents of the Hengyang science and Technology Bureau (2021)51-129].

REFERENCES

- Abu Rmilah, A. A., Zhou, W., and Nyberg, S. L. (2020). Hormonal Contribution to Liver Regeneration. *Mayo Clin. Proc. Innov. Qual. Outcomes* 4 (3), 315–338. doi:10.1016/j.mayocpiqo.2020.02.001
- Ajdukovic, M., Vucic, T., and Cvijanovic, M. (2021). Effects of Thiourea on the Skull of Triturus Newts during Ontogeny. *PeerJ* 9, e11535. doi:10.7717/peerj.11535
- Altan, N., Sepici-Dinçel, A., Sahin, D., Kocamanoglu, N., Kosova, F., and Engin, A. (2010). Oxidative DNA Damage: the Thyroid Hormone-Mediated Effects of Insulin on Liver Tissue. *Endocrine* 38 (2), 214–220. doi:10.1007/s12020-010-9376-7
- Alvarado, T. F., Puliga, E., Preziosi, M., Poddar, M., Singh, S., Columbano, A., et al. (2016). Thyroid Hormone Receptor β Agonist Induces β -Catenin-Dependent Hepatocyte Proliferation in Mice: Implications in Hepatic Regeneration. *Gene Expr.* 17 (1), 19–34. doi:10.3727/105221616x691631
- Anastasiou, O., Sydor, S., Sowa, J. P., Manka, P., Katsounas, A., Syn, W. K., et al. (2015). Higher Thyroid-Stimulating Hormone, Triiodothyronine and Thyroxine Values Are Associated with Better Outcome in Acute Liver Failure. *PLoS One* 10 (7), e0132189. doi:10.1371/journal.pone.0132189
- Anyetei-Anum, C. S., Evans, R. M., Back, A. M., Roggero, V. R., and Allison, L. A. (2019). Acetylation Modulates Thyroid Hormone Receptor Intracellular

- Localization and Intranuclear Mobility. *Mol. Cel Endocrinol* 495, 110509. doi:10.1016/j.mce.2019.110509
- Anyetel-Anum, C. S., Roggero, V. R., and Allison, L. A. (2018). Thyroid Hormone Receptor Localization in Target Tissues. *J. Endocrinol.* 237 (1), R19–R34. doi:10.1530/JOE-17-0708
- Baek, J. Y., Morris, S. M., Campbell, J., Fausto, N., Yeh, M. M., and Grady, W. M. (2010). TGF-beta Inactivation and TGF-Alpha Overexpression Cooperate in an *In Vivo* Mouse Model to Induce Hepatocellular Carcinoma that Recapitulates Molecular Features of Human Liver Cancer. *Int. J. Cancer* 127 (5), 1060–1071. doi:10.1002/ijc.25127
- Bargi-Souza, P., Goulart-Silva, F., and Nunes, M. T. (2017). Novel Aspects of T3 Actions on GH and TSH Synthesis and Secretion: Physiological Implications. *J. Mol. Endocrinol.* 59 (4), R167–R178. doi:10.1530/JME-17-0068
- Barrera-Hernandez, G., Park, K. S., Dace, A., Zhan, Q., and Cheng, S. Y. (1999). Thyroid Hormone-Induced Cell Proliferation in GC Cells Is Mediated by Changes in G1 Cyclin/cyclin-dependent Kinase Levels and Activity. *Endocrinology* 140 (11), 5267–5274. doi:10.1210/endo.140.11.7145
- Bianco, A. C., and da Conceição, R. R. (2018). The Deiodinase Trio and Thyroid Hormone Signaling. *Methods Mol. Biol.* 1801, 67–83. doi:10.1007/978-1-4939-7902-8_8
- Bicicusa, V., Popescu, M., Petrescu, I. O., Stan, I. S., Durand, P., Petrescu, M., et al. (2020). Hepatic Pathological Features in Naive Patients with Chronic Hepatitis C Who Have Developed Thyroid Disorder. *Rom. J. Morphol. Embryol.* 61 (4), 1085–1097. doi:10.47162/RJME.61.4.11
- Bo, X., Mu, D., Wu, M., Xiao, H., and Wang, H. (2018). The Morphological Changes and Molecular Biomarker Responses in the Liver of Fluoride-Exposed *Bufo gargarizans* Larvae. *Ecotoxicol Environ. Saf.* 151, 199–205. doi:10.1016/j.ecoenv.2018.01.027
- Bockhorn, M., Frilling, A., Benko, T., Best, J., Sheu, S. Y., Trippler, M., et al. (2007). Tri-iodothyronine as a Stimulator of Liver Regeneration after Partial and Subtotal Hepatectomy. *Eur. Surg. Res.* 39 (1), 58–63. doi:10.1159/000098443
- Brent, G. A. (2012). Mechanisms of Thyroid Hormone Action. *J. Clin. Invest.* 122 (9), 3035–3043. doi:10.1172/JCI60047
- Bruck, R., Oren, R., Shirin, H., Aeed, H., Papa, M., Matas, Z., et al. (1998). Hypothyroidism Minimizes Liver Damage and Improves Survival in Rats with Thioacetamide Induced Fulminant Hepatic Failure. *Hepatology* 27 (4), 1013–1020. doi:10.1002/hep.510270417
- Bruinstroop, E., Zhou, J., Tripathi, M., Yau, W. W., Boelen, A., Singh, B. K., et al. (2021). Early Induction of Hepatic Deiodinase Type 1 Inhibits Hepatosteatosis during NAFLD Progression. *Mol. Metab.* 53, 101266. doi:10.1016/j.molmet.2021.101266
- Burra, P., Franklin, J. A., Ramsden, D. B., Elias, E., and Sheppard, M. C. (1992). Severity of Alcoholic Liver Disease and Markers of Thyroid and Steroid Status. *Postgrad. Med. J.* 68 (804), 804–810. doi:10.1136/pgmj.68.804.804
- Cesarone, C. F., Scarabelli, L., Demori, I., Balocco, S., and Fugassa, E. (2000). Poly(ADP-ribose) Polymerase Is Affected Early by Thyroid State during Liver Regeneration in Rats. *Am. J. Physiol. Gastrointest. Liver Physiol.* 279 (6), G1219–G1225. doi:10.1152/ajpgi.2000.279.6.G1219
- Chao, G., and Chen, L. (2021). Study on the Independent Effect of Thyroid Hormone Based on Uric Acid Level on NAFLD. *J. Health Popul. Nutr.* 40 (1), 21. doi:10.1186/s41043-021-00247-w
- Chaves, C., Bruinstroop, E., Refetoff, S., Yen, P. M., and Anselmo, J. (2021). Increased Hepatic Fat Content in Patients with Resistance to Thyroid Hormone Beta. *Thyroid* 31 (7), 1127–1134. doi:10.1089/thy.2020.0651
- Chen, C. Y., Wu, S. M., Lin, Y. H., Chi, H. C., Lin, S. L., Yeh, C. T., et al. (2019). Induction of Nuclear Protein-1 by Thyroid Hormone Enhances Platelet-Derived Growth Factor A Mediated Angiogenesis in Liver Cancer. *Theranostics* 9 (8), 2361–2379. doi:10.7150/thno.29628
- Chen, R. N., Huang, Y. H., Yeh, C. T., Liao, C. H., and Lin, K. H. (2008). Thyroid Hormone Receptors Suppress Pituitary Tumor Transforming Gene 1 Activity in Hepatoma. *Cancer Res.* 68 (6), 1697–1706. doi:10.1158/0008-5472.CAN-07-5492
- Cheng, S. Y. (2005). Thyroid Hormone Receptor Mutations and Disease: beyond Thyroid Hormone Resistance. *Trends Endocrinol. Metab.* 16 (4), 176–182. doi:10.1016/j.tem.2005.03.008
- Chi, H. C., Chen, S. L., Lin, S. L., Tsai, C. Y., Chuang, W. Y., Lin, Y. H., et al. (2017). Thyroid Hormone Protects Hepatocytes from HBx-Induced Carcinogenesis by Enhancing Mitochondrial Turnover. *Oncogene* 36 (37), 5274–5284. doi:10.1038/onc.2017.136
- Chi, H. C., Liao, C. H., Huang, Y. H., Wu, S. M., Tsai, C. Y., Liao, C. J., et al. (2013). Thyroid Hormone Receptor Inhibits Hepatoma Cell Migration through Transcriptional Activation of Dickkopf 4. *Biochem. Biophys. Res. Commun.* 439 (1), 60–65. doi:10.1016/j.bbrc.2013.08.028
- Chi, H. C., Tsai, C. Y., Tsai, M. M., Yeh, C. T., and Lin, K. H. (2019). Molecular Functions and Clinical Impact of Thyroid Hormone-Triggered Autophagy in Liver-Related Diseases. *J. Biomed. Sci.* 26 (1), 24. doi:10.1186/s12929-019-0517-x
- Chung, I. H., Chen, C. Y., Lin, Y. H., Chi, H. C., Huang, Y. H., Tai, P. J., et al. (2015). Thyroid Hormone-Mediated Regulation of Lipocalin 2 through the Met/FAK Pathway in Liver Cancer. *Oncotarget* 6 (17), 15050–15064. doi:10.18632/oncotarget.3670
- Ciana, P., Braliou, G. G., Demay, F. G., von Lindern, M., Baretino, D., Beug, H., et al. (1998). Leukemic Transformation by the V-ErbA Oncoprotein Entails Constitutive Binding to and Repression of an Erythroid Enhancer *In Vivo*. *EMBO J.* 17 (24), 7382–7394. doi:10.1093/emboj/17.24.7382
- Columbano, A., Simbula, M., Pibiri, M., Perra, A., Deidda, M., Locker, J., et al. (2008). Triiodothyronine Stimulates Hepatocyte Proliferation in Two Models of Impaired Liver Regeneration. *Cell Prolif* 41 (3), 521–531. doi:10.1111/j.1365-2184.2008.00532.x
- Cornejo, P., Vargas, R., and Videla, L. A. (2013). Nrf2-regulated Phase-II Detoxification Enzymes and Phase-III Transporters Are Induced by Thyroid Hormone in Rat Liver. *Biofactors* 39 (5), 514–521. doi:10.1002/biof.1094
- D'Ambrosio, R., Campi, I., Maggioni, M., Perbellini, R., Giammona, E., Stucchi, R., et al. (2021). The Relationship between Liver Histology and Thyroid Function Tests in Patients with Non-alcoholic Fatty Liver Disease (NAFLD). *PLoS One* 16 (4), e0249614. doi:10.1371/journal.pone.0249614
- D'Espeisses, A., Dossi, C., Intriago, G., Leiva, P., and Romanque, P. (2013). Hormonal Pretreatment Preserves Liver Regenerative Capacity and Minimizes Inflammation after Partial Hepatectomy. *Ann. Hepatol.* 12 (6), 881–891. doi:10.1016/s1665-2681(19)31293-1
- Dang, Y., Wang, Y., Ouyang, X., Wang, L., and Huang, Q. (2015). High Expression of lncRNA-PCNA-AS1 in Human Gastric Cancer and its Clinical Significances. *Clin. Lab.* 61 (11), 1679–1685. doi:10.7754/clin.lab.2015.150312
- Dawson, P. A., and Parini, P. (2018). Hepatic Thyroid Hormone Receptor β 1 Agonism: Good for Lipids, Good for Bile? *J. Lipid Res.* 59 (9), 1551–1553. doi:10.1194/jlr.C088955
- Deng, J., Guo, Y., Zhang, G., Zhang, L., Kem, D., Yu, X., et al. (2021). M2 Muscarinic Autoantibodies and Thyroid Hormone Promote Susceptibility to Atrial Fibrillation and Sinus Tachycardia in an Autoimmune Rabbit Model. *Exp. Physiol.* 106 (4), 882–890. doi:10.1113/EP089284
- Du, J., Chai, S., Zhao, X., Sun, J., Zhang, X., and Huo, L. (2021). Association between Thyroid Hormone Levels and Advanced Liver Fibrosis in Patients with Type 2 Diabetes Mellitus and Non-alcoholic Fatty Liver Disease. *Diabetes Metab. Syndr. Obes.* 14, 2399–2406. doi:10.2147/DMSO.S313503
- Erhardttsen, E., Rasmussen, D. G. K., Frederiksen, P., Leeming, D. J., Shevell, D., Gluud, L. L., et al. (2021). Determining a Healthy Reference Range and Factors Potentially Influencing PRO-C3 - A Biomarker of Liver Fibrosis. *JHEP Rep.* 3 (4), 100317. doi:10.1016/j.jhepr.2021.100317
- Erion, M. D., Cable, E. E., Ito, B. R., Jiang, H., Fujitaki, J. M., Finn, P. D., et al. (2007). Targeting Thyroid Hormone Receptor-Beta Agonists to the Liver Reduces Cholesterol and Triglycerides and Improves the Therapeutic index. *Proc. Natl. Acad. Sci. U S A.* 104 (39), 15490–15495. doi:10.1073/pnas.0702759104
- Fanti, M., Singh, S., Ledda-Columbano, G. M., Columbano, A., and Monga, S. P. (2014). Tri-iodothyronine Induces Hepatocyte Proliferation by Protein Kinase A-dependent β -catenin Activation in Rodents. *Hepatology* 59 (6), 2309–2320. doi:10.1002/hep.26775
- Feng, X., and Shi, X. F. (2018). Research Progress in Prognostic Factors of Hepatitis B Virus-Associated End-Stage Liver Disease. *Zhonghua Gan Zang Bing Za Zhi* 26 (8), 626–629. doi:10.3760/cma.j.issn.1007-3418.2018.08.014
- Fernández, V., Castillo, I., Tapia, G., Romanque, P., Uribe-Echevarría, S., Uribe, M., et al. (2007). Thyroid Hormone Preconditioning: protection against Ischemia-Reperfusion Liver Injury in the Rat. *Hepatology* 45 (1), 170–177. doi:10.1002/hep.21476

- Fernández, V., Tapia, G., Varela, P., Cornejo, P., and Videla, L. A. (2009). Upregulation of Liver Inducible Nitric Oxide Synthase Following Thyroid Hormone Preconditioning: Suppression by N-Acetylcysteine. *Biol. Res.* 42 (4), 487–495. doi:10.4067/S0716-97602009000400010
- Ferrara, S. J., Bourdette, D., and Scanlan, T. S. (2018). Hypothalamic-Pituitary-Thyroid Axis Perturbations in Male Mice by CNS-Penetrating Thyromimetics. *Endocrinology* 159 (7), 2733–2740. doi:10.1210/en.2018-00065
- Fonseca, T. L., Fernandes, G. W., Bocco, B. M. L. C., Keshavarzian, A., Jakate, S., Donohue, T. M., et al. (2019). Hepatic Inactivation of the Type 2 Deiodinase Confers Resistance to Alcoholic Liver Steatosis. *Alcohol. Clin. Exp. Res.* 43 (7), 1376–1383. doi:10.1111/acer.14027
- Fonseca, T. L., Garcia, T., Fernandes, G. W., Nair, T. M., and Bianco, A. C. (2021). Neonatal Thyroxine Activation Modifies Epigenetic Programming of the Liver. *Nat. Commun.* 12 (1), 4446. doi:10.1038/s41467-021-24748-8
- Frau, C., Loi, R., Petrelli, A., Perra, A., Menegon, S., Kowalik, M. A., et al. (2015). Local Hypothyroidism Favors the Progression of Preneoplastic Lesions to Hepatocellular Carcinoma in Rats. *Hepatology* 61 (1), 249–259. doi:10.1002/hep.27399
- Fu, N., Yang, X., and Chen, L. (2018). Nucleophagy Plays a Major Role in Human Diseases. *Curr. Drug Targets* 19 (15), 1767–1773. doi:10.2174/1389450119666180518112350
- Gautherot, J., Claudel, T., Cuperus, F., Fuchs, C. D., Falguières, T., and Trauner, M. (2018). Thyroid Hormone Receptor β 1 Stimulates ABCB4 to Increase Biliary Phosphatidylcholine Excretion in Mice. *J. Lipid Res.* 59 (9), 1610–1619. doi:10.1194/jlr.M084145
- Gor, R., Siddiqui, N. A., Wijeratne Fernando, R., Sreekantan Nair, A., Illango, J., Malik, M., et al. (2021). Unraveling the Role of Hypothyroidism in Non-alcoholic Fatty Liver Disease Pathogenesis: Correlations, Conflicts, and the Current Stand. *Cureus* 13 (5), e14858. doi:10.7759/cureus.14858
- Gozcaci, D., Murakami, Y., Saigo, K., Chami, M., Mugnier, C., Lagorce, D., et al. (2001). Identification of Human Cancer-Related Genes by Naturally Occurring Hepatitis B Virus DNA Tagging. *Oncogene* 20 (43), 6233–6240. doi:10.1038/sj.onc.1204835
- Grover, G. J., Mellström, K., and Malm, J. (2007). Therapeutic Potential for Thyroid Hormone Receptor-Beta Selective Agonists for Treating Obesity, Hyperlipidemia and Diabetes. *Curr. Vasc. Pharmacol.* 5 (2), 141–154. doi:10.2174/157016107780368271
- Gu, J. X., Zhang, X., Miao, R. C., Xiang, X. H., Fu, Y. N., Zhang, J. Y., et al. (2019). Six-long Non-coding RNA Signature Predicts Recurrence-free Survival in Hepatocellular Carcinoma. *World J. Gastroenterol.* 25 (2), 220–232. doi:10.3748/wjg.v25.i2.220
- Gu, Y., Wu, X., Zhang, Q., Liu, L., Meng, G., Wu, H., et al. (2021). High-normal Thyroid Function Predicts Incident Non-alcoholic Fatty Liver Disease Among Middle-Aged and Elderly Euthyroid Subjects. *J. Gerontol. A. Biol. Sci. Med. Sci.* 77 (1), 197–203. doi:10.1093/gerona/glab037
- Harrison, S. A., Bashir, M., Moussa, S. E., McCarty, K., Pablo Frias, J., Taub, R., et al. (2021). Effects of Resmetirom on Noninvasive Endpoints in a 36-Week Phase 2 Active Treatment Extension Study in Patients with NASH. *Hepatol. Commun.* 5 (4), 573–588. doi:10.1002/hep4.1657
- Hernandez, A. (2019). Thyroid Hormone and Alcoholic Fatty Liver: The Developmental Input. *Alcohol. Clin. Exp. Res.* 43 (9), 1834–1837. doi:10.1111/acer.14145
- Hirose-Kumagai, A., Oda-Tamai, S., and Akamatsu, N. (1995). The Interaction between Nucleoproteins and Thyroid Response Element (TRE) during Regenerating Rat Liver. *Biochem. Mol. Biol. Int.* 35 (4), 881–888.
- Hossain, M. G., Akter, S., Ohsaki, E., and Ueda, K. (2020). Impact of the Interaction of Hepatitis B Virus with Mitochondria and Associated Proteins. *Viruses* 12 (2), 175. doi:10.3390/v12020175
- Hu, J., Wang, Y., Jiang, G., Zheng, J., Chen, T., Chen, Z., et al. (2020). Predictors of Inflammatory Activity in Treatment-Naïve Hepatitis B E-Antigen-Negative Patients with Chronic Hepatitis B Infection. *J. Int. Med. Res.* 48 (11), 300060520969582. doi:10.1177/0300060520969582
- Hu, Q., Ma, X., Li, C., Zhou, C., Chen, J., and Gu, X. (2021). Downregulation of THRSP Promotes Hepatocellular Carcinoma Progression by Triggering ZEB1 Transcription in an ERK-dependent Manner. *J. Cancer* 12 (14), 4247–4256. doi:10.7150/jca.51657
- Huang, M. J., Tsai, S. L., Huang, B. Y., Sheen, I. S., Yeh, C. T., and Liaw, Y. F. (1999). Prevalence and Significance of Thyroid Autoantibodies in Patients with Chronic Hepatitis C Virus Infection: a Prospective Controlled Study. *Clin. Endocrinol. (Oxf)* 50 (4), 503–509. doi:10.1046/j.1365-2265.1999.00686.x
- Huang, P. S., Lin, Y. H., Chi, H. C., Chen, P. Y., Huang, Y. H., Yeh, C. T., et al. (2017). Thyroid Hormone Inhibits Growth of Hepatoma Cells through Induction of miR-214. *Sci. Rep.* 7 (1), 14868. doi:10.1038/s41598-017-14864-1
- Huang, Y. H., Lin, Y. H., Chi, H. C., Liao, C. H., Liao, C. J., Wu, S. M., et al. (2013). Thyroid Hormone Regulation of miR-21 Enhances Migration and Invasion of Hepatoma. *Cancer Res.* 73 (8), 2505–2517. doi:10.1158/0008-5472.CAN-12-2218
- Huang, Y. Y., Gusdon, A. M., and Qu, S. (2013). Cross-talk between the Thyroid and Liver: a New Target for Nonalcoholic Fatty Liver Disease Treatment. *World J. Gastroenterol.* 19 (45), 8238–8246. doi:10.3748/wjg.v19.i45.8238
- Ignatova, T. M., Aprosina, Z. G., Serov, V. V., Mukhin, N. A., Krel', P. E., Semenkov, E. N., et al. (1998). Extrahepatic Manifestations of Chronic Hepatitis C. *Ter Arkh* 70 (11), 9–16.
- Ikeda, T., Ito, Y., Murakami, I., Mokuda, O., Tominaga, M., and Mashiba, H. (1986). Conversion of T4 to T3 in Perfused Liver of Rats with Carbontetrachloride-Induced Liver Injury. *Acta Endocrinol. (Copenh)* 112 (1), 89–92. doi:10.1530/acta.0.1120089
- Ishii, S., Amano, I., and Koibuchi, N. (2021). The Role of Thyroid Hormone in the Regulation of Cerebellar Development. *Endocrinol. Metab. (Seoul)* 36 (4), 703–716. doi:10.3803/EnM.2021.1150
- Israel, Y., Walfish, P. G., Orrego, H., Blake, J., and Kalant, H. (1979). Thyroid Hormones in Alcoholic Liver Disease. Effect of Treatment with 6-N-Propylthiouracil. *Gastroenterology* 76 (1), 116–122. doi:10.1016/s0016-5085(79)80137-7
- Jazdzewski, K., Boguslawska, J., Jendrzewski, J., Liyanarachchi, S., Pachucki, J., Wardyn, K. A., et al. (2011). Thyroid Hormone Receptor Beta (THRB) Is a Major Target Gene for microRNAs Deregulated in Papillary Thyroid Carcinoma (PTC). *J. Clin. Endocrinol. Metab.* 96 (3), E546–E553. doi:10.1210/jc.2010.1594
- Jerzak, K. J., Cockburn, J., Pond, G. R., Pritchard, K. I., Narod, S. A., Dhesy-Thind, S. K., et al. (2015). Thyroid Hormone Receptor α in Breast Cancer: Prognostic and Therapeutic Implications. *Breast Cancer Res. Treat.* 149 (1), 293–301. doi:10.1007/s10549-014-3235-9
- Ji, S., Jin, C., Höxtermann, S., Fuchs, W., Xie, T., Lu, X., et al. (2016). Prevalence and Influencing Factors of Thyroid Dysfunction in HIV-Infected Patients. *Biomed. Res. Int.* 2016, 3874257. doi:10.1155/2016/3874257
- Jing, W., Liu, J., and Liu, M. (2020). Eliminating Mother-To-Child Transmission of HBV: Progress and Challenges in China. *Front. Med.* 14 (1), 21–29. doi:10.1007/s11684-020-0744-2
- Ju, L., Li, X., Shao, J., Lu, R., Wang, Y., and Bian, Z. (2018). Upregulation of Thyroid Hormone Receptor Interactor 13 Is Associated with Human Hepatocellular Carcinoma. *Oncol. Rep.* 40 (6), 3794–3802. doi:10.3892/or.2018.6767
- Kagawa, T., Kozai, M., Masuda, M., Harada, N., Nakahashi, O., Tajiri, M., et al. (2018). Sterol Regulatory Element Binding Protein 1 Trans-activates 25-hydroxy Vitamin D3 24-hydroxylase Gene Expression in Renal Proximal Tubular Cells. *Biochem. Biophys. Res. Commun.* 500 (2), 275–282. doi:10.1016/j.bbrc.2018.04.058
- Kannt, A., Wohlfart, P., Madsen, A. N., Veidal, S. S., Feigh, M., and Schmoll, D. (2021). Activation of Thyroid Hormone Receptor- β Improved Disease Activity and Metabolism Independent of Body Weight in a Mouse Model of Non-alcoholic Steatohepatitis and Fibrosis. *Br. J. Pharmacol.* 178 (12), 2412–2423. doi:10.1111/bph.15427
- Kansu, A., Kuloğlu, Z., Demirçeken, F., and Girgin, N. (2004). Autoantibodies in Children with Chronic Hepatitis B Infection and the Influence of Interferon Alpha. *Turk J. Gastroenterol.* 15 (4), 213–218. https://pm.yuntsg.com/details.html?pmid=16249973&key=16249973
- Karimian, A., Ahmadi, Y., and Yousefi, B. (2016). Multiple Functions of P21 in Cell Cycle, Apoptosis and Transcriptional Regulation after DNA Damage. *DNA Repair (Amst)* 42, 63–71. doi:10.1016/j.dnarep.2016.04.008
- Karwowska, K., Wernik, J., and Abdulgater, A. (2018). New Possibilities for the Newborn's protection against Vertical HBV Transmission - a Case Report. *Pol. Merkuri Lekarski* 45 (269), 192–194. https://pm.yuntsg.com/details.html?pmid=30531668&key=30531668
- Kelly, M. J., Pietranico-Cole, S., Larigan, J. D., Haynes, N. E., Reynolds, C. H., Scott, N., et al. (2014). Discovery of 2-[3,5-Dichloro-4-(5-Isopropyl-6-Oxo-1,6-

- Dihydropyridazin-3-Yloxyphenyl]-3,5-Dioxo-2,3,4,5-Tetrahydro[1,2,4] triazine-6-Carbonitrile (MGL-3196), a Highly Selective Thyroid Hormone Receptor β Agonist in Clinical Trials for the Treatment of Dyslipidemia. *J. Med. Chem.* 57 (10), 3912–3923. doi:10.1021/jm4019299
- Kester, M. H., Toussaint, M. J., Punt, C. A., Matondo, R., Aarnio, A. M., Darras, V. M., et al. (2009). Large Induction of Type III Deiodinase Expression after Partial Hepatectomy in the Regenerating Mouse and Rat Liver. *Endocrinology* 150 (1), 540–545. doi:10.1210/en.2008-0344
- Knabl, J., de Maiziere, L., Hüttenbrenner, R., Hutter, S., Jückstock, J., Mahner, S., et al. (2020). Cell Type- and Sex-specific Dysregulation of Thyroid Hormone Receptors in Placentas in Gestational Diabetes Mellitus. *Int. J. Mol. Sci.* 21 (11), 4056. doi:10.3390/ijms21114056
- Kostopanagiotou, G., Kalimeris, K., Mourouzis, I., Kostopanagiotou, K., Arkadopoulos, N., Panagopoulos, D., et al. (2009). Thyroid Hormones Alterations during Acute Liver Failure: Possible Underlying Mechanisms and Consequences. *Endocrine* 36 (2), 198–204. doi:10.1007/s12020-009-9210-2
- Kowalik, M. A., Columbano, A., and Perra, A. (2018). Thyroid Hormones, Thyromimetics and Their Metabolites in the Treatment of Liver Disease. *Front. Endocrinol. (Lausanne)* 9, 382. doi:10.3389/fendo.2018.00382
- Ladenson, P. W., Kristensen, J. D., Ridgway, E. C., Olsson, A. G., Carlsson, B., Klein, I., et al. (2010a). Use of the Thyroid Hormone Analogue Eprotirome in Statin-Treated Dyslipidemia. *N. Engl. J. Med.* 362 (10), 906–916. doi:10.1056/NEJMoa0905633
- Ladenson, P. W., McCarren, M., Morkin, E., Edson, R. G., Shih, M. C., Warren, S. R., et al. (2010b). Effects of the Thyromimetic Agent Diiodothyropropionic Acid on Body Weight, Body Mass Index, and Serum Lipoproteins: a Pilot Prospective, Randomized, Controlled Study. *J. Clin. Endocrinol. Metab.* 95 (3), 1349–1354. doi:10.1210/jc.2009-1209
- Lee, J. W., Choi, H. S., Gyuris, J., Brent, R., and Moore, D. D. (1995). Two Classes of Proteins Dependent on Either the Presence or Absence of Thyroid Hormone for Interaction with the Thyroid Hormone Receptor. *Mol. Endocrinol.* 9 (2), 243–254. doi:10.1210/mend.9.2.7776974
- Li, L., Lei, Q. S., Kong, L. N., Zhang, S. J., and Qin, B. (2017). Gene Expression Profile after Knockdown of USP18 in Hepg2.2.15 Cells. *J. Med. Virol.* 89 (11), 1920–1930. doi:10.1002/jmv.24819
- Lin, Y. H., Huang, Y. H., Wu, M. H., Wu, S. M., Chi, H. C., Liao, C. J., et al. (2013a). Thyroid Hormone Suppresses Cell Proliferation through Endoglin-Mediated Promotion of P21 Stability. *Oncogene* 32 (33), 3904–3914. doi:10.1038/ncr.2013.5
- Lin, Y. H., Liao, C. J., Huang, Y. H., Wu, M. H., Chi, H. C., Wu, S. M., et al. (2013b). Thyroid Hormone Receptor Represses miR-17 Expression to Enhance Tumor Metastasis in Human Hepatoma Cells. *Oncogene* 32 (38), 4509–4518. doi:10.1038/ncr.2013.309
- Lin, Y. H., Lin, K. H., and Yeh, C. T. (2020a). Thyroid Hormone in Hepatocellular Carcinoma: Cancer Risk, Growth Regulation, and Anticancer Drug Resistance. *Front. Med. (Lausanne)* 7, 174. doi:10.3389/fmed.2020.00174
- Lin, Y. H., Wu, M. H., Huang, Y. H., Yeh, C. T., Chi, H. C., Tsai, C. Y., et al. (2018). Thyroid Hormone Negatively Regulates Tumorigenesis through Suppression of BC200. *Endocr. Relat. Cancer* 25 (12), 967–979. doi:10.1530/ERC-18-0176
- Lin, Y. H., Wu, M. H., Huang, Y. H., Yeh, C. T., and Lin, K. H. (2020b). TUG1 Is a Regulator of AFP and Serves as Prognostic Marker in Non-hepatitis B Non-hepatitis C Hepatocellular Carcinoma. *Cells* 9 (2), 262. doi:10.3390/cells9020262
- Lin, Y. H., Wu, M. H., Liao, C. J., Huang, Y. H., Chi, H. C., Wu, S. M., et al. (2015). Repression of microRNA-130b by Thyroid Hormone Enhances Cell Motility. *J. Hepatol.* 62 (6), 1328–1340. doi:10.1016/j.jhep.2014.12.035
- Liu, W., Zeng, M., and Fu, N. (2021). Functions of Nuclear Receptors SUMOylation. *Clin. Chim. Acta* 516, 27–33. doi:10.1016/j.cca.2021.01.007
- Liu, Y. C., Yeh, C. T., and Lin, K. H. (2019). Molecular Functions of Thyroid Hormone Signaling in Regulation of Cancer Progression and Anti-apoptosis. *Int. J. Mol. Sci.* 20 (20), 4986. doi:10.3390/ijms20204986
- Liu, Y. Y., and Brent, G. A. (2018). Posttranslational Modification of Thyroid Hormone Nuclear Receptor by Sumoylation. *Methods Mol. Biol.* 1801, 47–59. doi:10.1007/978-1-4939-7902-8_6
- LiverTox (2012). “Antithyroid Agents,” in *LiverTox: Clinical and Research Information on Drug-Induced Liver Injury* (Bethesda (MD): National Institute of Diabetes and Digestive and Kidney Diseases).
- Lopes, D., and Samant, H. (2021). “Hepatic Failure,” in *StatPearls* (Treasure Island (FL): StatPearls Publishing).
- López-Fontal, R., Zeini, M., Través, P. G., Gómez-Ferrería, M., Aranda, A., Sáez, G. T., et al. (2010). Mice Lacking Thyroid Hormone Receptor Beta Show Enhanced Apoptosis and Delayed Liver Commitment for Proliferation after Partial Hepatectomy. *PLoS One* 5 (1), e8710. doi:10.1371/journal.pone.0008710
- Luongo, C., Dentice, M., and Salvatore, D. (2019). Deiodinases and Their Intricate Role in Thyroid Hormone Homeostasis. *Nat. Rev. Endocrinol.* 15 (8), 479–488. doi:10.1038/s41574-019-0218-2
- Malik, R., Saich, R., Rahman, T., and Hodgson, H. (2006). During Thioacetamide-Induced Acute Liver Failure, the Proliferative Response of Hepatocytes to Thyroid Hormone Is Maintained, Indicating a Potential Therapeutic Approach to Toxin-Induced Liver Disease. *Dig. Dis. Sci.* 51 (12), 2235–2241. doi:10.1007/s10620-006-9275-1
- Malm, J. (2004). Thyroid Hormone Ligands and Metabolic Diseases. *Curr. Pharm. Des.* 10 (28), 3525–3532. doi:10.2174/1381612043382873
- Manka, P., Coombes, J. D., Boosman, R., Gauthier, K., Papa, S., and Syn, W. K. (2018). Thyroid Hormone in the Regulation of Hepatocellular Carcinoma and its Microenvironment. *Cancer Lett.* 419, 175–186. doi:10.1016/j.canlet.2018.01.055
- Mardones, M., Valenzuela, R., Romanque, P., Covarrubias, N., Anghileri, F., Fernández, V., et al. (2012). Prevention of Liver Ischemia Reperfusion Injury by a Combined Thyroid Hormone and Fish Oil Protocol. *J. Nutr. Biochem.* 23 (9), 1113–1120. doi:10.1016/j.jnutbio.2011.06.004
- Martínez-Escudé, A., Pera, G., Costa-Garrido, A., Rodríguez, L., Arteaga, I., Expósito-Martínez, C., et al. (2021). TSH Levels as an Independent Risk Factor for NAFLD and Liver Fibrosis in the General Population. *J. Clin. Med.* 10 (13), 2907. doi:10.3390/jcm10132907
- Méndez-Sánchez, N., and Díaz-Orozco, L. E. (2021). Editorial: International Consensus Recommendations to Replace the Terminology of Non-alcoholic Fatty Liver Disease (NAFLD) with Metabolic-Associated Fatty Liver Disease (MAFLD). *Med. Sci. Monit.* 27, e933860. doi:10.12659/MSM.933860
- Minakhina, S., Bansal, S., Zhang, A., Brotherton, M., Janodia, R., De Oliveira, V., et al. (2020). A Direct Comparison of Thyroid Hormone Receptor Protein Levels in Mice Provides Unexpected Insights into Thyroid Hormone Action. *Thyroid* 30 (8), 1193–1204. doi:10.1089/thy.2019.0763
- Mishima, E., Sato, E., Ito, J., Yamada, K. I., Suzuki, C., Oikawa, Y., et al. (2020). Drugs Repurposed as Antiferroptosis Agents Suppress Organ Damage, Including AKI, by Functioning as Lipid Peroxyl Radical Scavengers. *J. Am. Soc. Nephrol.* 31 (2), 280–296. doi:10.1681/ASN.2019060570
- Mishkin, S. Y., Pollack, R., Yalovsky, M. A., Morris, H. P., and Mishkin, S. (1981). Inhibition of Local and Metastatic Hepatoma Growth and Prolongation of Survival after Induction of Hypothyroidism. *Cancer Res.* 41 (8), 3040–3045.
- Moutzouri, E., Lyko, C., Feller, M., Blum, M. R., Adam, L., Blum, S., et al. (2021). Subclinical Thyroid Function and Cardiovascular Events in Patients with Atrial Fibrillation. *Eur. J. Endocrinol.* 185 (3), 375–385. doi:10.1530/eje-20-1442
- Niedowicz, D. M., Wang, W.-X., Price, D. A., and Nelson, P. T. (2021). Modulating Thyroid Hormone Levels in Adult Mice: Impact on Behavior and Compensatory Brain Changes. *J. Thyroid Res.* 2021, 1–13. doi:10.1155/2021/9960188
- Nomura, S., Pittman, C. S., Chambers, J. B., Buck, M. W., and Shimizu, T. (1975). Reduced Peripheral Conversion of Thyroxine to Triiodothyronine in Patients with Hepatic Cirrhosis. *J. Clin. Invest.* 56 (3), 643–652. doi:10.1172/JCI108134
- Obata, T., and Aomine, M. (2009). Changes in Monoamine Oxidase Activity in Hepatic Injury: a Review. *Res. Commun. Mol. Pathol. Pharmacol.* 122–123, 51–63.
- Onigata, K., and Szinnai, G. (2014). Resistance to Thyroid Hormone. *Endocr. Dev.* 26, 118–129. doi:10.1159/000363159
- Oren, R., Dabeva, M. D., Karnezis, A. N., Petkov, P. M., Rosencrantz, R., Sandhu, J. P., et al. (1999). Role of Thyroid Hormone in Stimulating Liver Repopulation in the Rat by Transplanted Hepatocytes. *Hepatology* 30 (4), 903–913. doi:10.1002/hep.510300418
- Orságová, I., Rožnovský, L., Petroušová, L., Konečná, M., Kabieszová, L., Šafářčík, K., et al. (2014). Thyroid Dysfunction during Interferon Alpha Therapy for Chronic Hepatitis B and C - Twenty Years of Experience. *Klin Mikrobiol Infekc Lek* 20 (3), 92–97. https://pm.yuntsg.com/details.html?pmid=25702290&key=25702290

- Ortiga-Carvalho, T. M., Sidhaye, A. R., and Wondisford, F. E. (2014). Thyroid Hormone Receptors and Resistance to Thyroid Hormone Disorders. *Nat. Rev. Endocrinol.* 10 (10), 582–591. doi:10.1038/nrendo.2014.143
- Oura, K., Morishita, A., and Masaki, T. (2020). Molecular and Functional Roles of MicroRNAs in the Progression of Hepatocellular Carcinoma—A Review. *Int. J. Mol. Sci.* 21 (21), 8362. doi:10.3390/ijms21218362
- Papineni, J. K., Pinnelli, V. B. K., and Davanum, R. (2017). Thyroid Hormone Levels in Chronic Alcoholic Liver Disease Patients before and after Treatment. *J. Clin. Diagn. Res.* 11 (7), BC13–BC16. doi:10.7860/JCDR/2017/24552.10276
- Paterlini-Bréchet, P., Saigo, K., Murakami, Y., Chami, M., Gozuacik, D., Mugnier, C., et al. (2003). Hepatitis B Virus-Related Insertional Mutagenesis Occurs Frequently in Human Liver Cancers and Recurrently Targets Human Telomerase Gene. *Oncogene* 22 (25), 3911–3916. doi:10.1038/sj.onc.1206492
- Perra, A., Kowalik, M. A., Cabras, L., Runfola, M., Sestito, S., Migliore, C., et al. (2020). Potential Role of Two Novel Agonists of Thyroid Hormone Receptor- β on Liver Regeneration. *Cel Prolif* 53 (5), e12808. doi:10.1111/cpr.12808
- Piqué, D. G., Grealley, J. M., and Mar, J. C. (2020). Identification of a Novel Subgroup of Endometrial Cancer Patients with Loss of Thyroid Hormone Receptor Beta Expression and Improved Survival. *BMC Cancer* 20 (1), 857. doi:10.1186/s12885-020-07325-y
- Puhr, H. C., Wolf, P., Berghoff, A. S., Schoppmann, S. F., Preusser, M., and Ilhan-Mutlu, A. (2020). Elevated Free Thyroxine Levels Are Associated with Poorer Overall Survival in Patients with Gastroesophageal Cancer: A Retrospective Single Center Analysis. *Horm. Cancer* 11 (1), 42–51. doi:10.1007/s12672-019-00374-1
- Raza, S., Rajak, S., Upadhyay, A., Tewari, A., and Anthony Sinha, R. (2021). Current Treatment Paradigms and Emerging Therapies for NAFLD/NASH. *Front. Biosci. (Landmark Ed.)* 26, 206–237. doi:10.2741/4892
- Ridruejo, E., Romero Caimi, G., Miret, N., Obregón, M. J., Randi, A., Deza, Z., et al. (2021). TGF- β 1 Mediates Cell Proliferation and Development of Hepatocarcinogenesis by Downregulating Deiodinase 1 Expression. *Medicina (B Aires)* 81 (3), 346–358.
- Ritter, M. J., Amano, I., and Hollenberg, A. N. (2020). Thyroid Hormone Signaling and the Liver. *Hepatology* 72 (2), 742–752. doi:10.1002/hep.31296
- Rodríguez-Castelán, J., Corona-Pérez, A., Nicolás-Toledo, L., Martínez-Gómez, M., Castelán, F., and Cuevas-Romero, E. (2017). Hypothyroidism Induces a Moderate Steatohepatitis Accompanied by Liver Regeneration, Mast Cells Infiltration, and Changes in the Expression of the Farnesoid X Receptor. *Exp. Clin. Endocrinol. Diabetes* 125 (3), 183–190. doi:10.1055/s-0042-112367
- Rosen, M. D., and Privalsky, M. L. (2011). Thyroid Hormone Receptor Mutations in Cancer and Resistance to Thyroid Hormone: Perspective and Prognosis. *J. Thyroid Res.* 2011, 361304. doi:10.4061/2011/361304
- Ruiz-Llorente, L., Ardila-González, S., Fanjul, L. F., Martínez-Iglesias, O., and Aranda, A. (2014). microRNAs 424 and 503 Are Mediators of the Anti-proliferative and Anti-invasive Action of the Thyroid Hormone Receptor Beta. *Oncotarget* 5 (10), 2918–2933. doi:10.18632/oncotarget.1577
- Russo, S. C., Salas-Lucia, F., and Bianco, A. C. (2021). Deiodinases and the Metabolic Code for Thyroid Hormone Action. *Endocrinology* 162 (8), bqab059. doi:10.1210/endo/bqab059
- Salman, M. A., Rabiee, A., Salman, A., Qassem, M. G., Ameen, M. A., Hassan, A. M., et al. (2021). Laparoscopic Sleeve Gastrectomy Has A Positive Impact on Subclinical Hypothyroidism Among Obese Patients: A Prospective Study. *World J. Surg.* 45 (10), 3130–3137. doi:10.1007/s00268-021-06201-5
- Saponaro, F., Sestito, S., Runfola, M., Rapposelli, S., and Chiellini, G. (2020). Selective Thyroid Hormone Receptor-Beta (TR β) Agonists: New Perspectives for the Treatment of Metabolic and Neurodegenerative Disorders. *Front. Med. (Lausanne)* 7, 331. doi:10.3389/fmed.2020.00331
- Senese, R., Cioffi, F., Petito, G., Goglia, F., and Lanni, A. (2019). Thyroid Hormone Metabolites and Analogues. *Endocrine* 66 (1), 105–114. doi:10.1007/s12020-019-02025-5
- Simon-Giavarotti, K. A., Giavarotti, L., Gomes, L. F., Lima, A. F., Veridiano, A. M., Garcia, E. A., et al. (2002). Enhancement of Lindane-Induced Liver Oxidative Stress and Hepatotoxicity by Thyroid Hormone Is Reduced by Gadolinium Chloride. *Free Radic. Res.* 36 (10), 1033–1039. doi:10.1080/1071576021000028280
- Sinha, R. A., You, S. H., Zhou, J., Siddique, M. M., Bay, B. H., Zhu, X., et al. (2012). Thyroid Hormone Stimulates Hepatic Lipid Catabolism via Activation of Autophagy. *J. Clin. Invest.* 122 (7), 2428–2438. doi:10.1172/JCI60580
- Sousa Domínguez, A. (2015). Severe Acute Liver Failure and Thyrotoxicosis: an Unusual Association. *Rev. Esp. Enferm. Dig.* 107 (9), 575–576. doi:10.17235/reed.2015.3607/2014
- Sun, Y., Deng, X., Li, W., Yan, Y., Wei, H., Jiang, Y., et al. (2007). Liver Proteome Analysis of Adaptive Response in Rat Immediately after Partial Hepatectomy. *Proteomics* 7 (23), 4398–4407. doi:10.1002/pmic.200600913
- Szilagy, A., Lerman, S., and Resnick, R. H. (1983). Ethanol, Thyroid Hormones and Acute Liver Injury: Is There a Relationship? *Hepatology* 3 (4), 593–600. doi:10.1002/hep.1840030420
- Taki-Eldin, A., Zhou, L., Xie, H. Y., Chen, K. J., Zhou, W. H., Zhang, W., et al. (2011). Tri-iodothyronine Enhances Liver Regeneration after Living Donor Liver Transplantation in Rats. *J. Hepatobiliary Pancreat. Sci.* 18 (6), 806–814. doi:10.1007/s00534-011-0397-2
- Tan, Y., Tang, X., Mu, P., Yang, Y., Li, M., Nie, Y., et al. (2021). High-Normal Serum Thyrotropin Levels Increased the Risk of Non-alcoholic Fatty Liver Disease in Euthyroid Subjects with Type 2 Diabetes. *Diabetes Metab. Syndr. Obes.* 14, 2841–2849. doi:10.2147/DMSO.S313224
- Tanase, D. M., Gosav, E. M., Neculau, E., Costea, C. F., Ciocoiu, M., Hurjui, L. L., et al. (2020). Hypothyroidism-Induced Nonalcoholic Fatty Liver Disease (HIN): Mechanisms and Emerging Therapeutic Options. *Int. J. Mol. Sci.* 21 (16), 5927. doi:10.3390/ijms21165927
- Taub, R., Chiang, E., Chabot-Blanchet, M., Kelly, M. J., Reeves, R. A., Guertin, M. C., et al. (2013). Lipid Lowering in Healthy Volunteers Treated with Multiple Doses of MGL-3196, a Liver-Targeted Thyroid Hormone Receptor- β Agonist. *Atherosclerosis* 230 (2), 373–380. doi:10.1016/j.atherosclerosis.2013.07.056
- Turan, E., and Turksoy, V. A. (2021). Selenium, Zinc, and Copper Status in Euthyroid Nodular Goiter: A Cross-Sectional Study. *Int. J. Prev. Med.* 12, 46. doi:10.4103/ijpvm.IJPVM_337_19
- Vargas, R., and Videla, L. A. (2017). Thyroid Hormone Suppresses Ischemia-Reperfusion-Induced Liver NLRP3 Inflammasome Activation: Role of AMP-Activated Protein Kinase. *Immunol. Lett.* 184, 92–97. doi:10.1016/j.imlet.2017.01.007
- Ventura-Holman, T., Mamoon, A., Subauste, M. C., and Subauste, J. S. (2011). The Effect of Oncoprotein V-erbA on Thyroid Hormone-Regulated Genes in Hepatocytes and Their Potential Role in Hepatocellular Carcinoma. *Mol. Biol. Rep.* 38 (2), 1137–1144. doi:10.1007/s11033-010-0211-2
- Wang, F., Zhang, B., Xu, X., Zhu, L., and Zhu, X. (2020). TRIP6 Promotes Tumorigenic Capability through Regulating FOXC1 in Hepatocellular Carcinoma. *Pathol. Res. Pract.* 216 (4), 152850. doi:10.1016/j.prp.2020.152850
- Wang, L., Yu, W., Cao, W., and Lu, W. (2017). The Abnormality of Thyroid Hormones in Patients with Type A Hepatic Encephalopathy. *Oncotarget* 8 (40), 67821–67828. doi:10.18632/oncotarget.18869
- Wang, R., and Mu, J. (2021). Arbutin Attenuates Ethanol-Induced Acute Hepatic Injury by the Modulation of Oxidative Stress and Nrf-2/HO-1 Signaling Pathway. *J. Biochem. Mol. Toxicol.* 35, e22872. doi:10.1002/jbt.22872
- Wu, C. H., Yeh, C. T., and Lin, K. H. (2020). Thyroid Hormones Suppress FOXM1 Expression to Reduce Liver Cancer Progression. *Oncol. Rep.* 44 (4), 1686–1698. doi:10.3892/or.2020.7716
- Wu, D., Sun, Z., Liu, X., Rao, Q., Chen, W., Wang, J., et al. (2018). HINT: a Novel Prognostic Model for Patients with Hepatitis B Virus-Related Acute-On-Chronic Liver Failure. *Aliment. Pharmacol. Ther.* 48 (7), 750–760. doi:10.1111/apt.14927
- Wu, S. M., Cheng, W. L., Liao, C. J., Chi, H. C., Lin, Y. H., Tseng, Y. H., et al. (2015). Negative Modulation of the Epigenetic Regulator, UHRF1, by Thyroid Hormone Receptors Suppresses Liver Cancer Cell Growth. *Int. J. Cancer* 137 (1), 37–49. doi:10.1002/ijc.29368
- Yamamoto, M. (1995). Liver Injury. *Ryokibetsu Shokogun Shirizu* 8, 487–492.
- Yan, L. D., Thomas, D., Schwartz, M., Reich, J., and Steenkamp, D. (2017). Rescue of Graves Thyrotoxicosis-Induced Cholestatic Liver Disease without Antithyroid Drugs: A Case Report. *J. Endocr. Soc.* 1 (3), 231–236. doi:10.1210/js.2016.1065
- Yang, J., Wang, Y., Sui, M., Liu, F., Fu, Z., and Wang, Q. X. (2015). Tri-iodothyronine Preconditioning Protects against Liver Ischemia Reperfusion Injury through the

- Regulation of Autophagy by the MEK/ERK/mTORC1 axis. *Biochem. Biophys. Res. Commun.* 467 (4), 704–710. doi:10.1016/j.bbrc.2015.10.080
- Yang, Q., Liu, W., Sun, D., Wang, C., Li, Y., Bi, X., et al. (2020). Yinning Tablet, a Hospitalized Preparation of Chinese Herbal Formula for Hyperthyroidism, Ameliorates Thyroid Hormone-Induced Liver Injury in Rats: Regulation of Mitochondria-Mediated Apoptotic Signals. *J. Ethnopharmacol.* 252, 112602. doi:10.1016/j.jep.2020.112602
- Zeng, F., Takaya, T., Yoshida, N., Ito, T., Suto, M., Hatani, Y., et al. (2017). A Case of Fatal Heart and Liver Failure Accompanied by Thyroid Storm Treated with Prompt Plasma Exchange. *J. Cardiol. Cases* 15 (3), 100–103. doi:10.1016/j.jccase.2016.11.001
- Zeng, M., Liu, W., Hu, Y., and Fu, N. (2020). Sumoylation in Liver Disease. *Clin. Chim. Acta* 510, 347–353. doi:10.1016/j.cca.2020.07.044
- Zhang, L., Zeyu, W., Liu, B., Jang, S., Zhang, Z., and Jiang, Y. (2021). Pyroptosis in Liver Disease. *Rev. Esp. Enferm. Dig.* 113 (4), 280–285. doi:10.17235/reed.2020.7034/2020
- Zhang, P., Shi, L., Song, L., Long, Y., Yuan, K., Ding, W., et al. (2020). LncRNA CRNDE and lncRNA SNHG7 Are Promising Biomarkers for Prognosis in Synchronous Colorectal Liver Metastasis Following Hepatectomy. *Cancer Manag. Res.* 12, 1681–1692. doi:10.2147/CMAR.S233147
- Zhang, X., Li, R., Chen, Y., Dai, Y., Chen, L., Qin, L., et al. (2020). The Role of Thyroid Hormones and Autoantibodies in Metabolic Dysfunction Associated Fatty Liver Disease: TgAb May Be a Potential Protective Factor. *Front. Endocrinol. (Lausanne)* 11, 598836. doi:10.3389/fendo.2020.598836
- Zhang, Y., Zhan, C., Chen, G., and Sun, J. (2018). Label-free Quantitative Proteomics and Bioinformatics Analyses of Alcoholic Liver Disease in a Chronic and Binge Mouse Model. *Mol. Med. Rep.* 18 (2), 2079–2087. doi:10.3892/mmr.2018.9225
- Zhao, L. F., Iwasaki, Y., Han, B. L., Wang, J., Zhang, Y., Han, J., et al. (2020). Triiodothyronine Activates Glycerol-3-Phosphate Acyltransferase 3 via Aggta-Like-Direct-Repeat-4 Type Thyroid Hormone Response Element. *Acta Endocrinol. (Buchar)* 16 (2), 129–135. doi:10.4183/aeb.2020.129
- Zhao, W., Dai, Y., Dai, T., Xie, T., Su, X., Li, J., et al. (2017). TRIP6 Promotes Cell Proliferation in Hepatocellular Carcinoma via Suppression of FOXO3a. *Biochem. Biophys. Res. Commun.* 494 (3–4), 594–601. doi:10.1016/j.bbrc.2017.10.117

Conflict of Interest: The authors declare that the research was conducted in the absence of any commercial or financial relationships that could be construed as a potential conflict of interest.

Publisher's Note: All claims expressed in this article are solely those of the authors and do not necessarily represent those of their affiliated organizations, or those of the publisher, the editors, and the reviewers. Any product that may be evaluated in this article, or claim that may be made by its manufacturer, is not guaranteed or endorsed by the publisher.

Copyright © 2022 Tang, Zeng, Chen and Fu. This is an open-access article distributed under the terms of the Creative Commons Attribution License (CC BY). The use, distribution or reproduction in other forums is permitted, provided the original author(s) and the copyright owner(s) are credited and that the original publication in this journal is cited, in accordance with accepted academic practice. No use, distribution or reproduction is permitted which does not comply with these terms.

GLOSSARY

TH/TR axis thyroid hormone/thyroid hormone receptor axis

T4 thyroid hormones 3,5,3',5'- tetraiodothyronine or thyroxine

T3 3,5,3'-triiodothyronine

AEV avian erythroblastosis virus

TRE thyroid hormone-response element

TSH thyroid-stimulating hormone

PCNA proliferating cell nuclear antigen

cdk2 cyclin-dependent kinase 2

PARP Poly (ADP-ribose) polymerase

PH partial hepatectomy

MAFLD metabolic-associated fatty liver disease

HCC hepatocellular carcinoma

HBV hepatitis B virus

HCV hepatitis C virus

ALF acute liver failure

GC-1 sobetosome

Eprotriome KB2115

MetS metabolic syndrome

TPOAb thyroid peroxidase antibody

SBP systolic blood pressure

DBP diastolic blood pressure

FBG fasting blood glucose

TG triglyceride

HDLC high-density lipoprotein

ALT alanine aminotransferase

AST aspartate aminotransferase

BUN urea nitrogen

CR creatinine

Dio iodothyronine deiodinases

HIF-1 α hypoxia-inducible factor 1 α

NCD normal chow diet

H sites sites of *de novo* DNA hypermethylation

CDK cyclin-dependent kinase

miRNAs microRNAs

lncRNA long non-coding RNA

Hh Hedgehog

PIM-1 the proto-oncogene serine/threonine-protein kinase-1

HCB hexachlorobenzene

FOXMI forkhead box M1

R-H model resistance-hepatocyte rat model

SCLM synchronous colorectal liver metastasis

BC200 brain cytoplasmic RNA 1

TUG1 taurine upregulated gene 1

TRIP Thyroid hormone receptor-interacting proteins

PTTG1 pituitary tumor-transforming gene 1

Lcn2 lipocalin 2

NUPR1 nuclear protein 1

THRSP thyroid hormone responsive

DKK 4 dickkopf 4

USP18 ubiquitin-specific protease 18

TRUP thyroid hormone uncoupling protein

ALF acute liver failure

HE hepatic encephalopathy

CLF chronic liver disease

CHC chronic hepatitis C

TD thyroid disease

PRO-C3 N-terminal type III collagen pro-peptide

PBC primary biliary cirrhosis

ftT3 TH-free T3

EMR ethanol metabolic rate

AF alcohol-feed

PF pair-feed

8-OHdG 8-hydroxy-2-deoxyguanosine

PCO protein carbonyl content

AOPPs advanced oxidation protein products

MP methylprednisolone

n-3 PUFA n-3 polyunsaturated fatty acid

IR ischemia-reperfusion

STAT3 signal transducer and activator of transcription 3

Nrf2 nuclear transcription factor erythroid 2-related factor 2

Eh1 epoxide hydrolase 1

NQO1 NADPH-quinone oxidoreductase 1

GST glutathione-S-transferases

MRP multidrug resistance-associated proteins

GdCl3 gadolinium chloride

PC preconditioning

AMPK AMP-activated protein kinase

MAO monoamine oxidase

R243Q substitution of glycine by arginine at position 243

SUMO small ubiquitin-like modifier

OA oleic acid



Multi-Omics Reveals Inhibitory Effect of Baicalein on Non-Alcoholic Fatty Liver Disease in Mice

Ping Li^{1,2}, Jianran Hu², Hongmei Zhao², Jing Feng³ and Baofeng Chai^{1*}

¹Institute of Loess Plateau, Shanxi University, Taiyuan, China, ²Department of Biological Science and Technology, Jinzhong University, Jinzhong, China, ³Department of Gastroenterology, Shanxi Provincial People's Hospital Affiliated to Shanxi Medical University, Taiyuan, China

OPEN ACCESS

Edited by:

Francisco Javier Cubero,
Complutense University of Madrid,
Spain

Reviewed by:

Douglas Maya Miles,
Institute of Biomedicine of Seville
(CSIC), Spain
Ignacio Benedicto,
Centro Nacional de Investigaciones
Cardiovasculares (CNIC), Spain

*Correspondence:

Baofeng Chai
bfchai@sxu.edu.cn

Specialty section:

This article was submitted to
Gastrointestinal and Hepatic
Pharmacology,
a section of the journal
Frontiers in Pharmacology

Received: 21 April 2022

Accepted: 06 May 2022

Published: 15 June 2022

Citation:

Li P, Hu J, Zhao H, Feng J and Chai B
(2022) Multi-Omics Reveals Inhibitory
Effect of Baicalein on Non-Alcoholic
Fatty Liver Disease in Mice.
Front. Pharmacol. 13:925349.
doi: 10.3389/fphar.2022.925349

Non-alcoholic fatty liver disease (NAFLD) is the most common chronic liver disease, whose etiology is poorly understood. Accumulating evidence indicates that gut microbiota plays an important role in the occurrence and progression of various human diseases, including NAFLD. In this study, NAFLD mouse models were established by feeding a high-fat diet (HFD). Baicalein, a natural flavonoid with multiple biological activities, was administered by gavage, and its protective effect on NAFLD was analyzed by histopathological and blood factor analysis. Gut microbiota analysis demonstrated that baicalein could remodel the overall structure of the gut microbiota from NAFLD model mice, especially *Anaerotruncus*, *Lachnospirillum*, and *Mucispirillum*. Transcriptomic analysis showed baicalein restored the expressions of numerous genes that were upregulated in hepatocytes of NAFLD mice, such as *Apoa4*, *Pla2g12a*, *Elovl7*, *Slc27a4*, *Hilpda*, *Fabp4*, *Vldlr*, *Gpld1*, and *Apom*. Metabolomics analysis proved that baicalein mainly regulated the processes associated with lipid metabolism, such as alpha-Linolenic acid, 2-Oxocarboxylic acid, Pantothenate and CoA biosynthesis, and bile secretion. Multi-omics analysis revealed that numerous genes regulated by baicalein were significantly correlated with pathways related to lipid metabolism and biosynthesis and secretion of bile acid, and baicalein might affect lipid metabolism in liver via regulating the ecological structure of gut microbiota in NAFLD mice. Our results elucidated the correlated network among diet, gut microbiota, metabolomic, and transcriptional profiling in the liver. This knowledge may help explore novel therapeutic approaches against NAFLD.

Keywords: baicalein, gut microbiota, transcriptomic profiling, metabolomic profiling, integrated analysis

INTRODUCTION

Non-alcoholic fatty liver disease (NAFLD) is a common liver disease worldwide. NAFLD affects both children and adults because of the dramatic rise in the prevalence of obesity, diabetes (Vuppalanchi and Chalasani, 2009; Majumdar et al., 2021), hypertension (Ryoo et al., 2014), and dyslipidemia (Katsiki et al., 2016). Between 2009 and 2019, the incidence rate of liver complications related to NAFLD increased in most Asian countries. In 2019, there were 170,000 incident cases and 168,959 deaths worldwide. Of these, 48.3% of the incident cases and 46.2% of the deaths occurred in Asia (Golabi et al., 2021). Recent research has demonstrated ingestion of high fat and intestinal dysbiosis may trigger NAFLD (Lambertz et al., 2017). Excess dietary fats might induce the accumulation of non-esterified fatty acids and then result in potential lipotoxins (Ferramosca and Zara, 2014).

Increasing evidence shows that disturbances in the gut microbiota may result in liver diseases including NAFLD (Tokuhara, 2021), since nutrients and microbiota-related components transfer from the intestines to the liver directly through the portal tract (Chen et al., 2019; Hong et al., 2019; Suk and Kim, 2019; Yuan et al., 2019). Gut microbiota has been proved to modulate a variety of physiological processes, such as the digestion of dietary fiber, the absorption of monosaccharides, the secretion of glucagon-like peptide-1, the suppression of bile acid production, and inflammation (Doulberis et al., 2012). The excess sugar and lipids associated with hepatic steatosis could be regulated by gut microbiota (Gkolfakis et al., 2015). Therefore, gut microbiota could be the potential therapeutic target to alleviate NAFLD.

Some natural compounds such as coffee (and its components), tormentic acid, verbascoside, and silymarin showed protective effects in ameliorating the critical pathological events involved in NAFLD. For example, silymarin has been widely used in the treatment of various liver disorders because of its hepatoprotective properties, including anti-inflammatory, antiproliferative, immunomodulatory, and anticholesterolemic properties (Salvoza et al., 2022). Baicalein, a bioactive flavone, is isolated from *Scutellariae baicalensis*, which is a traditional Chinese herb. Growing evidence shows that baicalein has a variety of pharmacological activities, such as anti-inflammatory, anticancer, and anti-oxidant effect (Pu et al., 2012; Li et al., 2020). Baicalein was also proved to be a promising compound for NAFLD and could be used as a dietary supplement to reduce hepatic fat accumulation and to ameliorate NAFLD-related biochemical abnormalities. Hepatic lysosomal acidification may be the potential target of baicalein (Zhu et al., 2020), and the mTOR pathway (Zhu et al., 2020), the AMPK pathway, SREBP1 signaling, and the synthesis of hepatic fat were proved to be affected by baicalein (Sun et al., 2020). Thus, the mechanism of baicalein against NAFLD might involve multiple targets and pathways.

Here, we identified the effects of baicalein ameliorating NAFLD. To explore the mechanism systematically, transcriptomics and metabolomics in the liver and metagenomics analysis in the high-fat diet (HFD)-fed mouse model (C57BL/6n) were combined, and bioinformatics analysis was carried out. Overall, these results should contribute new insight into the molecular mechanism of baicalein against NAFLD and suggest specific targets and pathways for the development of novel treatments that have the same beneficial effects.

METHODS AND MATERIALS

Mice and Reagent

Healthy male C57BL/6N mice (15–20 g, 4 weeks old) were purchased from Beijing Vital River Laboratory Animal Technology Co., Ltd. All animal experiments were strictly in accordance with published National Institutes of Health guidelines and approved by the Committee on the Ethics of Scientific Research of Shanxi Medical University (Shanxi, China).

The mice were randomized into five groups ($n = 10$): 1) Control (C, gavaged with equal volume saline), 2) Model (M, gavaged with equal volume saline), 3) Positive (P, gavaged with silymarin 200 mg/kg), 4) baicalein with high concentration (H, gavaged with baicalein 200 mg/kg/day), and 5) baicalein with low concentration (L, gavaged with baicalein 100 mg/kg/day). The C group was administered a normal basal diet and drinking water, whereas all the other groups were fed purified diets containing 60 kcal% (Research Diets, D12492, high fat diet; HFD) for 5 weeks. Body weights were measured weekly. The levels of blood glucose and insulin were determined after 12 h of fasting using an ELISA kit (Nanjing Jiancheng, Nanjing, China), respectively. At experiment completion, all mice were terminated by cervical dislocation. Blood was collected, and plasma was obtained after centrifugation (4°C; 1,500 × g, 10 min) and stored at −20°C. Liver tissue for RNA extraction and metabolic analysis and luminal contents of the cecum were flash-frozen in liquid nitrogen and stored at −80°C.

Baicalein, 5,6,7-Trihydroxyflavone ($C_{15}H_{10}O_5$, HPLC > 98%), was purchased from Sigma-Aldrich (St. Louis, MO, United States).

Histopathological Analysis

The paraffin-embedded liver tissue was cut into 4-μm-thick sections that were stained with hematoxylin and eosin (H&E). All stained liver slides were observed using a light microscope and evaluated for the NAFLD activity score (NAS), according to the previous report (Kleiner et al., 2005). Briefly, hepatic steatosis, lobular inflammation, and hepatic ballooning were investigated. In brief, steatosis was scored on a scale of 0–3 according to the following criteria: 0 (<5%), 1 (5%–33%), 2 (33%–66%), or 3 (>66%). Lobular inflammation was scored on a scale of 0–3 according to the following criteria: 0 (No foci), 1 (<2 foci per 20× optical field), 2 (2–4 foci per 20× optical field), or 3 (>4 foci per 20× optical field). Hepatocellular ballooning was scored on a scale of 0–2 according to the following criteria: 0 (none), 1 (mild, few), or 2 (moderate, many). The levels of TC, TG, LDL-C, HDL-C, ALT, and AST were detected using commercial kits (Nanjing Jiancheng, Nanjing, China).

Transcriptomic Analysis and Real-Time PCR

Total RNA was extracted from mouse liver tissue using TRIzol agent according to the manufacturer's protocols. RNA was further quantified using agarose gel electrophoresis, a NanoPhotometer spectrophotometer, and an Agilent 2100 bioanalyzer. Oligo (dT) magnetic beads were used to enrich the total RNA with Poly A structure. RNA seq libraries were generated using a NEBNext® Ultra™ RNA Library Prep Kit for Illumina® (NEB, United States). The library quality was assessed on the Agilent Bioanalyzer 2100 system. Sequencing was performed by generating 50 base reads on an Illumina HiSeq platform (Illumina). Clean data were obtained by removing reads containing adapters, reads containing poly-N and low-quality reads from raw data. The paired-end clean reads were aligned to the reference genome using Hisat2 v2.0.5. The original readcount

is normalized, mainly to correct the sequencing depth. Differential expression analysis was performed using the DESeq2 R package (1.16.1). p -values were adjusted using Benjamini and Hochberg's approach for controlling the false discovery rate. Genes with $|\log_2(\text{FoldChange})| > 0$ and $\text{Padj} < 0.05$ found using DESeq2 were assigned as differentially expressed. The FDR value was obtained by multiple hypothesis test correction. Gene Ontology (GO) and KEGG (Kyoto Encyclopedia of Genes and Genomes) enrichment analysis were determined using the clusterProfiler R package.

A High Capacity cDNA Reverse Transcription Kit (Applied Biosystems, United States) was used to synthesize cDNA. The real-time PCR was conducted using the SYBR@Premix Ex Taq™ (Perfect Real Time) (Takara, China) by the StepOne Real-Time PCR system (Thermo Fisher Scientific, United States). The primers are listed in **Supplementary Table S1**. The results are presented as the means \pm standard deviation (SD). Statistical analysis was performed using GraphPad Prism 5.0 (GraphPad, San Diego, CA, United States). Student's two-tailed t -test was used as appropriate. p -value < 0.05 was considered statistically significant.

Metabolomic Analysis

Liver tissues (100 mg) were individually grounded with liquid nitrogen, and the homogenate was resuspended with prechilled 80% methanol and 0.1% formic acid by well vortexing. The samples were incubated on ice for 5 min and were then centrifuged at 15,000 rpm and 4°C for 5 min. Supernatant was diluted to the final concentration containing 60% methanol by LC-MS grade water. The samples were subsequently transferred to a fresh Eppendorf tube with a 0.22- μm filter and were then centrifuged at 15,000 g and 4°C for 10 min. LC-MS/MS analyses were performed using a Vanquish UHPLC system (Thermo Fisher) coupled with an Orbitrap Q Exactive series mass spectrometer (Thermo Fisher).

These metabolites were annotated using the KEGG database, HMDB database, and Lipidmaps database. Principal components analysis (PCA) and partial least squares discriminant analysis (PLS-DA) were performed at metaX (Wen et al., 2017). Univariate analysis (t -test) was used to calculate the p value. The metabolites with $\text{VIP} > 1$ and p -value < 0.05 and fold change ≥ 2 or $\text{FC} \leq 0.5$ were considered to be differential metabolites. Volcano plots were used to filter metabolites of interest which were based on $\log_2(\text{FC})$ and $-\log_{10}(p\text{-value})$ of metabolites.

Gut Microbiota Analysis

Total genome DNA from luminal content of the cecum was extracted using the CTAB/SDS method. The 16S rRNA V3-V4 region was amplified using a specific primer (16S V4: 515F-806R) with the barcode. Sequencing libraries were generated using the Ion Plus Fragment Library Kit (Thermo Scientific, United States) following the manufacturer's recommendations. The library quality was assessed on a Qubit@ 2.0 Fluorometer (Thermo Scientific). At last, the library was sequenced on an Ion S5TM XL platform. The clean reads were obtained by using the Cutadapt and UCHIME algorithm. Sequences analysis was performed using Uparse software (Uparse v7.0.1001, <http://drive5.com/uparse/>). To

investigate the phylogenetic relationship of different OTUs and the difference of the dominant species in different groups, multiple sequence alignment was conducted using MUSCLE software. Alpha diversity and beta diversity were calculated using QIIME software (Version 1.7.0). Principal component analysis (PCA), UniFrac distance-based non-metric multidimensional scaling (NMDS), and the unweighted pair-group method with arithmetic means (UPGMA) were performed using R software. Tax4Fun functional prediction was achieved using the nearest neighbor method based on the minimum 16S rRNA sequence similarity by extracting the KEGG database prokaryotic whole genome 16S rRNA gene sequence and aligning it to the SILVA SSU Ref NR database using the BLASTN algorithm (BLAST Bitscore > 1500) to establish a correlation matrix and map the prokaryotic whole genome functional information of the KEGG database annotated by UProC and PAUDA to the SILVA database to implement the SILVA database function annotation.

Integrative Analysis of Multi-Omics Data

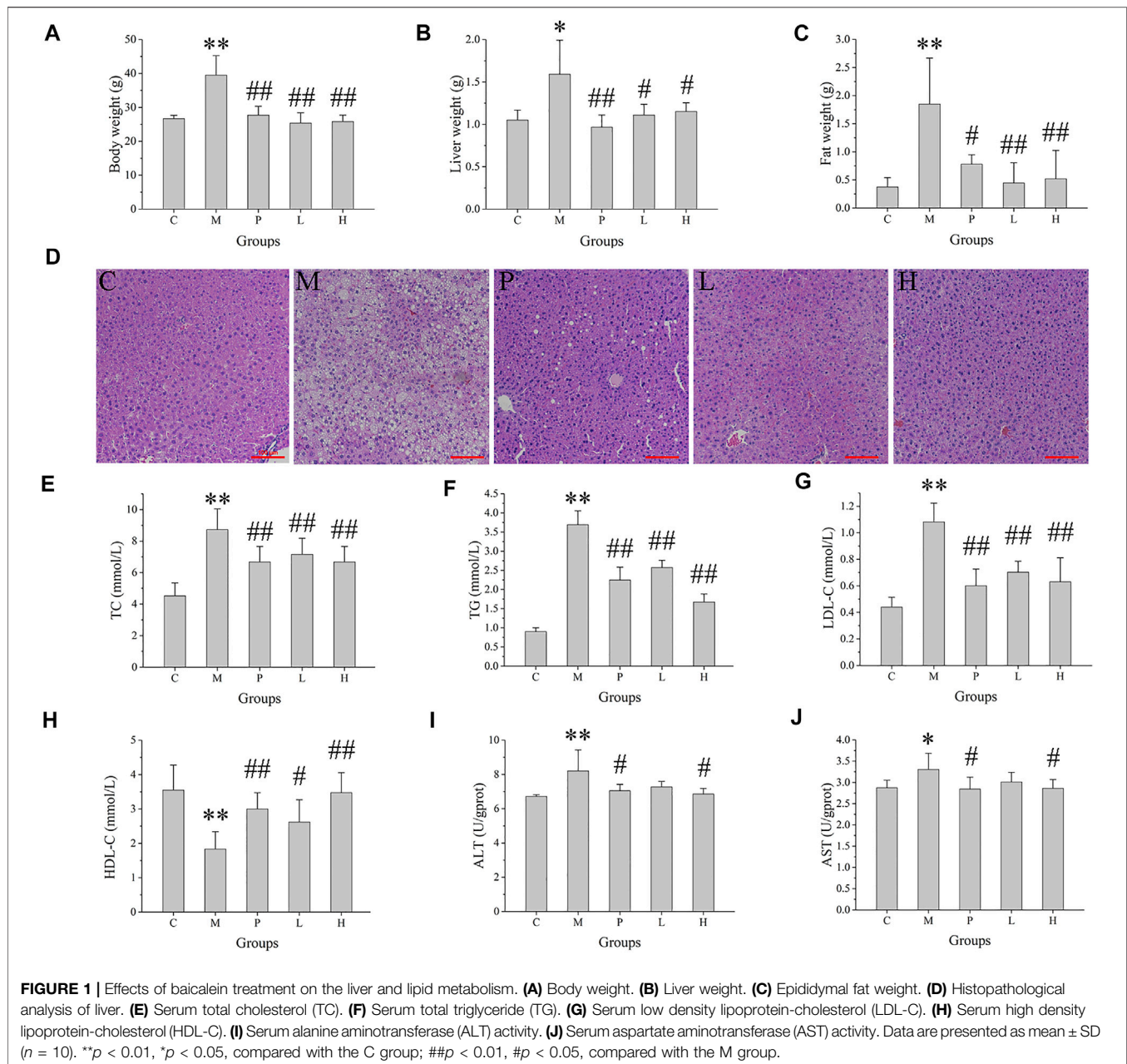
Correlation between the top 100 DEGs and top 50 differential metabolites was analyzed using the Pearson statistical method, and the correlation coefficient R^2 and p value were calculated. Red color indicates the positive correlation, and the blue color means the negative correlation.

The Pearson statistical method was used to access the correlation between the top 20 differential bacteria and top 10 differential metabolites. The correlation coefficients ρ ($|\rho| \geq 0.8$) and p value ($p \leq 0.05$) were calculated. Red color indicates the positive correlation, and the blue color means the negative correlation. The flatness of the ellipse represents the absolute value of the correlation.

RESULTS

Hepatoprotective Effect of Baicalein on High-Fat Diet-Induced Non-Alcoholic Fatty Liver Disease in Mice

To access the protective effect of baicalein on NAFLD, body weight, liver weight, and epididymal fat weight were determined. There was no significant difference in the initial body weight of each group. The mice fed with high-fat diet (M group) continuously for 5 weeks showed a clear increase in body weight ($p < 0.01$), compared with the control groups (fed with normal basal diet) (**Figure 1A**). Administration of silymarin (P group) or baicalein (L and H group) clearly decreased the body weight ($p < 0.01$), compared with the M group. In addition, the liver weight and the epididymal fat weight in NAFLD mice (M group) were elevated ($p < 0.01$) by 3.4- and 4.9-fold, relative to the control mice, respectively, and treatment of silymarin (P group) or baicalein (L and H group) could significantly decrease this HFD-induced increase in liver weight and epididymal fat weight (**Figures 1B,C**). Pathological examination of liver tissues revealed frequent incidence of macrosteatosis and hepatocyte ballooning in NAFLD mice, which was ameliorated in livers of silymarin- and baicalein-treated mice (**Figure 1D**). Compared with the C group, the liver tissue of mice in the M

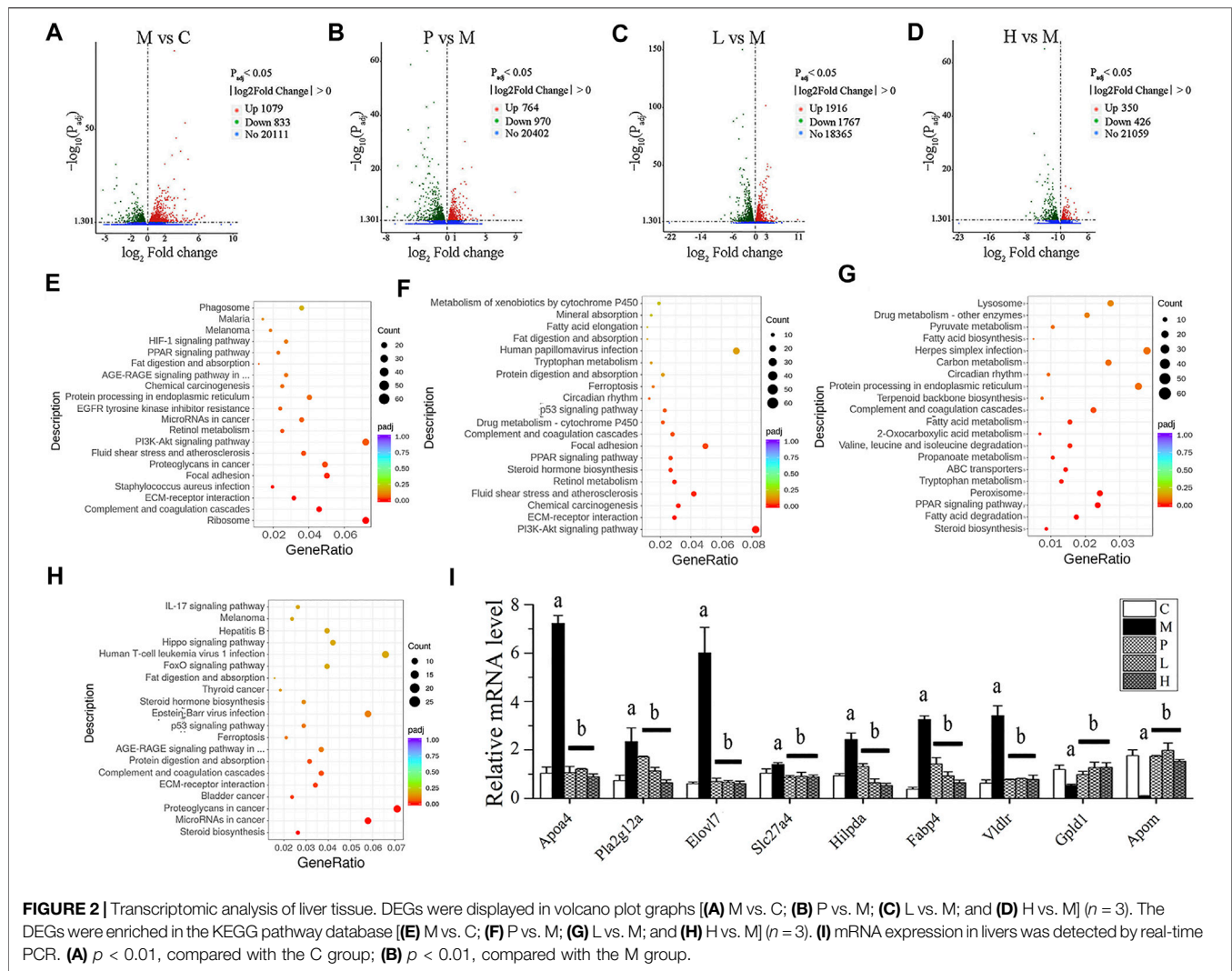


group obtained higher scores of steatosis, hepatocyte ballooning, lobular inflammation, and NAS score, indicating that the NAFLD model was successfully established. Compared with the M group, the scores of the P group decreased significantly, while the scores of the L and H groups were lower (Supplementary Figure S1A). Additionally, compared with the C group, the fasting blood glucose ($p < 0.01$) and insulin ($p < 0.01$) were extremely high in the M group and decreased in silymarin- and baicalein-treated mice (P, L, and H groups, $p < 0.01$) (Supplementary Figures S1B,C). After all mice were sacrificed, several blood factors were determined by ELISA assay. As shown in Figures 1E–J, NAFLD mice exhibited higher serum TC, TG, LDL-C, ALT, and AST and lower serum HDL-C, indicating metabolic disorders and NAFLD symptoms.

After treatment with silymarin (P group) or baicalein (L and H groups), the levels of serum TC, TG, LDL-C, ALT, and AST decreased significantly, while the levels of HDL-C increased ($p < 0.01$). Therefore, silymarin and baicalein could both improve the disorder of lipid metabolism in NAFLD mice, while baicalein exhibited a better effect.

Variations of Global Transcriptional Profiling in Liver of Non-Alcoholic Fatty Liver Disease Mice

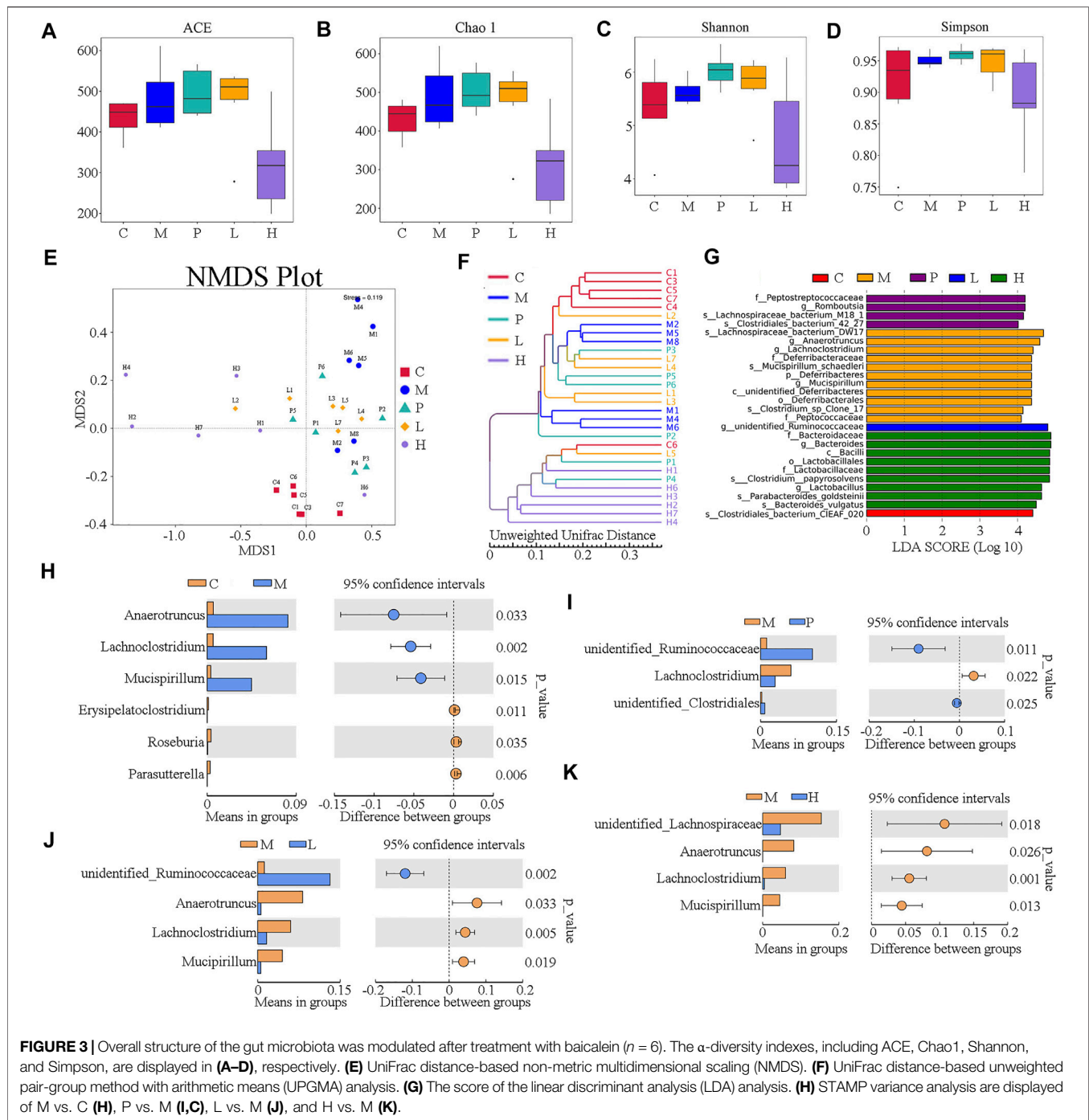
Transcriptomic analysis was conducted on the mRNA from the livers of C, M, P, L, and H groups. The DEGs were illustrated in a



heatmap (Supplementary Figure S2A), and the overlapped ones from three comparisons (P vs. M, L vs. M, and H vs. M) were shown in a Venn diagram (Supplementary Figure S2B). Compared with the C group, the M group had 1,912 DEGs (Supplementary Table S2), of which 1,079 were upregulated (Figure 2A; Supplementary Table S3), and 833 were downregulated (Figure 2A; Supplementary Table S4). After the treatment of silymarin, 1,734 DEGs were found (Supplementary Table S2), including 764 upregulated (Figure 2B; Supplementary Table S5) and 970 downregulated (Figure 2B; Supplementary Table S6), of which 214 transcripts were restored, with regard to the expression level of the C group (Supplementary Table S7). Similarly, compared with the M group, 3,683 DEGs with $|\log_2\text{fold change}| \geq 1$ and $\text{Padj} < 0.05$ were screened in the L group (Supplementary Table S2), presenting as volcano plot graphs (Figure 2C). 1,916 of them were upregulated (Supplementary Table S8) and 1,767 of them were downregulated (Supplementary Table S9), and expressions of 46 transcripts of them were similar to those in the C group (Supplementary Table S10). Additionally, DEGs containing 350

upregulated (Supplementary Table S11 and 426 downregulated (Supplementary Table S12) were revealed in the H group vs. the M group (Figure 2D), and the expression of 21 of them were similar to those in the C group (Supplementary Table S13). 640 of the DEGs in the L group vs. the M group and the H group vs. the M group were overlapped (Supplementary Figure S2B; Supplementary Table S14), and 278 of them were positively regulated by baicalein (Supplementary Table S15), while 362 were negatively regulated by baicalein (Supplementary Table S16). Therefore, these 640 transcripts might play an important role in the process of baicalein against NAFLD. Notably, 476 of these 640 transcripts also showed consistent alterations under silymarin treatment (Supplementary Figure S2B) and number 1–476 in Supplementary Table S16), indicating that these transcripts might be the common critical genes of silymarin and baicalein in alleviating NAFLD symptoms.

To further investigate characterization of DEGs, we performed enrichment analysis using the GO and KEGG pathway database. Supplementary Figures S3A,D depicts the enriched biological processes (BPs), cellular components (CCs), and molecular



functions (MFs) of the targets, which are mainly associated with response to baicalein. As shown in **Figure 2E**, the DEGs in the M group vs. the C group involved in the BPs related to angiogenesis, cell movement, extracellular matrix organization, and so on; the coding products of DEGs were mainly distributed in CCs, including the ribosome, extracellular matrix, cytosolic part, and basement membrane; as to the enriched MFs, the target proteins were mainly connected with structural constituent of ribosome, structural molecule activity, glycosaminoglycan

binding, growth factor binding, heparin binding, sulfur compound binding, extracellular matrix binding, platelet-derived growth factor binding, calcium ion binding, and cell adhesion molecule binding. In the treated groups (**Figures 2F–H**), compared with the M group, most of the BPs, CCs, and MFs related to DEGs which were affected by baicalein; especially the high-dose baicalein and silymarin were overlapped (**Supplementary Table S17**). **Figures 2E–H** show KEGG pathway enrichment analysis of DEGs. The results

indicated that baicalein exerting its protective effects against NAFLD was closely related to steroid biosynthesis, fatty acid degradation, the PPAR signaling pathway, peroxisome, tryptophan metabolism, ABC transporters, propanoate metabolism, valine, leucine and isoleucine degradation, 2-Oxocarboxylic acid metabolism, fatty acid metabolism, complement and coagulation cascades, ECM–receptor interaction, protein digestion and absorption, etc.

To verify the results of transcriptomic analysis, the expression of overlapped DEGs from three comparisons (P vs. M, L vs. M, and H vs. M) were detected by real-time PCR (**Figure 2I**). The expressions of *Apoa4*, *Pla2g12a*, *Elovl7*, *Slc27a4*, *Hilpda*, *Fabp4*, and *Vldlr* were all increased in the M group and reduced by the treatment of silymarin or baicalein. In contrast, the levels of *Gpld1* and *Apom* mRNA were decreased in the M group and positively regulated by silymarin or baicalein. The pathways associated with these genes were listed in **Supplementary Table S1**. Gene annotation, GO, and KEGG pathway analysis revealed that lipid metabolism–related pathways were significantly affected by baicalein.

Baicalein Changes Gut Microbiota in Non-Alcoholic Fatty Liver Disease Mice

The gut microbiome was assessed by 16S rRNA amplicon gene sequencing on an IonS5TMXL platform using specimen colonic luminal content samples of mice from C, M, P, L, and H groups. The α -diversity indexes including ACE, Chao1, Shannon, and Simpson were used to determine the ecological diversity within the microbial community. The ACE index reflecting the number of OTUs were 483.12 ± 78.15 , 473.83 ± 98.86 , and 318.11 ± 109.97 in M, L, and H groups, respectively (**Figure 3A**). The Chao1 indexes reflecting community richness were 489.72 ± 85.24 , 474.84 ± 102.03 , and 309.88 ± 112.08 in M, L, and H groups, respectively (**Figure 3B**). The Shannon indexes indicating both the species richness and evenness were 5.63 ± 0.24 , 5.75 ± 0.55 , and 4.71 ± 1.06 in M, L, and H groups, respectively (**Figure 3C**). Simpson indexes reflecting community evenness were 0.95 ± 0.01 , 0.95 ± 0.03 , and 0.89 ± 0.07 in M, L, and H groups, respectively (**Figure 3D**). β -diversity analysis was used to investigate the overall community structure. As shown in PCoA (**Supplementary Figure S4A**) and NMDS (**Figure 3E**), the M group was separated from the C group significantly, and the baicalein-treated groups (L and H) were separated from the M group; especially H groups were isolated from the M group completely. In line with these results, unweighted UPGMA indicated that significant separation appeared between the C, M, P, L, and H groups (**Figure 3F**). These analyses confirmed the effect of baicalein on the microbiome structure remodeling in NAFLD mice.

To investigate the dominant microorganisms in response to the baicalein treatment, we analyzed the relative abundance in the phylum (**Supplementary Figure S4B**) and genus level (**Supplementary Figure S4C**) of each group and the species with significantly different abundances in the different groups using the linear discriminant analysis (LDA) effect size (LEfSe) method (**Supplementary Figure S4D**; **Figure 3G**). In the comparison of the baicalein-treated groups and the NAFLD model group at different taxonomic levels (**Supplementary**

Figure S4D), the successive circles corresponding to five phylogenetic levels (phylum, class, family, class, and genus) indicated that the microbiota belonging to the *Deferribacteraceae* family, *Deferribacteraceae* order, unidentified_*Deferribacteres*, and *Peptococcaceae* family were enriched in the mice of the M group, whereas those belonging to the *Bacteroidaceae* family, *Lactobacillaceae* family, *Lactobacillales* order, and *Bacilli* class were enriched in the H group. In the P group, the *Peptostreptococcaceae* family was enriched. These results were also described in the LEfSe bar (**Figure 3G**). Also, the microbiota belonging to the *Clostridiales_bacterium_CIEAF_020* (the C group) and the unidentified_*Ruminococcaceae* genus (the L group) were found to be enriched (**Figure 3G**). Notably, there were four different bacterial genera between the M group and the L or H group (**Figures 3J,K**), of which three were the same (*Anaerotruncus*, *Lachnoclostridium*, and *Mucispirillum*). Besides, the abundance of *Lachnoclostridium* was also increased in P group (**Figure 3I**). Interestingly, these three genera significantly increased in the M group compared with the C group (**Figure 3H**) were all drastically decreased following baicalein treatment. These findings indicated an appreciable capability of the baicalein to recover the gut microbiota profile altered by the high-fat diet.

To reveal whether functional genes change with the structure of the gut microbiota, Tax4fun was employed to predict the bacterial functions of the members among different groups based on KEGG Orthology (KO) terms. According to the functional annotation and abundance information of samples in the database, the top 35 metabolic pathways, which were level 3 KEGG pathways, were selected to establish the heat map (**Supplementary Figure S4E**). The abundances of 10 unique pathways (K01955, K03088, K00936, K01153, K03046, K02004, K02003, K09687, K02470, and K02337) were higher in the M group than in the C group, while the remaining 25 pathways were lower, as determined by Student's *t*-test (*p*-value < 0.05). However, silymarin and low and high concentration of baicalein could restore the abundances of five pathways (K02004, K01153, K02337, K03046, and K07497), while the abundances of 12 pathways, including K03088, K03763, K03737, K04759, K06147, K02529, K03798, K03657, K02026, K02027, K02025, and K03406, were restored by silymarin or low concentration of baicalein.

Variations of Metabolomic Profiling in Liver of Non-Alcoholic Fatty Liver Disease Mice

To investigate the effects of baicalein on the metabolic profiling in NAFLD mice, LC-MS was used to analyze the extract from liver tissue of each group. Under the positive ion mode, data of 845 metabolites were used in partial least squares discriminant analysis (PLS-DA). As shown in **Figure 4A**, the M group and the C group could be clearly separated in the *x*-axis direction. The model quality was determined by parameters R2Y and Q2Y (R2Y = 0.99, Q2Y = 0.94). In addition, under the negative analysis ion mode, the PLS-DA score plot also showed a clear separation between the M and C groups (R2Y = 1.0 and Q2Y = 0.95) (**Supplementary Figure S5A**). Similarly, the significant

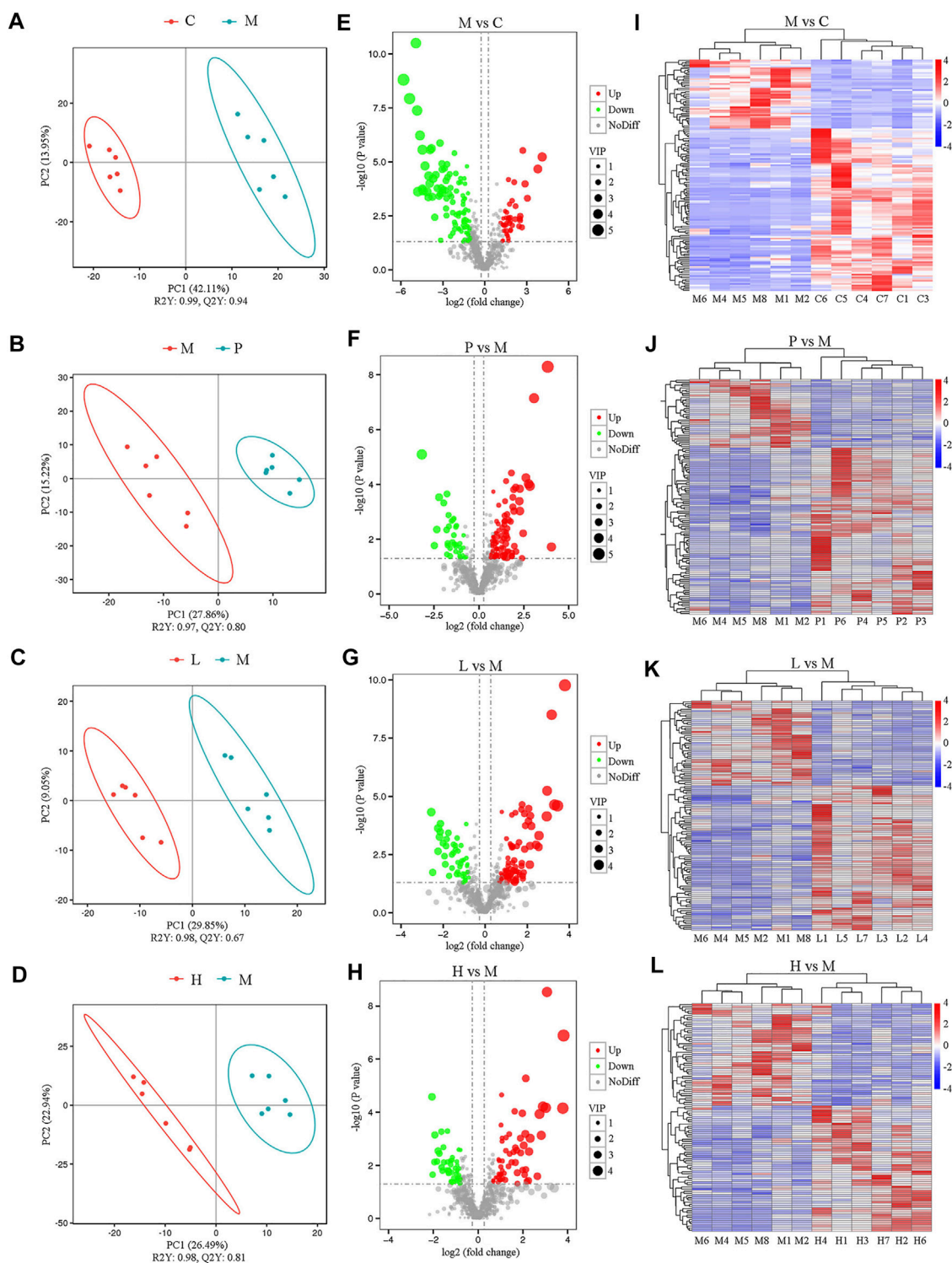


FIGURE 4 | Metabolomic analysis among five groups under the positive ion mode ($n = 6$). The separation of two groups was accessed by partial least square-discriminate analysis (PLS-DA) [(A) M vs. C; (B) P vs. M; (C) L vs. M; and (D) H vs. M]. Volcano plot indicates the differentially expressed metabolites between the groups [(E) M vs. C; (F) P vs. M; (G) L vs. M; and (H) H vs. M]. Heat map shows the differential expression of metabolites between groups [(I) M vs. C; (J) P vs. M; (K) L vs. M; and (L) H vs. M].

separation was also observed between the M group and the P, L, or H group (Figures 4B–D). Besides, under the negative ion mode, the PLS-DA score plot also showed a clear separation between the M group and treatment groups (P, L, and H groups) (Supplementary Figures S5B–D). Therefore, the PLS-DA model could sufficiently explain the variance between these two groups.

Furthermore, significantly differential metabolites were identified according to the following criteria: PLS-DA VIP (variable importance in the projection) > 1, fold change > 1.5 and FDR < 0.05. We identified 148 metabolites that were differentially expressed in the M group as compared with the C group under the positive ion mode (Supplementary Table S18). Among significantly differential metabolites, 44 metabolites (Urobilinogen, 13-deoxydanolide, 8-Azaadenosine, UROBILIN, Patidegib, p-Hydroxyketorolac, Bicyclomycin, S-[(1Z)-N-Hydroxy-5-(methylsulfanyl)pentanimidoyl]cysteine, Perflubron, Meptin, and so forth) were upregulated, while the remaining compounds were downregulated in the M group (Supplementary Table S18). Compared with the M group, there were 88, 77, and 58 metabolites upregulated and 36, 45, and 47 metabolites downregulated in the P (Supplementary Table S19), L (Supplementary Table S20), and H (Supplementary Table S21) groups, respectively. All these metabolites were included in the multivariate analysis, as shown in volcano plots (Figures 4E–H) and heatmaps (Figures 4I–L). Similar results were also observed under the negative analysis ion mode (Supplementary Figures S5E–L). These results suggested that baicalein treatment led to significant metabolic alterations in mouse liver.

KEGG pathway enrichment analysis was performed to determine the effect of baicalein on related pathways in NAFLD mice (Supplementary Figure S6). Compared with the C group, there were 11 related metabolic pathways under positive ion mode, and 13 related metabolic pathways in negative mode in the M group. The results indicated that primary bile acid biosynthesis ($p = 3.98 \times 10^{-2}$) and alpha-Linolenic acid metabolism ($p = 3.98 \times 10^{-2}$) were both downregulated in the M group and restored by silymarin (P group, $p = 5.73 \times 10^{-2}$) and baicalein (L group, $p = 3.21 \times 10^{-2}$). Additionally, silymarin and low concentration of baicalein might modulate 2-Oxocarboxylic acid metabolism ($p = 5.73 \times 10^{-2}$ in the P group and $p = 3.21 \times 10^{-2}$ in the L group). Interestingly, high concentration of baicalein could affect 2-Oxocarboxylic acid metabolism ($p = 1.91 \times 10^{-2}$ in positive ion mode), Pantothenate and CoA biosynthesis ($p = 2.41 \times 10^{-2}$ in negative ion mode), and bile secretion ($p = 4.96 \times 10^{-2}$ in negative ion mode) (Supplementary Figures S6D,H). Taken together, baicalein was closely associated with altered alpha-Linolenic acid, 2-Oxocarboxylic acid, Pantothenate and CoA biosynthesis, and bile secretion.

Integrated Analysis of the Mechanism of Baicalein Treated Mice From Metabolomic and Transcriptomic Data

To explore the potential relationship between DEGs and differential metabolites in the liver, metabolomic and transcriptomic data were integrated. Compared with the C

group, a total of 12 pathways were listed under the negative ion mode (as shown in Supplementary Figure S7A, such as Porphyrin and chlorophyll metabolism, Platelet activation, Drug metabolism—cytochrome P450, Protein digestion and absorption, Cholesterol metabolism, Steroid hormone biosynthesis, and so forth) and 11 ones (as shown in Figure 5A, such as Primary bile acid biosynthesis, alpha-Linolenic acid metabolism, Retinol metabolism, and Cholesterol metabolism) in the positive ion mode in the M group. Compared with the M group, the significantly differential metabolites in the P (Figure 5B), L (Figure 5C), and H (Figure 5D) groups were involved in 17, 11, and 8 pathways, respectively, under the positive ion mode, while there were 8 (Supplementary Figure S7B), 13 (Supplementary Figure S7C), and 13 (Supplementary Figure S7D) pathways, respectively, under the negative ion mode. Among them, steroid hormone biosynthesis, cholesterol metabolism, primary bile acid biosynthesis, bile secretion, and drug metabolism—cytochrome P450 might play an important role in the process of baicalein and silymarin ameliorating NAFLD symptoms. Besides, low concentration of baicalein affected three pathways (including Serotonergic synapse, Protein digestion, and absorption and Platelet activation), which were also altered in the M group. Notably, low and high dose of baicalein both affected fatty acid biosynthesis, and high dose of baicalein also modulated some different pathways, such as fatty acid degradation, fat digestion, and absorption, pantothenate and CoA biosynthesis, vitamin digestion and absorption, beta-alanine metabolism, ferroptosis, starch and sucrose metabolism, cholinergic synapse, and retrograde endocannabinoid signaling. There is also a heat map of integrated analysis between differential metabolite expression patterns and transcriptomics under the positive ion mode (Figures 5E–H) and negative ion mode (Supplementary Figures S7E–H). Taken together, baicalein mainly targeted the pathways associated with biosynthesis and secretion of bile acid, such as cholesterol metabolism and steroid hormone biosynthesis and the pathways related to lipid metabolism including fatty acid degradation, fat digestion and absorption, and so on. These were consistent with the results of real-time PCR described above (Figure 2I). For example, *Apoa4* plays a role in fat digestion and absorption, cholesterol metabolism, and atherosclerosis; *Pla2g12a* functions in Glycerophospholipid metabolism, ether lipid metabolism, arachidonic acid metabolism, linoleic acid metabolism, and fat digestion and absorption; *Elovl7*, *Slc27a4*, *Hilpda*, and *Fabp4* are all involved in lipid metabolism (Supplementary Table S1).

Association of the Non-Alcoholic Fatty Liver Disease-Induced Gut Microbial Dysbiosis With Dysregulation Metabolites

To further explore the potential association between gut microbiota and liver metabolome in NAFLD mice, the top 20 differentially expressed metabolites and the top 10 altered microbial genera between two groups were analyzed by Pearson's correlation analysis. As Figure 6 displayed, the typical metabolites of physiological function were highly linked

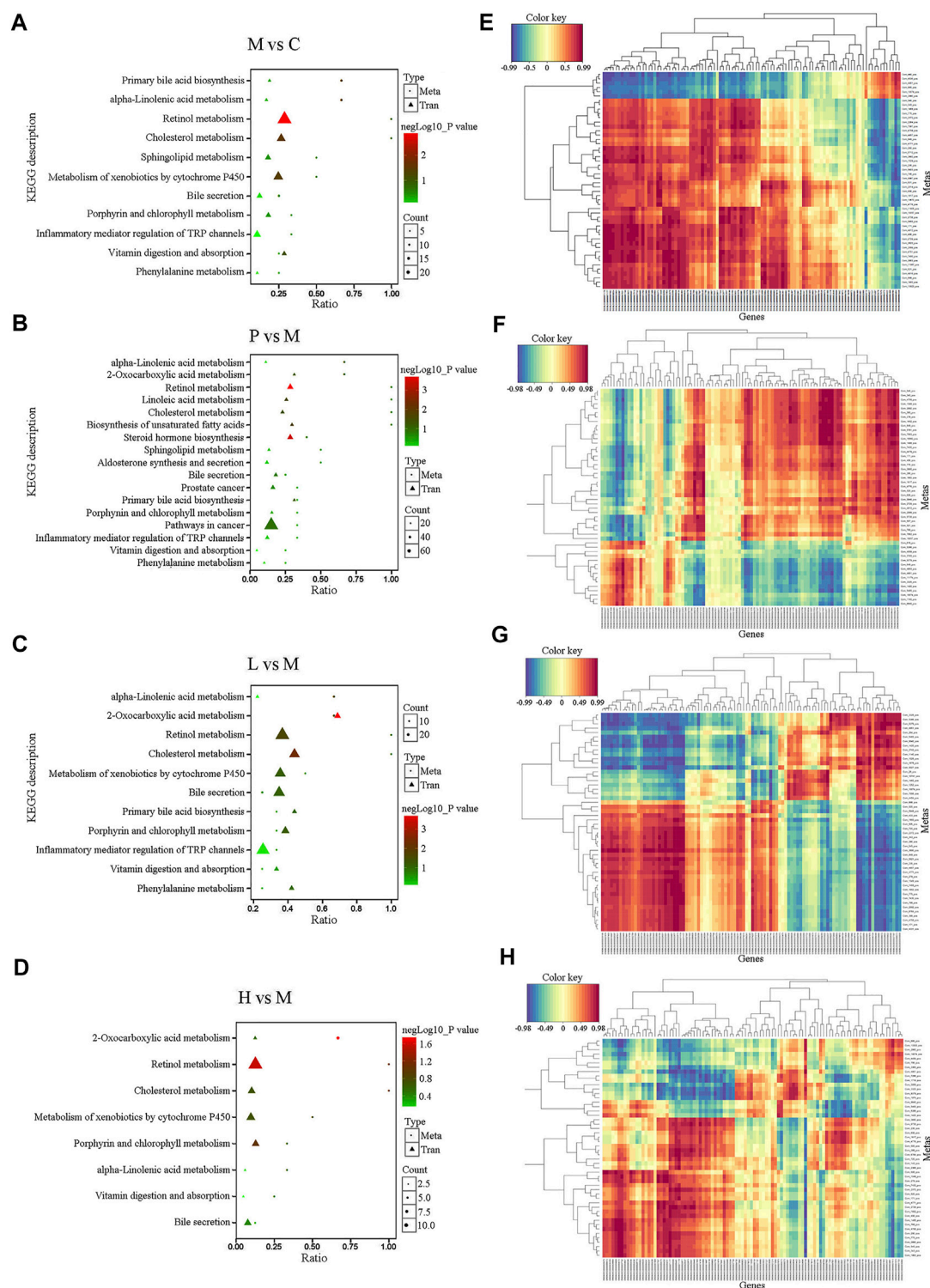


FIGURE 5 | Integrated analysis of the metabolomic and transcriptomic data under the positive ion mode. **(A–D)** Integrated altered metabolic pathways according to the metabolomic and transcriptomic data. The horizontal axis shows the ratio of differential expressed genes and the vertical axis indicated the pathway name [**(A)** M vs. C; **(B)** P vs. M; **(C)** L vs. M; and **(D)** H vs. M]. **(E–H)** Integrated analysis using metabolomic and transcriptomic data. The horizontal axis shows the clustering of differential expressed transcripts and the vertical axis indicated the clustering of differential expressed metabolites. The red depth represents the strength of the positive correlation. The blue depth represents the negative correlation [**(E)** M vs. C; **(F)** P vs. M; **(G)** L vs. M; and **(H)** H vs. M].

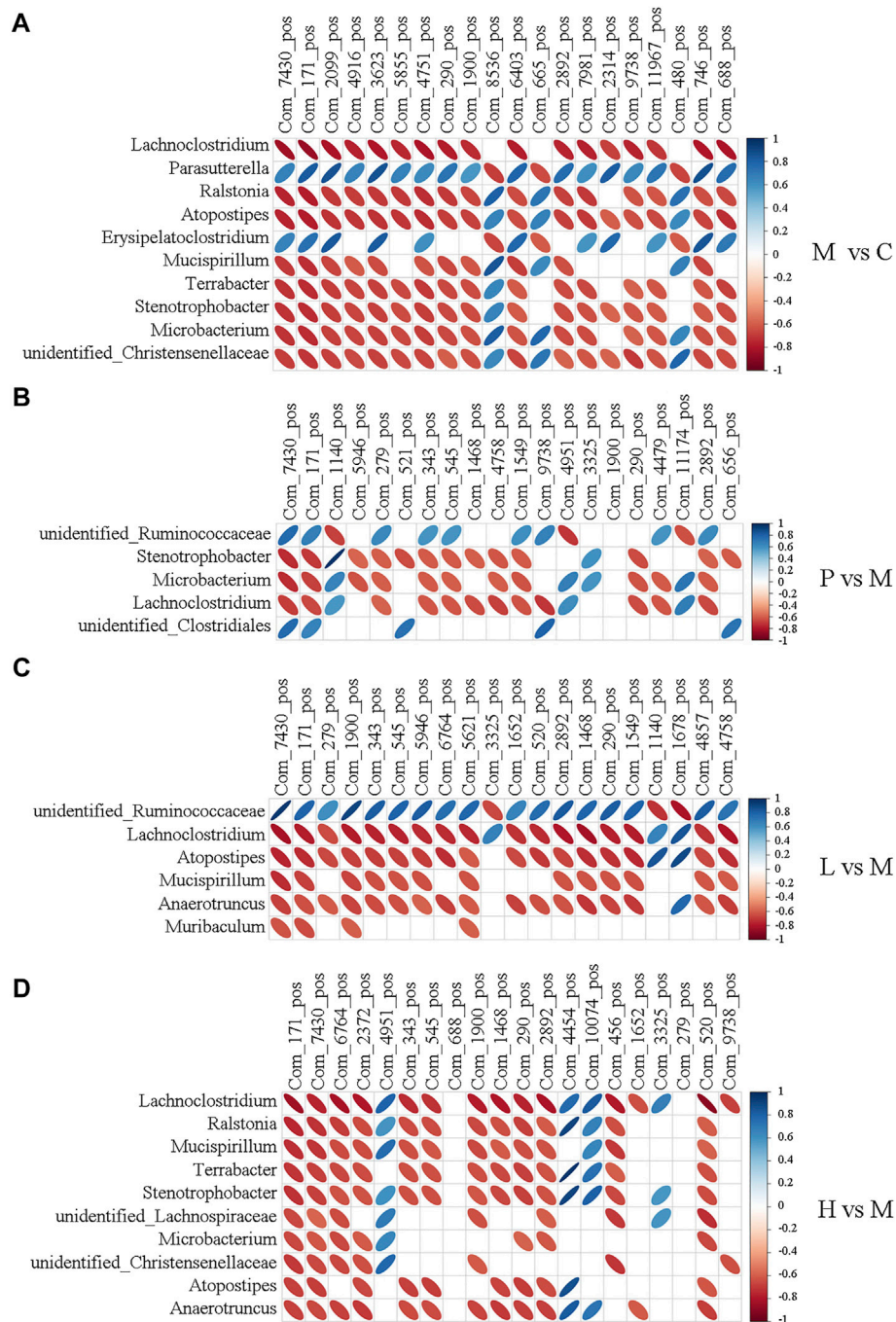


FIGURE 6 | Heatmap describing the correlation analysis of relative abundance of gut microbiota in the genus level and liver metabolite levels under the positive ion mode. **(A)** M vs. C; **(B)** P vs. M; **(C)** L vs. M; and **(D)** H vs. M. The horizontal axis shows the top 20 of the differential metabolites in the comparison pair, the left vertical axis shows the differential bacteria, and the right means the correlation coefficient. Blue indicates positive correlation and red indicates negative correlation.

to specific gut bacteria by calculating Pearson's correlation coefficient. For instance, compared with the C group, the abundance of *Lachnospirillum* showed a significantly negative correlation with 17 metabolites except Patidegib, urobilinogen, and 13-deoxytendanolide in the M group. 2-Hydroxyimipramine and L-Ergothioneine, which decreased to

less than 4% and 2% in the C group, were positively associated with *Parasutterella* ($r = 0.665$ and 0.822) and *Erysipelatoclostridium* ($r = 0.657$ and 0.739) and negatively correlated with *Lachnospirillum* ($r = -0.83$ and -0.857), *Microbacterium* ($r = -0.718$ and -0.736), *Ralstonia* ($r = -0.755$ and -0.774), *Atopostipes* ($r = -0.752$ and -0.773),

Mucispirillum ($r = -0.697$ and -0.72), *Terrabacter* ($r = -0.717$ and -0.738), *Stenotrophobacter* ($r = -0.716$ and -0.739), and unidentified_*Christensenellaceae* ($r = -0.682$ and -0.703). Notably, baicalein treatment clearly regulated the level of 2-Hydroxyimipramine and L-Ergothioneine. They were negatively associated with *Lachnoclostridium*, *Atopostipes*, *Mucispirillum*, *Anaerotruncus*, and *Muribaculum* except unidentified_*Ruminococcaceae* in the L group. However, they were negatively associated with *Lachnoclostridium*, *Ralstonia*, *Mucispirillum*, *Terrabacter*, *Stenotrophobacter*, unidentified_*Lachnospiraceae*, *Microbacterium*, unidentified_*Christensenellaceae*, *Atopostipes*, and *Anaerotruncus* in the H group. The abundances of *Lachnoclostridium*, *Atopostipes*, *Mucispirillum*, and *Anaerotruncus* were all decreased in the L and H groups (Figures 3J,K), and the first three were increased in the M group (Figure 3H). The results were also observed under the negative ion mode (Supplementary Figure S8). L-Ergothioneine, which is a metabolite with anti-oxidant activity, protects the liver against lipid peroxidation and is also involved in histidine metabolism. Our findings indicated that the abundance of L-Ergothioneine was affected by some microbial genera which were regulated by baicalein. Therefore, baicalein affected lipid metabolism in the liver by regulating the ecological structure of gut microbiota in NAFLD mice.

DISCUSSION

The pathogenesis of NAFLD is complex. Nowadays, the “multiple-hit model” is the theory widely accepted. The metabolic dysfunction induced by the genetic defects, environmental factors, and abnormal interaction of the organs and tissues is identified as the direct cause of NAFLD. However, fat accumulation in the liver seems to be the “first hits” (Fang et al., 2018). Triglycerides derived from the esterification of glycerol and free fatty acids (FFAs) are the main form of fat accumulated in the liver (Musso et al., 2013). Insulin resistance (IR) is a critical stage and risk factor in the progression of NAFLD. IR promotes liver lipid synthesis and inhibits liver fatty acid β -oxidation and lipolysis of fat. Consequently, lipids accumulate in the liver, and finally, hepatocyte fatty lesions occur (Stols-Gonçalves et al., 2019).

However, the available therapeutic options are very limited so far. Currently, the main treatment strategies against NAFLD include lifestyle change (diet and exercise), anti-oxidant treatment (such as vitamin 4), and regulation of body metabolism and lipid regulation. Silymarin, which is a complex mixture of flavonolignan isomers, namely, silybin, isosilybin, silydianin, and silychristin, from *Silybum marianum* (milk thistle), has been proved to be effective in treating liver diseases including NAFLD. Silymarin has been widely used in the treatment of acute or chronic hepatitis (Tighe et al., 2020). Baicalein is also a natural flavonoid extracted from plants. Growing evidence has indicated the anti-oxidant, anti-inflammatory, and antitumor activities of baicalein. In this study, we proved that baicalein significantly protected liver

function against HFD-induced NAFLD (Figure 1). In terms of therapeutic effect, baicalein is slightly stronger than silymarin.

Gut microbiota, including bacteria, fungi, parasites, and viruses, inhabits the gastrointestinal tract. Increasing evidence indicated that gut microbiota plays an important role in maintaining the integrity of the intestinal epithelium, defense against pathogens, regulating the host immunity, harvesting energy, and regulating metabolism. In healthy adults, *Firmicutes*, *Bacteroidetes*, *Actinobacteria*, and *Proteobacteria* are the top 4 phyla in abundance. The abundance of these bacterial phyla is usually related to some pathologic conditions, including NAFLD. In NAFLD, the microbial diversity is usually decreased, with the increased relative abundance of species of the *Proteobacteria* and *Bacteroidetes* phyla and the *Enterobacteriaceae* family and the *Escherichia* genera and reduced relative abundance of the *Firmicutes* phylum and the *Prevotellaceae* family. Consequently, lipopolysaccharide (LPS) translocation is increased, short-chain fatty acids (SCFA) produced by gut microbiota are decreased, and the production of endogenous ethanol is increased, and then inflammations occur. Le Roy and colleagues believed that intestinal microbiota allows the transfer of disease phenotype and liver steatosis by conducting gut microbiota transplant experiments (Le Roy et al., 2013). Alterations of gut microbiota composition affect the expression of intestinal and hepatic genes related to the metabolic process and the onset of inflammation (Membrez et al., 2008). In this study, we identified that the composition of gut microbiota was extremely changed in NAFLD mice compared with the control group, and the treatment of baicalein as well as silymarin could restore the abundance of some genera, especially the abundances of *Anaerotruncus*, *Lachnoclostridium*, and *Mucispirillum* that were decreased under the treatment of silymarin and low or high dose of baicalein (Figure 3). The abundance of *Anaerotruncus* and *Mucispirillum* were proved increased in high-fat/high-cholesterol-fed mice and related to NAFLD-associated hepatocellular carcinoma development (Zhang et al., 2021). The relative abundance of *Lachnoclostridium* associated with inflammation-mediated obesity (Rondina et al., 2013) was remarkably higher in the HFD group than in the control group and positively correlated with the fructose levels in feces (Jo et al., 2021). Therefore, gut microbiota seems to be the potential therapeutic target of baicalein against NAFLD.

Recently, gut microbiota is considered to be an important “organ” of the body, which can affect a variety of physiological processes. Dao et al. (2021) believed that gut microbiota altered by high-fat diet could modulate the retinal transcriptome, and they proposed a diet-microbiome-retina axis to reveal how diet affects the pathogenesis and severity of retinal diseases. Another report showed that gut microbiota from young donors could reprogram the circadian clock of the lacrimal gland by transcriptomic analysis (Jiao et al., 2021). A study on NAFLD demonstrated that appropriate WLT supplementation could regulate gut microbial composition, reduce intestinal permeability and liver inflammation, and then prevent NAFLD (Chen et al., 2021). Therefore, gut microbiota can affect the gene expression of a variety of tissues, including the liver, and then play

a regulatory role in human diseases. In this study, we found that compared with the control mice, the gut microbial composition of NAFLD mice was changed significantly, and baicalein could restore the relative abundance of some bacteria. Based on the analysis of liver transcriptome, we found that many transcripts changed by baicalein overlapped with those changed by silymarin. Silymarin is considered a natural drug that can effectively resist liver inflammation and is used clinically in the treatment of NAFLD. The expressions of several genes related to lipid metabolism were verified by real-time PCR to confirm the alteration of liver metabolites (**Figure 2I**). For example, *Apoa4*, *Pla2g12a*, and *Slc27a4*, which all promote fat digestion and absorption, were negatively regulated by silymarin and baicalein. *Gpld1* and *Apom*, which are both the positive regulators of lipid metabolism, were increased by baicalein. Therefore, compared with silymarin, we believe that baicalein has a similar function of alleviating NAFLD, and there might be a crosstalk in the mechanism.

Gut microbiota also regulate the choline metabolism and then affect the accumulation level of hepatic triglycerides (Panasevich et al., 2017). The bile acid-farnesoid X receptor (FXR) may be an important participant in the process of gut microbiota modulating body weight and hepatic steatosis in mice (Parséus et al., 2017). The fasting-induced adipocyte factor (FIAF) reduced by gut microbiota was proved to exacerbate the accumulation of hepatic triglycerides (Roopchand et al., 2015). Besides, gut microbiota-mediated excess of short-chain fatty acids (SCFAs) in the liver reduces the activity of adenosine-monophosphate activated protein kinase (AMPK), leading to the accumulation of hepatic free fatty acids (Wang et al., 2020). With the analysis of liver metabolome, we found that primary bile acid biosynthesis and alpha-linolenic acid metabolism were downregulated in NAFLD mice and restored by baicalein and silymarin. Previous studies have proved that fatty acids, bile acids, and amino acids are involved in the development of hyperlipidemia (Li et al., 2018; Liu et al., 2019). The pathogenesis of NAFLD is due to the accumulation of excessive lipid in hepatocytes, which is induced by the transfer of excessive NEFA from adipose tissue to the liver, the increase in fat synthesis, the reduction of fatty acid β -oxidation, and bile acid excretion (Tang et al., 2019). Bile acids are produced from cholesterol in hepatocytes and regulate insulin secretion and glycolipid metabolism. Guo et al. (2020) found that Ganoderic acid A ameliorated hyperlipidemia and gut microbiota dysbiosis in HFD-induced hyperlipidemic mice, and bile acid metabolism was positively regulated by Ganoderic acid A. Alpha-linolenic acid is a metabolite with antioxidant activity. Lianqun et al. found that alpha-linolenic acid metabolism was significantly downregulated in hyperlipidemia model mice. After ginsenoside Rb1 intervention, gut microbiota of mice was remarkably changed and alpha-linolenic acid metabolism was clearly upregulated (Lianqun et al., 2021). In the research on human schizophrenia, Fan et al. (2022) discovered a significant correlation between serum differential metabolites and differential intestinal bacteria between the patients with schizophrenia and the healthy individuals, while the metabolism of anti-inflammatory metabolites (such as alpha-linolenic acid) might be the regulatory target of gut microbiota.

Therefore, the primary bile acid biosynthesis and alpha-linolenic acid metabolism are closely related to lipid metabolism. In the integrative analysis of multi-omics, we found that there was a significant correlation between the relative abundance of altered intestinal bacterial genera and the levels of various metabolites. For example, the relative abundance of *Lachnocostridium*, *Atopodipes*, *Mucispirillum*, and *Anaerotruncus* was significantly restored to the normal level in the baicalein treatment group and had a clear negative correlation with the level of some metabolites. For example, L-Ergothioneine was enriched in Histidine metabolism, and Traumatic acid was enriched in alpha-linolenic acid metabolism. Thus, baicalein intervention could significantly improve a considerable number of pathways, including the primary bile acid biosynthesis and alpha-linolenic acid metabolism, and the associated mechanisms might be the direct regulation by baicalein, indirect modulation by baicalein *via* gut microbiota, or the comprehensive effect of multiple mechanisms affected by baicalein.

In conclusion, baicalein may affect the microbial community structure in the intestine on the one hand and affect the expression of liver transcriptome through its own metabolism on the other hand and then affect the hepatic fatty acid metabolism against NAFLD. However, this study only focused on intestinal bacteria, and the role of intestinal fungi and other microorganisms in NAFLD is unknown. Moreover, the mechanism of how intestinal microorganisms respond to baicalein and then affect the expression of liver transcripts is unclear. Therefore, we will further investigate the intestinal fungi and other microorganisms in NAFLD mice and analyze the role of intestinal endothelial cells in the function of gut microbiota, hoping to uncover the molecular mechanism of baicalein in alleviating NAFLD.

DATA AVAILABILITY STATEMENT

The datasets presented in this study can be found in online repositories. The names of the repository/repositories and accession number(s) can be found in the article/**Supplementary Material**.

ETHICS STATEMENT

The animal study was reviewed and approved by the Committee on the Ethics of Scientific Research of Shanxi Medical University.

AUTHOR CONTRIBUTIONS

Conceptualization, PL and BC. Methodology, PL, JH, and BC. Validation, PL and JH. Formal analysis, PL, JH, and JF. Investigation, PL and JH. Resources, PL and JH. Data curation, PL, JH, and HZ. Writing—original draft preparation, PL. Writing—review and editing, BC. Visualization, PL and JH.

Supervision, BC. Project administration, BC. Funding acquisition, PL and BC. All authors have read and agreed to the published version of the manuscript.

FUNDING

This research was funded by grants from the National Natural Science Foundation of China (No. 31772450) and the Special Foundation for Postdoctoral in Shanxi Province.

SUPPLEMENTARY MATERIAL

The Supplementary Material for this article can be found online at: <https://www.frontiersin.org/articles/10.3389/fphar.2022.925349/full#supplementary-material>

Supplementary Figure S1 | Effects of baicalein on high-fat diet-induced hyperglycemia. **(A)** Scores of steatosis, inflammation and ballooning, and Liver NAS score. **(B)** Fasting blood glucose (mM); **(C)** Fasting serum insulin (mU/mL). Data are presented as mean \pm SD ($n=10$). ** $p < 0.01$, * $p < 0.05$, compared with the C group; ## $p < 0.01$, # $p < 0.05$, compared with the M group.

Supplementary Figure S2 | DEGs involved in C, M, P, L, and H groups ($n=3$). **(A)** The heatmap showing the DEGs involved in five groups. **(B)** The Venn diagram indicating the DEGs overlapped in three comparisons, M vs. P, M vs. L, and M vs. H.

Supplementary Figure S3 | DEGs were enriched in the GO database ($n=3$). **(A)** M vs. C; **(B)** P vs. M; **(C)** L vs. M; **(D)** H vs. M.

Supplementary Figure S4 | Community composition of gut microbiota was regulated after treatment with baicalein ($n=6$). **(A)** Principal coordinate analysis (PCoA) based on the unweighted UniFrac analysis calculated using QIIME software. Effects of baicalein on the composition of the microbiota at phylum **(B)** and genus **(C)** levels. **(D)** LefSe analysis based on the linear discriminant analysis (LDA). **(E)** Heatmap showing the specific annotated information of each KEGG orthologous group (KO) in the metabolic pathway.

Supplementary Figure S5 | Metabolic alterations after baicalein treatment in the liver under the negative ion mode ($n=6$). Partial least squares discriminant analysis (PLS-DA) was used to show the separation between two groups, including M and C **(A)**, P and M **(B)**, L and M **(C)**, and H and M **(D)**. The differential metabolites were displayed in the volcano plots **(E)** M vs. C; **(F)** P vs. M; **(G)** L vs. M; **(H)** H vs. M and heatmaps **(I)** M vs. C; **(J)** P vs. M; **(K)** L vs. M; **(L)** H vs. M.

Supplementary Figure S6 | KEGG pathway enrichment analysis under the positive and the negative ion mode ($n=6$). **(A–D)** showed the differential metabolites between M and C, P and M, L and M, and H and M, respectively, under the positive ion mode. **(E–H)** indicated the differential metabolites under the negative ion mode.

Supplementary Figure S7 | Integrated analysis of the relationship between DEGs and differential metabolites in the liver under the negative ion mode. **(A–D)** Integrated altered metabolic pathways according to the metabolomic and transcriptomic data. The horizontal axis shows the ratio of differential expressed genes and the vertical axis indicated the pathway name **(A)** M vs. C; **(B)** P vs. M; **(C)** L vs. M; **(D)** H vs. M. **(E–H)** Integrated analysis using metabolomic and transcriptomic data. The horizontal axis shows the clustering of differential expressed transcripts and the vertical axis indicated the clustering of differential expressed metabolites. The red depth represents the strength of the positive correlation. The blue depth represents the negative correlation **(E)** M vs. C; **(F)** P vs. M; **(G)** L vs. M; **(H)** H vs. M.

REFERENCES

Chen, J., Thomsen, M., and Vitetta, L. (2019). Interaction of Gut Microbiota with Dysregulation of Bile Acids in the Pathogenesis of Nonalcoholic Fatty Liver

Supplementary Figure S8 | Heatmap describing the correlation analysis of relative abundance of gut microbiota in the genus level and liver metabolite levels under the negative ion mode. **(A)** M vs. C; **(B)** P vs. M; **(C)** L vs. M; **(D)** H vs. M. The horizontal axis shows the top 20 of the differential metabolites in the comparison pair, the left vertical axis shows the differential bacteria, and the right means the correlation coefficient. Blue indicates positive correlation and red indicates negative correlation.

Supplementary Table S1 | Genes detected by real-time PCR.

Supplementary Table S2 | Number of DEGs between groups.

Supplementary Table S3 | Transcripts upregulated in the M group compared with the C group.

Supplementary Table S4 | Transcripts downregulated in the M group compared with the C group.

Supplementary Table S5 | Transcripts upregulated in the P group compared with the M group.

Supplementary Table S6 | Transcripts downregulated in the P group compared with the M group.

Supplementary Table S7 | Transcripts restored to the normal level in the P group.

Supplementary Table S8 | Transcripts upregulated in the L group compared with the M group.

Supplementary Table S9 | Transcripts downregulated in the L group compared with the M group.

Supplementary Table S10 | Transcripts restored to the normal level in the L group.

Supplementary Table S11 | Transcripts upregulated in the H group compared with the M group.

Supplementary Table S12 | Transcripts downregulated in the H group compared with the M group.

Supplementary Table S13 | Transcripts restored to the normal level in the H group.

Supplementary Table S14 | DEGs overlapped in the L group vs the M group and the H group vs the M group.

Supplementary Table S15 | Transcripts positively regulated by baicalein.

Supplementary Table S16 | Transcripts negatively regulated by baicalein.

Supplementary Table S17 | GO pathways overlapped in P, L, and H groups.

Supplementary Table S18 | Differential metabolites in the M and C groups under the positive ion model.

Supplementary Table S19 | Differential metabolites in the P and M groups under the positive ion model.

Supplementary Table S20 | Differential metabolites in the L and M groups under the positive ion model.

Supplementary Table S21 | Differential metabolites in the H and M groups under the positive ion model.

Supplementary Table S22 | Information of the top 20 correlated differential metabolites in M vs C.

Supplementary Table S23 | Information of the top 20 correlated differential metabolites in P vs M.

Supplementary Table S24 | Information of the top 20 correlated differential metabolites in L vs M.

Supplementary Table S25 | Information of the top 20 correlated differential metabolites in H vs M.

Disease and Potential Therapeutic Implications of Probiotics. *J. Cell Biochem.* 120 (3), 2713–2720. doi:10.1002/jcb.27635

Chen, L., Kan, J., Zheng, N., Li, B., Hong, Y., Yan, J., et al. (2021). A Botanical Dietary Supplement from White Peony and Licorice Attenuates Nonalcoholic Fatty Liver Disease by Modulating Gut Microbiota and

- Reducing Inflammation. *Phytomedicine* 91, 153693. doi:10.1016/j.phymed.2021.153693
- Dao, D., Xie, B., Nadeem, U., Xiao, J., Movahedan, A., D'Souza, M., et al. (2021). High-Fat Diet Alters the Retinal Transcriptome in the Absence of Gut Microbiota. *Cells* 10 (8), 2119. doi:10.3390/cells10082119
- Doulberis, M., Kotronis, G., Gialampirinou, D., Kountouras, J., and Katsinelos, P. (2012). Non-alcoholic Fatty Liver Disease: An Update with Special Focus on the Role of Gut Microbiota. *Metabolism* 71, 182–197. doi:10.1016/j.metabol.2017.03.013
- Fan, Y., Gao, Y., Ma, Q., Yang, Z., Zhao, B., He, X., et al. (2022). Multi-Omics Analysis Reveals Aberrant Gut-Metabolome-Immune Network in Schizophrenia. *Front. Immunol.* 13, 812293. doi:10.3389/fimmu.2022.812293
- Fang, Y. L., Chen, H., Wang, C. L., and Liang, L. (2018). Pathogenesis of Non-alcoholic Fatty Liver Disease in Children and Adolescence: From "two Hit Theory" to "multiple Hit Model". *World J. Gastroenterol.* 24 (27), 2974–2983. doi:10.3748/wjg.v24.i27.2974
- Ferramosca, A., and Zara, V. (2014). Modulation of Hepatic Steatosis by Dietary Fatty Acids. *World J. Gastroenterol.* 20 (7), 1746–1755. doi:10.3748/wjg.v20.i7.1746
- Gkolafakis, P., Dimitriadis, G., and Triantafyllou, K. (2015). Gut Microbiota and Non-alcoholic Fatty Liver Disease. *Hepatobiliary Pancreat. Dis. Int.* 14 (6), 572–581. doi:10.1016/s1499-3872(15)60026-1
- Golabi, P., Paik, J. M., AlQahtani, S., Younossi, Y., Tuncer, G., and Younossi, Z. M. (2021). Burden of Non-alcoholic Fatty Liver Disease in Asia, the Middle East and North Africa: Data from Global Burden of Disease 2009–2019. *J. Hepatol.* 75 (4), 795–809. doi:10.1016/j.jhep.2021.05.022
- Guo, W. L., Guo, J. B., Liu, B. Y., Lu, J. Q., Chen, M., Liu, B., et al. (2020). Ganoderic Acid A from *Ganoderma lucidum* Ameliorates Lipid Metabolism and Alters Gut Microbiota Composition in Hyperlipidemic Mice Fed a High-Fat Diet. *Food Funct.* 11 (8), 6818–6833. doi:10.1039/d0fo00436g
- Hong, M., Han, D. H., Hong, J., Kim, D. J., and Suk, K. T. (2019). Are Probiotics Effective in Targeting Alcoholic Liver Diseases? *Probiotics Antimicrob. Proteins* 11 (2), 335–347. doi:10.1007/s12602-018-9419-6
- Jiao, X., Pei, X., Lu, D., Qi, D., Huang, S., He, S., et al. (2021). Microbial Reconstitution Improves Aging-Driven Lacrimal Gland Circadian Dysfunction. *Am. J. Pathol.* 191 (12), 2091–2116. doi:10.1016/j.ajpath.2021.08.006
- Jo, J. K., Seo, S. H., Park, S. E., Kim, H. W., KimKim, E. J. J. S., Kim, J. S., et al. (2021). Gut Microbiome and Metabolome Profiles Associated with High-Fat Diet in Mice. *Metabolites* 11 (8), 482. doi:10.3390/metabo11080482
- Katsiki, N., Mikhailidis, D. P., and Mantzoros, C. S. (2016). Non-alcoholic Fatty Liver Disease and Dyslipidemia: An Update. *Metabolism* 65 (8), 1109–1123. doi:10.1016/j.metabol.2016.05.003
- Kleiner, D. E., Brunt, E. M., Van Natta, M., Behling, C., Contos, M. J., Cummings, O. W., et al. (2005). Design and Validation of a Histological Scoring System for Nonalcoholic Fatty Liver Disease. *Hepatology* 41 (6), 1313–1321. doi:10.1002/hep.20701
- Lambertz, J., Weiskirchen, S., Landert, S., and Weiskirchen, R. (2017). Fructose: A Dietary Sugar in Crosstalk with Microbiota Contributing to the Development and Progression of Non-alcoholic Liver Disease. *Front. Immunol.* 8, 1159. doi:10.3389/fimmu.2017.01159
- Le Roy, T., Llopis, M., Lepage, P., Bruneau, A., Rabot, S., Bevilacqua, C., et al. (2013). Intestinal Microbiota Determines Development of Non-alcoholic Fatty Liver Disease in Mice. *Gut* 62 (12), 1787–1794. doi:10.1136/gutjnl-2012-303816
- Li, C., Cao, J., Nie, S.-P., Zhu, K.-X., Xiong, T., and Xie, M.-Y. (2018). Serum Metabolomics Analysis for Biomarker of *Lactobacillus Plantarum* NCU116 on Hyperlipidaemic Rat Model Fed by High Fat Diet. *J. Funct. Foods* 42, 171–176. doi:10.1016/j.jff.2017.12.036
- Li, P., Hu, J., Shi, B., and Tie, J. (2020). Baicalein Enhanced Cisplatin Sensitivity of Gastric Cancer Cells by Inducing Cell Apoptosis and Autophagy via Akt/mTOR and Nrf2/Keap 1 Pathway. *Biochem. Biophys. Res. Commun.* 531 (3), 320–327. doi:10.1016/j.bbrc.2020.07.045
- Lianqun, J., Xing, J., Yixin, M., Si, C., Xiaoming, L., Nan, S., et al. (2021). Comprehensive Multiomics Analysis of the Effect of Ginsenoside Rb1 on Hyperlipidemia. *Aging (Albany NY)* 13 (7), 9732–9747. doi:10.18632/aging.202728
- Liu, Y., Li, Q., Wang, H., Zhao, X., Li, N., Zhang, H., et al. (2019). Fish Oil Alleviates Circadian Bile Composition Dysregulation in Male Mice with NAFLD. *J. Nutr. Biochem.* 69, 53–62. doi:10.1016/j.jnutbio.2019.03.005
- Majumdar, A., Verbeek, J., and Tsochatzis, E. A. (2021). Non-alcoholic Fatty Liver Disease: Current Therapeutic Options. *Curr. Opin. Pharmacol.* 61, 98–105. doi:10.1016/j.coph.2021.09.007
- Membrez, M., Blancher, F., Jaquet, M., Bibiloni, R., Cani, P. D., Burcelin, R. G., et al. (2008). Gut Microbiota Modulation with Norfloxacin and Ampicillin Enhances Glucose Tolerance in Mice. *FASEB J.* 22 (7), 2416–2426. doi:10.1096/fj.07-102723
- Musso, G., Gambino, R., and Cassader, M. (2013). Cholesterol Metabolism and the Pathogenesis of Non-alcoholic Steatohepatitis. *Prog. Lipid Res.* 52 (1), 175–191. doi:10.1016/j.plipres.2012.11.002
- Panasevich, M. R., Peppler, W. T., Oerther, D. B., Wright, D. C., and Rector, R. S. (2017). Microbiome and NAFLD: Potential Influence of Aerobic Fitness and Lifestyle Modification. *Physiol. Genomics* 49 (8), 385–399. doi:10.1152/physiolgenomics.00012.2017
- Parséus, A., Sommer, N., Sommer, F., Caesar, R., Molinaro, A., Ståhlman, M., et al. (2017). Microbiota-induced Obesity Requires Farnesoid X Receptor. *Gut* 66 (3), 429–437. doi:10.1136/gutjnl-2015-310283
- Pu, P., Wang, X. A., Salim, M., Zhu, L. H., Wang, L., Chen, K. J., et al. (2012). Baicalein, a Natural Product, Selectively Activating AMPK α 2 and Ameliorates Metabolic Disorder in Diet-Induced Mice. *Mol. Cell. Endocrinol.* 362 (1–2), 128–138. doi:10.1016/j.mce.2012.06.002
- Rondina, M. T., Weyrich, A. S., and Zimmerman, G. A. (2013). Platelets as Cellular Effectors of Inflammation in Vascular Diseases. *Circ. Res.* 112 (11), 1506–1519. doi:10.1161/CIRCRESAHA.113.300512
- Roopchand, D. E., Carmody, R. N., Kuhn, P., Moskal, K., Rojas-Silva, P., Turnbaugh, P. J., et al. (2015). Dietary Polyphenols Promote Growth of the Gut Bacterium *Akkermansia muciniphila* and Attenuate High-Fat Diet-Induced Metabolic Syndrome. *Diabetes* 64 (8), 2847–2858. doi:10.2337/db14-1916
- Ryoo, J. H., Suh, Y. J., Shin, H. C., Cho, Y. K., Choi, J. M., and Park, S. K. (2014). Clinical Association between Non-alcoholic Fatty Liver Disease and the Development of Hypertension. *J. Gastroenterol. Hepatol.* 29 (11), 1926–1931. doi:10.1111/jgh.12643
- Salvoza, N., Giraudi, P. J., Tiribelli, C., and Rosso, N. (2022). Natural Compounds for Counteracting Nonalcoholic Fatty Liver Disease (NAFLD): Advantages and Limitations of the Suggested Candidates. *Int. J. Mol. Sci.* 23 (5), 2764. doi:10.3390/ijms23052764
- Stols-Gonçalves, D., Hovingh, G. K., Nieuwdorp, M., and Holleboom, A. G. (2019). NAFLD and Atherosclerosis: Two Sides of the Same Dysmetabolic Coin? *Trends Endocrinol. Metab.* 30 (12), 891–902. doi:10.1016/j.tem.2019.08.008
- Suk, K. T., and Kim, D. J. (2019). Gut Microbiota: Novel Therapeutic Target for Nonalcoholic Fatty Liver Disease. *Expert. Rev. Gastroenterol. Hepatol.* 13 (3), 193–204. doi:10.1080/17474124.2019.1569513
- Sun, W., Liu, P., Wang, T., Wang, X., Zheng, W., and Li, J. (2020). Baicalein Reduces Hepatic Fat Accumulation by Activating AMPK in Oleic Acid-Induced HepG2 Cells and High-Fat Diet-Induced Non-insulin-resistant Mice. *Food Funct.* 11 (1), 711–721. doi:10.1039/c9fo02237f
- Tang, Y., Zhang, J., Li, J., Lei, X., Xu, D., Wang, Y., et al. (2019). Turnover of Bile Acids in Liver, Serum and Caecal Content by High-Fat Diet Feeding Affects Hepatic Steatosis in Rats. *Biochim. Biophys. Acta Mol. Cell Biol. Lipids* 1864 (10), 1293–1304. doi:10.1016/j.bbalip.2019.05.016
- Tighe, S. P., Akhtar, D., Iqbal, U., and Ahmed, A. (2020). Chronic Liver Disease and Silymarin: A Biochemical and Clinical Review. *J. Clin. Transl. Hepatol.* 8 (4), 454–458. doi:10.14218/JCTH.2020.00012
- Tokuhara, D. (2021). Role of the Gut Microbiota in Regulating Non-alcoholic Fatty Liver Disease in Children and Adolescents. *Front. Nutr.* 8, 700058. doi:10.3389/fnut.2021.700058
- Vuppalanchi, R., and Chalasani, N. (2009). Nonalcoholic Fatty Liver Disease and Nonalcoholic Steatohepatitis: Selected Practical Issues in Their Evaluation and Management. *Hepatology* 49 (1), 306–317. doi:10.1002/hep.22603

- Wang, W. W., Wang, J., Zhang, H. J., Wu, S. G., and Qi, G. H. (2020). Supplemental *Clostridium Butyricum* Modulates Lipid Metabolism through Shaping Gut Microbiota and Bile Acid Profile of Aged Laying Hens. *Front. Microbiol.* 11, 600. doi:10.3389/fmicb.2020.00600
- Wen, B., Mei, Z., Zeng, C., and Liu, S. (2017). metaX: a Flexible and Comprehensive Software for Processing Metabolomics Data. *BMC Bioinforma.* 18 (1), 183. doi:10.1186/s12859-017-1579-y
- Yuan, J., Chen, C., Cui, J., Lu, J., Yan, C., Wei, X., et al. (2019). Fatty Liver Disease Caused by High-Alcohol-Producing *Klebsiella pneumoniae*. *Cell Metab.* 30 (4), 1172–1688. doi:10.1016/j.cmet.2019.11.006
- Zhang, X., Coker, O. O., Chu, E. S., Fu, K., Lau, H. C. H., Wang, Y. X., et al. (2021). Dietary Cholesterol Drives Fatty Liver-Associated Liver Cancer by Modulating Gut Microbiota and Metabolites. *Gut* 70 (4), 761–774. doi:10.1136/gutjnl-2019-319664
- Zhu, X., Yao, P., Liu, J., Guo, X., Jiang, C., and Tang, Y. (2020). Baicalein Attenuates Impairment of Hepatic Lysosomal Acidification Induced by High Fat Diet via Maintaining V-ATPase Assembly. *Food Chem. Toxicol.* 136, 110990. doi:10.1016/j.fct.2019.110990

Conflict of Interest: The authors declare that the research was conducted in the absence of any commercial or financial relationships that could be construed as a potential conflict of interest.

Publisher's Note: All claims expressed in this article are solely those of the authors and do not necessarily represent those of their affiliated organizations, or those of the publisher, the editors, and the reviewers. Any product that may be evaluated in this article, or claim that may be made by its manufacturer, is not guaranteed or endorsed by the publisher.

Copyright © 2022 Li, Hu, Zhao, Feng and Chai. This is an open-access article distributed under the terms of the Creative Commons Attribution License (CC BY). The use, distribution or reproduction in other forums is permitted, provided the original author(s) and the copyright owner(s) are credited and that the original publication in this journal is cited, in accordance with accepted academic practice. No use, distribution or reproduction is permitted which does not comply with these terms.

Advantages of publishing in Frontiers



OPEN ACCESS

Articles are free to read
for greatest visibility
and readership



FAST PUBLICATION

Around 90 days
from submission
to decision



HIGH QUALITY PEER-REVIEW

Rigorous, collaborative,
and constructive
peer-review



TRANSPARENT PEER-REVIEW

Editors and reviewers
acknowledged by name
on published articles

Frontiers

Avenue du Tribunal-Fédéral 34
1005 Lausanne | Switzerland

Visit us: www.frontiersin.org

Contact us: frontiersin.org/about/contact



REPRODUCIBILITY OF RESEARCH

Support open data
and methods to enhance
research reproducibility



DIGITAL PUBLISHING

Articles designed
for optimal readership
across devices



FOLLOW US

@frontiersin



IMPACT METRICS

Advanced article metrics
track visibility across
digital media



EXTENSIVE PROMOTION

Marketing
and promotion
of impactful research



LOOP RESEARCH NETWORK

Our network
increases your
article's readership